# THE INFLUENCE OF FLUTE FORM ON DRILL DESIGN AND PERFORMANCE

by

MANUEL DOS SANTOS PAIS, MSc (England),
Lic.Eng.Mec, CEng, MEOrEng (Portugal).

A Doctoral Thesis

Submitted in partial fulfilment of the
requirements for the award of the degree of
Doctor of Philosophy
of the Loughborough University of Technology

July 1982

Supervisor: D J Billau, PhD, MSc, CEng, MIMechE,
FIProdE
Department of Engineering Production

## ACKNOWLEDGEMENTS

I would like to express my gratitude to the Instituto Nacional de Investigação Científica - INIC - for the financial support that made this thesis possible.

I am also obliged to the following people:

Professor R J Sury, Head of the Department of Engineering Production and my Director of Research for the interest he took in my studies in England;

Dr D J Billau, my supervisor, for his constant encouragement, advice and assistance;

Osborn-Mushet Tools Limited, Sheffield, and Marsh Brothers and Co. Ltd, Engineers, Sheffield for the drills manufacture;

Mr D G Johnson, from the Department of Management Studies, for helping with the statistical design of the experiments;

Mr R E Phelps, from the Centre for Industrial Studies, for his assistance with the analysis and heat treatment of the materials;

Mr K Pugh and Mr M Frost for the photographs, and

All the other people, mainly in the Computer Centre and in CIS, who contributed to making this work come true.

The text was typed by Mrs J Smith whose help is also acknowledged.

*"... an ordinary twist drill ... is extremely complex, geometrically".*

*Shaw and Oxford*

*"... when you cannot express it in numbers, your knowledge is of a meagre and unsatisfactory kind".*

*Lord Kelvin*

# THE INFLUENCE OF FLUTE FORM ON DRILL DESIGN AND PERFORMANCE

# THE INFLUENCE OF FLUTE FORM ON DRILL DESIGN AND PERFORMANCE


## SYNOPSIS

Many modifications have been made in the past to the conventional drill points and references to the better performance of curved lip drills when cutting cast iron can be found. Similar drill points do not seem to be as successful with steel.

The objective of this research was set to analyse drill design and to study the effect on drill performance of changing the drill conventional flute form when cutting steel.

Changing the conventional flute form has an immediate effect on the shape of the drill lip - it is no longer a straight cutting edge.

A new range of problems arises when the drill lip is a curved line as the available expressions in literature for drill cutting angles calculation are not valid except for straight lines. However, to be able to calculate and to predict the cutting angles with a non-conventional flute drill is a matter of necessity, especially if the new flute design is based or specified upon some condition relative to these angles.

The drill lip shape is also influenced by the flank surface. Thus the analysis of the drill lip shape and the calculation of the cutting angles cannot be made without studying both the flute and the flank surfaces.

Geometric surfaces are better dealt with by computing techniques and computers. Thus the shape of a drill lip - the intersection of the flute with the point flank - and the cutting angles, are analysed by means of computer design aids for both varying flute and point flank surfaces.

First, the conventional flute face design is revised as far as its design parameters and profiles normal to the drill axis are concerned. The flute heel is analysed and incorporated with the mathematical model for the flute face. Additionally, as a matter of interest for the flute cutter design, the flute sections normal to the flute direction are computed from the mathematical model for the flute.

The cylindrical grinding concept is analysed and mathematically modelled in order to simulate the capabilities of many cylindrical grinding machines in industry and the one available to the author. The name "extended cylindrical grinding" is proposed as the orthodox cylindrical grinding concept is extended to allow for free selection of all drill point features generally available with conical grinding.

A mathematical model for the extended cylindrical grinding is built up, the parameters defined, and the equations implemented in a computer program for the analysis of the effect of these parameters on the drill point features by numerical investigation, and by simulation by computer aided design.

To make possible the complete simulation of the drill point, the chisel edge - the intersection of two point flanks symmetric relatively to the drill axis - is also analysed.

The intersection of the modelled cylindrical flank surface with any modelled flute - conventional or non-conventional - yields the drill lip which is simulated for shape and analysed for the cutting angles such as rake angle, inclination angle, clearance angle and wedge angle.

By varying the flute form, the law to each cutting angle along the lip is altered. Reciprocally, to each pre-fixed law to some of the cutting angles along the drill lip corresponds to a different flute form.

One method to compute the flute form, given a law to the selected cutting angle along the drill lip, is presented, analysed and used for designing a new drill flute.

Based on the assumption that the effective rake angle is the important rake angle in cutting, and that it may be nearly unaltered when a decrease in the normal rake angle is compensated by an increase in the inclination angle, an attempt is made to increase drill life by designing a special flute with increased wedge angle (known as *"heat sinking"* at many workshops) at the outer corner.

Drills were manufactured according to the new flute design by drill manufacturers.

Tests were run with steel in order to compare the performance of a conventional fluted drill and the non-conventional design put forward.

The wear was measured at several points on the lips of the tested drills and appeared to be more uniform along the lips of the new design drill type than along the lips of the conventional one. Lip wear rate however, tended to be higher for the new design drill type than for the conventional one.

Comparing the drilling forces, the drilling thrust values for the new design drill type were smaller than for the conventional one; the drilling torque values however, were smaller for the conventional type than for the new design one.

Chips produced by both drill types were also analysed as a further aspect of drill performance.

The rigid body concept - a mechanics concept - was introduced for chip flow mathematically modelling and for computer aided analysis in order to study the influence of flute form on chip kinematics. The potential of this approach by the author for drilling chip analysis is shown by means of geometrical simulation, chip flow angle prediction and chip length ratio prediction. This approach also allows for other predictions which correlate with experimental data already reported in literature.

The suggestion is made for drill design to be based on specifications established according to rigid body drilling chip production.

# NOMENCLATURE

## i) Notations

| | |
|---|---|
| (BSj) | British Standards specification number j |
| (C.j) | Catalogue number j |
| [D.j] | Definition number j |
| i.j | Equation number j in Chapter i. |
| (j) | Bibliographic reference number j. |
| (j,k) | Bibliographic reference numbers j and k. |
| 3D | Three dimensional |

## ii) Vectors and Vectorial Operations

Vectors and vectorial operations are represented as in (78). A summary of those representations used throughout the present work is given in this section.

| | | |
|---|---|---|
| $\vec{OP}$ | - | Vector with original point at O and terminal point at P |
| $\vec{A}$ | - | Vector A |
| $\vec{a}$ | - | Unit vector a |
| A or $\lvert\vec{A}\rvert$ | | Magnitude of vector A |
| $\lvert\vec{a}\rvert$ | = | 1 |
| $\vec{A}$ | = | $A\,\vec{a} = \lvert\vec{A}\rvert\,\vec{a}$ |
| $\vec{A}.\vec{B}$ | = | $\lvert\vec{A}\rvert\lvert\vec{B}\rvert\cos\psi$ - dot product of vectors A and B; $\psi$ is the angle between $\vec{A}$ and $\vec{B}$ |
| $\vec{A}\times\vec{B}$ | = | $\lvert\vec{A}\rvert\lvert\vec{B}\rvert\sin\psi\,\vec{c}$ - cross product of vectors A and B; $\psi$ is the angle between $\vec{A}$ and $\vec{B}$; $\vec{c}$ is a unit vector perpendicular to vectors A and B |
| $\vec{i},\vec{j},\vec{k}$ | | Unit vectors in the directions of the axes of a 3D rectangular coordinate system |
| $\vec{a}$ | = | $(a_1, a_2, a_3)$ - components of vector a in the directions of the axes of a 3D rectangular coordinate system |
| $\vec{i}$ | = | $(1,0,0)$; $\vec{j} = (0,1,0)$; $\vec{k} = (0,0,1)$ |

$$\vec{A}.\vec{B} = |\vec{A}||\vec{B}|\ \vec{a}.\vec{b} = |\vec{A}||\vec{B}|\ (a_1\ b_1 + a_2\ b_2 + a_3\ b_3)$$

$$\vec{A}x\vec{B} = |\vec{A}||\vec{B}|\ \vec{a}x\vec{b} = |\vec{A}||\vec{B}| \begin{vmatrix} \vec{i} & \vec{j} & \vec{k} \\ a_1 & a_2 & a_3 \\ b_1 & b_2 & b_3 \end{vmatrix}$$

$$= |\vec{A}||\vec{B}|\ (a_2\ b_3 - a_3\ b_2)\vec{i} + (a_3 b_1 - a_1\ b_3)\vec{j} + (a_1 b_2 - a_2 b_1)\vec{k}$$

$$= |\vec{A}||\vec{B}|\ (a_2 b_3 - a_3 b_2,\ a_3 b_1 - a_1 b_3,\ a_1 b_2 - a_2 b_1)$$

The following symbols are also used:

$\vec{t}$ - unit vector tangent to a line or surface
$\vec{n}$ - unit vector normal to a surface
$\vec{e}$ - vector tangent to a cutting edge

iii) List of Symbols

| | | |
|---|---|---|
| A,B,C,D,E, F,G,H,I,J | - | coefficients to the equations of the surfaces representing the drill flanks |
| $A_{h1}$, $B_{h1}$, $C_{h1}$ | - | coefficients to the equation of the drill heel contour |
| $b_1$ | - | uncut chip width |
| $b_2$ | - | chip width |
| $C_1$, $C_2$, $C_3$, $C_4$ | - | coefficients to the equation of a plane in a 3D referential system |
| $d_o$ | - | drill diameter |
| $d_{og}$, $\nu_g$, $ex_g$, $\kappa_g$ | | parameters to mathematical model of drill flank surface generated by cylindrical grinding |

$D_{og}$, $V_g$, $Ex_g$, $RK_g$ - the same as ($d_{og}$, $\nu_g$, $ex_g$, $\kappa_g$) used in the FORTRAN computer programs (appendices)

$ex_g$, $Ex_g$ - see $d_{og}$ and $D_{og}$ entries, respectively

$K_1, K_2, \ldots$ - numerical constants

$\ell$ - drill flute lead

$\ell_1$ - uncut chip length

$\ell_2$ - chip length

$r$ - radial distance on a drill

$r_c$ - radial distance on a chip

$r_\ell$ - cutting length ratio

$r_o$, $2W'$, $\gamma_f$, $\kappa$ - parameters to the conventional flute face mathematical model

$R_o$, Web, $H_o$, $R_k$ - equivalent to ($r_o$, $2W'$, $\gamma_f$, $\kappa$) used in the FORTRAN computer programs (appendices)

$s$ - variable length measured along the drill lip

$t_1$ - uncut chip thickness

$t_2$ - chip thickness

$T, T_1, T_2, T_3$ - coordinate transformation matrices

$T_h$ - drilling thrust

$T_o$ - drilling torque

$V$ - cutting speed

$V_c$ - chip speed

$X_p, Y_p, Z_p$ - coordinates of point P in a referential system with axes X, Y and Z

XCHI, YCHI, ZCHI - chisel edge coordinates used in the FORTRAN computer programs (appendices)

$X'$, $Y'$, $Z'$
$X''$, $Y''$, $Z''$
$X^*$, $Y^*$, $Z^*$ - coordinates in auxiliary referential systems

$W, W'$ - half web thickness and half lip spacing, respectively

$Z_{dc}$ - distance of chisel point (dead centre) to referential plane XY

$\alpha_n$ - normal clearance angle

$\beta_n$ - normal wedge angle

$\gamma_n$, $\gamma_e$ - normal and effective rake angle, respectively

$\gamma_f$ - drill helix angle (at periphery) - refer to entry $r_o$

$\eta$ - chip flow angle

$\kappa$ - half drill design point angle - refer to entry $r_o$

$\kappa_g$ - half drill ground point angle - refer to entry $d_{og}$

$\lambda$ - inclination angle

$\mu$,X - parameters to heel equation

$\nu_g$ - refer to entry $d_{og}$

$\xi$ - rotation angle

$\phi$,r,z - cylindrical coordinates

$\psi$ - chisel edge angle

$\psi'$ - chisel edge angular distance to X axis of referential system

iv) Definitions

Writers in the area of drilling do not use always the same terms when referring to similar drill and drilling concepts. To avoid ambiguity, a glossary of the terms used throughout this work is presented in this section. Terms are given in alphabetical order.

[D.1] - Body - the part of the drill extending from the chisel edge to the shank end of the flute (3) (Figure 1.1)

[D.2] - Body clearance - the part of the body surface reduced in diameter to provide diametral clearance (3) (Figures 1.1 and 1.2)

[D.3] - Built up edge, BVE - a thin crusted layer on the tool face, adjacent to the cutting edge (4)

[D.4] - chip flow angle, $\eta$ - Section 4.4

[D.5] - chip length ratio, $r_\ell$ - Section 8.6.3

[D.6] - chisel edge - Section 3.4

[D.7] - chisel edge angle, $\psi$ - the obtuse angle between the tangent to the projection of the chisel edge at the chisel point and the projection of the lips on a plane normal to the drill axis (67) (Figure 1.3).

[D.8] - clearance angle, lip, $\alpha_f$ - the same as nominal relief angle

[D.9] - clearance angle, normal, $\alpha_n$ - Section 4.3.2.

[D.10] - contact length, chip - length of tool - chip contact (79)

[D.11] - cylindrical grinding, extended - drill point grinding by generation of a cylinder surface which, for convenience, can be positioned in such a way that allows for free selection of all drill point features generally available with conical grinding

[D.12] - face, flute (rake) - part of the flute on which the chip impinges as it is cut from the work and which, together with the flank surface, determines the drill lip (Figure 1.1)

[D.13] - flank (surface) - the surface of a drill point which extends behind the lip to the following flute (Figure 1.2)

[D.14] - flute (surface) - Section 2.1

[D.15] - flute face, conventional - a flute face which is a ruled surface - Section 2.7

[D.16] - flute face, non-conventional - Section 2.7

[D.17] - heel flute (surface) - the surface which, together with the flute face completes the flute surface (Figure 1.1)

[D.18] - heel drill point contour - intersection of heel flute surface with flank surface (Figure 4.1)

[D.19] - inclination angle, $\lambda$ - Section 4.3.4

[D.20] - lands - the cylindrical ground surfaces on the leading edges of the drill flute (3) - (Figure 1.2)

[D.21] - lip - Section 4.1 (Figure 4.1)

[D.22] - lip height, relative - distance between two planes normal to the drill axis each one containing one of the two drill outer corners

[D.23] - lip spacing, 2W' - distance between the projections on a plane normal to the drill axis of the tangents to the drill lips at a radial distance r

[D.20] - margin - same as land

[D.24] - point angle, flute design, $2\kappa$ - Section 2.2

[D.25] - point angle, ground, $2\kappa_g$ - Section 3.2.1

[D.26] - rake angle, effective, $\gamma_e$ - Section 4.5

[D.27] - rake angle, normal, $\gamma_n$ - Section 4.3.1

[D.28] - relief angle, nominal - the angle between the drill point surface and a plane perpendicular to the drill axis, measured in a plane parallel to the drill axis and perpendicular to a radius. The angle is usually measured from the lip (3)

[D.29] - rigid body - a material system for which the distance between any pair of points is a constant with respect to time (80)

[D.30] - ruled surface - surface which is generated by a moving straight line (62)

[D.31] - web thickness, 2W - Section 2.4.2

[D.32] - wedge angle, normal, $\beta_n$ - the angle between the face and the flank measured in a plane normal to the cutting edge

v) Units

Where it is not referred to otherwise, the distances are measured in mm and the angles in degrees.

CONTENTS

Page No

APPENDICES ... continued — Page No

*"The complex nature of conventional twist drills and their cutting action has challenged research workers for many years"*

*Armarego*

# 1. GENERAL INTRODUCTION

## 1.1 General Literature Survey

Drilling is one of the oldest (1,2) and most widely used operations(1,2,3,4,5,6,7,8,9,10) in the manufacturing process.

Kahng and Ham estimated hole-making to be more than 30% of the total metal cutting business (9). Billau quotes a PERA survey according to which 28.2% of the total general engineering industry in Britain consisted of work carried out on drilling machines (6). Ernst and Haggerty estimated about 20% of the machine tools in the USA were drilling machines (2). Drilling, however, can also be done on turning machines and other machine tools capable of providing a relative rotation of workpiece and cutting tool (8).

The drilling operation is affected by many factors (3) and its success depends mainly on the performance of the drilling tool.

To meet the requirements of the manufacturing process there are several types of drilling tools which may be as different as those referred to in Table 1.1.

The twist drill, Figure 1.1, a two lipped diametrically opposed helical fluted tool - is currently made of high speed steel and it is the most commonly used drilling tool (5).

According to Billau (11) the twist drill was invented in 1863 by Martignoni, and Wiriyacosol and Armarego (12) also refer to Morse as having patented a twist drill in 1863.

Twist drills have been produced since a century ago (10), and their development has been dependent on manufacturers incentives (6,10). However, for Billau, the development of alternative designs by drill manufacturers *"has not proved fertile ground for the academic researcher"* (6).

Specifications for the twist drill - also known as conventional drill (13), regular twist drill (14), standard drill (3) and orthodox

| | Twist drill | Half-round drill | Pivot (micro) | Spade | Indexable insert drill | Gundrill | BTA system | Ejector drill | Trepanning |
|---|---|---|---|---|---|---|---|---|---|
| Diameter typical range (mm) | 0.51-51 | 0.15-6.35 | 0.025-0.51 | 25.4-152 | 15.9-76 | 2-25.4 | 11-203 | 19-57 | 44.5-254 |
| Depth/ diameter ratio common maximum | 5-10 | > 10(horiz) | 3-10 | >40(horiz) | 2-3 | 100 | 100 | 50 | 100 |

TABLE 1.1: Drilling Tools (8)

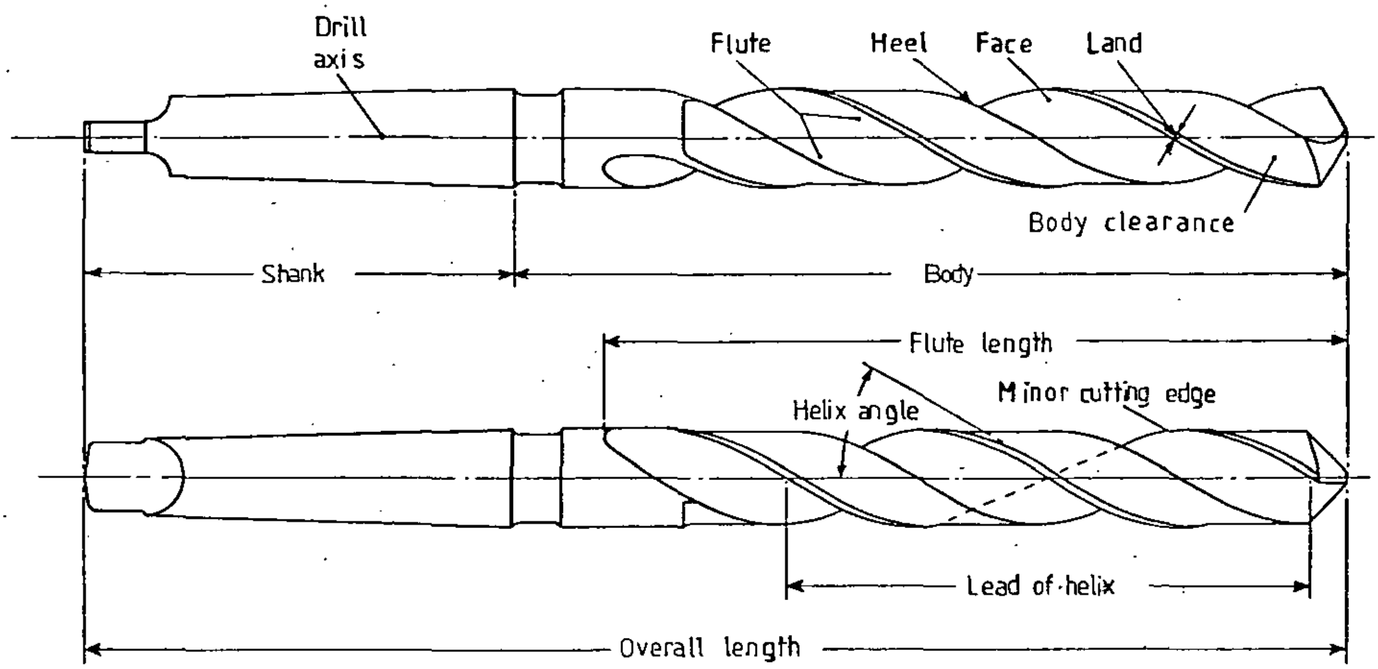


FIGURE 1.1: Twist drill [(BS 328),with alterations]

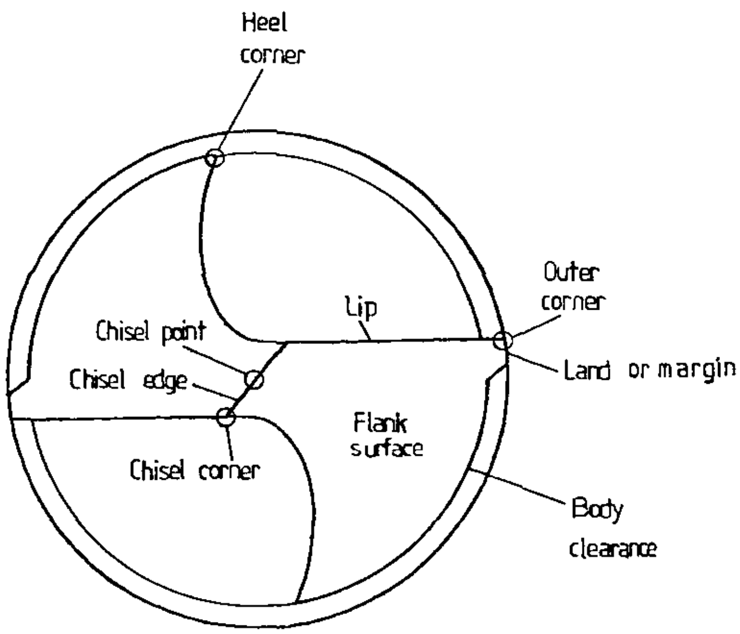


FIGURE 1.2: Twist drill point

drill (15) - have been issued by several national standard organizations (16, 17, 19, BS328).

A two fluted twist drill is generally considered to be geometrically complex (16, 20, 21, 22), and its main active surfaces are as follows (Figure 1.1 and Figure 1.2):

- two flanks (the surfaces produced by the drill user at the drill point)
- two flutes (the helical canals along the body of the drill)
- two margins (3,18) or lands (3, BS328) [they belong to the cylindrical (3) surface determining the leading edges of the flutes].

The intersection of the two flank surfaces yields the chisel edge.

Each flute comprises two parts:

- the face - the leading side where the chip formation occurs
- the heel - the trailing side which is the chip former.

Each flank intersects both flutes: the face of one flute and the heel of the other one. The intersections of the flank surfaces with the flute faces determine the lips (BS 328) or major cutting edges (BS 5533). The intersections of the flute faces with the margins determine the minor cutting edges (Figure 1.1) (BS 5533).

According to Armarego and Wright there are six features commonly specified in handbooks for twist drills (Figure 1.3) (16):

- the point angle, [D.25], $2\ \kappa g$
- the chisel edge angle, [D.7],
- the lip clearance angle at the outer corner, [D.8], $\alpha_f$
- the web thickness, [D.31], 2W
- the helix angle at the outer corner, $\gamma_f$
- the drill diameter, $d_o$.

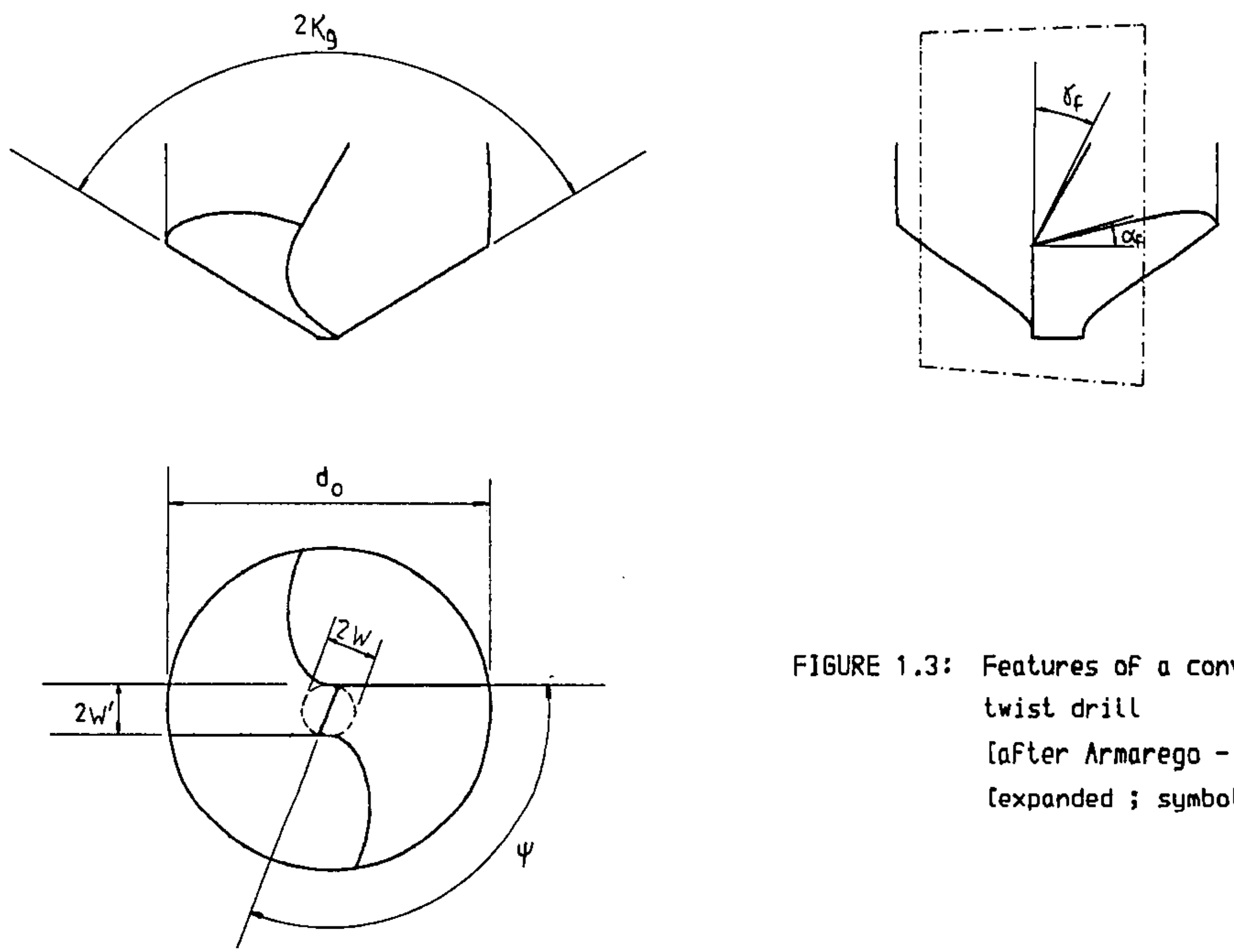


FIGURE 1.3: Features of a conventional twist drill
[after Armarego - (16)]
[expanded ; symbols altered]

Three of the above listed features are determined at the manufacture stage: $d_o$, 2W and $\gamma_f$; the other three can be selec-ted by the user at the drill point grinding stage.

For Shaw (discussion of paper 20), the important features are: the point angle, the helix angle and the web thickness.

As far as the point angle is concerned the author would prefer to make a distinction between the (conventional) flute design point angle, [D.24], $2\kappa$, and the actual ground point angle, [D.25], $2\kappa g$, for they may be different.

As shown in Chapter 2, it is necessary to define a point angle to design a conventional flute. If the ground point angle at the grinding machine is different to that for the flute design, the lips will be curve shaped (either convex or concave - Figure 1.4) as it is known in the workshop, and has been referred to, for instance, by Galloway (3).

To measure the actual drill point angle by measuring the angle of two curved lips becomes slightly ambiguous as it varies from point to point along the lips.

Also the relative position of the chisel edge to the curved lip ($\psi$, Figure 1.3) is open to reconsideration as the direction of the lip varies from point to point.

The web thickness, 2W, is taken equal to the lip spacing [D.23], 2W' (Figure 1.3), by several workers (3, 12, 16), however, the author did not find in the many works in literature any reference to the actual difference between 2W and 2W'. Furthermore, the lip spacing feature is open to clarification too, when the lips are curved.

Most research work on twist drills was aimed at finding how drill performance correlates with the twist drill features, usually one at a time (23).

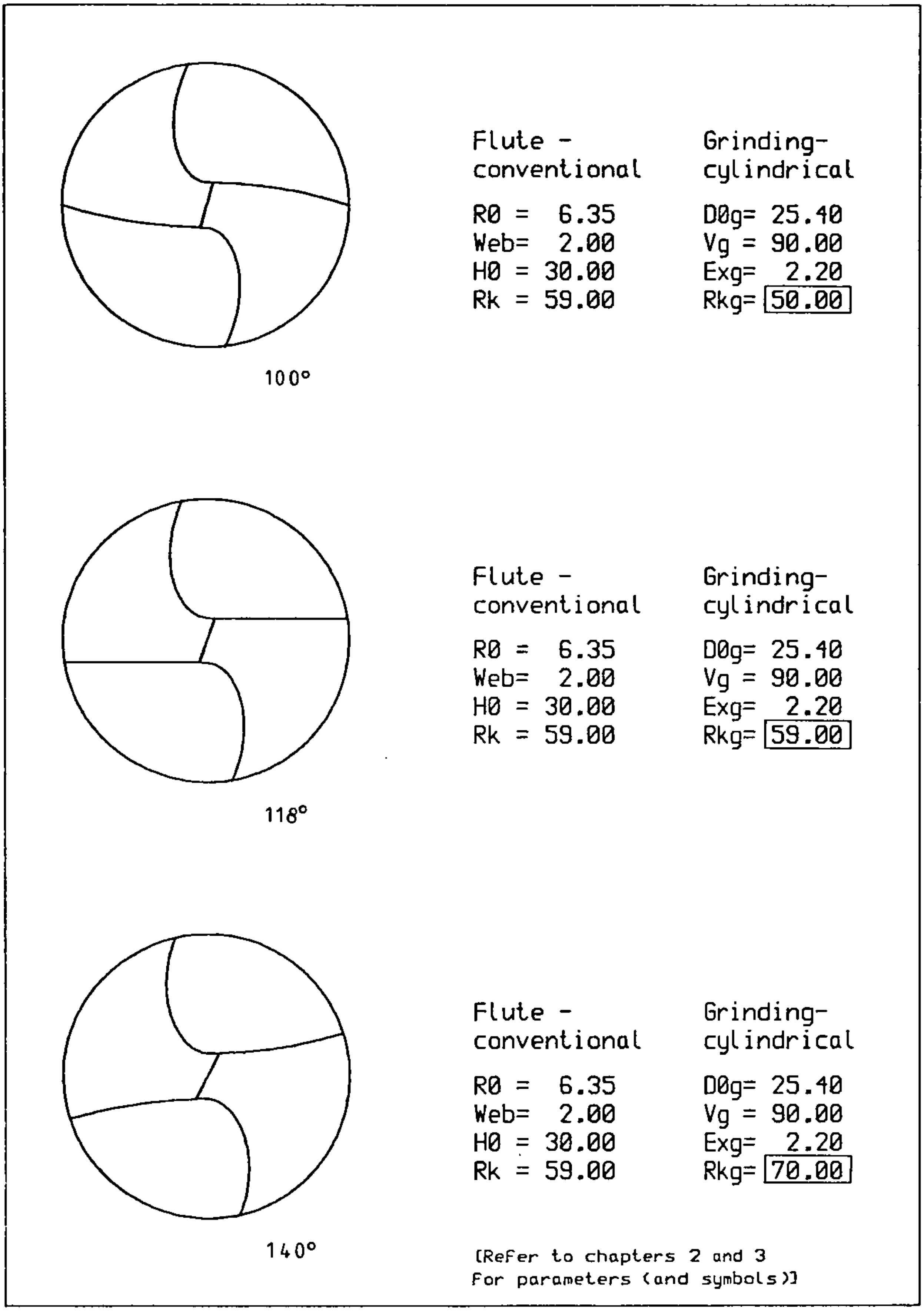


FIGURE 1.4: Conventional twist drill ground to three different point angles

The influence of point angle variation on drill life has been reported by Galloway (3) and PERA (24), for example. Its influence on drilling forces was studied by Galloway (3), Galloway and Morton (10), Wiriyacosol (12), Micheletti (23), Bhattacharyya and co-workers (25,26) and Oxford and Shaw (27). Micheletti (23) also quotes Codron, Bird and Fairfield.

The effect of the chisel edge angle on drilling forces was referred to by Micheletti (23).

The influence of the lip clearance angle [D.8] on drill life was investigated by Lorenz (28); on drill life and drilling forces, by Galloway and Morton (10) and PERA (24).

The web thickness has been reported to influence the drilling forces (3, 10, 20), and the helix angle to influence drill life (3, 29, 31, 32) and drilling forces (10, 27).

The effect of drill diameter on drilling forces has also been reported (10, 12, 27).

According to Micheletti (23), Tourret (32) would have reviewed most of the papers on drill performance published up to 1957.

Drill performance, according to many research workers in the drilling area, varies a great deal, for nominally similar twist drills, and for each set of cutting conditions. According to the same research workers such variation is due to the inaccuracies of drill geometry (3, 20, 28, 33, 34).

Inaccuracies of symmetry of the two fluted twist drill can occur at the manufacture stage (flute spacing inaccuracy, for example), and/or at the point grinding stage (flank positioning error, for example).

One frequently referred to error of twist drill symmetry is the relative lip height [D.22] (3, 9, 10, 33, 34, 35, 37, C.1) as it can diminish drill life. Some other errors of symmetry are:

- eccentricity of web (1, 17)

- eccentricity of chisel edge (9, 35)
- unequal lip spacing (1, 17)
- defective drill straightness (17)

Many attempts to improve drill performance consisted of modifying the conventional drill point:

- spiral point (2, 17)
- four facets point (17)
- six facets point (17)
- double cone (17, 38)
- split point (2, 17)
- point thinning (3, 10, 17, 38, 39)

However, special flank surface shapes cannot be implemented except with special grinding machines and/or by expert toolmakers. Additionally, the performance improvement with these altered drill points is frequently limited to some drilling conditions, and some drill point forms alter the shape of the lips and are bound to affect the mechanics of cutting along these cutting edges (3).

Encouragement for the analysis of the drilling process to be made with a cutting mechanics approach has come from a great deal of workers who have suggested that there is no fundamental difference between the cutting process of complex tools such as drills and other simpler tools such as the single point cutting tool.

- Oxford and Shaw stated that an ordinary twist drill operates in the same way as a single point tool (27);
- Dagnell underlines the similarities between the drill lip action and the lathe single point cutting tool (40);
- Wiriyacosol and Armarego predicted some drilling performance characteristics by approaching the drill lip and the chisel edge to a certain number of elementary single point cutting tools (12);
- Kumar et al are of the opinion that the drill lip action is *"more or less an inclined and oblique cutting process"* (25).

The same opinion is shared by Bera and co-workers (26).

- Wu et al employed photoelastic techniques in the analysis of drill stress and found that at drill periphery their results suggested an action analogous to orthogonal cutting (41).
- Venkataraman attempted a theory of tool simulation consisting of one to one correspondence of the cutting angles along the drill lip with that of a shaper tool (42).
- Oxley and Palmer think that the shape of any tool is connected with the orthogonal cut case (43).

The influence of such angles as the rake angle [D.26, D.27] and/or the inclination angle [D.19], for example, on the mechanics of cutting has been emphasized by Merchant (44), Stabler (45, 81), Shaw (77, discussion of paper 20), Armarego and Brown (46), Lee and Shaffer (47), Hirota and Usui (48), Ramalingam (49), Catrina et al (50) and others (51, 52).

Some workers such as Galloway (3), Oxford (53), Williams (54) and Amaradasa (55) have presented expressions for the calculation of such angles as, the rake angle, the inclination angle and the clearance angle along the straight twist drill lips. These expressions are usually based on the features of the twist drills and the referred to cutting angles may be calculated for each point at a radial distance r selected on the straight drill lip.

By using the referred to expressions the following facts may be established for the straight lip of a conventional flute twist drill:

- normal rake angle [D.27] is maximum at the outer corner
- inclination angle [D.19] is minimum at the outer corner
- normal wedge angle [D.32] is minimum at the outer corner

It is also easy to find that:

- cutting speed is maximum at the outer corner
- the outer half of the drill removes 75% of the material from the hole.

Yokoyama and Watanabe made a thermal analysis of the drilling process and found calculated temperature to increase with radial distance on the drill lip and claimed good agreement with the experiments (56). Wu and co-workers have also analysed drill temperature distribution by numerical solutions (57) and found the higher values to be near the outer corner; they claimed good agreement with experiments too.

Oxford measured the chip flow angle along the drill lip and found the smaller values to be at the outer corner (20).

## 1.2 Statement and Approach to Problem

The outer corner (Figure 1.2) is the part of a conventional twist drill most subject to wear, according to Bhattacharyya (38, 58). Also Galloway (34) and Kanai and Kanda (33) referred to the wear near the outer corner and suggested it to be used as a drill life criterion.

The relatively quicker wear near the outer corner of a conventional drill may be attributed, at a first approach, to an unfavourable combination of high temperature and small wedge angle (*"heat sink"*), for, as suggested by Galloway (34), the amount of metal supporting the drill lips may influence drill life.

In an early preliminary numerical investigation on the expressions available in the literature, and measurements made by Amaradasa (55), the author found the wedge angle with conventional twist drills to vary from about $50^0$ at the outer corner up to about $80^0$ near the chisel corner.

The hypothesis is put forward that the flute face, which is produced at the manufacture stage, can possibly by changed in order to yield a more uniform wedge angle along the drill lip than that with the conventional flute, and a more uniform wear along the new drill lip may be obtained while leaving the grinding process unaltered.

Drill lip wear may possibly be diminished at the outer corner by making the wedge angle bigger than that of a conventional flute drill, even at the expense of the normal rake angle. This would probably not impair drill efficiency as the effective rake angle [D.26] - the angle that in the field of oblique cutting replaces the normal rake angle in orthogonal cutting, according to Shaw and co-workers (59) and Yokoyama and co-workers (56) - depends on the normal rake angle and inclination angle, according to Stabler (45), and a decrease in the normal rake angle can be compensated by an increase in the inclination angle (Figure 1.5).

Any departure from the conventional flute (rake) face [D.15] - a ruled surface [D.30] - has an immediate effect on the shape of the drill lip: it is no longer a straight cutting edge.

To deal with non-conventional flute faces [D.16]or, in general, with non-straight drill lips, arises a new range of problems as the available expressions in the literature for drill lip cutting angles calculations are not valid except for straight lips.

The analysis of cutting variables such as rake angle, clearance angle and inclination angle along curved lips cannot be made without defining the surfaces which determine the drill lips - the flute face and the flank surface.

These two rather complex surfaces can be mathematically modelled and their properties and mutual intersections determining the cutting edges can be analysed by computer design aids.

A numerical investigation and geometrical simulation is to be performed in this work, as far as it is needed, for lip shape determination and cutting angles computation when the lips are not straight.

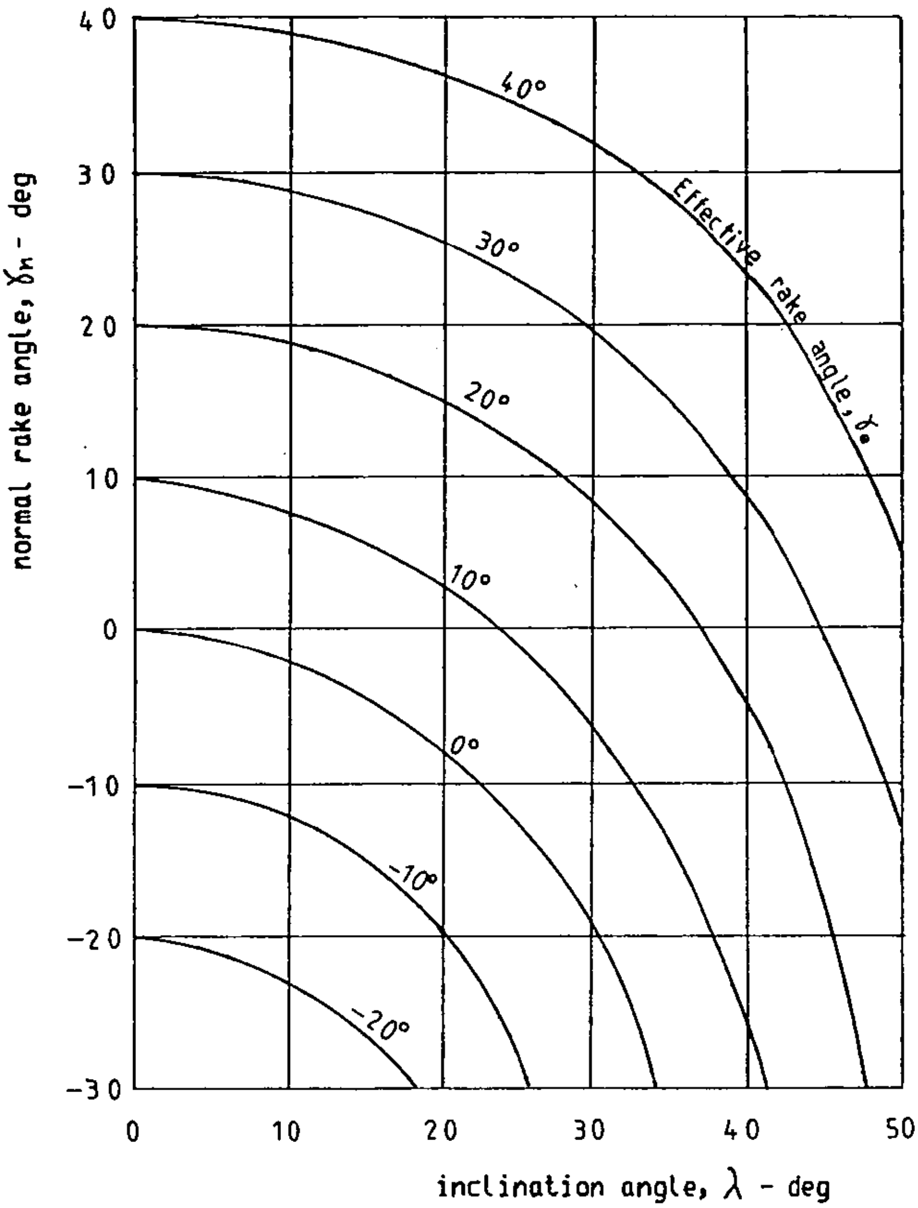


FIGURE 1.5: Effective rake angle computed from the normal rake angle and inclination angle.
[After Stabler (45);also Shaw (77) and others (25)]

To design a method for designing drill flutes specified by the cutting angles along the lip is also one of the author's purposes; especially to design a drill with such a flute that the lips would comply with the condition of uniform wedge angle.

The author's objectives can be summarised as follows:

- to analyse the influence of flute form on drill point design
- to design a new flute that hypothetically may improve drill performance
- to study the influence of flute form on drill performance (chips included) when cutting steel.

For these purposes the drill lip geometry is to be analysed by means of the cutting angles by computer aided design.

*"It is ordinary thought that the shape of the drill flute should be such that the cutting lip will be a straight line"*

*Moore*

## 2. CONVENTIONAL TWIST DRILL FLUTE DESIGN

## 2.1 Introduction

Galloway and Morton (10) defined the drill flute as a chip disposal groove extending from the drill point towards the shank. Tsai (5) points out the following functions to the flute:

i) form the cutting edges on the drill point
ii) allow the chip to escape
iii) cause the chips to curl
iv) permit cutting coolant to reach the cutting edges.

For Shaw and Oxford (27) the flute-shape details may be ignored for a *"normally functioning drill"*. According to Cetim (17), the flute form affects the shape of the drilling chips. Shaw (21) refers to the influence of flute form on lip shape, chip flute space and drill torsional rigidity. Billau (11) also refers to the flute as providing a cutting lip after point grinding, assisting the removal of chips, and affecting drill rigidity.

## 2.2 Conventional Flute Face Design and Parameters

One half of the flute - the face - is commonly determined in order to yield a straight cutting edge (3, 20, 21, 60). The other half - the heel - is chosen in such a way that drill strength (3), drill rigidity (11, 21, 61) and space for chip conveyance (3, 21, 31) are at a compromise.

A straight line - the conventional drill main cutting edge - can be defined by two parameters relatively to an axis - the drill axis (Figure 2.1):

W' - the distance to the drill axis (half of drill lip spacing)
$\kappa$ - angle to the drill axis (half of drill point angle)

An helical movement of this straight line around the drill axis generates a ruled surface - the conventional flute face. The locus of a point on the generating line, at a distance $r_0$ (= $d_0/2$) from the drill axis, is an helical line with angle $\gamma_f$ - the drill helix angle.

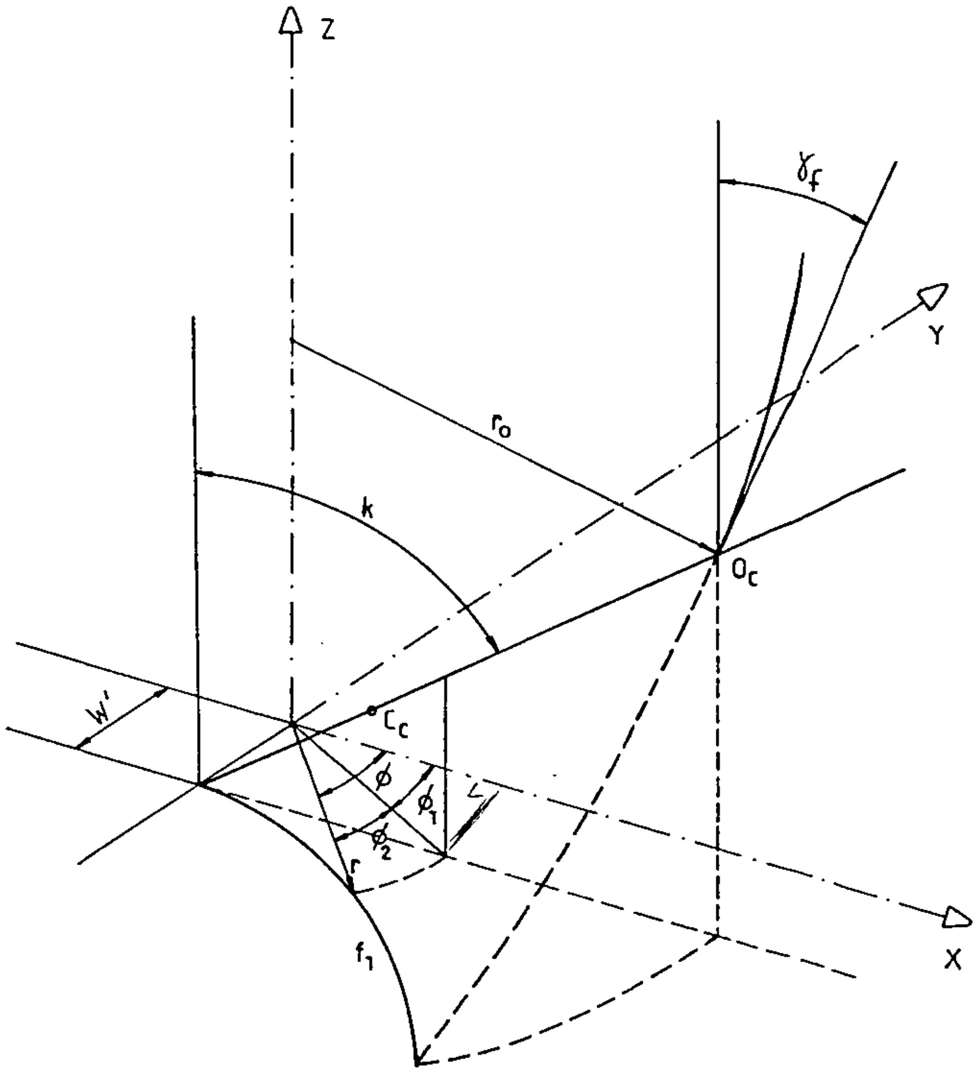


Z - drill axis
$f_1$ - flute face cross section
Cc - chisel corner
Oc - outer corner
Cc-Oc - drill lip
$2r_o, w', \gamma_f, k$ - parameters to the conv. flute face model

FIGURE 2.1: Twist drill conventional flute face generation and parameters

The four parameters, $r_0$, $W'$, $\gamma_f$ and $\kappa$ define mathematically the conventional drill flute face as no further paremeters are needed.

Galloway (3) has already developed the parametric equations to the conventional flute face and from his analysis Tsai and Wu (60) deduced the mathematical model of the flute shape. As a matter of necessity the author presents the analysis by Galloway, further studied by Tsai, for the conventional flute mathematical model.

For the mathematical model reference, a coordinate system of rectangular cartesian axes is defined (Figure 2.1):

Z - drill axis, pointing to the shank ;

XY - plane normal to the drill axis at the point where the distance from the drill axis to the flute generating line is measured ;

X - axis parallel to the projection of the flute generating line on the plane XY, pointing to the same direction as that referred to projection ;

Y - axis in the plane XY, normal to X, orientated in such a way that the reference system XYZ is a right-hand coordinate system.

From Figure 2.1 it can be seen that:

$$\measuredangle \phi = \measuredangle \phi_1 + \measuredangle \phi_2 \tag{2.1}$$

where $$\measuredangle \phi_1 = \sin^{-1} (W'/r) \tag{2.2}$$

$$\measuredangle \phi_2 = (r^2 - W'^2)^{\frac{1}{2}} \tan \gamma_f \cot \kappa / r_0 \tag{2.3}$$

where r and $\phi$ are the polar coordinates of a selected point on the flute profile in the plane XY.

The flute cross-section can be determined numerically and/ or geometrically if $r_0$, $W'$, $\gamma_f$ and $\kappa$, or some relationships between them, are known.

$2W'$ is close to the web thickness, as it will be shown, and the web thickness, $2W$, is usually specified according to the drill diameter, $d_0$, (17, 36, C.1). In (C.1) for instance, the recommended minimum web thickness reads approximately

$$2W = 0.2\ (d_0)^{0.283} \qquad 2.4$$

from a graphical relationship.

The classical helix angle, $\gamma_f$, has been $27\frac{1}{2}^o$, according to Lorenz (29), and in his opinion this was inherited from the past when milling machines tables for flute cutting had a swivel of $55^o$.

For the parameter $2\kappa$, the point angle, $118^o$ is the most common value (3, BS 328).

The influence of the referred to parameters on the flute form is better shown graphically. For this purpose and according to one of the author's aims, a computer program, to be extended, is built up and its flow diagram shown in Figure 2.2.

Figure 2.3 shows the influence of the parameters to the conventional flute mathematical model on its cross-section.

## 2.3 Conventional Flute Face Mathematical Model

The flute cross-section at a distance $\ell$ from the XY plane, equal to the drill lead, projects on this plane confounded with the cross-section in this plane. The projection of any cross-section between these two can be found by rotating the cross-section in the XY plane by an angle $\zeta$ (Figure 2.4).

The angle of rotation, $\zeta$, of two distinct flute normal cross-sections, distant Z from each other, can be obtained from the geometric

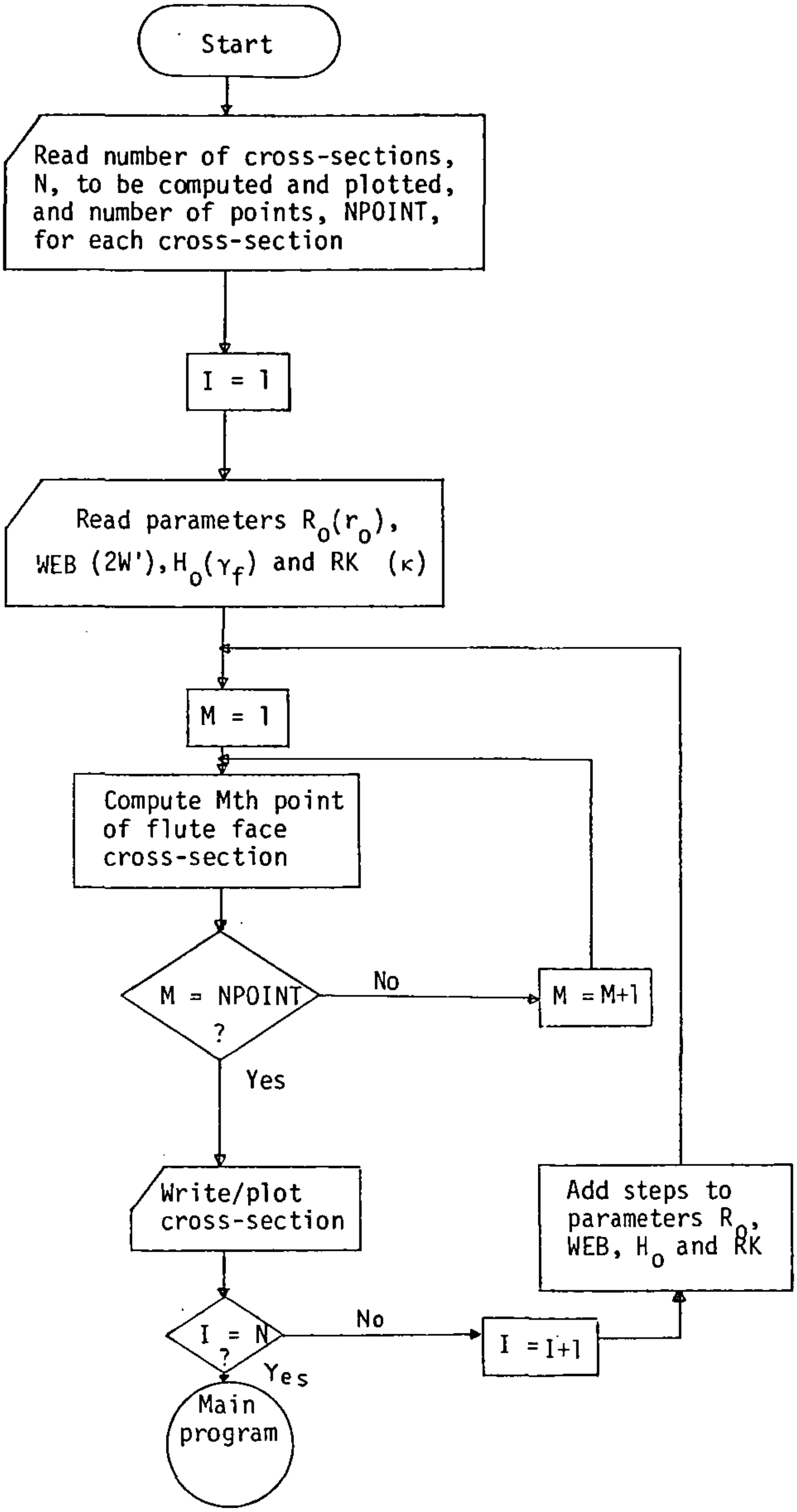


FIGURE 2.2: Flow diagram of the computer program segment to compute and plot (Figure 2.3) conventional flute (face) cross-sections

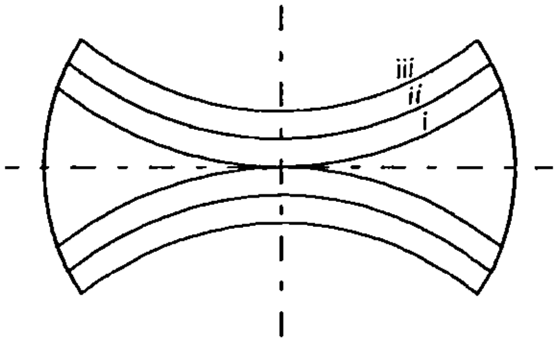


2W' | 0.0 mm (i)
1.5 mm (ii)
3.0 mm (iii)

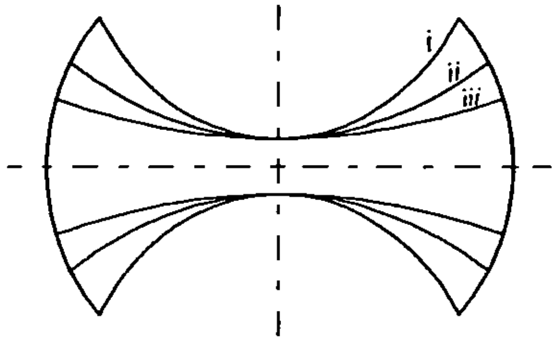


2K | 90° (i)
118° (ii)
146° (iii)

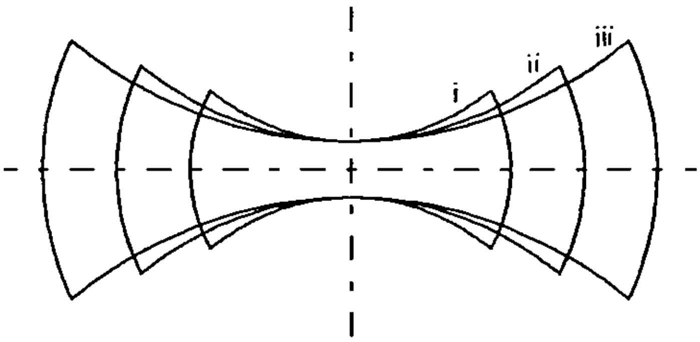


$d_o$ | 8.7 mm (i)
12.7 mm (ii)
16.7 mm (iii)

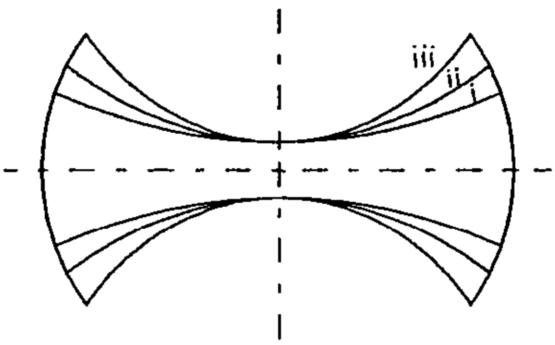


$\gamma_f$ | 20° (i)
30° (ii)
40° (iii)

Central set of parameters:

| do | 2w' | $\gamma_f$ | 2K |
|---|---|---|---|
| 12.7 | 1.5 | 30 | 118 |

FIGURE 2.3: Computer analysis of the influence of the conventional flute design parameters on the flute face cross section.

analysis of helices (62):

$$\zeta = \frac{\tan \gamma_f}{r_o} Z \tag{2.5}$$

where $\gamma_f$ is the helix angle at a radial distance $r_o$.

The angle, $\phi_z$, for a point on the flute contour distant $Z$ from the XY plane, at a radial distance r from the drill axis, can be computed from the angle, $\phi$, for a point on the flute contour in the XY plane at the same radial distance, r, from the drill axis as follows:

$$\phi_z = \phi + \zeta \quad \text{or}$$

$$\phi_z = \mathrm{Sin}^{-1} (W'/r) + (r^2 - W'^2)^{\frac{1}{2}} \tan \gamma_f \cot \kappa/r_o + \tan \gamma_f Z/r_o \tag{2.6}$$

This equation, of the form $f(r,\phi, Z) = 0$, represents the points of the conventional flute face in cylindrical coordinates and it is the mathematical model to this surface.

## 2.4 Flute Heel Analysis

### 2.4.1 Flute heel mathematical model

For commodity, in the computer plots in Figure 2.3, the flute heel has been given the same law as the face of the flute. However, the drill cross-section influences the drill torsional rigidity and this affects drill life as referred by several workers (3, 6, 21, 31, 63, 64). It also affects the conveyance of drilling chips, and the design solution to the conflicting aspects of chip clogging properties and drill rigidity is usually based on a compromise between these two effects.

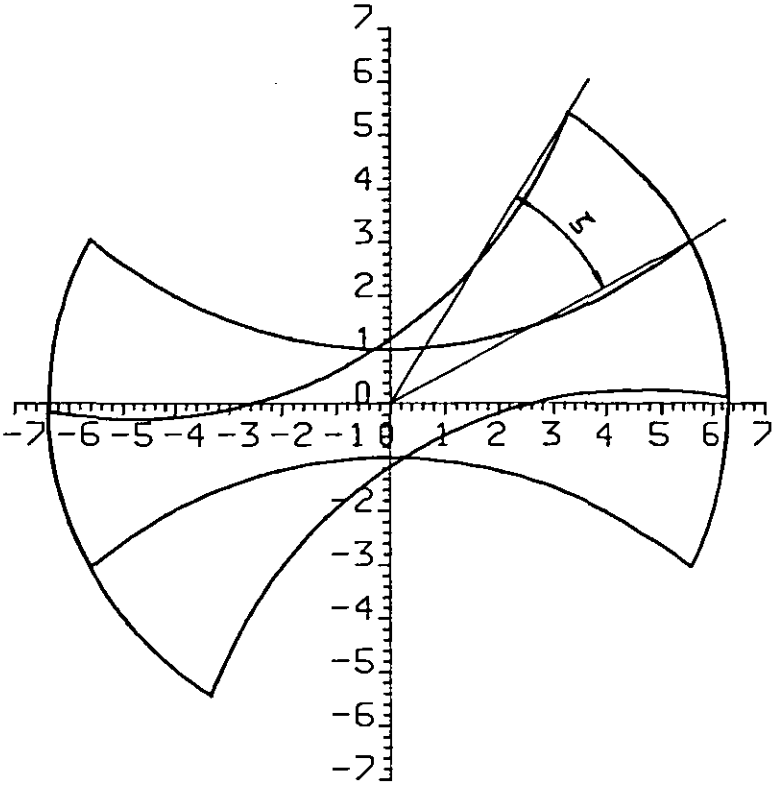


FIGURE 2.4: Two flute cross sections distant Z, projected on a plane normal to the drill axis.

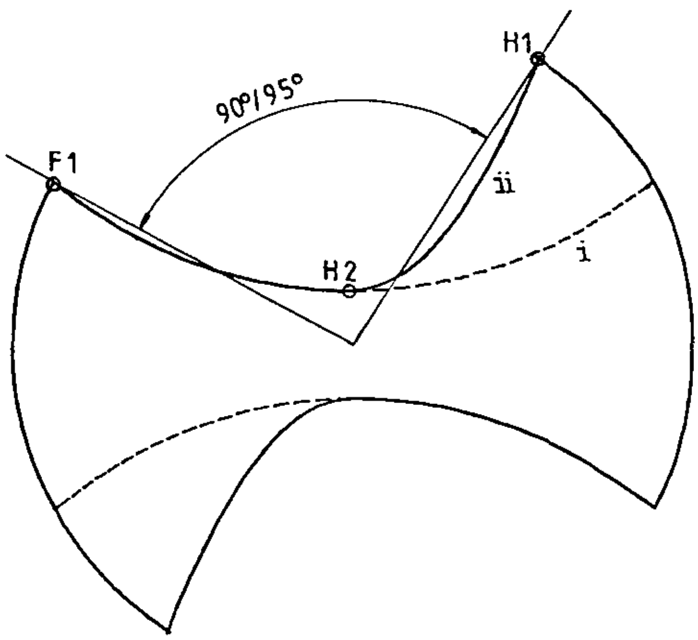


FIGURE 2.5: Comparing the heel designed according to the same law as to the flute face (i), to the heel designed according to a more realistic law (ii) [refer to FIG. 2.6]

According to Armarego (16), there is no full specification for the *"drill point heel shape"* (heel point contour- Figure 1.2) and the heel corner position.

For the purpose of mathematical modelling of the complete flute surface, the heel surface is approached in this work on a geometrical basis.

For simplicity, and because the heel is not critical (3), its cross-section in the XY plane is given, in this work, the law:

$$Y = A_{h1} X^2 + B_{h1} X + C_{h1} \tag{2.7}$$

which proved to describe satisfactorily the actual heel cross-sections produced, projected, magnified and studied by the author for all drills observed.

The flute normal cross-section resembles two circular sectors diametrically opposed (Figure 2.6i). From his observations the author found the contour heel corner, $H_1$ (Figure 2.5), to be $90^0$/ $95^0$ apart of the contour face corner, $F_1$ (Figure 2.5), on the flute contour.

The heel design is approached in the following way:

i) the body clearance is neglected
ii) the heel contour corner, $H_1$, is determined from the face corner, $F_1$, on the basis of the empirical observations
iii) the heel contour joins the face contour at point $H_2$ (Figure 2.5) that originates the chisel corner, after grinding, by smooth transition.
iv) the heel contour in plane XY is represented by a second degree polynomial $Y = h_1(X)$ such as it complies with the following conditions:

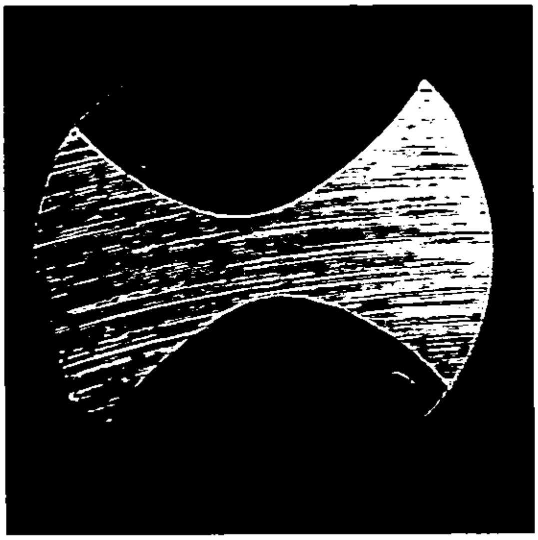

FIGURE 2.6 (i): Cross section (view from the drill point) of a conventional drill, normal to axis, with the following features:
do=12.7 mm, 2w=2.0 mm, $\gamma_f$ =31°, Kg=60°

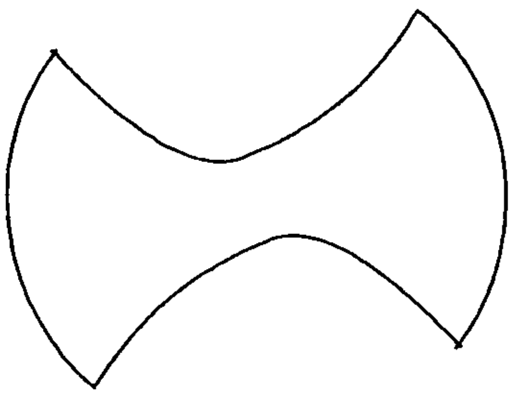

FIGURE 2.6(ii): Computer simulated cross section for a conventional flute face with the following values to the paramters:
do=12.7 mm, 2w'=2.0 mm, $\gamma_f$ =31°, K=60°,
and heel according to a second degree polynomial model.

a) contains point $H_1$
b) contains point $H_2$
c) has a common tangent with the flute face at point $H_2$

To determine numerically and geometrically the shape of the heel contour is to find $A_{h1}$, $B_{h1}$ and $C_{h1}$ to Equation 2.7.

The conditions established above lead to the following equations:

$$A_{h1}X_1{}^2 + B_{h1}X_1 + C_{h1} - Y_1 = 0$$

$$A_{h1}X_2{}^2 + B_{h1}X_2 + C_{h1} - Y_2 = 0$$

$$2A_{h1}X_2 + B_{h1} - [\frac{dY}{dX}]_{H_2} = 0$$

where $(X_1, Y_1)$ and $(X_2, Y_2)$ are the coordinates of point $H_1$ and point $H_2$ respectively and $[dY/dX]_{H_2}$ is the slope of the tangent to the flute face at point $H_2$.

Figure 2.5(ii) shows a flute heel profile plotted after being computed according to the above introduced criterion compared to the one that follows the same law as the conventional flute face profile.

An actual flute profile is shown in Figure 2.6(i). Figure 2.6(ii) shows the computer plot of the flute profile simulated according to the mathematical approach presented above and according to the specifications referred to in Figure 2.6(i).

The heel surface, like the face, is an helical surface and it is better represented by cylindrical coordinates, r, $\phi$ and Z, which can be written in parametric form

$$r = (Y^2 + X^2)^{\frac{1}{2}} = ((A_{h1}X^2+B_{h1}X+C_{h1})^2+ X^2)^{\frac{1}{2}} \qquad 2.8$$

$$\phi = \tan^{-1}(Y/X) + (\tan\gamma_f/r_o)\mu = \tan^{-1}((A_{h1}X^2+B_{h1}X+C_{h1})/X)$$
$$+ (\tan\gamma_f/r_o)\mu \qquad 2.9$$

$$Z = \mu \qquad 2.10$$

where $\mu$ and X are the parameters to the coordinates r, $\phi$ and Z.

### 2.4.2 Web thickness

Oxford (53) defines the web as *"the minimum section of metal between the two flutes"*.

Figure 2.3 (face and heel profiles computed from equations 2.1 to 2.3) suggests that the web thickness, 2W, is measured along one of the axes of the flute profile. Analysis of equations 2.1 to 2.3 shows that the minimum radial distance for the points of the flute occurs for $\phi = 90^o$ and therefore 2W = 2W'.

Figure 2.5(ii), representing a more realistic heel contour than Figure 2.3, suggests that 2W' might be different from 2W.

According to the definition, W can be found by determining the minimum distance from the heel to the drill axis:

$$r = (X^2 + Y^2)^{\frac{1}{2}} \qquad 2.11$$

where $\quad Y = A_{h1}X^2 + B_{h1}X + C_{h1}$.

From the condition dr/dX = 0 it results:

$$X = -\frac{B_{h1}}{A_{h1} + 1} \qquad 2.12$$

and W can be computed.

Numerical investigation revealed that 2W is slightly higher than 2W' and the difference seems to be irrelevant for many purposes.

As an example, the web thickness was computed for the conditions

$$2W' = 2 \text{ mm}; \quad \gamma_f = 30^o; \quad \kappa = 59^o; \quad d_o = 12.7 \text{ mm}$$

and it was found $2W = 2.008$ mm, i.e. a difference of less than 1%.

## 2.5 Flute Contour in a Plane Normal to the Helical Direction of Drill Flute

The flute cutter design is better dealt with if the cross-section of the flute profile perpendicular to its helical direction is known.

A method for determining such a section should be available if a new flute form is to be designed and manufactured.

The solution to this problem is approached as follows:

i) A plane $p_1$ (Figure 2.7) normal to the helical direction of the flute is defined and represented by:

$$C_1X + C_2Y + C_3Z + C_4 = 0 \tag{2.13}$$

in the coordinate system (X, Y, Z).

ii) For each point P (Figure 2.7) of the flute contour in the plane XY, a point Q belonging to the same helical line on the flute surface as P, and on the plane $p_1$, is found by computing the intersection point of the helical line with plane $p_1$.

iii) The set of points Q belonging to the flute surface and to the plane $p_1$ are better represented in graphical form if a new coordinate system (X', Y', Z'), is defined such as the plane X'Y' coincides with the plane $p_1$ (Figure 2.7).

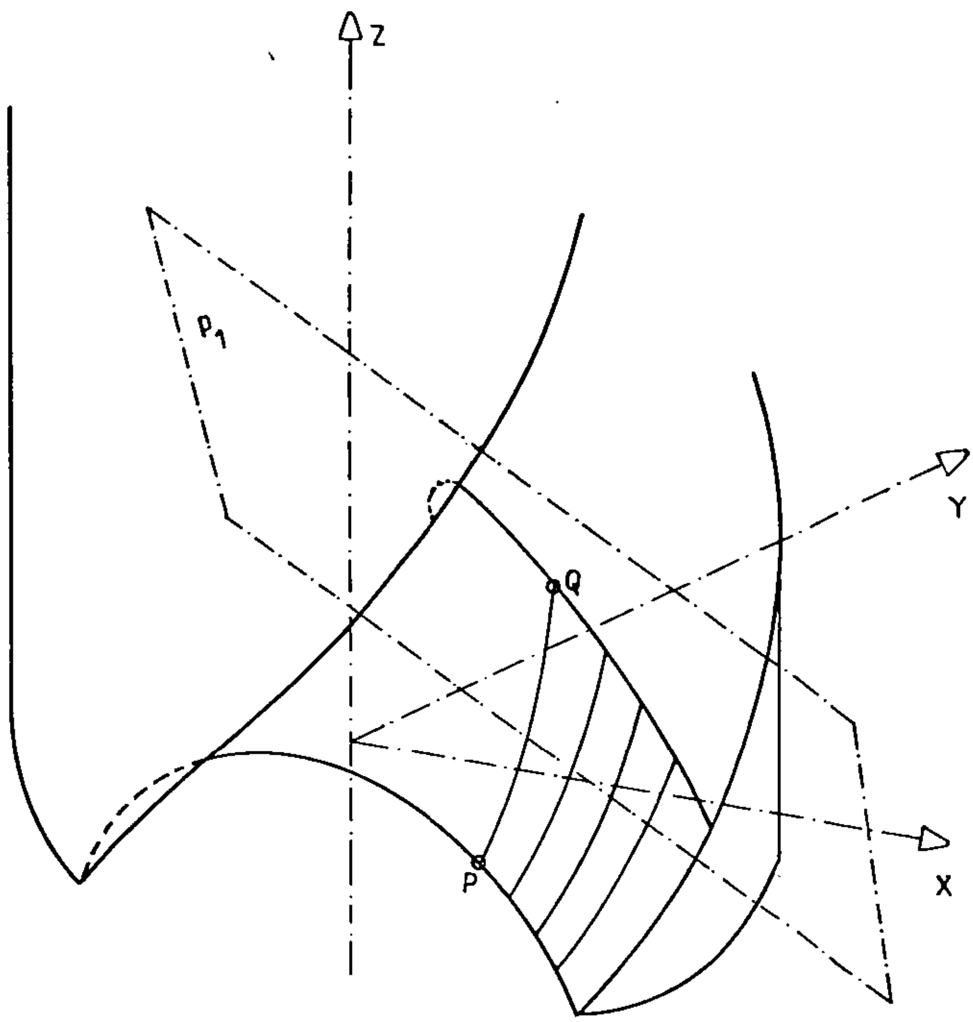


FIGURE 2.7: Flute cross section in a plane normal to the flute helical direction.

iv) The coordinates of each point Q, ($X_Q$, $Y_Q$, $Z_Q$) are transformed into the new coordinates ($X_Q'$, $Y_Q'$, $Z_Q'$).
Note: Transformations of coordinates are dealt with in Chapter 3, Section 3.2.1. To avoid repetitions and as the subject is analysed in the referred to section no further details are given here. (See Figure 2.8 for flow diagram of computer program segment).

The flow diagram of the computer program segment (see Appendix 1) for the computation of the above referred to sections is shown in Figure 2.8.

Cross-sections perpendicular to the helical direction of the flute, for several values of the parameters of the conventional flute and heel mathematical models are shown in Figure 2.9.

## 2.6 Some Alterations to Conventional Flutes

Many works in literature refer to some deviations from the conventional flutes, usually due to manufacture inaccuracies and/or manufacturing variations. Some variations are introduced for the purpose of creating special drilling characteristics such as the ones to implement a stronger chip breaking effect than that yielded by the regular flute (Figure 2.10).

Drill flute variations have been referred to by Galloway (3, 34), Galloway and Morton (10) and Lorenz (29), for instance. Arshinov and Aleksev (4) also refer to flute deviations and point a cause for them. According to these workers, for each set of the drill flute features, $r_o$,2W', $\gamma_f$ and $\kappa$, a proper flute profile cutter should be designed and used. This, however, would require a great many cutters for cutting the flutes of a given range and the manufacturers frequently use the same flute cutter within a certain drill diameter range. The influence of these flute deviations on the cutting angles such as the normal rake angle inclination angle, for instance, will be shown later when a method for finding the drill lip cutting geometry is presented.

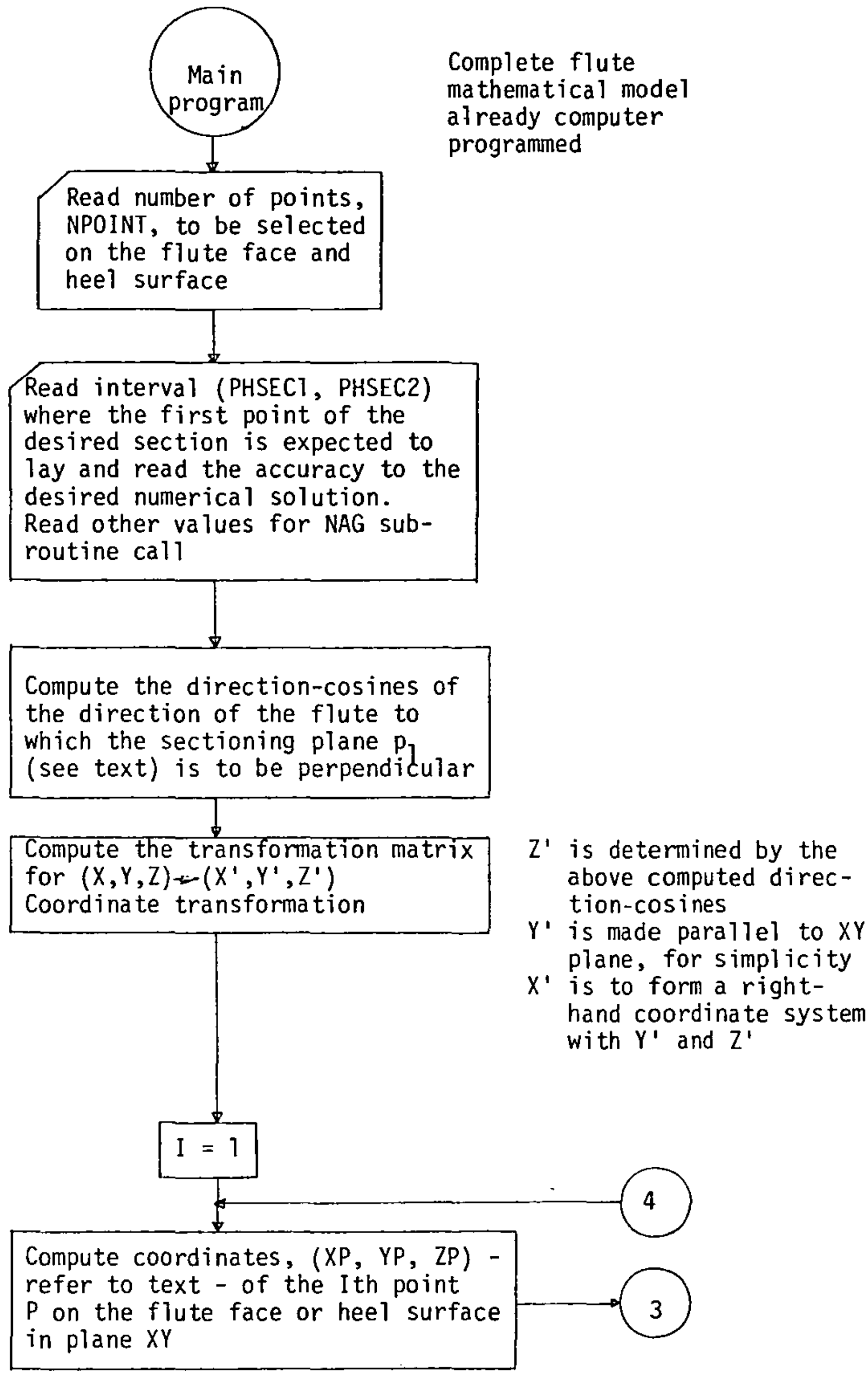


FIGURE 2.8 (continued)

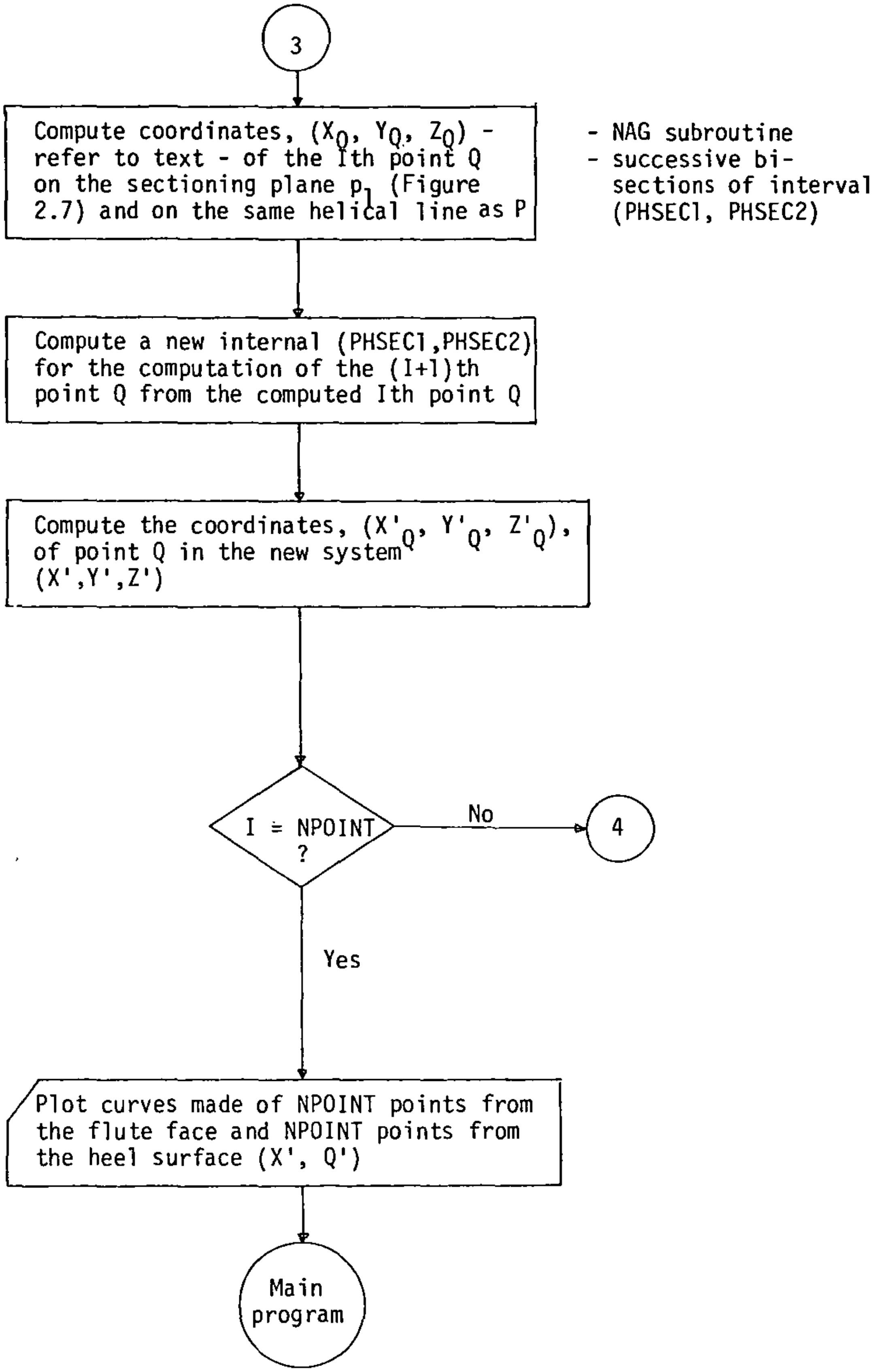


FIGURE 2.8: Flow diagram of the computer program (refer to Appendix 1) for the computation of the flute cross-section perpendicular to the helical direction of the flute

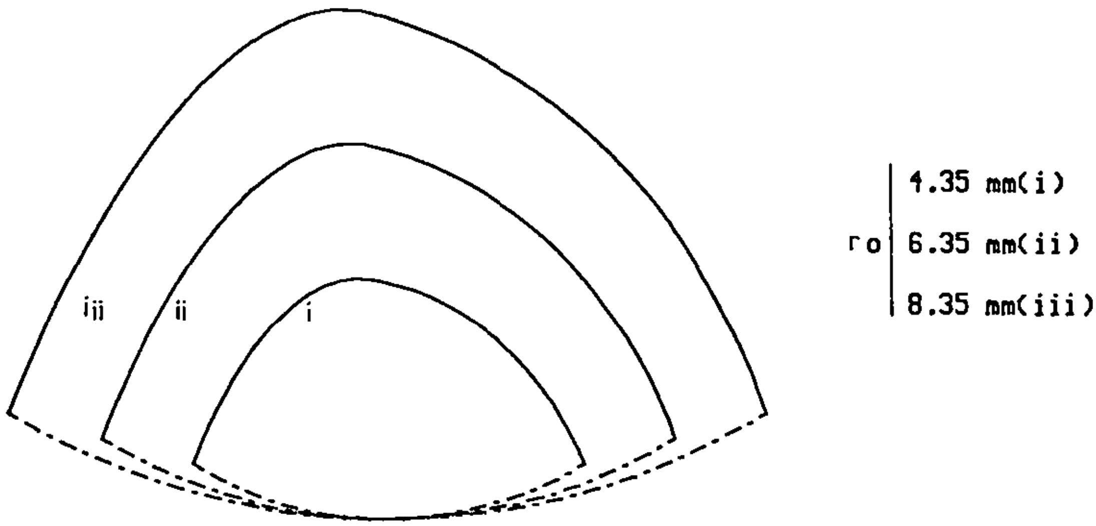


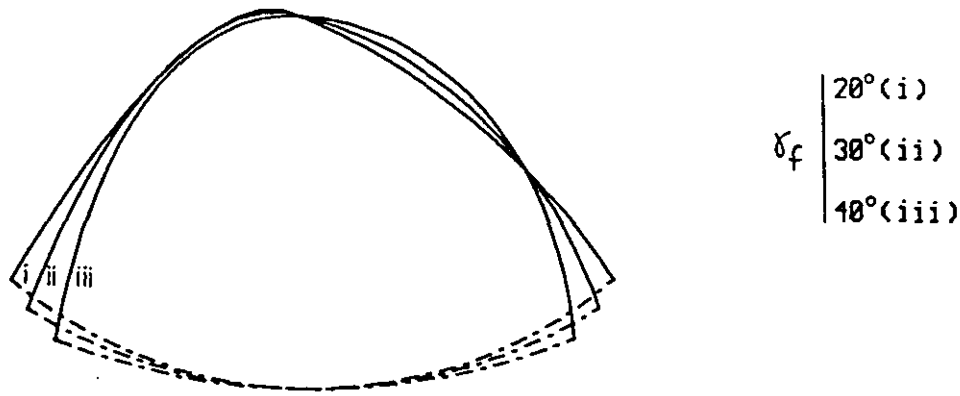


Central set of parameters :

| 2 ro = do | 2w | $\gamma_f$ | 2k |
|---|---|---|---|
| 12.7 | 1.5 | 30 | 118 |

FIGURE 2.9 (continued)

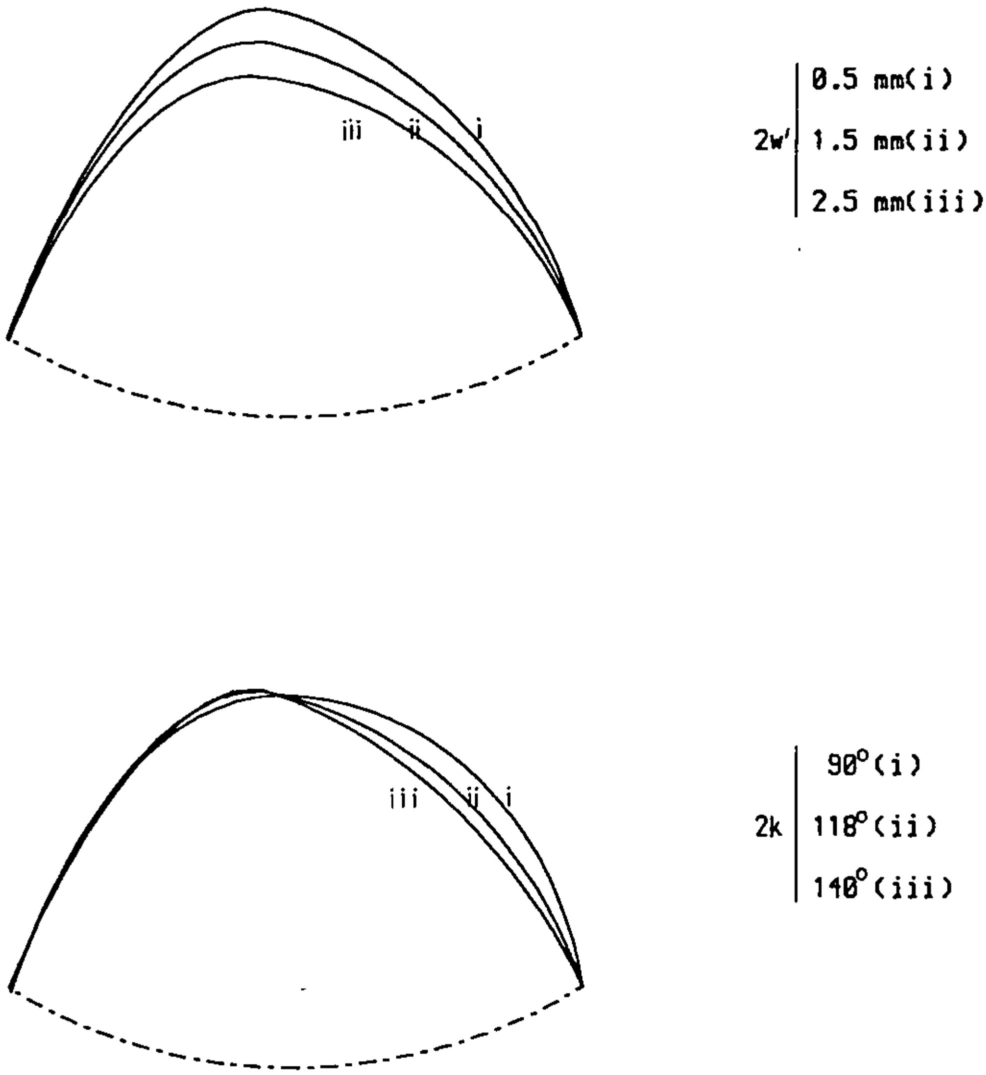


FIGURE 2.9: Computer analysis of the flute sections normal to the flute helical direction by varying the conventional flute model parameters.[refer to previous page].

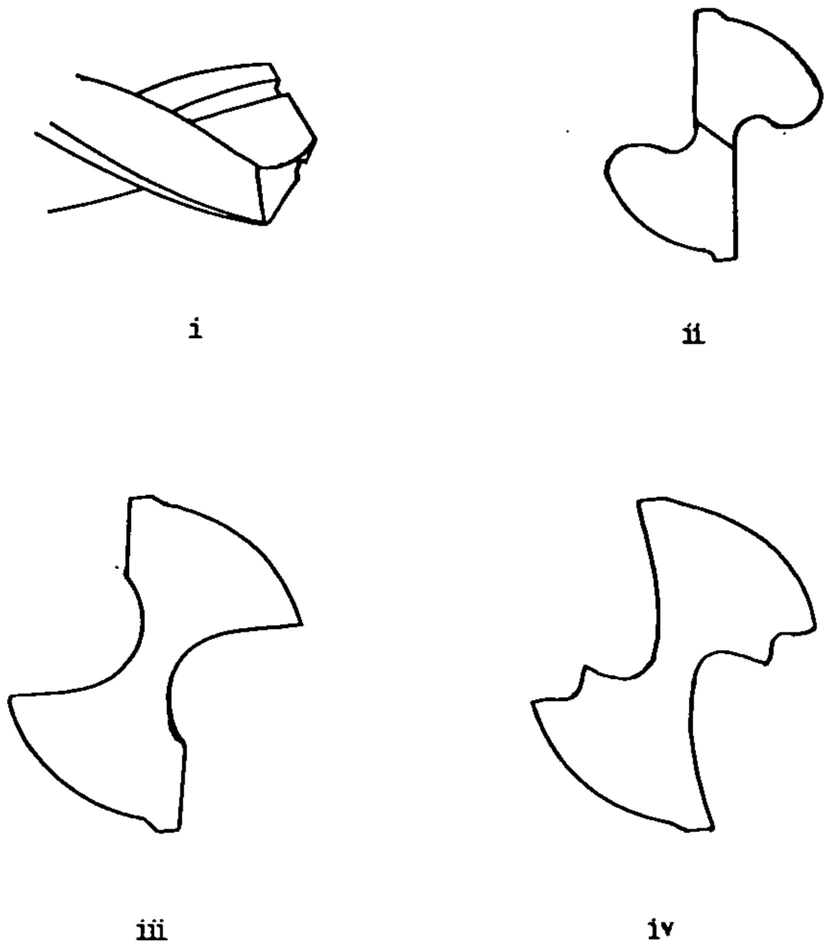


FIGURE 2.10: Modified Flutes :

(i) Chip breaking grooves (15,38)

(ii) Typical chip breaking drill (15,17)

(iii) Self-thinned heavy duty drill (21,38)

(iv) Crisp design chip breaker (21,38)

## 2.7 Flute Design Classification

The flutes which are ruled surfaces generated as shown above, according to the parameters $r_o$, $2W'$, $\gamma_f$ and $\kappa$ are designated in this work by conventional flutes. The conventional flutes for which $2\kappa = 118^o$ are designated standard flutes as this is the point angle specified in (BS 328).

Any flute which is not designed to comply with the condition to yield a straight lip is called non-conventional flute.

The following classification of drill flutes is proposed:

Drill flutes
- conventional flutes: designed to be ruled surfaces
  - standard flutes $2\kappa = 118^o$
  - non-standard flutes $2\kappa \neq 118^o$
- non-conventional flutes: designed according to other criterion rather than yielding a straight lip

## 2.8 Chapter Closure

The conventional drill flute is determined on the basis of a very simple condition: the linearity of the drill lip.

It seems fortunate that such a criterion could serve the many different drilling conditions - drill sizes, feeds, speeds and materials, for example - and has succeeded for the many years the conventional drills have been used in industry.

The flute face, however, is curved and it has never been proved that a straight li e lip is better than any other shape. Furthermore, reports are found from time to time referring to the improved performance of drills ground to curved lips as for drilling cast iron.

Nearly all research work took this flute form for granted and has generated an important body of information data that applies only to such forms.

*"The effects of the grinding parameters on the drill geometry are complex"*

*Fujii*

# 3. MATHEMATICAL MODEL TO ANY-DRILL POINT YIELDED BY CYLINDRICAL GRINDING

## 3.1 Introduction

For complete determination of the drill point geometry and cutting lip geometry it is necessary to define the flank surfaces.

The drill surfaces are usually machine produced. In some cases, in industry, the drill points are manually ground, however, this is uncommon in drilling research. The author came across in the literature with just one case, by Lorenz (7), where drills manually ground were compared, for drill performance, against drills ground at a drill grinding machine.

Assessing drill sharpening methods and proposing *"acceptable grinder criteria"*, Armarego (16) compares three drill grinding points: 'conical flank', 'cylindrical flank' and the 'plane flank'.

The conical grinding method was first (65) dealt with by Galloway (3) and further analysed by Fujii and co-workers (65,66), Tsai and Wu (60) and Armarego and Rotenberg (22, 66, 68).

A cylindrical drill grinding machine was available to the author and many similar machines are used in industry.

It is unfortunate that the cylindrical grinding method is scarcely dealt with in the literature, and, according to Armarego (16), this method is *"unsuitable for general purpose drill point sharpening"*.

At the time the author started his work, the paper by Armarego (16, Annals of CIRP 29/1/1980) was not available to him. Later, when the paper was available, the author found the analysis of Armarego to be a particular case, with a major simplification, of the one made by the author. In fact the analysis of the author considers four parameters while Armarego considers only three. However, the analysis by the author further aims at:

- building a mathematical model for drill cylindrical grinding;
- including in this model all setting possibilities usually available in current practice of drill cylindrical grindings;

- implementing the mathematical model in a computer program in order that it can be analysed by computer aided design.

## 3.2 Cylindrical Grinding Analysis

In a previous work (11), Billau manufactured a perspex model representing the mechanism of the type of the grinding machine available to the author (Figure 6.4) and has shown that the flank point surface is of cylindrical form.

In this work the author approaches the cylindrical grinding in an analytical way, in order to build up a mathematical model to be dealt with by computing methods and computer design aids.

### 3.2.1 Setting parameters

From the study of the work by Billau (11, 69) and further analysis of the referred to grinding machine, the following grinding setting parameters were established by the author (Figure 3.1):

$d_{og}$ - ($= 2\ r_{og}$) diameter of the cylinder generated by grinding

$\nu_g$ - angle for the position of the flute relative to the generated cylinder by grinding

$ex_g$ - distance between the axis of the generated cylinder by grinding and the drill axis

$\kappa_g$ - angle between the axis of the cylinder generated by grinding and the drill axis.

### 3.2.2 Mathematical model for cylindrical flank surface

For reference of the mathematical model, referential systems are needed.

One referential system (X, Y, Z), has already been defined in the previous chapter, for flute and drill reference. This will always be, for consistency, the ultimate reference system (Figure 3.2).

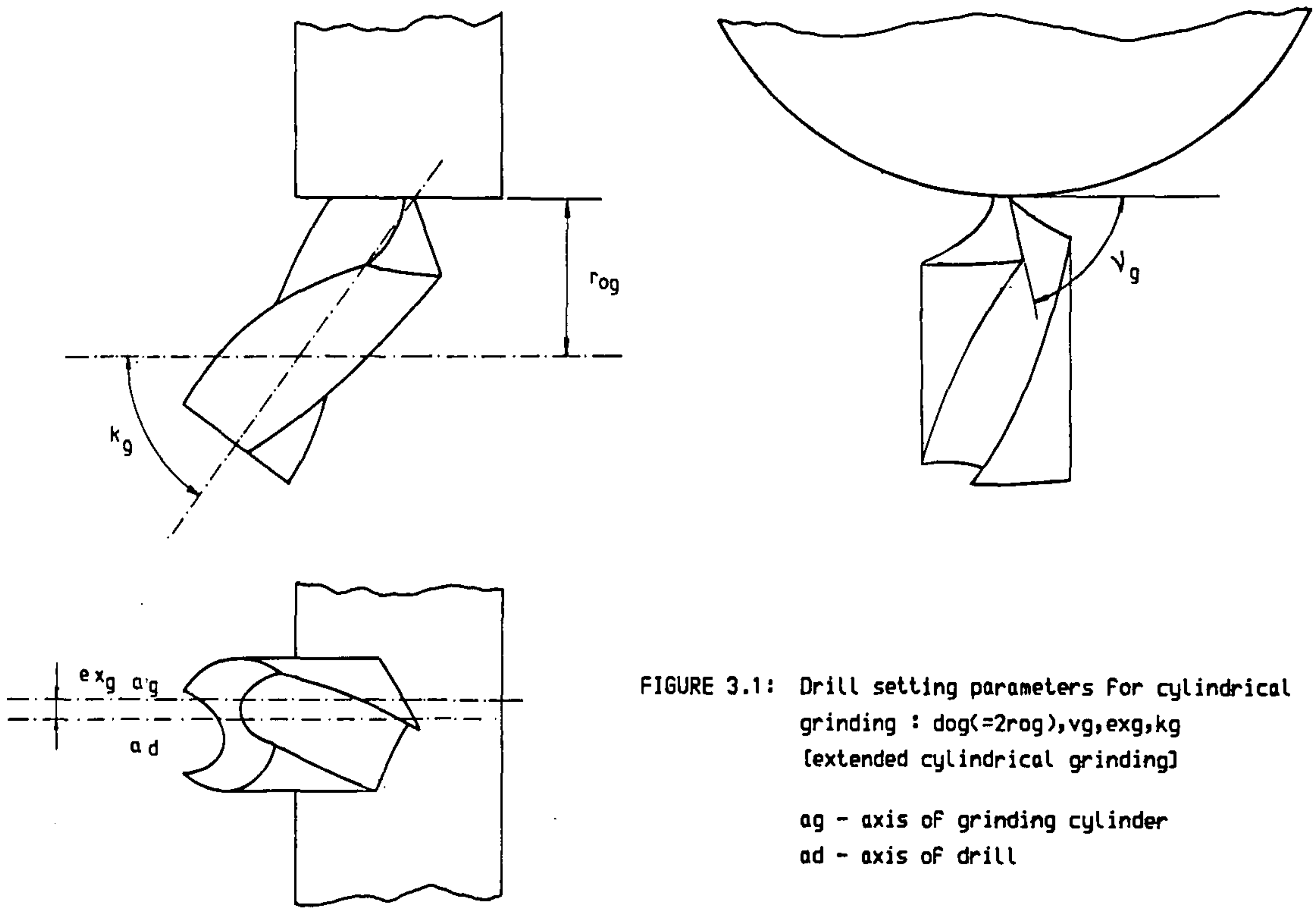


FIGURE 3.1: Drill setting parameters for cylindrical grinding : dog(=2rog),vg,exg,kg [extended cylindrical grinding]

ag - axis of grinding cylinder
ad - axis of drill

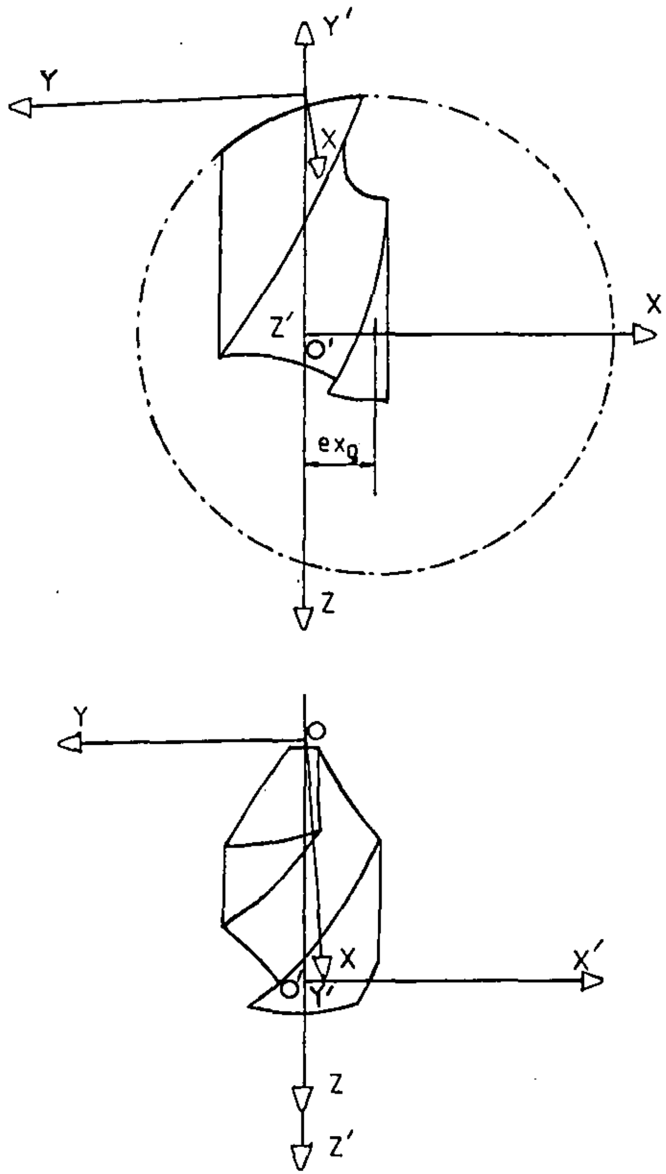


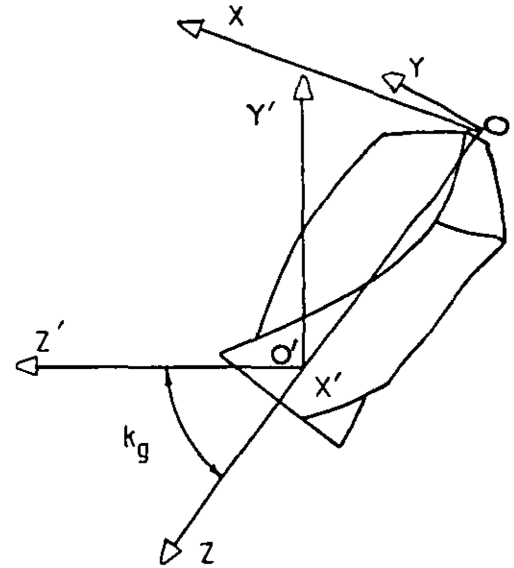


FIGURE 3.2: coordinate reference systems

X Y Z -Drill reference system

X'Y'Z' -Drill holding device reference system

However, for analysis simplicity, other referential systems are also considered.

The cylinder generated by grinding is firstly referred to an auxiliary referential system (X', Y', Z') attached to the drill holding device (Figure 3.2).

For clarity, the generated cylinder by grinding and system (X', Y', Z') attached to it are further represented in Figure 3.3.

From Figure 3.3 the cylindrical surface can be described as follows:

$$(X' - ex_g)^2 + Y'^2 = r_{og}^2 \tag{3.1}$$

Z' any real number

For consistency, this cylinder surface - one drill flank surface - shall be referred to the referential system (X, Y, Z). To help with the coordinates transformation,two auxiliary referential systems, (X", Y", Z") and (X*, Y*, Z*), are introduced. The referred to four systems are shown in Figure 3.4 which shows also their geometrical relationships.

The system (X*, Y*, Z*) has its X* axis coincident with the axis X' of system (X', Y', Z'); Y* and Z* are in the same plane as the Y' and Z' axes but rotated $\kappa_g$ - the grinding point angle - relatively to these axes.

From Figure 3.4:

$$X' = X^*$$
$$Y' = Y^* \cos \kappa g = Z^* \operatorname{Sin} \kappa g$$
$$Z' = Y^* \operatorname{Sin} \kappa g + Z^* \operatorname{Cos} \kappa g$$ or, in other form:

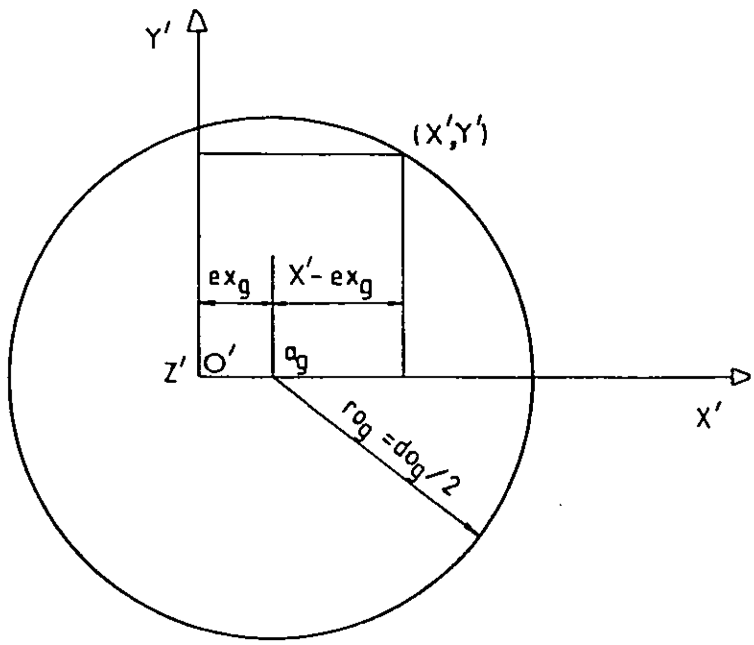


FIGURE 3.3: Generated grinding cylinder of axis ag [refer to FIG 3.1 and FIG 3.2]

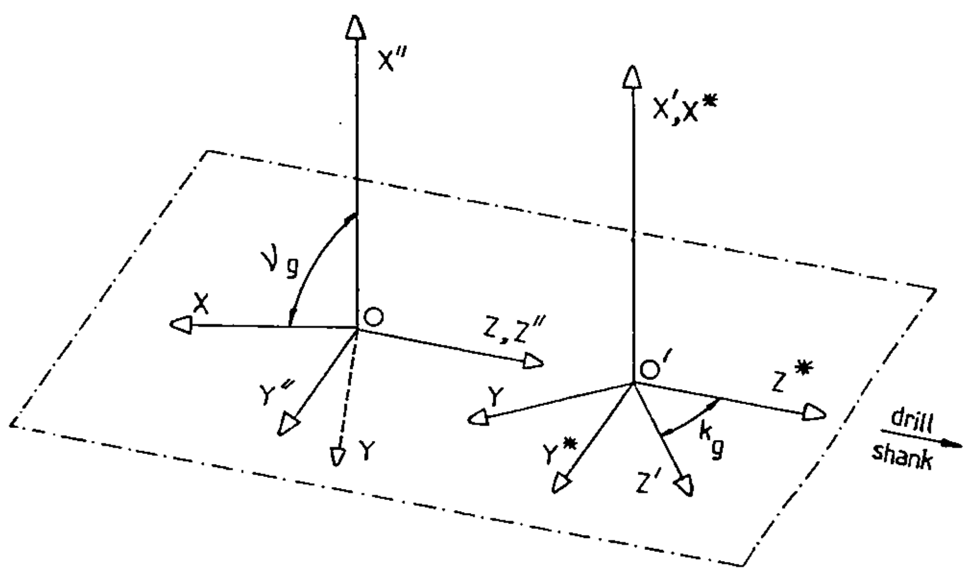


FIGURE 3.4: Drill referential system (X,Y,Z) ; Drill holding device referential system (X′,Y′,Z′) ; Auxiliary referential systems (X″,Y″,Z″) and (X*,Y*,Z*).

$$\begin{vmatrix} X' \\ Y' \\ Z' \end{vmatrix} = \begin{vmatrix} 1 & 0 & 0 \\ 0 & \text{Cos } \kappa g & -\text{Sin } \kappa g \\ 0 & \text{Sin } \kappa g & \text{Cos } \kappa g \end{vmatrix} \begin{vmatrix} X^* \\ Y^* \\ Z^* \end{vmatrix} = T_1 \begin{vmatrix} X^* \\ Y^* \\ Z^* \end{vmatrix} \qquad 3.2$$

where $T_1$ is the coordinates transformation matrix:

$$T_1 = \begin{vmatrix} 1 & 0 & 0 \\ & \text{Cos } \kappa g & -\text{Sin } \kappa g \\ 0 & \text{Sin } \kappa g & \text{Cos } \kappa g \end{vmatrix}$$

The system (X", Y", Z") is a translation of system (X*, Y*, Z*) and they are apart from the distance $Z_o$ (distance from 0 to 0') measured either along Z" or Z*:

$$X^* = X''$$
$$Y^* = Y''$$
$$Z^* = Z'' - Z_o \qquad \text{or, in other form,}$$

$$\begin{vmatrix} X^* \\ Y^* \\ Z^* \end{vmatrix} = \begin{vmatrix} 1 & 0 & 0 \\ 0 & 1 & 0 \\ 0 & 0 & 1 \end{vmatrix} \begin{vmatrix} X'' \\ Y'' \\ Z'' \end{vmatrix} + \begin{vmatrix} 0 \\ 0 \\ -Z_o \end{vmatrix} = T_2 \begin{vmatrix} X'' \\ Y'' \\ Z'' \end{vmatrix} + \begin{vmatrix} 0 \\ 0 \\ -Z_o \end{vmatrix} \qquad 3.3$$

Finally, the referential system (X, Y, Z) attached to the drill has its Z axis coincident with Z"; the XY plane is the same as the plane X"Y" and X axis is rotated $\psi g$ relatively to the X' axis.

From Figure 3.4:

$$X'' = X \cos \nu g - Y \sin \nu g$$
$$Y'' = X \sin \nu g + Y \cos \nu g$$
$$Z'' = Z$$

or:
$$\begin{vmatrix} X'' \\ Y'' \\ Z'' \end{vmatrix} = \begin{vmatrix} \cos \nu g & -\sin \nu g & 0 \\ \sin \nu g & \cos \nu g & 0 \\ 0 & 0 & 1 \end{vmatrix} \begin{vmatrix} X \\ Y \\ Z \end{vmatrix} = T_3 \begin{vmatrix} X \\ Y \\ Z \end{vmatrix} \qquad 3.4$$

The cylindrical surface can now be expressed in terms of X, Y and Z. In fact from 3.3 and 3.4:

$$\begin{vmatrix} X' \\ Y' \\ Z' \end{vmatrix} = T_1 \; T_2 \; T_3 \begin{vmatrix} X \\ Y \\ Z \end{vmatrix} + T_1 \begin{vmatrix} 0 \\ 0 \\ -Z_0 \end{vmatrix} \qquad 3.5$$

and this leads to

$$X' = X \cos \nu g - Y \sin \nu g$$
$$Y' = (X \sin \nu g + Y \cos \nu g) \cos \kappa g - (Z - Z_0) \sin \kappa g$$
$$Z' = (X \sin \nu g + Y \cos \nu g) \sin \kappa g + (Z - Z_0) \cos \kappa g.$$

Substituting X' and Y' in Equation 3.1 it results a an equation of the form:

$$f_{\alpha 1}(X,Y,Z) = AX^2 + BY^2 + CZ^2 + DXY + EXZ + FYZ +$$
$$+ GX + HY + IZ + \quad = 0 \qquad 3.6$$

where: $A = \cos^2 \nu g + \sin^2 \nu g \cos^2 \kappa g$

$B = \sin^2 \nu g + \cos^2 \nu g \cos^2 \kappa g$

$C = \sin^2 \kappa g$

$$D = -2\ \mathrm{Cos}\ \nu g\ \mathrm{Sin}\ \nu g + 2\ \mathrm{Sin}\ \nu g\ \mathrm{Cos}\ \nu g\ \mathrm{Cos}^2\ \kappa g$$

$$E = -2\ \mathrm{Sin}\ \kappa g\ \mathrm{Cos}\ \kappa g\ \mathrm{Sin}\ \nu g$$

$$F = -2\ \mathrm{Sin}\ \kappa g\ \mathrm{Cos}\ \kappa g\ \mathrm{Cos}\ \nu g$$

$$G = 2\ \mathrm{Sin}\ \kappa g\ \mathrm{Cos}\ \kappa g\ \mathrm{Sin}\ \nu g\ Z_0 - 2\ ex_g\ \mathrm{Cos}\ \nu g$$

$$H = 2\ \mathrm{Sin}\ \kappa g\ \mathrm{Cos}\ \kappa g\ \mathrm{Cos}\ \nu g\ Z_0 + 2\ ex_g\ \mathrm{Sin}\ \nu g$$

$$I = -\ 2\ Z_0\ \mathrm{Sin}^2\ \kappa g$$

$$J = ex_g^{\ 2} + Z_0^{\ 2}\ \mathrm{Sin}^2\ \kappa g - r_{og}^2$$

$$Z_0 = (r_{og}^{\ 2} - (ex_g - W)^2)^{\frac{1}{2}} / \mathrm{Sin}\ \kappa g$$

This equation represents the model of one flank whose parameters are, $r_{og}$, $\nu g$, $ex_g$ and $\kappa g$ which determine completely the coefficients A to J of function $f_{\alpha 1}$.

A two-fluted drill point is made of two similar flanks and one flank substitutes the other when the drill is rotated $180^0$. For each point $P_1 = (X,Y,Z)$ on the flank represented by equation $f_{\alpha 1}$ there is a diametrically opposed point $P_2 = (-X, -Y, Z)$ on the other flank. The equation $f_{\alpha 2}$ for this flank can be found from $f_{\alpha 1}$ by substituting X for -X and Y for -Y:

$$f_{\alpha 2} = AX^2 + BY^2 + CZ^2 + DXY - EXZ - FYZ -$$
$$- GX - HY + IZ + J = 0 \qquad 3.7$$

## 3.3 Computing Approach

The equations dealt with in the previous sections can be easily dealt with by computing methods.

The implementation of these equations in a computer program do not present any particular problem and the respective flow diagram is omitted from this writing.

The segment computer program relative to the drill flank point can be seen in the computer program shown in Appendix 1.

Figures 3.5 to 3.8 show computer plotted cross-sections through both flank surfaces, normal to the drill axis. Each figure shows the effect of one of the four grinding parameters on the size or on the position of the flank surface relative to the referential system attached to the drill.

## 3.4 The Chisel Edge

The intersection of the two flank surfaces forms the chisel edge. To find the chisel edge is to find the common solution to $f_{\alpha 1}$ and $f_{\alpha 2}$ at the drill point region.

The chisel edge can be found geometrically and numerically from the successive cross-sections on both flank surfaces yielded along the drill axis: Figures 3.5 to 3.8.

The chisel edge intersects the drill axis at the chisel point (dead centre), $(0, 0, Z_{dc})$, where $Z_{dc}$ can be found from either $f_{\alpha 1}$ or $f_{\alpha 2}$ by making $X = Y = 0$. In doing so, $Z_{dc}$ is found from the equation:

$$CZ_{dc}^2 + IZ_{dc} + J = 0 \qquad 3.8$$

which results from $f_{\alpha 1}(0, 0, Z) = f_{\alpha 2}(0, 0, Z) = 0$.

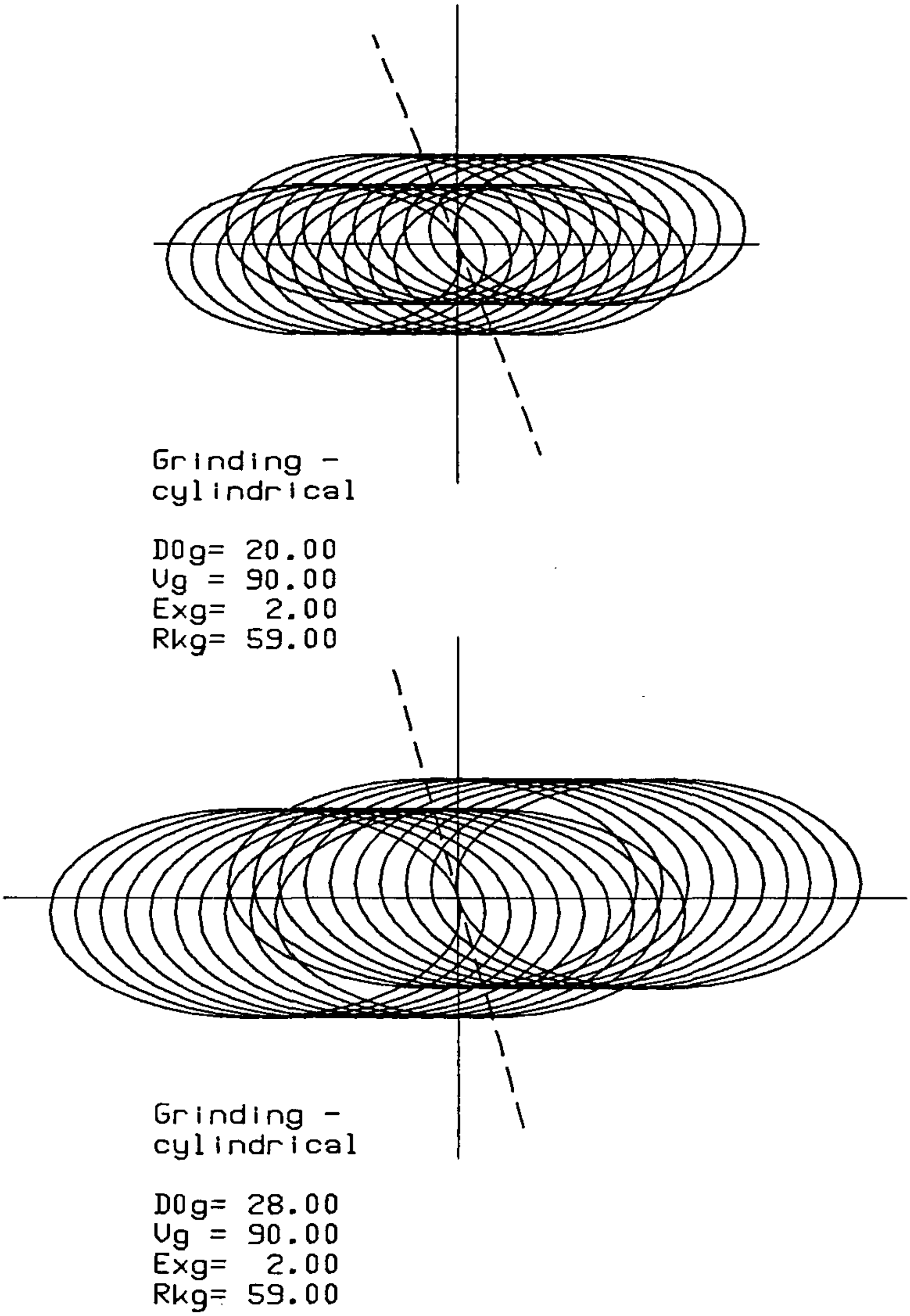


FIGURE 3.5: Computer plotted cross sections of the flank surfaces normal to the drill axis. Effect of Dog

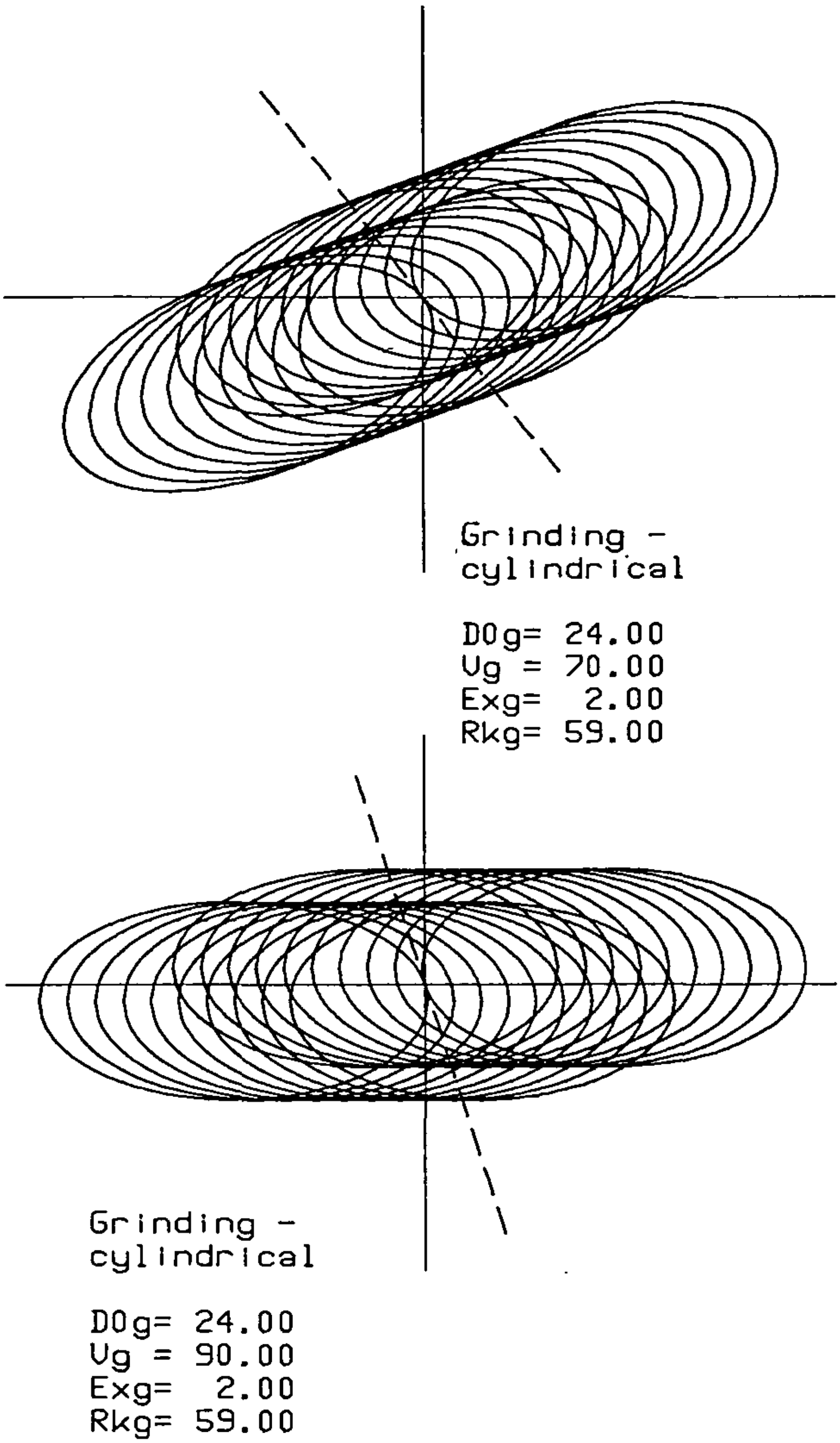


FIGURE 3.6: Computer plotted cross sections of the flank surfaces normal to the drill axis.
Effect of Vg

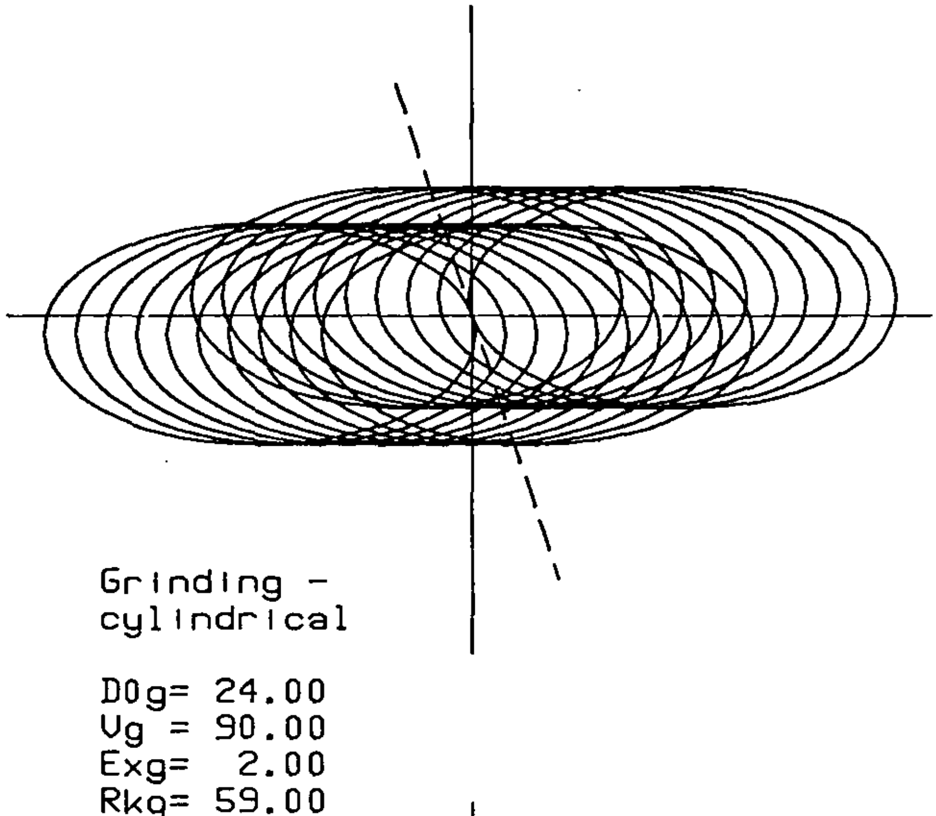


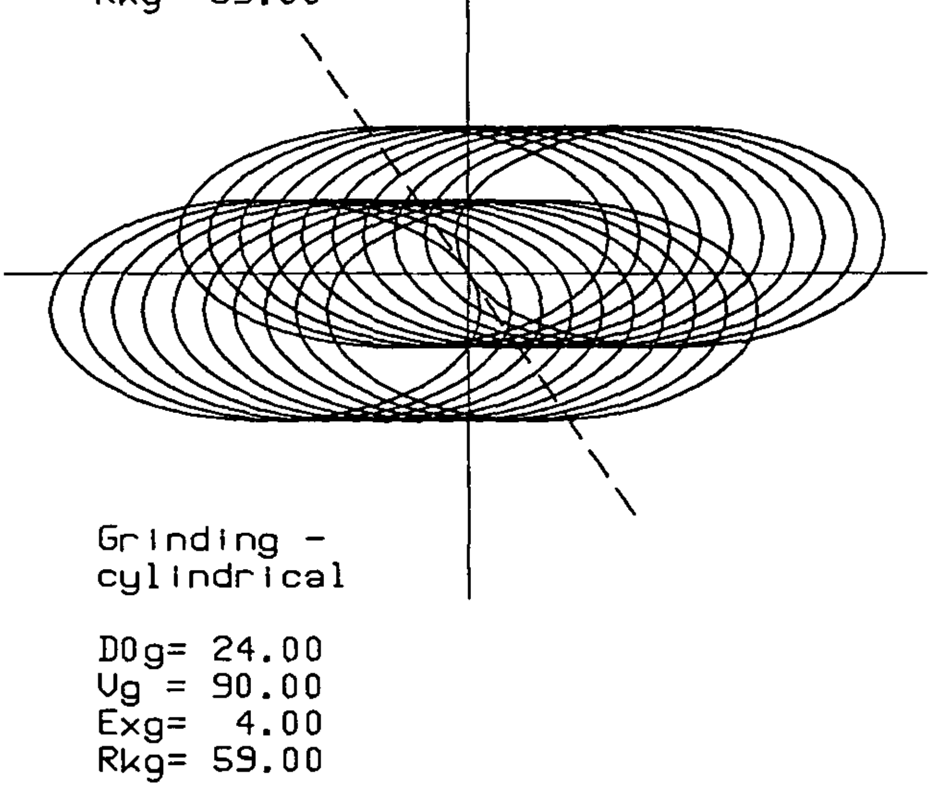


FIGURE 3.7: Computer plotted cross sections of the flank surfaces normal to the drill axis.
Effect of Exg

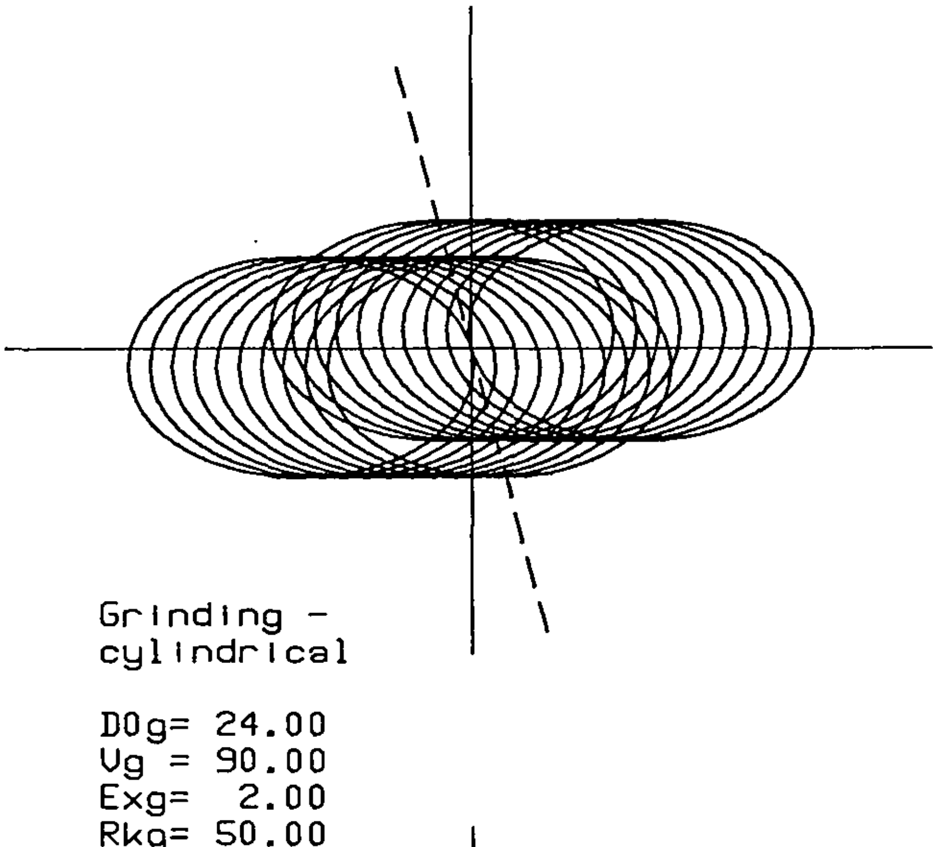


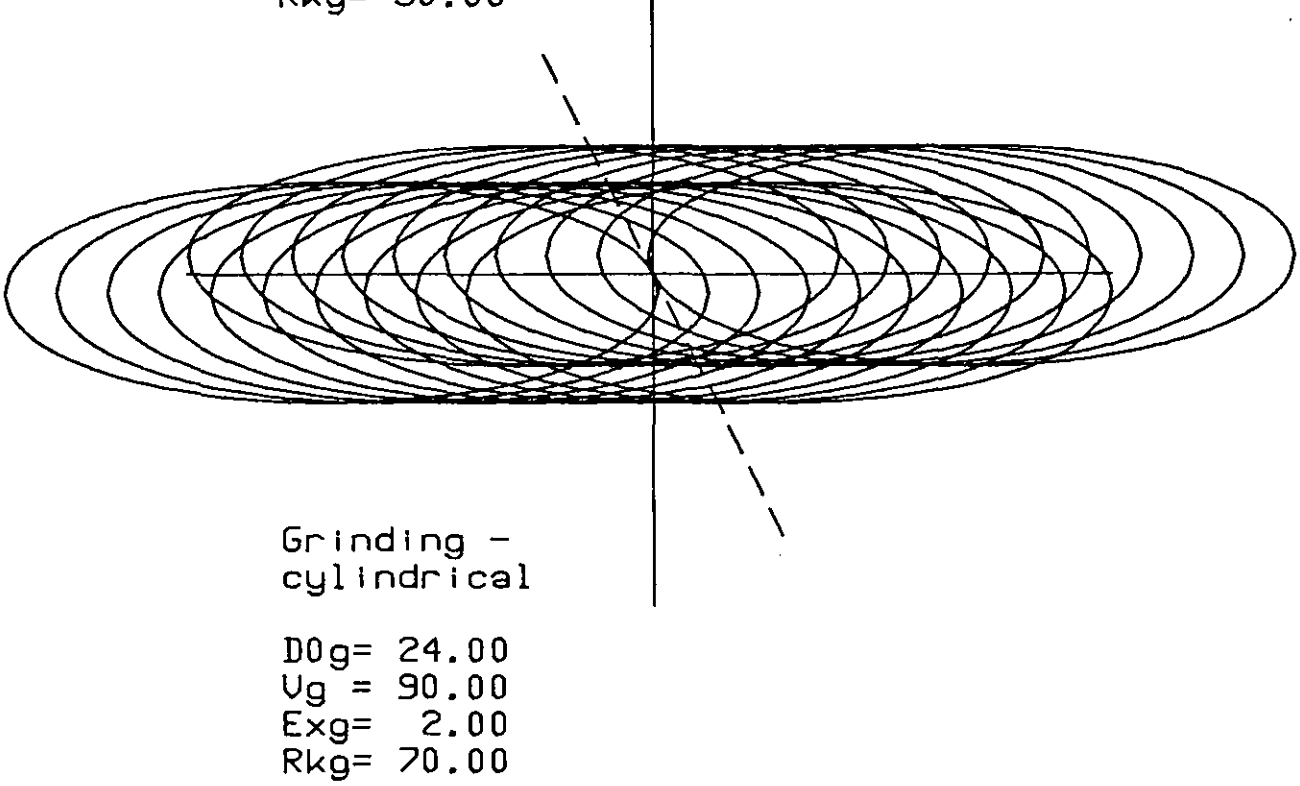


FIGURE 3.8: Computer plotted cross sections of the flank surfaces nomal to the drill axis.
Effect of Rkg

The direction of the chisel edge at the chisel point is given by the tangent to the chisel edge at this point.

Let $S_{\alpha 1}$ be the flank surface represented by equation $f_{\alpha 1}$; from geometry, the normal vector, $\vec{n}_1$, to surface $S_{\alpha 1}$ at one point (X, Y, Z) is in the same direction as the vector $(\partial f_{\alpha 1}/\partial X,\ \partial f_{\alpha 1}/\partial Y,\ \partial f_{\alpha 1}/\partial Z)$:

$$N_1\vec{n}_1 = (\partial f_{\alpha 1}/\partial X,\ \ \partial f_{\alpha 1}/\partial Y,\ \ \partial f_{\alpha 1}/\partial Z) \qquad 3.9$$

In the same way, for flank $S_{\alpha 2}$:

$$N_2\vec{n}_2 = (\partial f_{\alpha 2}/\partial X,\ \ \partial f_{\alpha 2}/\partial Y,\ \ \partial f_{\alpha 2}/\partial Z) \qquad 3.10$$

At the chisel edge, $\vec{n}_1$ and $\vec{n}_2$ are both normal to the tangent to this line; then the tangent to the chisel edge is in the direction of vector $\vec{n}_1 \times \vec{n}_2$, that is, normal to both $\vec{n}_1$ and $\vec{n}_2$.

At the chisel point, $(0, 0, Z_{dc})$,

$$N_1\vec{n}_1 = (EZ_{dc} + G,\ \ FZ_{dc} + H,\ \ 2CZ_{dc} + I) \qquad 3.11$$

$$N_2\vec{n}_2 = (-EZ_{dc} - G,\ \ -FZ_{dc} - H,\ \ 2CZ_{dc} + I) \qquad 3.12$$

$$N_1N_2\vec{n}_1 x\vec{n}_2 = \begin{vmatrix} \vec{i} & \vec{j} & \vec{k} \\ EZ_{dc} + G & FZ_{dc} + H & 2CZ_{dc}+I \\ -EZ_{dc} - G & -FZ_{dc} - H & 2CZ_{dc}+I \end{vmatrix} \qquad 3.13$$

where $\vec{i}$, $\vec{j}$ and $\vec{k}$ are the unit vectors associated with the axes of the referential system (X, Y, Z).

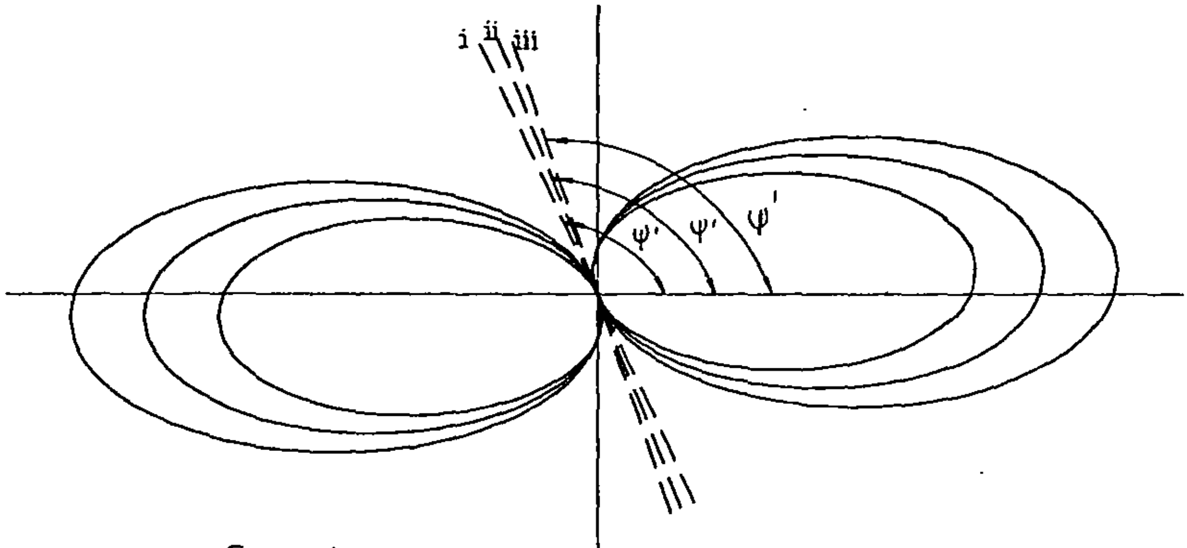


Grinding -
cylindrical

DOg= ▭
Vg = 90.00
Exg= 2.50
Rkg= 59.00

| | |
|---|---|
| i | 8.70 |
| ii | 10.70 |
| iii | 12.70 |

FIGURE 3.9: Effect of Dog on the chisel edge angle

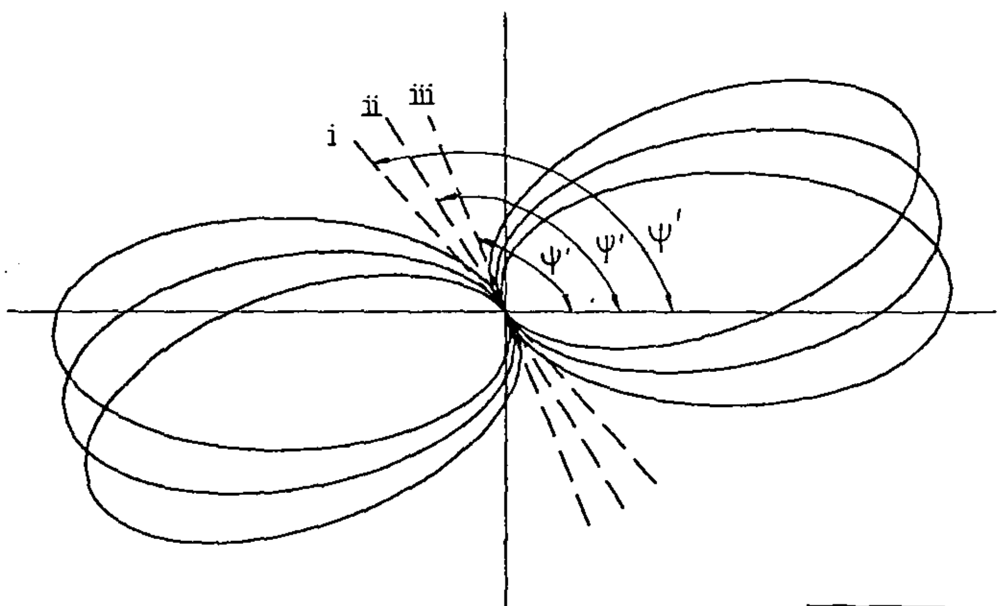


Grinding -
cylindrical

DOg= 25.40
Vg = ▭
Exg= 2.50
Rkg= 59.00

| | |
|---|---|
| i | 70,00 |
| ii | 80,00 |
| iii | 90,00 |

FIGURE 3.10: Effect of Vg on the chisel edge angle

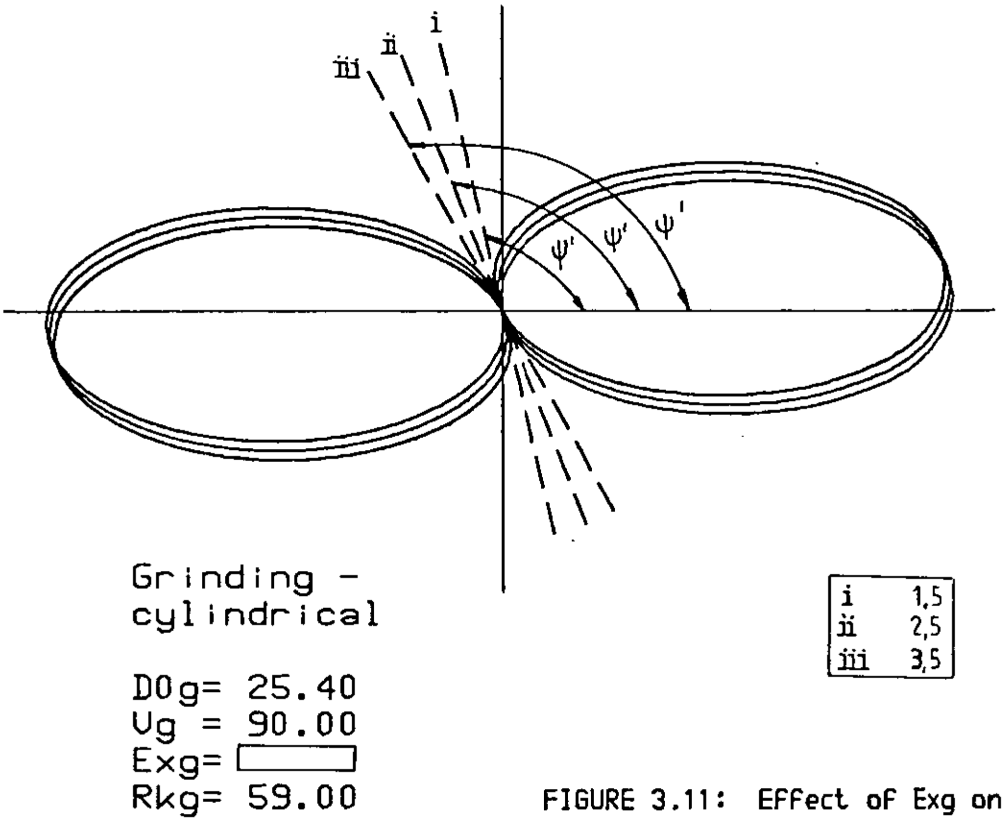


FIGURE 3.11: Effect of Exg on the chisel edge angle

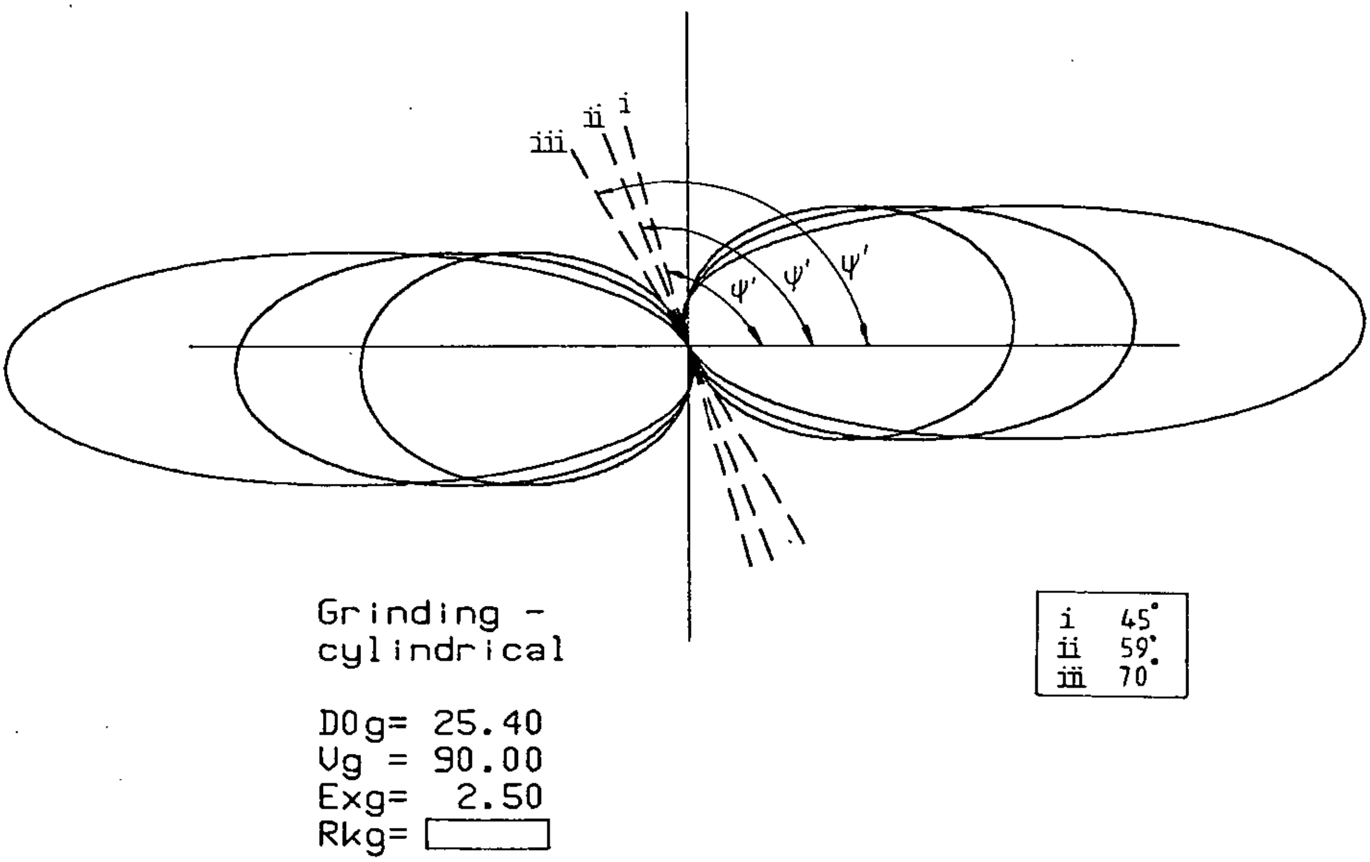


FIGURE 3.12: Effect of Rkg on the chisel edge angle

$$N_1N_2\vec{n_1}x\vec{n_2} = (EZ + G)(2(FZ_{dc} + H)(2CZ_{dc} + I),$$

$$- 2(FZ_{dc} + H)(2\ CZ_{dc} + I),\ 0) \qquad 3.13$$

As expected, the $\vec{n_1}$ x $\vec{n_2}$ vector is normal to the drill axis (third component null), i.e. the tangent to the chisel edge at the drill chisel point is normal to the drill axis.

This tangent makes an angle $\psi'$ (Figures 3.9 to 3.12) with the X axis, which is the same as the chisel edge angle, $\psi$, when the drill lip is a straight line.

Let $\vec{c}$ be the unit vector in the direction of $N_1N_2\vec{n_1}$ x $\vec{n_2}$, or, in the chisel edge direction; let $\vec{i}$ be the unit vector along the X axis:

$$\vec{c}.\vec{i} = |\vec{c}|.|\vec{i}|.\ \mathrm{Cos}\ \ \psi' \ = \mathrm{Cos}\ \ \psi' \qquad 3.14$$

The variation of angle $\psi'$ with the flank model parameters is shown in Figures 3.9 to 3.12 which reveal the parameter $\nu g$ to have in general a greater influence than the other parameters.

Numerical investigation, not included in this work, also revealed the direction of the tangent along the chisel edge to vary very little: less than 1% at a point 1 mm away from the chisel point.

## 3.5 Chapter Closure

In building up the novel model of the cylindrical grinding and implementing it in a computer program, the author aimed at designing a 'tool' to be used in flute design. Thus the analysis was carried out just up to the stage that was needed for that purpose. However, the analysis has been brought to a point that makes easy any further numerical and geometrical investigation on the cylindrical flank surfaces.

*"The drill is geometrically the most complex tool to be found in the workshop and offers a real challenge to anyone attempting to visualize the effective rake angle or other quantities of fundamental importance".*

*Milton Shaw*

# 4. DRILL POINT GEOMETRIC SIMULATION AND CUTTING ANGLES ALONG ANY SHAPED DRILL LIP

## 4.1 Introduction

In attempting to design a new drill flute based on the pre-fixed values of the cutting angles along a drill lip, the author found himself committed to the task of devising and designing analytical and computing 'tools' not available so far. Designing, developing and implementing these 'tools' has been a major task in his work to achieve the main purpose, and, as a result, an extensive, quite complex computer program was built up.

One objective with this computer program was to design it in order that it could simulate any drill point either for any flute form or for any set of the setting parameters of a drill point cylindrical grinding machine.

Simulation of the drill point by computer aided design presents the following advantages:

- it is an additional design aid in drill design;
- it allows for visualization of drill point before flute manufacture and/or actual drill point grinding;
- it can offer an overall view of the drill point configuration represented by its complete contour, for example;
- it allows for elimination of undesired configurations;
- it eliminates trial and error grindings for a set of desired features;
- it reveals design details not immediately available from the traditional set of features used to characterize a drill point;
- it offers a useful approach in unusual situations as the one referring to non-conventional flute design;
- it allows for finding, by comparison with the actual drill points, the error and/or deviations of the flute form and/or the ground surfaces.

## 4.2 Drill Point Geometric Simulation

The geometry of the drill point is determined by the flutes and flanks and their mutual intersections. The drill surfaces are designated as follows (Figure 4.1):

- $S_{\alpha 1}$ - represented by a function $f_{\alpha 1}$ - is the flank surface extending towards the positive semi-axis X
- $S_{\alpha 2}$ - represented by a function $f_{\alpha 2}$ - is the flank surface extending towards the negative semi-axis X and symmetric to $S_{\alpha 1}$ relative to the drill axis (Z axis)
- $S_{\gamma 1}$ - represented by a function $f_{\gamma 1}$ - is the flute face which, with $S_{\alpha 1}$, determines the lip 1
- $S_{\gamma 2}$ - represented by a function $f_{\gamma 2}$ - is the flute face which, with $S_{\alpha 2}$, determines the lip 2
- $S_{h1}$ - represented by a function $f_{h1}$ - is the heel surface that, together with $S_{\gamma 1}$, completes one flute surface
- $S_{h2}$ - represented by a function $f_{h2}$ - is the heel surface that, together with $S_{\gamma 2}$, completes the second flute surface
- $S_{\alpha f}$ - represented by a function $f_{\alpha f}$ - is the drill external cylindrical surface

For the sake of simplicity and without any relevant loss of geometric information, the drill body clearance is not considered and therefore the drill margin (land) is not simulated.

The flow diagram of the computer program segment for drill point simulation is presented in Figure 4.2. The computer program itself, to which belong the referred to segment and other segments already referred to in previous chapters, is presented in Appendix 1 and has been the source for other computer programs the author developed and used throughout his work.

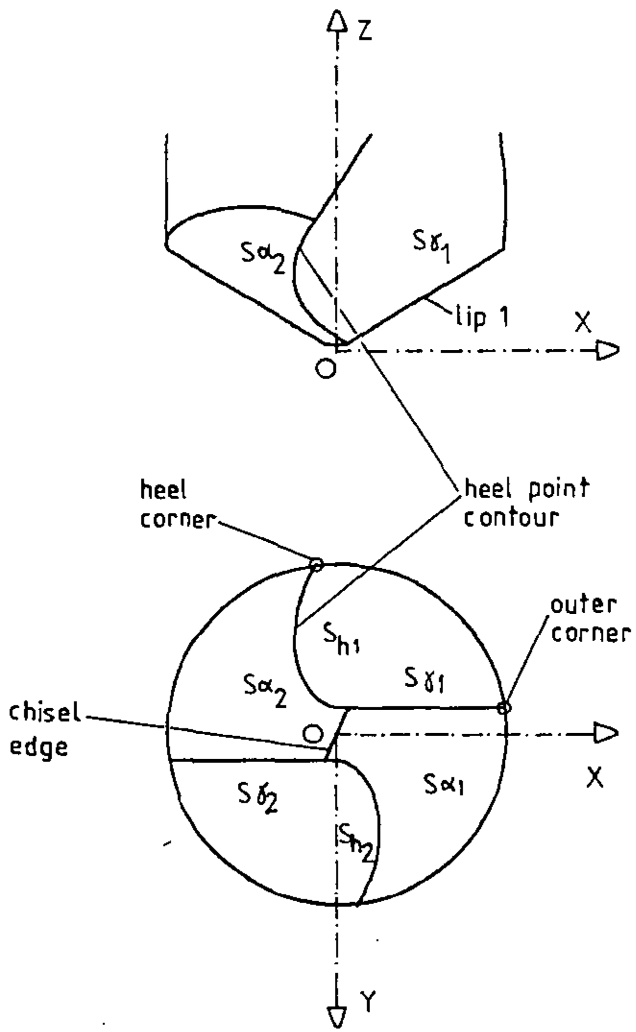


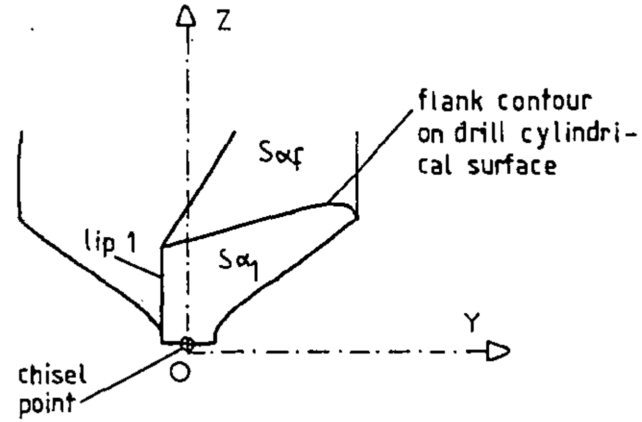


FIGURE 4.1: Drill point surfaces and drill point contour lines .

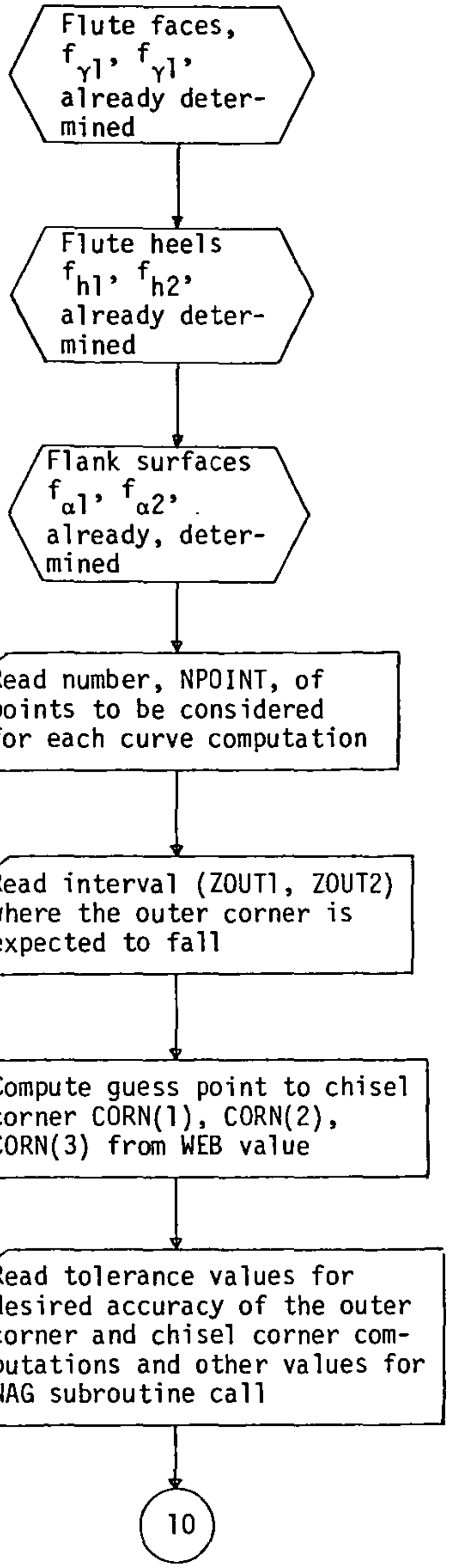


FIGURE 4.2 (continued)

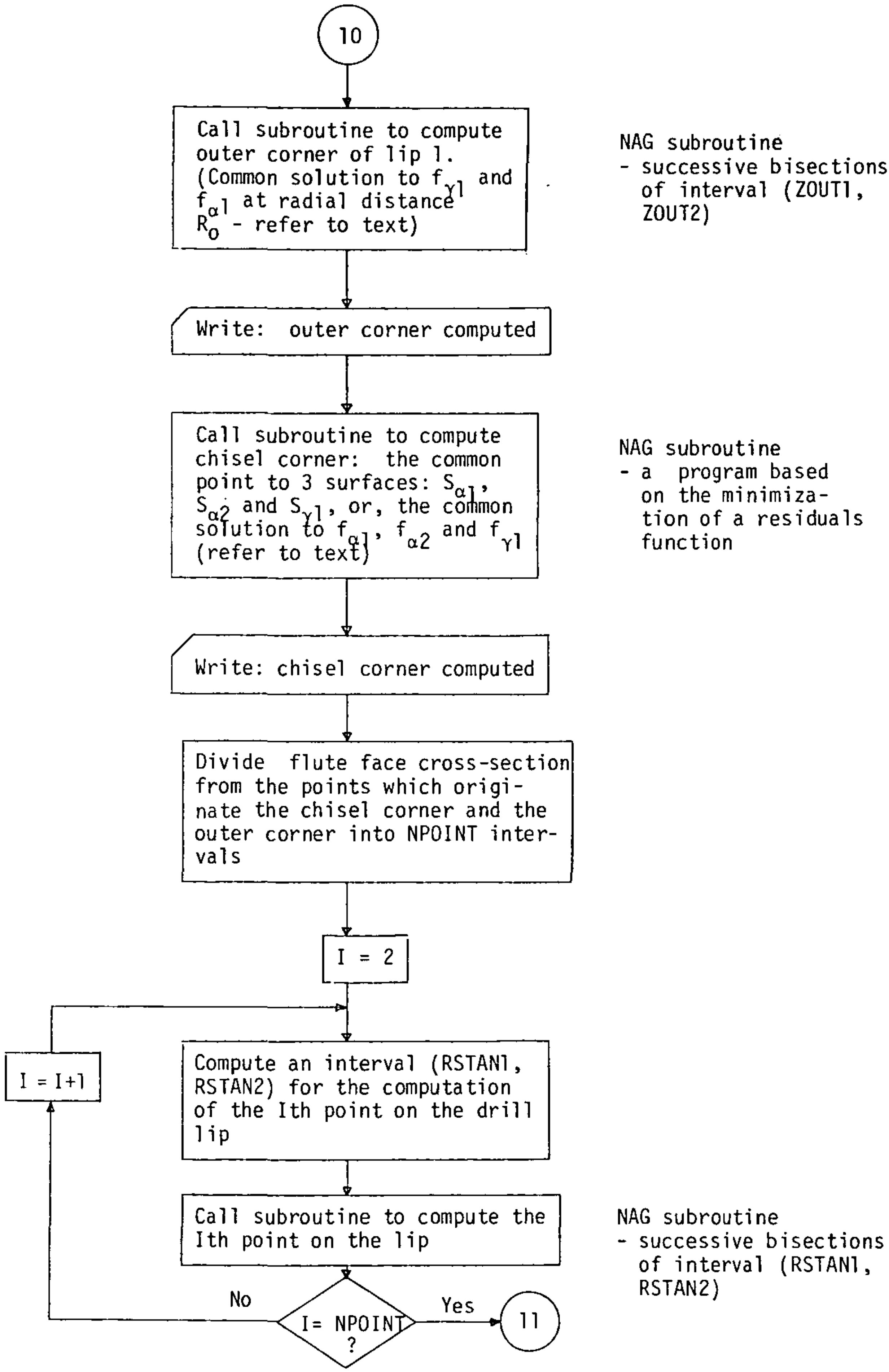
10
Call subroutine to compute outer corner of lip 1. (Common solution to $f_{\gamma 1}$ and $f_{\alpha 1}$ at radial distance $R_o$ - refer to text)
NAG subroutine - successive bisections of interval (ZOUT1, ZOUT2)
Write: outer corner computed
Call subroutine to compute chisel corner: the common point to 3 surfaces: $S_{\alpha 1}$, $S_{\alpha 2}$ and $S_{\gamma 1}$, or, the common solution to $f_{\alpha 1}$, $f_{\alpha 2}$ and $f_{\gamma 1}$ (refer to text)
NAG subroutine - a program based on the minimization of a residuals function
Write: chisel corner computed
Divide flute face cross-section from the points which originate the chisel corner and the outer corner into NPOINT intervals
I = 2
I = I+1
Compute an interval (RSTAN1, RSTAN2) for the computation of the Ith point on the drill lip
Call subroutine to compute the Ith point on the lip
NAG subroutine - successive bisections of interval (RSTAN1, RSTAN2)
No
I= NPOINT ?
Yes
11

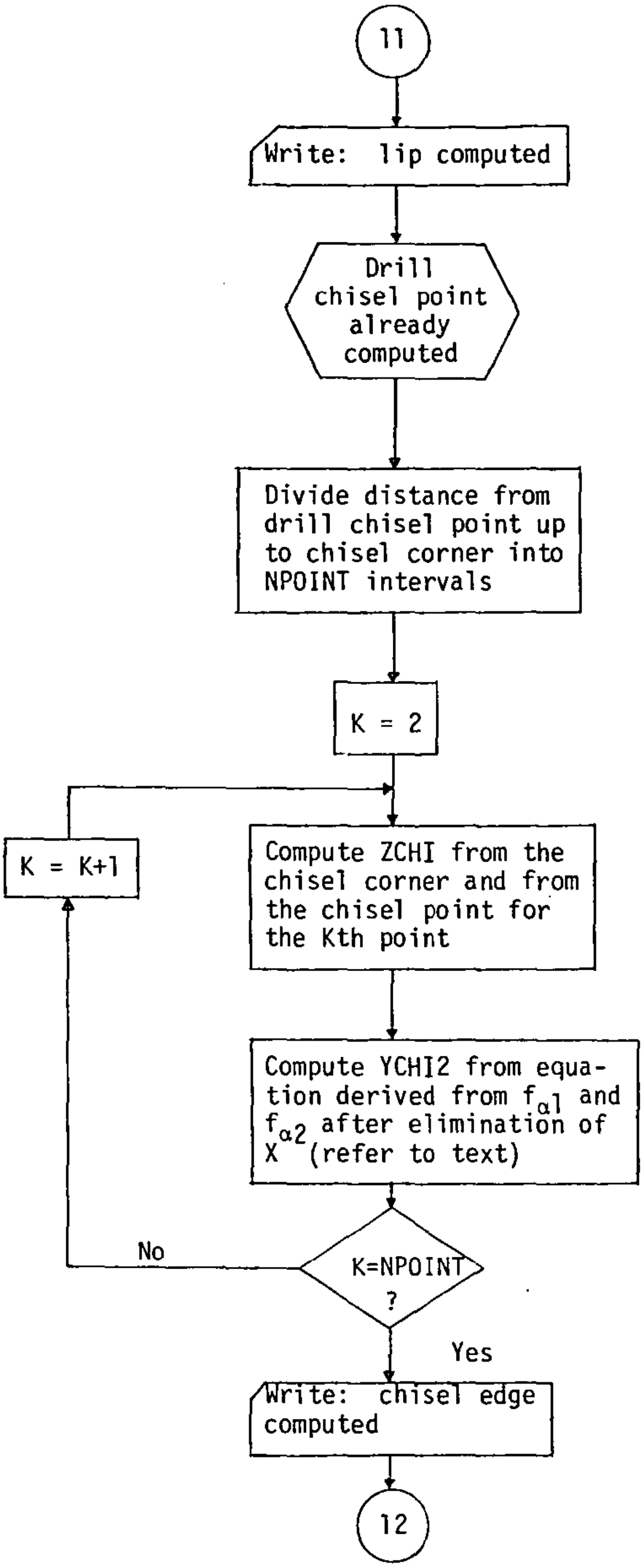
11
Write: lip computed
Drill chisel point already computed
Divide distance from drill chisel point up to chisel corner into NPOINT intervals
K = 2
K = K+1
Compute ZCHI from the chisel corner and from the chisel point for the Kth point
Compute YCHI2 from equation derived from $f_{\alpha 1}$ and $f_{\alpha 2}$ after elimination of $X^2$ (refer to text)
No
K=NPOINT ?
Yes
Write: chisel edge computed
12

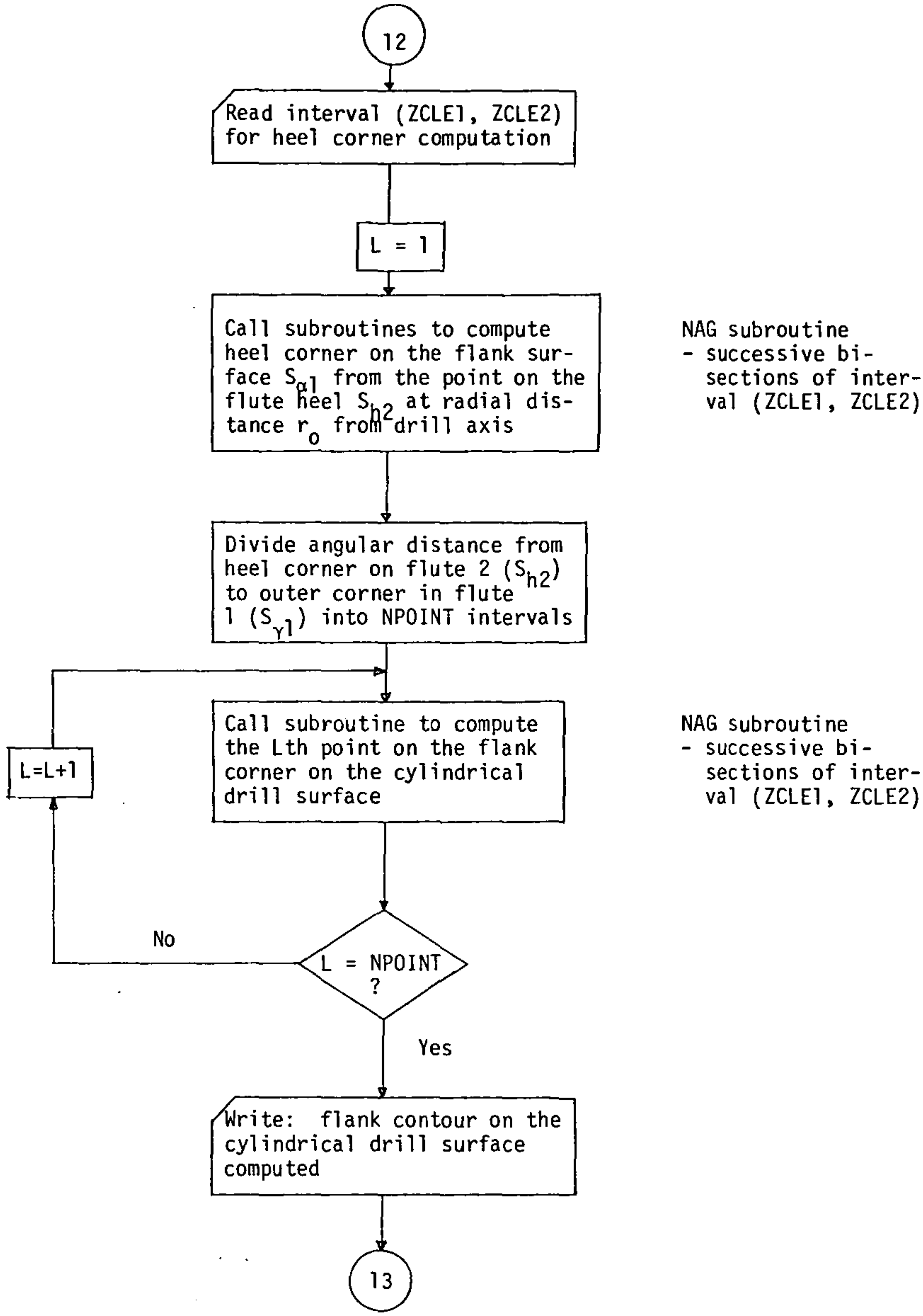

12
Read interval (ZCLE1, ZCLE2) for heel corner computation
L = 1
Call subroutines to compute heel corner on the flank surface $S_{\alpha 1}$ from the point on the flute heel $S_{h2}$ at radial distance $r_o$ from drill axis
NAG subroutine - successive bisections of interval (ZCLE1, ZCLE2)
Divide angular distance from heel corner on flute 2 ($S_{h2}$) to outer corner in flute 1 ($S_{\gamma 1}$) into NPOINT intervals
Call subroutine to compute the Lth point on the flank corner on the cylindrical drill surface
NAG subroutine - successive bisections of interval (ZCLE1, ZCLE2)
L=L+1
No
L = NPOINT ?
Yes
Write: flank contour on the cylindrical drill surface computed
13

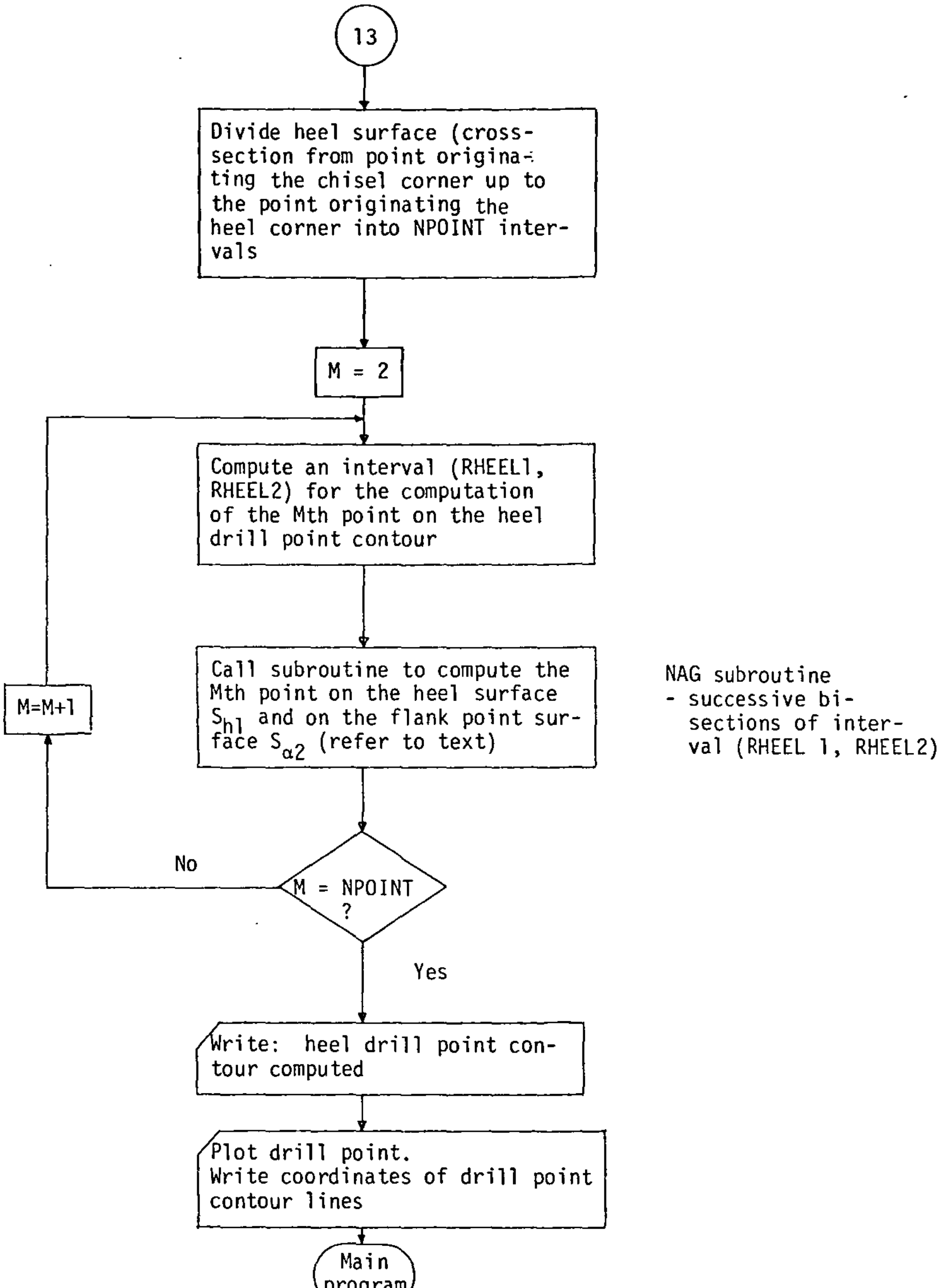


FIGURE 4.2: Flow diagram of computer program segment for drill point geometric simulation

From the computer program implemented numerical model for the drill point, many simulations either numeric (Table 4.1) or geometric (Figure 4.3) were done with two purposes:

i) numerical and geometrical investigation
ii) for comparison with actual drill points produced on the grinding machine available to the author, with drills mainly from the shelf.

Figure 4.3 shows a simulated drill point of a 19.05 mm (¾") diameter conventional flute drill for which the cylindrical grinding parameters were selected as follows:

$d_{og} = 38$ mm; $\nu_g = 65^o$; $ex_g = 3$ mm; $\kappa_g = 59^o$

Figure 4.4 shows the actual drill point, after grinding, of a conventional flute drill without margins which has been manufactured for research purposes, with the features used for the simulation shown in Figure 4.3.

Figures 4.5 to 4.10 are presented to illustrate drill point simulation for one conventional flute ground to three different point angles. The effect of the other cylindrical grinding parameters and the conventional flute design parameters is illustrated in Appendix 2.

## 4.3 Lip Geometry Related Cutting Angles Along Any Shape Drill Lip

Drill features, as presented in Chapter 1, are inadequate to take account of the differences between flute forms which influence the length and shape of the lips and the chisel edge length together with the cutting angles along the lips.

Lip length and chisel edge length can be put in evidence from the computations presented in the previous section (Table 4.1 and geometric simulations).

| 1 | | | | 2 | 3 | | | 4 | | | |
|---|---|---|---|---|---|---|---|---|---|---|---|
| RADI | X | Y | Z | S | XCHI | YCHI | ZCHI | XCLE | YCLE | ZCLE | PHCL (deg) |
| 9.52 | 9.44 | -1.20 | 4.90 | 0.00 | 1.39 | -1.53 | 0.33 | 0.78 | 9.49 | 7.08 | 85.32 |
| 9.04 | 8.95 | -1.26 | 4.60 | 0.59 | 1.35 | -1.48 | 0.33 | 1.79 | 9.35 | 7.14 | 79.15 |
| 8.55 | 8.45 | -1.31 | 4.29 | 1.17 | 1.30 | -1.42 | 0.32 | 2.79 | 9.10 | 7.13 | 72.97 |
| 8.06 | 7.94 | -1.36 | 3.99 | 1.77 | 1.25 | -1.37 | 0.31 | 3.75 | 8.75 | 7.06 | 66.80 |
| 7.56 | 7.43 | -1.40 | 3.68 | 2.36 | 1.19 | -1.31 | 0.30 | 4.67 | 8.30 | 6.95 | 60.63 |
| 7.06 | 6.92 | -1.43 | 3.38 | 2.96 | 1.14 | -1.25 | 0.29 | 5.53 | 7.75 | 6.80 | 54.46 |
| 6.56 | 6.39 | -1.46 | 3.07 | 3.56 | 1.08 | -1.18 | 0.28 | 6.33 | 7.11 | 6.64 | 48.28 |
| 6.05 | 5.87 | -1.49 | 2.77 | 4.17 | 1.02 | -1.12 | 0.28 | 7.06 | 6.38 | 6.46 | 42.11 |
| 5.54 | 5.33 | -1.51 | 2.47 | 4.79 | 0.95 | -1.05 | 0.27 | 7.71 | 5.59 | 6.27 | 35.94 |
| 5.03 | 4.80 | -1.52 | 2.16 | 5.41 | 0.88 | -0.97 | 0.26 | 8.26 | 4.73 | 6.08 | 29.77 |
| 4.52 | 4.25 | -1.53 | 1.86 | 6.03 | 0.80 | -0.88 | 0.25 | 8.72 | 3.81 | 5.89 | 23.59 |
| 4.00 | 3.69 | -1.54 | 1.55 | 6.67 | 0.72 | -0.79 | 0.24 | 9.08 | 2.85 | 5.69 | 17.42 |
| 3.49 | 3.13 | -1.54 | 1.25 | 7.31 | 0.62 | -0.68 | 0.23 | 9.34 | 1.86 | 5.50 | 11.25 |
| 2.99 | 2.56 | -1.54 | 0.94 | 7.95 | 0.51 | -0.56 | 0.23 | 9.48 | 0.84 | 5.31 | 5.08 |
| 2.51 | 1.98 | -1.54 | 0.64 | 8.61 | 0.36 | -0.40 | 0.22 | 9.52 | -0.18 | 5.11 | -1.10 |
| 2.07 | 1.39 | -1.53 | 0.33 | 9.27 | 0.00 | -0.00 | 0.21 | 9.44 | -1.20 | 4.90 | -7.27 |

TABLE 4.1: Computer printout for drill point (an example)
[Refer to FIGURES 4.3 and 4.4]

1 - Radial distance and coordinates along the drill lip (from the outer corner)

2 - Distance along the drill lip (from the outer corner)

3 - Half-chisel edge coordinates (from the chisel corner to the chisel point)

4 - Circumferential drill flank contour coordinates and angle (from heel corner)

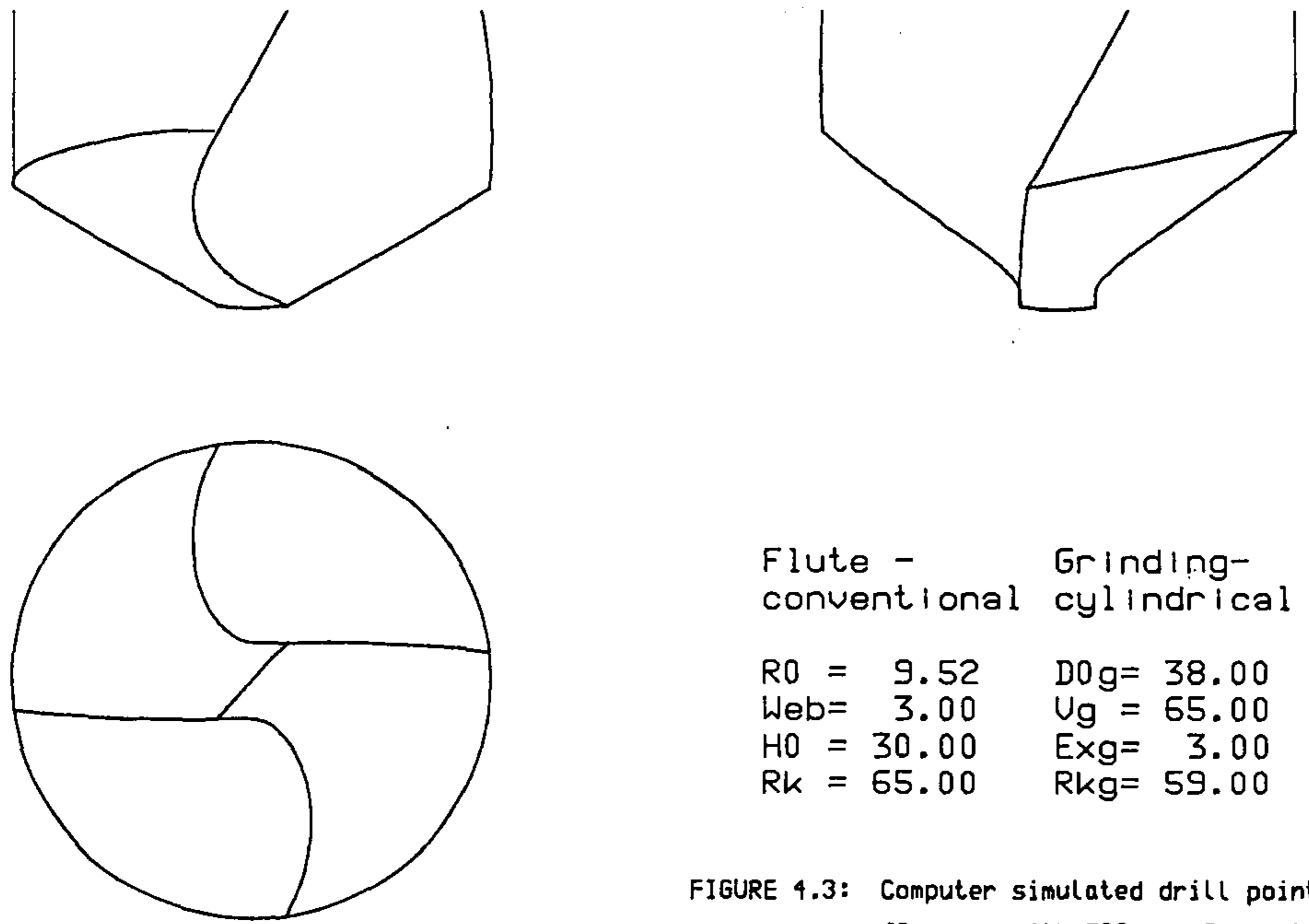


FIGURE 4.3: Computer simulated drill point [Compare with FIG 4.4 for actual drill point]

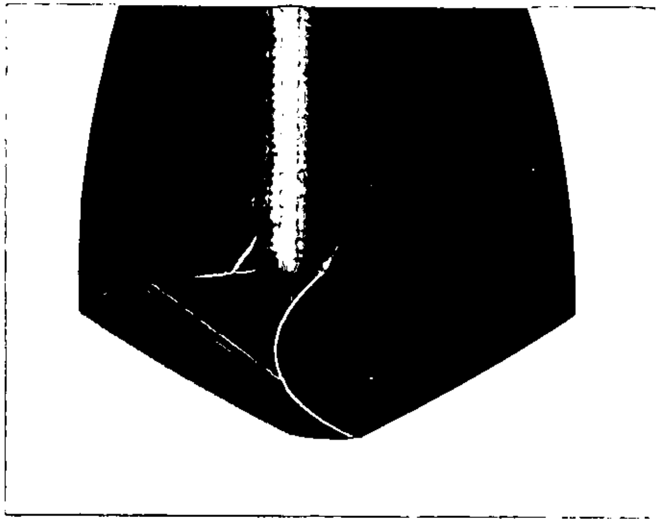

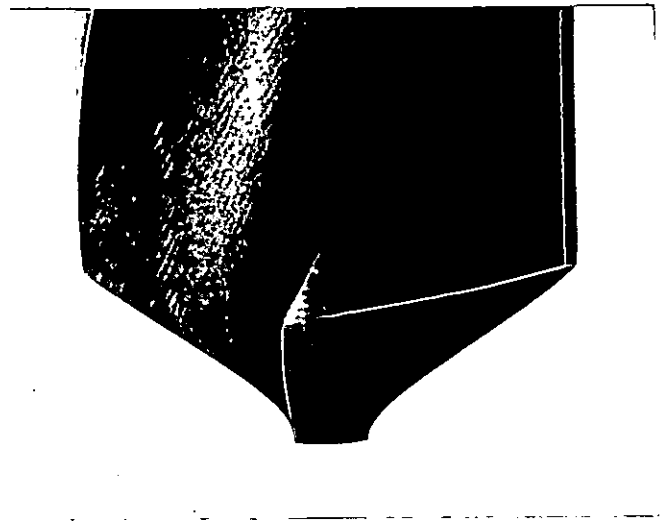

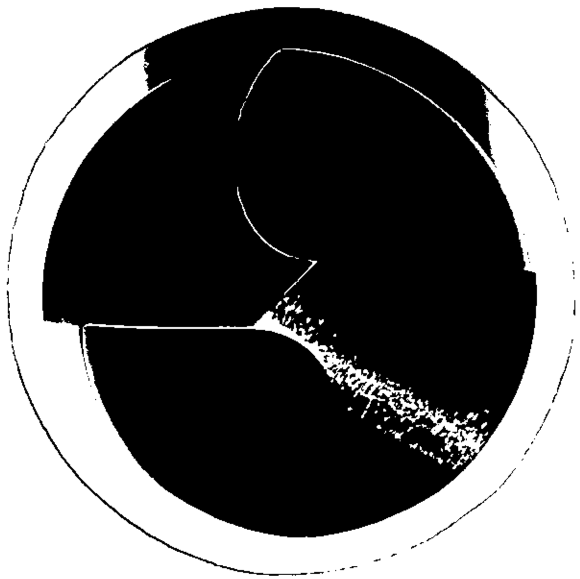

Flute - conventional

RO = 9.52
Web= 3.00
HO = 30.00

Grinding- cylindrical

DOg= 38.00
Vg = 65.00
Exg= 3.00
Rkg= 59.00

FIGURE 4.4: Actual drill point
[Compare with FIG 4.3 for computer simulated drill point]

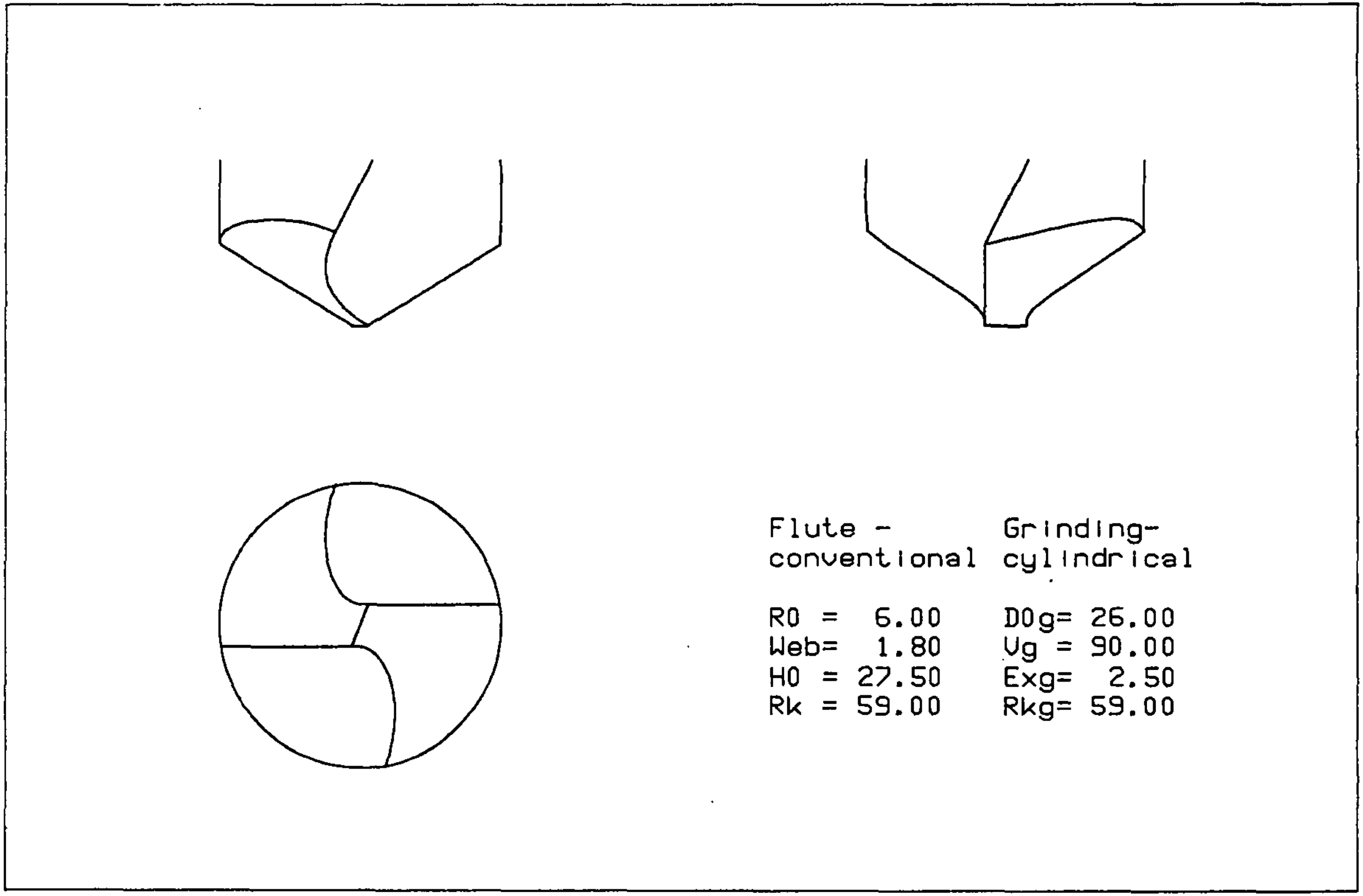


FIGURE 4.5: Computer simulation of drill point.

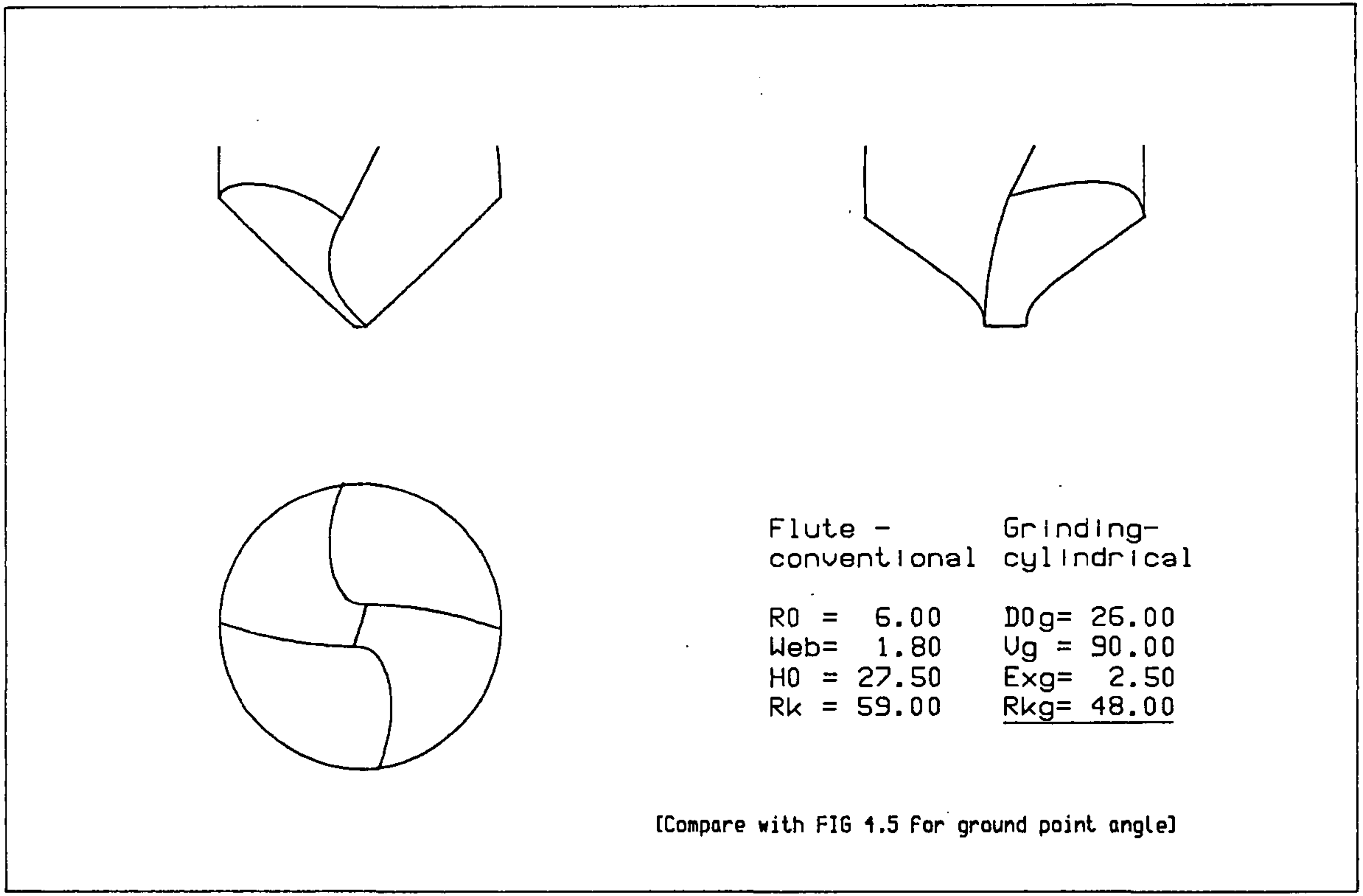


FIGURE 4.6: Computer simulation of drill point.

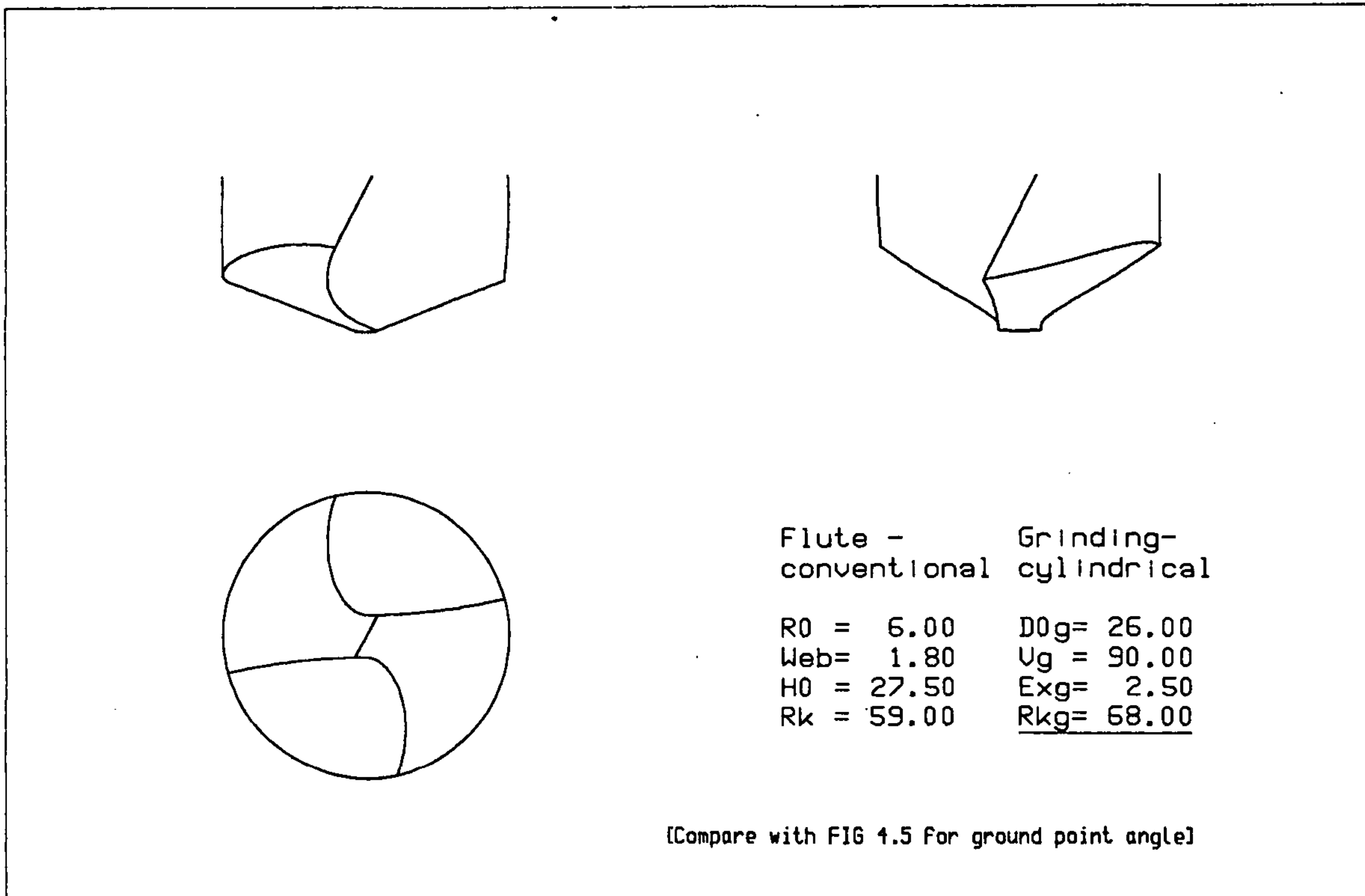


FIGURE 4.7: Computer simulation of drill point.

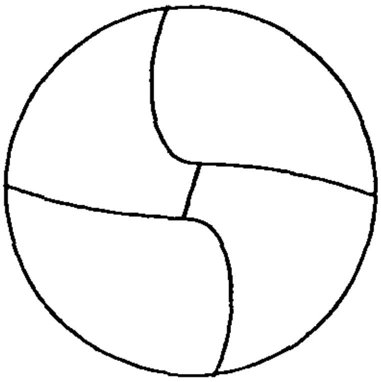

| Flute - conventional | Grinding- cylindrical |
|---|---|
| R0 = 6.00 | D0g= 26.00 |
| Web= 1.80 | Vg = 90.00 |
| H0 = 27.50 | Exg= 2.50 |
| Rk = 59.00 | Rkg= 48.00 |

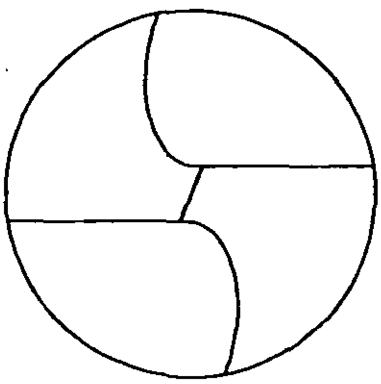

| Flute - conventional | Grinding- cylindrical |
|---|---|
| R0 = 6.00 | D0g= 26.00 |
| Web= 1.80 | Vg = 90.00 |
| H0 = 27.50 | Exg= 2.50 |
| Rk = 59.00 | Rkg= 59.00 |

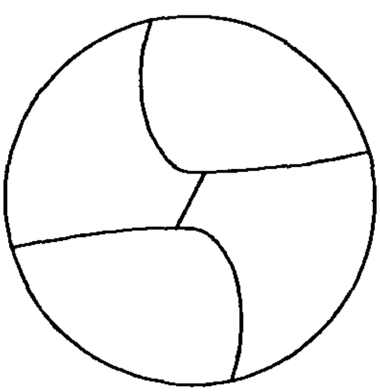

| Flute - conventional | Grinding- cylindrical |
|---|---|
| R0 = 6.00 | D0g= 26.00 |
| Web= 1.80 | Vg = 90.00 |
| H0 = 27.50 | Exg= 2.50 |
| Rk = 59.00 | Rkg= 68.00 |

FIGURE 4.8: Comparing similar views of computer simulated drill points ground to three different point angles (refer to FIG 4.5 to FIG 4.7).

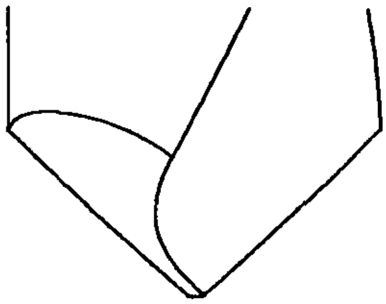

| Flute - conventional | Grinding- cylindrical |
|---|---|
| R0 = 6.00 | D0g= 26.00 |
| Web= 1.80 | Vg = 90.00 |
| H0 = 27.50 | Exg= 2.50 |
| Rk = 59.00 | Rkg= 48.00 |

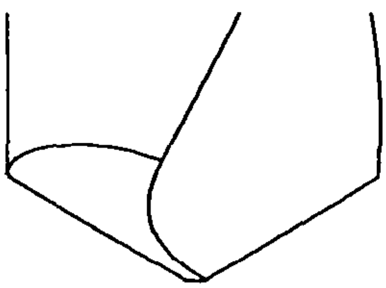

| Flute - conventional | Grinding- cylindrical |
|---|---|
| R0 = 6.00 | D0g= 26.00 |
| Web= 1.80 | Vg = 90.00 |
| H0 = 27.50 | Exg= 2.50 |
| Rk = 59.00 | Rkg= 59.00 |

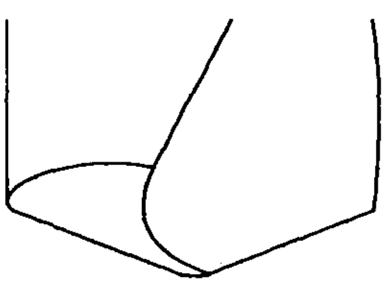

| Flute - conventional | Grinding- cylindrical |
|---|---|
| R0 = 6.00 | D0g= 26.00 |
| Web= 1.80 | Vg = 90.00 |
| H0 = 27.50 | Exg= 2.50 |
| Rk = 59.00 | Rkg= 68.00 |

FIGURE 4.9: Comparing similar views of computer simulated drill points ground to three different point angles (refer to FIG 4.5 to FIG 4.7).

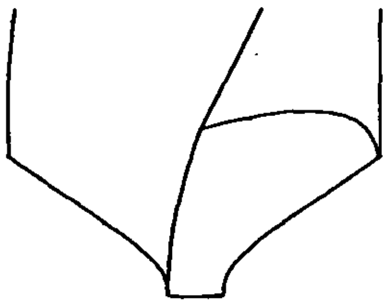

| Flute - conventional | Grinding- cylindrical |
|---|---|
| R0 = 6.00 | D0g= 26.00 |
| Web= 1.80 | Vg = 90.00 |
| H0 = 27.50 | Exg= 2.50 |
| Rk = 59.00 | Rkg= 48.00 |

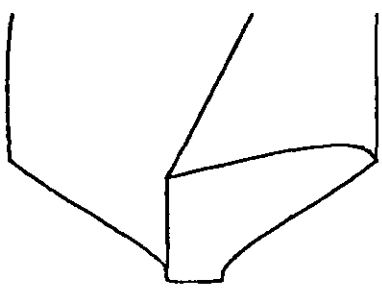

| Flute - conventional | Grinding- cylindrical |
|---|---|
| R0 = 6.00 | D0g= 26.00 |
| Web= 1.80 | Vg = 90.00 |
| H0 = 27.50 | Exg= 2.50 |
| Rk = 59.00 | Rkg= 59.00 |

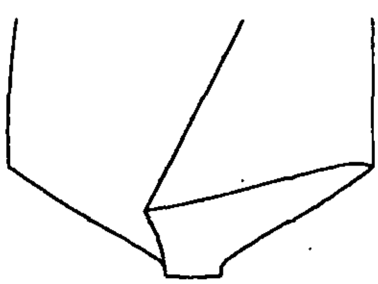

| Flute - conventional | Grinding- cylindrical |
|---|---|
| R0 = 6.00 | D0g= 26.00 |
| Web= 1.80 | Vg = 90.00 |
| H0 = 27.50 | Exg= 2.50 |
| Rk = 59.00 | Rkg= 68.00 |

FIGURE 4.10: Comparing similar views of computer simulated drill points ground to three different point angles (refer to FIG 4.5 to FIG 4.7).

For a more complete knowledge of a drill cutting capability, the cutting geometry along its edges must be known.

Single point cutting tools are usually dealt with in terms of rake angles, inclination angle and clearance angle, for example. These angles are the concepts which eventually should be used in comparing such different tools as drills and single point cutting tools.

To design new drill flutes according to prefixed conditions such as a uniform wedge angle along the drill lip, it is not possible before a method is available to compute such an angle along the cutting edge.

Galloway (3) and others presented expressions to calculate some basic cutting angles along the drill lips. These expressions are not valid except for straight lips.

Drill curved lips are reported from time to time to perform better than the straight ones, at least in special cases - with cast iron, for instance.

Approaching the cutting angles of curved edges could be made, according to Stabler (45), in the same way as for straight cutting edges by taking the tangent at the selected point to the curved cutting edge. This approach is considered in the following analysis and computations.

### 4.3.1 Rake angle

The rake angle has always received a great deal of attention which is expressed in the number of papers which deal with this particular variable, and in the many designations used with the same basic concept.

The many designations used with the rake angle derive mainly from the oblique cutting case as for this case the definition of rake is dependent on the selection of the reference plane and measurement plane.

The normal rake angle is a basic angle, for the many works reporting on its influence upon cutting performance and for being a basic variable for the calculation of other rake angles such as the velocity rake and the effective rake.

The normal rake angle (Figure 4.11), $\gamma_n$, is measured in a plane perpendicular to the cutting edge, $p_n$, between the face ($S_{\gamma 1}$ or $S_{\gamma 2}$) and the normal to the plane defined by the cutting edge and the cutting velocity.

The vector simultaneously normal to the cutting edge vector, $\vec{e}$, and velocity vector, $\vec{v}$, is designated by $\vec{n}_m$ (Figures 4.11 and 4.12). The vector on the rake face, normal to the cutting edge is designated by $\vec{t}_{\gamma 1}$.

From Figure 4.11:

$$\vec{n}_m \cdot \vec{t}_{\gamma 1} = |\vec{n}_m| \cdot |\vec{t}_{\gamma 1}| \cos \gamma_n = \cos \gamma_n \qquad 4.1$$

Computing $\vec{n}_m$ and $\vec{t}_{\gamma 1}$:
From Figure 4.12:

$$N_n \, \vec{n}_m = \vec{e} \times \vec{v} \qquad 4.2$$

$$\vec{v} = (- \sin \phi, \cos \phi, 0) \qquad 4.3$$

where $N_m = |\vec{e} \times \vec{v}|$

Vector $\vec{v}$ is normal to radial vector $\vec{r}$ and parallel to the XY plane (Figure 4.12). Vector $\vec{e}$ is computed from the vector, $\vec{n}_{\alpha 1}$, normal to the flank at point P, and from the vector $\vec{n}_{\gamma 1}$, normal to the rake face (Figure 4.13):

$$E \, \vec{e} = \vec{n}_{\gamma 1} \times \vec{n}_{\alpha 1} \qquad 4.4$$

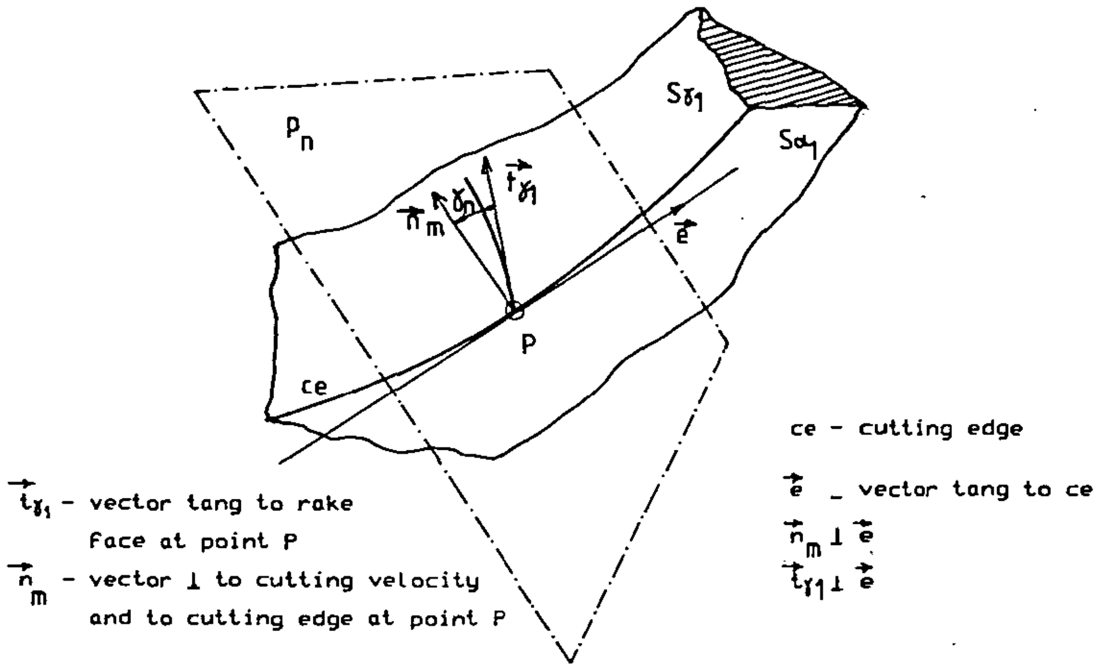


FIGURE 4.11: Normal rake angle definition

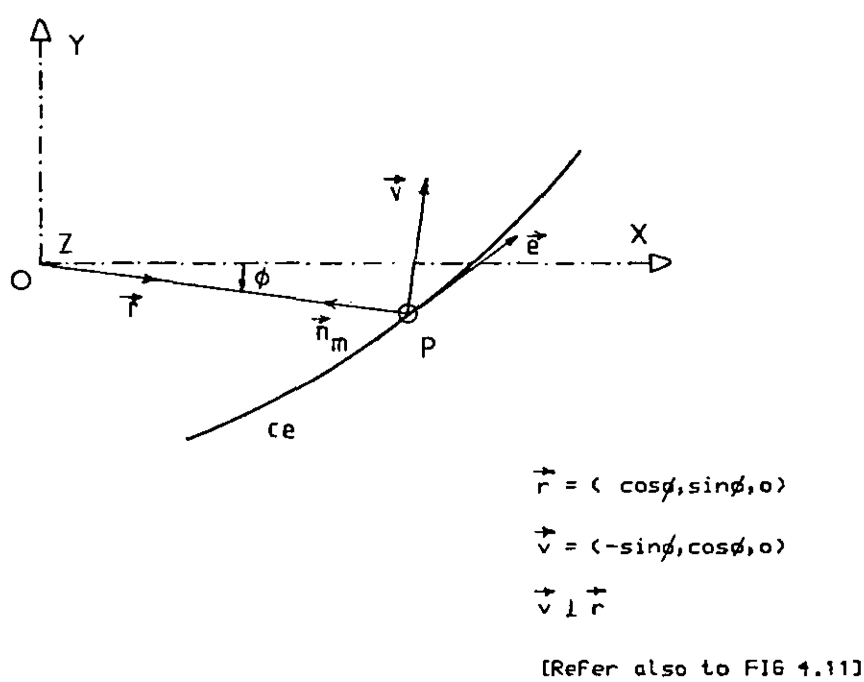


FIGURE 4.12: Definition of vector normal to the cutting edge and to cutting velocity , $\vec{n}_m$

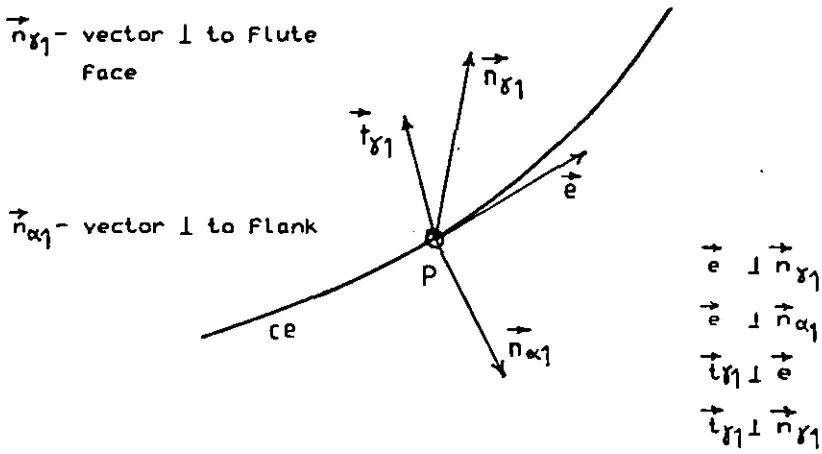


FIGURE 4.13: Determination of vector $\vec{e}$ and cutting edge direction.

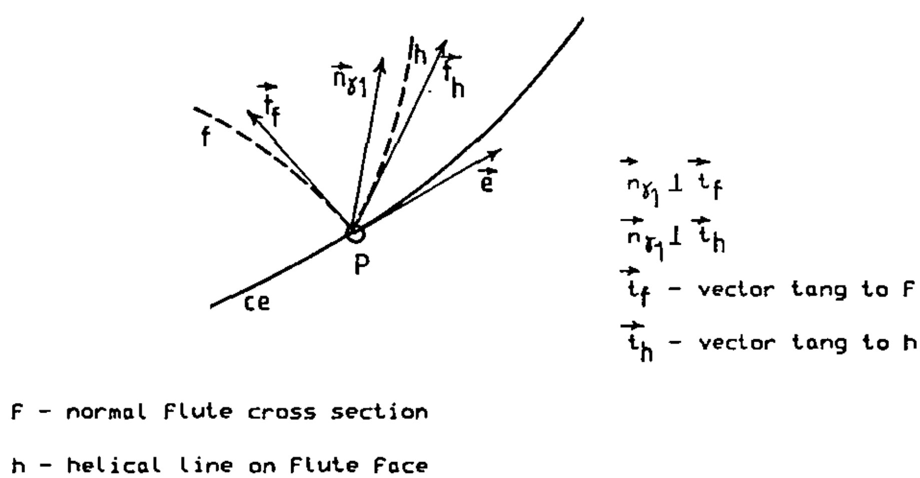


FIGURE 4.14: Determination of vector, $\vec{n}_{\gamma 1}$, normal to the rake face.

[Refer to previous FIGS.].

where $E = |\vec{n}_{\gamma 1} \times \vec{n}_{\alpha 1}|$

and $\quad N_{\alpha 1} \cdot \vec{n}_{\alpha 1} = (\partial f_{\alpha 1}/\partial X,\ \partial f_{\alpha 1}/\partial Y,\ \partial f_{\alpha 1}/\partial Z)$ 4.5

where $f_{\alpha 1}$ is the expression for the mathematical model of flank $S_{\alpha 1}$ and $N_{\alpha 1}$ is the length of the vector on the right side of the equation.

Vector $\vec{n}_{\gamma 1}$ is computed from the vector, $\vec{t}_h$, tangent to the helix containing P, and from the vector, $\vec{t}_f$, tangent to the flute cross-section at point P (Figure 4.14).

From Figure 4.14:

$$N_{\gamma 1} \cdot \vec{n}_{\gamma 1} = \vec{t}_h \times \vec{t}_f \tag{4.6}$$

where $\quad N_{\gamma 1} = |\vec{t}_h \times \vec{t}_f|$

The vector $\vec{t}_h$, tangent to helix h (Figure 4.15) can be computed from vector, $\vec{v}$, normal to $\vec{r}$ at P and from the helix angle $\gamma_h$ at point P.

From Figure 4.15:

$$T_h \cdot \vec{t}_h = \vec{v} + \cot \gamma_h \cdot \vec{K} \tag{4.7}$$

Vector $\vec{t}_f$ can be computed as shown in Figure 4.16:

$$\vec{t}_f = \left(-\cos\left(\tan^{-1}\left(\frac{dY}{dX}\right)_{Z=0} - \xi\right),\ -\sin\left(\tan^{-1}\left(\frac{dY}{dX}\right)_{Z=0} - \xi\right), 0\right) \tag{4.8}$$

Finally, $\vec{t}_{\gamma 1}$ is computed from $\vec{n}_{\gamma 1}$ and $\vec{e}$ (Figure 4.13):

$$T_{\gamma 1}\ \vec{t}_{\gamma 1} = \vec{n}_{\gamma 1} \times \vec{e} \tag{4.9}$$

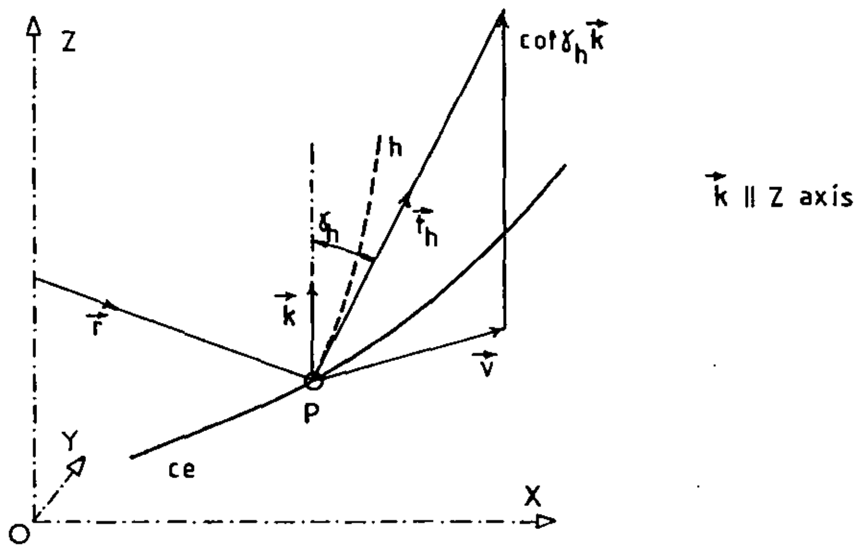


FIGURE 4.15: Determination of tangent to helix h, $\vec{t}_h$, from the normal to radial vector and from the helix angle.

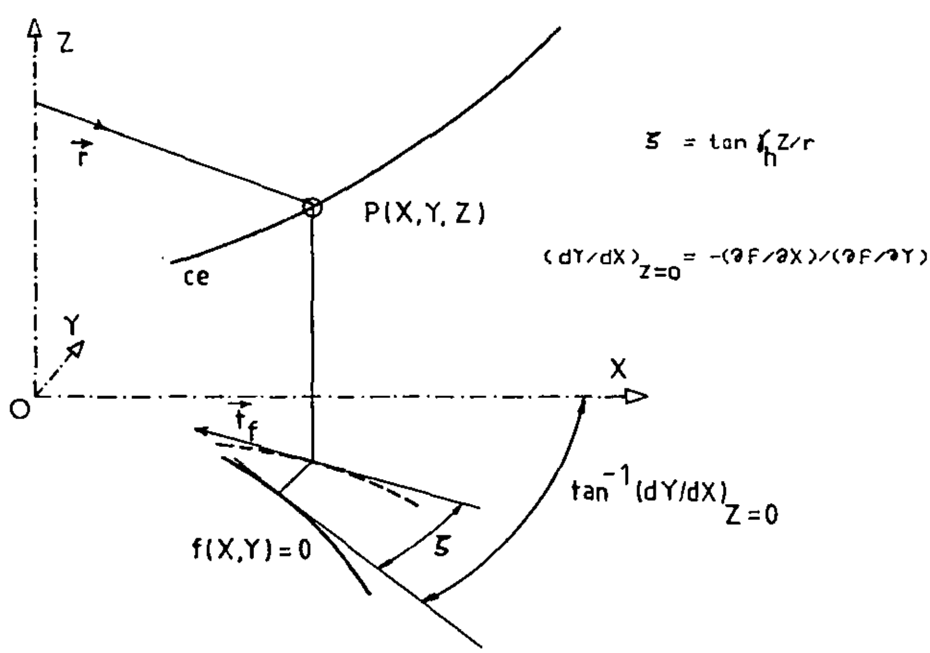


$$\vec{t}_f = (\cos(\tan^{-1}(dY/dX)_{Z=0} - \xi), \sin(\tan^{-1}(dY/dX)_{Z=0} - \xi), 0)$$

FIGURE 4.16: Determination of tangent, $\vec{t}_f$, to flute cross section at point P.

where $T_{\gamma 1} = |\vec{n}_{\gamma 1} \times \vec{e}|$

$\vec{v}$, $\vec{n}_{\alpha 1}$, $\vec{t}_h$ and $\vec{t}_f$ are computed directly from Equations 4.3, 4.5, 4.7 and 4.8 respectively. From $\vec{v}$, $\vec{n}_{\alpha 1}$, $\vec{t}_h$ and $\vec{t}_f$, the algorithm to compute the normal rake angle is devised as follows:

$\vec{t}_f, \vec{t}_h \rightarrow \vec{n}_{\gamma 1}$ (Equation 4.6)

$\vec{n}_{\gamma 1}, \vec{n}_{\alpha 1} \rightarrow \vec{e}$ (Equation 4.4)

$\vec{e}, \vec{v} \rightarrow \vec{n}_m$ (Equation 4.2)

$\vec{n}_{\gamma 1}, \vec{e} \rightarrow \vec{t}_{\gamma 1}$ (Equation 4.9)

$\vec{t}_{\gamma 1}, \vec{n}_m \rightarrow \gamma_n$ (Equation 4.1)

For computing purposes the variables which are vectors must be represented by their components in a referential system, as shown in Section 'Nomenclature'.

The flow diagram of the computer program (Appendix 1) segment to compute the normal rake angle is given in Figure 4.17.

The above presented method was tested, for straight lips, against the expression for the normal rake angle, $\gamma_n$, given by Galloway (3):

$$\tan \gamma_n = \frac{(\rho^2 - \sigma^2 \operatorname{Sin}^2 \kappa)}{(\rho^2 - \sigma^2)^{\frac{1}{2}} \operatorname{Sin} \kappa} \tan \gamma_f - \frac{\sigma \operatorname{Cos} \kappa}{(\rho^2 - \sigma^2)^{\frac{1}{2}}} \qquad 4.10$$

where $\rho = \frac{r}{r_o}$ and $\sigma = \frac{W'}{r_o}$

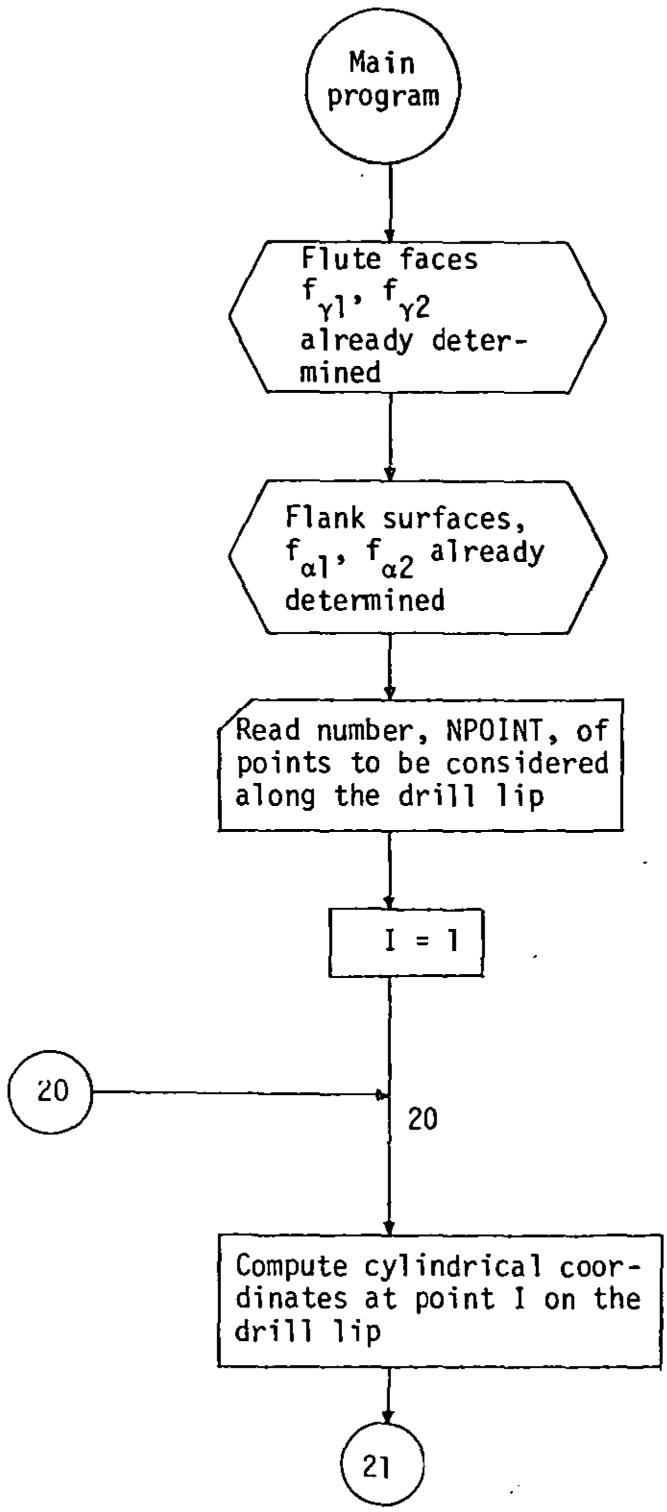


FIGURE 4.17 (continued)

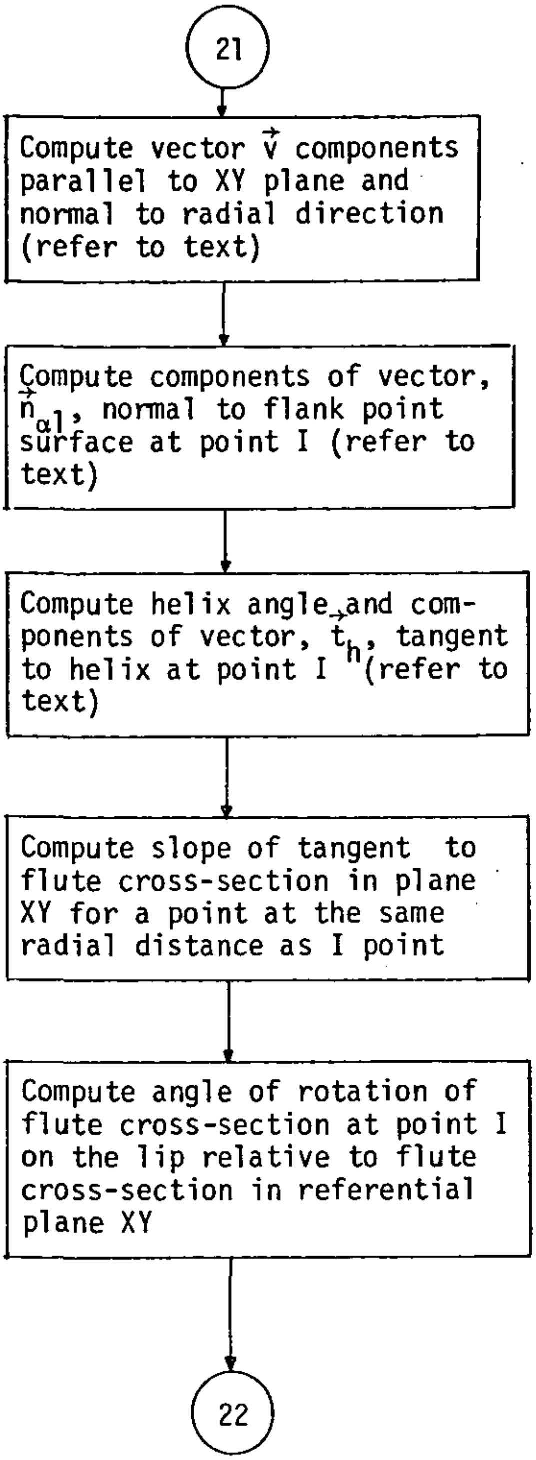


FIGURE 4.17 (continued)

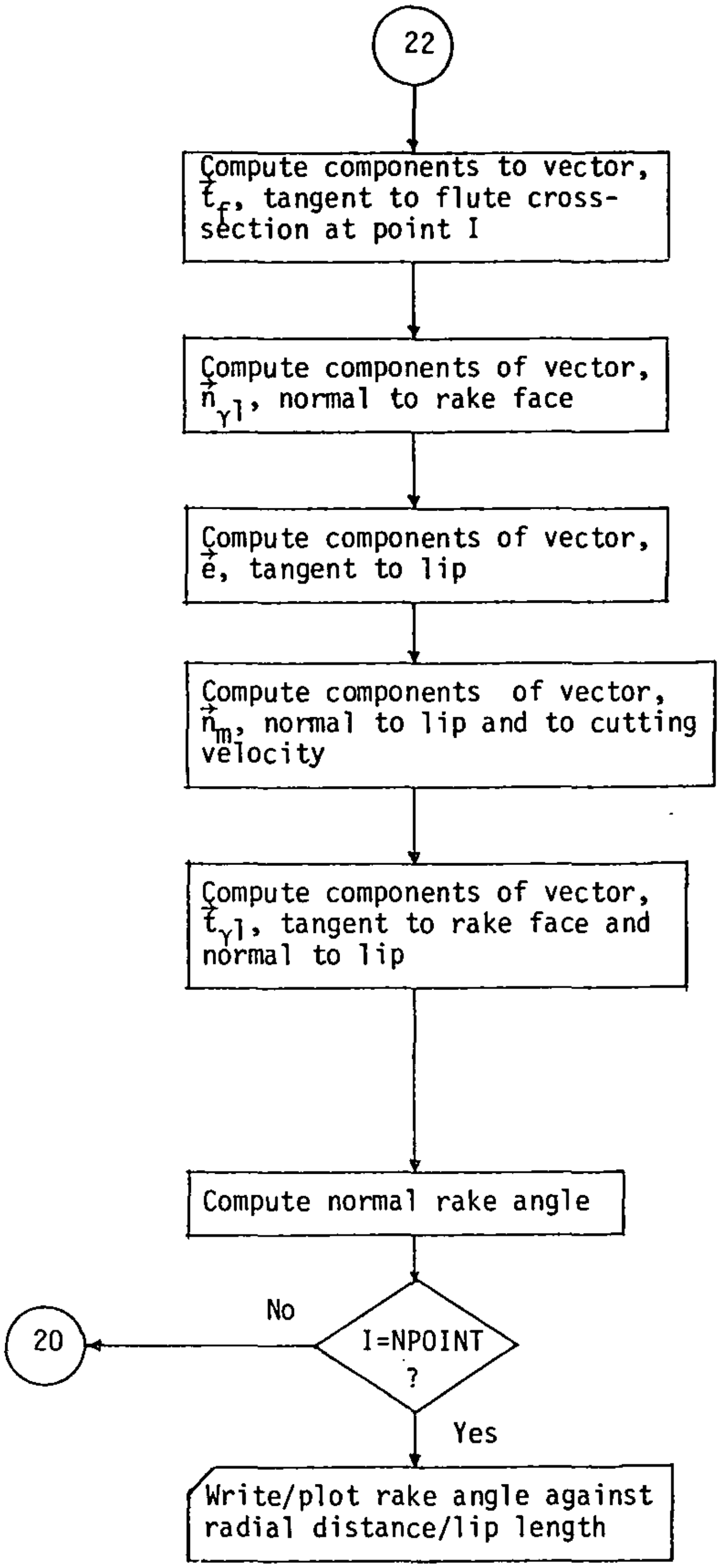


FIGURE 4.17: Flow diagram of computer program segment to compute the normal rake angle

The normal rake angle, $\gamma_n$, was calculated both with the formulae by Galloway and with the algorithm by the author for the case of straight lips. Large ranges of parameters, $r_o$, W', $\kappa$ and $\gamma_f$ and varying radial distances, r, were investigated and the results were coincident.

The need and advantage of the present method refers mainly to the cases where the lips are curved and for which Equation 4.10 cannot be applied.

The present algorithm allows for numerical and graphical investigation of the normal rake angle for any practical range of the grinding parameters - $d_{og}$, $\nu_g$, $ex_g$, $\kappa_g$ -, for any practical range of the conventional flute parameters - $r_o$, W', $\gamma_f$, $\kappa$ - and for other flutes defined by their cross-sections in the XY plane.

In Figure 4.18 it is shown the variation of the normal rake angle with the radial distance for three different conventional flutes; the flutes have different design point angles and are ground accordingly (Figure 4.5 and Appendix 2).

In Figure 4.19 it is shown the variation of the normal rake angle with the radial distance for one conventional flute and three different ground point angles (Figures 4.5, 4.6 and 4.7).

One curve from Figure 4.18 - $48^0$ design point angle flute and $48^0$ ground point angle - is compared with one curve from Figure 4.19 - $59^0$ design point angle flute and $48^0$ ground point angle - in Figure 4.20.

The influence of the conventional flute design parameters other than $\kappa$, and the influence of the cylindrical grinding parameters other than $\kappa_g$ on the normal rake angle is shown in Appendix 3.

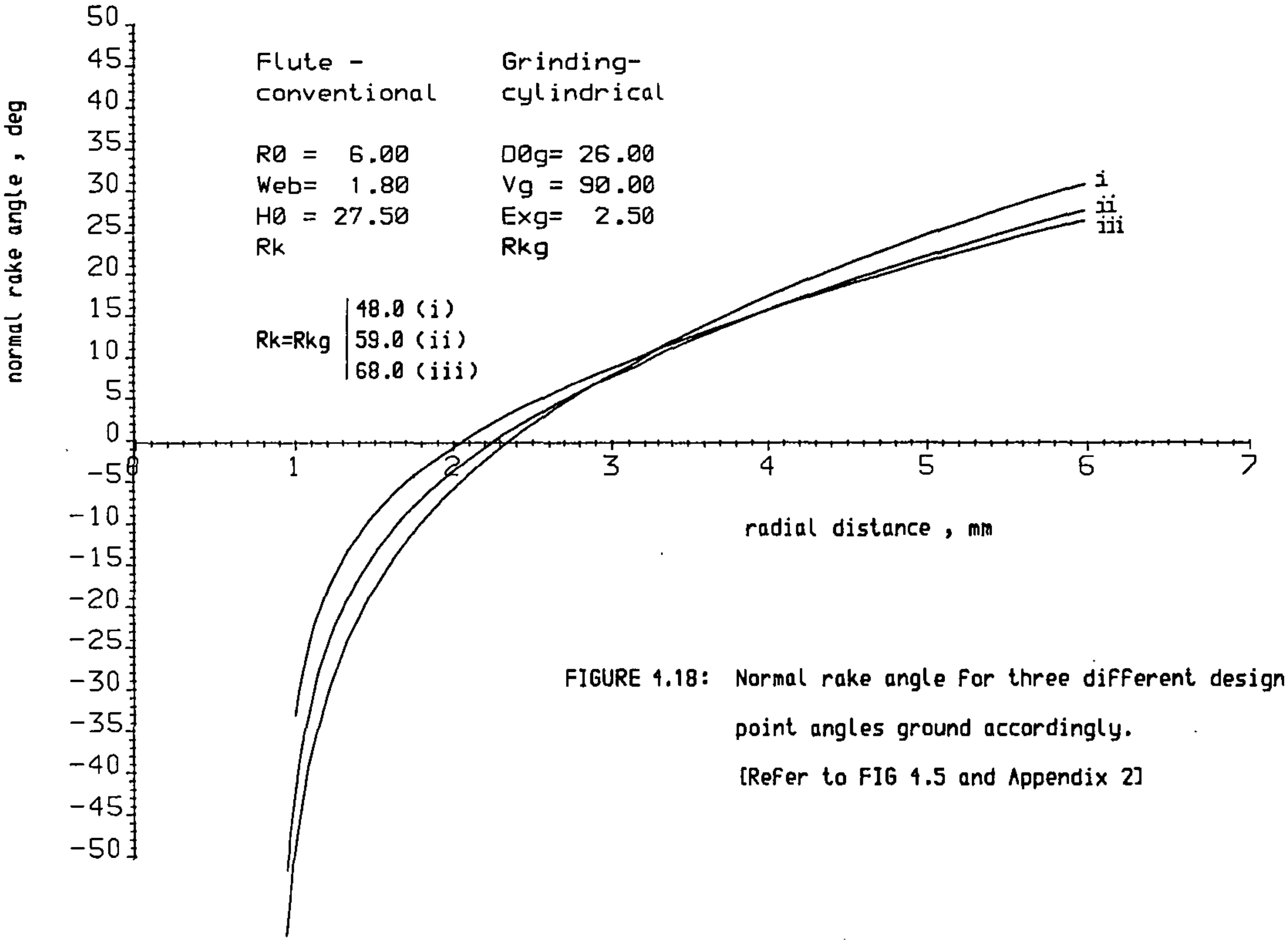


FIGURE 4.18: Normal rake angle for three different design point angles ground accordingly.

[Refer to FIG 4.5 and Appendix 2]

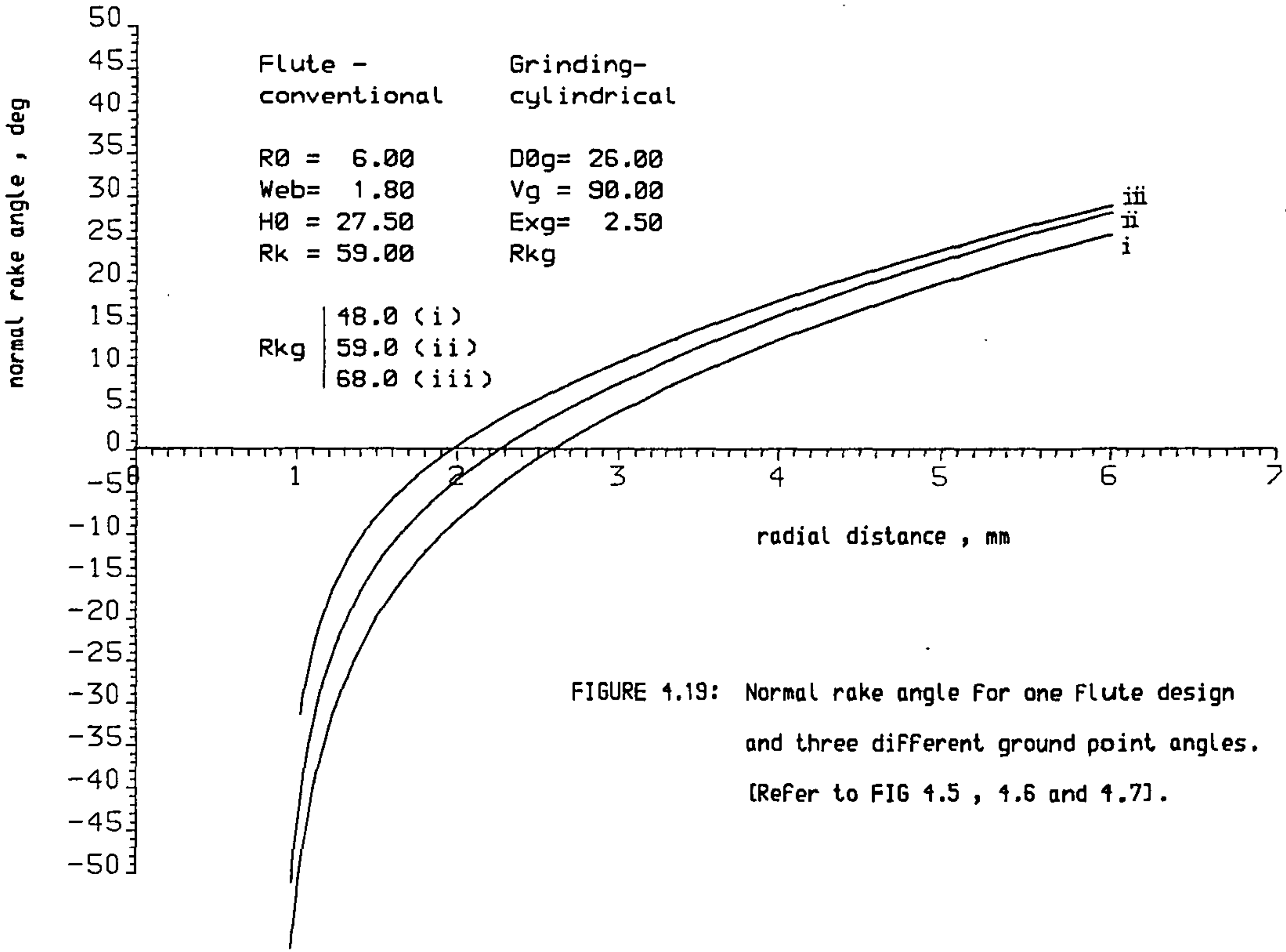


FIGURE 4.19: Normal rake angle for one flute design and three different ground point angles. [Refer to FIG 4.5 , 4.6 and 4.7].

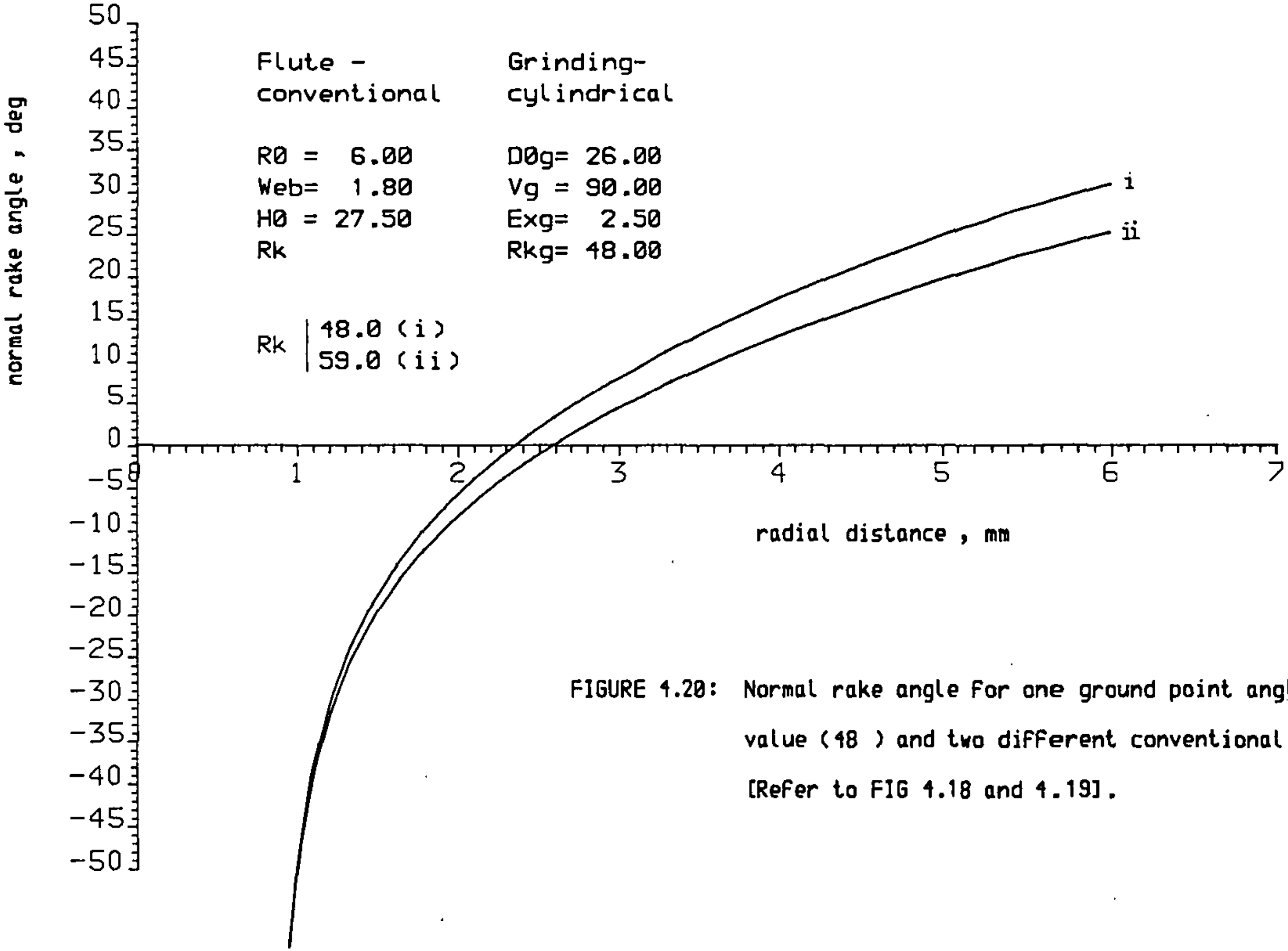


FIGURE 4.20: Normal rake angle for one ground point angle value (48 ) and two different conventional flutes. [Refer to FIG 4.18 and 4.19].

### 4.3.2 Clearance angle

The space between the flank of a cutting tool and the machined surface is usually measured by the clearance angle.

To produce a cutting edge with an excessive clearance angle weakens the lip (10); to make it minute increases interference between tool and machined surface (17).

The clearance angle may be measured in a number of different measurement planes through the cutting edge, and several definitions of clearance angle are possible. As for the rake angle, all possible definitions can usually be referred to and calculated from the normal clearance angle.

The normal clearance angle, (Figure 4.21), $\alpha_n$, is measured in a plane perpendicular to the cutting edge, $p_n$, between the flank ($S_{\alpha 1}$ or $S_{\alpha 2}$) and the plane defined by the cutting edge and the cutting velocity (Figure 4.21).

From Figure 4.21

$$\vec{t}_m . \vec{t}_{\alpha 1} = |\vec{t}_m||\vec{t}_{\alpha 1}| \cos \alpha_n = \cos \alpha_n \qquad 4.11$$

where $\vec{t}_m$ and $\vec{t}_{\alpha 1}$ are both normal to the cutting edge, the first being tangent to the machined surface and the second being tangent to the flank.

$\vec{t}_m$ can be computed from $\vec{e}$ and from $\vec{n}_m$ (Figure 4.22) which have already been determined:

$$T_m \vec{t}_m = \vec{n}_m \times \vec{e} \qquad 4.12$$

where $T_m = |\vec{n}_m \times \vec{e}\ |$

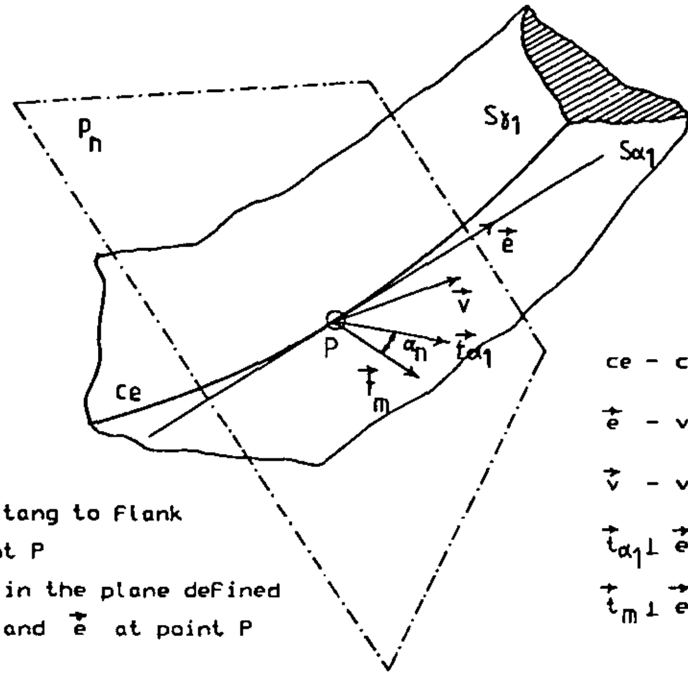


ce - cutting edge

$\vec{e}$ - vector tang to ce

$\vec{v}$ - velocity vector

$\vec{t}_{\alpha 1} \perp \vec{e}$

$\vec{t}_m \perp \vec{e}$

$\vec{t}_{\alpha 1}$ - vector tang to flank at point P

$\vec{t}_m$ - vector in the plane defined by $\vec{v}$ and $\vec{e}$ at point P

FIGURE 4.21: Normal clearance angle definition

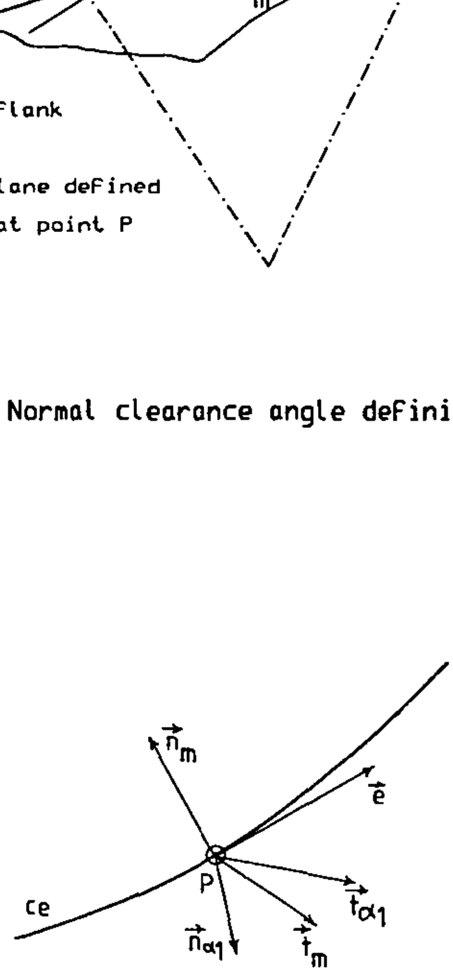


$\vec{t}_{\alpha 1} \perp \vec{n}_{\alpha 1}$

$\vec{t}_{\alpha 1} \perp \vec{e}$

$\vec{t}_m \perp \vec{n}_m$

$\vec{t}_m \perp \vec{e}$

$\vec{n}_m$ - vector normal to machined surface at point P

$\vec{n}_{\alpha 1}$ - vector normal to flank ($S_{\alpha 1}$) at point P

FIGURE 4.22: Determination of vector, $\vec{t}_m$, tangent to the machined surface.

[Refer to FIG 4.12 and 4.21]

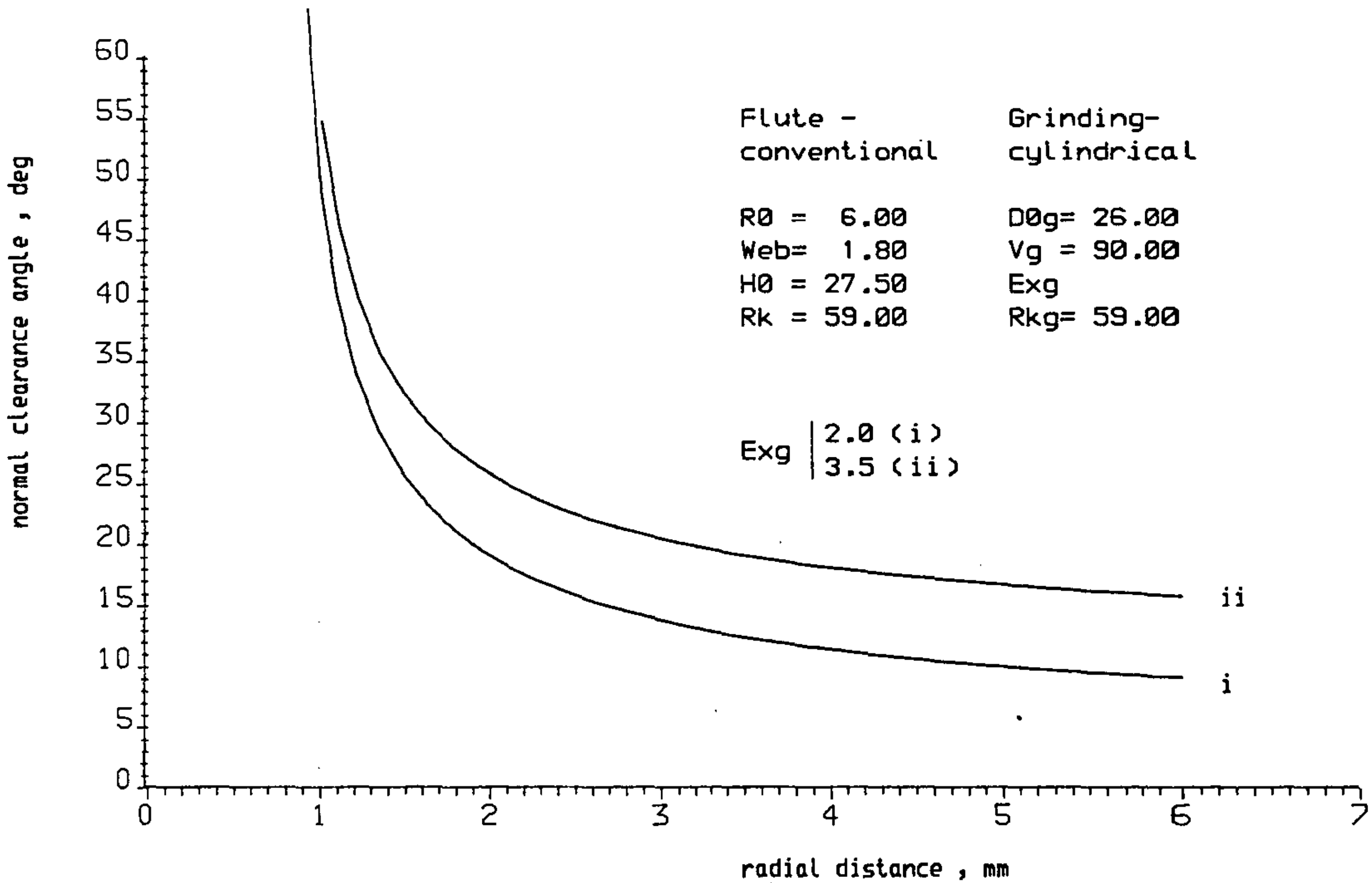


FIGURE 4.23: Normal clearance angle and the effect of the grinding parameter Exg. [Refer to Appendix 4 for the other parameters]

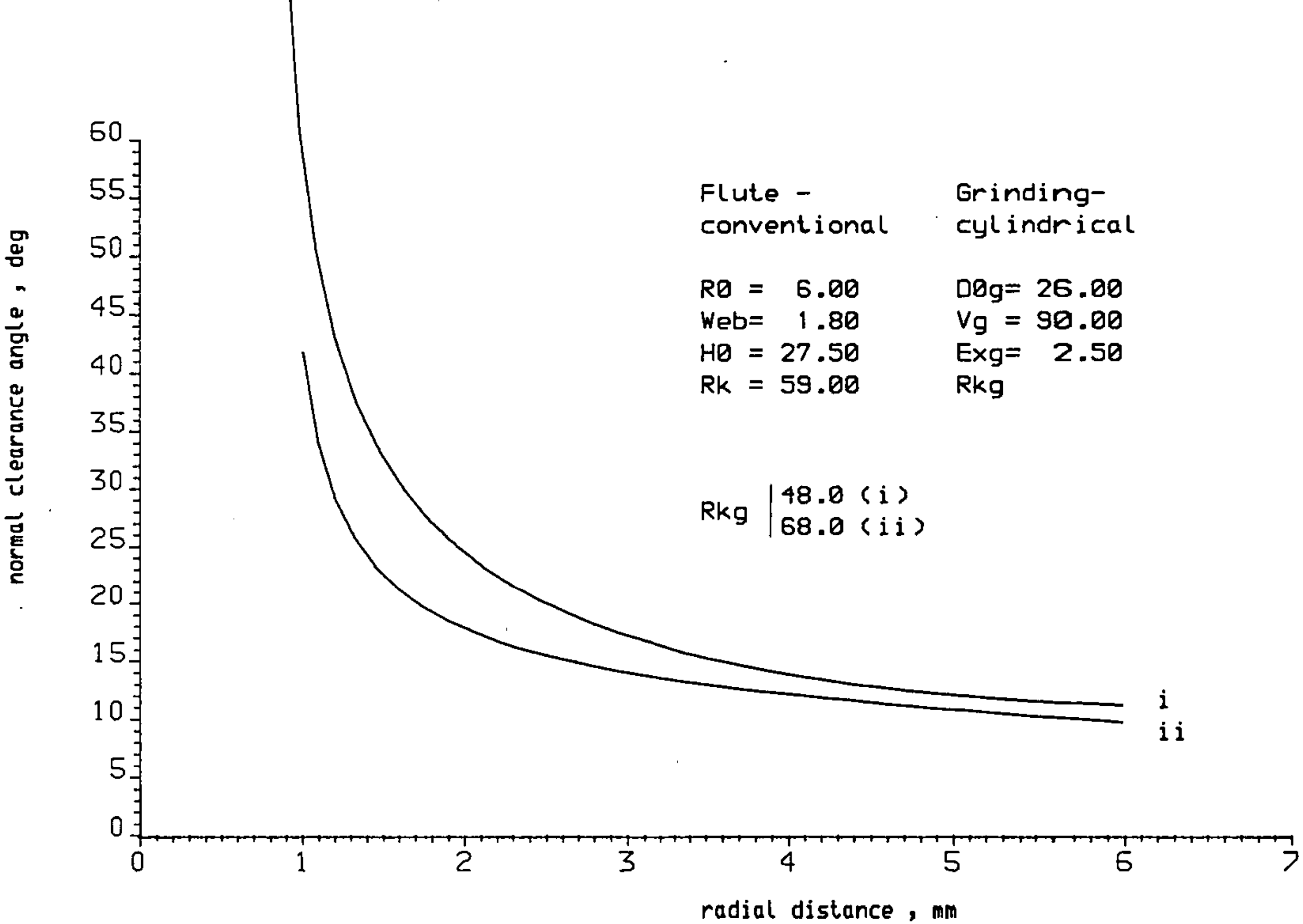


FIGURE 4.24: Normal clearance angle and the effect of the grinding point angle,Rkg. [Refer to Appendix 4 for the other parameters]

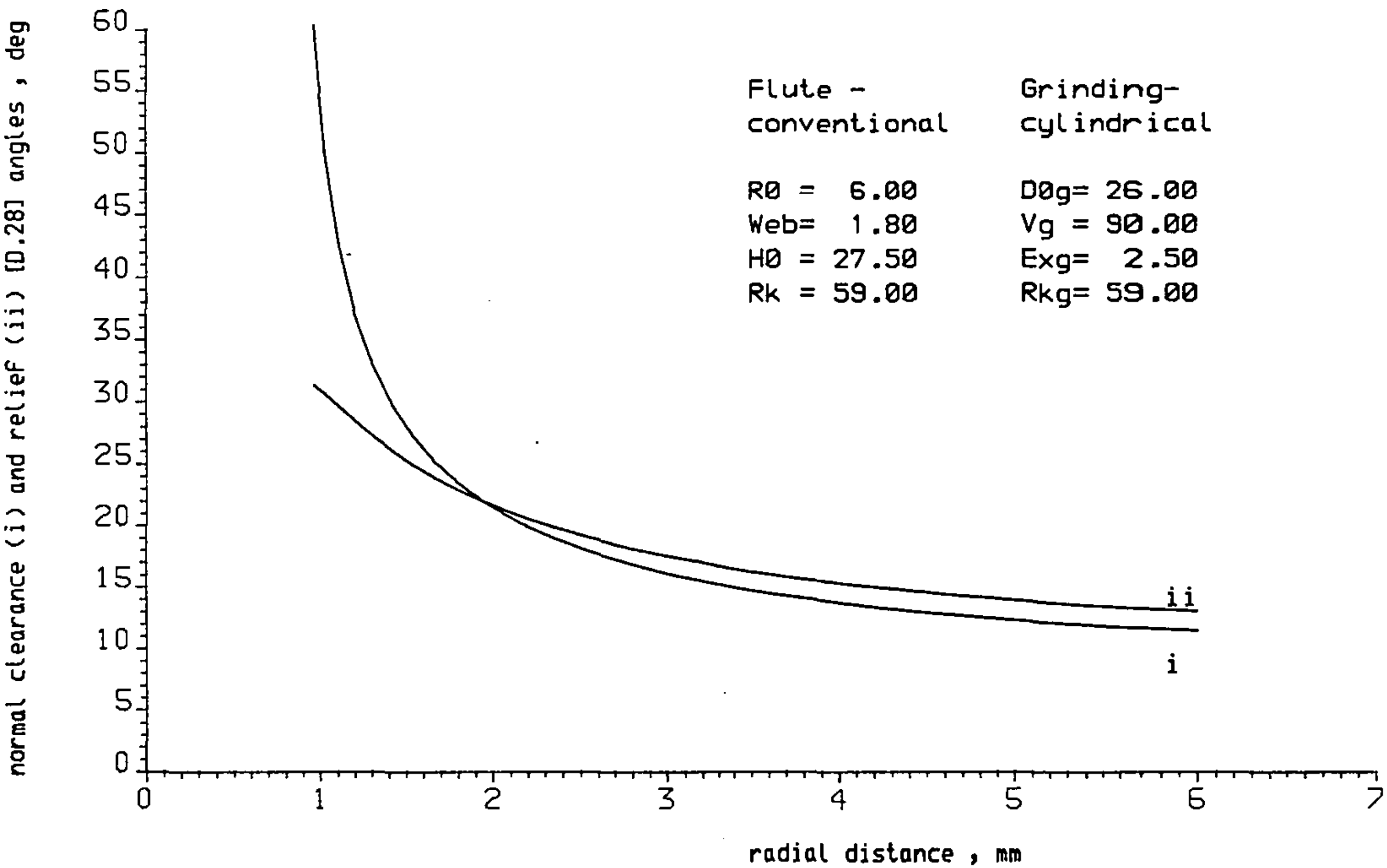


FIGURE 4.25: Comparing the normal clearance to the relief angle.

$\vec{t}_{\alpha 1}$ can also be computed from $\vec{e}$ and $\vec{n}_{\alpha 1}$ which have been determined too:

$$T_{\alpha 1}\ \vec{t}_{\alpha 1} = \vec{e} \times \vec{n}_{\alpha 1} \tag{4.13}$$

where $T_{\alpha 1} = |\vec{e} \times \vec{n}_{\alpha 1}|$

Computation of the normal clearance angle was carried out according to a similar method as for the normal rake angle. Thus the author thinks it unnecessary to repeat an identical flow diagram to that in Figure 4.17 of the computer program segment (refer to Appendix 1) for this computation.

Figure 4.23 shows the influence of the grinding parameter $ex_g$ (refer to Appendix 2 for simulated drill points) on the normal clearance angle. This grinding parameter, as the author found from numerical investigation, has a strong effect on the clearance angle without influencing so strongly the other drill point features.

The influence of the ground point angle, $\kappa_g$, on the normal clearance angle is also shown in Figure 4.24 (refer to Appendix 2 for simulated drill point).

The influence of the other cylindrical grinding parameters and the influence of the conventional flute design parameters is shown in Appendix 4.

The nominal relief angle, as defined by Galloway [D.28] is compared with the normal clearance angle in Figure 4.25.

### 4.3.3 Wedge angle

The wedge angle is a measure of the amount of metal supporting the cutting edge.

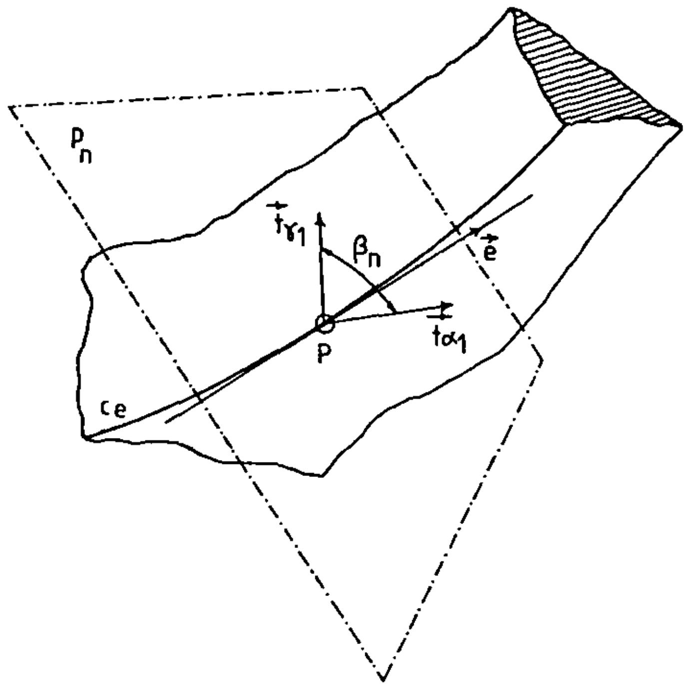


FIGURE 4.26: Definition of the normal wedge angle

[Refer to FIG 4.11 and 4.21]

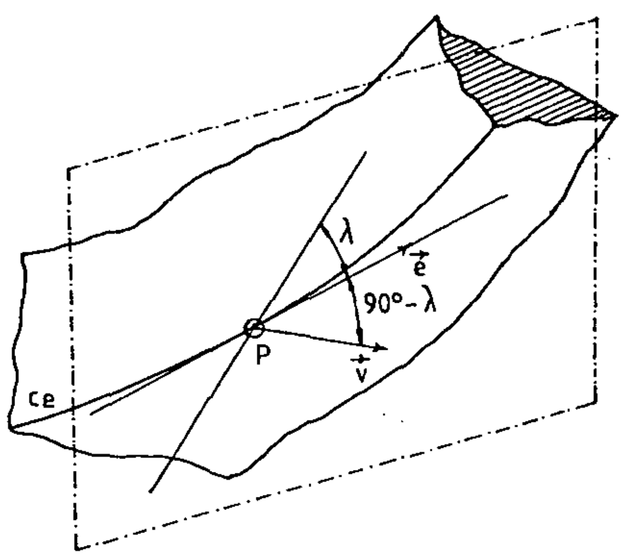


FIGURE 4.27: Definition of the inclination angle

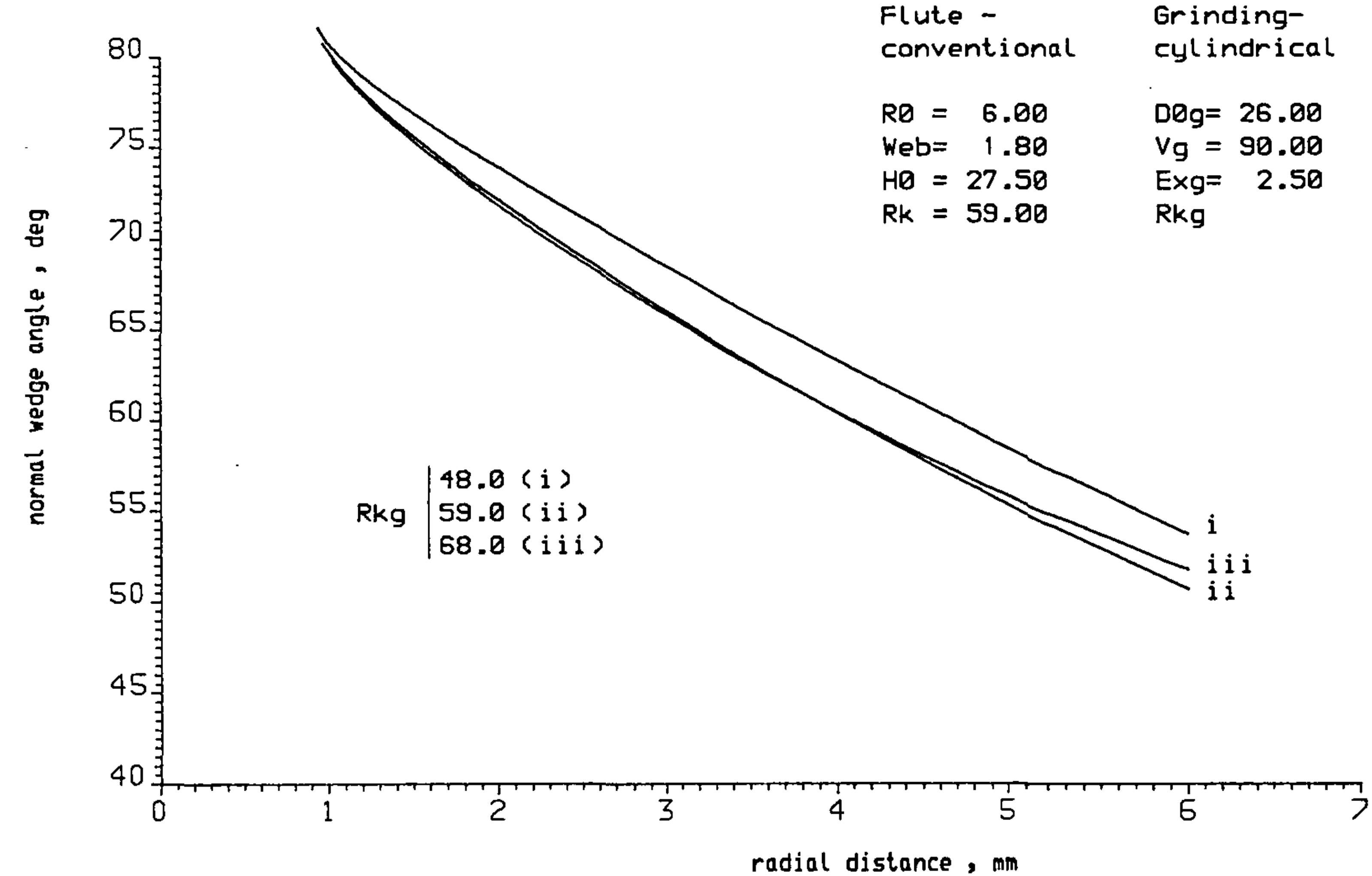


FIGURE 4.28: Normal wedge angle for one flute and three different ground point angles. [Refer to FIG 4.5 to 4.7]

The normal wedge angle, $\beta_n$, is measured in a plane normal to the cutting edge between the face and the flank (Figure 4.26).

From Figure 4.26:

$$\vec{t}_{\gamma 1} \cdot \vec{t}_{\alpha 1} = |\vec{t}_{\gamma 1}||\vec{t}_{\alpha 1}| \text{ Cos } \beta_n = \text{Cos } \beta_n \qquad 4.14$$

where $\vec{t}_{\gamma 1}$ and $\vec{t}_{\alpha 1}$ have already been defined in the previous sections.
Also: (BS 5533):

$$\beta_n = \pi/2 - \gamma_n - \alpha_n \qquad 4.15$$

Computing $\beta_n$ from equation 4.14 serves as a verification for the computations with equation 4.15.

Figure 4.28 shows the variation of the normal wedge angle along the drill lip when one conventional flute is ground to three different point angles (refer to Figures 4.5 to 4.7 for drill point simulation).

### 4.3.4 Inclination angle

The angle of inclination has received a great deal of attention since Stabler (45). It has a major influence upon the chip flow and affects the cutting efficiency in several ways.

The inclination angle is measured in the plane determined by the cutting edge and the cutting velocity, between the normal to the velocity in this plane and the cutting edge (Figure 4.27).

From Figure 4.27:

$$\vec{v} \cdot \vec{e} = |\vec{e}||\vec{v}| \text{ Cos } (90^o - \lambda),$$

$$\vec{v} \cdot \vec{e} = \text{Sin } \lambda \qquad 4.16$$

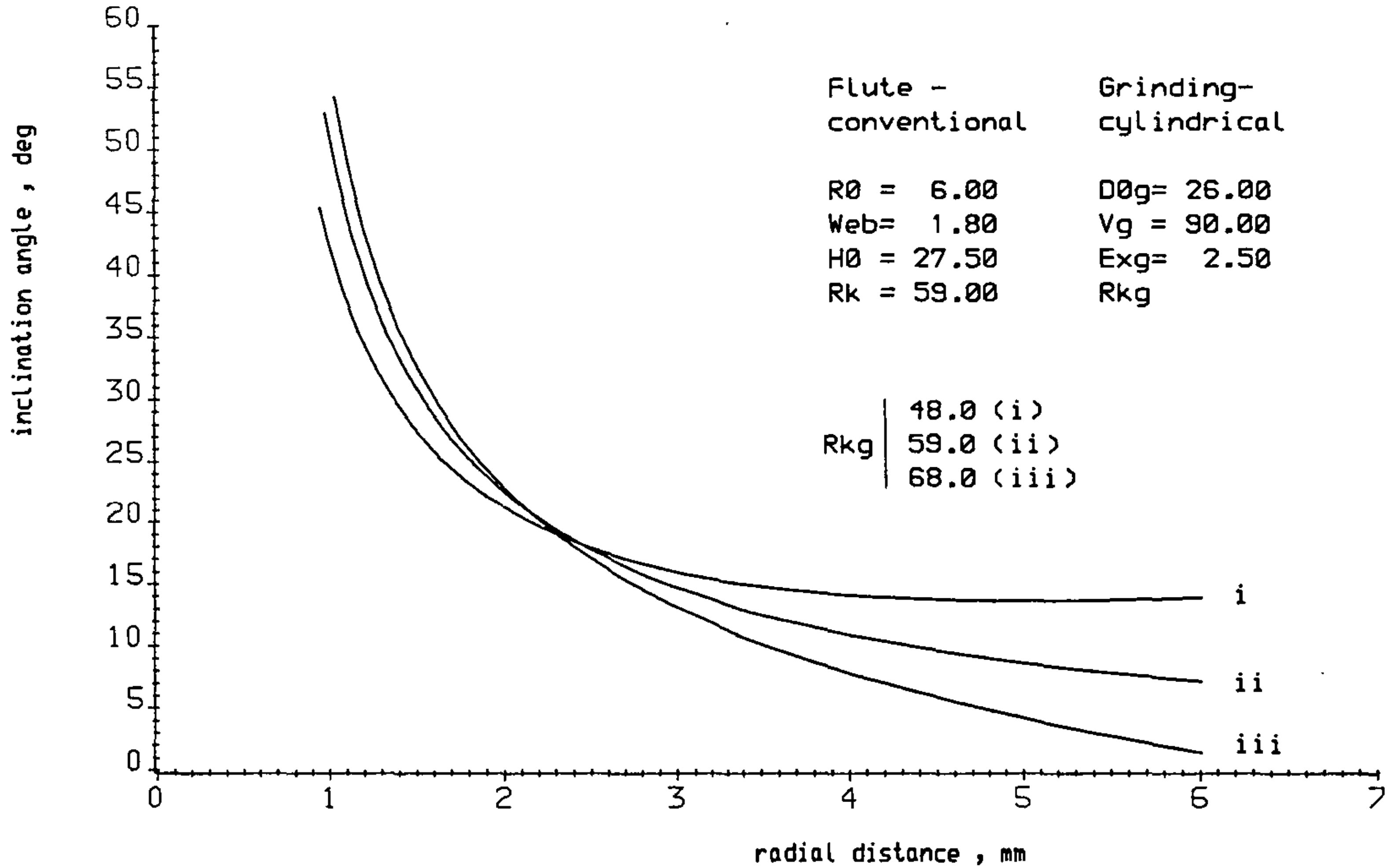


FIGURE 4.29: Inclination angle for one conventional drill flute and three different ground point angles.[Refer to FIG 4.5 to 4.7]

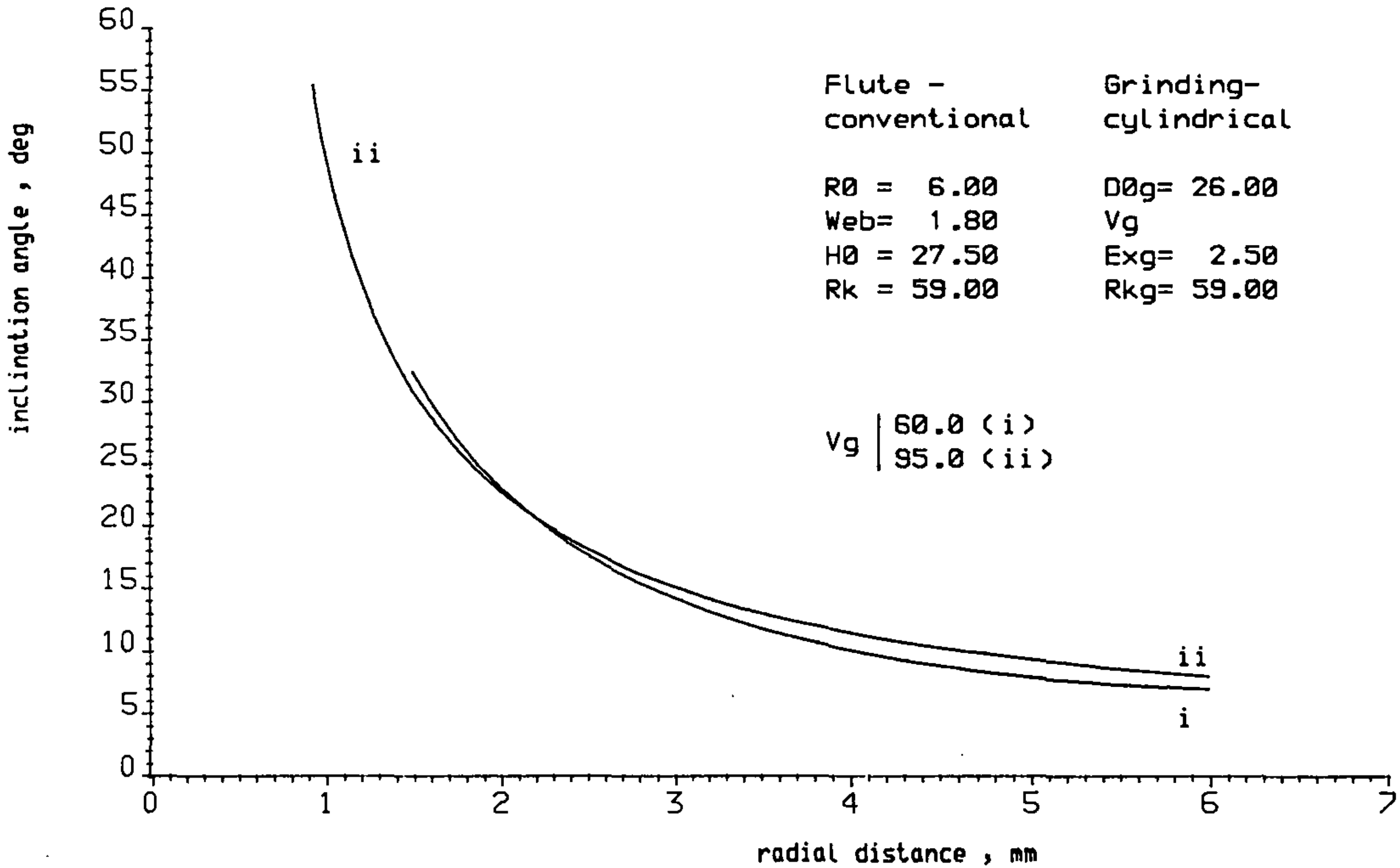


FIGURE 4.30: Effect of the grinding parameter Vg on the inclination angle.

[Refer to Appendix 2: varying Vg]

Figure 4.29 shows the inclination angle variation with the radial distance for the same conventional flute drill, ground to three different point angles.

The influence of the grinding parameter $\nu_g$ is also shown in Figure 4.30 where it can be seen to be relatively small.

The influence of other cylindrical grinding parameters other than $\kappa_g$ and $\nu_g$ and the influence of the conventional flute design parameters is shown in Appendix 5.

## 4.4 Chip Flow Angle

The chip flow angle, as the inclination angle, has received a lot of attention since the paper (45) by Stabler. Workers such as Colwell (51), Spaans (73), Usui and Hirota (48) and others (46, 70, 71, 72) have also dealt with this variable for the oblique cutting.

Apart from the need for the effective rake angle calculation, the importance of the chip flow angle arises from the interest in chip flow control.

As the author will refer to the chip flow angle, later in this work, some laws are revised in the present section.

The chip flow angle is measured on the rake face, between the normal to the cutting edge and the chip flow velocity (16) - Figure 4.31.

Several methods to determine the chip flow angle have been reviewed and shortly discussed by Venuvinod and Shing (74). Prediction rules (45, 48, 51) have also been reported.

The most well known prediction rule is the one due to Stabler, for the number of papers referring to it and for the number of reported experiments carried out to test it. This is an empirical rule and reads:

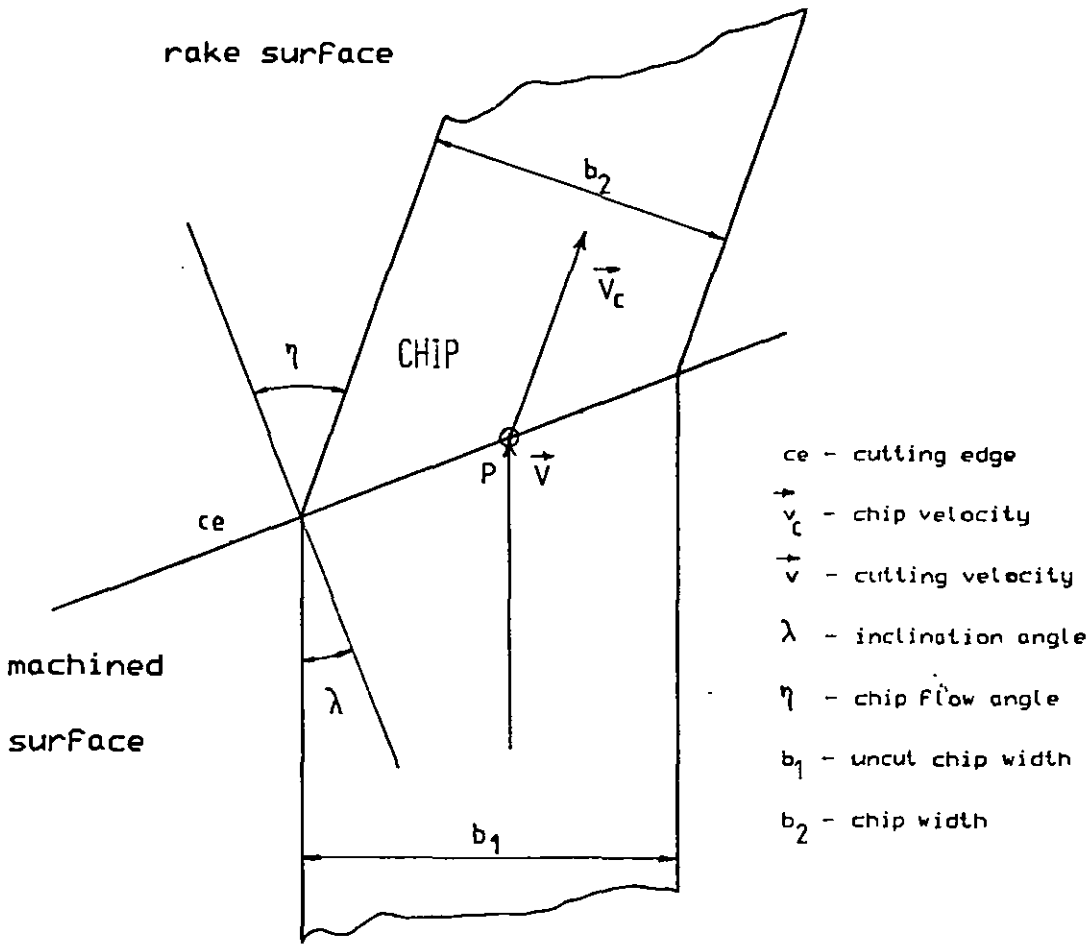


FIGURE 4.31: Definition of chip flow angle.

$$\eta = \lambda \qquad 4.17$$

where $\eta$ - chip flow angle
$\lambda$ - inclination angle

According to Stabler (75), the rule expressed by equation 4.17 has been challenged by Shaw, Cook and Smith, Rapier and Wilkinson, among others.

Stabler himself, after further experimental work, later proposed an alteration to the previous rule which should now read (75):

$$\eta = K\lambda \qquad 4.18$$

where K is a constant: $0.9 \div 0.95$.

Spaans, in a recent doctoral thesis (73), found that K could vary from 0.6 to 1.4 and Rapier and Wilkinson, according to Russell and Brown (70), reported that $\eta$ is often greater than $\lambda$.

Spaans (73) also found that if the rake angle and/or the inclination angle differ from zero, the chip flow angle is material dependent.

Armarego and Cheng (72) suggested that chip flow angle is either entirely dependent on the inclination angle and slightly influenced by the normal rake angle. Brown and co-workers (46), Russell and co-workers (70) and Armarego and Cheng (72) found the expression

$$\eta = \tan^{-1} (\tan\lambda \, \mathrm{Cos}\, \gamma_n) \qquad 4.19$$

to correlate satisfactory with the results of some experiments.

Very recently, Usui and Hirota (48) approached the mechanics of oblique cutting from the point of view of the theory of plasticity,

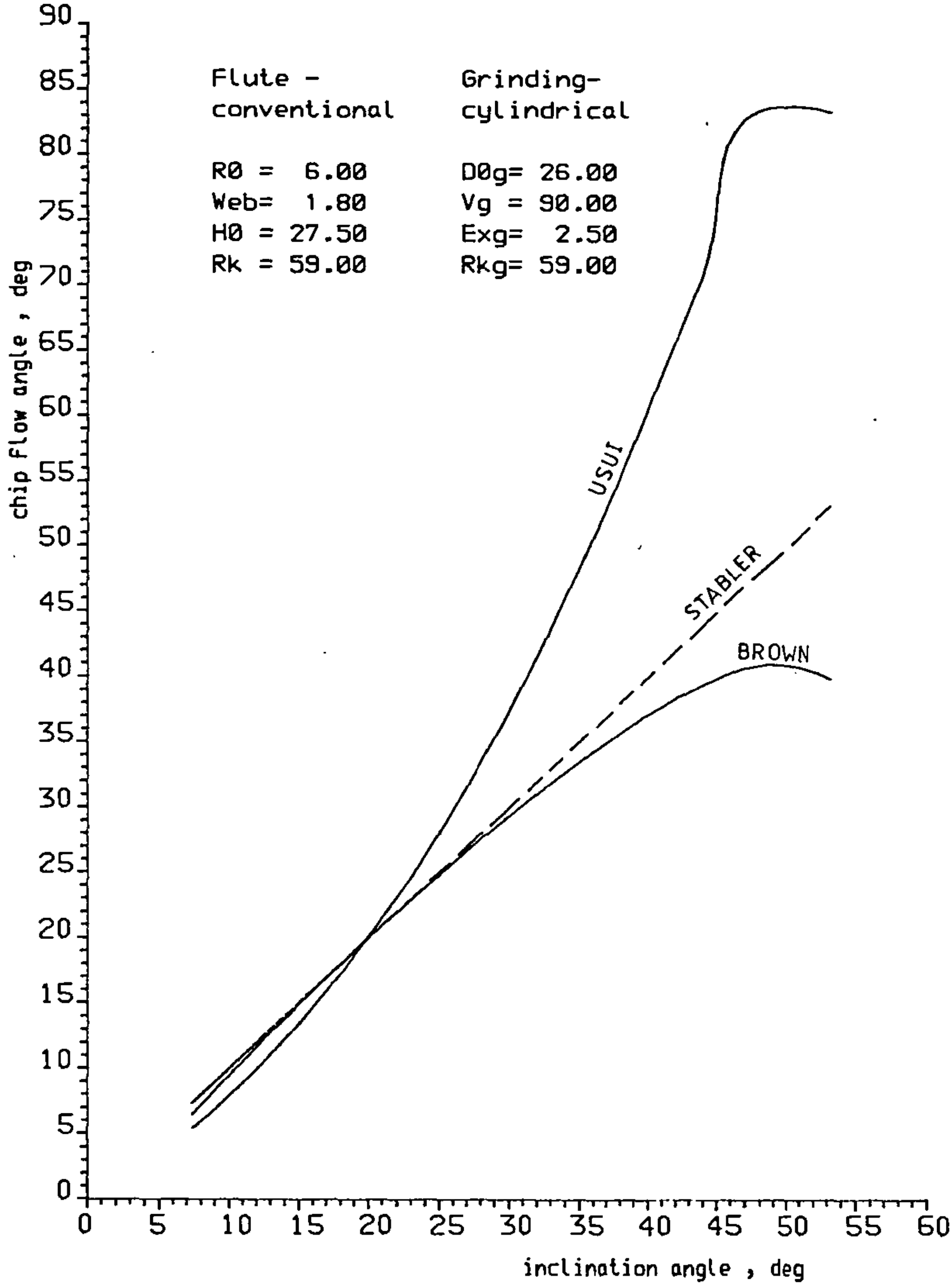


FIGURE 4.32: Chip flow angle against inclination angle along a drill lip,according to laws to oblique cutting,by three workers

in a similar way as Lee and Shaffer (47) did for the orthogonal cutting, and derived the following expression for the chip flow angle:

$$\eta = \tan^{-1}\left[\frac{\tan\lambda}{\operatorname{Sin}\gamma_n + \operatorname{Cos}\gamma_n}\right] \qquad 4.20$$

The laws by Stabler, by Brown and by Usui if used with a drill lip would result in the curves shown in Figure 4.32.

## 4.5 Effective Rake Angle

As referred to in the general introduction, some authors believe that with oblique cutting the effective rake angle replaces the normal rake angle as used with orthogonal cutting.

The effective rake angle, $\gamma_e$, can be computed from the normal rake angle, the inclination angle and the chip flow angle. The geometrical relationship between these variables has been referred to by Stabler (45), Oxford (20) and Armarego and co-workers (46) and reads:

$$\operatorname{Sin}\gamma_e = \operatorname{Sin}\lambda \operatorname{Sin}\eta + \operatorname{Cos}\lambda \operatorname{Cos}\eta \operatorname{Sin}\gamma_n \qquad 4.21$$

Equation 4.21 shows that, for a given cutting edge, the effective rake angle, $\gamma_e$, depends on the chip flow angle, $\eta$.

Figure 4.33 shows the variation of the effective rake angle with the radial distance, computed according to three chip flow angle laws referred to in the previous section.

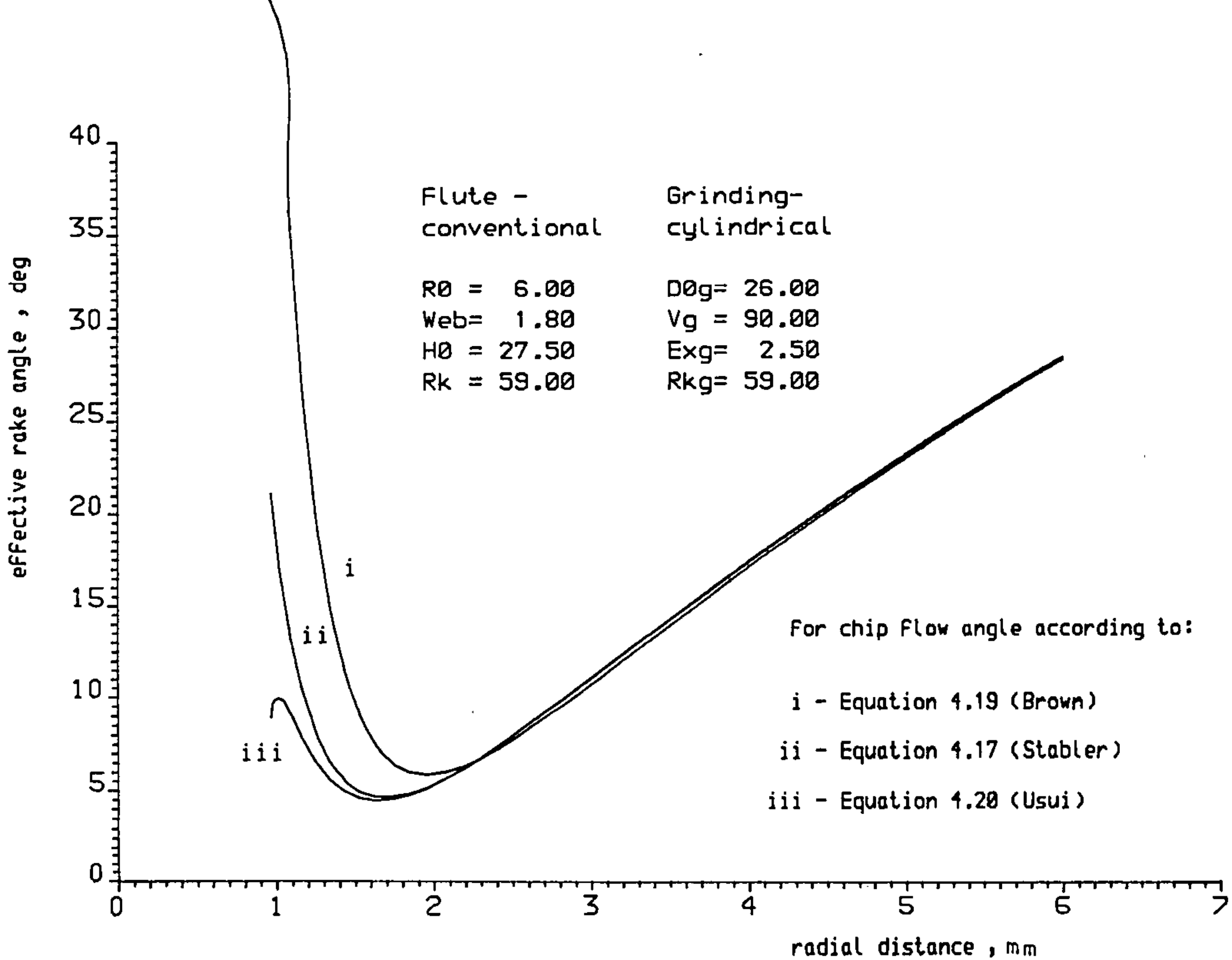


FIGURE 4.33: Effective rake angle for several chip flow laws

### 4.6 Chapter Closure

For all the drill points ground according to the parameters utilised for geometric simulation, the author found very good agreement between the predicted contour and the actual drill point contour. Very small observed deviations, however, may be attributed to flute manufacture deviations and/or very small errors in setting the grinding machine, together with measurement errors.

A very well known drill point error, nearly always present, is the relative lip height. The simulation here presented is rigorously symmetric and does not take any account of this error, or web eccentricity, or other drill errors such as those referred to in the general introduction. The author could easily simulate these errors with his computing approach by introducing assymetrics either in the flutes shapes or in the flank point surfaces and simulating accordingly. This however is not included in this project as it is out of purpose.

An extensive piece of work could be set, in another project, for assessing the significance of the small deviations between the actual drill points and the simulated ones in order to gain information on the accuracy of the drill grinding machine type available to the author. In the same work the objective could be set to find the relative influence of each parameter upon the different types of deviations.

*"The flute geometry behind the cutting edge mainly influences the conveyance of chips and assumes an important role only when chips tend to jam in the flutes".*

*Shaw and Oxford.*

# 5. AN APPROACH TO NON-CONVENTIONAL DRILL FLUTE DESIGN

## 5.1 Introduction

As referred to in Chapter 2, the flute profile is usually designed in order to yield a straight cutting edge. However, some workers (13, 58, 76) have reported on the better performance of the drill curved lips - as those yielded by grinding the drill to a point angle different to the one relative to the flute design (refer to Chapter 4, Figure 4.6).

The condition for the drill lip to be straight seems to stem from tradition and from empirical grounds.

The specifications for drill flute design may be given in terms of the cutting angles along the drill lip.

This chapter deals with the problem of designing a drill flute which, together with the flank surface, yields a lip with uniform wedge angle.

## 5.2 General Mathematical Approach to Flute Design

As in the previous chapters, the symbol $S_{\alpha 1}$ is used for the flank surface and the symbol $S_{\gamma 1}$ for the flute face. Also the equations expressing the properties of the coordinates for each surface are designated by $f_{\alpha 1}$ and $f_{\gamma 1}$ respectively.

$f_{\alpha 1}$ has been dealt with in Chapter 3. $f_{\gamma 1}$ is to be found according to the specifications to the drill lip.

Let a current point on the cutting edge, Q, be represented by (x, y, z) - Figure 5.1 - and any point on $S_{\alpha 1}$, or $S_{\gamma 1}$, to be represented by (X, Y, Z).

As the drill lip is one intersection of surfaces $S_{\gamma 1}$ and $S_{\alpha 1}$, the equations:

$$f_{\gamma 1}\ (X,Y,Z) = 0$$

$$f_{\alpha 1}\ (X,Y,Z) = 0$$

have a common solution for the points (x, y, z).

The unit vector tangent to the drill lip is represented by:

$$\vec{e} = (e_1, e_2, e_3)$$

and the perpendicular to $S_{\alpha 1}$ is represented by

$$\begin{aligned}\vec{n}_{\alpha 1} &= (n_{\alpha 11}, n_{\alpha 12}, n_{\alpha 13}) \\ &= (\partial f_{\alpha 1}/\partial X,\ \partial f_{\alpha 1}/\partial Y,\ \partial f_{\alpha 1}/\partial Z)\end{aligned}$$

where $f_{\alpha 1}$ is a continuous function of X, Y and Z (Chapter 3).

The condition for $\vec{e}$ to be tangent to $S_{\alpha 1}$ is:

$$\vec{e}.\vec{n}_{\alpha 1} = 0 \qquad 5.1$$

If s is chosen to represent the length from a reference point on the drill lip to (x, y, z), measured along the lip, vector $\vec{e}$ may be further represented by:

$$\vec{e} = (dx/ds,\ dy/ds,\ dz/ds)$$

where x = x(s), y = y(s) and z = z(s) are the parametric equations for the coordinates of point (x, y, z).

Equation 5.1 may be rewritten as follows:

$$(\partial f_{\alpha 1}/\partial X,\ \partial f_{\alpha 1}/\partial Y,\ \partial f_{\alpha 1}/\partial Z)_{x,y,z}\ (dx/ds,\ dy/ds,\ dz/ds) = 0 \qquad 5.1'$$

or

$$[\frac{\partial f_{\alpha 1}}{\partial X}]_{x,y,z} \cdot \frac{dx}{ds} + [\frac{\partial f_{\alpha 1}}{\partial Y}]_{x,y,z} \cdot \frac{dy}{ds} + [\frac{\partial f_{\alpha 1}}{\partial Z}]_{x,y,z} \cdot \frac{dz}{ds} = 0 \qquad 5.1''$$

where:

$$(dx/ds)^2 + (dy/ds)^2 + (dz/ds)^2 = 1 \qquad 5.2$$

as

$$(ds)^2 = (dx)^2 + (dy)^2 + (dz)^2$$

A third relationship independent of the above two is needed for finding points (x, y, z) of the cutting edge. This will be given by considering the vector $\vec{v}$ with the same direction as the cutting velocity:

$$\vec{v} = (v_1,\ v_2,\ v_3)$$

By definition of inclination angle (equation 4.16):

$$\vec{v}.\vec{e} = \text{Sin}\ \lambda \qquad \text{(Equation 4.16), or}$$

in other notation:

$$(v_1, v_2, v_3).(dx/ds,\ dy/ds,\ dz/ds) = \text{Sin}\lambda \qquad 4.16'$$

The tangent to the cutting edge is tangent to the flank surface and makes an angle $\pi/2 - \lambda$ with the cutting velocity, so, the components

$$(e_1, e_2, e_3) = (dx/ds,\ dy/ds,\ dz/ds),$$

of the unit vector in the direction of the tangent to the cutting edge must be a solution to the following equations:

$$[\partial f_{\alpha 1}/\partial X]_{x,y,z} \frac{dx}{ds} + [\partial f_{\alpha 1}/\partial Y]_{x,y,z} \frac{dy}{ds} + [\partial f_{\alpha 1}/\partial Z]_{x,y,z} \frac{dz}{ds} = 0 \qquad 5.1''$$

$$V_1 \frac{dx}{ds} + V_2 \frac{dy}{ds} + V_3 \frac{dz}{ds} = \mathrm{Sin}\lambda \qquad 4.16''$$

$$(\frac{dx}{ds})^2 + (\frac{dy}{ds})^2 + (\frac{dz}{ds})^2 = 1 \qquad 5.2$$

The points (x,y,z) on the cutting edge can be found by integration of dx/ds, dy/ds and dz/ds.

## 5.3 Computation of a Non-conventional Drill Flute Profile

### 5.3.1 Analysis for computation

The drill specifications for the drill with a new flute design are as follows:

- body

  $d_o$ - drill diameter (12.7 mm) (½")
  
  2W - web thickness (2 mm)
  
  $\gamma_f$ - helix angle at drill periphery ($30^o$)

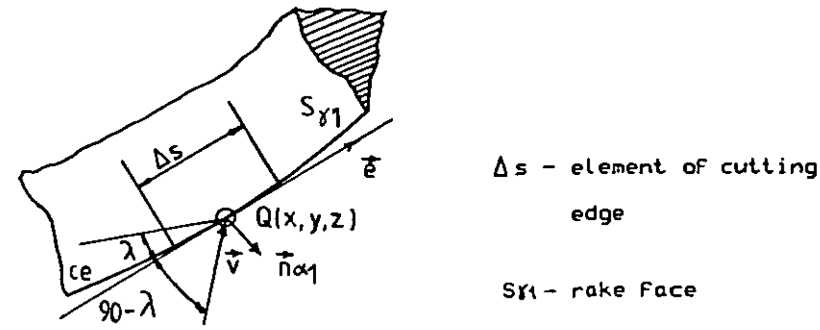


FIGURE 5.1: Geometric elements for the analysis of the drill lip.

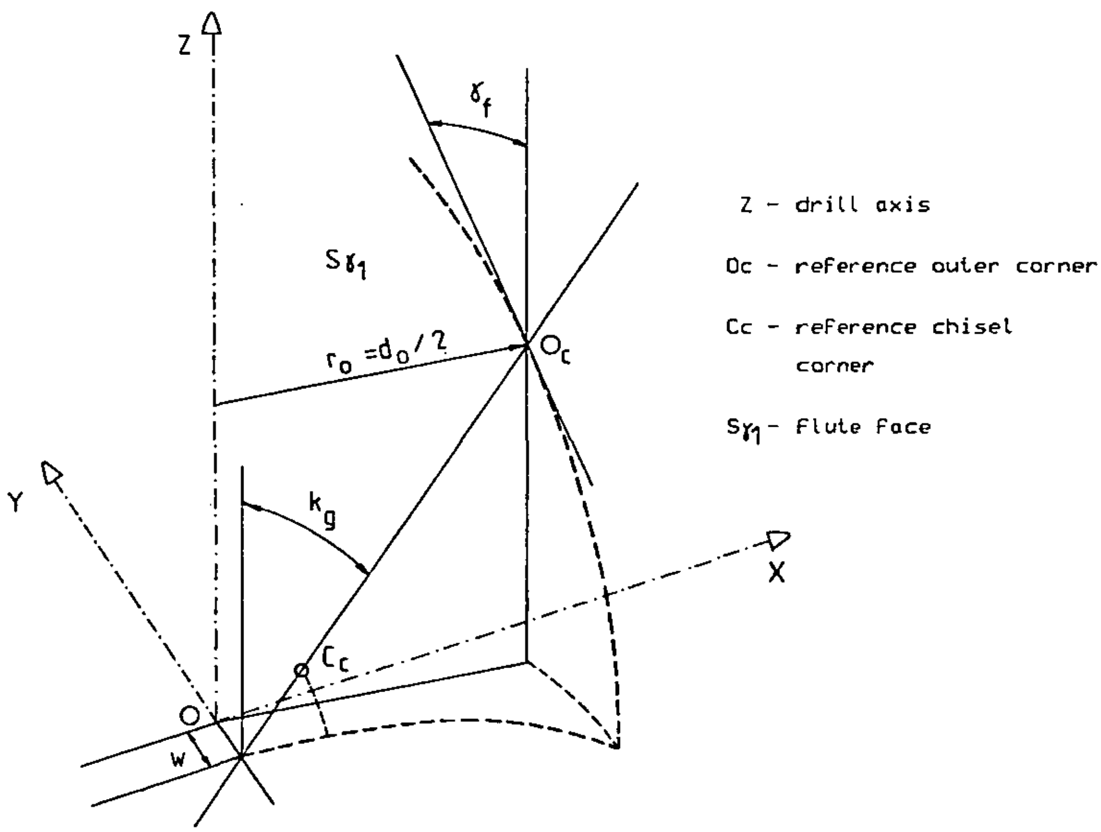


FIGURE 5.2: Specification parameters and geometric reference elements for the new flute design.

- point (cylindrical grinding parameters)

  $d_{og}$ - grinding cylinder diameter (28 mm)
  $\nu_g$ - grinding cylinder rotation ($90^o$)
  $ex_g$ - distance from grinding cylinder axis to drill axis (3 mm)
  $2\kappa_g$ - grinding point angle ($118^o$)

- flute

  face - designed in order to yield, together with the flank point, a uniform wedge angle
  heel - determined as for the conventional flute (Chapter 2)

The flute to be designed will be referred to as a referential system of Cartesian coordinates (X, Y, Z).

The outer corner, $0_c$, of the new design drill is defined as if it belonged to a conventional flute drill with the following design parameters: $d_o$, 2W, $\gamma_f$ and $\kappa$ (Figures 5.2 and 5.3). For reference, the chisel corner, $C_c$, that would be yielded with such a conventional flute drill is also considered (Figure 5.2).

Let Q (x,y,z) be a point on the lip of the new design drill such that it is on the same helix as P(X,Y,0) of the new flute profile in the plane XY (Figure 5.3).

Let $\vec{v} = (v_1, v_2, 0)$ to be parallel to the rotational velocity at point Q and

$$|\vec{v}| = 1$$

From Figure 5.3

$$\phi_1 = \tan^{-1} (y/x) \qquad 5.3$$

$$r = \sqrt{x^2 + y^2} \qquad 5.4$$

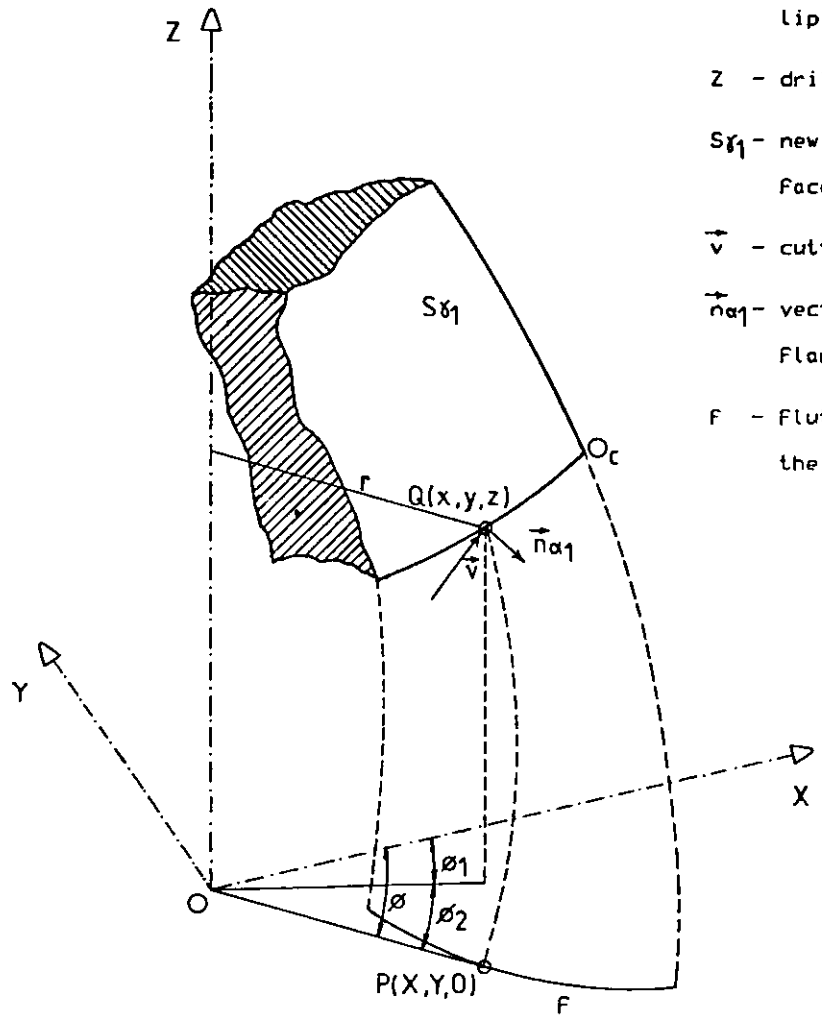


$O_c$ - outer corner

Q - current point on the lip

Z - drill axis

$S_{\gamma 1}$ - new design flute face

$\vec{v}$ - cutting velocity

$\vec{n}_{\alpha 1}$ - vector normal to flank $S_{\alpha 1}$

f - flute section in the plane XY

FIGURE 5.3: Geometric elements for the analysis of a new flute design

$$z = r_o \, \phi_2/\tan \gamma_f \qquad 5.5$$

where $\phi_1$, r and z are the cylindrical coordinates of point Q.

Also from Figure 5.3:

$$v_1 = \sin \phi_1 \qquad 5.6$$

$$v_2 = \cos \phi_1 \qquad 5.7$$

$$v_3 = 0$$

where $(v_1, v_2, 0)$ is in the direction of the rotational velocity at point Q.

Equation $f_{\alpha 1} = 0$ has already been dealt with in Chapter 3:

$$f_{\alpha 1}(X,Y,Z) = AX^2 + BY^2 + CZ^2 + DXY + EXZ + FYZ$$

$$+ GX + HY + IZ + J = 0 \qquad 3.6$$

where coefficients from A to J depend on the grinding parameters $d_{og}$, $\nu_g$, $ex_g$ and $\kappa_g$ and have also been given.

From equation 3.6:

$$[\partial f_{\alpha 1}/\partial X]_{x,y,z} = 2Ax + Dy + Ez + G \qquad 5.8$$

$$[\partial f_{\alpha 1}/\partial Y]_{x,y,z} = 2By + Dx + Iz + H \qquad 5.9$$

$$[\partial f_{\alpha 1}/\partial Z]_{x,y,z} = 2Cz + Ex + Fy + I \qquad 5.10$$

All terms in the system of equations, Equations 5.1", 4.16" and 5.2, except $\lambda$, have been expressed in terms of the coordinates (x,y,z) of point Q on the drill lip.

To express the inclination angle, $\lambda$, immediately in terms of the coordinates $(x,y,z)$, $\lambda = \lambda(x,y,z)$, is not possible as, in the present situation, the lip is not specified in terms of the nornal wedge angle. One solution however, is to proceed by successive approximations, by investigating different laws to the angle $\lambda$, till the desired values for the normal wedge angle are arrived at. This procedure can be implemented in a computer program and quickly and properly done by computers.

A relationship between the inclination angle, $\lambda$, and the point Q position along the cutting edge may be expressed as

$$\lambda = \lambda(K_1, K_2, K_3, \ldots, r)$$

where $K_1$, $K_2$, $K_3$, ... are constants and r is the radial distance from Q to the drill axis.

As $\lambda$ enters in Equation 4.16" under the form of Sin$\lambda$ it appears more reasonable to think of a relationship with the form

$$\text{Sin}\lambda = \lambda(K_1, K_2, K_3, \ldots r)$$

or, rather,

$$r \text{ Sin}\lambda = \lambda(K_1, K_2, K_3, \ldots r)$$

as, by doing $\lambda(K_1, K_2, K_3, \ldots r) = \text{const}$, the law

$r \text{ Sin}\lambda = \text{const}$ is similar to

$r \text{ Sin}\lambda = W \sin\kappa = \text{const}$ for

a conventional drill.

As a matter of simplicity and as the result of computer aided numerical investigation, the polynomial law

$$r \sin\lambda = K_1 r^3 + K_2 r^2 + K_3 r + K_4 \qquad 5.11$$

was selected. If $r \neq 0$ this equation becomes:

$$\sin\lambda = K_1 r^2 + K_2 r + K_3 + K_4/r \qquad 5.11'$$

### 5.3.2 Non-conventional drill flute profiles

In order to solve numerically the problem above analysed, a computer program was designed and built.

The flow diagram for this computer program is presented in Figure 5.4 and the program itself is shown in Appendix 6.

For the purpose of the computation, the cylindrical grinding surface was selected, as it would be for grinding a regular conventional drill point.

In order to decide the range of wedge angles that could be reasonably selected for the present computation, the wedge angle for a 12.7 mm (½") diameter conventional drill with the same parameters $R_0$, $2W$, $\gamma_f$, as for the non-conventional flute, and the standard point $118^0$ was analysed - Figure 5.5.

Several wedge angle values, mainly within the range falling in the middle of curve in Figure 5.5, were tested by means of the computer program referred to above. As an example, Figures 5.6 and 5.7 show the computer plots for flutes yielding a $65^0$ and $60^0$ normal wedge angle respectively.

Observing the computer plots as shown in Figures 5.6 and 5.7 it can be noticed a "gap" between the special flute (a) and the heel (c) near the point that yields the chisel corner. This "gap" increases with the selected wedge angle, and the modification to be made to the flute at this area in order to bridge the flute face with the heel surface, for manufacture, becomes larger.

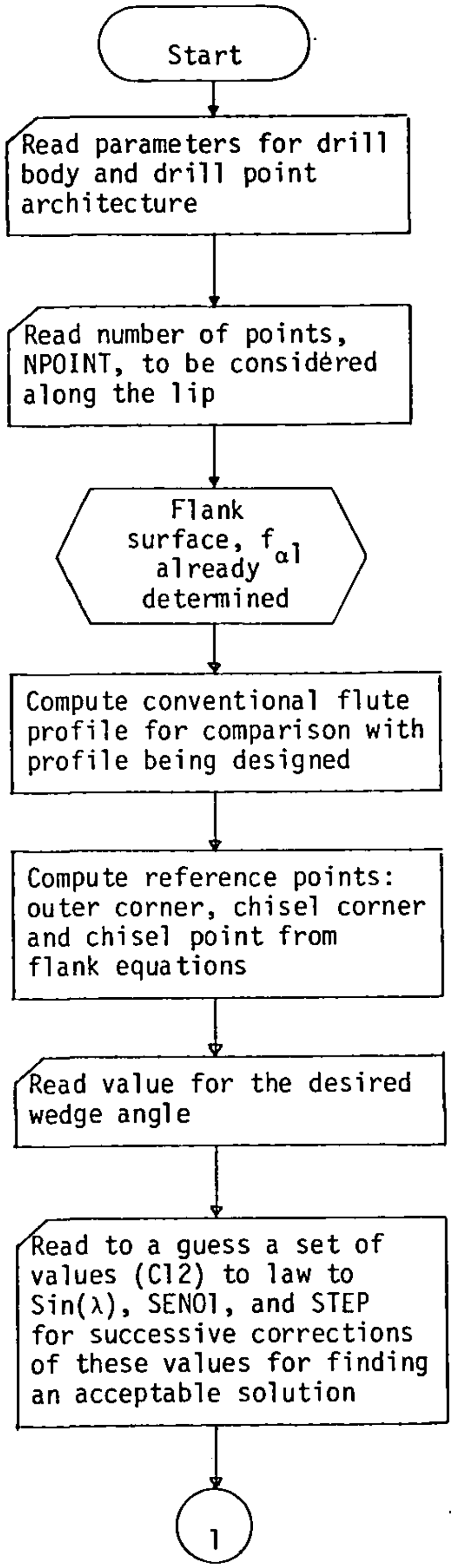


FIGURE 5.4 (continued)

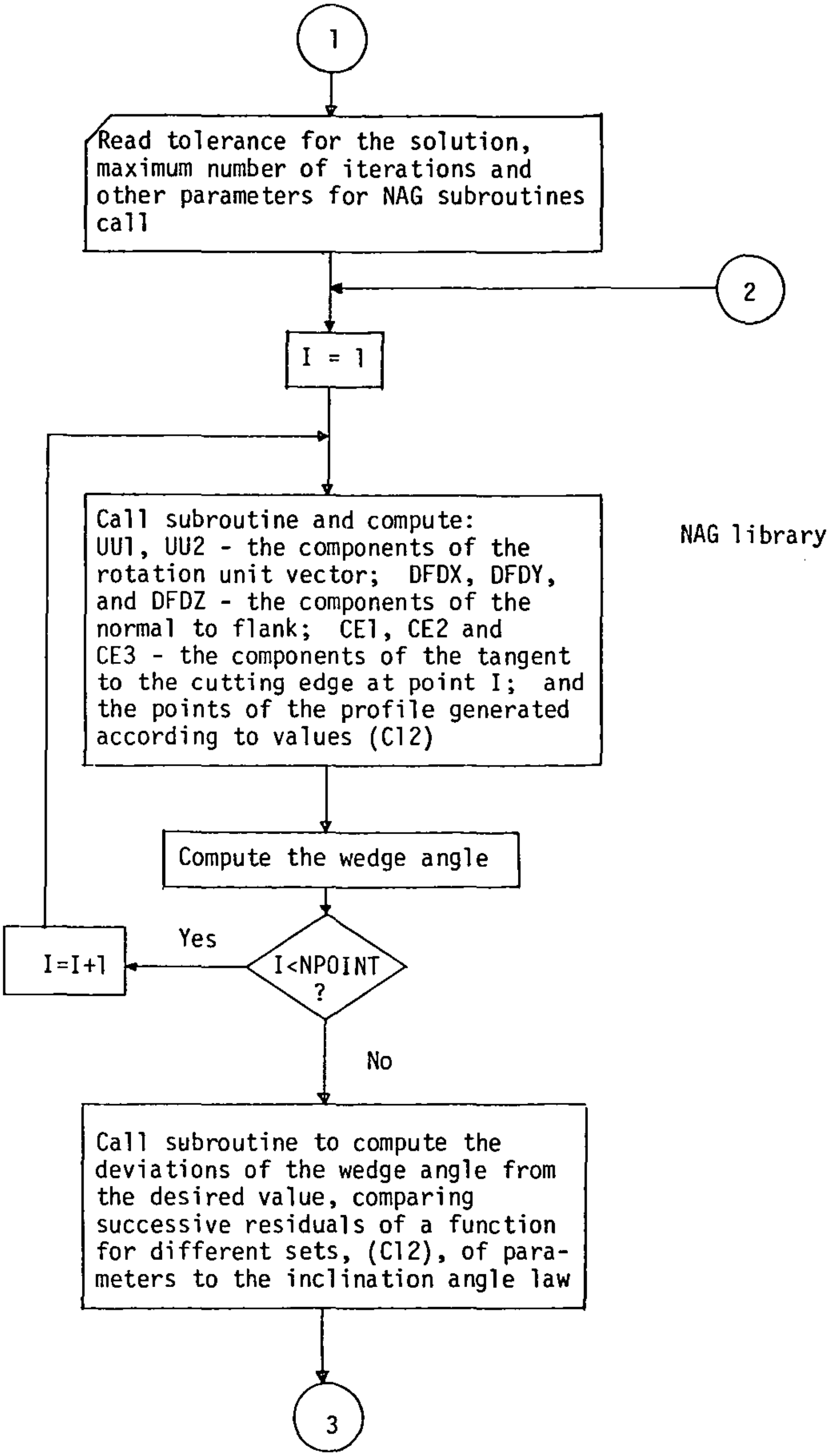


FIGURE 5.4 (continued)

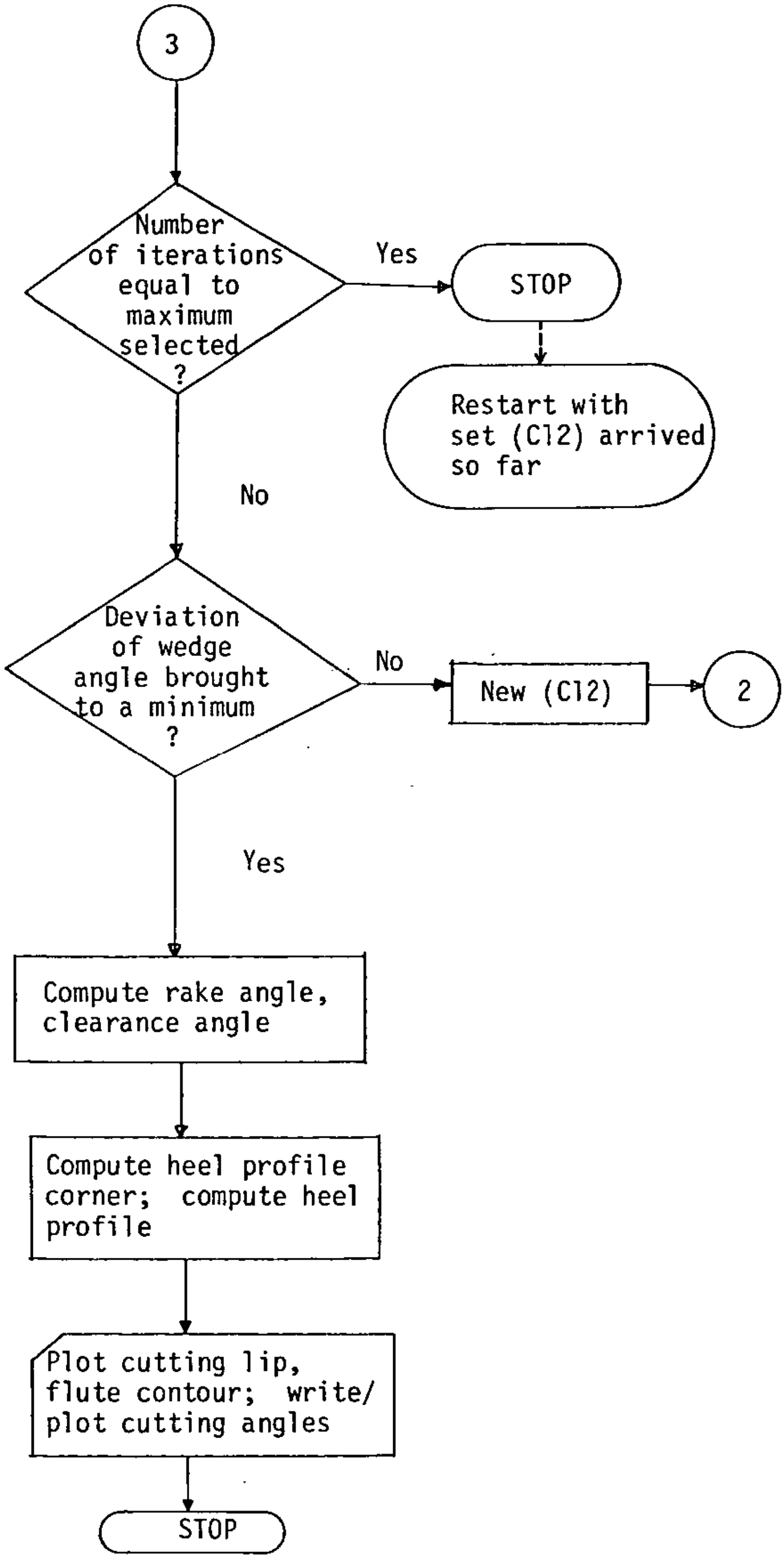


FIGURE 5.4: Flow diagram for the computer program for finding a non-conventional flute

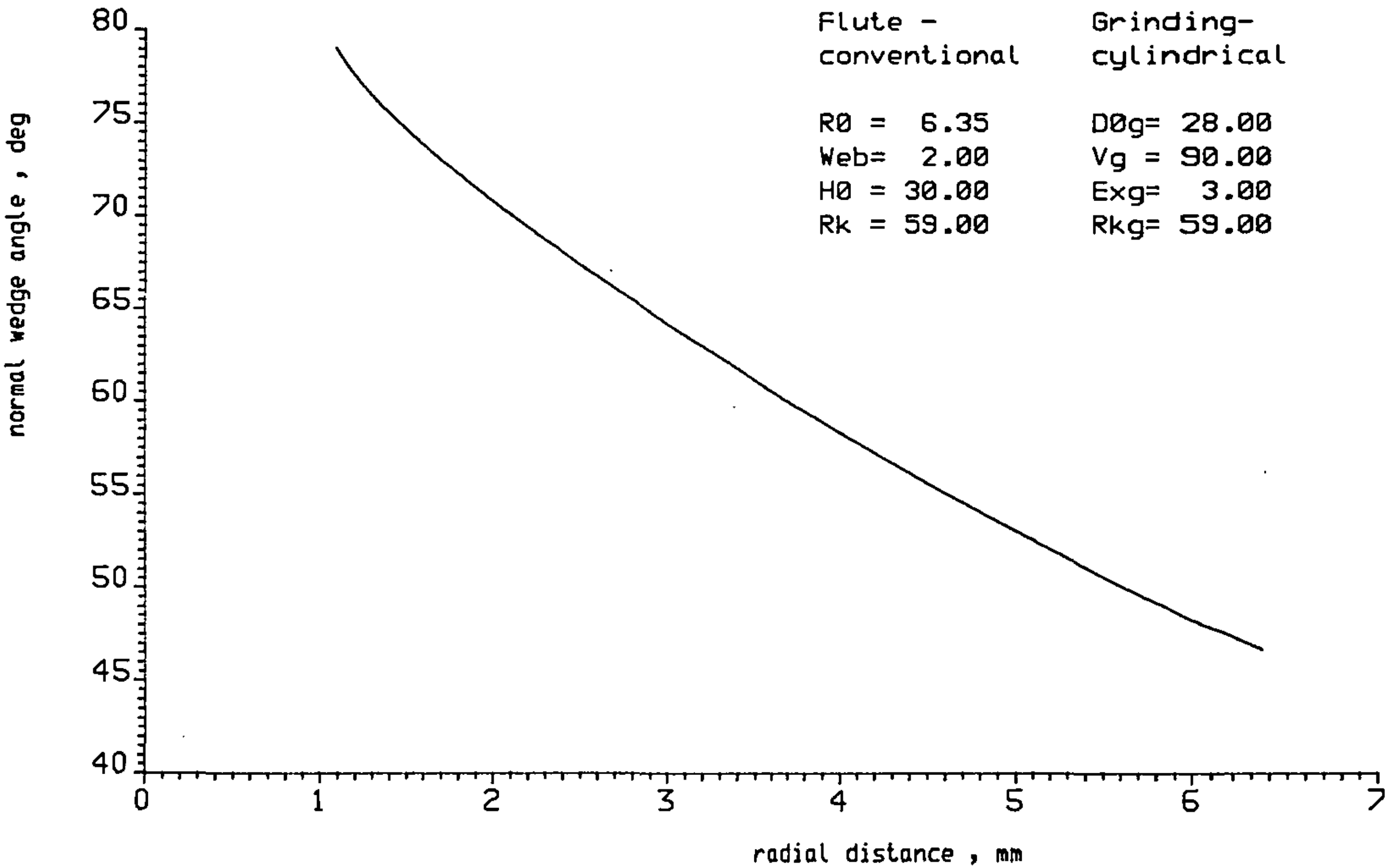


FIGURE 5.5: Normal wedge angle for conventional drill

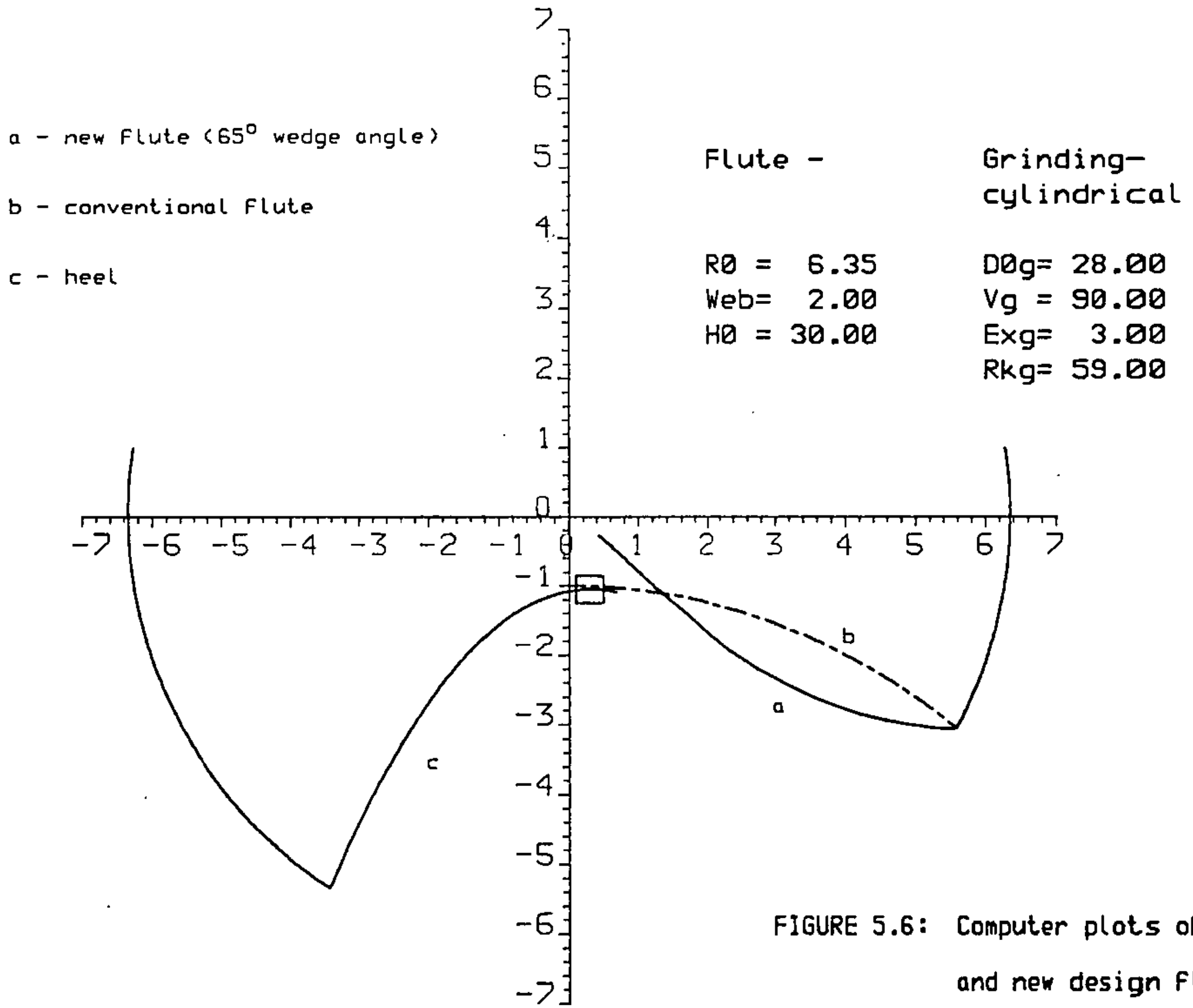


FIGURE 5.6: Computer plots of conventional and new design flutes.

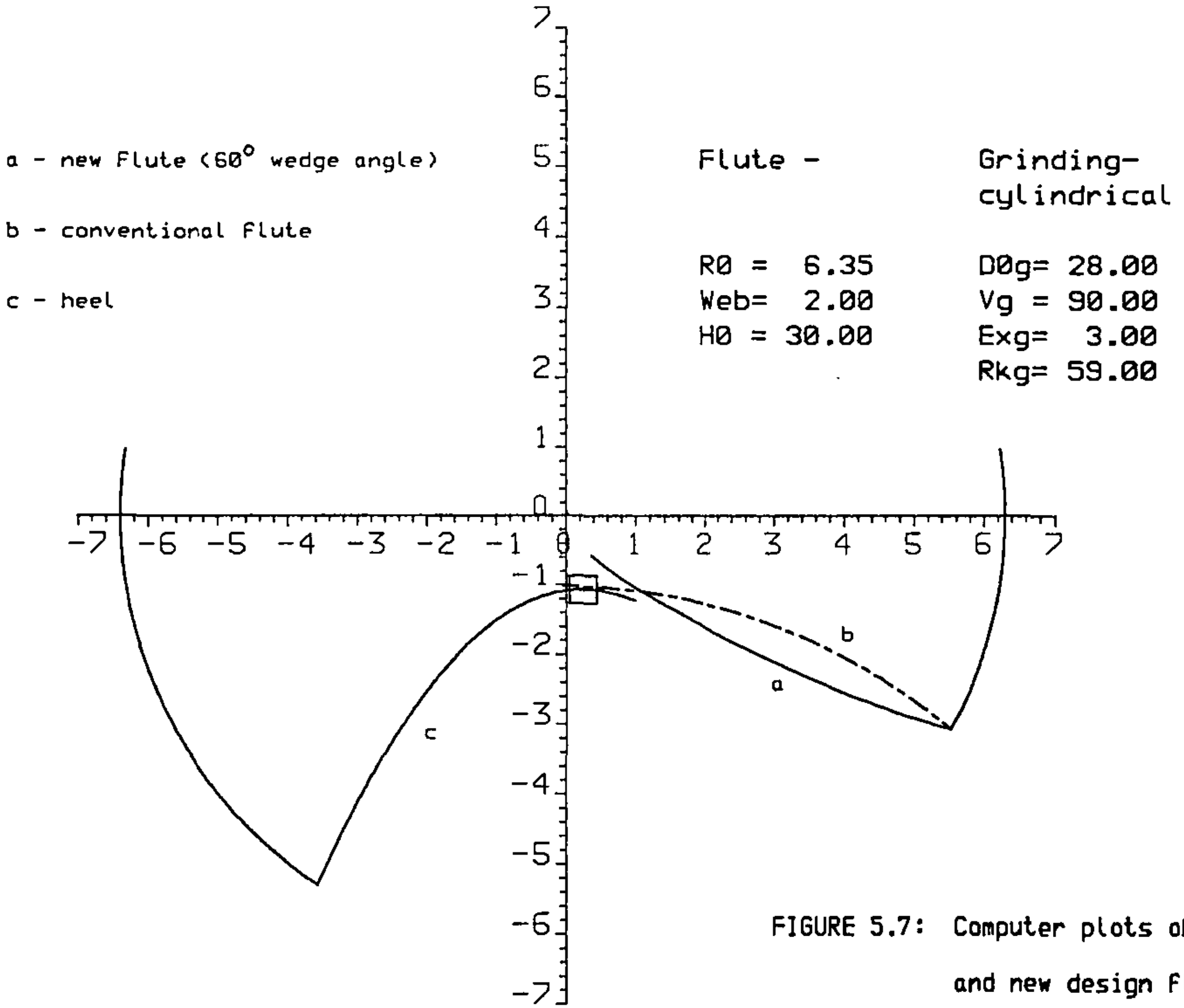


FIGURE 5.7: Computer plots of conventional and new design flutes.

From his numerical investigations and his observations, the author decided to select the wedge angle to be $60^{o}$, as it is well above the wedge angle at the outer corner of the conventional drill (Figure 5.5) and it yields a flute face (Figure 5.7) for which the normal wedge angle is nearly constant (Figure 5.8). Additionally, the inclination angle (Figure 5.9) and the normal rake angle (Figure 5.10) are such that the effective rake angle, after Stabler (45), is very close to the one to the conventional drill (Figure 5.11). Finally, the alteration necessary to be made to the flute face, for manufacture, in order to bridge it with the heel surface at the region of the chisel corner is small (Figure 5.7).

## 5.4 Drill Prototype Manufacture

Drill prototype manufacture involved the collaboration of drill manufacturers and was not controlled by the author.

The drill normal cross-section design, after the computer plot shown in Figure 5.7, is presented in Figure 5.12.

The geometric simulation of the drill point according to new design (Figure 5 .12) is shown in Figure 5.14.

The flute cross-section, normal to flute helical direction, for flute cutter design (at the drill's manufacture) is shown in Figure 5.13.

The author has had two lots of prototypes of the new drill design build, one after the other, from two different drill manufacturers.

Drills belonging to one lot presented a web weakness and some of them split into pieces, after a few dozen holes. Drills belonging to the other lot have been made by another drill manufacturer, and they have shown (Figures 5.15, 5.16 and 5.17) to be closer to the design by the author (Figure 5.12) than the ones from the first batch.

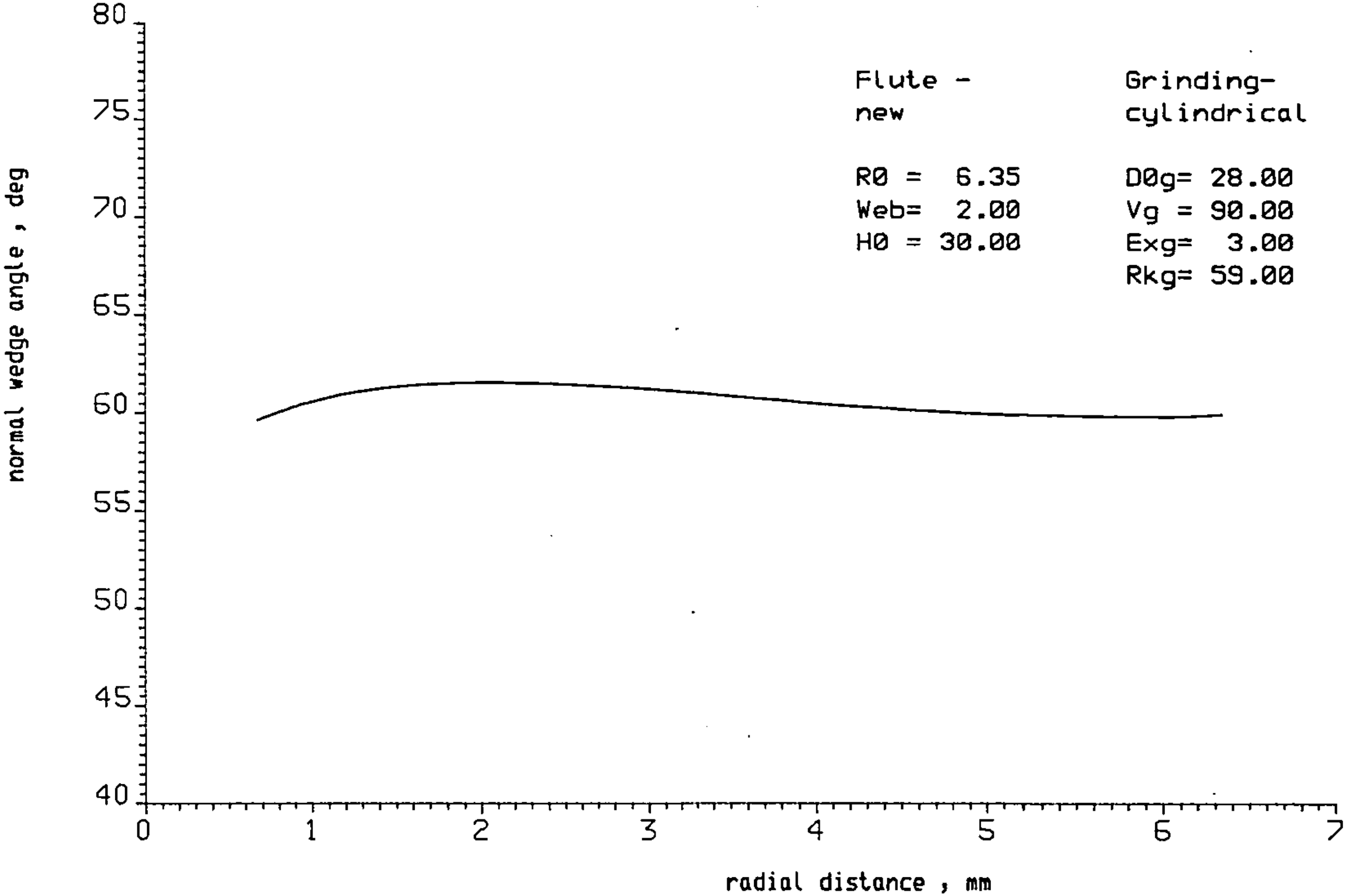


FIGURE 5.8: Normal wedge angle for the new flute design.

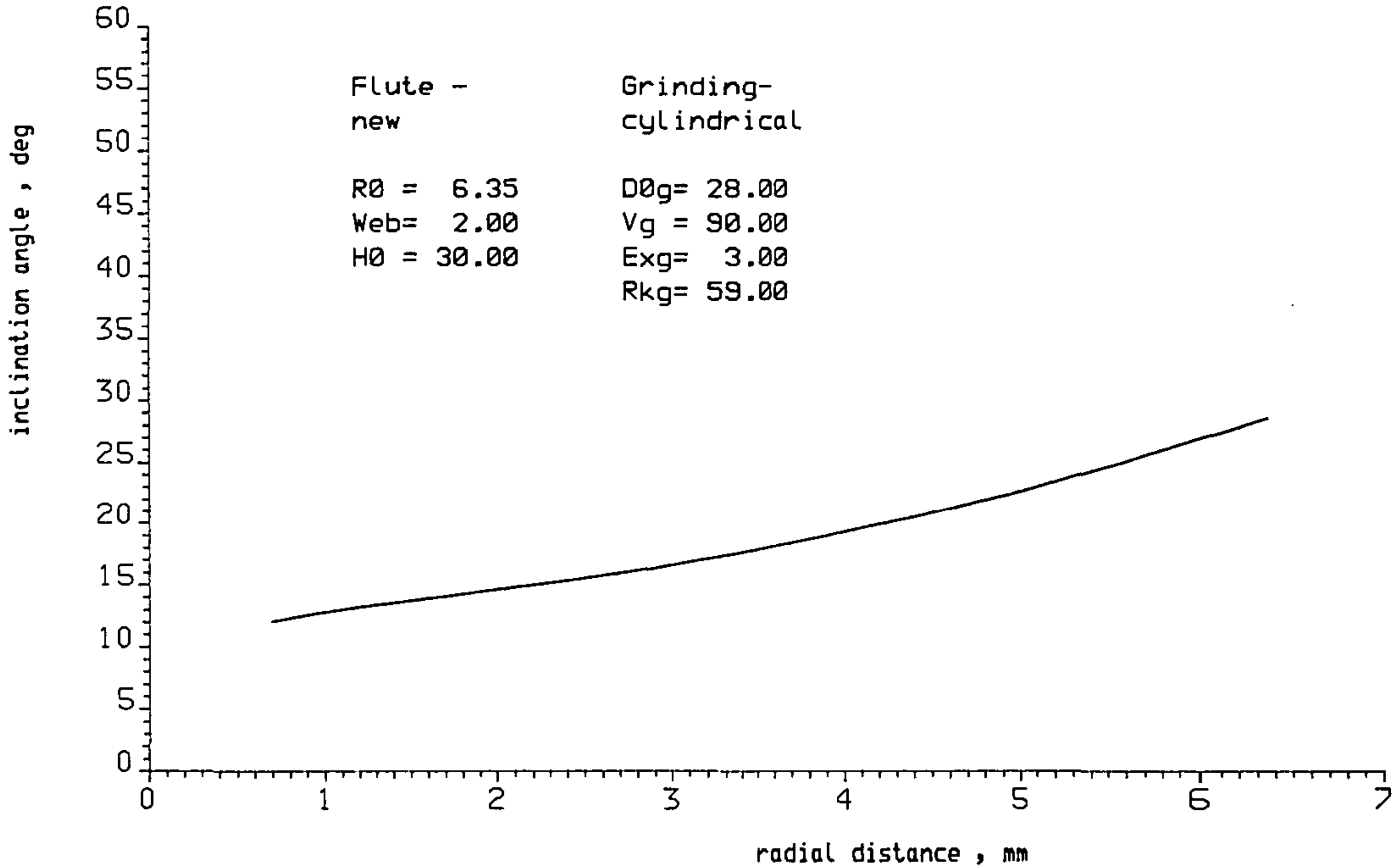


FIGURE 5.9: Inclination angle for the new flute design.

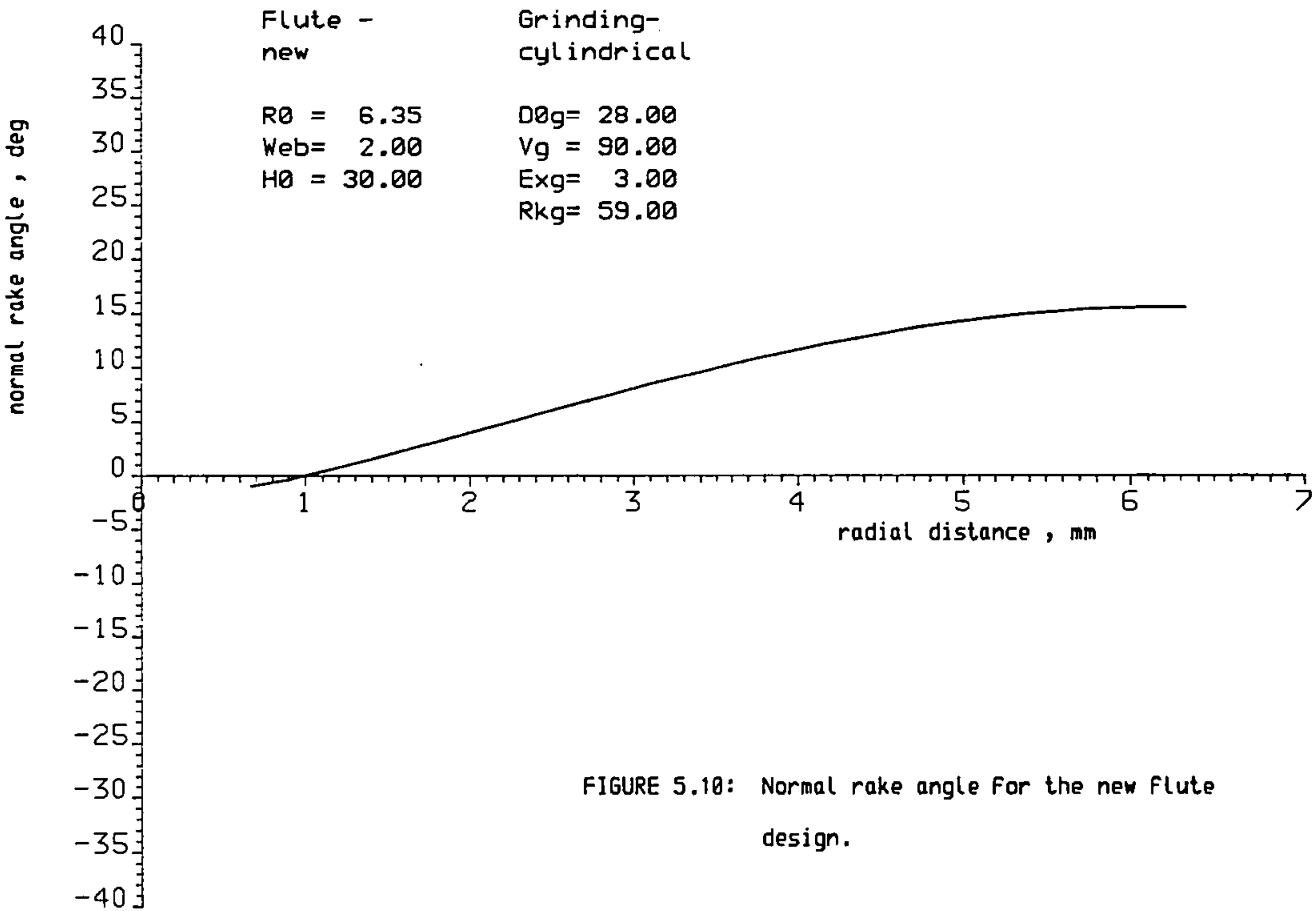


FIGURE 5.10: Normal rake angle for the new flute design.

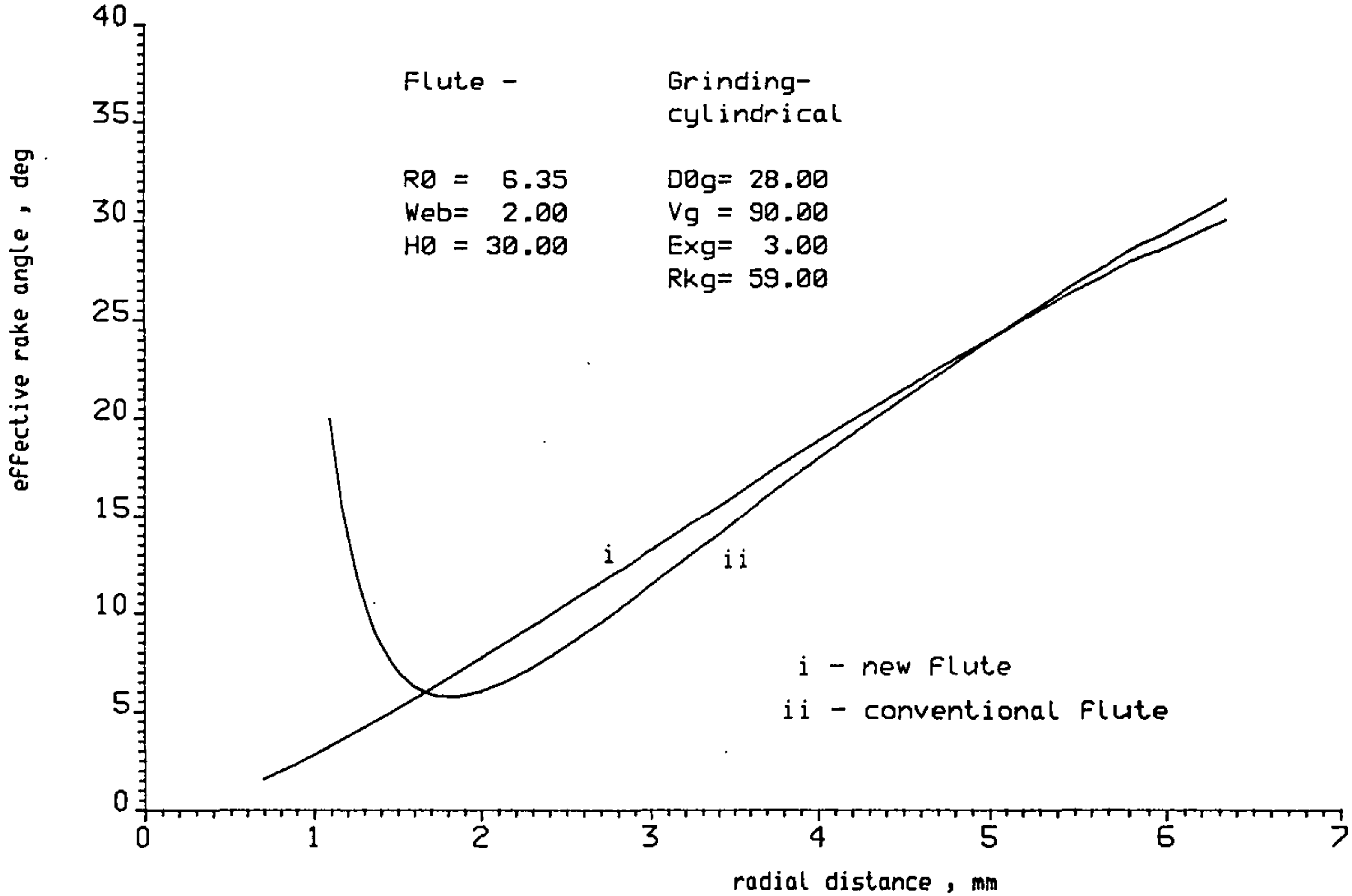


FIGURE 5.11: Effective rake angle computed for chip flow angle law according to Stabler's rule for oblique cutting.

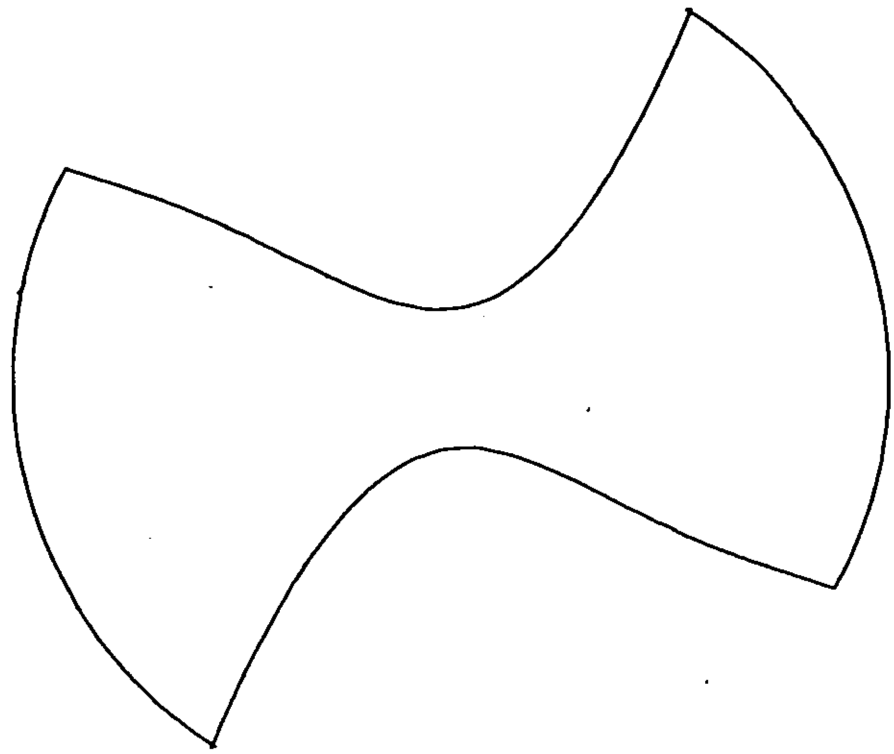

FIGURE 5.12: Drill cross section designed after FIG 5.7

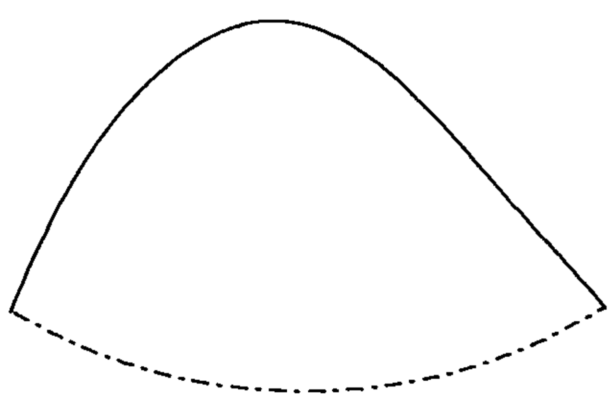

FIGURE 5.13: Flute cross section normal to the flute helical direction for the new flute design [FIG 5.12]

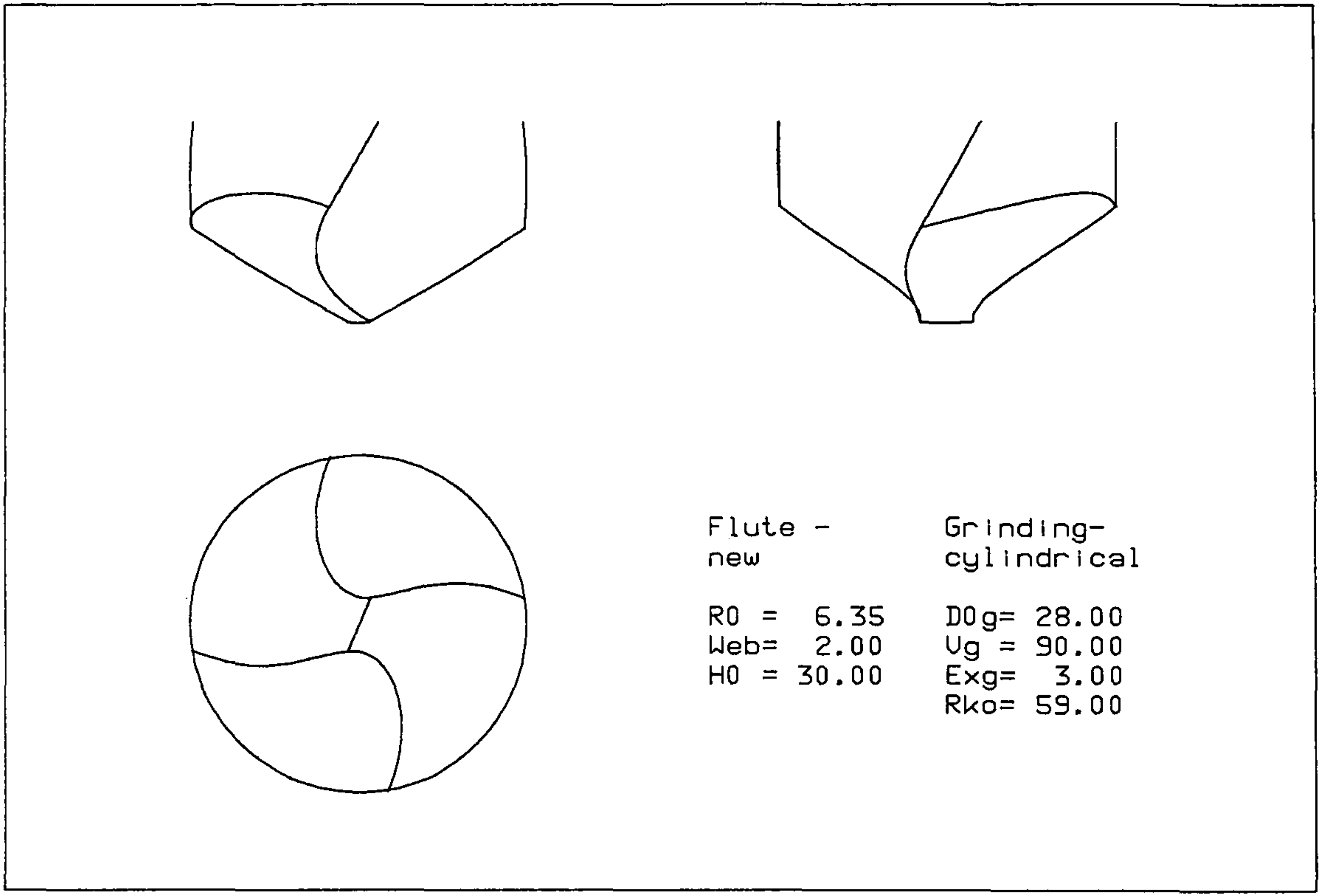


FIGURE 5.14: Computer geometric simulation of drill point according to design shown in FIG 5.12

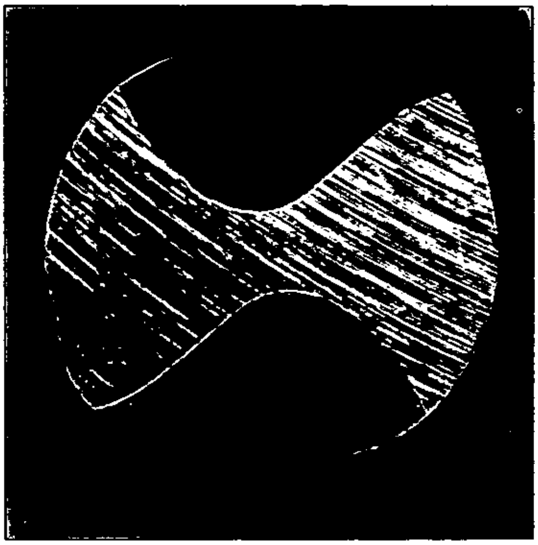

FIGURE 5.15
New design drill cross section - view from the drill point

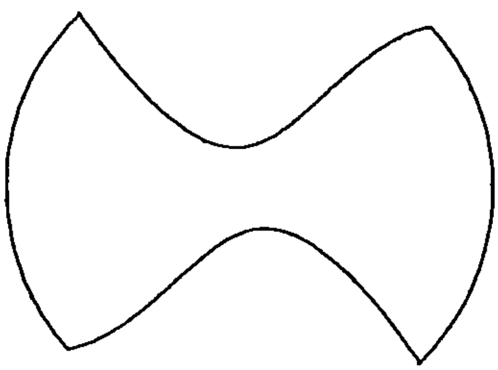

FIGURE 5.16
Computer simulated cross section after manufactured new design drill (FIG 4.15) - view from the drill point

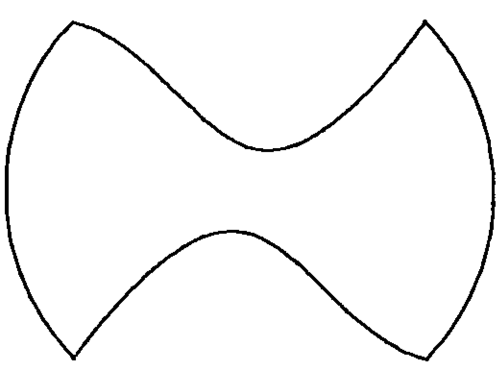

FIGURE 5.17
As in FIG 5.16 -
- view from the drill shank

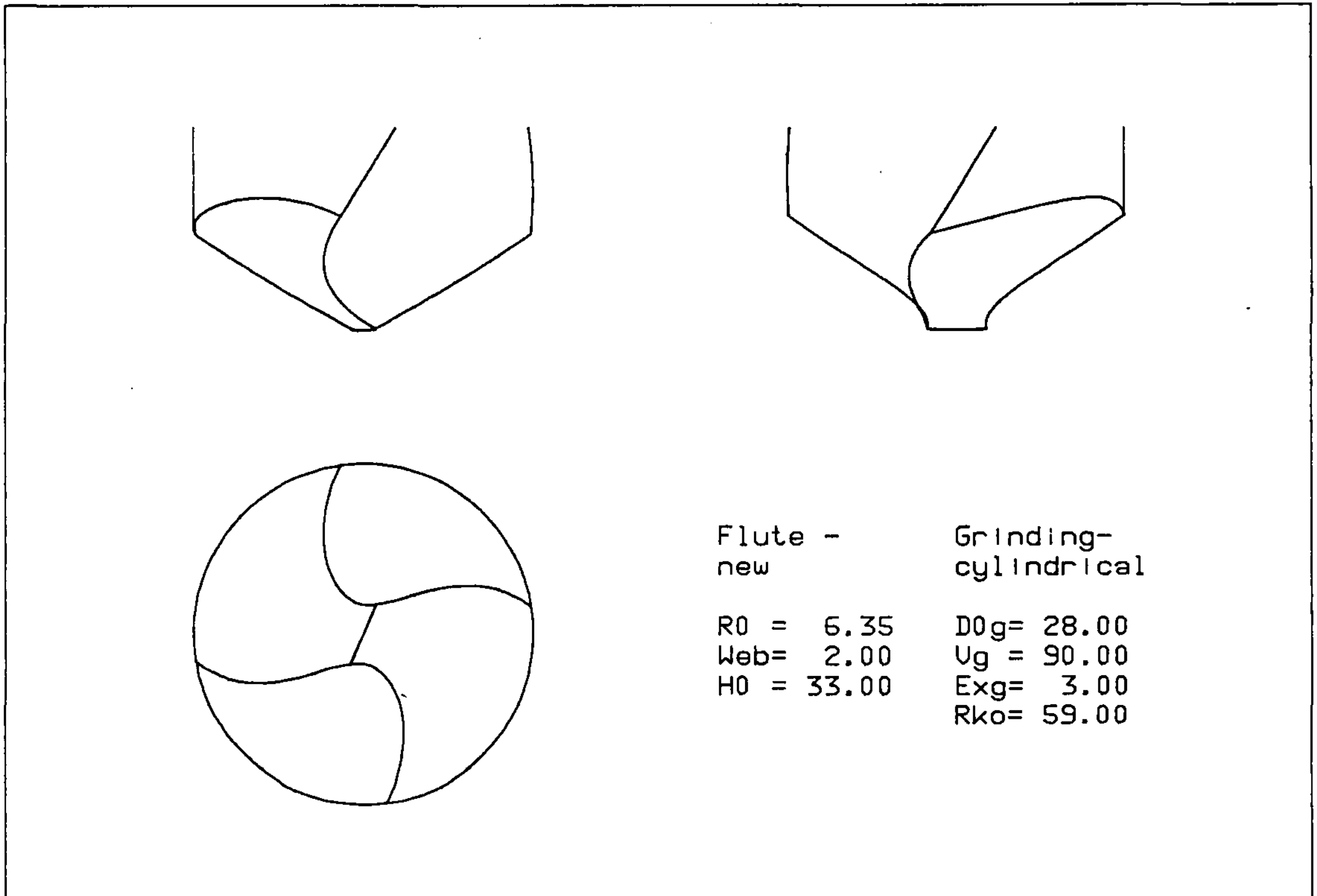


FIGURE 5.18: Computer geometric simulation of drill point as manufactured. [Refer to FIG 5.16 and 5.17]

Drills belonging to the referred to second lot will be designated by new design drills, or new flute drills and the simulation for this actual new design drill point is shown in Figure 5.18.

*"No man ought to be discouraged if the experiments he puts in practice answer not his expectations; for what succeeds pleases more, but what succeeds not many times informs no less".*

*Bacon*

# 6. PERFORMANCE TESTS - COMPARING LIP WEAR ON CONVENTIONAL AND NEW DESIGN DRILL

## 6.1 Introduction

### 6.1.1 Review of drill performance concept

The author did not find in the literature a generally accepted drill performance measure. He rather found that the drill performance concept comprehends several aspects. For convenience some drill performance aspects will be revised concisely.

For Waller (31) the aspect of drill performance most emphasized in the past was drill life. Lorenz (28,29) also refer to drill life when he reports on drill performance. Valery (82) reported upon durability of drills.

Micheletti and Levi (23) restrained the analysis of drill performance to the study of drilling forces, and so did Fujii and coworkers (37).

Billau (11) emphasized the hole quality with the double margin drill. Burant and Skingle (83) looked for high metal-removal rates when testing different drills for the determination of optimum drilling conditions for an Al-Si alloy.

Ernest and Haggerty (2) investigated drill performance by considering the following aspects: (i) torque and thrust, (ii) drill life and (iii) hole oversize.

Galloway and Morton (10) have listed the main objectives of drill users:

i) high rate of penetration;
ii) long drill life;
iii) accuracy of holes;
iv) high drilling efficiency.

Later, Galloway (3) considered drilling performance criteria as follows:

i) rate of penetration;
ii) drill life;

iii) efficiency of metal removal;
iv) hole accuracy;
v) hole surface finish.

Kanai and Kanda (33), in a contribution for the development of a standardized drill test, recommended the wear at the drill outer corner to be measured and to be used as a drill performance index.

Farnworth (84) defined a drilling performance index based on economic factors where drill life is one of the variables accounting for the index calculation.

Nakayama (66), Arshinov and Aleksev (4), CETIM (85) and others (83) referred to chip geometry in assessing machining performance.

### 6.1.2 Drill life

In spite of being very frequently used as a performance criterion, drill life definition is still open to discussion.

According to Singpurwalla and Kuebler (86) drill life could mean different things to different people. Galloway and Morton (10) found it difficult to recommend means to determine the end of drill life but based on personal judgement. Also Valery (82) stated that drill life is somewhat vague and Williams and McGilchrist (87) referred that no current drill life criterion provides a unique measure of drill failure. Burant and Skingle (83) referred to the fact that drill life was determined more or less subjectively.

The author found in some reports (86,87) the writer's referring that they relied on the personal opinions of drilling operators rather than on any objective criterion to judge upon the end of drill life.

Frequently, squeaking (82,88), crying (86), screaming (89) and screeching (11,35) during drill is taken as an indication of drill failure. Singpurwalla and Kuebler (86) and PERA (24) determined the end of drill life by a change in sound during drilling. Iwata and Moriwaki (90) and Weller and co-workers (91) studied acoustic emission from the cutting process in order to find some useful information about the cutting state.

The change in colour of the drill during drilling has also been suggested by Singpurwalla and Kuebler (86) as a (subjective) method for drill life criterion.

Drilling torque and thrust have been suggested by Galloway (3), Galloway and Morton (10) and others (89), as indicators of drill dulling. Also (BS 5623) refers to the cutting forces used as a basis for tool life criterion in scientific research and in adaptive control systems. However, some doubts on the methods based upon the use of dynamometers and upon the variations of drilling forces in assessing drill life have been put forward by Oxford (discussion of paper (3)), Williams and McGilchrist (87) and Billau (35).

### 6.1.3 Drill wear

To allow a drill to reach the state of complete failure can lead to irreparable damages or long lasting regrinding operations. Thus Oxford (92) and others (93) recommended that excessive drill wear should be avoided as a matter of cost effectiveness.

Frequently drill life (and in general tool life) is associated with flank wear by some workers. (Billau (35) found the "wear rate"/"life" to correspond favourably with the "screech"/"life" for the drills and conditions he tested. For Valery (82), the end of drill life appears to be related to an area of wear at the drill lip. Burant and Skingle (83) decided that drill life would be ended at the point at which the *"wear pattern changes to an increasing rate"*. Šoloja and Toko (64) also based drill life upon wear criteria. Subramanian and Cook (94) reported that the limit of the economical life of a tool is determined by the extent of wear on the tool, and according to Tseng and Noujaim (95) the wear land width *"is considered by many to be the most dependable guide of tool life"*.

Frequently tool life is defined in terms of a pre-determined wear land width (Figure 6.1) (1, 88, 95, 97, 98, BS 5623), and one great advantage of such a method consists of not being dependent on individual judgement.

Subramanian and Cook (94) and Kanai and Kanda (33) find the drill flank wear to be relatively easy to measure, however, Lorenz (88), considers that it is very time consuming.

Billau (11), Subramanian and Cook (94), among others, established that drill lip flank wear develops in three stages (Figure 6.2);

A - rapid and non-linear increase of the wear land width due to the removal of the sharp edge.

B - slow, long and uniform rate of wear.

C - accelerated wear rate leading to increase of noise and drill failure.

In order to monitor and to assess as objectively as possible the decreasing ability of drill lips to cut, as drilling progresses, the drills dealt with in this work will be tested for wear.

## 6.2 Experimental Design

The aim for the experiments to be made is to compare two drill types - conventional and new design - for wear at the neighbourhood of the drill outer corner with the number of holes drilled.

### 6.2.1 Drill test type

A great selection of drilling speeds and feeds are usually available to drilling researchers and drill users. Lorenz (28), Lenz (99), Galloway and Morton (10), Valery (82), Williams (87), Singpurwalla and Kuebler (86) and Billau (35), among others, reported on the influence of speed and feed on drill life and they found the drill life to decrease with increasing speeds and feeds.

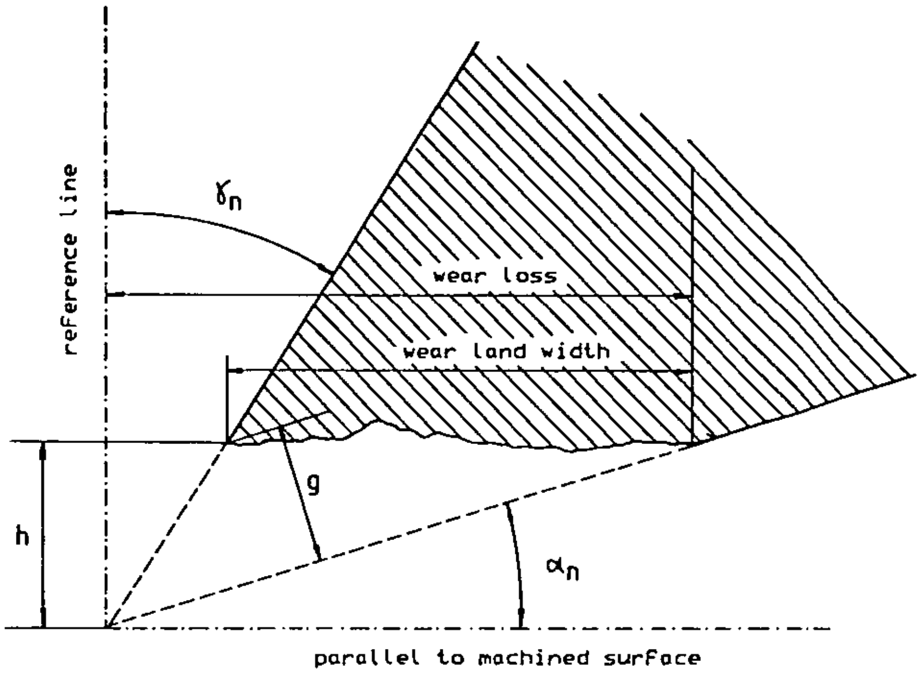


FIGURE 6.1: Geometry of a worn cutting edge

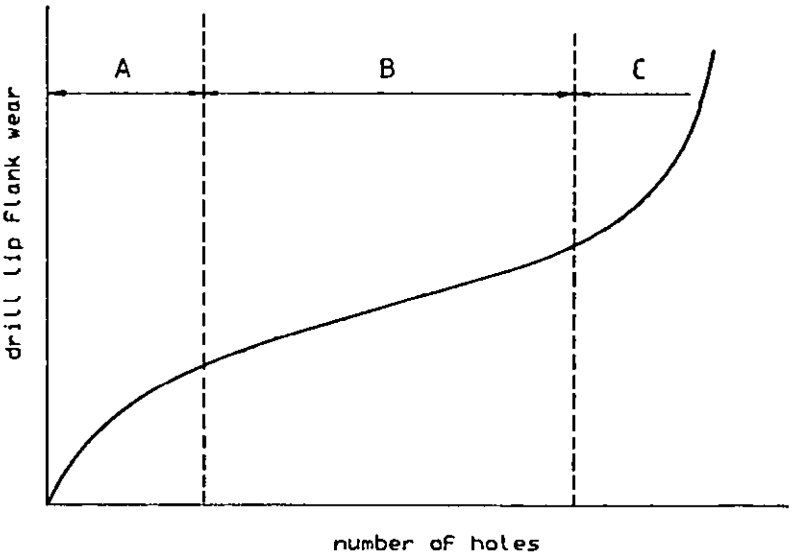


FIGURE 6.2: Drill lip wear pattern (11)

[Refer to text for phases A,B and C]

As a matter of economy and because resources to researchers are usually scarce, tests should be as short as possible. However, there is no general agreement on the acceptance of accelerated life testing (100). Some workers (101) argue that the same phenomena (thermic, dynamic, structural) are present during cutting, either during slow or accelerated cutting; others (10) think that the mechanism of drill failure or wear varies with the cutting conditions.

Drilling tests may be divided into three types (3,10):

- short duration tests - up to approximately 30 holes, each two diameters deep
- medium duration tests - up to approximately 40-140 holes, each two diameters deep
- long duration tests - more than 150 holes, each two diameters deep.

A literature survey revealed that many reported drilling tests (3, 5, 28, 29, 87, 88, 89, 94) are medium duration tests as they are frequently roughly centred at 100 holes. For Galloway (3), the knowledge gained through medium-duration life tests could be used in the workshop.

In view of the above, the author decided to perform medium duration drilling tests.

### 6.2.2 Factors selection

The author thought it to be necessary to investigate the two different flute designs response to the variation of (i) speed, (ii) feed and (iii) point angle as these are the variables with a major influence on drill performance and over which the user has usually a wide control. Limitations to these variables may be imposed by the available range of speeds and feeds in the drilling machine and by the maximum point angle that can be set in the grinding machine.

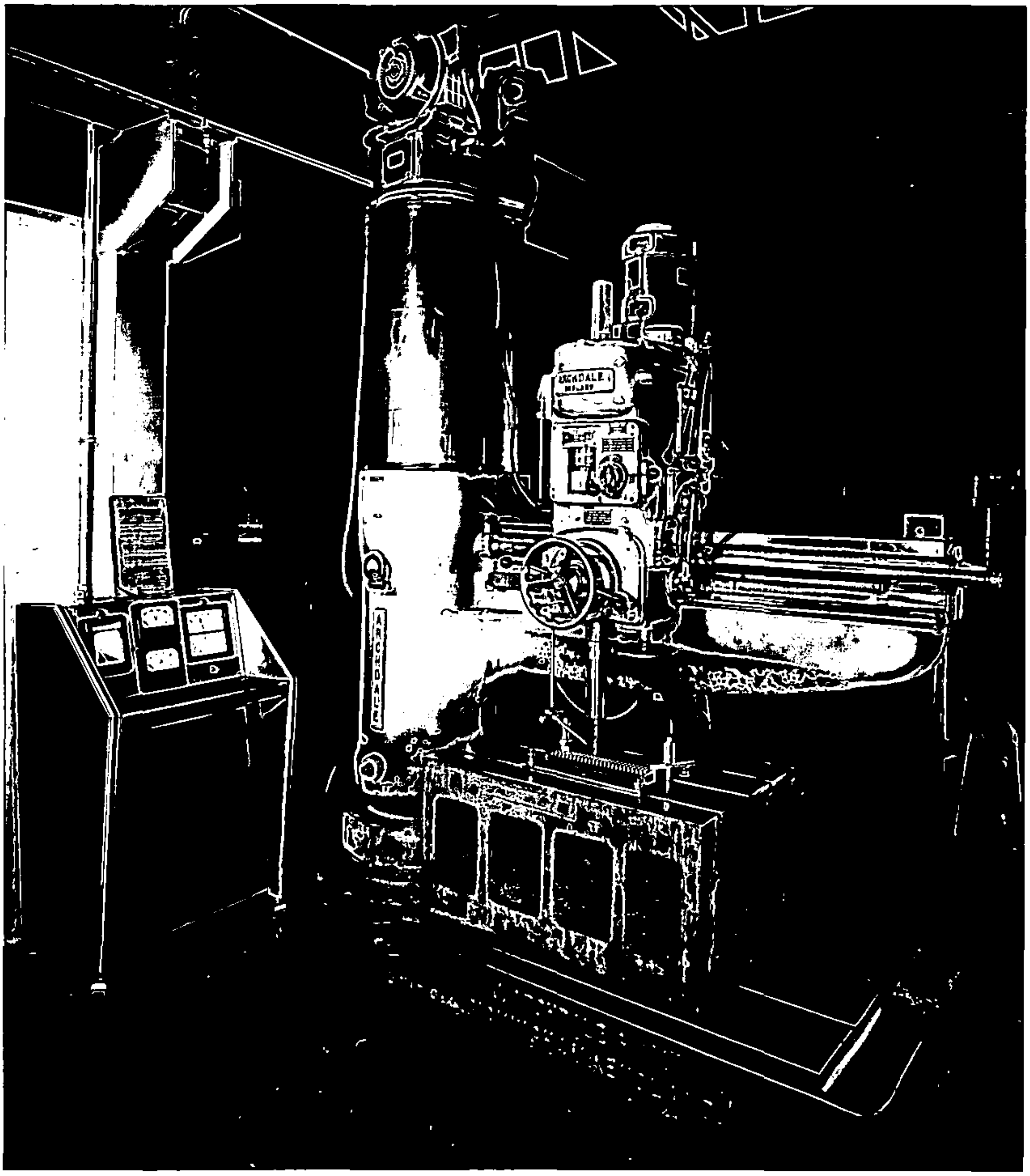

FIGURE 6.3: Radial arm drilling machine

The very limited amount of experience on the new design drill and also the limited resources available to the author prevented the inclusion of a larger number of variables.

### 6.2.3 Equipment

The drilling machine, the coolant, other equipment, the drills and other factors were involved in close control.

#### 6.2.3.1 Drilling machine

A radial drilling machine (Figure 6.3) was used for all drilling tests relating to this project. Its features are as follows:

| | |
|---|---|
| Manufacturer: | Archdale Limited |
| Type: | 6 ft radial arm |
| Power: | 5 HP motor |
| Spindle: | 2.5 inch diameter - No 5 internal Morse tape |
| Speeds: | 60 85 110 140 197 260 |
| | 350 490 640 820 1140 1500 rev/min |
| Penetration: | 30 45 70 103 157 240 rev/in |
| Coolant supply: | 5 l/min (≈ 1.1 gallons/minute) |

To produce a portal frame-like structure an adjustable brace was fixed to the free end of the arm.

The machine was checked for alignment. The speeds were checked with a stroboscope device and the feeds by a dial gauge.

#### 6.2.3.2 Drill grinding machine

A Dormer model 84 drill grinding machine was used in this work for the preparation and regrinding of the drill points (Figure 6.4).

Billau (11) has investigated with a perspex model the shape of the flank face produced by this grinding machine and found it to be of a cylindrical form.

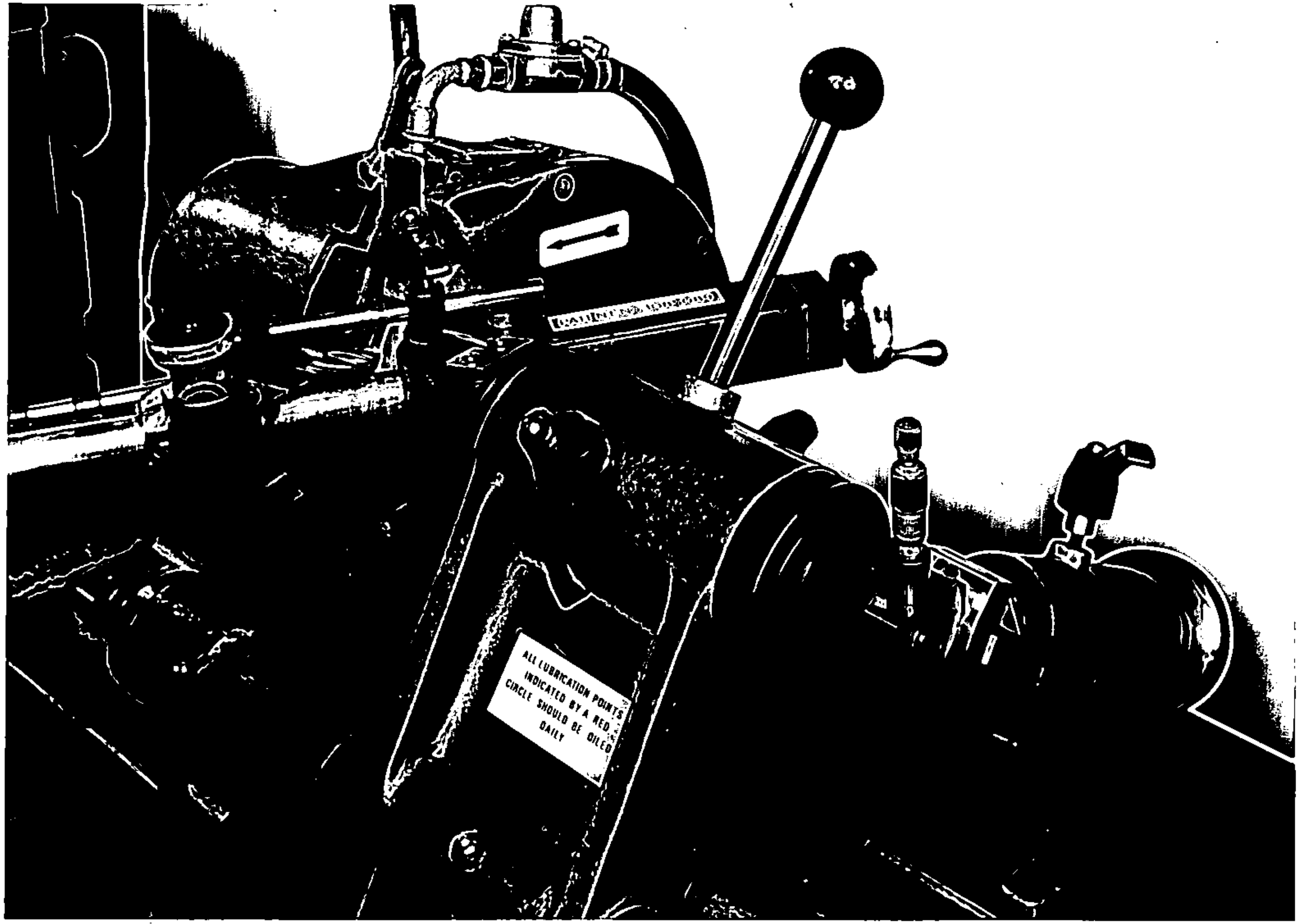


FIGURE 6.4: Drill point grinding machine

The relevant technical data for this machine is as follows:

| | |
|---|---|
| Grinding wheel, diameter: | 203 mm |
| width: | 25 mm |
| bore: | 102 mm |
| Maximum peripheral speed: | 30 m/sec |
| Range of drill diameters: | 3 mm - 32 mm |
| Maximum overall length of drill: | 420 mm |
| Range of point angles: | $90^o$ - $140^o$ |

With the machine available to the author, the point angle could not be larger than about $135^o$.

6.2.3.3 Drill geometry measurement machine

Much of the drill geometrical accuracy depends on the careful control of quality during the manufacture stage. Careful drill point grinding however is as much important as the manufacture.

The drills reported in this work have been manufactured under special control and the drill grinding by the author has been made and controlled in the most careful way. For the control of the geometrical drill features, before any test, a Dormer model 94 goniometer drill inspection unit was used (Figure 6.5). The angles can be measured to the 5' and the distances to the 0.01 mm.

For proper positioning of the drill in the goniometer and for more accurate results, the main vee block as from the manufacturer was provided with a clamping system in order the drill could be properly set and held during measurement (Figure 6.5).

6.2.3.4 Microscope

For the wear measurement on the flank face of the drills a Hilger and Watts microscope provided with a table operated by two perpendicular micrometer screws was used. The normal eyepiece of the microscope was replaced by a micrometer graticule type of eyepiece (Figure 6.6).

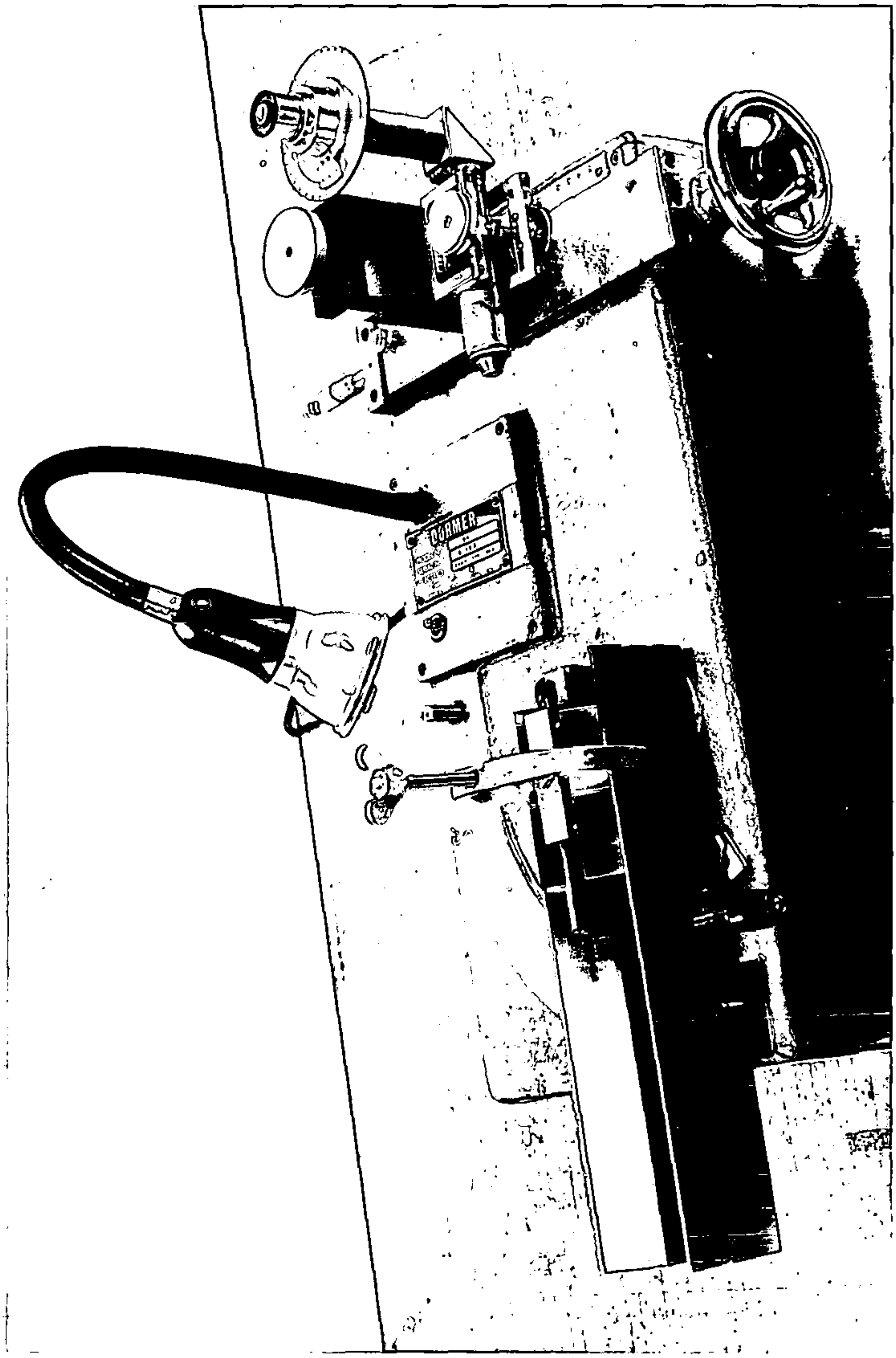


FIGURE 6.5: Drill geometry measurement machine

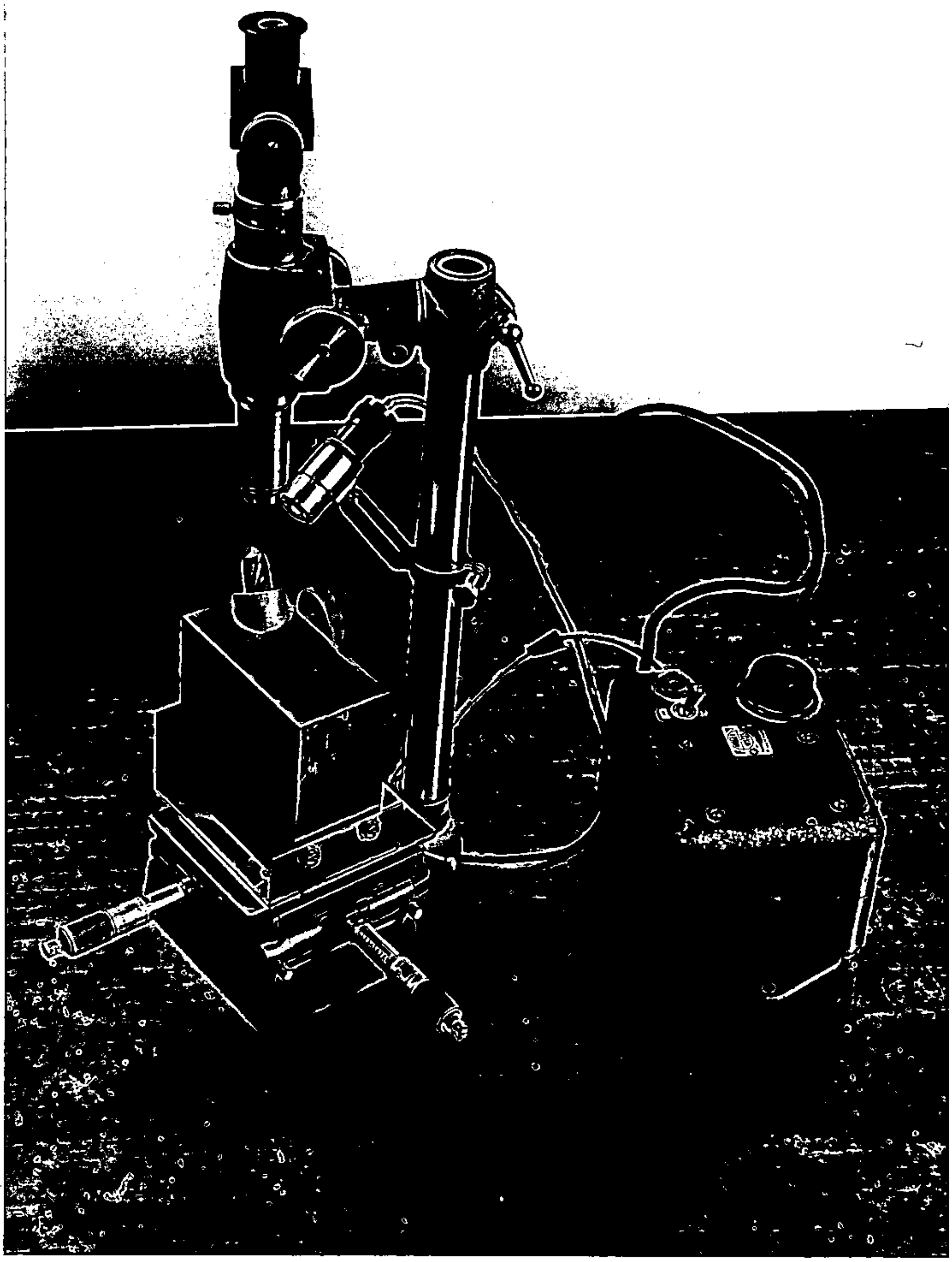

FIGURE 6.6: Hilger and Watts microscope adapted for drill lip wear measurement

The position of the points on the cutting edge and the position of the points on the line determining the wear land on the flank were measured relatively to a reference line etched on the flank (Section 6.3.1). Measurements were made at five equally spaced points near the outer corners, on both lips of each drill (Section 6.3.1).

### 6.2.4 Preliminary life tests for selection of values of factors

In order to establish the cutting conditions for the main wear testing the author: (i) surveyed technical data available for the conventional drills (mainly reports on drill life), (ii) ran preliminary tests with both drill types.

The preliminary tests were run to determine the penetration rates which would lead to medium-duration tests (see Section 6.2.1). The results were used to select the cutting speed and drilling feed values shown in the next section.

### 6.2.5 Statistical design of experiments

In designing the experimental work for the drill wear tests the following objectives were considered:

- investigate the difference (if any) between the conventional and the new design drill when speed, feed and point angle are varied

- design the experiments in order that statistical analysis can be exercised with the data collected

- plan statistically the experimental sequence and the combination of factors for each experiment

- provide for conclusions relating to the interaction between factors

- make the series of experiments as economical as possible

The advantages of statistical design of experiments have been emphasized in many works by statisticians (103, 104, 105) and by some researchers in the drilling area (87, 88).

Each drill type is tested for combinations of some values of the factors referred to in Section 6.2.2 : (i) cutting speed, (ii) drilling feed and (iii) point angle.

As a matter of efficiency, a factorial design experiment will be used in the present investigation, and for statistical analysis the experiments relating to the same drill type are arranged in separate blocks.

According to the factorial design, each factor is given two values: one conventionally called low and the other high. To use a special notation similar to the one frequently found in books on statistics (102, 105) the symbols shown in Table 6.1 were adopted.

TABLE 6.1: Symbols for Factor Levels

| Factor \ Level | Low | High |
|---|---|---|
| Speed (S) | 1 | s |
| Feed (F) | 1 | f |
| Point angle ($\kappa$) | 1 | $\kappa$ |

The following factors levels were considered:

Speed 1 - 32.72 m/min (820 rpm)

s - 45.48 m/min (1140 rpm)

Feed 1 - 0.106 mm/rev (240 RPI)
f - 0.162 mm/rev (157 RPI)
Point 1 - $118^o$
$\kappa$ - $134^o$

The different combinations of the above factors levels for wear testing are shown in Table 6.2.

TABLE 6.2: Combination of Factors Levels for Wear Testing

| Symbol | Factors | | |
|---|---|---|---|
| | S (rpm) | F(RPI) | $\kappa$(deg) |
| 1 | 820 | 240 | 118 |
| s | 1140 | 240 | 118 |
| f | 820 | 157 | 118 |
| $\kappa$ | 820 | 240 | 134 |
| sf | 1140 | 157 | 118 |
| s$\kappa$ | 1140 | 240 | 134 |
| f$\kappa$ | 820 | 157 | 134 |
| sf$\kappa$ | 1140 | 157 | 134 |

## 6.3 Drill Wear Testing

### 6.3.1 Testing procedure

The aim of the wear testing was to compare the performance of two drill types differing by the flute form. For the purpose of eliminating the effect of any difference between drills other than the flute profile shape, only one drill of each type was used. To use more than one drill of each type would introduce additional geometric differences such as minor flute shape differences among the drills of the same type as well as differences in web thickness, web eccentricity, relative lip height and drill straightness which would affect the variability of the results of the drilling tests (Chapter

1). To use only one drill was found in literature (3, 87) to be acceptable.

Two drills, one of each type, were selected with the most approximate web thicknesses, helix angles and drill diameters (Section 6.3.2).

The decreasing length of the drills with the successive drill regrindings could be compensated by a special drill holder (Figure 6.7) that allows for control of drill projection length.

To keep to a minimum any discrepancies from drill regrindings, the tests were run first for one point angle. After completion of these tests the grinding machine was set for the other angle and this set-up was kept until all the tests had been run.

After each drill regrinding the web thickness and the drill diameter of each drill were checked for differences due to possible web taper and to the negligible drill diameter taper (Tables 6.3 and 6.4). The differences were found to be within the measurement error for the drill length removed by regrinding during all drilling tests.

After each test the drills were observed for any change of colour that could affect drill material hardness and structure and drill regrinding was made carefully as recommended in (35) to avoid drill burning. Drill hardness was measured on the drill margins after each regrinding and was found to be within the measured values as received (Section 6.3.2).

Each hole was 3 drill diameters deep and the drill wear was measured at five points, on both lips of each drill, numbered as shown in Figure 6.8. Point 5 is coincident with the outer corner and each point is 0.508 mm (0.02") distant to the next one.

With this procedure, not only the wear at the outer corner but also along a length of about 1/3 of the whole lip length was measured, and in this way it will be possible to monitor and to compare the pattern of wear in the neighbourhood of the outer corner for both drill types.

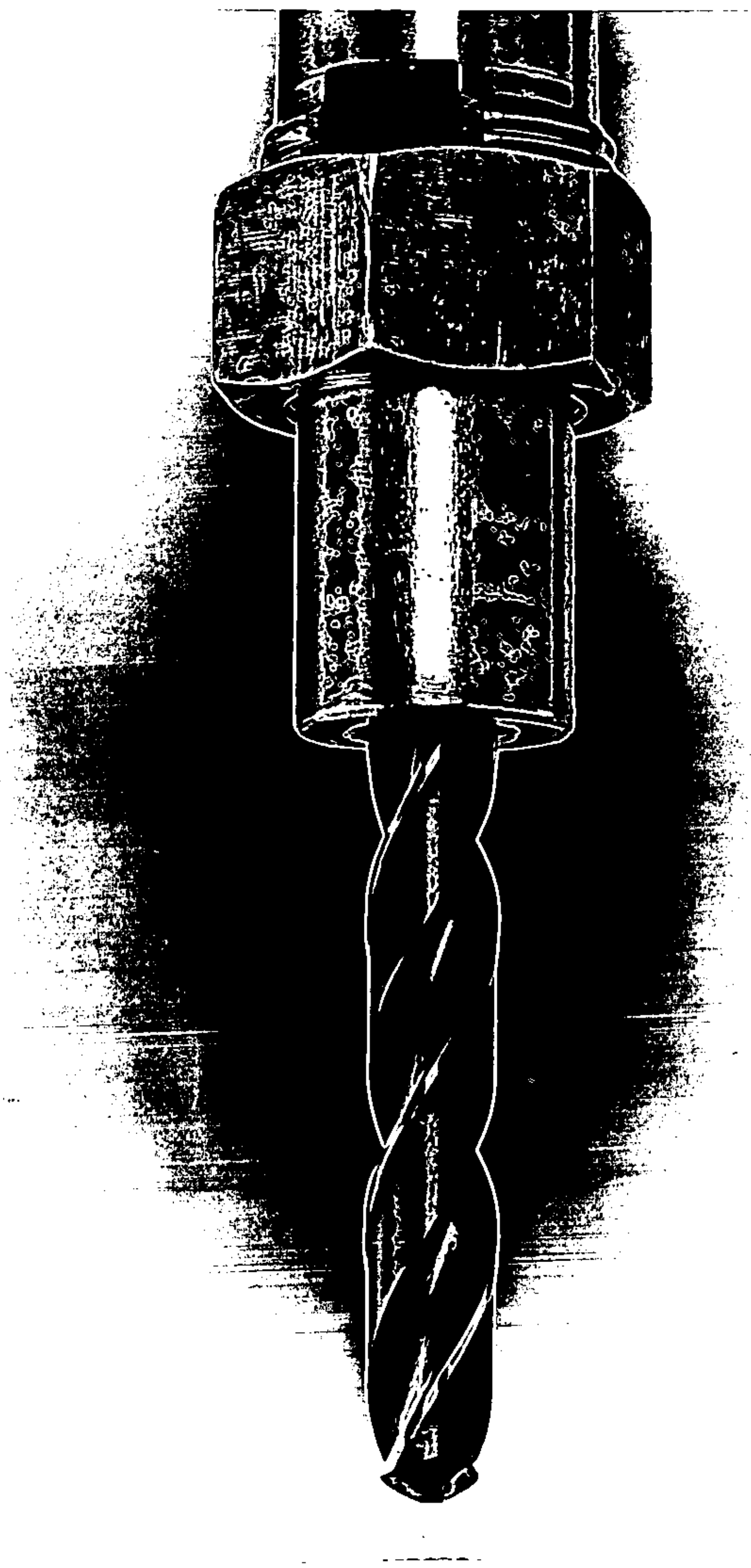

FIGURE 6.7: Bristol Erickson chuck for variable drill length projection

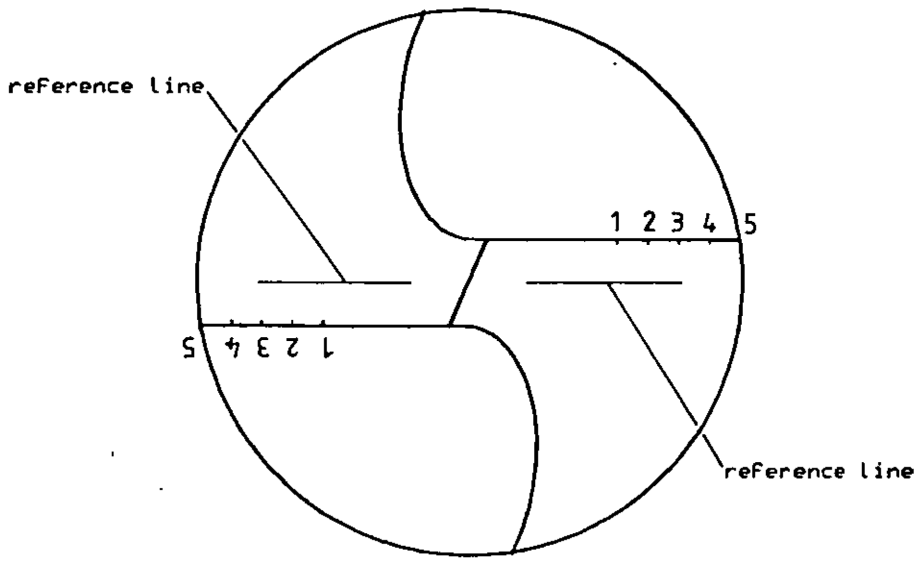


FIGURE 6.8: Wear measurement points on drill lips in the neighbourhood of the outer corner

FIGURE 6.9
Etched line on the drill flank surface for wear measurement reference

The wear was measured after the fifth, tenth, fifteenth, and twentieth holes and each ten holes after the twentieth. Wear measurements were carried out until the drill failed, or, until the 150th hole if failure had not occurred before.

For measurement reference, etched lines were produced on the flanks, parallel to the line defined by the outer corner and the chisel corner (Figure 6.9).

For reading accuracy three readings were taken at each measurement point.

### 6.3.2 Drill features

As it has already been referred to, the tests were run with two types of drills: conventional and new design. For this purpose, together with the new design drills, some conventional drills were also manufactured from the same lot of material and according to the same production and treatment processes, in a way that only the differences in the flute geometries would be expected (Figure 6.10).

The drills were manufactured from the same lot of M2 high speed steel whose nominal composition is:

| C(%) | W(%) | Mo(%) | Cr(%) | V(%) |
|---|---|---|---|---|
| 0.83 | 6 | 5 | 4 | 2 |

The drills were heat treated as follows:

| | | |
|---|---|---|
| Pre-heat | 800 - 850$^{o}$C | |
| High heat | 1220 - 1240$^{o}$C | |
| Temperature | 550 - 560$^{o}$C | - one hour twice |
| Steam temperature | 470$^{o}$- for half an hour | |

All the drills, especially manufactured, both conventional and new design, are straight shank drills and are held in a Bristol Erikson chuck (Figure 6.7).

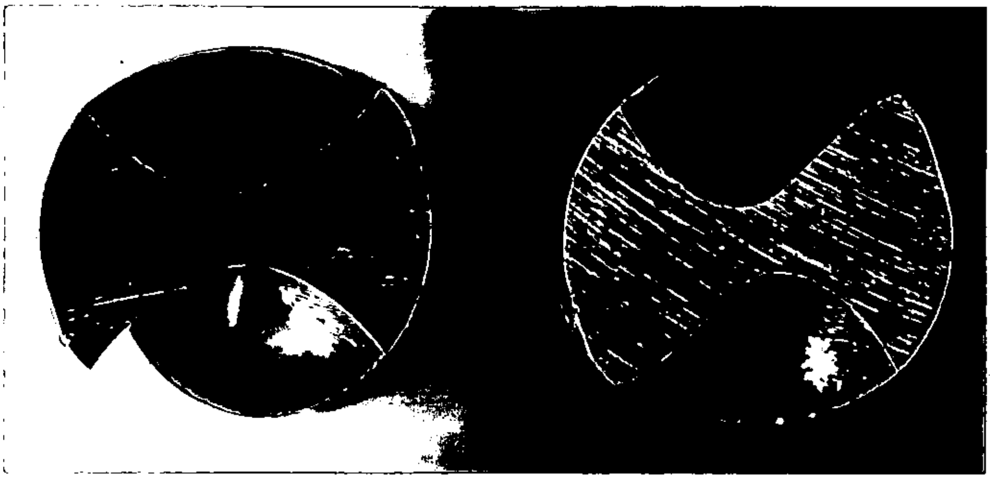

i ii

FIGURE 6.10: Cross sections of conventional (i) and new design (ii) drill - view from the drill point

Drill hardness was measured on the drill margins, near the drill point, in a Vickers Armstrong pyramid hardness testing machine and all results were found to be within the interval 64-66 $HR_c$ (Rockwell C scale)

Drill nominal relief angle [D.28], chisel edge angle and heel corner elevation (height of the heel corner relative to the outer corner), were the same as for the design of the new drill (Chapter 5) (Tables 6.3 and 6.4).

The point angle was selected for two values: $118^{o}$ and $134^{o}$; the first being the standard point angle (BS 328), and the second being the maximum possible within the grinding machine available to the author.

Two drills of each type were chosen and their cross-sections projected and magnified. For each drill type the differences found between the two sections were within the measurement errors.

For the new design drill, the differences between the designed profile and the profile as manufactured were found to be small (Chapter 5). However, for drill point geometric simulation and for all other computing purposes, as a matter of accuracy, the new drill flute profile as manufactured is used instead of the designed one.

For the purpose of mathematical representation of the profile as manufactured, a set of points with coordinates (X,Y) was taken by superimposing a graticule to the projected profile. This set of points was further represented by a polynomial law that better fitted their coordinates in order that the profile could be mathematically dealt with as a continuous curve.

The conventional drill profiles as manufactured were also compared to the conventional computed profiles and appeared to be similar.

Simulations for both drill types and both drill point angles are shown from Figures 6.11 to 6.14 and the actual features as measured are shown in Tables 6.3 and 6.4.

TABLE 6.3: Drill Specification for Drills Used with Tests for $118^{o}$ Nominal Point Angle

| Grinding Parameters | $d_{og}$(mm) | $\nu_g$(deg) | exg(mm) | $\kappa_g$(deg) |
|---|---|---|---|---|
| | 28 | 90 | 3.0 | ≈59 |

DRILL SPECIFICATION

| Item | Dimension | |
|---|---|---|
| | Conventional Drill | New Design Drill |
| Shank | Straight | Straight |
| Overall length (mm) (before first test for $118^{o}$ point | 150.5 | 151.0 |
| Flute length (mm) (before first test) for $118^{o}$ point | 101.0 | 102.0 |
| Drill diameter (mm) | 12.70 | 12.70 |
| Web thickness (mm) | 1.95 | 1.95 |
| Helix angle (deg) | 33.0 | 33.2 |
| Point angle - outer corner/chisel corner line (deg) | 118.1 | 117.8 |
| Nominal relief angle (deg) | 14.2 | 14.6 |
| Chisel edge angle - outer corner/chisel corner line (deg) | 113.6 | 112.0 |
| Width of margin (mm) | 0.90 | 0.90 |
| Back taper at margin (%) | 0.00 | 0.00 |
| Elevation of the heel corner relative to the outer corner (mm) | 0.48 | 0.54 |
| Lip length - outer corner/chisel corner distance (mm) | 6.85 | 6.75 |
| Chisel edge length (mm) | 2.10 | 2.40 |
| Eccentricity of chisel (mm) | 0.02 | 0.01 |
| Lip height difference (mm) | 0.02 | 0.03 |
| Flute spacing | <5' | <5' |

TABLE 6.4: Drill Specification for Drills Used with Tests for 134$^o$ Nominal Point Angle

| Grinding Parameters | $d_{og}$(mm) | $\nu_g$(deg) | exg(mm) | $\kappa_g$(deg) |
|---|---|---|---|---|
| | 34 | 100 | 3.8 | ≈67 |

DRILL SPECIFICATION

| Item | Dimension | |
|---|---|---|
| | Conventional Drill | New Design Drill |
| Shank | Straight | Straight |
| Overall length (mm) (before first test for 134$^o$ point) | 144.5 | 145.5 |
| Flute length (mm) | 95 | 96.5 |
| Drill diameter (mm) | 12.70 | 12.70 |
| Web thickness (mm) | 1.95 | 1.95 |
| Helix angle (deg) | 33.0 | 33.2 |
| Point angle - outer corner/ chisel corner line (deg) | 133.8 | 133.5 |
| Nominal relief angle (deg) | 13.6 | 13.8 |
| Chisel edge angle - outer corner/chisel corner line (deg) | 117.5 | 116.2 |
| Width of margin (mm) | 0.90 | 0.90 |
| Back taper at margin | 0.00 | 0.00 |
| Elevation of the heel corner relative to the outer corner (mm) | 0.65 | 0.69 |
| Lip length - outer corner/ chisel corner line (mm) | 6.35 | 6.40 |
| Chisel edge length (mm) | 2.10 | 2.35 |
| Eccentricity of chisel (mm) | 0.01 | 0.01 |
| Lip height difference (mm) | 0.01 | 0.02 |
| Flute spacing (deg) | <5' | <5' |

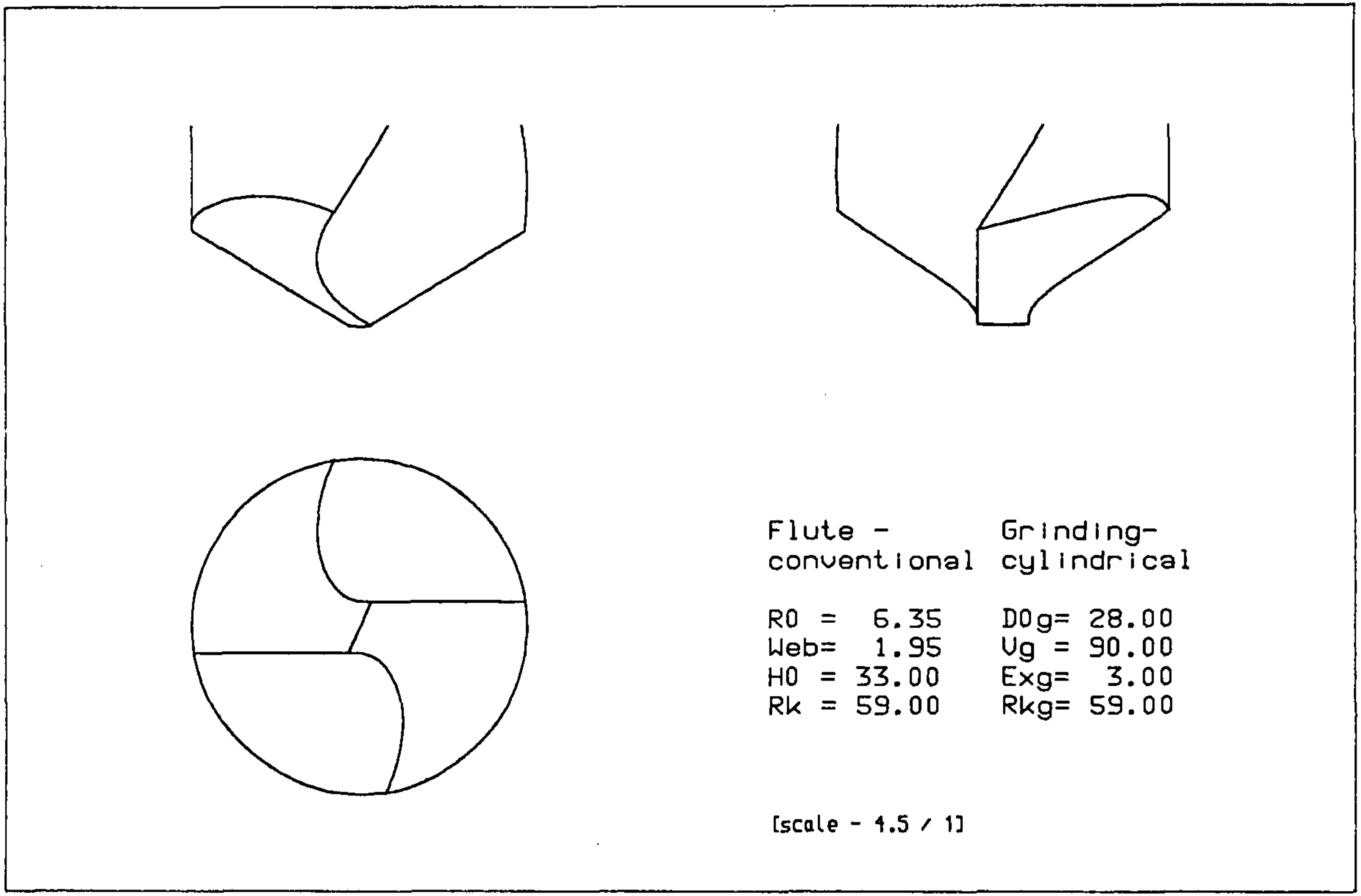


FIGURE 6.11: Computer geometric simulation of conventional flute drill point.[Refer to TABLE 6.3]

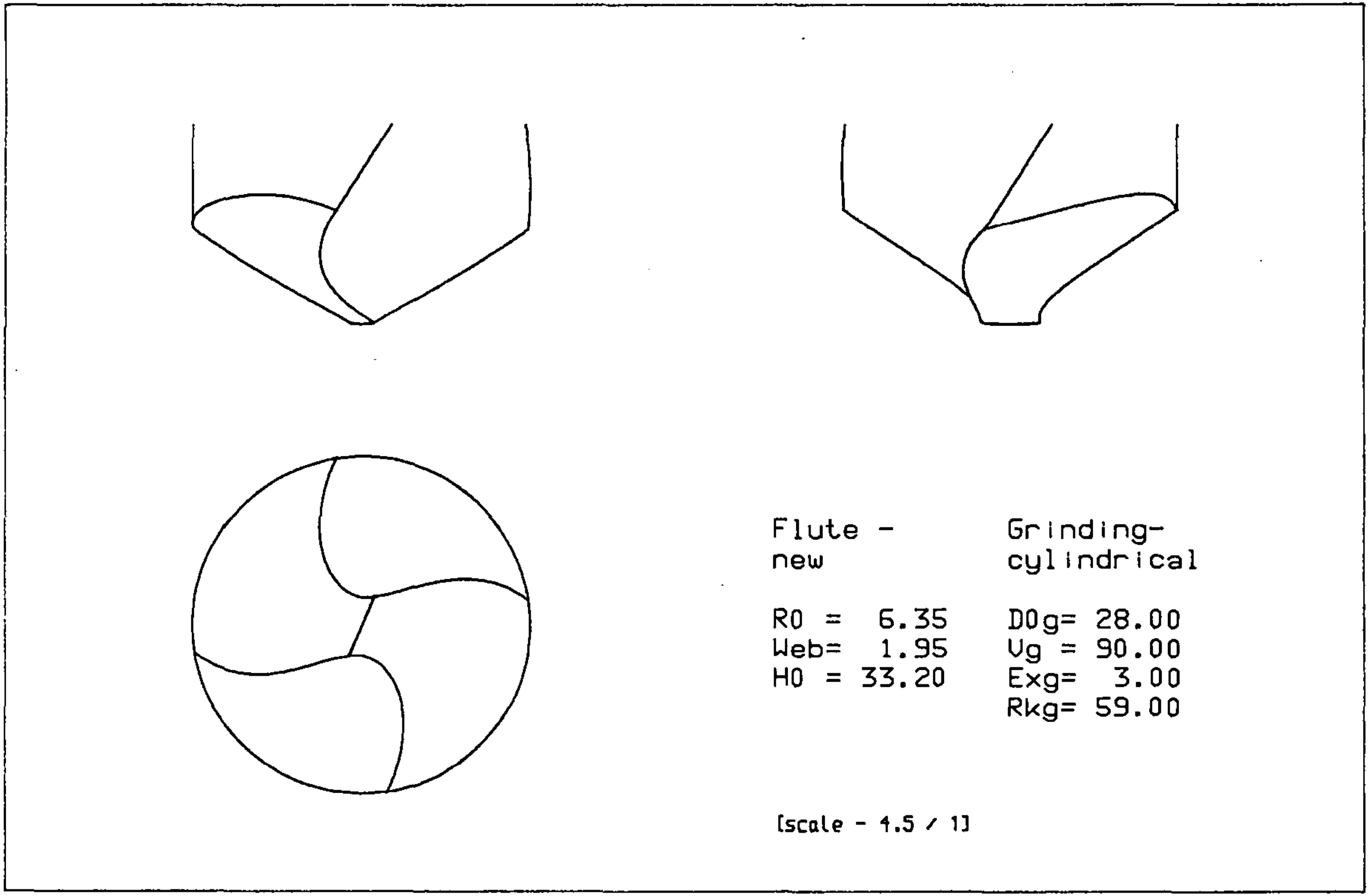


FIGURE 6.12: Computer geometric simulation of new design Flute drill point.[Refer to TABLE 6.3]

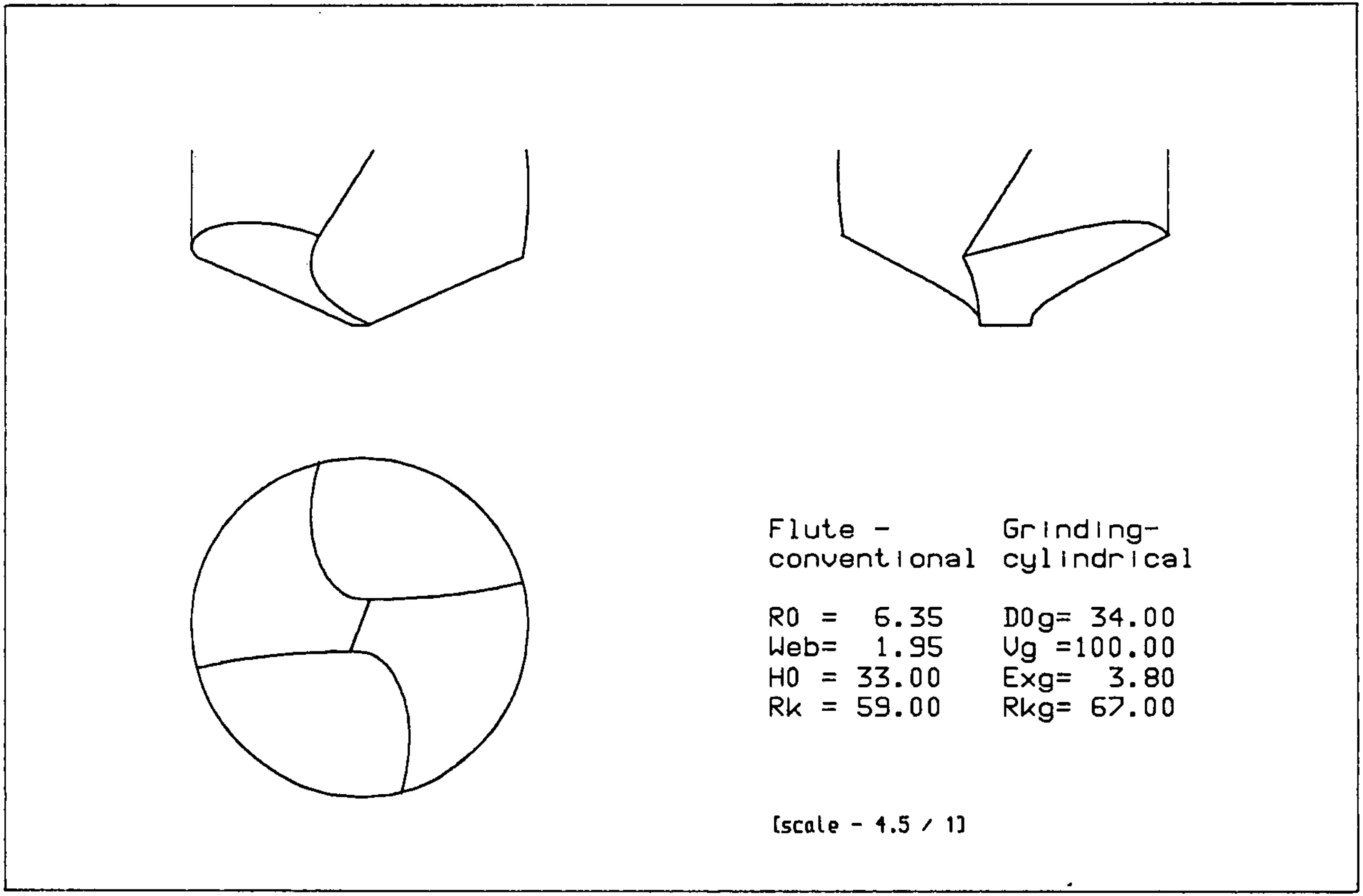


FIGURE 6.13: Computer geometric simulation of conventional flute drill point. [Refer to TABLE 6.4]

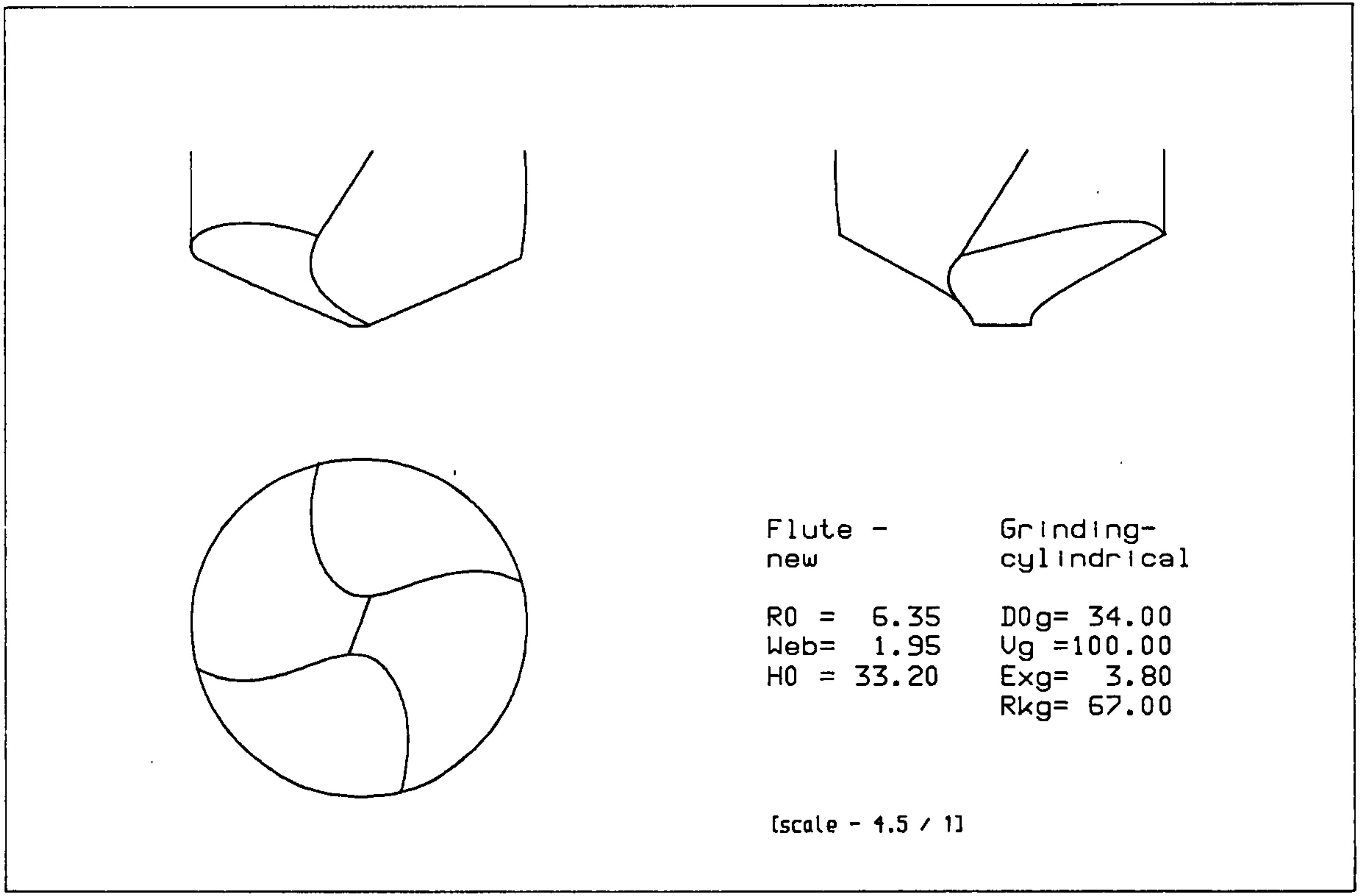


FIGURE 6.14: Computer geometric simulation of new design flute drill point.[Refer to TABLE 6.4]

### 6.3.3 Material

Selection of the testing material was limited to existing stocks in CIS (Centre for Industrial Studies, Loughborough University).

152 mm x 152 mm x 77 mm (6" x 6" x 3") blocks of EN43 steel in the normalised condition were used for the wear tests. The nominal chemical composition for this steel is:

| C(%) | Si(%) | Mn(%) | S(%) | P(%) |
|---|---|---|---|---|
| 0.45/0.50 | 0.05/0.35 | 0.7/1.0 | 0.06 Max. | 0.06 Max |

A sample analysis indicated that the material was within the chemical specifications.

The blocks were machined on both faces for parallelism and surface roughness uniformity. The hardness was measured on all blocks, on both faces and it was found that approximately 90% of the readings fall in the interval 180 HB - 190 HB.

The blocks were drilled on both faces.

## 6.4 Wear Tests Results

The "screech" many times referred to in literature (Section 6.1.2) and observed in the workshop was the criterion to decide that the drilling operation should not be continued.

When "screech" occurred the bottom of the hole presented radial marks of the type already referred to by Singpurwalla and co-workers (86), and the electric power input to the drilling machine increased by a significant amount as also reported in (89).

"Screech" occurred in the following cases:

| | |
|---|---|
| $118^o$ x 1140 rpm x 240 RPI | Conventional drill - 90 holes<br>New design drill - 84 holes |
| $118^o$ x 1140 rpm x 157 RPI | Conventional drill - 77 holes<br>New design drill - 60 holes |
| $134^o$ x 1140 rpm x 240 RPI | Conventional drill - 50 holes<br>New design drill - 69 holes |
| $134^o$ x 1140 rpm x 157 RPI | Conventional drill - 31 holes<br>New design drill - 42 holes |

The results for the wear loss (Figure 6.1) at point 1 (Figure 6.8) against the number of holes drilled, for each set of drilling conditions, and for both drill types are shown from Figure 6.15 to Figure 6.22. Similar results for the outer 4 points selected along the drill lips are shown in Appendix 7.

The variation of the wear loss with point position along each lip of each drill type, at the neighbourhood of the outer corner, at the end of the 150th hole, or shortly before drill failure, is represented from Figures 6.23 to 6.30 for all sets of drilling conditions tested.

## 6.5 Analysis of the Results

The wear curves shown in Figures 6.15 to 6.22 and in Appendix 7 appear to fit phases A and B of the typical wear curve shown in Figure 6.2. Phase C of the referred to typical curve hardly could be noticed with point 5 (Appendix 7) for one experiment leading to drill failure ($134^o$ x 1140 rpm x 157 RPI).

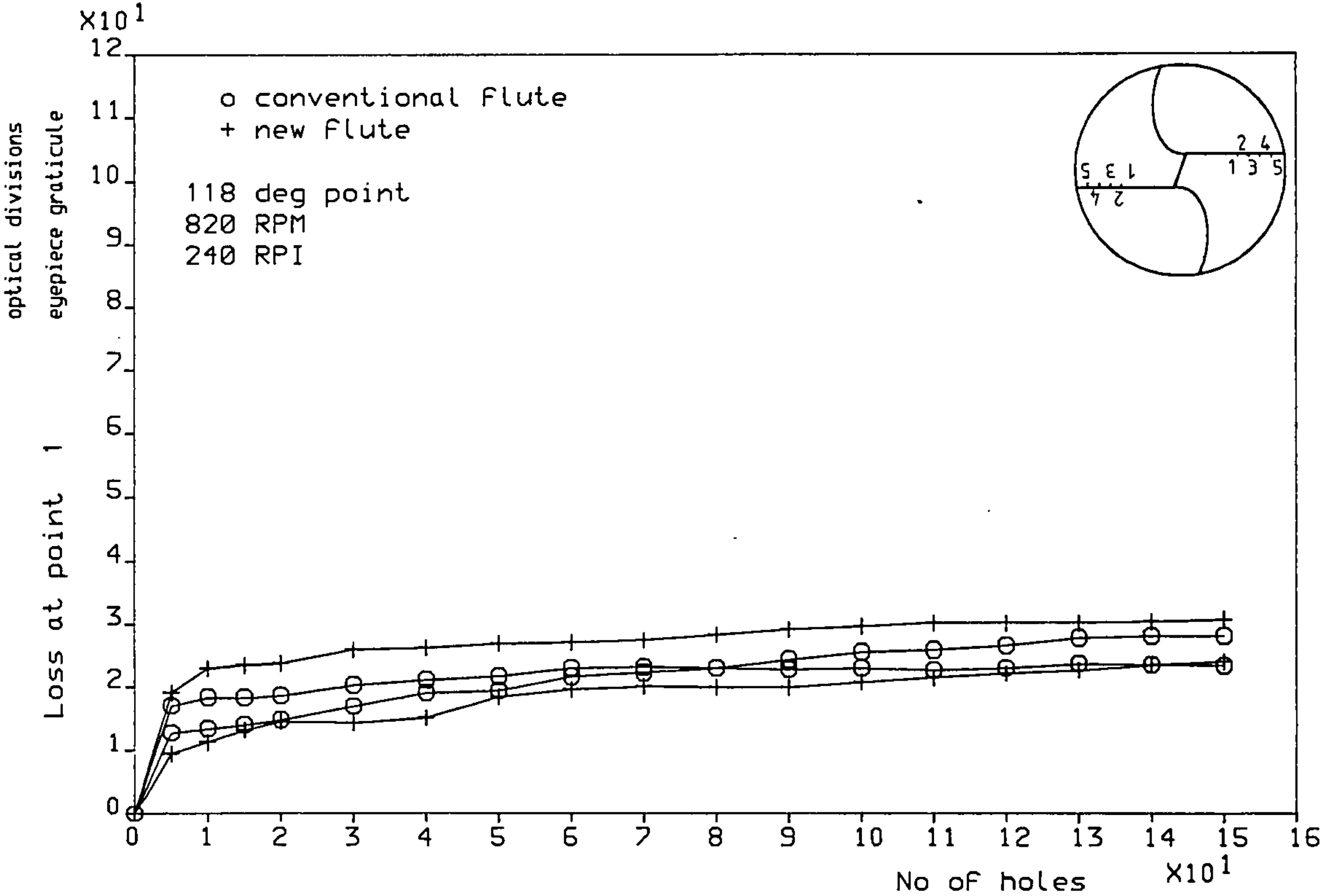


FIGURE 6.15: Wear loss at point 1 of each drill lip

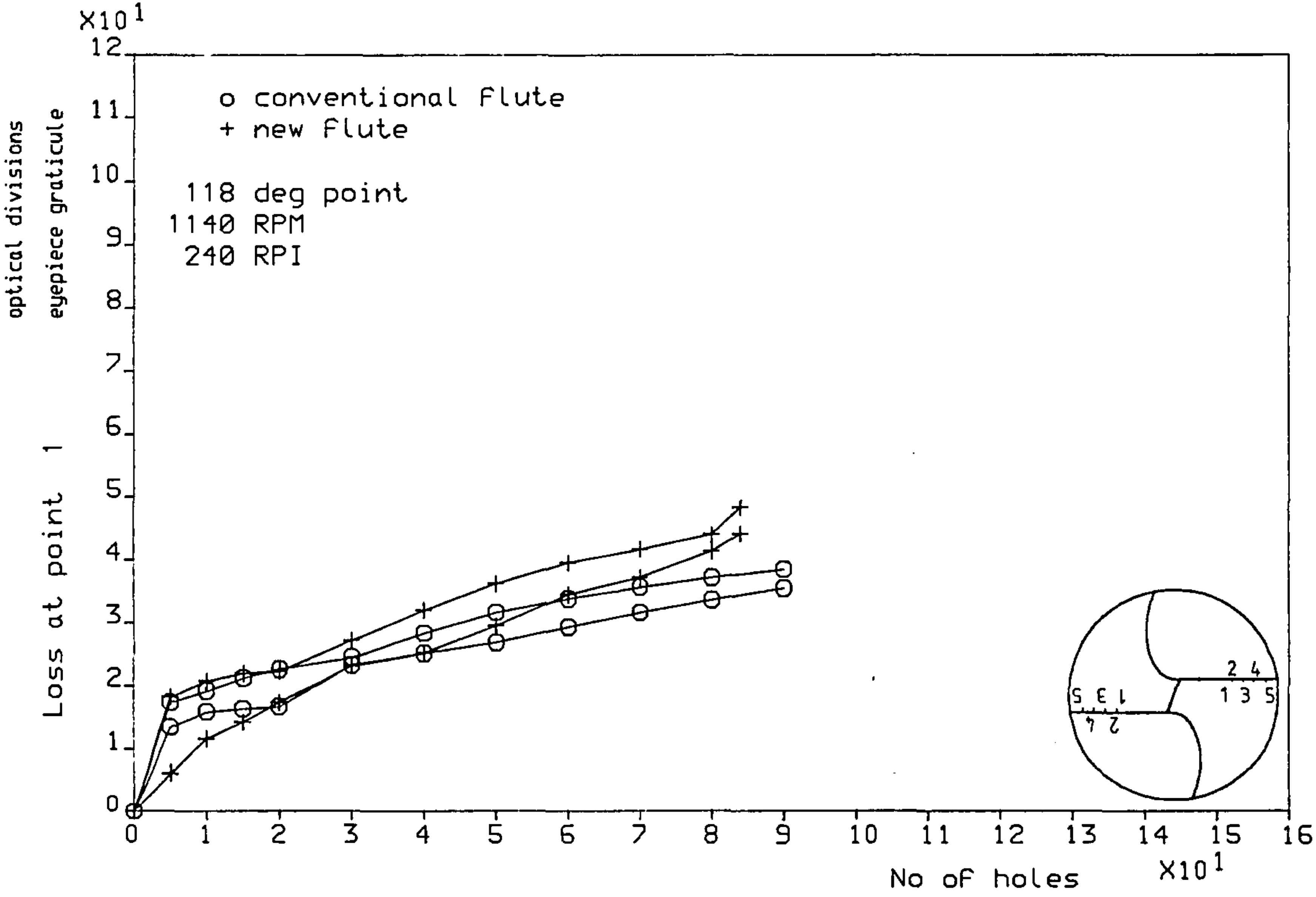


FIGURE 6.16: Wear loss at point 1 of each drill lip

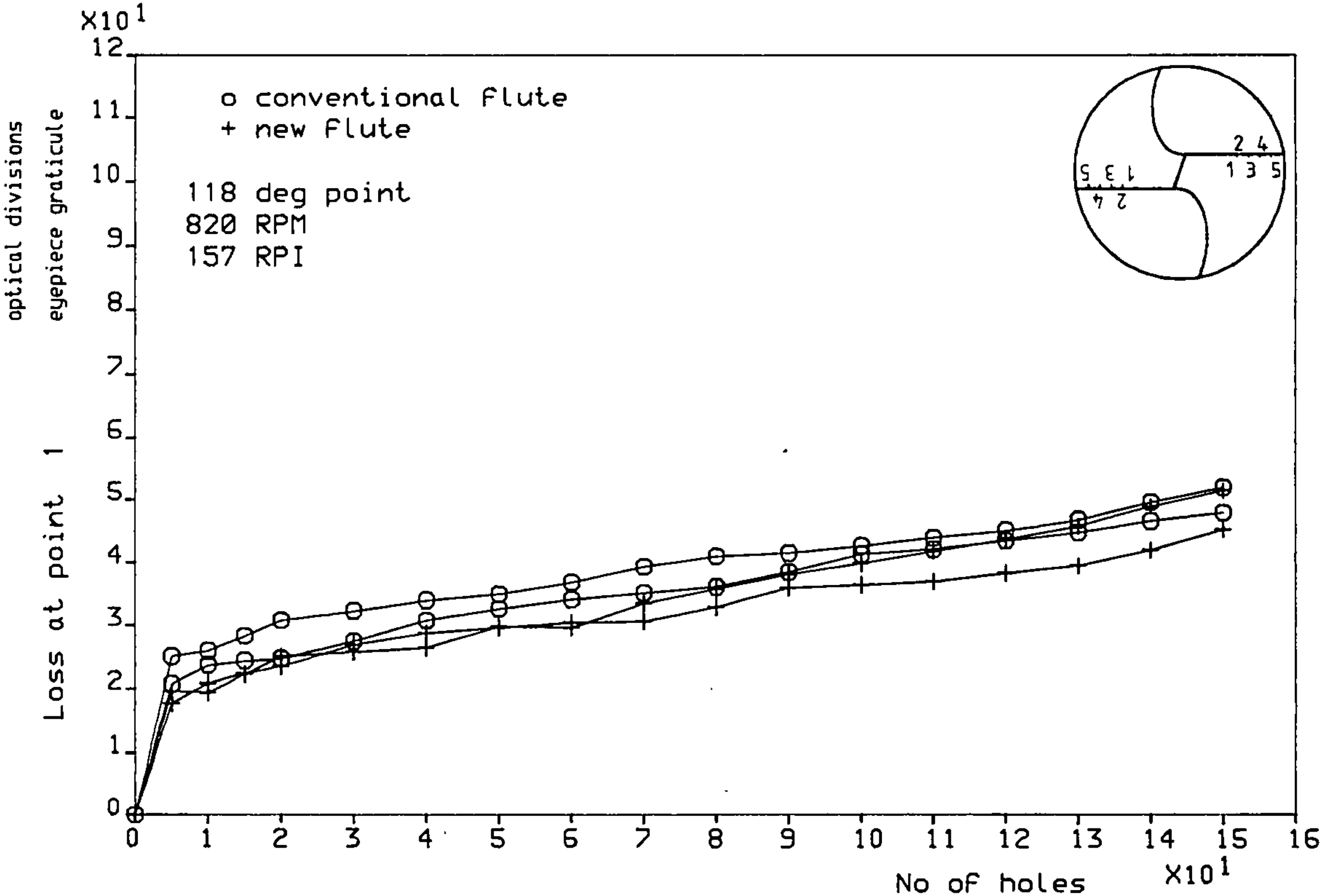


FIGURE 6.17: Wear loss at point 1 of each drill lip

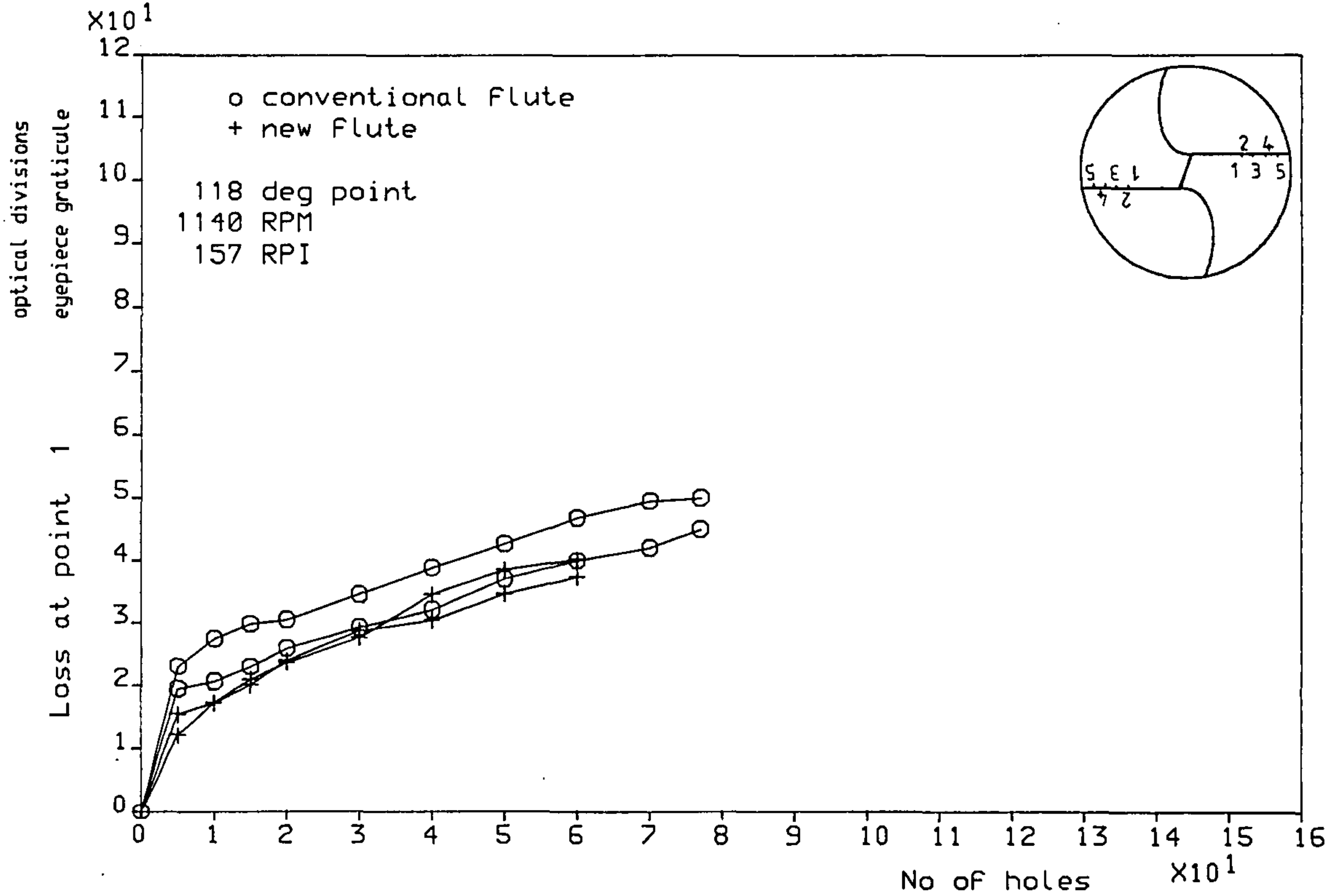


FIGURE 6.18: Wear loss at point 1 of each drill lip

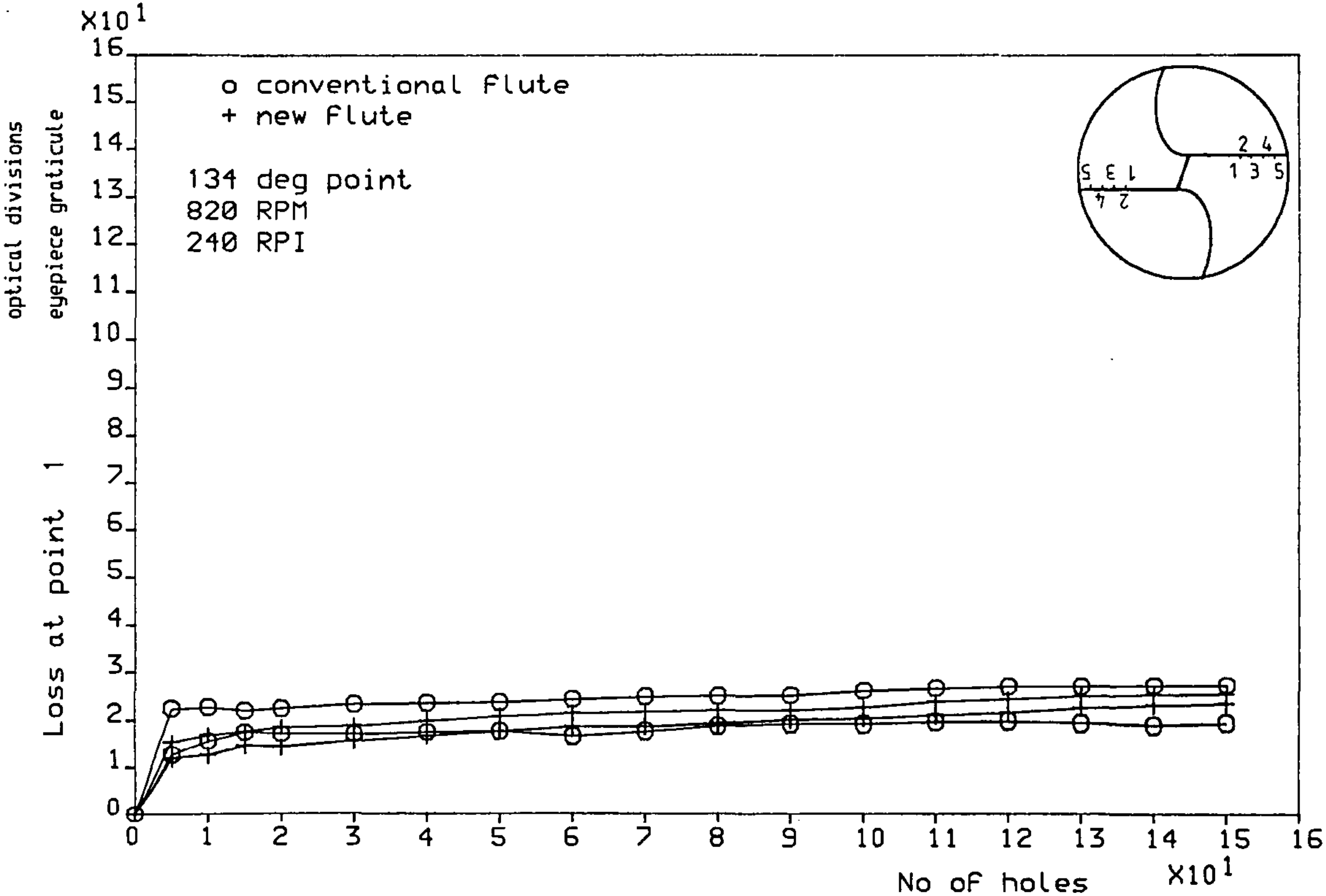


FIGURE 6.19: Wear loss at point 1 of each drill lip

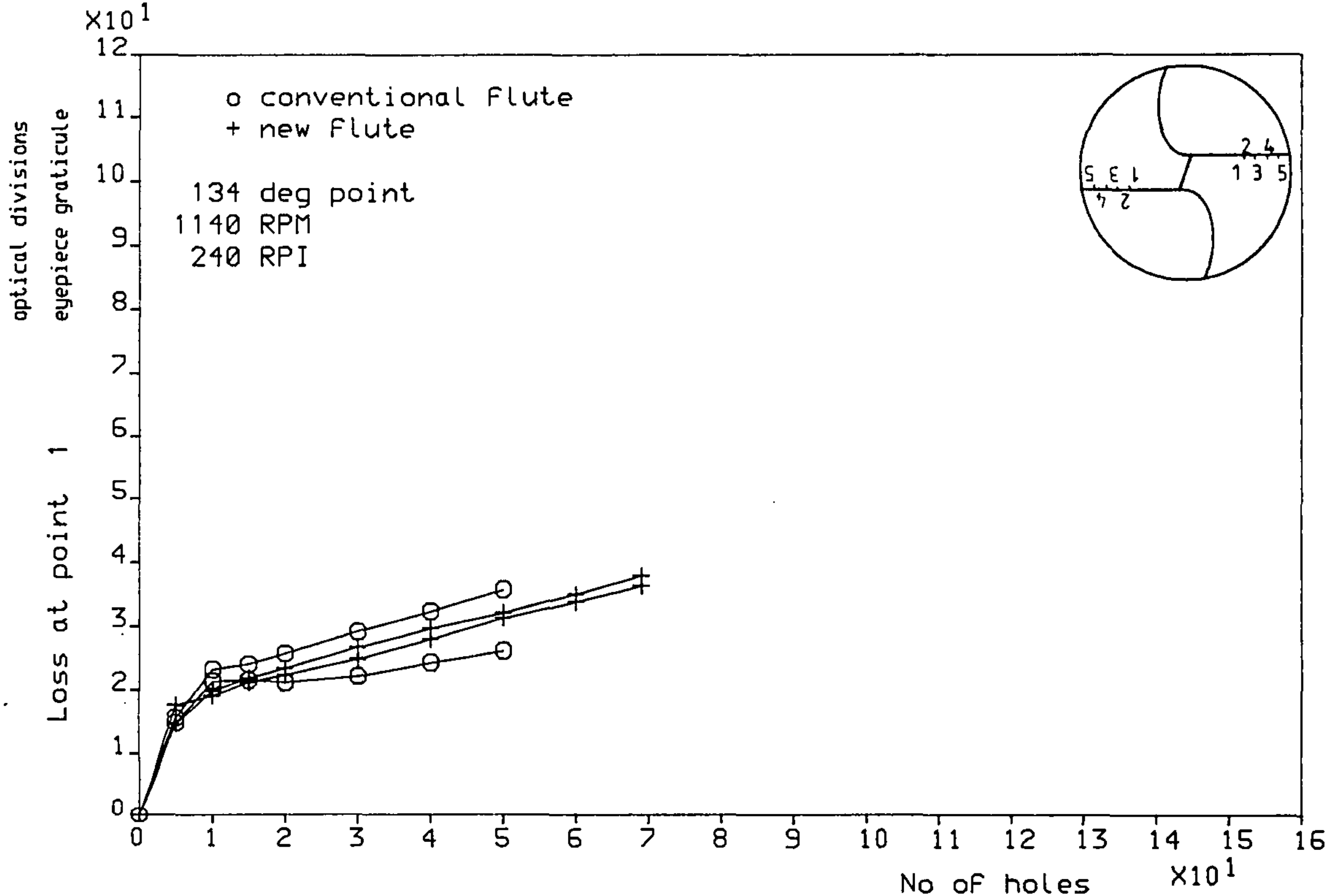


FIGURE 6.20: Wear loss at point 1 of each drill lip

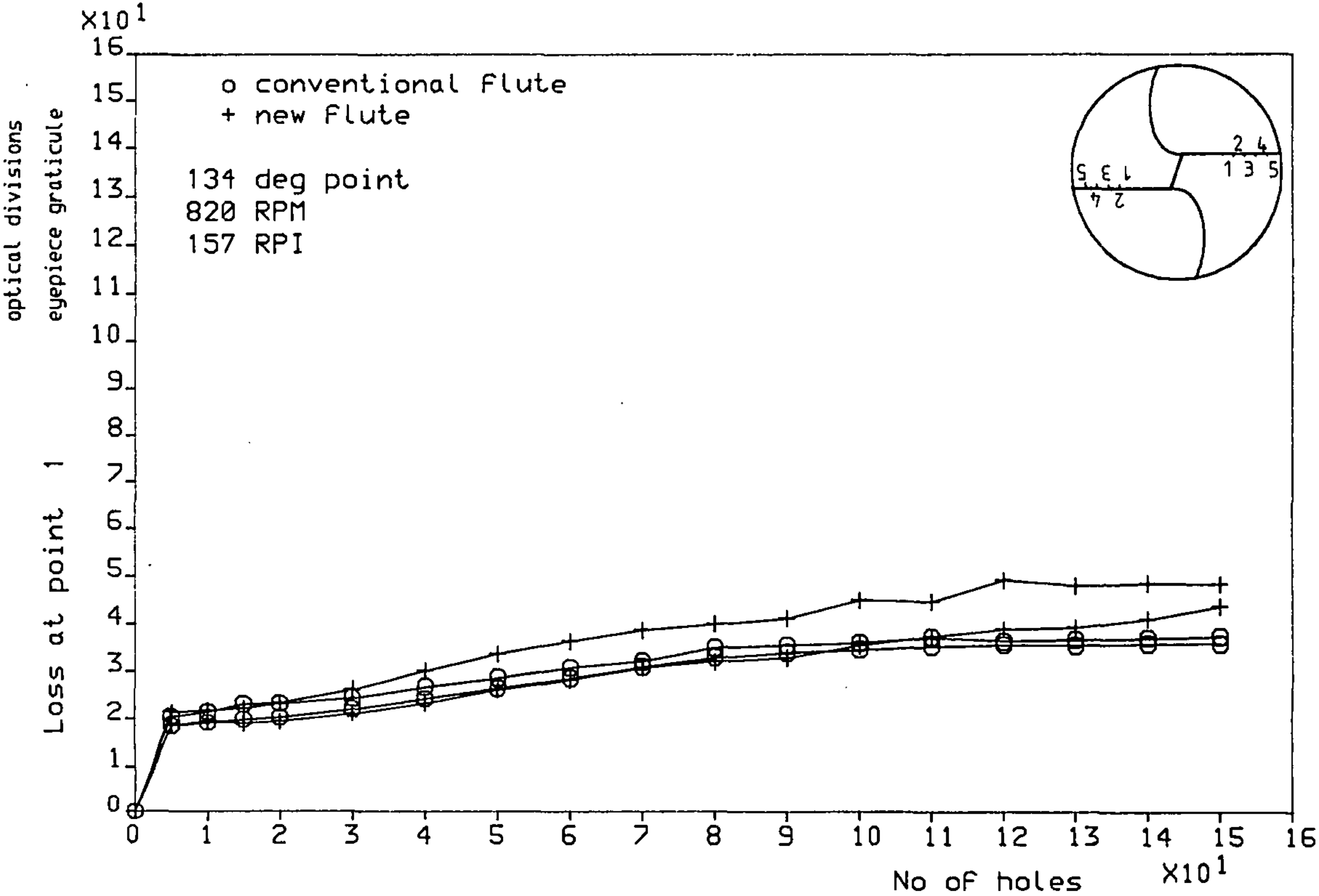


FIGURE 6.21: Wear loss at point 1 of each drill lip

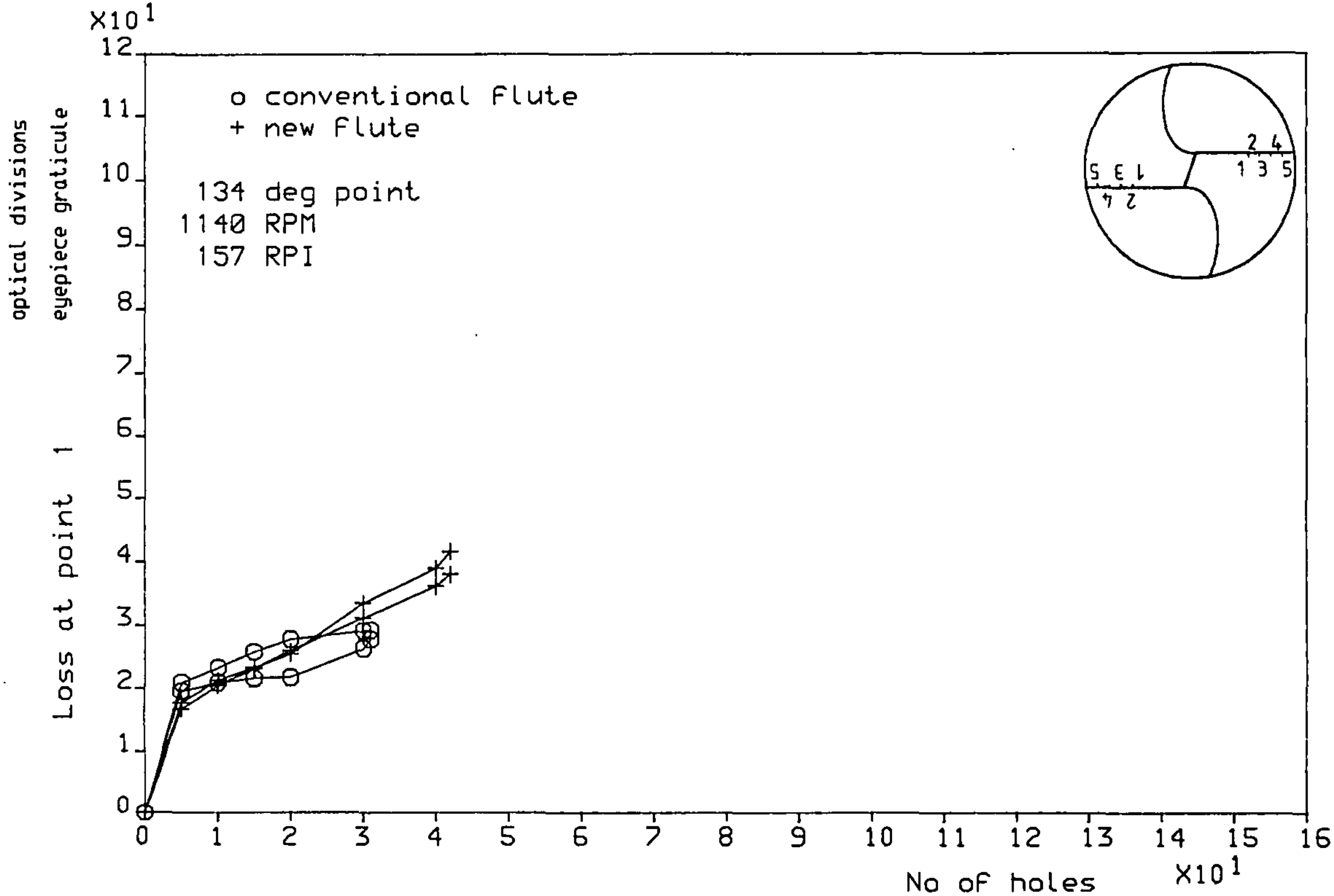


FIGURE 6.22: Wear loss at point 1 of each drill lip

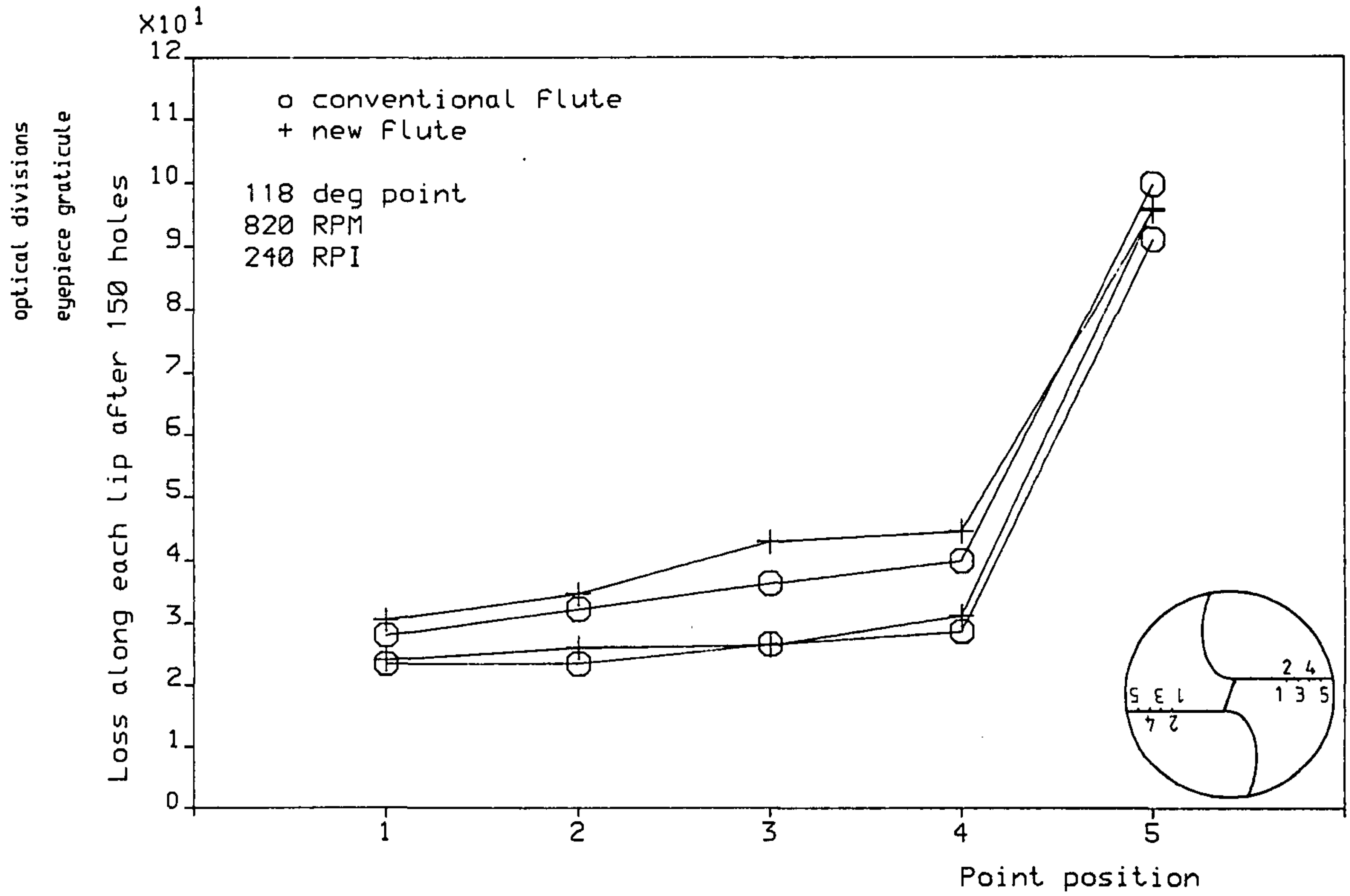


FIGURE 6.23: Wear loss at five points along each drill lip

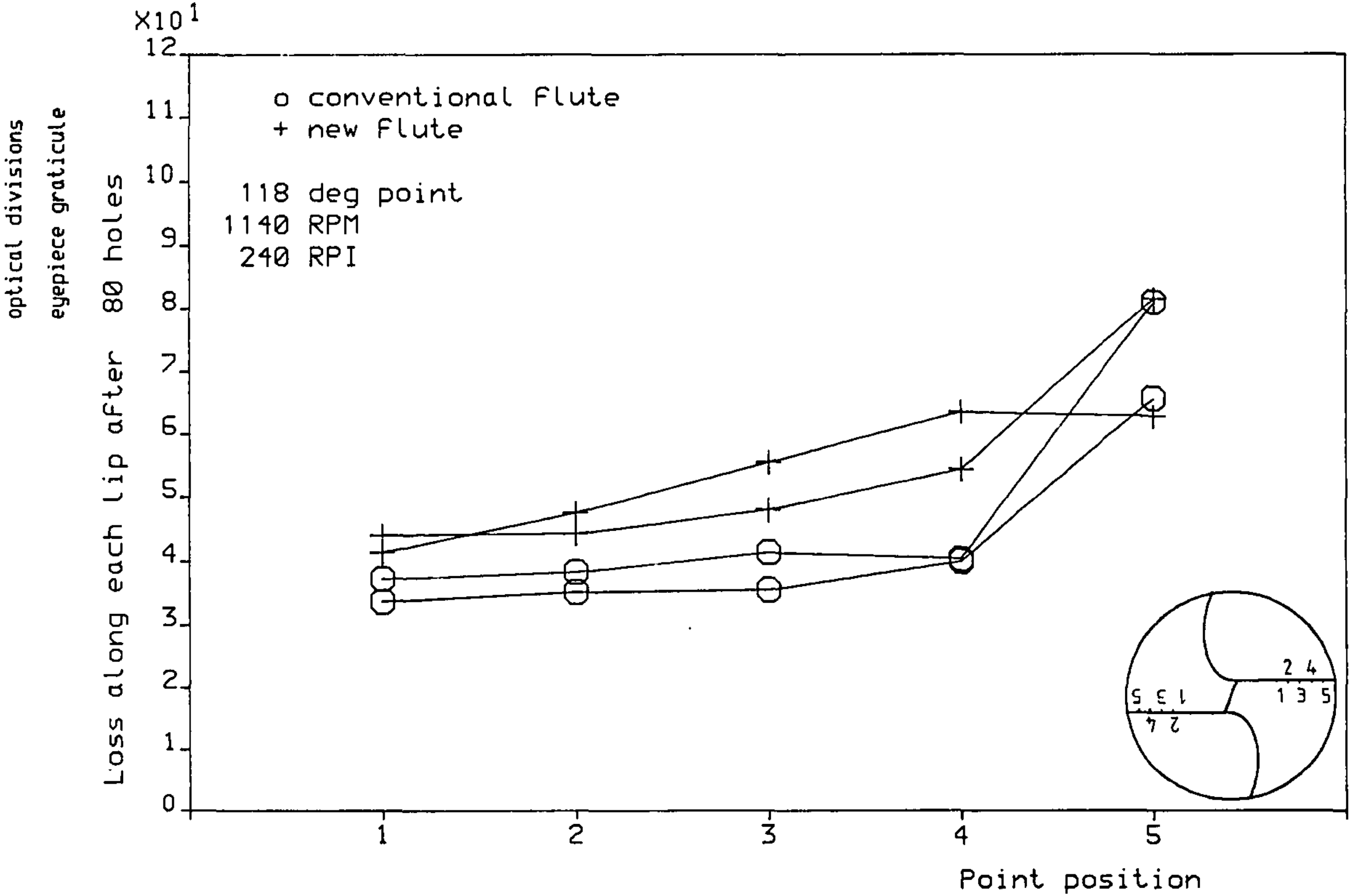


FIGURE 6.24 Wear loss at five points along each drill lip

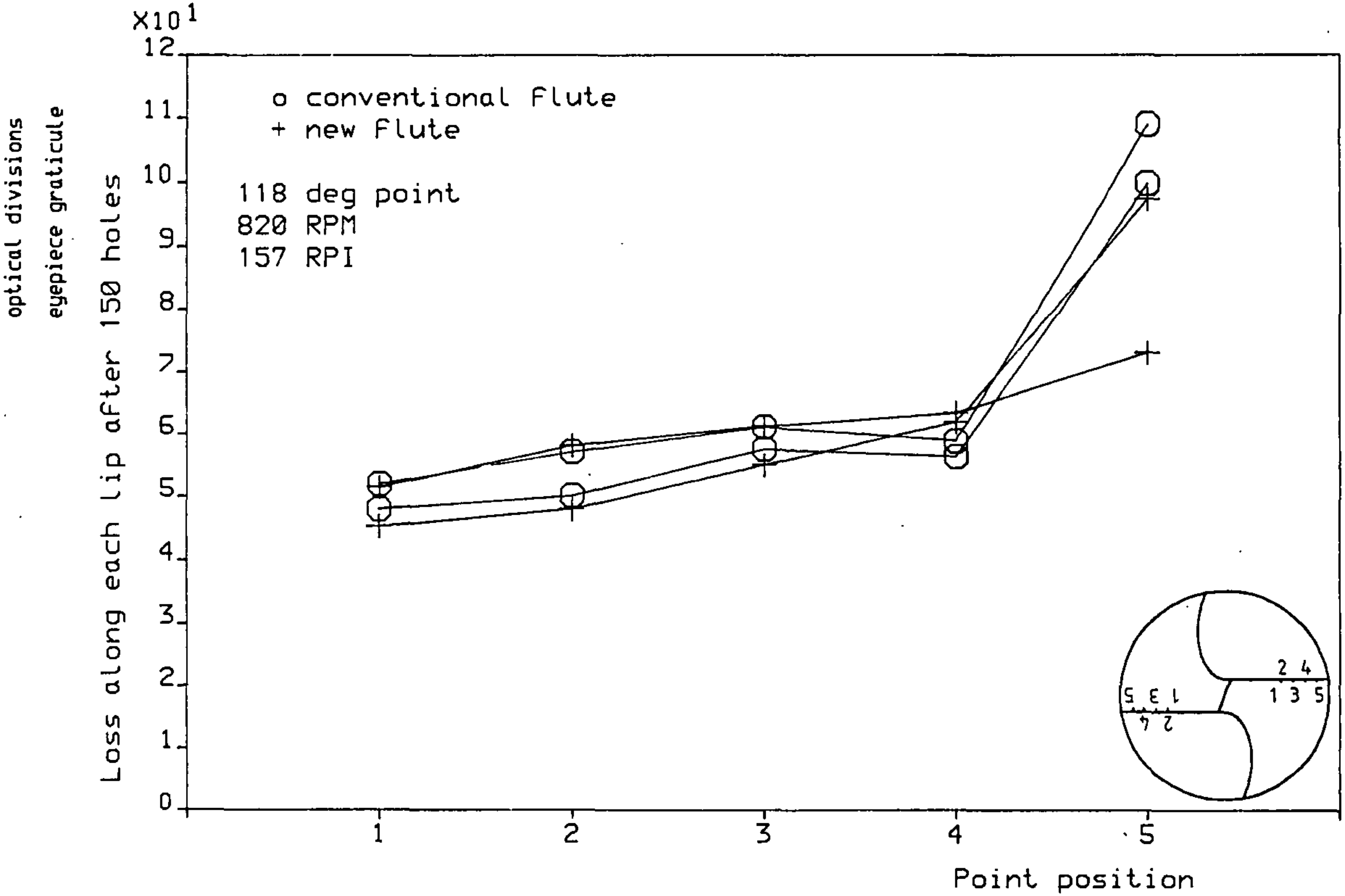


FIGURE 6.25: Wear loss at five points along each drill lip

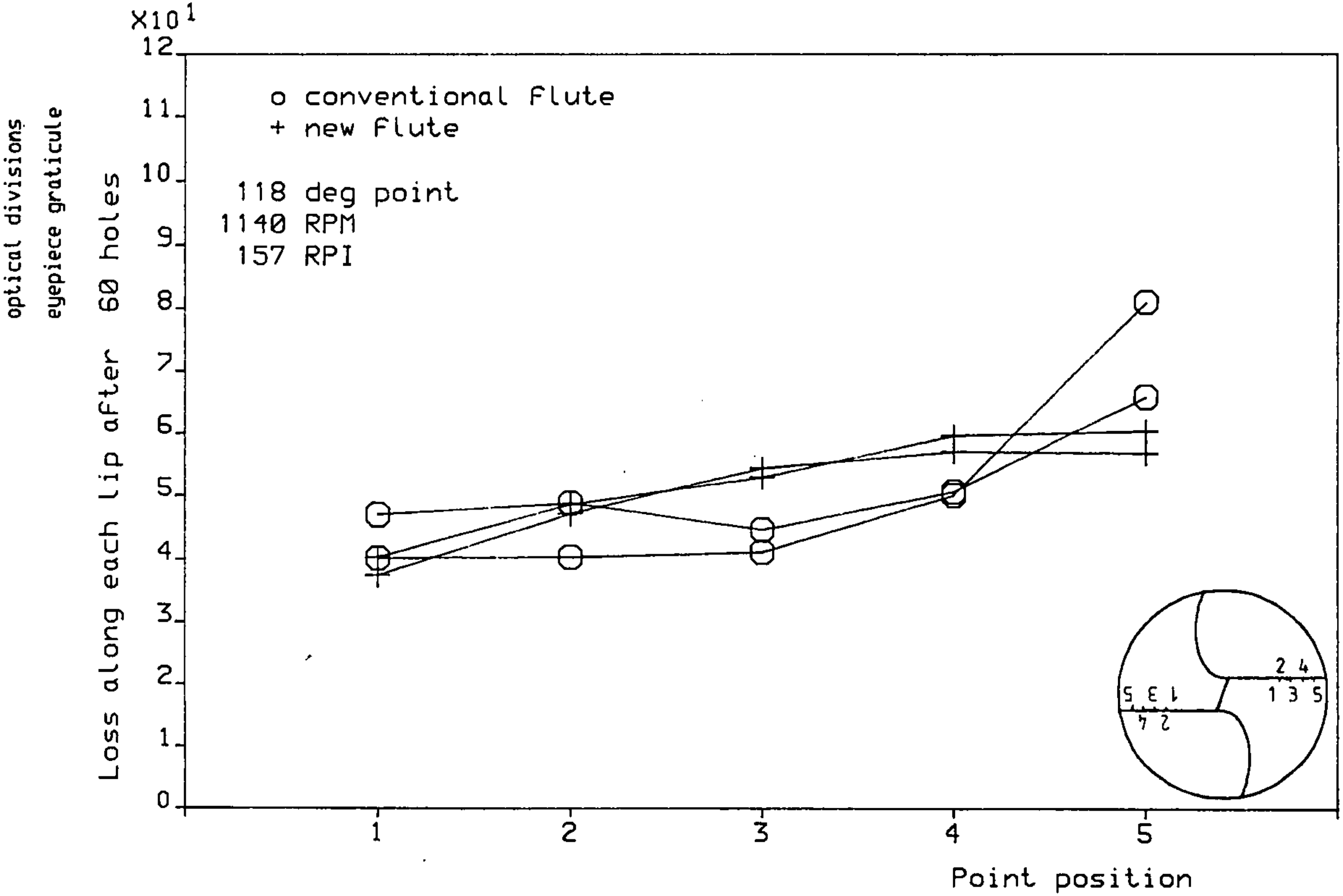


FIGURE 6.26: Wear loss at five points along each drill lip

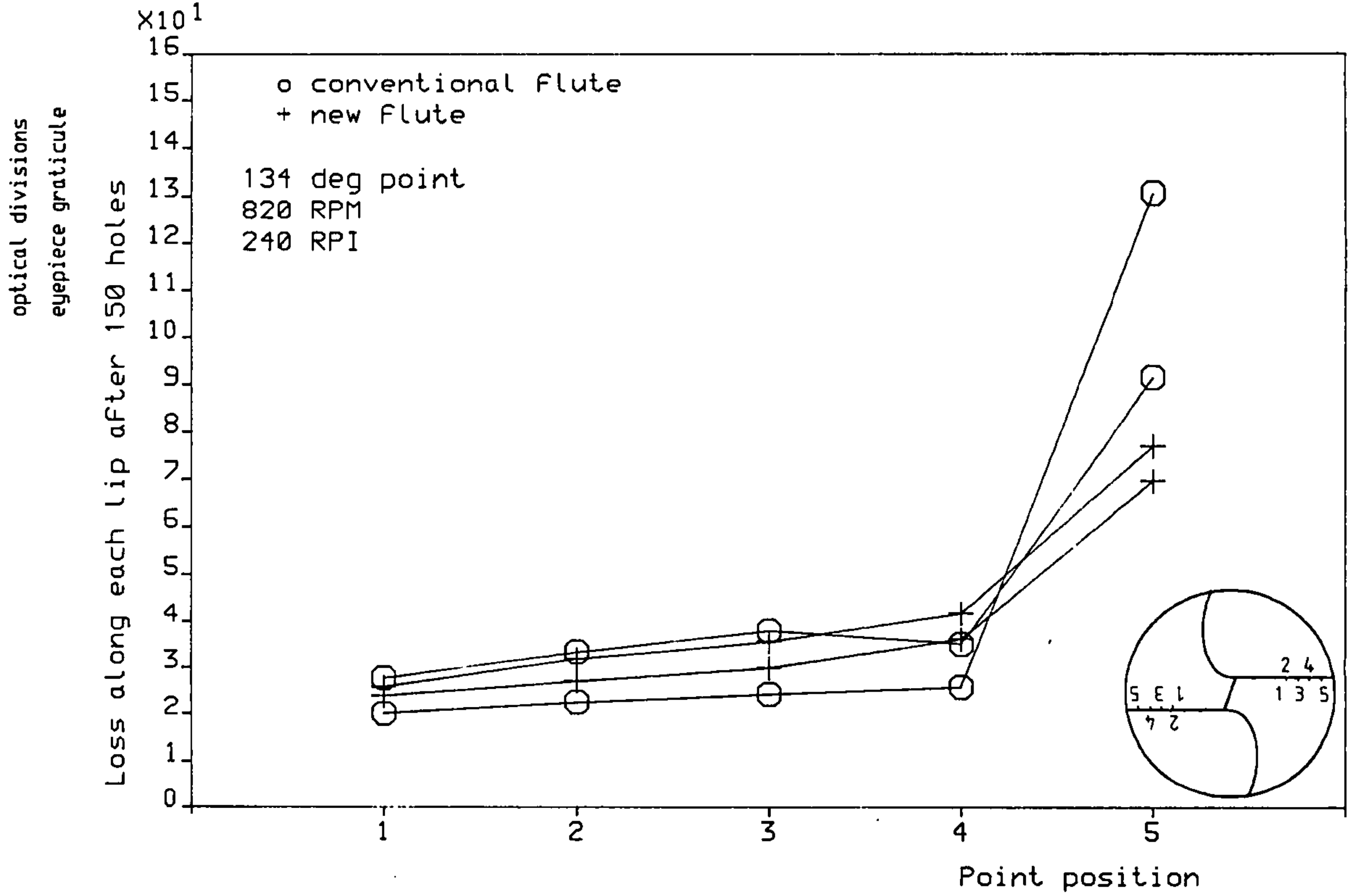


FIGURE 6.27: Wear loss at five points along each drill lip

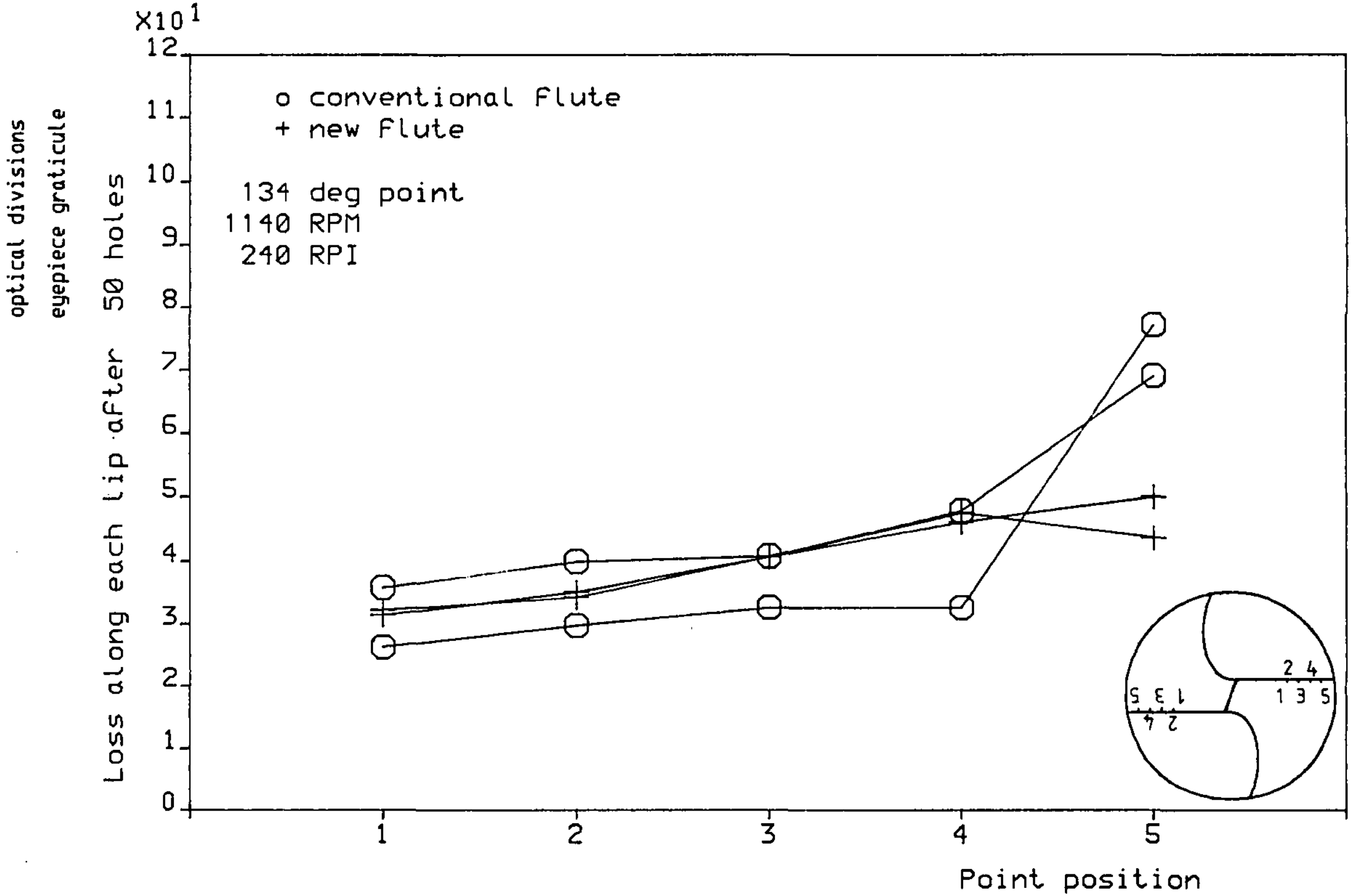


FIGURE 6.28: Wear loss at five points along each drill lip

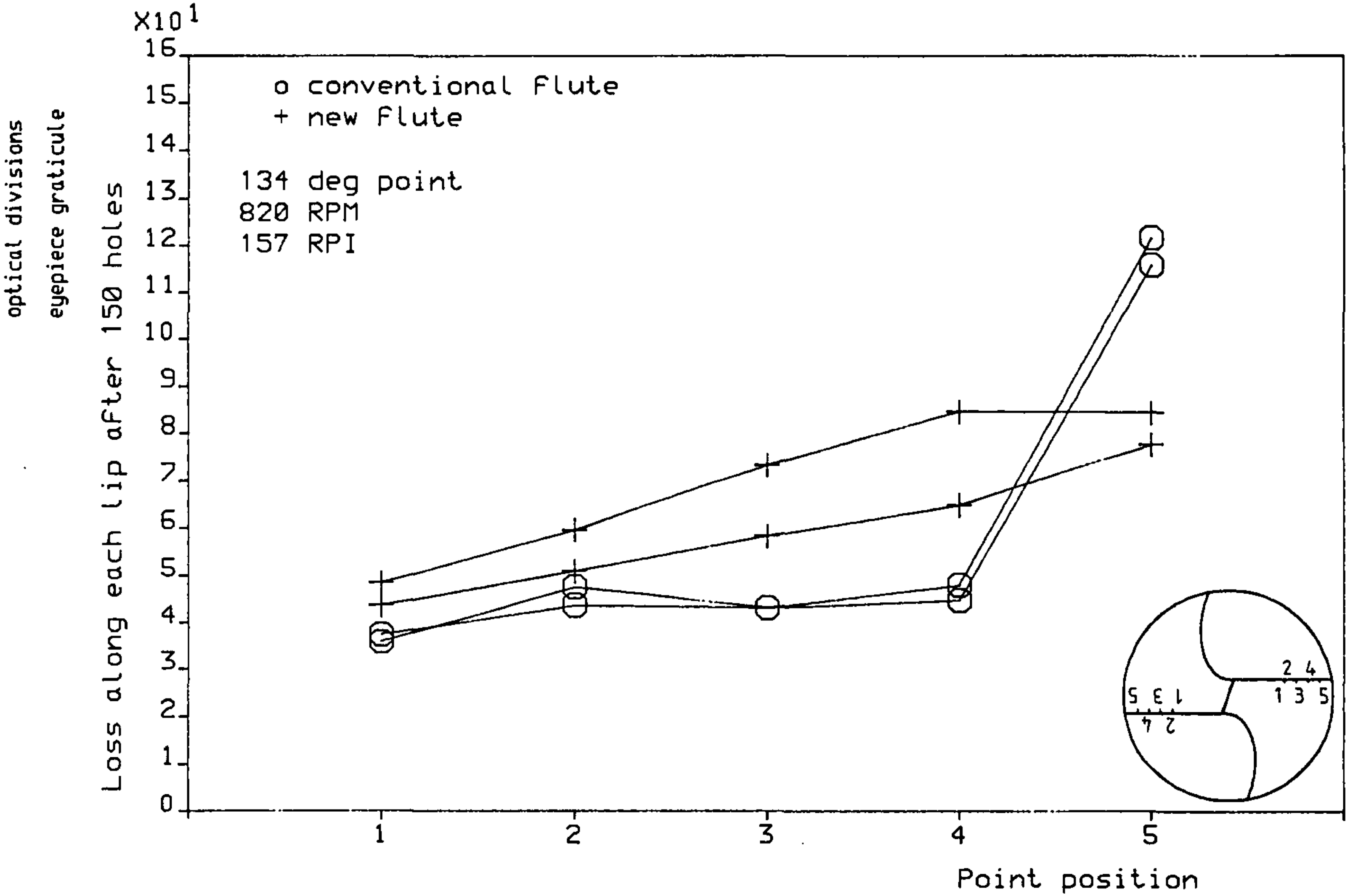


FIGURE 6.29: Wear loss at five points along each drill lip

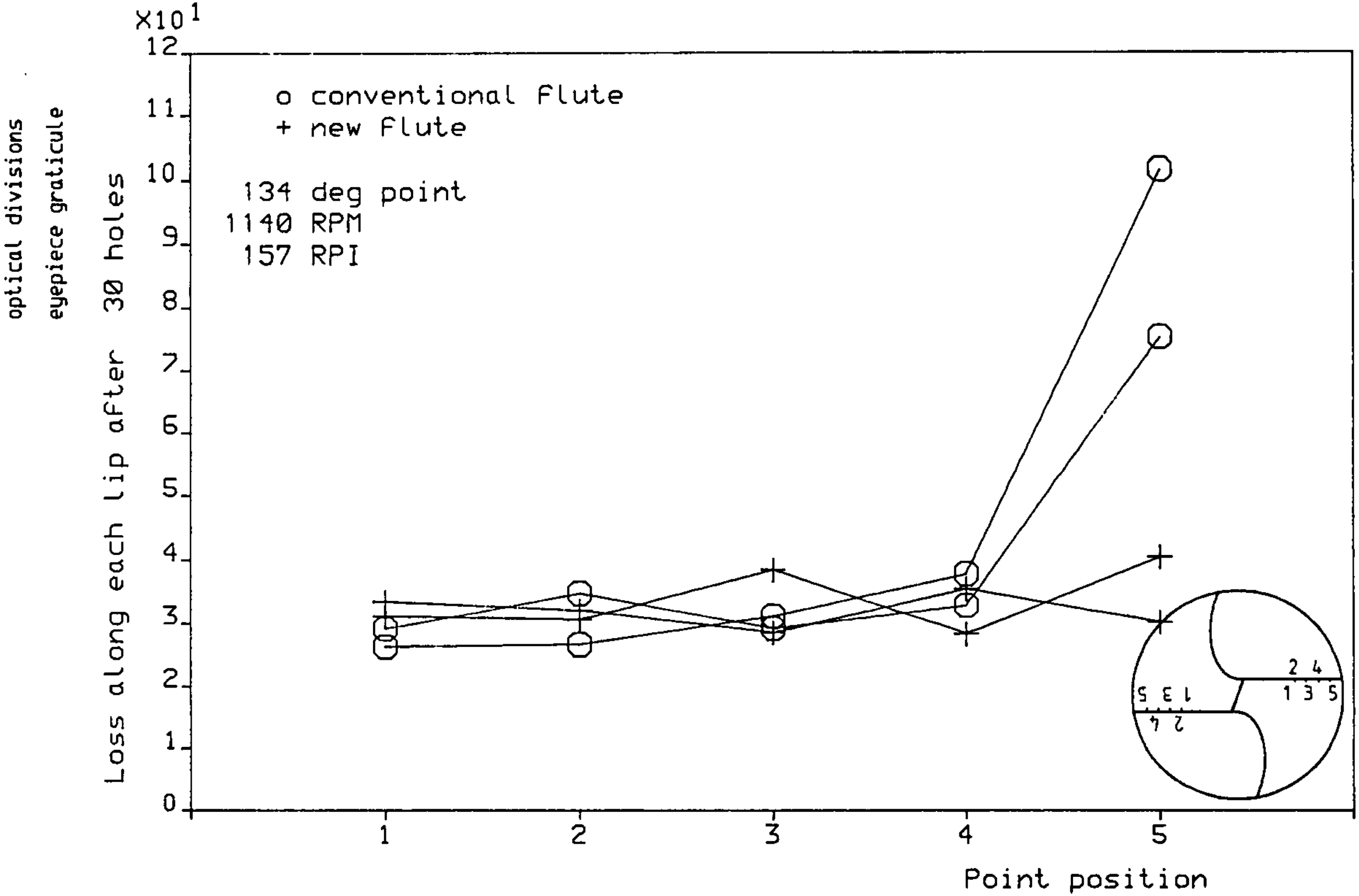


FIGURE 6.30: Wear loss at five points along each drill lip

There is an immediate detectable difference between the wear profiles referring to the new design drill and those for the conventional one: the initial phase A for the conventional drills portrays a more intense wear than that for the new design drill, especially with points 3, 4 and 5 (Appendix 7). For point 5, for instance, the wear loss relative to phase A of the wear curves is 2 to 3 times bigger with the conventional drill than with the new design drill.

Phase B is longer than phase A and it is expected to reflect more consistently the wear performance of each drill type.

To compare the wear performance of both drill types, the wear rate, measured by the slope of the straight line that better fits phase B of each wear curve (Figures 6.15 to 6.22 and Appendix 7), was computed and averaged for each pair of lips of each drill and for each set of drilling conditions. The results are shown in Table 6.5.

With few exceptions, all values shown in Table 6.5 appear to be higher for the new design drill than for the conventional one, for the same drilling conditions. Comparing the values for the new design drill with those for the conventional drill shown in Table 6.5, the minimum ratio was found to be 0.51 and the maximum 2.52. However, on average, the values of the wear rate for the new design drill are approximately 50% higher than those for the conventional drill, for the same speed, feed and point angle.

In order to test the statistical significance of the differences between the values shown in Table 6.5 an analysis of variance has been carried out on these values.

The results of the tests are arranged in two separate blocks: one referring to the conventional drill and another to the new design drill.

The results for point 1 (Figure 6.8) on the lips are taken from Table 6.5, multiplied by 10 for convenience of the calculations, and

TABLE 6.5: Wear Rate

In optical divisions per hole (Average for two lips. After Figures 6.15 - 6.22 and Appendix 7)

| Drill Type | Point Angle (deg) | RPI | RPM | Point 1 | Point 2 | Point 3 | Point 4 | Point 5 |
|---|---|---|---|---|---|---|---|---|
| Conventional | 118 | 240 | 820 | 0.071 | 0.053 | 0.066 | 0.088 | 0.350 |
| | | | 1140 | 0.230 | 0.250 | 0.298 | 0.316 | 0.345 |
| | | 157 | 820 | 0.168 | 0.180 | 0.184 | 0.159 | 0.350 |
| | | | 1140 | 0.335 | 0.380 | 0.391 | 0.436 | 0.465 |
| | 134 | 240 | 820 | 0.036 | 0.052 | 0.048 | 0.066 | 0.370 |
| | | | 1140 | 0.233 | 0.278 | 0.348 | 0.308 | 0.645 |
| | | 157 | 820 | 0.114 | 0.132 | 0.132 | 0.128 | 0.355 |
| | | | 1140 | 0.387 | 0.446 | 0.551 | 0.756 | 1.275 |
| New | 118 | 240 | 820 | 0.044 | 0.068 | 0.087 | 0.121 | 0.465 |
| | | | 1140 | 0.375 | 0.407 | 0.464 | 0.550 | 0.660 |
| | | 157 | 820 | 0.176 | 0.207 | 0.276 | 0.289 | 0.415 |
| | | | 1140 | 0.371 | 0.468 | 0.614 | 0.690 | 0.720 |
| | 134 | 240 | 820 | 0.064 | 0.084 | 0.104 | 0.146 | 0.325 |
| | | | 1140 | 0.292 | 0.342 | 0.390 | 0.456 | 0.440 |
| | | 157 | 820 | 0.186 | 0.248 | 0.280 | 0.322 | 0.340 |
| | | | 1140 | 0.590 | 0.639 | 0.608 | 0.664 | 0.650 |

presented in Table 6.6 (refer to Section 6.2.5 for the meaning of the symbols).

TABLE 6.6: Wear Rate (x 10)

Point 1 on the lips

Block C (Conventional drill)

| Treatment (drilling condition) | Yield (wear rate x 10) |
|---|---|
| (1) | 0.71 |
| s | 2.30 |
| f | 1.68 |
| sf | 3.35 |
| $\kappa$ | 0.36 |
| s$\kappa$ | 2.33 |
| f$\kappa$ | 1.14 |
| sf$\kappa$ | 3.87 |
| Total: | 15.74 |

Block N (New design Drill)

| Treatment (drilling condition) | Yield (wear rate x 10) |
|---|---|
| (1) | 0.44 |
| s | 3.75 |
| f | 1.76 |
| sf | 3.71 |
| $\kappa$ | 0.64 |
| s$\kappa$ | 2.92 |
| f$\kappa$ | 1.86 |
| sf$\kappa$ | 5.90 |
| Total: | 20.98 |

Total Sum: 15.74 + 20.98 = 36.72

TABLE 6.7: Sum of Squares (Ref to Table 6.6)

Point 1 on the lips

Block C

| Treatment | Yield |
|---|---|
| (1) | 0.504 |
| s | 5.290 |
| f | 2.822 |
| sf | 11.222 |
| κ | 0.130 |
| sκ | 5.429 |
| fκ | 1.300 |
| sfκ | 14.977 |
| Total: | 41.674 |

Block N

| Treatment | Yield |
|---|---|
| (1) | 0.194 |
| s | 14.063 |
| f | 3.098 |
| sf | 13.764 |
| κ | 0.410 |
| sκ | 8.526 |
| fκ | 3.460 |
| sfκ | 34.810 |
| Total: | 78.325 |

Sum of square (Table 6.7):

Sum of squares within Block C:

$$41.674 - \frac{(15.74)^2}{8} = 10.706$$

Sum of squares within Block N:

$$78.325 - \frac{(20.98)^2}{8} = 23.305$$

Total sum of squares $= 41.674 + 78.325 - \frac{(36.72)^2}{16} = 35.727$

Between blocks sum of squares:

$$\frac{(15.74)^2}{8} + \frac{(20.98)^2}{8} - \frac{(36.72)^2}{16} = 1.716$$

Total sum of squares within blocks:

$$10.706 + 23.305 = 34.011$$

Analysis of variance between and within blocks is shown in Table 6.8.

TABLE 6.8: Analysis of Variance
Point 1 on the lips

| Source | Sum of Squares | Degrees of Freedom |
|---|---|---|
| Between blocks | 1.716 | 1 |
| Within blocks | 34.011 | 14 |
| Total: | 35.727 | 15 |

TABLE 6.9: Treatment Sum of Squares (refer to Table 6.6)
Point 1 on the lips
Block C + Block N

| Treatment | Yield C + Yield N | (Yield C + Yield N)$^2$ |
|---|---|---|
| (1) | 1.15 | 1.3225 |
| s | 6.05 | 36.6025 |
| f | 3.44 | 11.8336 |
| sf | 7.06 | 49.8436 |
| κ | 1.00 | 1.0000 |
| sκ | 5.25 | 27.5625 |
| fκ | 3.00 | 9.0000 |
| sfκ | 9.77 | 95.4529 |
| | Total: | 232.6176 |

Treatment sum of squares (Table 6.9:

$$\frac{232.6176}{2} - \frac{(36.72)^2}{16} = 32.036$$

Table 6.10 shows the sum of squares relative to residual treatments and between blocks.

TABLE 6.10: Analysis of Variance
Point 1 on lips

| Source | Sum of Squares | Degrees of Freedom |
|---|---|---|
| Between blocks | 1.716 | 1 |
| Treatments | 32.036 | 7 |
| Residual | 1.975 | 7 |
| Total: | 35.727 | 15 |

According to a common algorithm (105, 124) the effect of factor S, for instance, can be represented as follows:

$$(s - (1))\ (f + (1))\ (\kappa + (1)) = sf\kappa + sf + s\kappa$$

$$- f\kappa + s - f - \kappa - (1)$$

Similar "expressions" can be used for the other cases. The effects of the different combinations of factors are presented in Table 6.11. In Table 6.12 is presented the analysis of variance for all factors and their interactions.

Proceeding in a similar way as for point 1 for the analysis of variance of the wear rate at points 2, 3, 4 and 5, the effects of the different factors and their interactions were computed and presented in Tables 6.13, 6.14, 6.15 and 6.16 respectively.

TABLE 6.11: Treatment Effect

Point 1 on the lips

| Effect of | sfκ | f | sκ | fκ | s | f | κ | (1) | Total | Square | Sum of Squares |
|---|---|---|---|---|---|---|---|---|---|---|---|
| S | 9.77 | +7.06 | +5.25 | -3.00 | +6.05 | -3.44 | -1.00 | -1.15 | 19.54 | 381.812 | 23.863 |
| F | 9.77 | +7.06 | -5.25 | +3.00 | -6.05 | +3.44 | -1.00 | -1.15 | 9.82 | 36.432 | 6.027 |
| SF | 9.77 | +7.06 | -5.25 | -3.00 | -6.05 | -3.44 | +1.00 | +1.15 | 1.24 | 1.5383 | 0.096 |
| κ | 9.77 | -7.06 | +5.25 | +3.00 | -6.05 | -3.44 | +1.00 | -1.15 | 1.32 | 1.742 | 0.109 |
| Sκ | 9.77 | -7.06 | +5.25 | -3.00 | -6.05 | +3.44 | -1.00 | +1.15 | 2.50 | 6.25 | 0.391 |
| Fκ | 9.77 | -7.06 | -5.25 | +3.00 | +6.05 | -3.44 | -1.00 | +1.15 | 3.22 | 10.368 | 0.648 |
| SFκ | 9.77 | -7.06 | -5.25 | -3.00 | +6.05 | +3.44 | +1.00 | -1.15 | 3.80 | 14.44 | 0.902 |

TOTAL 32.036

TABLE 6.12: Analysis of Variance (Refer to Tables 6.10 and 6.11)
Point 1 on the lips

| Source<br>(i) | Sum of Squares<br>(ii) | | Degrees of Freedom<br>(iii) | | Variance Estimate Mean Square<br>(iv)=(ii)/(iii) | Variance Ratio<br>(v) | |
|---|---|---|---|---|---|---|---|
| Between Blocks | | 1.716 | | 1 | 1.716 | 6.09 | * |
| Treatments | | 32.036 | | 7 | | | |
| s | 23.863 | | 1 | | 23.863 | 84.62 | *** |
| f | 6.027 | | 1 | | 6.027 | 21.37 | ** |
| κ | 0.109 | | 1 | | 0.109 | 0.39 | n.s. |
| sf | 0.096 | | 1 | | 0.096 | 0.34 | n.s. |
| sκ | 0.391 | | 1 | | 0.391 | 1.39 | n.s. |
| fκ | 0.648 | | 1 | | 0.648 | 2.30 | n.s. |
| sfκ | 0.902 | | 1 | | 0.902 | 3.20 | n.s. |
| Residual | | 1.975 | | 7 | 0.282 | 1.00 | |
| Total: | | 35.727 | | 15 | | | |

*** Significant at 0.1% level (highly significant (105))

** Significant at 1% level (significant (105))

* Significant at 5% level (probably significant (105))

n.s. Not significant at 5% level (non-significant(105))

TABLE 6.13: Analysis of Variance

Point 2 on the lips

| Source (i) | Sum of Squares (ii) | | Degrees of Freedom (iii) | | Variance Estimate Mean Square (iv)=(ii)/(iii) | Variance Ratio (v) | |
|---|---|---|---|---|---|---|---|
| Between blocks | | 2.993 | | 1 | 2.993 | 14.29 | ** |
| Treatments | | 39.942 | | 7 | | | |
| s | 29.866 | | 1 | | 29.866 | 142.63 | *** |
| f | 8.497 | | 1 | | 8.497 | 40.58 | *** |
| κ | 0.270 | | 1 | | 0.270 | 1.29 | n.s. |
| sf | 0.133 | | 1 | | 0.133 | 0.64 | n.s. |
| sκ | 0.230 | | 1 | | 0.230 | 1.10 | n.s. |
| fκ | 0.397 | | 1 | | 0.397 | 1.90 | n.s. |
| sfκ | 0.548 | | 1 | | 0.548 | 2.62 | n.s. |
| Residual | | 1.466 | | 7 | 0.209 | 1.00 | |
| Total: | | 44.401 | | 15 | | | |

*** Significant at 0.1% level (highly significant (105))

** Significant at 1% level (significant (105))

n.s. Not significant at 5% level (non-significant (105))

TABLE 6.14: Analysis of Variance

Point 3 on the lips

| Source<br>(i) | Sum of Squares<br>(ii) | | Degrees of Freedom<br>(iii) | | Variance Estimate Mean Square<br>(iv)=(ii)/(iii) | Variance Ratio<br>(v) | |
|---|---|---|---|---|---|---|---|
| Between Blocks | | 4.050 | | 1 | 4.050 | 16.09 | ** |
| Treatments | | 48.852 | | 7 | | | |
| s | 38.657 | | 1 | | 38.657 | 153.57 | *** |
| f | 9.471 | | 1 | | 9.471 | 37.63 | *** |
| κ | 0.041 | | 1 | | 0.041 | 0.16 | n.s. |
| sf | 0.059 | | 1 | | 0.059 | 0.23 | n.s. |
| sκ | 0.201 | | 1 | | 0.201 | 0.80 | n.s. |
| fκ | 0.107 | | 1 | | 0.107 | 0.43 | n.s. |
| sfκ | 0.316 | | 1 | | 0.316 | 1.26 | n.s. |
| Residual | | 1.762 | | 7 | 0.252 | 1.00 | |
| Total: | | 54.664 | | 15 | | | |

*** Significant at 0.1% level (highly significant (105))

** Significant at 1% level (significant (105))

n.s. Not significant at 5% level (non-significant (105))

TABLE 6.15: Analysis of Variance

Point 4 on the lips

| Source (i) | Sum of Squares (ii) | | Degrees of Freedom (iii) | | Variance Estimate Mean Square (iv)=(ii)/(iii) | Variance Ratio (v) | |
|---|---|---|---|---|---|---|---|
| Between Blocks | | 6.015 | | 1 | 6.015 | 9.22 | * |
| Treatments | | 66.769 | | 7 | | | |
| s | 51.015 | | 1 | | 51.015 | 78.17 | *** |
| f | 12.128 | | 1 | | 12.128 | 18.58 | ** |
| κ | 0.243 | | 1 | | 0.243 | 0.37 | n.s. |
| sf | 1.205 | | 1 | | 1.205 | 1.85 | n.s. |
| sκ | 0.219 | | 1 | | 0.219 | 0.33 | n.s. |
| fκ | 0.975 | | 1 | | 0.975 | 1.49 | n.s. |
| sfκ | 0.984 | | 1 | | 0.984 | 1.51 | n.s. |
| Residual | | 4.568 | | 7 | 0.653 | 1.00 | |
| Total | | 77.352 | | 15 | | | |

*** Significant at 0.1% level (highly significant (105))

** Significant at 1% level (significant (105))

* Significant at 5% level (probably significant (105)

n.s. Not significant at 5% level (non-significant (105))

TABLE 6.16: Analysis of Variance

Point 5 on the lips

| Source (i) | Sum of Squares (ii) | Degrees of Freedom (iii) | Variance Estimate Mean Square (iv)=(ii)/(iii) | Variance Ratio (v) | |
|---|---|---|---|---|---|
| Between Blocks | 0.056 | 1 | 0.056 | 0.01 | n.s. |
| Treatments | 59.692 | 7 | | | |
| s | 32.348 | 1 | 32.348 | 7.27 | * |
| f | 5.348 | 1 | 5.348 | 1.20 | n.s. |
| κ | 2.848 | 1 | 2.848 | 0.64 | n.s. |
| sf | 7.770 | 1 | 7.770 | 1.75 | n.s. |
| sκ | 5.820 | 1 | 5.820 | 1.31 | n.s. |
| fκ | 3.563 | 1 | 3.563 | 0.80 | n.s. |
| sfκ | 1.995 | 1 | 1.995 | 0.45 | n.s. |
| Residual | 31.167 | 7 | 4.452 | 1.00 | |
| Total: | 90.915 | 15 | | | |

* Significant at 5% level (probably significant (105))

n.s. Not significant at 5% level (non-significant (105))

TABLE 6.17: Summary of Tables 6.12 to 6.16 for Statistical Analysis of Significance

| Factors | Point 1 | Point 2 | Point 3 | Point 4 | Point 5 |
|---|---|---|---|---|---|
| Drill type | * | ** | ** | * | n.s. |
| Drilling speed | *** | *** | *** | *** | * |
| Drilling feed | ** | *** | *** | ** | n.s. |
| Drill point | n.s. | n.s. | n.s. | n.s. | n.s. |
| Intersection of factors | n.s. | n.s. | n.s. | n.s. | n.s. |

*** Significant at 0.1% level (highly significant (105))

** Significant at 1% level (significant (105))

* Significant at 5% level (probably significant (105))

n.s. Not significant at 5% level (non-significant (105))

For the ranges of the drilling factors tested, the analysis of tables 6.12 to 6.16 reveals that the difference between the drill types is significant (1% level) for points 2 and 3; the difference is probably significant (5% level) for points 1 and 4. For point 5, the probability of the difference between drill types to occur by chance is greater than 5% and it can be considered non-significant.

For the ranges of the drilling factors tested, the effect of speed is highly significant (0.1% level) for points 1, 2, 3 and 4 (Tables 6.12 to 6.15) and probably significant (5% level) for point 5 (Table 6.16). The effect of drilling feed is highly significant (0.1% level) for points 2 and 3 (Tables 6.13 and 6.14), is significant (1% level) for points 1 and 4 (Tables 6.12 and 6.15) and non-significant for point 5 (Table 6.16).

These results are summarised in Table 6.17.

Surprisingly, the effects of the drilling factors (Table 6.17) do not mirror significantly at point 5, the outer corner, with the exception of drilling speed (probably significant). This might be taken, on a purely statistical basis, as meaning that the wear rate at the outer corner is independent of the drilling factors tested (except for drilling speed). However, this is not true as it is known by the workers in the drilling area. The reason for this result should be looked for in the residual for point 5 (Table 6.16) which is much higher than those for the other points 1, 2, 3 and 4 and reflects a large variability in the wear rate at this point. Therefore, inner points to the outer corner on the drill lip must be selected when wear rate performance measurement is intended.

The above analysis of the drill wear results reveals that the expectations built upon the hypothesis of better drill wear performance, with a new flute yielding a better *"heat sink"* while maintaining approximately the same effective rake angle as the conventional one, did not succeed. However, the observation of Figures

6.23 to 6.30 shows a more uniform wear for the new design drill than for the conventional one as, for the majority of cases, the transition from point 4 to point 5, for the wear curves, is smoother for the first drill type than for the second one.

It can also be noted that for the tests which ended with "screech", the wear loss is greater for the conventional drill than for the new design drill at point 5 (outer corner), where the wear is shown to vary from approximately 0% ($118^{o}$ x 1140 rpm x 240 RPI) to more than +50% ($134^{o}$ x 1140 rpm x 157 RPI) relatively to the new design drill (Appendix 7). The reverse appears to happen with the other points, especially points 3 and 4, for which the wear loss with the new design drill varies from approximately 0% (point 4, $118^{o}$ x 1140 rpm x 157 RPI) to more than +20% (point 4, $118^{o}$ x 1140 rpm x 240 RPI) (Appendix 7).

The tests reported in this chapter have been set to investigate the drills wear performance, however, on the basis of reported work in literature (35) on drill life, and on the higher wear rate for the new drill design, a shorter life, according to the "screech" criterion (Section 6.1.2), might be expected with the new design drill. Nevertheless, the tests which ended with "screech" (Section 6.4) do not allow such a definitive statement.

*"Mechanical efficiency in drilling operations can be expressed in terms of torque and total thrust on the drill".*

*Galloway*

## 7. PERFORMANCE TESTS - COMPARING DRILLING FORCES ON CONVENTIONAL AND NEW DESIGN DRILL

## 7.1 Introduction

Many papers (3, 12, 17, 23, 24, 25, 26, 27, 106, 107) report on drilling forces measurement.

The importance of drilling forces derives from the need to compute drilling power consumption and stress and/or strain on working elements such as the components being drilled, component holders, drill holders and drilling machine spindle. Drilling forces can also be important in comparing drill performance for different drill designs.

It is usual to measure drilling torque and thrust and many drilling variables have been investigated for their influence on drilling forces.

Drilling forces have been studied for the variation of helix angle (3, 23, 27, 42), point angle (3, 17, 23, 42), clearance angle (3, 23), point shape (2, 17), chisel edge length (3), drill diameter (3, 5, 27, 42), feed (5, 23, 27, 42, 53, 99), speed (42), workpiece material (3, 5, 23, 27, 42, 53), depth of hole (42) and number of holes (3) and with and without pilot holes (25).

## 7.2 Experimental Design

The author aimed at designing an experiment to compare, for drilling forces, 12.7 mm (½") drills of two types - a conventional drill and the new flute design drill. To define the number and the range of the variables to be tested was one of his targets.

To exclude the cutting speed as a testing factor was justified on the basis of the reports of some workers who found the influence of the cutting speed on drilling forces to be negligible (27), insignificant (12) or null (107).

### 7.2.1 Factors selection

Each drill type is to be tested for the drilling forces with varying drill point angle and drilling feed.

As a result of the conditions fixed for the wear tests, and the drilling feeds range available in the drilling machine used by the author, the combinations of drilling factors shown in Table 7.1 were selected for testing.

TABLE 7.1:
Drilling Factors Combinations Used with the Drilling Forces Tests

| Drill Type | Drill point angle, deg | Revolutions per inch penetration |
|---|---|---|
| Conventional | 118 | 240<br>157<br>103<br>70 |
| | 134 | 240<br>157<br>103<br>70 |
| Wear design | 118 | 240<br>157<br>103<br>70 |
| | 134 | 240<br>157<br>103<br>70 |

### 7.2.2 Equipment

The drilling machine, the grinding machine and the geometry measurement machine have already been described in Chapter 6 (Section 6.2.3).

### 7.2.2.1 Dynamometer

A Kistler two-component measuring platform type 9271A was used in this work (C.2).

This measuring platform is a piezo-electric transducer which measures simultaneously a force parallel to the transducer axis, $F_Z$, and a moment in the plane normal to the line of application of the force, $M_Z$ (Figure 7.1).

Each channel comprises a charge amplifier and a galvo-amplifier, driving a recording galvonometer in an ultraviolet oscillograph. The charge amplifier converts the electrical charge into a proportional voltage, taking into account the individual transducer sensitivity, so that the output voltage is an even scale of N/V. In addition, the desired range can be selected over four decades in steps of 1, 2, 5. The set up is shown in Figure 7.2.

The technical specification for the dynamometer is as follows:

| | |
|---|---|
| Maximum measuring range: | $F_Z$: - 5000 to 20,000N |
| | $M_Z$: ± 100 Nm |
| Overload capacity: | ± 50% |
| Resolution: | $F_Z$: 0.02N |
| | $M_Z$: 0.0002 Nm |
| Cross sensitivity: | $F_Z \rightarrow M_Z \leqslant \pm$ 0.0002 Nm/N |
| | $M_Z \rightarrow F_Z \leqslant \pm$ 1.0 N/Nm |
| Linearity: | $\leqslant$ ± 1% full scale output |
| Hysteresis: | $\leqslant$ ± 0.5% full scale output |
| Resonant frequency: | ≈ 3.5 KHz |
| Rigidity: | $F_Z$: ≈6500 N/μm |
| | $M_Z$: ≈0.5 Nm/μrad |
| Sensitivity: | $F_Z$: 2.0 $p_c$/N |
| | $M_Z$: 150 $p_c$/Nm |
| Working temperature range: | $0^o$ to $70^oC$ |
| Mass: | 2.9 Kg |

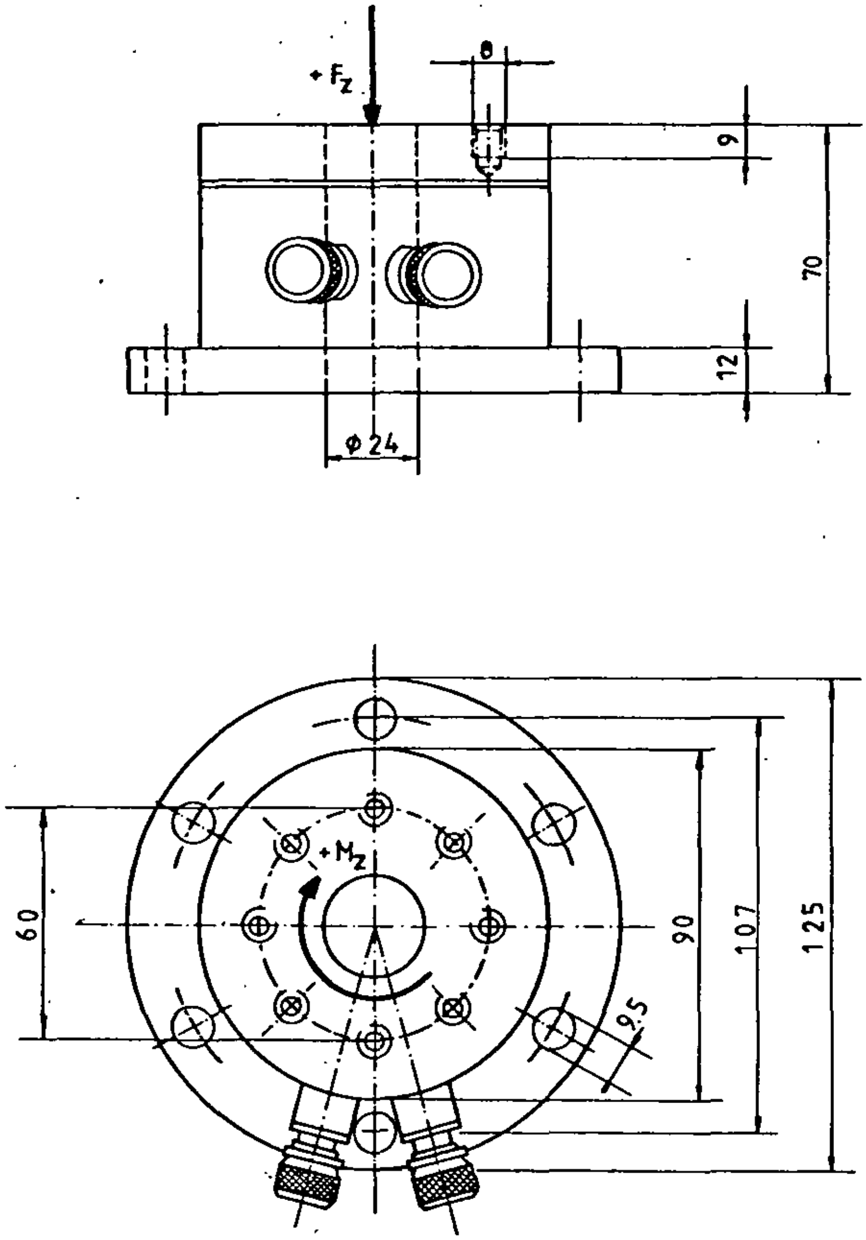


FIGURE 7.1: Kistler thrust (Fz) and torque (Mz) measuring platform

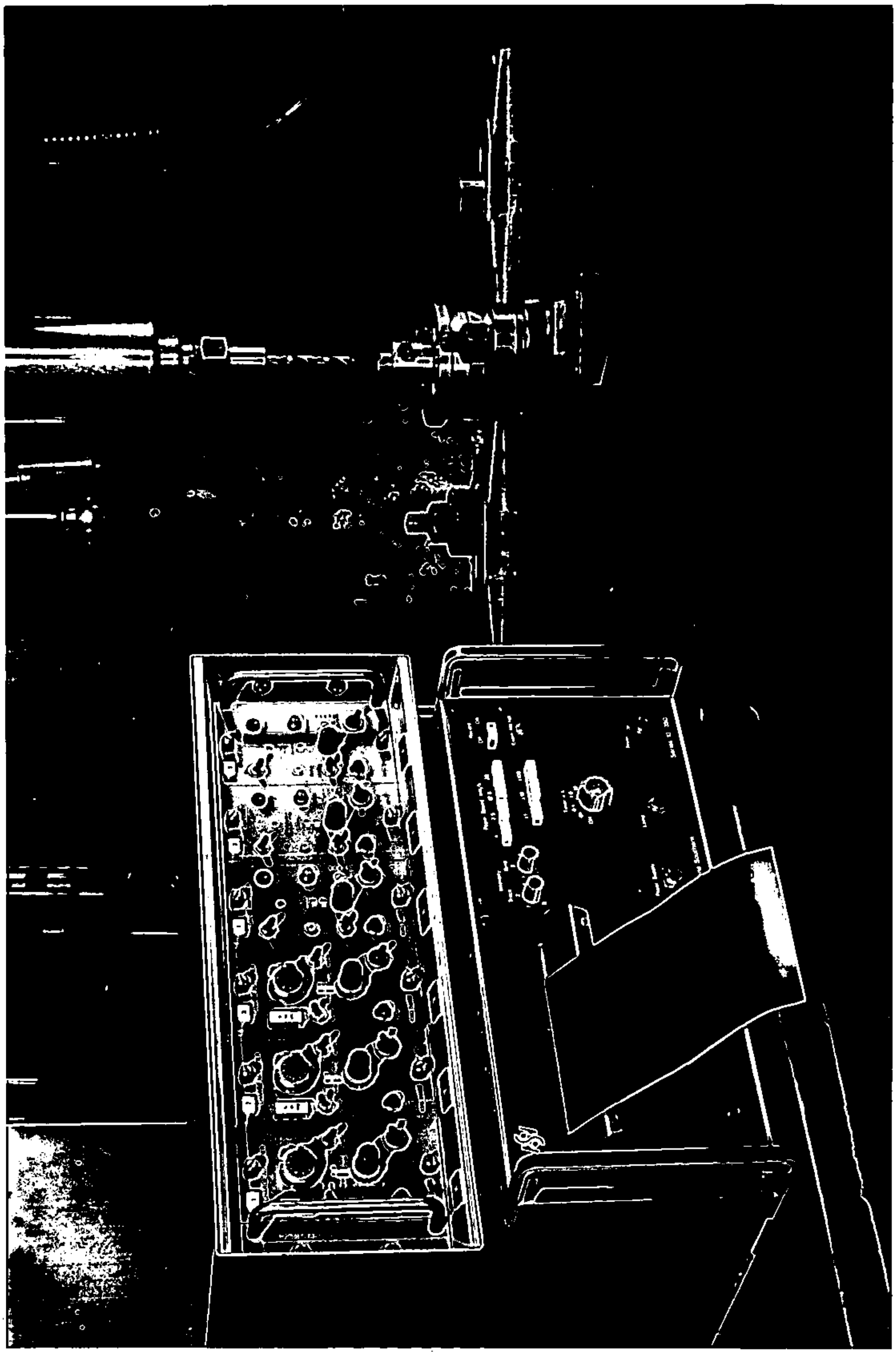

FIGURE 7.2: Set-up for drilling forces measurement

The oscillograph was a Southern Instruments direct reading ultra-violet unit series M1300 with the following specifications:

| | |
|---|---|
| Galvanometer: | SMI/N 100 c/s |
| Number of data channels: | 10 |
| Datum traces: | 2 |
| Writing speed: | 762 mm/s |
| Max. deflection: | 152 mm |
| Recording material: | Kodak linagraph direct print paper 120 mm wide |
| Paper speeds: | 3.8, 7.6, 12.7, 25.4, 38.1, 76.2, 254, 762, 1270, 2540 mm/s |
| Speed stability: | better than ±5% |
| Timing lines: | 0.01, 0.1, or 10s |

Galvanometer specification:

| | |
|---|---|
| Natural frequency: | 1000 c/s |
| Terminal resistance | 35Ω |
| d.c. sensitivity: | 0.05 mA/mm, 1.75 mV/mm |
| Maximum safe current: | 50 mA |
| Maximum safe voltage | 1.75V |

Calibration of the dynamometer:

The dynamometer was calibrated by directly applying a proving ring in the axial direction and loading a lever arm for the calibration of the torque component as reported in (84). A torsion balance was also used for moment calibration, as indicated by the manufacturer [C.2], and similar results as for the arm were obtained.

Calibration charts and calibration set-up pictures are not presented for dynamometer calibration procedures for drilling forces measurement are already well established (3, 5, 35, 84, 125).

### 7.2.3 Preliminary work

The purpose of the experiments reported in this chapter was to test the effect of flute form on drilling forces with steel.

The author considered, as for the wear tests, two point angles - 118° and 134° - and tested the whole range of drilling feeds available with the drilling machine.

Some tests were performed with two materials: EN3 and EN8 steels.

The results of the experiments with EN3 steel with the conventional drill appeared to be unexpectedly much higher than the values predicted by the simplified formula equations 7.1 and 7.2 after Oxford and Shaw (27):

$$T_o = 0.087\ HBf^{0.8}\ d_o^{1.8} \qquad 7.1$$

$$T_h = 0.195\ HBf^{0.8}\ d_o^{0.8} + 0.0022\ H_B\ d_o^{2} \qquad 7.2$$

where $T_o$ = drilling torque, lb.in
$T_h$ = drilling thrust, lb
HB = workpiece hardness, psi
f = drilling feed, in/rev
$d_o$ = drill diameter, in
(units as given in (27)).

Close inspection of the drill after drilling EN3 steel revealed the presence of an important built-up-edge (BUE) on the lip and for this situation - large BUE - Oxford and Shaw had found no good agreement between their formula and the experimental data. Thus EN3 steel was discarded from the main drilling forces tests.

To specify a cutting speed was conditioned by the absence of coolant and by the heaviest feed to be tested. The author found the speed 260 rpm, within the range available, to be the more appropriate to the drilling forces tests.

## 7.3 Main Drilling Forces Tests

### 7.3.1 Testing procedure

The tests for drilling forces measurement were run dry to protect the dynamometer, to simplify the testing procedure and to avoid possible effects due to the variation in the cutting fluid and its action.

The number of drills tested was as for the wear tests (Section 6.3.1).

As for the wear tests, the drilling forces tests were first run for one drill point angle (Section 6.3.1). To eliminate any possible systematic error, the tests were run in a random sequence for the combination of the remaining factors. After completion of the tests with one point angle, the grinding machine was set for the other point angle and testing procedure was as for the first point angle.

For each set of drilling conditions and each drill type, tests were run four times in order to eliminate, by averaging, the effect of experimental random deviations. Drilling torques and thrusts were recorded by a UV recorder as specified in Section 7.2.2.1.

### 7.3.2 Drills features

Drills features were as for the wear tests (Section 6.3.2).

### 7.3.3 Material

The work material, EN8 steel, supplied in 3.05 m (10") lengths of 19.05 mm (¾") diameter bar was a nominal 0.40% carbon steel with the following limits to chemical composition:

| | C | Si | Mn | S | P |
|---|---|---|---|---|---|
| min | 0.35 | 0.05 | 0.60 | - | - |
| max | 0.45 | 0.35 | 1.00 | 0.060 | 0.060 |

A material sample was submitted for chemical analysis and the result proved it to be within the specified composition.

The bars were cut into pieces 30 mm long and the end pieces had been discarded.

The specimens were normalized and cleaned, and the tops were ground. The specimens were numbered and ten pieces were selected at random for hardness tests at each top.

A Rockwell hardness tester was used for testing the specimens hardness and the hardness numbers obtained after the readings fell in the interval 197 HB - 206 HB.

The pieces for drilling tests were selected in a random sequence and drilled with a 25 mm ($\approx 2\ d_o$) deep hole.

## 7.4 Experimental Results

The results of the experiments are shown in Tables 7.2 (thrust) and 7.3 (torque). These results are presented graphically in Figure 7.3 (thrust for $118^o$ point angle), Figure 7.4 (thrust for $134^o$ point angle), Figure 7.5 (torque for $118^o$ point angle) and Figure 7.6 (torque for $134^o$ point angle).

TABLE 7.2: Thrust (N)

| RPI (rev/in) | Feed (mm/rev) | Conventional Drill | | New Design Drill | |
|---|---|---|---|---|---|
| | | Ground point angle | | Ground point angle | |
| | | $118^o$ | $134^o$ | $118^o$ | $134^o$ |
| 240 | 0.106 | 1610 | 1943 | 1521 | 1668 |
| | | 1697 | 1999 | 1603 | 1617 |
| | | 1648 | 1952 | 1572 | 1626 |
| | | 1627 | 1982 | 1553 | 1647 |
| 157 | 0.162 | 2456 | 2502 | 2262 | 2187 |
| | | 2359 | 2540 | 2241 | 2179 |
| | | 2406 | 2471 | 2311 | 2129 |
| | | 2351 | 2556 | 2232 | 2213 |
| 103 | 0.247 | 3375 | 3447 | 3186 | 3015 |
| | | 3429 | 3437 | 3085 | 3017 |
| | | 3329 | 3510 | 3153 | 2956 |
| | | 3469 | 3369 | 3134 | 3042 |
| 70 | 0.363 | 4802 | 4694 | 4248 | 4155 |
| | | 4824 | 4877 | 4294 | 4259 |
| | | 4887 | 4727 | 4381 | 4127 |
| | | 4709 | 4807 | 4208 | 4293 |

TABLE 7.3: Torque (N.cm)

| RPI (rev/in) | Feed (mm/rev) | Conventional Drill | | New Design Drill | |
|---|---|---|---|---|---|
| | | Ground point angle | | Ground point angle | |
| | | 118° | 134° | 118° | 134° |
| 240 | 0.106 | 642.0 | 751.6 | 622.8 | 711.0 |
| | | 671.4 | 743.7 | 694.0 | 784.4 |
| | | 645.4 | 738.1 | 636.3 | 738.1 |
| | | 653.3 | 757.3 | 648.8 | 732.4 |
| 157 | 0.162 | 1060 | 1135 | 1082 | 1267 |
| | | 1017 | 1122 | 1076 | 1157 |
| | | 1066 | 1099 | 1113 | 1191 |
| | | 1041 | 1159 | 1053 | 1231 |
| 103 | 0.247 | 1485 | 1507 | 1631 | 1717 |
| | | 1537 | 1637 | 1635 | 1683 |
| | | 1499 | 1552 | 1568 | 1635 |
| | | 1550 | 1573 | 1672 | 1755 |
| 70 | 0.363 | 2221 | 2254 | 2204 | 2502 |
| | | 2140 | 2287 | 2316 | 2281 |
| | | 2212 | 2224 | 2281 | 2400 |
| | | 2199 | 2320 | 2201 | 2355 |

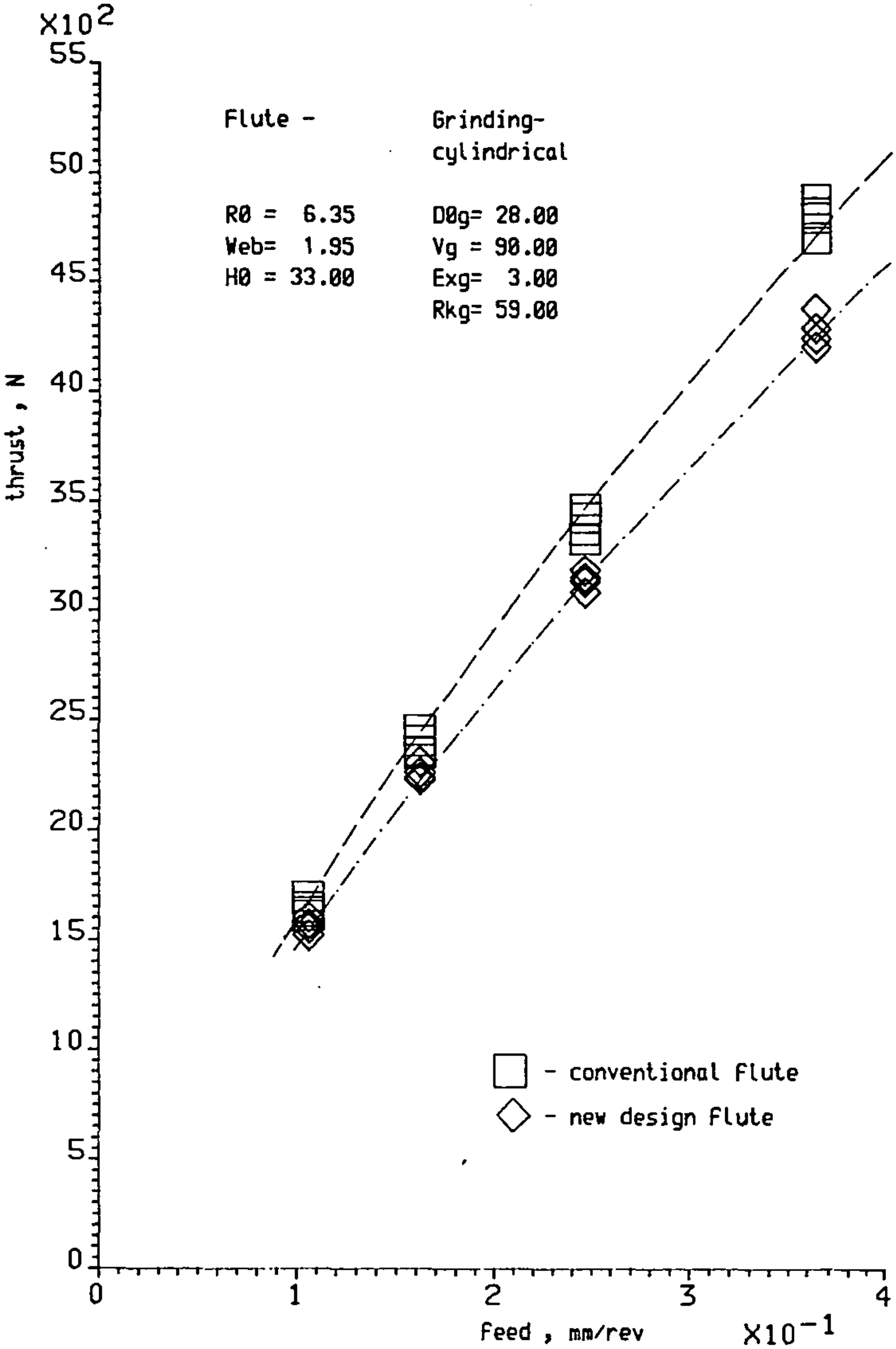


FIGURE 7.3: Drilling thrust for 118° point angle
[four tests with each drilling feed]

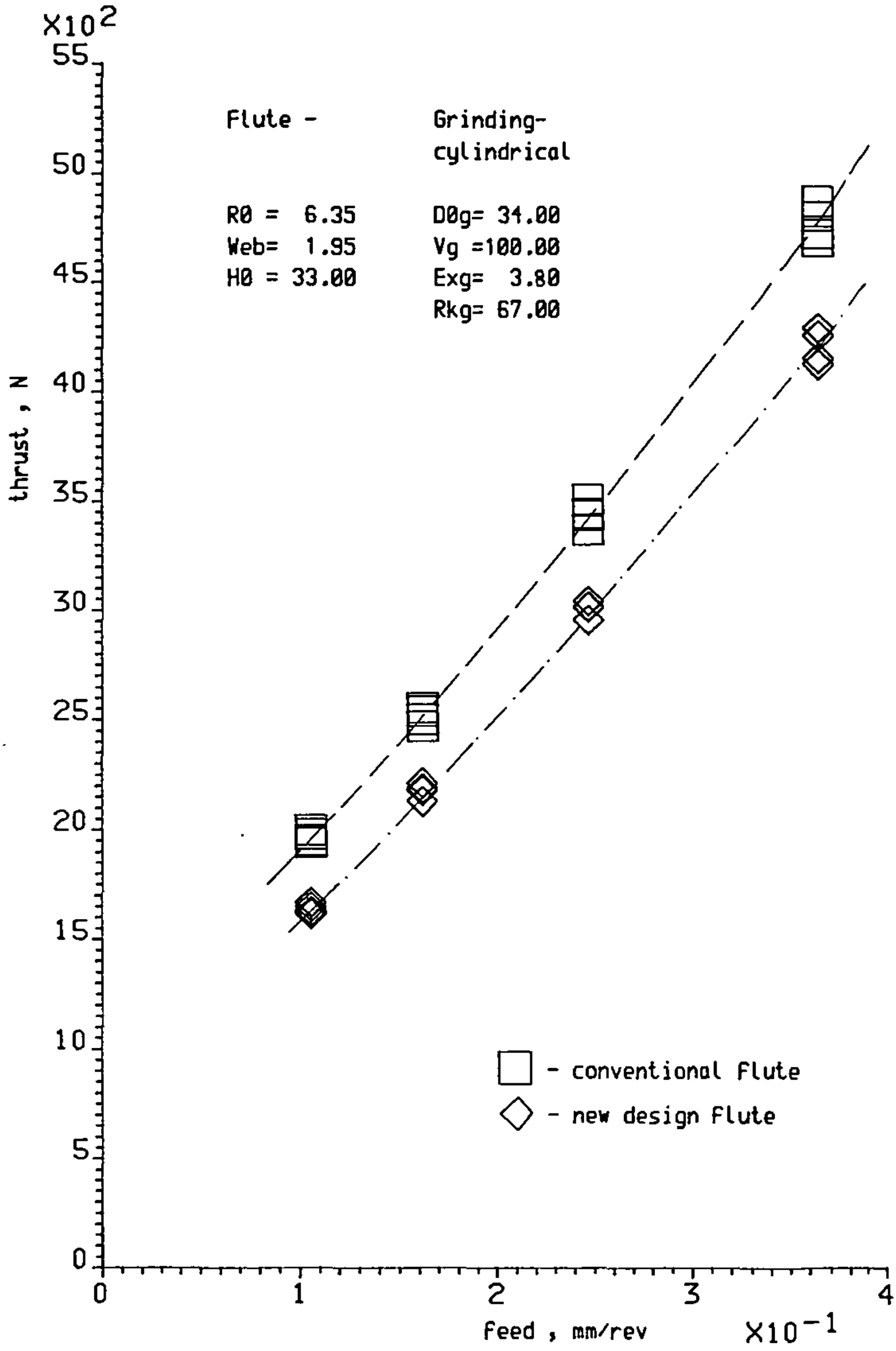


FIGURE 7.4: Drilling thrust for 134° point angle
[Four tests with each drilling feed]

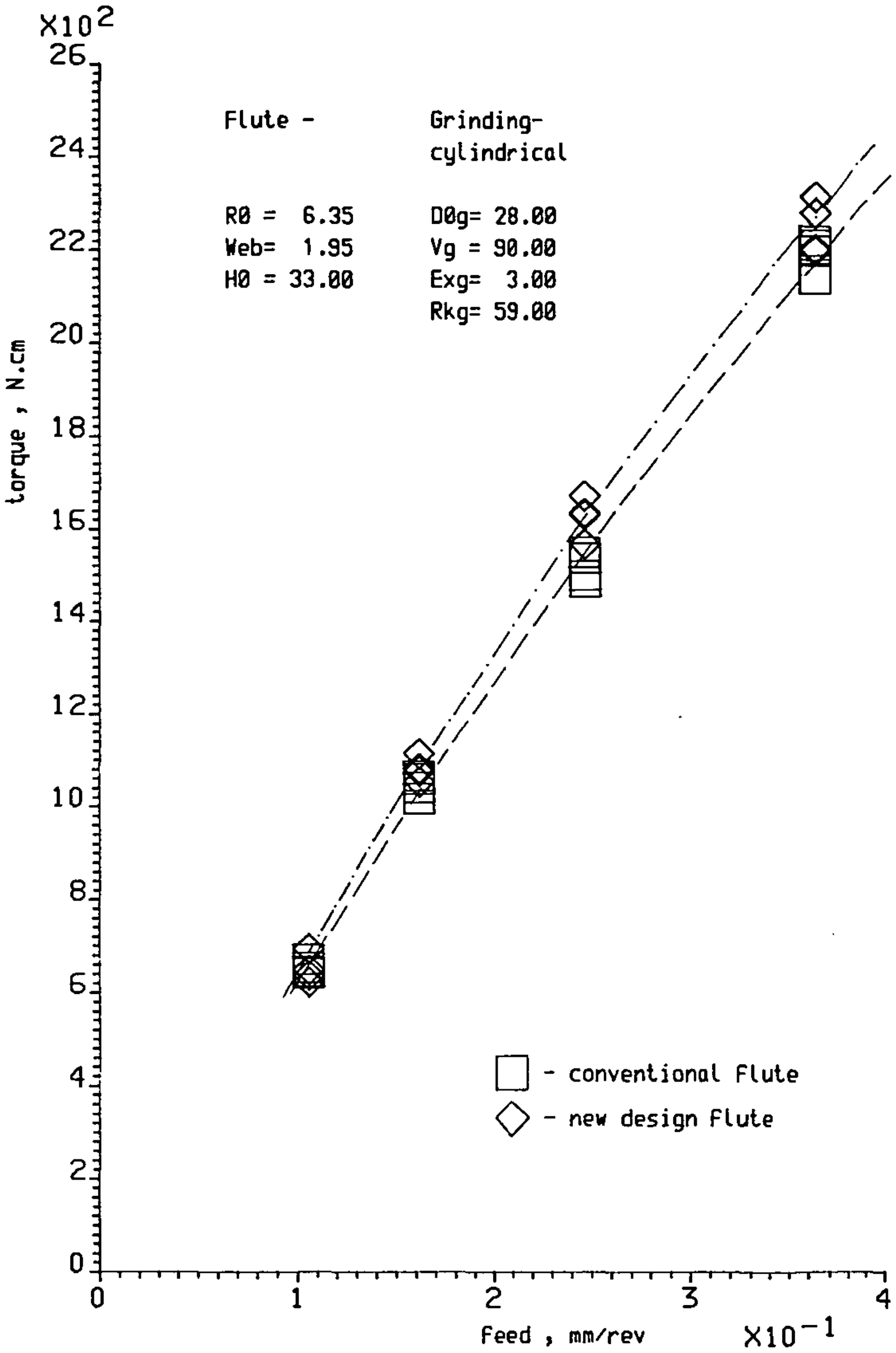


FIGURE 7.5: Drilling torque for 118° point angle
[Four tests with each drilling feed]

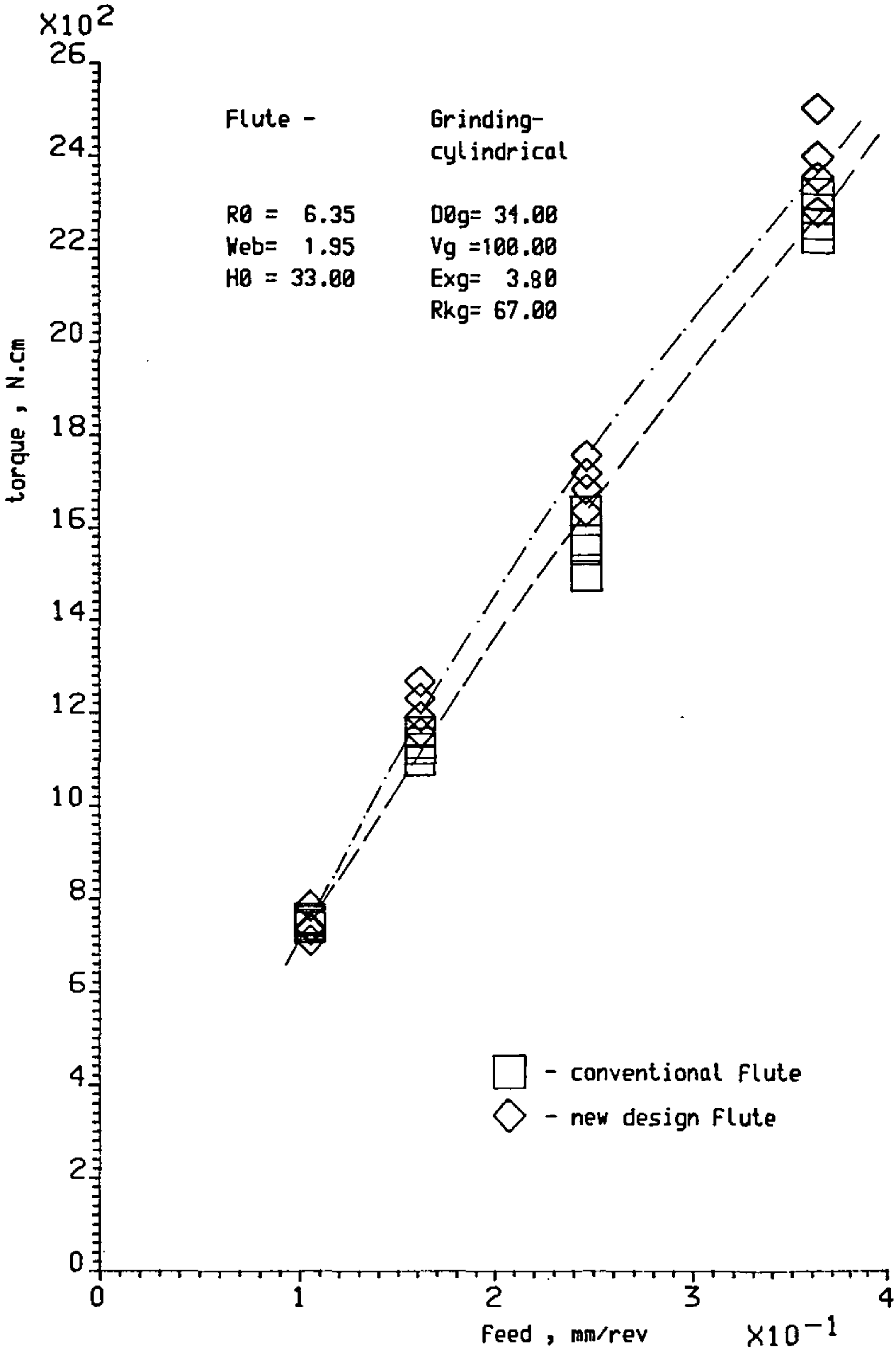


FIGURE 7.6: Drilling torque for 134° point angle
[Four tests with each drilling feed]

## 7.5 Analysis of Results

The drilling forces were averaged for each set of cutting conditions and the results presented in Table 7.4 (thrust) and Table 7.5 (torque).

Graphics from Figures 7.3 to 7.6 and Tables 7.4 and 7.5 show that, for both drill types, drilling forces increase with feed, as expected. They also show some differences between the conventional drill and the new design drill.

For each feed, the thrust value relative to the $118^{o}$ point angle conventional drill has been given the value 100 and the thrust values for the other cases have been computed accordingly; the results are shown in Table 7.6. The same procedure has been adopted for the torque values and the results are shown in Table 7.7.

Table 7.6 shows that, for the $118^{o}$ point angle, the thrust is 5 to 10% (depends on the feed) lower for the new design drill than for the conventional one. For the $134^{o}$ point angle, the thrust for the new design drill is 10 to 20% lower than for the conventional one.

Table 7.7 shows that the reverse happens with the drilling torque: the new design drill yields a drilling torque approximately 0 to 10% bigger than the conventional one for either drill point.

An analysis of variance on the drilling forces results has been done in order to find if the effects of the tested drilling factors are statistically significant. Let drilling thrust be considered first and let all the drilling factors tested be analysed.

The following symbols are used:

$d_1$ - conventional drill
$d_2$ - new design drill
$f_1$, $f_2$, $f_3$, $f_4$ - the feeds corresponding to 240, 157, 103 and 70 RPI respectively

TABLE 7.4: Thrust (N) Averages (refer to Table 7.2)

| RPI (rev/in) | Feed (mm/rev) | Conventional Drill | | New Design Drill | |
|---|---|---|---|---|---|
| | | Ground point angle | | Ground point angle | |
| | | 118° | 134° | 118° | 134° |
| 240 | 0.106 | 1646 | 1969 | 1562 | 1640 |
| 157 | 0.162 | 2393 | 2517 | 2261 | 2177 |
| 103 | 0.247 | 3400 | 3441 | 3139 | 3007 |
| 70 | 0.363 | 4806 | 4776 | 4283 | 4209 |

TABLE 7.5: Torque (N.cm) Averages (refer to Table 7.3)

| RPI (rev/in) | Feed (mm/rev) | Conventional Drill | | New Design Drill | |
|---|---|---|---|---|---|
| | | Ground point angle | | Ground point angle | |
| | | 118° | 134° | 118° | 134° |
| 240 | 0.106 | 653 | 748 | 651 | 741 |
| 157 | 0.162 | 1047 | 1129 | 1082 | 1211 |
| 103 | 0.247 | 1518 | 1568 | 1626 | 1698 |
| 70 | 0.363 | 2193 | 2272 | 2250 | 2385 |

TABLE 7.6: Comparative Drilling Thrusts

| RPI (rev/min) | Feed (mm/rev) | Conventional Drill | | New Design Drill | |
|---|---|---|---|---|---|
| | | Ground point angle | | Ground point angle | |
| | | 118° | 134° | 118° | 134° |
| 240 | 0.106 | 1646N= 100 | 120 | 95 | 100 |
| 157 | 0.162 | 2394N= 100 | 105 | 94 | 91 |
| 103 | 0.247 | 3400N= 100 | 101 | 92 | 88 |
| 70 | 0.363 | 4806= 100 | 99 | 89 | 88 |

TABLE 7.7: Comparative Drilling Torques

| RPI (rev/min) | Feed (mm/rev) | Conventional Drill | | New Design Drill | |
|---|---|---|---|---|---|
| | | Ground point angle | | Ground point angle | |
| | | 118° | 134° | 118° | 134° |
| 240 | 0.106 | 653 N.cm= 100 | 115 | 100 | 113 |
| 157 | 0.162 | 1047 N.cm= 100 | 108 | 103 | 116 |
| 103 | 0.247 | 1518 N.cm= 100 | 103 | 107 | 112 |
| 70 | 0.363 | 2193 N.cm= 100 | 104 | 103 | 109 |

$\kappa_1$, $\kappa_2$ - the point angles 118° and 134° respectively.

The drilling thrust averages (Table 7.4) for each set of drilling conditions are divided by 1000, for the sake of simplification of the calculations, and presented in Table 7.8.

TABLE 7.8: Thrust-related Values (refer to Table 7.4)

| Feed | $d_1$ | | $d_2$ | | TOTALS |
|---|---|---|---|---|---|
| | $\kappa_1$ | $\kappa_2$ | $\kappa_1$ | $\kappa_2$ | |
| $f_1$ | 1.646 | 1.969 | 1.562 | 1.640 | 6.817 |
| $f_2$ | 2.394 | 2.517 | 2.261 | 2.177 | 9.349 |
| $f_3$ | 3.400 | 3.441 | 3.139 | 3.007 | 12.987 |
| $f_4$ | 4.806 | 4.777 | 4.283 | 4.209 | 18.075 |
| TOTALS: | 12.246 | 12.704 | 11.245 | 11.033 | 47.228 |

Grand total = 47.228

Sum of squares for feed effect, SSF (Table 7.8):

$$SSF = \frac{1}{16}(6.817^2 + 9.349^2 + 12.987^2 + 18.075^2) - \frac{47.228^2}{64} = 4.47638$$

Summing for the factor drill type (Table 7.8):

| $d_1$ | $d_2$ |
|---|---|
| 24.950 | 22.278 |

Sum of squares for drill type effect, SSD:

$$SSD = \frac{1}{32}(24.950^2 + 22.278^2) - \frac{47.228^2}{64} = 0.11156$$

Summing for the factor drill point (Table 7.8):

| $\kappa_1$ | $\kappa_2$ |
|---|---|
| 23.491 | 23.737 |

Sum of squares for point angle effect, SSP:

$$SSP = \frac{1}{32}(23.491^2 + 22.737^2) - \frac{47.228^2}{64} = 0.00095$$

Summing for the cross effect of drill type and feed (Table 7.8):

| | $d_1$ | $d_2$ |
|---|---|---|
| $f_1$ | 3.615 | 3.202 |
| $f_2$ | 4.911 | 4.438 |
| $f_3$ | 6.841 | 6.146 |
| $f_4$ | 9.583 | 8.492 |

Sum of squares for cross effect drill type and feed, SSDF:

$$SSDF = \frac{1}{8}(3.615^2 + 3.202^2 + 4.911^2 + 4.438^2 + 6.841^2 + 6.146^2 +$$

$$9.583^2 + 8.492^2) - 0.111556 - 4.47638 - \frac{47.228^2}{64} = 0.01767$$

Sum of squares for drill type and point angle cross effect (Table 7.8), SSDP:

$$SSDP = \frac{1}{16}(12.246^2 + 12.704^2 + 11.245^2 + 11.033^2) -$$

$$- 0.11156 - 0.00095 - \frac{47.228^2}{64} = 0.00700$$

Summing for the cross-effect of point angle and feed (Table 7.8):

| | $\kappa_1$ | $\kappa_2$ |
|---|---|---|
| $f_1$ | 3.208 | 3.609 |
| $f_2$ | 4.655 | 4.694 |
| $f_3$ | 6.539 | 6.448 |
| $f_4$ | 9.089 | 8.986 |

Sum of squares for point angle and feed cross-effect, SSPF:

$$SSPF = \frac{1}{8}(3.208^2 + 3.609^2 + 4.655^2 + 4.694^2 + 6.539^2 + 6.448^2$$

$$+ 9.089^2 + 8.986^2) -$$

$$- 0.00095 - 4.47638 - \frac{47.228^2}{64} = 0.01038$$

Sum of squares for the three factors cross-effect, (Table 7.8):

$$\frac{1}{4}(1.646^2 + 1.969^2 + \dots + 4.209^2) - 4.47638 - 0.11156 -$$

$$- 0.00095 - 0.01767 - 0.00700 - 0.01038 - \frac{47.228^2}{64} = 0.00143$$

Total sum of squares (Table 7.2): 4.63013

The analysis of variance for drilling thrust is presented in Table 7.9.

TABLE 7.9: Analysis of Variance for Drilling Thrust

| Effect | Sum of Squares | Degrees of Freedom | Variance Estimate | Variance Ratio |
|---|---|---|---|---|
| Drill type | 0.11156 | 1 | 0.11156 | 1115 |
| Drill point | 0.00095 | 1 | 0.00095 | 9.5 |
| Feed | 4.47638 | 3 | 1.49213 | 14,921 |
| Type x point | 0.00700 | 1 | 0.00700 | 70.0 |
| Type x feed | 0.01767 | 3 | 0.00589 | 58.9 |
| Point x feed | 0.01038 | 3 | 0.00346 | 34.6 |
| Type x point x feed | 0.00143 | 3 | 0.00048 | 4.8 ** |
| Error | 0.00476 | 48 | 0.00010 | |
| Total: | 4.63013 | 63 | | |

** Significant at 1% level

Observing Table 7.9, the interaction of the three tested drilling factors appears to be significant, (terminology as in Section 6.5). In such a case separate analyses on the original data should be done (105) to test statistically the effect of the drilling factors.

It is well established that feed has an important effect on the drilling forces (Section 7.1), thus let us first do a breakdown analysis by drilling feeds. Tables 7.10 to 7.13 present the analysis of variance for the data of Table 7.2 separated according to the feed value.

TABLE 7.10: Analysis of Variance for Drilling Thrust for 240 RPI

| Effect | Sum of Squares | Degrees of Freedom | Variance Estimate | Variance Ratio | |
|---|---|---|---|---|---|
| Point angle | 3.4468 | 1 | 3.4468 | 64.03 | *** |
| Drill type | 0.0078 | 1 | 0.0078 | 0.15 | n.s. |
| Interaction pointxtype | 0.0012 | 1 | 0.0012 | 0.02 | n.s. |
| Error | 0.6460 | 12 | 0.0538 | | |
| Total: | 4.1018 | 15 | | | |

TABLE 7.11: Analysis of Variance for Drilling Thrust for 157 RPI

| Effect | Sum of Squares | Degrees of Freedom | Variance Estimate | Variance Ratio | |
|---|---|---|---|---|---|
| Point angle | 4.5478 | 1 | 4.5478 | 45.39 | *** |
| Drill type | 1.3867 | 1 | 1.3867 | 13.84 | ** |
| Interaction pointxtype | 0.2278 | 1 | 0.2278 | 2.27 | n.s. |
| Error | 1.2024 | 12 | 0.1002 | | |
| Total: | 7.3467 | 15 | | | |

*** Significant at 0.1% level

** Significant at 1% level

* Significant at 5% level

n.s. Not significant at 5% level

TABLE 7.12: Analysis of Variance for Drilling Thrust for 103 RPI

| Effect | Sum of Squares | Degrees of Freedom | Variance Estimate | Variance Ratio | |
|---|---|---|---|---|---|
| Point angle | 1.4522 | 1 | 1.4522 | 6.98 | * |
| Drill type | 5.7119 | 1 | 5.7119 | 27.44 | *** |
| Interaction pointxtype | 0.0459 | 1 | 0.0459 | 0.22 | n.s. |
| Error | 2.4980 | 12 | 0.2082 | | |
| Total: | 9.7080 | 15 | | | |

(See previous page for symbols)

TABLE 7.13: Analysis of Variance for Drilling Thrust for 70 RPI

| Effect | Sum of Squares | Degrees of Freedom | Variance Estimate | Variance Ratio | |
|---|---|---|---|---|---|
| Point angle | 4.5078 | 1 | 4.5078 | 12.13 | ** |
| Drill type | 2.9180 | 1 | 2.9180 | 7.85 | * |
| Interaction pointxtype | 0.3086 | 1 | 0.3086 | 0.83 | n.s. |
| Error | 4.4590 | 12 | 0.3716 | | |
| Total: | 12.1934 | 15 | | | |

(See previous page for symbols)

Analysis of Tables 7.10 to 7.13 shows that the interaction between drill type and point angle is probably not significant for any feed. The effect of point angle is highly significant for the low to moderate feeds (240 RPI and 157 RPI, Tables 7.10 and 7.11), and significant (Table 7.13) or probably significant (Table 7.12) for the moderate to high feeds.(70 RPI and 103 RPI). The analysis of the same tables also shows that the effect of drill type on drilling thrust is highly significant (Table 7.12), or significant (Table 7.11), for moderate feeds (103 RPI and 157 RPI, respectively) and probably not significant for low feeds (Table 7.10). For high feeds the effect of drill type on drilling thrust is probably significant (Table 7.13).

In Table 7.14 is presented a resumé of Tables 7.10 to 7.13.

TABLE 7.14: Resume of Analysis of Variance for Drilling Thrust, by Drilling Feeds (refer to Tables 7.10 to 7.13). Variance Ratios

| Effect | 240 RPI | 157 RPI | 103 RPI | 70 RPI |
|---|---|---|---|---|
| Point angle | 64.03 *** | 45.39 *** | 6.98 * | 12.13 ** |
| Drill type | 0.15 n.s. | 13.84 ** | 27.44 *** | 7.85 * |
| Interaction point x type | 0.02 n.s. | 2.27 n.s. | 0.22 n.s. | 0.83 n.s. |

(See Tables 7.10 and 7.11 for symbols)

Two further breakdown analyses for the effects on drilling thrust were done by drill point angles (Tables 7.15 and 7.16) and by drill types (Tables 7.17 to 7.18).

TABLE 7.15: Analysis of Variance for Drilling Thrust for $118^0$ Point Angle

| Effect | Sum of Squares | Degrees of Freedom | Variance Estimate | Variance Ratio | |
|---|---|---|---|---|---|
| Feed | 38.7422 | 3 | 12.9141 | 4562.46 | |
| Drill type | 0.4987 | 1 | 0.4987 | 176.17 | |
| Interaction Feed x Type | 0.2325 | 3 | 0.0775 | 27.39 | *** |
| Error | 0.0680 | 24 | 0.0628 | | |
| Table: | 39.5414 | 31 | | | |

(See Tables 7.10 and 7.11 for symbols)

TABLE 7.16: Analysis of Variance for Drilling Thrust for $134^0$ Point Angle

| Effect | Sum of Squares | Degrees of Freedom | Variance Estimate | Variance Ratio | |
|---|---|---|---|---|---|
| Feed | 33.0329 | 3 | 11.0110 | 4065.43 | |
| Drill type | 1.3958 | 1 | 1.3958 | 515.34 | |
| Interaction Feed x Type | 0.0731 | 3 | 0.0243 | 8.99 | *** |
| Error | 0.0650 | 24 | 0.0027 | | |
| Total: | 34.5668 | 31 | | | |

TABLE 7.17: Analysis of Variance for Drilling Thrust for Conventional Drill

| Effect | Sum of Squares | Degrees of Freedom | Variance Estimate | Variance Ratio | |
|---|---|---|---|---|---|
| Feed | 40.3805 | 3 | 13.4602 | 4282.16 | |
| Point angle | 0.1053 | 1 | 0.1053 | 33.50 | |
| Interaction Feed x Point | 0.1398 | 3 | 0.0466 | 14.83 | *** |
| Error | 0.0754 | 24 | 0.0031 | | |
| Total: | 40.7010 | 31 | | | |

(See Tables 7.10 and 7.11 for symbols)

TABLE 7.18: Analysis of Variance for Drilling Thrust for New Design Drill

| Effect | Sum of Squares | Degrees of Freedom | Variance Estimate | Variance Ratio | |
|---|---|---|---|---|---|
| Feed | 31.5111 | 3 | 10.5037 | 4375.24 | |
| Point angle | 0.0229 | 1 | 0.0229 | 9.55 | |
| Interaction Feed x Point | 0.0491 | 3 | 0.0164 | 6.82 | ** |
| Error | 0.0576 | 24 | 0.0024 | | |
| Total: | 31.6407 | 31 | | | |

(See tables 7.10 and 7.11 for symbols)

Analysis of Tables 7.15 and 7.16 reveals that the interaction of feed and drill type on drilling thrust is highly significant. Tables 7.17 and 7.18 show that the effect of the interaction between feed and point angle on drilling thrust is highly significant for the conventional drill (Table 7.17) and significant for the new design drill (Table 7.18).

Proceeding for the torque (Table 7.3) as for the thrust, the analysis of variance was also carried out and summarised in Table 7.19.

TABLE 7.19: Analysis of Variance for Drilling Torque

| Effect | Sum of Squares | Degrees of Freedom | Variance Estimate | Variance Ratio | |
|---|---|---|---|---|---|
| Drill type | 0.00416 | 1 | 0.00416 | 71 | |
| Point angle | 0.00837 | 1 | 0.00837 | 142 | *** |
| Feed | 1.37687 | 3 | 0.45896 | 7832 | |
| Type x Point | 0.00023 | 1 | 0.00023 | 3.8 | n.s. |
| Type x Feed | 0.00205 | 3 | 0.00068 | 11.6 | ** |
| Point x Feed | 0.00034 | 3 | 0.00011 | 1.9 | n.s. |
| Type x Point x Feed | 0.00014 | 3 | 0.000047 | 0.8 | n.s. |
| Error | 0.00281 | 48 | 0.000059 | | |
| Total: | 1.39497 | 63 | | | |

(See Tables 7.10 and 7.11 for symbols)

Table 7.19 shows that the effect of the interaction of the three factors, drill type x point angle x drilling feed, the effect of the interaction of drill type and point angle and the effect of the interaction of the point angle and drilling feed on the drilling torque are probably not significant. It also shows that the effect of the interaction of drill type and drilling feed on the drilling torque is significant while the effect of the point angle is highly significant.

To study the effect of the other factors, a breakdown analysis was done by feed and drill type. A resumé of the variance analysis by drilling feed is presented in Table 7.20

TABLE 7.20: Resumé of Analysis of Variance for Drilling Torque by Drilling Feed

Variance ratios

| Effect | 240 RPI | 157 RPI | 103 RPI | 70 RPI |
|---|---|---|---|---|
| Point angle | 64.03 *** | 45.39 *** | 6.98 * | 12.13 ** |
| Drill type | 0.15 n.s. | 13.84 ** | 27.94 *** | 7.85 * |
| Interaction point x type | 0.02 n.s. | 2.27 n.s. | 0.22 n.s. | 0.83 n.s. |

(See tables 7.10 and 7.11 for symbols)

Analysis of Table 7.20 shows that the effect of the interaction of point angle and drill type on drilling torque is probably not significant as already seen in Table 7.19. The effect of the drill type is highly significant (103 RPI) or significant (157 RPI) for moderate drilling feeds and probably significant for high feeds (70 RPI); for low feeds(240 RPI) the effect of drill type on the drilling torque is probably not significant. The effect of point angle on the drilling torque is highly significant for low to moderate feeds (240 RPI and 157 RPI) and probably significant to significant for moderate to high feeds (103 RPI to 70 RPI).

A resumé of the variance analysis by drill type is presented in Table 7.21.

TABLE 7.21: Resumé of Analysis of Variance for Drilling Torque, by Drill Type

Variance Ratios

| Effect | Conventional Drill | New Design Drill |
|---|---|---|
| Feed | 3355.89 *** | 1475.45 *** |
| Point angle | 45.08 *** | 34.52 *** |
| Interaction feed x point | 0.71 n.s. | 0.71 n.s. |

(See Tables 7.10 and 7.11 for symbols)

Analysis of Table 7.21 shows that the interaction of drilling feed and point angle on the drilling torque is probably not significant, as already shown in Talbe 7.19. It also shows that feed and point angle are highly significant for drilling torque, as expected.

*"...most of the information for the evaluation of cutting operations ... is closely related to the chip geometry".*

*Nakayama*

# 8. ANALYSIS OF THE INFLUENCE OF FLUTE FORM ON CHIP FLOW

## 8.1 Introduction

The new design drill has shown higher wear rates and higher torque (especially for stronger feeds) in spite of presenting a better "heat sink" and approximately the same effective rake angle as the conventional drill.

In an attempt to investigate the reasons for such a difference in the performance of the two compared drill types, and further to develop a better criterion for drill design, the author took the view that the chip characteristics, being specific to each drill type, should be considered in analysing the drilling operation and the drill action.

## 8.2 Common Approach to Machining Chips

Frequently machining chips are looked at as a nuisance for the inconveniences such as chip disposal and interruption of the machining operation. Some chip classifications reflect this approach and they show the chips grouped into two major classes (71, 108): acceptable and unfavourable.

Many chip classifications can be found in literature (71, 73, 108, 109, 110, 111, 112, 113) and even in a recent edition of a British Standard (BS 5623). Many times, however, these classifications focus mainly on the conveyance and disposal features of the chips.

There are many reports in the literature on the devices and on the cutting conditions for chip control with single point cutting tools. For drilling chip control, literature is more scarce. However, some drills with special chip breaking features have been reported by Bhattacharyya (38), Oxford (21) and CETIM (17) (refer to Chapter 2, too).

The influence of drilling conditions on chip form and size have been referred to by Nakayama and co-workers (14), CETIM (17) and Galloway and co-workers (10).

Some workers, such as Spaans (100), Nakayama et al (14) and others (114, 115, 116) take the view that chip geometry is related to cutting efficiency. The author also believes that the machining chips are an important source of a great deal of information data about the cutting process.

## 8.3 Chips and Rigid Body Concept

In many works the chip is either explicitly or implicitly referred to as a rigid body [D.19] .

Lee and Shaffer (47), in a paper on the orthogonal cutting, stated that the chip must leave the plastic region as a rigid body. For Dewhurst (117) the chip can be viewed as the continuous emergence of a rigid body. Spaans (73) assumes the chip to behave as a rigid body. Armarego and Cheng (72) make the assumption that the chip travels as a rigid body after shearing has occurred. Kronenberg (118) referred to the fact that it is customary to consider the chip as a stationary body in static equilibrium. Wallace (119) also assumed the chip to slide as a rigid body up the tool rake face.

The assumption that the chip is a rigid body is also implicit in works by Nakayama (120) and Henriksen (112), for instance.

## 8.4 Drilling Chips

Oxford (20) reported once on the chip formation mechanism along drill lips and found it to be similar to any other metal-cutting operation. He further measured the chip flow angle for several radial distances and for several drilling conditions.

Armarego and Cheng (121) measured the chip length ratio [D.5] for drilling chips.

Nakayama and co-workers (14), discussed, in qualitative terms, the factors which are supposed to influence the formation of drilling chips and would determine their shape and size. They observed that *"the basic form of the chip produced by twist drills is the conical helical chip with short pitch".* (Figures 8.1 and 8.2).

Observations by the author of the drilling chips and the drilling operation were complemented by a visual study of a high speed cine film (1000 frames per second) showing a 19.52 mm diameter conventional drill producing 38.1 mm deep holes in EN8 steel at 640 rpm and 0.25 mm/rev. In this film the drill entry stage can be seen with great detail and the chips emerging from the hole, along the flute, can also be seen during drill penetration (Figures 8.1 and 8.2).

The author believes that the rigid body concept can be used with the drilling chips for analysis of their shape and kinematic properties.

Rigid bodies have properties of their own which are likely to enlighten some drilling aspects and to help with some predictions otherwise difficult.

The rigid body concept is used in this work as an analytical approach which is surprisingly successful, as it will be shown, mainly for the correlations between its predictions and experimental results reported in literature (Sections 8.6.2, 8.6.3 and 8.6.4).

## 8.5 Mathematical Model of an Helical Rigid Body Chip

The rigid body concept is a physical one and it is more general than most of the machining concepts.

To use the rigid body concept for chip analysis allows for the utilization of mathematical models and for implementation in computer programs.

This approach permits geometrical simulation and numerical investigation to be carried out which is expected:

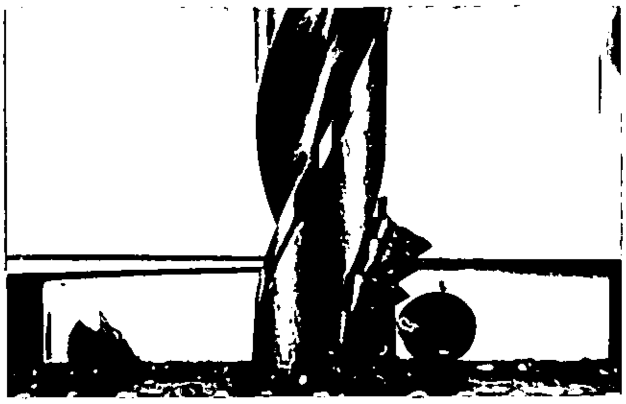

FIGURE 8.1: Drilling chip inside hole and drill flute. [Frame from high speed cine film]

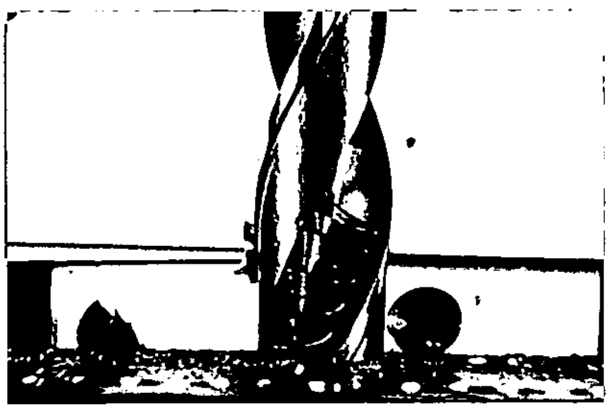

FIGURE 8.2: As in FIGURE 8.1 after drill rotated approximately 90 degrees

- to make possible to identify the parameters that govern the variation of chip flow along a drill lip
- to allow to identify the conditions and constraints the geometry of the flute drill imposes on the determination of chip form and size and chip flow
- to produce new information to be taken into account in the definition of a criterion for drill flute design.

### 8.5.1 Equations

The rigid body motion features are dealt with in many books on mechanics such as (80).

The motion of a rigid body can be regarded as a translation along a certain axis, a, and simultaneous rotation about it.

Let (Figure 8.3i):

| | | |
|---|---|---|
| a | - | the rigid body axis |
| O | - | any point on the axis a, |
| P | - | a current point on the rigid body, |
| $\vec{V}_t$ | - | the translation velocity of the rigid body along axis a |
| $\vec{W}_c$ | - | the angular velocity of the rigid body about axis a |
| $\vec{V}_c$ | - | Velocity of point P |

Let a drilling chip (Figures 8.1, 8.2 and 8.3) be a rigid body.

From the mechanics of rigid bodies (80):

$$\vec{V}_c = \vec{V}_t + \vec{W}_c \times \vec{OP}$$

This can also be written:

$$\vec{V}_c = \vec{V}_t + \vec{W}_c \times \vec{R}_c \qquad 8.1$$

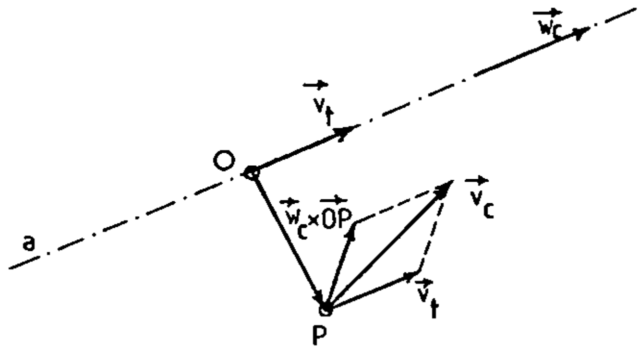


i

a - rigid body axis

$\vec{Vc}$ - chip velocity at point P

$\vec{Rc}$ - radial vector to point P

$\vec{Vt}$ - translation velocity

$\vec{Wc}$ - angular velocity

$\eta$ - chip flow angle

$S_\gamma$ - rake face

$S_\alpha$ - flank face

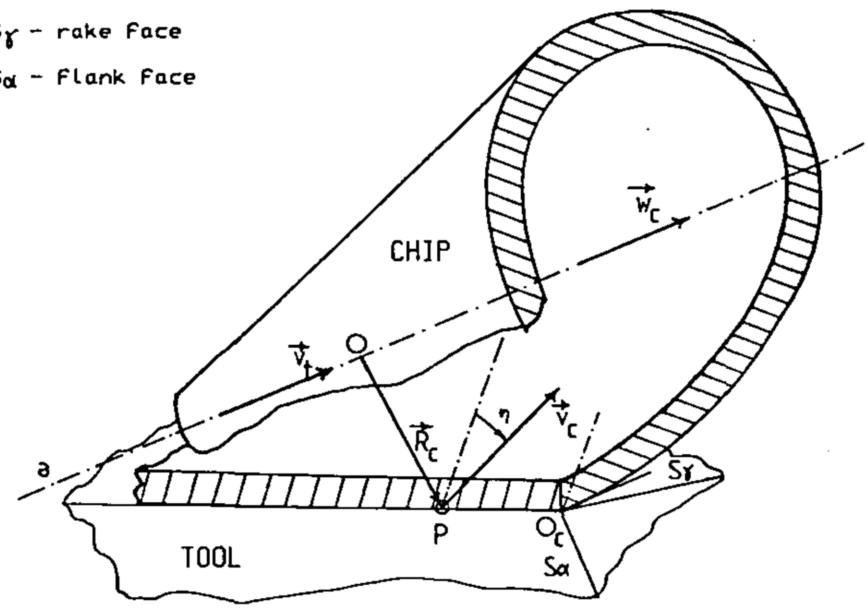


ii

FIGURE 8.3: Rigid body geometrical and kinematical variables (i) and rigid body chip (ii)

where $\vec{R}_c$ is the radial vector of point P referred to the chip axis.

The relevant geometrical features of an helical chip are shown in Figure 8.4 from where the following relationship can be written:

$$p_c = \pi d_{co} \cot \gamma_{co} \tag{8.2}$$

where $p_c$ - chip lead
$d_{co}$ - chip diameter
$\gamma_{co}$ - chip helix angle at radius $d_{co}/2$

The number of revolutions per time unit of the chip about its axis is designated by $N_c$ and the following expressions can be written:

$$W_c = 2\pi N_c \tag{8.3}$$

$$V_t = p_c N_c \tag{8.4}$$

where $W_c = |\vec{W}_c|$ and
$V_t = |\vec{V}_t|$

Let $\vec{a}$ be the unit vector on the chip instantaneous axis of rotation of the chip, then:

$$\vec{V}_t = p_c N_c \vec{a} \tag{8.5}$$

$$\vec{W}_c = 2\pi N_c \vec{a} \tag{8.6}$$

Also let

$$\vec{V}_c = V_c \vec{v}_c \qquad \text{where } |\vec{v}_c| = 1$$
$$\vec{R}_c = R_c \vec{r}_c \qquad \text{where } |\vec{r}_c| = 1$$

As $\vec{V}_t$ is normal to $\vec{W}_c \times \vec{R}_c$, from equation 8.1, it can be written

$$V_c = (V_t^2 + (|\vec{W}_c \times \vec{R}_c|)^2)^{\frac{1}{2}}$$

$$V_c = ((p_c\ N_c)^2 + (2\pi\ N_c\ R_c)^2)^{\frac{1}{2}} \qquad 8.7$$

If equations 8.5, 8.6 and 8.7 are substituted in equation 8.1 then

$$N_c\ (p_c^2 + (2\pi\ R_c)^2)^{\frac{1}{2}}\ \vec{v}_c = p_c\ N_c\ \vec{a} + 2\pi\ N_c\ \vec{a} \times (R_c\ \vec{r}_c)$$

$$\vec{v}_c = \frac{p_c}{(p_c^2 + (2\pi\ R_c)^2)^{\frac{1}{2}}}\ \vec{a} + \frac{2\pi\ R_c}{(p_c^2 + (2\pi\ R_c)^2)^{\frac{1}{2}}}\ \vec{a} \times \vec{r}_c \qquad 8.1'$$

Equation 8.1' is the mathematical model, in the vectorial form, for a helical chip with lead $p_c$ where $p_c$ depends on the external diameter, $d_{co}$, of the chip and on the helix angle, $\gamma_{co}$, at the chip periphery (Equation 8.2).

The mathematical model represented by equation 8.1' can be written in algebraic form if the components of $\vec{v}_c$, $\vec{a}$ and $\vec{r}_c$ in a referential system are known.

Let:

$$\vec{v}_c = (v_1, v_2, v_3)$$

$$\vec{a} = (a_1, a_2, a_3)$$

$$\vec{r}_c = (r_{c1}, r_{c2}, r_{c3})$$

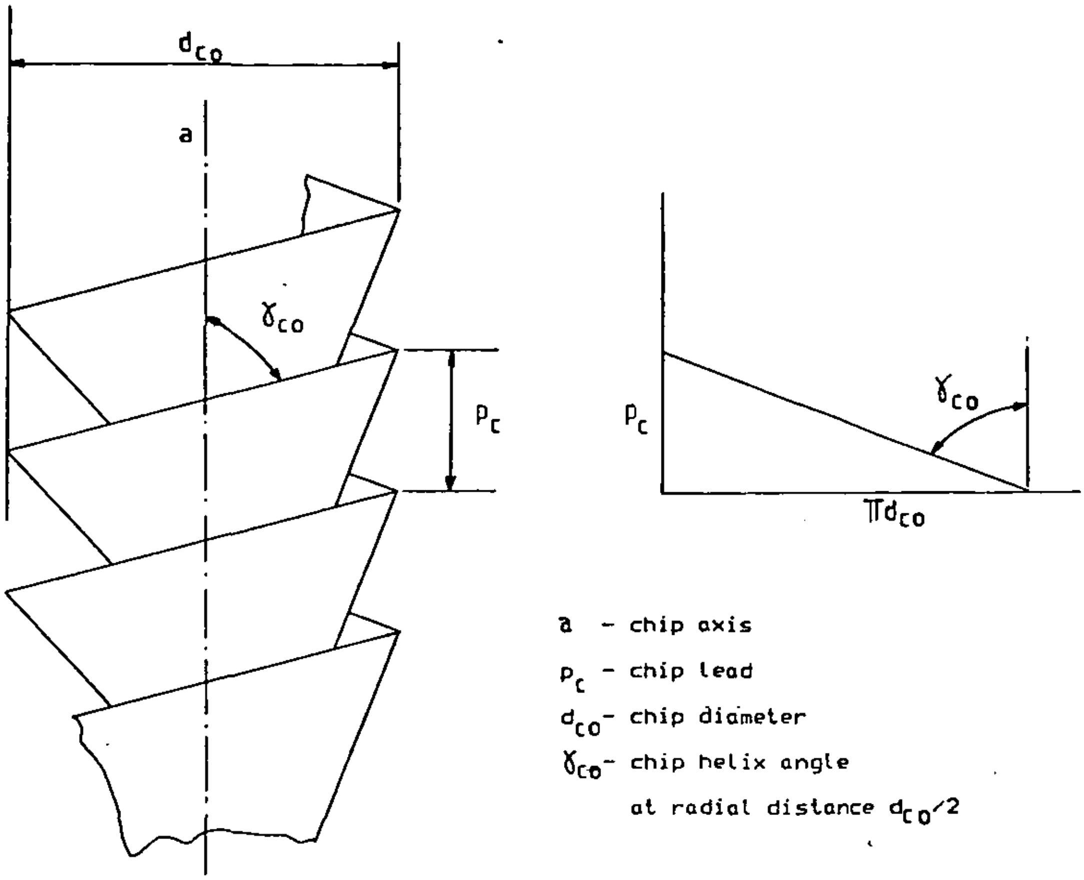


FIGURE 8.4: Geometrical features of an helical chip

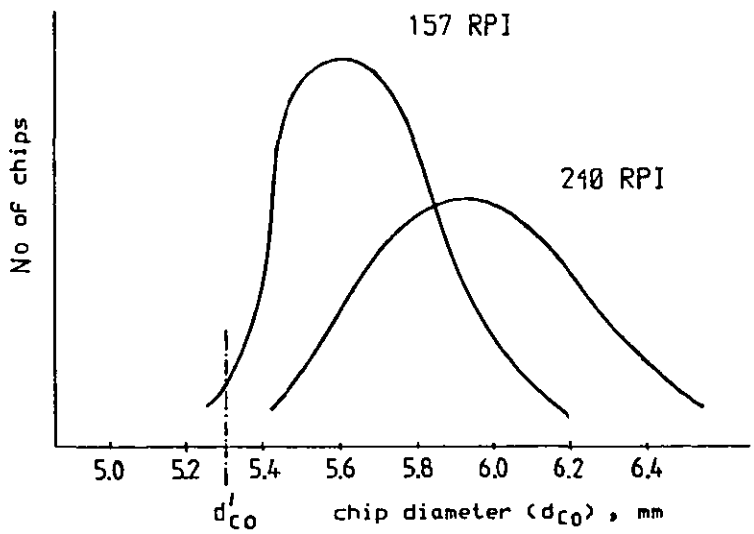


FIGURE 8.5: Steel drilling chips diameter distribution for 12.7 mm diameter conventional drill. [Refer to next FIG for $d'_{co}$]

So:

$$\vec{a} \times \vec{r}_c = \begin{vmatrix} \vec{i} & \vec{j} & \vec{k} \\ a_1 & a_2 & a_3 \\ r_{c1} & r_{c2} & r_{c3} \end{vmatrix} =$$

$$= (a_2\, r_{c3} - a_3\, r_{c2},\ \ a_3\, r_{c1} - a_1\, r_{c3},$$

$$a_1\, r_{c2} - a_2\, r_{c1})$$

where $\vec{i}$, $\vec{j}$, $\vec{k}$ are the unit vectors on the referential axes.
Then:

$$v_{c1} = M\,[p_c a_1 + 2\pi\, R_c\,(a_2 r_{c3} - a_3 r_{c2})] \qquad 8.1'a$$

$$v_{c2} = M\,[p_c a_2 + 2\pi\, R_c\,(a_3 r_{c1} - a_1 r_{c3})] \qquad 8.1'b$$

$$v_{c3} = M\,[p_c a_3 + 2\pi\, R_c\,(a_1 r_{c2} - a_2 r_{c1})] \qquad 8.1'c$$

where $\qquad M = \dfrac{1}{(p_c{}^2 + (2\pi\, R_c)^2)^{\frac{1}{2}}}$

Equations 8.1'a to 8.1'c represent, in algebraic form, the mathematical model for a helical chip with parameter $p_c$.

8.5.2 Analysis of parameter $p_c$

The rigid body chip lead, $p_c$, is related to the chip helix angle through the chip diameter as can be seen in equation 8.2 and Figure 8.4.

#### 8.5.2.1 Drilling chip diameter

From the earlier stages of this work many chips produced by different drill sizes, in different drilling conditions, for various steels, have been collected.

It was observed, and it has also been reported (17), that drilling chips produced by conventional drills tend to appear fragmented when feed increases and/or drill diameter decreases.

With 12.7 mm (½") conventional drills and for the feeds relative to 240 RPI and 157 RPI, many helical chips of full width (the length of the lip, from chisel corner to outer corner) could be collected. The diameters of these chips were measured and the respective distribution analysed (Figure 8.5).

The chips for the 240 RPI appeared to concentrate around the 5.9 mm diameter, and the ones for the 157 RPI around 5.6 mm diameter.

The author thought that these diameter values might be related to the space available inside the flute. This space was computed according to the biggest circle inside a section normal to the drill axis, as shown in Figure 8.6, and the computed value, $d'_{co}$, resulted to be 5.3 mm (refer to Figure 8.6).

The actual chip diameters appear to be somewhat over the computed value of $d'_{co}$ (refer to Figure 8.5): 5.9 mm and 5.6 mm against 5.3 mm for $d'_{co}$. This fact may be explained by the ability of the drilling chips to accommodate large elastic deformation as it can be checked by twisting, by hand, any drilling chip, by opening it (increases diameter) or closing it (decreases diameter). This is believed to be supported by the fact that different feeds (thus different chip thicknesses) yield chips of different average diameters (different compliance of the chips).

As a matter of chip diameter specification, for the computation with the chip model, a dimension of the space available inside the flute can be used as an approximation. Such a dimension can be, as a

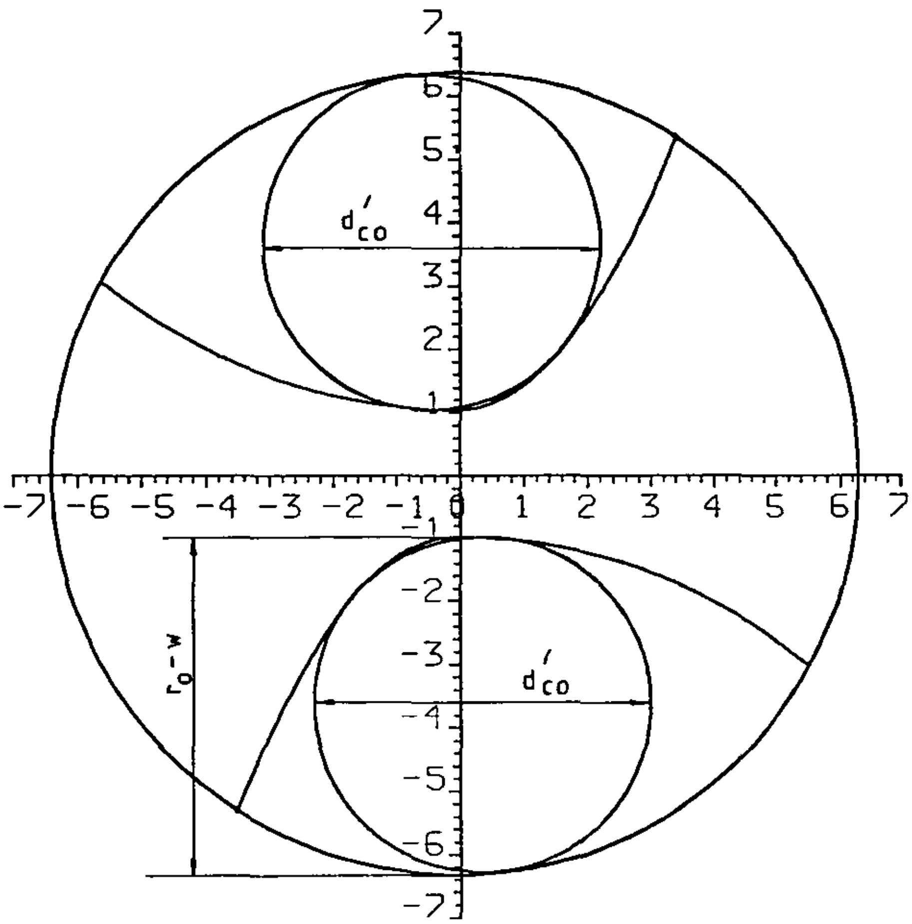


FIGURE 8.6: Maximum circle inside the drill flute in a section normal to the drill axis

matter of simplification relatively to the method illustrated in Figure 8.6, the computed difference between the drill radius ($r_o$) and the half web thickness (W): $r_o - W$ (Figure 8.6).

Nevertheless, the diameter of the chip decreases from the outer corner to the chisel corner mainly as a consequence of the decreasing cutting speed along the lip, from the periphery to the drill axis.

8.5.2.2 Drilling chip helix angle

The chip helix angle, $\gamma_{co}$ (Figure 8.4), can be related to the chip flow angle, $\eta_o$ (Figure 8.3), at the point $O_c$ (outer corner) as it will be shown.

If, as generally recognized in the field of oblique cutting, the inclination angle has an important influence on the determination of the chip flow angle, the chip helix angle will be equally determined by the inclination angle too.

By definition, the chip flow angle, $\eta$, is given by (Figure 8.3):

$$\cos(90 - \eta) = \frac{\vec{V}_c \cdot \vec{e}}{|\vec{V}_c||\vec{e}|} = \frac{\vec{V}_c \cdot \vec{e}}{V_c} \qquad 8.8$$

where $\vec{e}$ is assumed to be the unit vector on the tangent to the cutting edge at the selected point.

From equations 8.1 and 8.8:

$$\sin\eta = \frac{(\vec{V}_t + \vec{W}_c \times \vec{R}_c) \cdot \vec{e}}{V_c}$$

$$\sin\eta = \frac{\vec{V}_t \cdot \vec{e} + (\vec{W}_c \times \vec{R}_c) \cdot \vec{e}}{V_c} \qquad 8.9$$

Using equations 8.5 and 8.6 in equation 8.9 it results:

$$\sin\eta = \frac{N_c p_c\ \vec{a}.\vec{e} + (2\pi\ N_c\vec{a} \times \vec{R}_c).\vec{e}}{V_c} \qquad 8.9'$$

$$\sin\eta = N_c\ \frac{p_c \cos\kappa_c + 2\pi\ R_c\ (\vec{a} \times \vec{r}_c).\vec{e}}{V_c} \qquad 8.9''$$

where $\kappa_c$ (Figure 8.7) is the angle between the cutting edge at the selected point and the instantaneous axis of rotation of the chip, and $\vec{r}_c$ is the unit vector in the direction of $\vec{R}_c$, and $R_c$ the length of $\vec{R}_c$.

From vectorial analysis (78), the product $(\vec{a} \times \vec{r}_c).\vec{e}$ represents the volume of a parallelepiped having $\vec{a}$, $\vec{r}_c$ and $\vec{e}$ as edges.

$\vec{a}$ and $\vec{r}_c$ are unit vectors and normal to each other. From Figure 8.7:

$$\frac{HJ}{AH} = \frac{GI}{AG}\ ; \quad AH = 1; \quad HJ = \frac{GI}{AG}$$

$$\frac{AB}{AG} = \mathrm{Cos}\ \kappa_c; \quad AB = 1; \quad AG = \frac{1}{\mathrm{Cos}\ \kappa_c}\ ; \quad HJ = GI\ \mathrm{Cos}\ \kappa_c$$

$$GI = MN$$

$$\frac{MN}{AN} = \frac{g_c}{R_c}$$

$$MN = \frac{g_c}{R_c} AN; \quad AN = BG = \tan\kappa_c; \quad MN = \frac{g_c}{R_c}\tan\kappa_c = GI$$

$$HJ = GI\ \mathrm{Cos}\ \kappa_c = \frac{g_c}{R_c}\tan\kappa_c\ \mathrm{Cos}\ \kappa_c = \frac{g_c}{R_c}\mathrm{Sin}\ \kappa_c$$

$$\therefore \qquad (\vec{a} \times \vec{r}_c).\vec{e} = 1.1.HJ = HJ = \frac{g_c}{R_c}\mathrm{Sin}\ \kappa_c$$

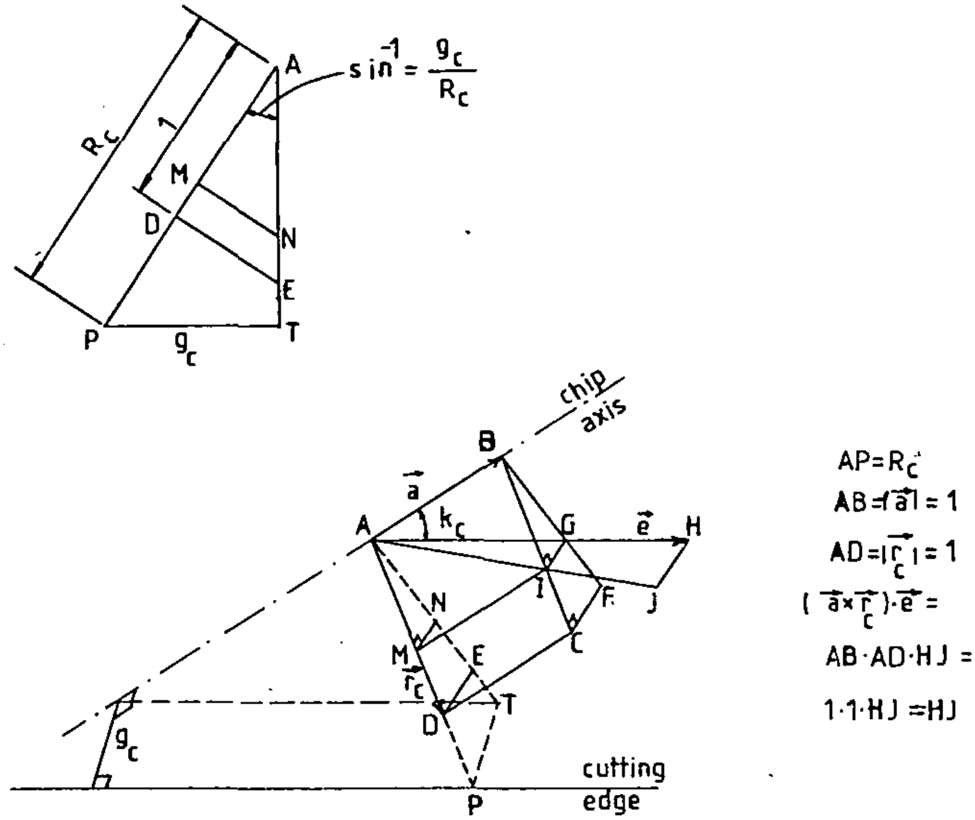


FIGURE 8.7: Position of the chip axis relative to the cutting edge

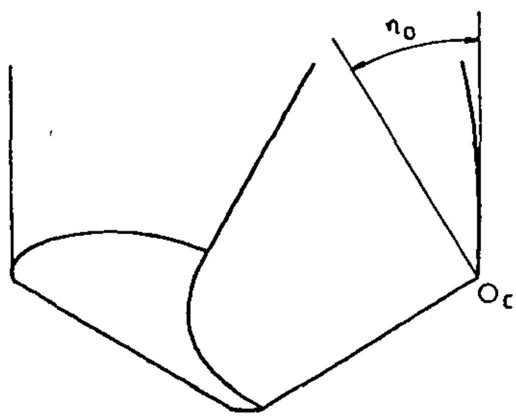


FIGURE 8.8: Maximum theoretical possible chip flow angle at the drill outer corner

Equation 8.9" can now be written in the following way:

$$\text{Sin}\,\eta = N_c \frac{p_c \,\text{Cos}\,\kappa_c + 2\pi\, R_c \frac{g_c}{R_c} \,\text{Sin}\,\kappa_c}{V_c} \qquad 8.9^{iii}$$

As $V_c$ is given by equation 8.7, then equation 8.9''' becomes:

$$\text{Sin}\,\eta = \frac{p_c \,\text{Cos}\,\kappa_c + 2\pi\, g_c \,\text{Sin}\,\kappa_c}{1/M} \qquad 8.9^{iv}$$

or

$$\text{Sin}\,\eta = p_c\, M \,\text{Cos}\,\kappa_c + 2\pi\, R_c M \frac{g_c}{R_c} \,\text{Sin}\,\kappa_c \qquad 8.9^{v}$$

From Figure 8.3 it can be seen that:

$$\text{Cos}\,\gamma_c = p_c\, M \qquad 8.10$$

$$\text{Sin}\,\gamma_c = 2\pi\, R_c M \qquad 8.11$$

where

$$M = \frac{1}{(p_c^{\,2} + (2\pi\, R_c)^2)^{\frac{1}{2}}}$$

Then

$$\text{Sin}\,\eta = \text{Cos}\,\gamma_c \,\text{Cos}\,\kappa_c + \text{Sin}\,\gamma_c \frac{g_c}{R_c} \,\text{Sin}\,\kappa_c \qquad 8.9^{vi}$$

where (Figure 8.7):

$\gamma_c$ - chip helix angle at the selected point

$R_c$ - chip radial distance from the selected point to the chip axis

$g_c$ - distance from the chip instantaneous axis of rotation to the tangent to the lip at the selected point

$\kappa_c$ - angle between the chip instantaneous axis of rotation and the tangent to the lip at the selected point.

At the outer corner, equation $8.9^{vi}$ is written:

$$\text{Sin } \eta_o = \text{Cos } \gamma_{co} \text{ Cos } \kappa_{co} + \text{Sin } \gamma_{co} \frac{g_{co}}{R_{co}} \text{ Sin } \kappa_{co} \qquad 8.9^{vii}$$

The maximum theoretically possible value of $\eta_o$ at the drill periphery is illustrated in Figure 8.8.

For one conventional drill with the features 2W' = 2 mm; $\gamma_f = 30^o$; $\kappa = 59^o$ and $d_o = 12.7$ mm (½") the angle $\eta_o$ was computed and found to be 30.9°.

Making $g_{co} = 0.1$ and $\kappa_{co} = 18^o$, which have been obtained from one example, and for one chip 5.3 mm diameter, the above equation $8.9^{vii}$ gives $\gamma_{co} = 60^o$ for $\eta_o = 30.9^o$. This corresponds to a chip lead of nearly 10 mm.

The chips referred to in the last section were also measured for chip lead. The results have shown a dispersed distribution with the majority of the values falling in the interval 3-5 mm. These values correspond to chip helix angles comprehended between approximately 80° and 73°.

## 8.6 Computing Approach to Drilling Chips

For computing approach purposes the following conditions are supposed to apply to drilling chips:

i) the chip is formed at the drill lip and it is born a rigid body;

ii) the chip is generated all along the lip, from the chisel corner up to the outer corner, and any lateral deformation is neglected;

iii) any action (by the hole wall or the flute heel, for example) on the chip formed at the lip is responded by the chip, for its permanent form and size, at its root, i.e. at the surface of separation chip/workpiece;

iv) the rigid body chip tends to be tangent to the rake face at the drill lip and the chip contact length [D.10] is neglected;

v) the chip diameter is governed by the space available in the drill flute and in the hole;

vi) chip radius decreases from the outer corner towards the chisel corner.

One condition is also assumed for the lip and for the flute face: the lip and the flute face are not altered either by wear or by built-up-edge [D.3] during drilling.

At this stage the instantaneous axis of rotation of the chip is not yet known. However, some conditions controlling the size and the flow of drilling chips have already been referred to.

It is possible to compute a chip rigid body motion, for a given chip lead, with the drill lip as a generator line, for an instantaneous axis selected to a guess. Then it is possible to compute the deviation of the computed rigid body to the pre-specified conditions: chip diameter and tangency to the rake face.

If the instantaneous axis is defined by two points, B and M, Figure 8.9, it is possible, starting from the points determined to a guess, to determine a set of pairs of points in the neighbourhood of the starting one and to define a set of instantaneous axes with each pair of points. The above referred to deviations can be computed for each new instantaneous axis and compared between each other in order to find the one which is nearer to the desired solution.

From the new instantaneous axis the process can proceed as indicated until the best axis is found as an exact solution may not be possible.

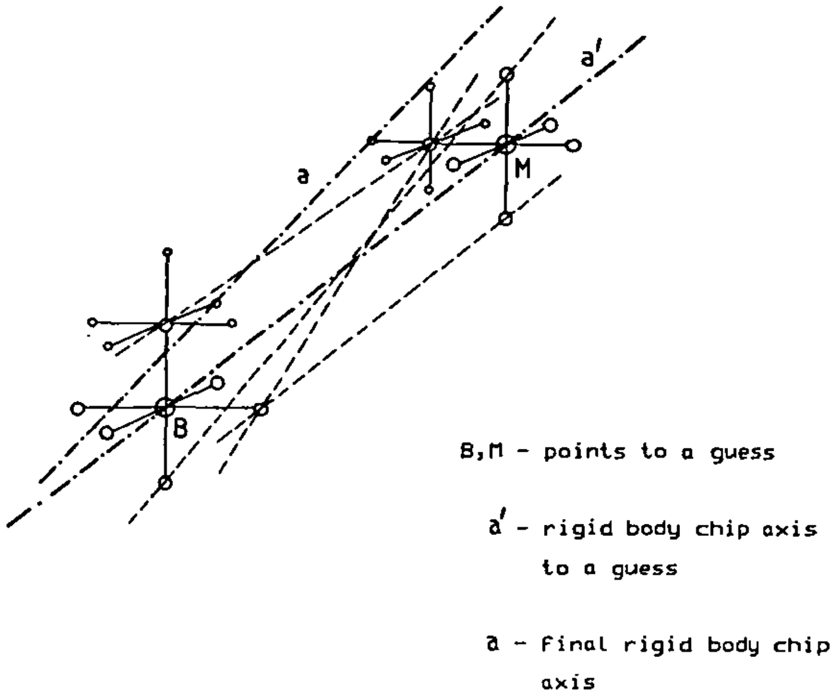


FIGURE 8.9: Strategy for numerical search of the best rigid body chip instantaneous axis. B,M - starting points.

A computer program (Appendix 8) was designed and built up, according to the described strategy, in order that the best rigid body chip complying to the specifications could be found.

A rigid body chip axis is presented in Figure 8.10 for one chip 4 mm lead, 6.4 mm diameter. For this example, the axis is 0.09 mm distant from the cutting edge and inclined 27.01° to the same edge as referred to the outer corner.

### 8.6.1 Drilling chip geometrical simulation

The above referred to computer program was developed in order to geometrically simulate the chip. Figure 8.11 shows the geometrically simulated rigid body chip for the same conditions as for Figure 8.10.

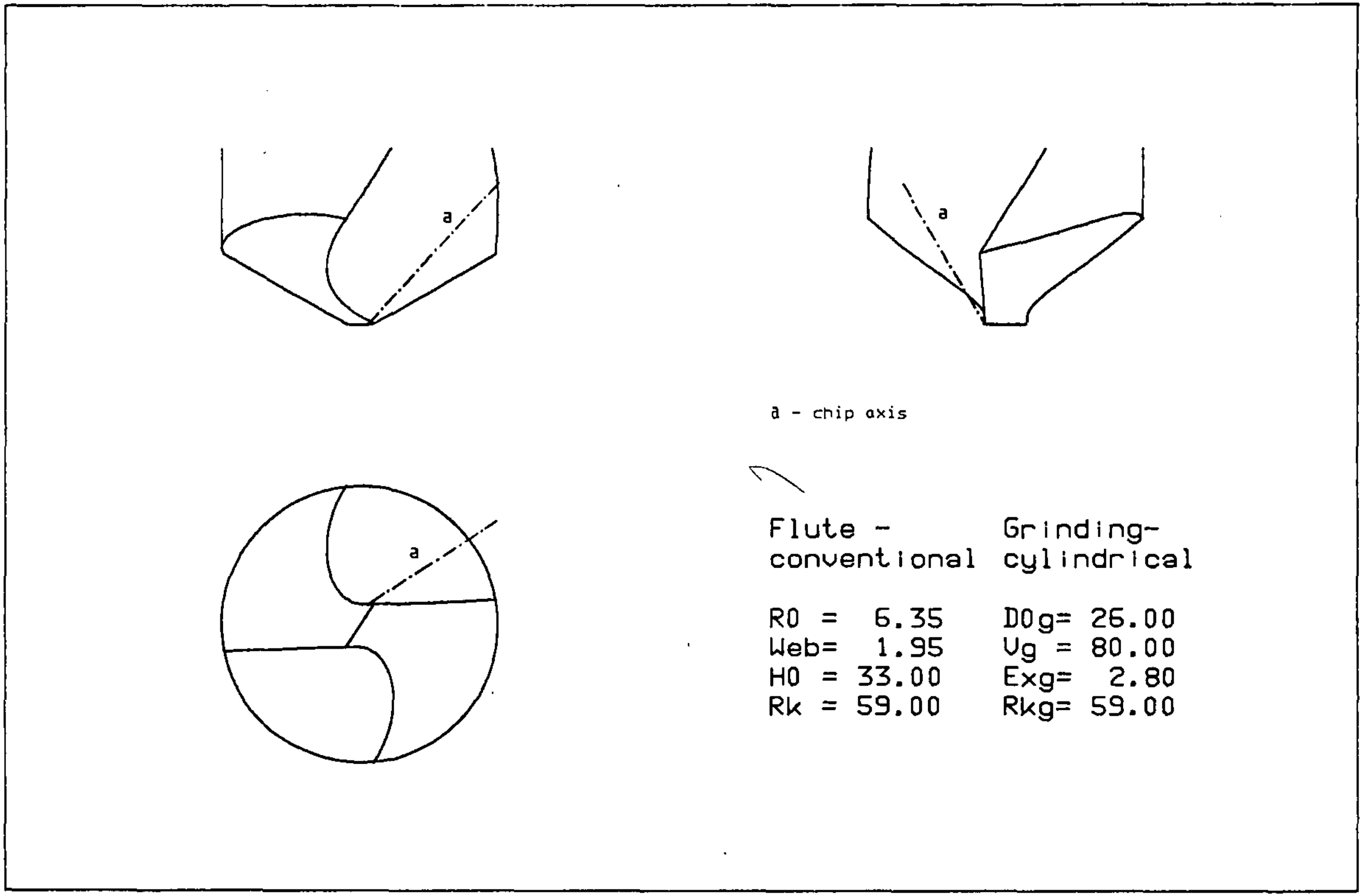


FIGURE 8.10: Computer generated drilling chip axis for one chip 4 mm lead and 6.4 mm diameter

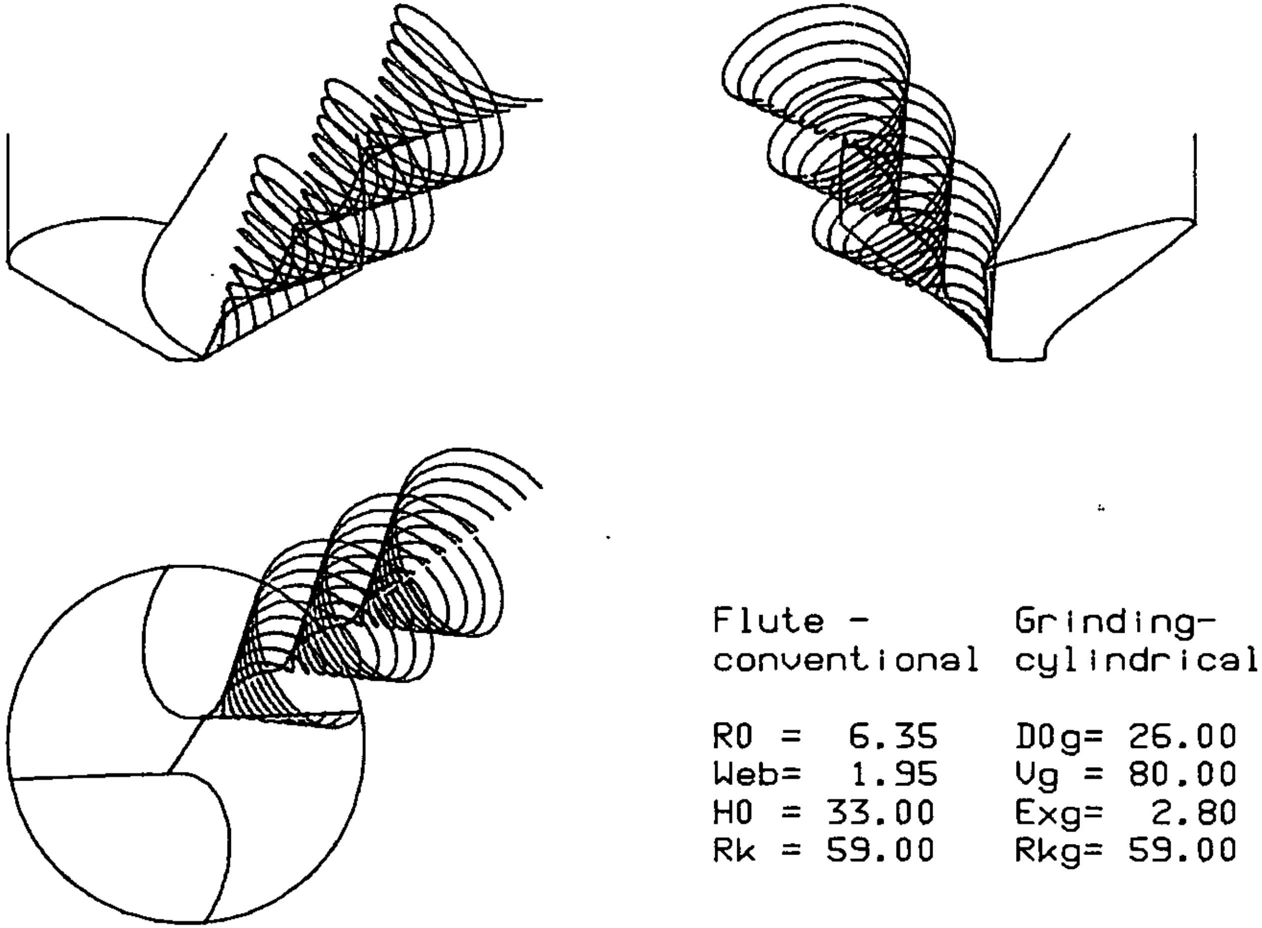


FIGURE 8.11: Computer geometrically simulated rigid body chip

For axis and conditions as in FIGURE 8.10

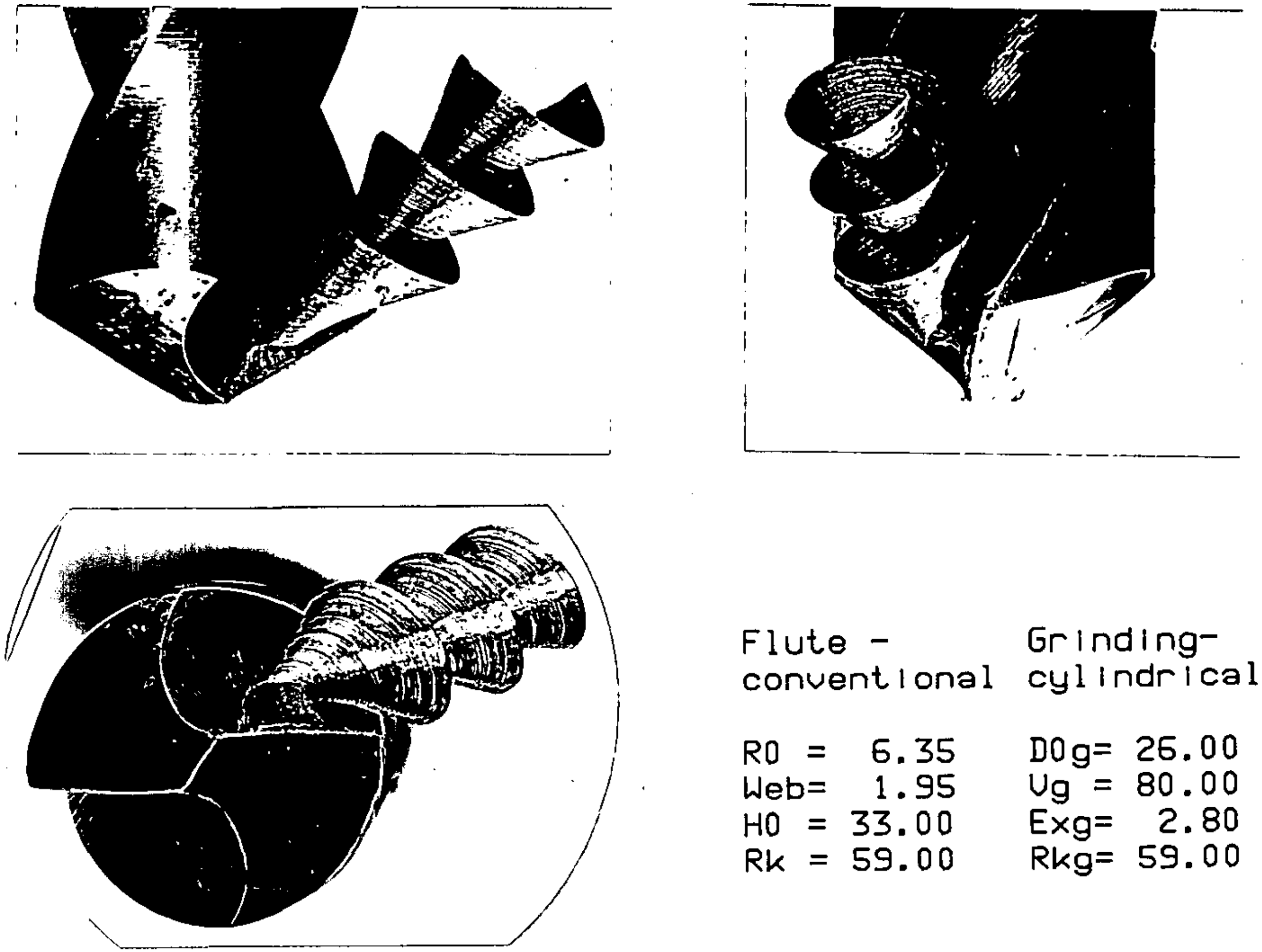


FIGURE 8.12: Views of drilling chip emerging from the drill lip
[Refer to FIGURE 8.11 - computer simulated chip]

Figure 8.12 shows an actual chip produced by a conventional drill with the features as for Figures 8.10 and 8.11, and for the following cutting conditions: 820 rpm, 240 RPI, EN43 steel, soluble oil as coolant.

Figure 8.13 shows the computed chip axis for the new design drill. A similar simulation to that in Figure 8.12 is shown in Figure 8.14 for this drill.

The main apparent difference between the simulated chip shown in Figure 8.11 and the one shown in Figure 8.14 refers to the geometric shape which is cone-like for the conventional flute and bell-like for the new design flute. Other major and more significant differences will be referred to in the sections ahead.

### 8.6.2 Chip flow angle: prediction by the present model compared to measurements by Oxford

Some workers, in studying the conventional drill lip action with the cutting mechanics approach, have made several assumptions for the chip flow angle.

Bhattacharyya (25) once assumed the empirical Stabler's rule:

$$\eta = \lambda \qquad 4.17$$

to be valid in the drilling operation.

Armarego and Cheng (72) made a study of conventional drills to which the rake face was made flat at the drill lip, by grinding, and attempted three different chip flow angle laws:

i) $\eta = \lambda$

ii) $\eta = \tan^{-1} (\tan\lambda \cos \gamma_n)$ 4.19

iii) $\eta = (0.9 - 0.2\ \gamma_n)\lambda$ 8.12

where the two last ones are arbitrary laws.

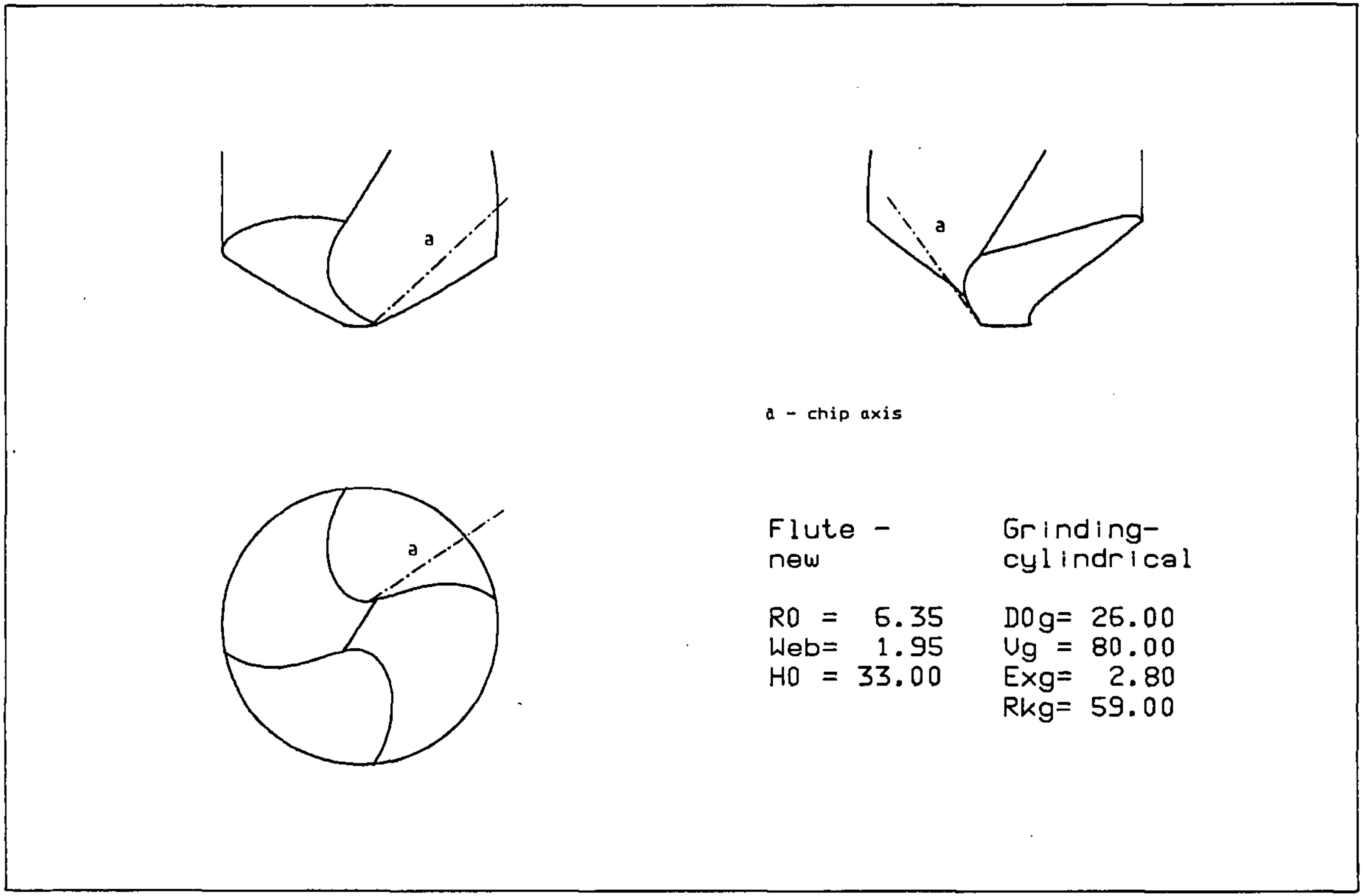


FIGURE 8.13: Computer generated drilling chip axis for one chip 4 mm lead and 6.4 mm diameter

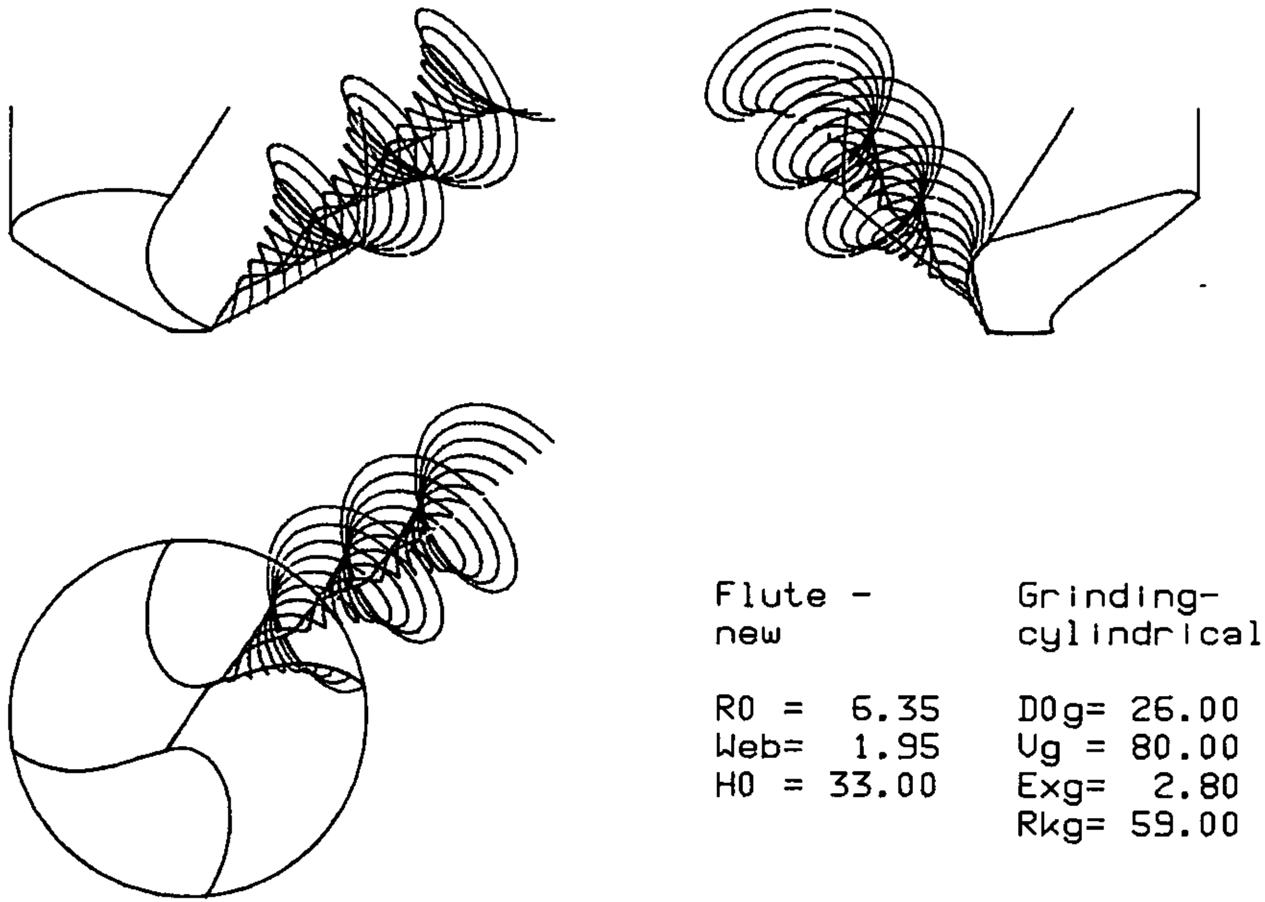


FIGURE 8.14: Computer geometrically simulated rigid body chip

For axis and conditions as in FIGURE 8.13

Laws (i) and (ii) have already been dealt with by the author in Chapter 4.

The law (iii) has shown to better serve the theoretical purposes of Armarego and Cheng who found it to yield smaller angles than those with the rule by Stabler.

For conventional drills, the same workers - Armarego and Cheng - assumed the chip velocity at each point to be on a plane parallel to the drill axis and normal to the radius at the selected point (72).

They further developed a formula for the calculation of this angle, which is, according to the assumption, the angle between the lip and the tangent to the helix, measured on the plane tangent to the rake face, at the selected point, and found

$$\eta = \mathrm{Sin}^{-1}\left(\mathrm{Cos}\gamma\ \mathrm{Cos}\kappa + \frac{W'}{r}\ \mathrm{Sin}\gamma\ \mathrm{Cos}\kappa\right) \qquad 8.13$$

where

$\eta$ :- chip flow angle at the selected point
$\gamma$ - helix angle at the selected point
$\kappa$ - ½ point angle
$2W'$- lip spacing
$r$ - radial distance.

The author computed this angle by the model presented in Chapter 4 and by means of vectorial analysis and found the values to coincide, as expected, with those by the above formula. Incidentally the author notes that the formula by Armarego and Cheng is unusable with curved lips.

Equation 4.17 (Stabler) and equation 8.13 (Armarego and Cheng) are presented in Figure 8.15 compared to drilling chip measurements by Oxford (20), (refer to Figure 8.16 ii).

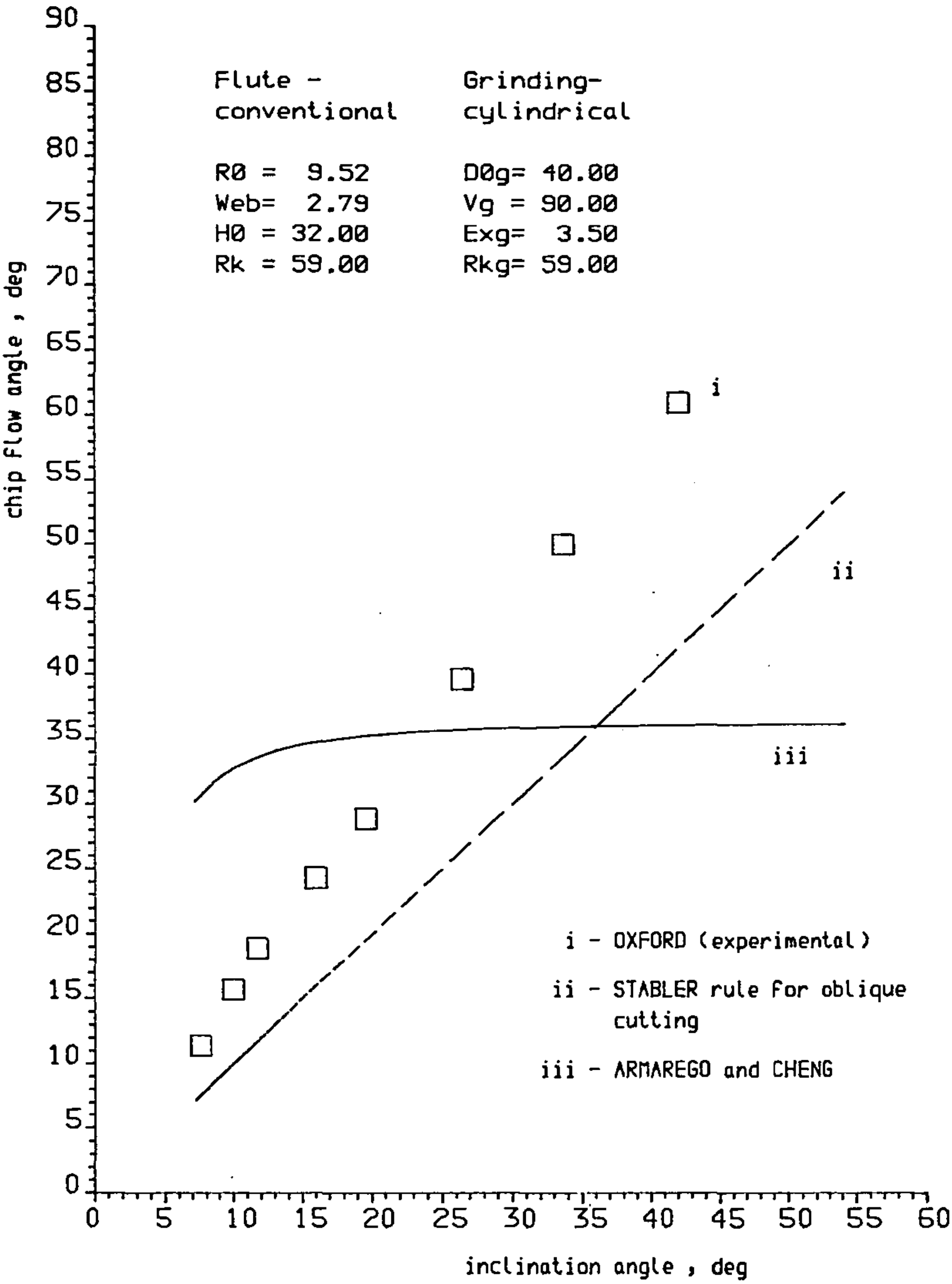


FIGURE 8.15: Drilling chip flow angle versus inclination angle from three sources : i (20) [refer to FIG 8.16ii] ; ii (45) ; iii (72)

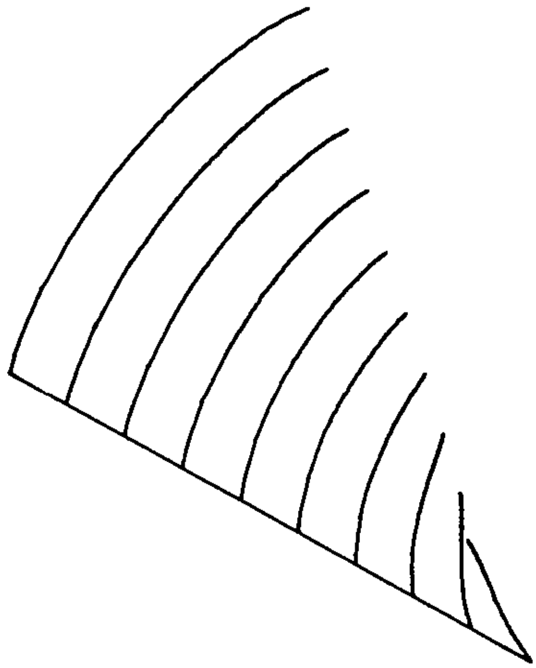

i

ii

FIGURE 8.16: Chip Flow lines :

i - Computer simulated (author's approach)

ii - Recorded by OXFORD (1,20)

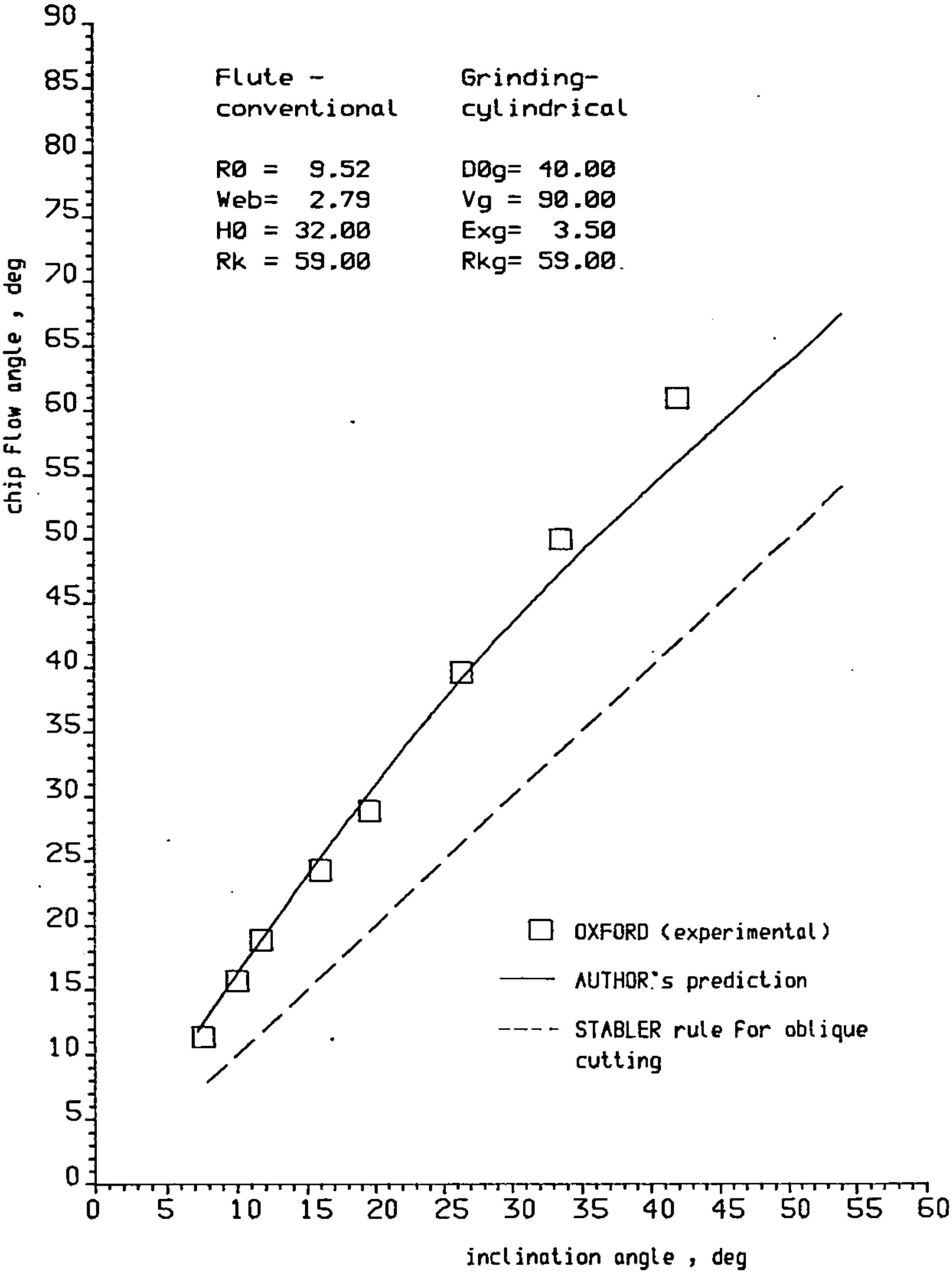


FIGURE 8.17: Drilling chip flow angle versus inclination angle as predicted by the author. [Compare with FIGURE 8.15]

The drill features to which Figure 8.15 refers to are (Oxford (20)): $r_o$ = 9.52 mm, 2W = 2.79 mm, $\gamma_f = 32^0$, $2\kappa = 118^0$.

The author used his rigid body approach for computing the chip flow angle (Figure 8.16) and for $d_{co}$ = 8 mm and $p_c$ = 5.5 mm (values that tests with 19.52 mm diameter conventional drills from the shelf confirmed to be representative) found the result shown in Figure 8.17.

The agreement between the experimental values and the prediction by the present model is not only qualitative but also quantitative.

The deviations of the predicted chip flow angle from the measured ones, for the higher values of the inclination angle (occurring close to the chisel corner) may be explained by the effect of the chisel edge chips, which has not been considered in the present approach, and may increase the chip flow angle of the lip produced chips by locally forcing them out (Figure 8.18). However, the chip flow near the chisel corner is likely to be so strongly complex and disturbed (there are two distinct processes of cut at the chisel corner neighbourhood - one by the lip and the other by the chisel edge) that a theoretical approach for this point could hardly succeed.

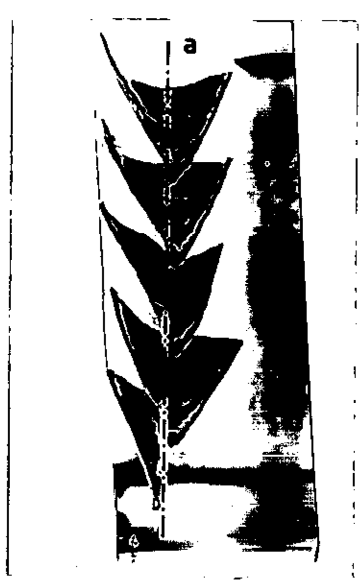


FIGURE 8.18
Drilling chip embeded in press moulded resin,cut along its axis,showing larger concentrations of material at the area closer to the chip axis(a)

To compare the conventional drill with the new design one, the rigid body approach was considered for both 12.7 mm diameter drill types.

Figure 8.19 shows the chip flow angle together with the inclination angle versus the distance along the lip for the conventional drill. The chip flow angle was also plotted against the inclination angle in Figure 8.20.

Figures 8.21 and 8.22 show similar representation to Figures 8.19 and 8.20 respectively, for the new design drill.

Figure 8.21 shows that the inclination angle is such that it has a minimum near the point at 3 mm from the chisel corner, and increases to either side of this point.

Figure 8.22 shows that for the conditions considered in the computation (chip diameter to be accommodated inside the flute) a rigid body chip would have two parts with two distinct performances: for one part the chip flow angle would increase together with the inclination angle, for the other the chip flow angle would decrease with increasing inclination angle.

If the inclination angle is the major variable controlling the chip flow angle for oblique cutting (14, 45, 73) (see equation 4.17, for example) the situation depicted in Figure 8.22 would be quite unusual as it shows two different tendencies for two distinct parts of the same chip. In fact, it is observed in Figure 8.26 (compare to Figure 8.24) and Figure 8.27i that, for the case analysed, the chip splits in two as if two chips were produced.

Apparently it could be asked if a rigid body that yields a chip flow angle as the one shown in Figures 8.28 and 8.29 - chip flow angle increases when the inclination angle increases and decreases with decreasing inclination angle - would be possible with the new design drill.

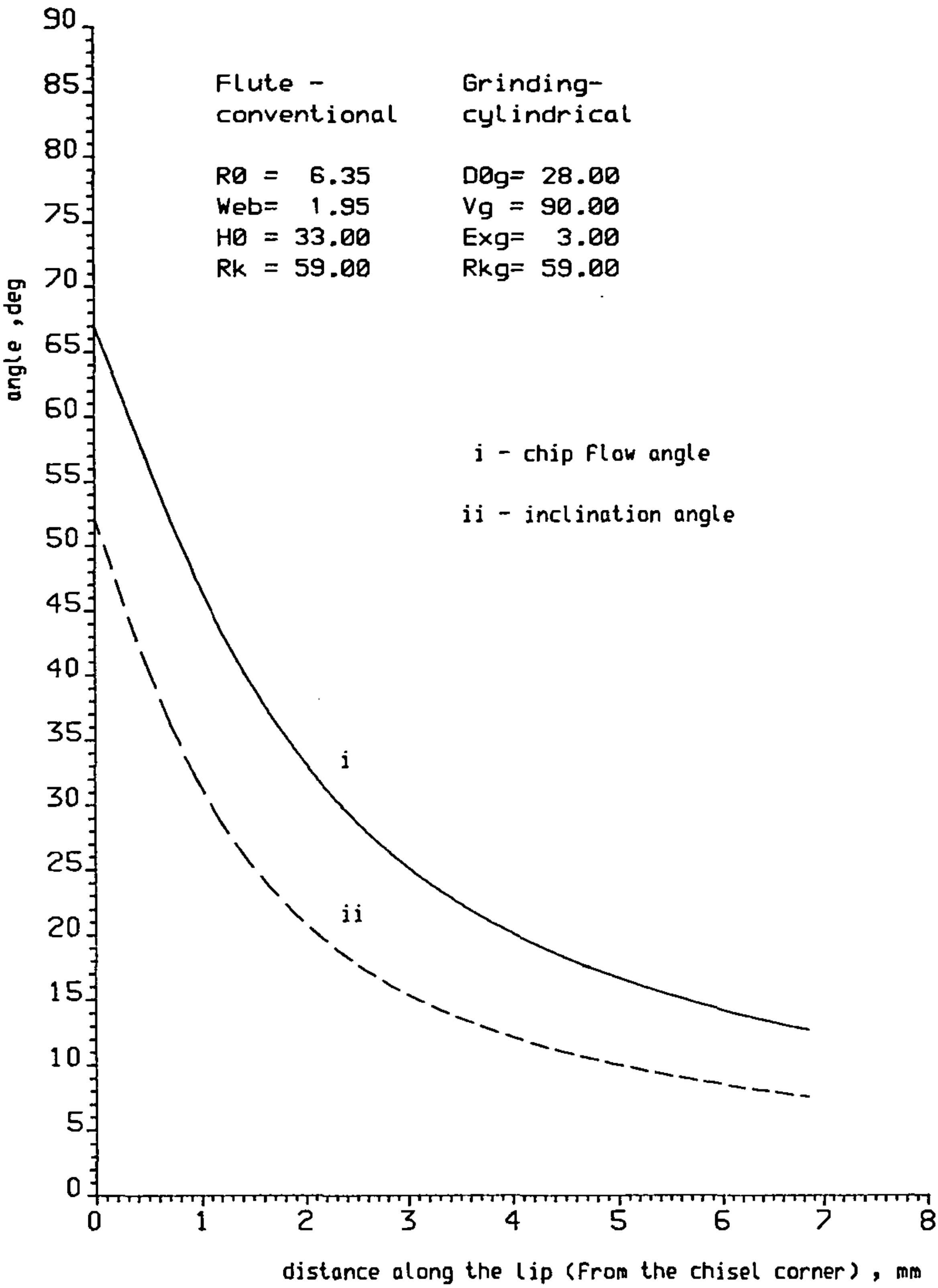


FIGURE 8.19: Drilling chip flow angle,from rigid body approach [5.4 mm chip diameter and 4 mm chip lead],and drill lip inclination angle

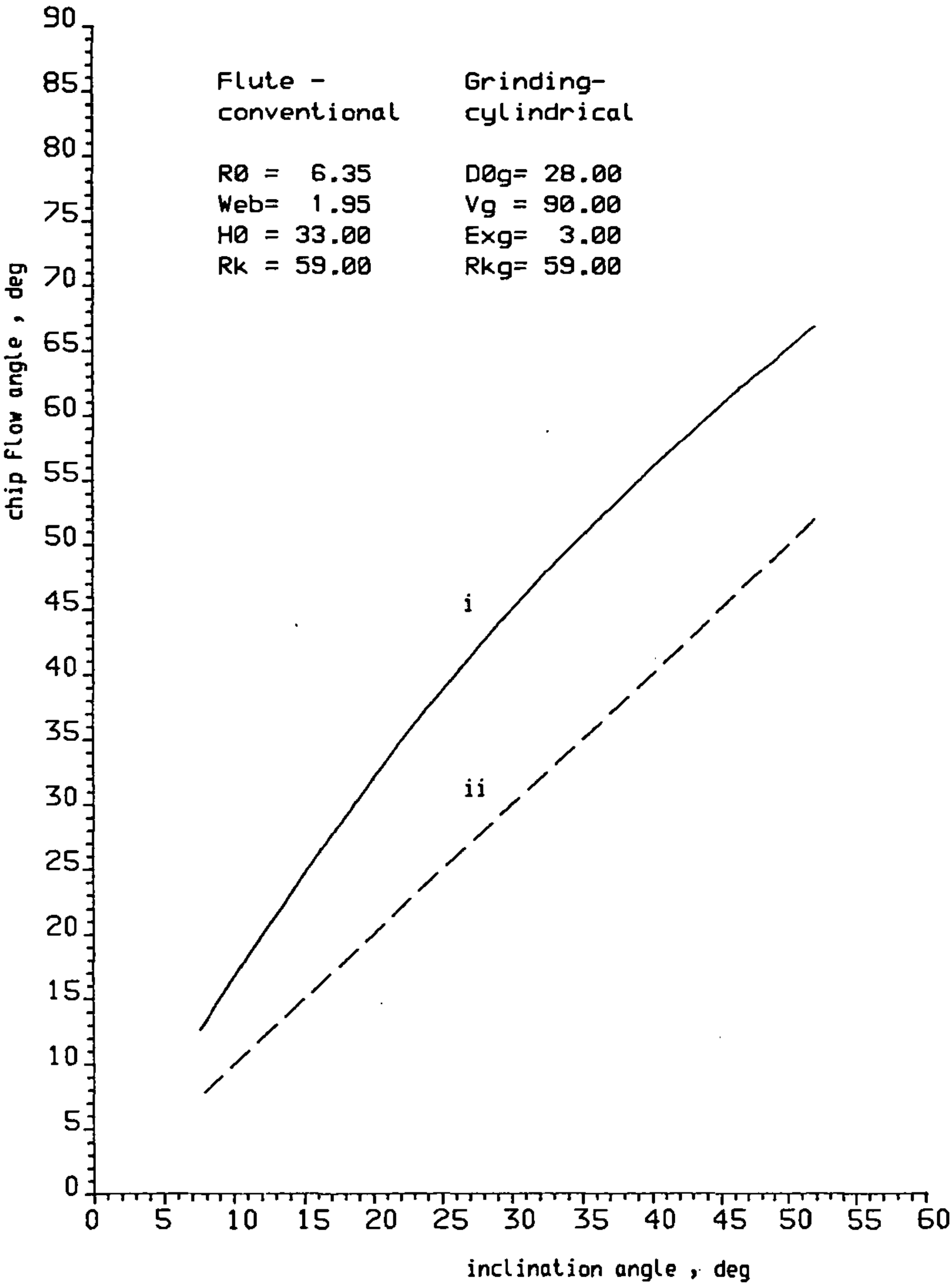


FIGURE 8.20: Drilling chip flow angle from rigid body approach (i) [refer to FIGURE 8.19] and STABLER's rule versus drill lip inclination angle

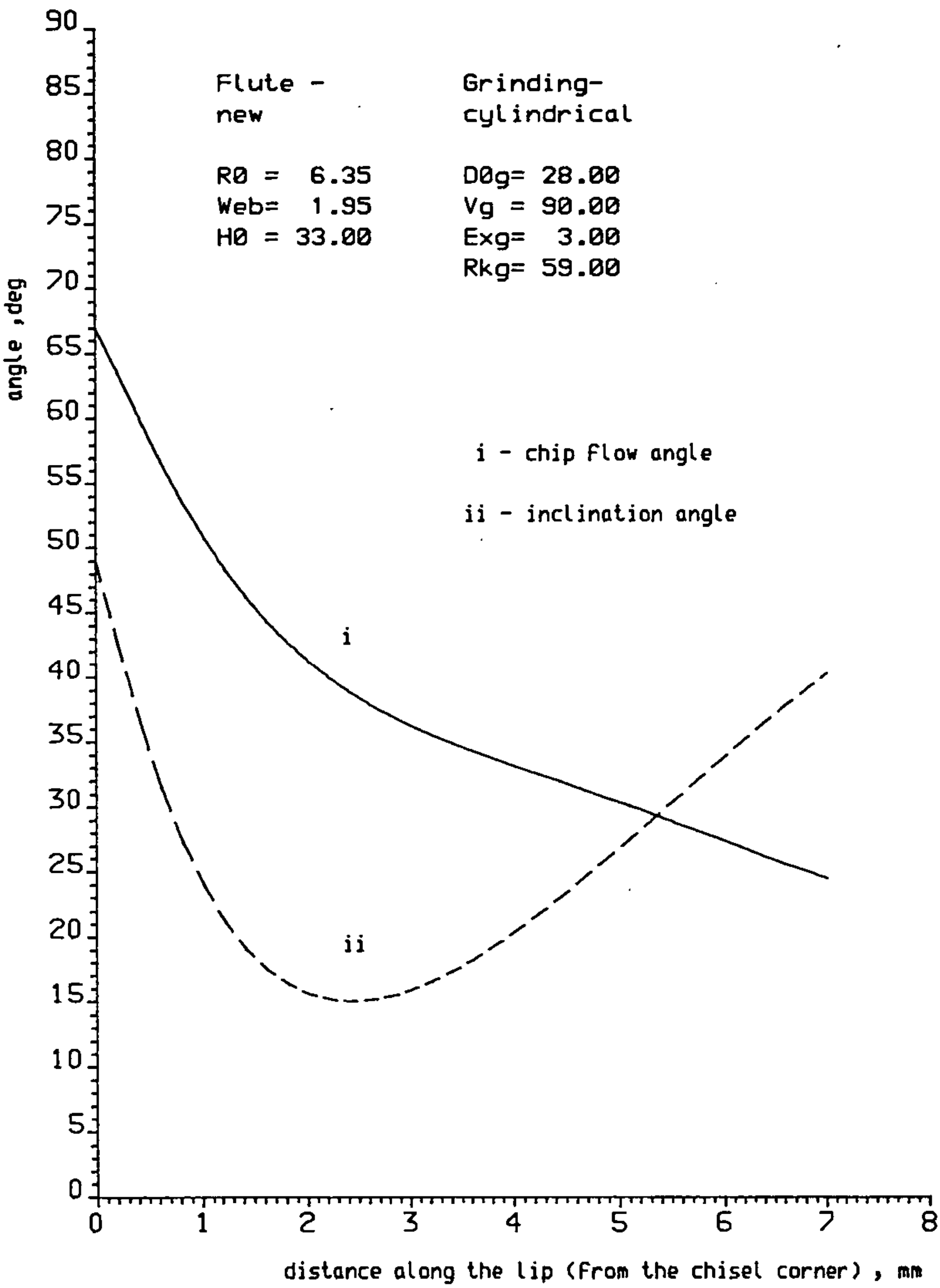


FIGURE 8.21: Drilling chip flow angle,from rigid body approach [5.4 mm chip diameter and 4 mm chip lead],and drill lip inclination angle

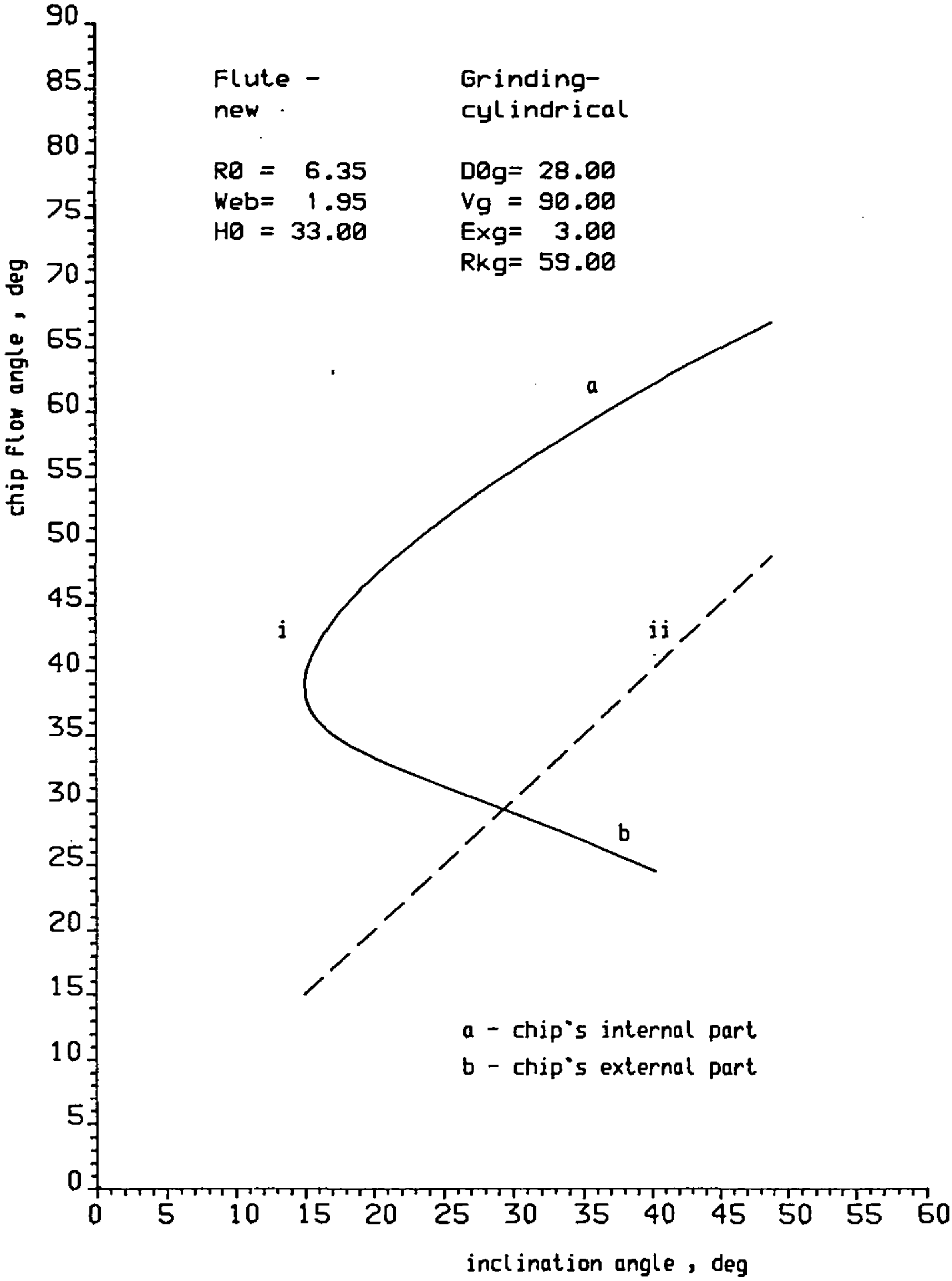


FIGURE 8.22: Drilling chip flow angle from rigid body approach (i) [refer to FIGURE 8.21] and STABLER's rule versus drill lip inclination angle

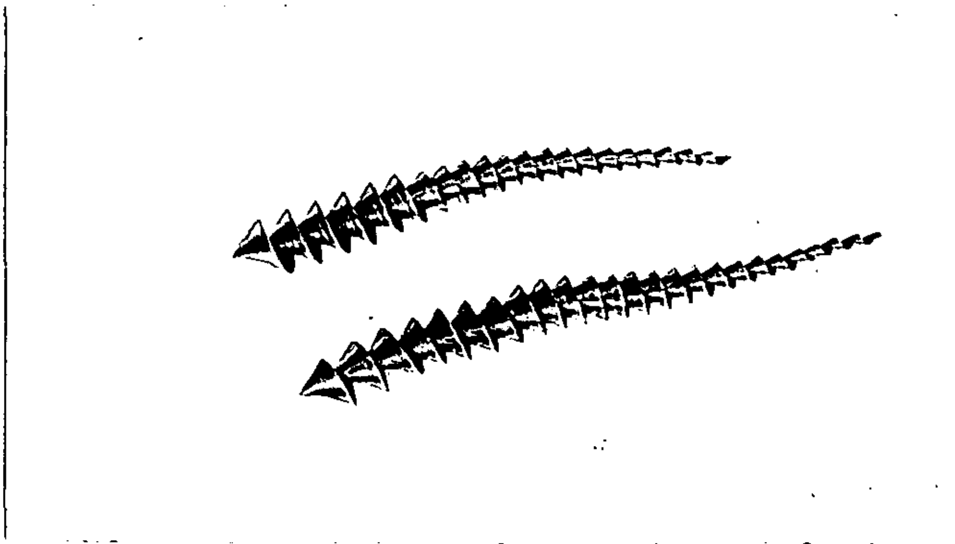

FIGURE 8.23: Cone-like chips produced on drill entry [1/2″ and 118° conventional drill;820 rpm and 157 rpi ; EN43 steel]

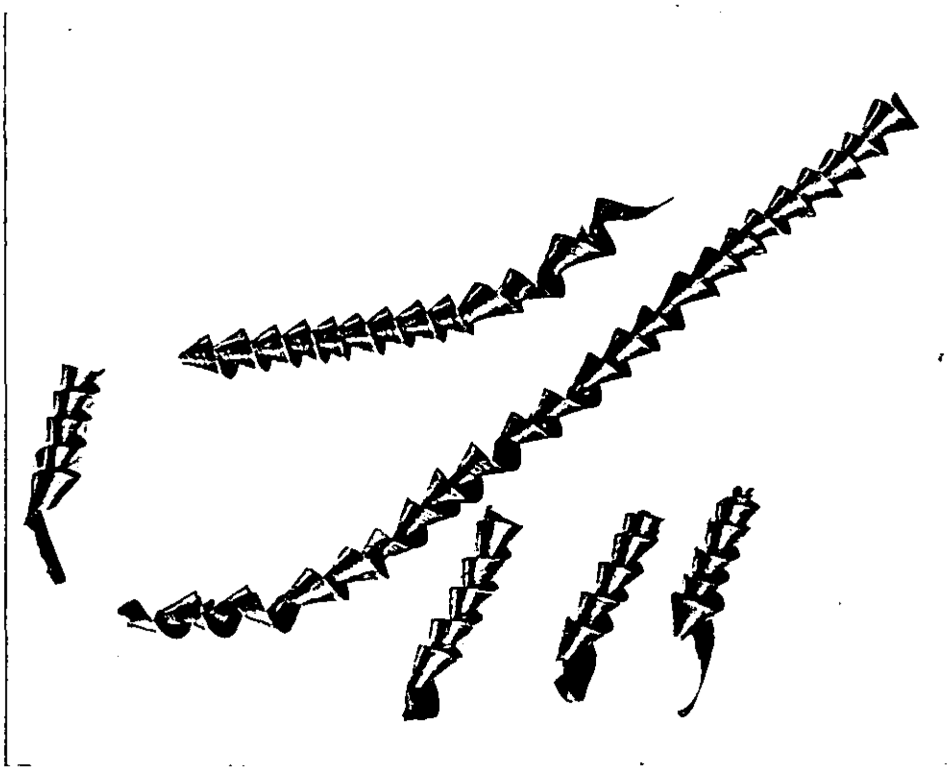

FIGURE 8.24: Conical helical drilling chips generated inside hole and flute - drill and conditions as for FIG 8.23 [Refer to FIG 8.1]

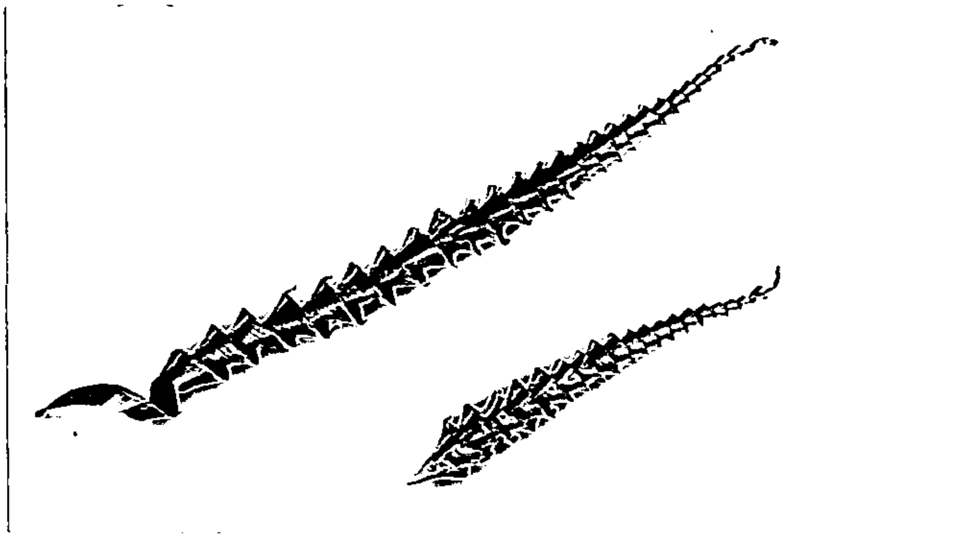

FIGURE 8.25: Bell-like chips produced on drill entry [1/2″ and 118° new design drill;820 rpm and 157 rpi ; EN43 steel]

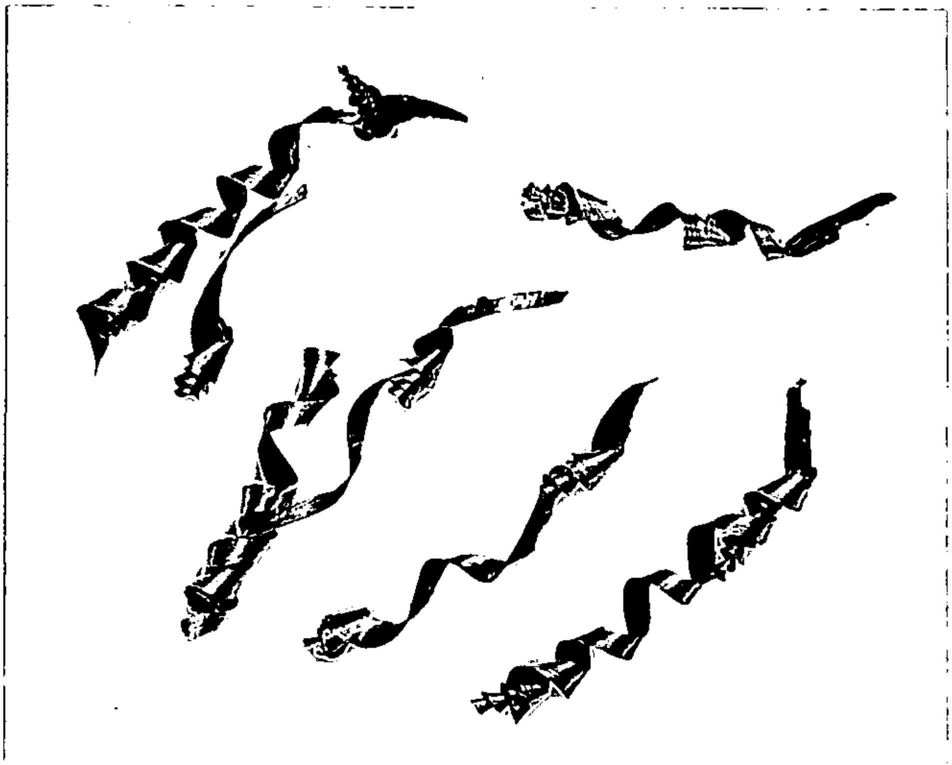

FIGURE 8.26: Split drilling chips generated inside hole and flute - drill and conditions as for FIG 8.25]

.i ii

FIGURE 8.27: Frozen drilling chips:
i) by non-conventional drill (split chip)
ii) by conventional drill

Such a chip flow angle was computed for a rigid body chip with parameters $d_{co}$ = 9 mm (chip diameter) and $p_c$ = 4 mm (chip lead) (Figure 8.30).

This rigid body would be possibly produced if enough space was provided for the chip to flow as it would require a "cylinder" at least approximately 9 mm diameter (the flute and hole "produce" a "cylinder" about only 5.4 mm).

Such a space is actually available at the entry of the drill where the chip is not constrained by the hole walls, Figure 8.25 (compare to Figure 8.23), and can proceed without splitting as a rigid body.

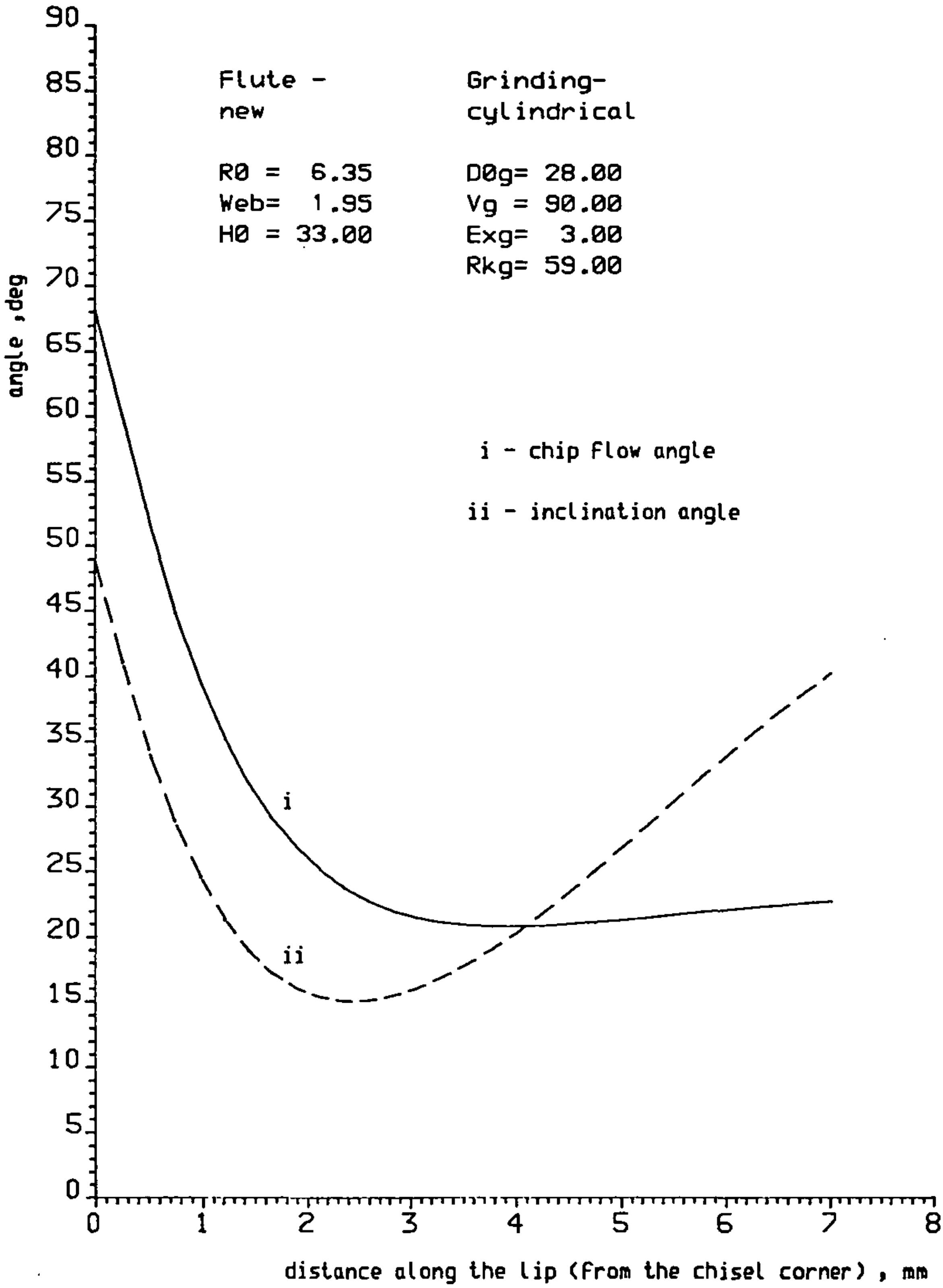


FIGURE 8.28: Drilling chip flow angle, from rigid body approach [9.0 mm chip diameter and 4 mm chip lead], and drill lip inclination angle

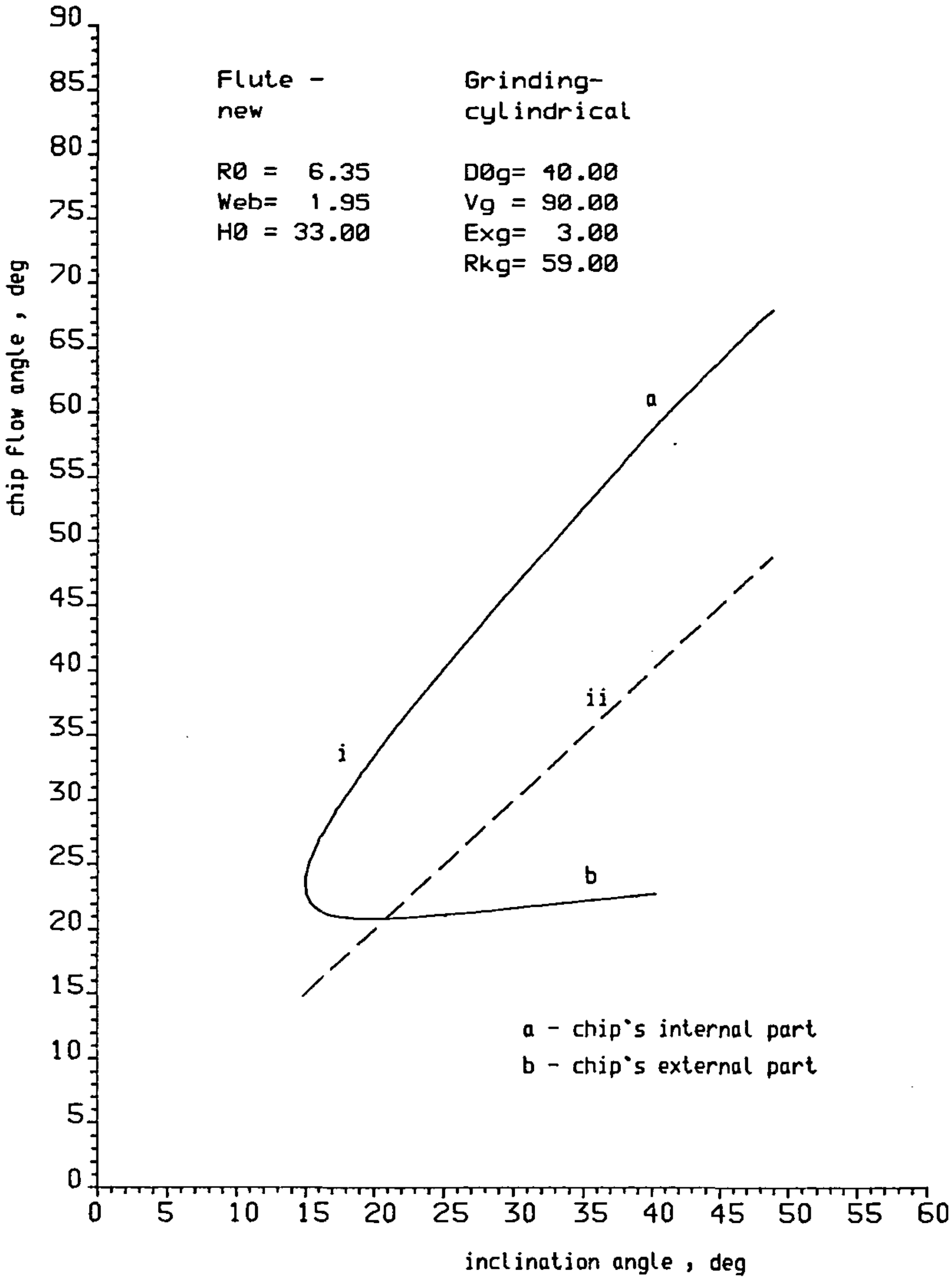


FIGURE 8.29: Drilling chip flow angle from rigid body approach (i) [refer to FIGURE 8.28] and STABLER`s rule versus drill lip inclination angle

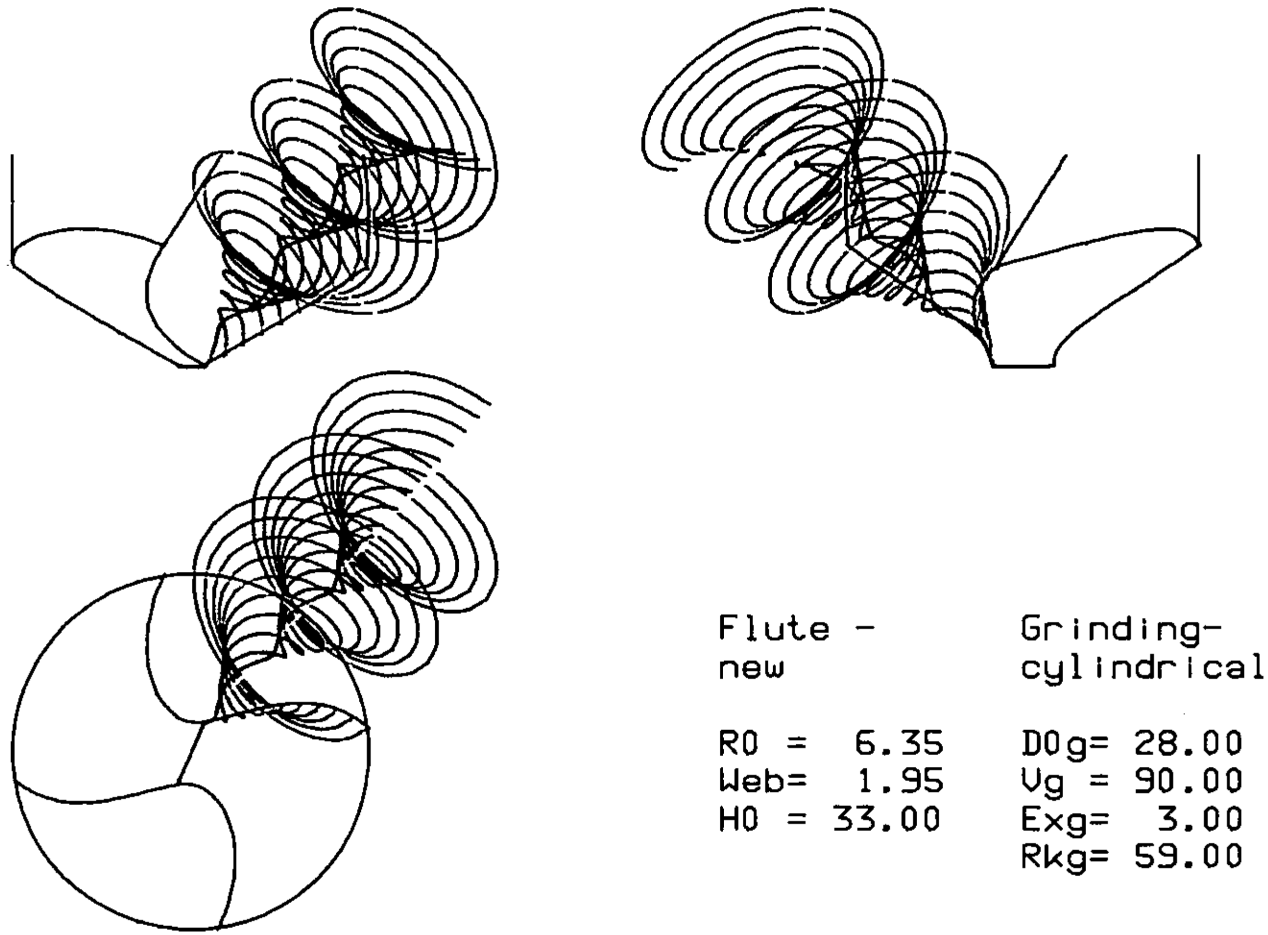


FIGURE 8.30: Computer geometrically simulated rigid body chip [drill entry] for the new design drill

### 8.6.3 Variation of the chip length ratio along drill lip. Prediction by the present model *versus* experimental data reported in literature

The cutting ratio is the ratio of the uncut chip thickness, $t_1$, to the chip thickness, $t_2$: $t_1/t_2$. Sometimes the reciprocal, $t_2/t_1$ - chip thickness ratio - is used instead.

In the cases where chip thickness is difficult to measure, another ratio is used: the chip length ratio, which is the chip length divided by the corresponding uncut length.

The cutting ratio has been analysed, measured and discussed by many workers in the area of machining (4, 12, 25, 43, 45, 47, 73, 119, 122). It depends on many factors, and reports in literature frequently refer to empirical correlations between the cutting ratio and the cutting factors . However, only one reference dealing with one sort of cutting ratio (chip length ratio) of the drilling chips was found in literature (121).

The chip length ratio (and the cutting ratio too) is difficult to predict, in general. Nevertheless it appears that it would be possible to predict its relative variation along a cutting edge such as a drill lip as regards to the lip cutting geometry variation, chip flow variation and material approaching speed variation.

From Figure 4.34 and admitting that there is no loss of material, neither material density variation across the lip, nor chip lateral deformation, it can be written:

$$\ell_1 \, t_1 \, b_1 = \ell_2 \, t_2 \, b_2 \qquad 8.14$$

where $\ell_1$ - length of uncut chip
$t_1$ - uncut chip thickness
$b_1$ - uncut chip width
$\ell_2$ - length of chip

$t_2$ - chip thickness
$b_2$ - chip width

If cutting time is equal to 1,equation 8.14 can be written:

$$V\ t_1\ b_1 = V_c\ t_2\ b_2 \qquad 8.15$$

when: $V$ - cutting speed
$V_c$ - chip speed

The chip length ratio is defined by:

$$r_\ell = \ell_2/\ell_1 = \frac{V_c}{V} \qquad 8.16$$

$V_c$ is proportional to the chip radial distance at the selected point on the lip, and $V$ is proportional to the drill radial distance at the same point.

Making $r_\ell = 1$ at the outer corner, the variation of $r_\ell$ along the lip can be referred to this value.

Armarego (121) once reported on the experimental determination of the chip length ratio of drilling chips by cutting and measuring annuli chips of different sizes. He used one drill with the following features: $r_o = 12.7$ mm, $2W = 3.2$ mm, $\gamma_f = 32^0$ and $\kappa_g = 122^0\ 50'$. His results are shown in Figure 8.31 by the points fitted by curve i.

The features of the drill utilized by Armarego were used with the rigid chip model and the relative chip length ratio was computed and computer plotted in Figure 8.31 (curve ii).

The model, in accordance with the experimental results which Armarego obtained by special methods, predicts a decrease in the chip length ratio along the lip, from the outer corner towards the chisel corner.

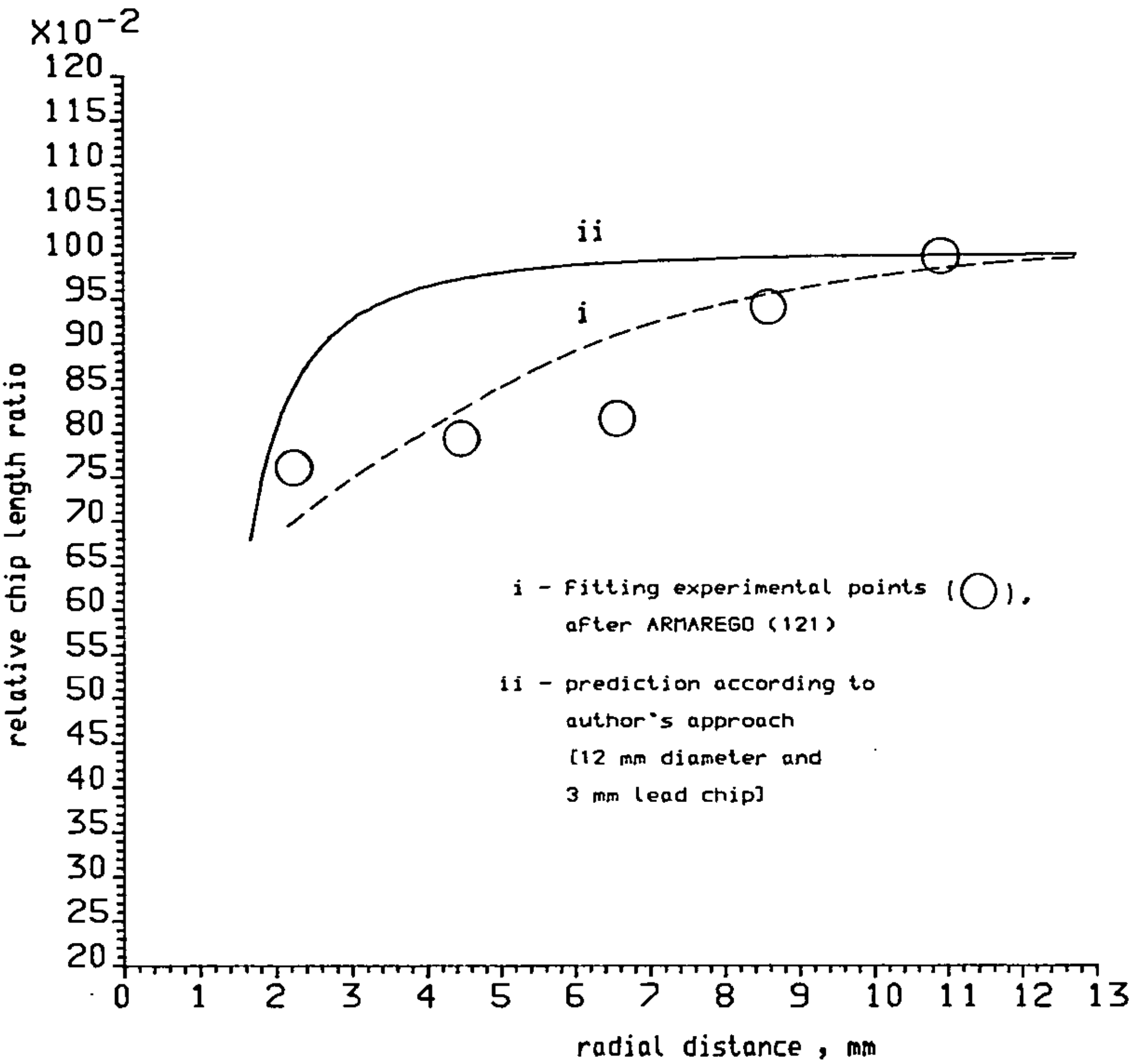


FIGURE 8.31: Variation of the relative chip length ratio along the drill lip. [Refer to text for drill features]

The author would like to consider the subject a little further, considering the cutting ratio too.

From Figure 4.34 it results:

$$\frac{b_1}{\cos\lambda} = \frac{b_2}{\cos\eta} \tag{8.16}$$

where: $\lambda$ - inclination angle

$\eta$ - chip flow angle

Then, from equation 8.15:

$$V\ t_1\ b_1 = V_c\ t_2 \frac{\cos\eta}{\cos\lambda} b_1$$

$$\therefore \qquad \frac{t_1}{t_2} = \frac{V_c}{V} \frac{\cos\eta}{\cos\lambda} \tag{8.17}$$

The variation of the cutting ratio along the lip is determined by the chip radial distance, drill radial distance, inclination angle and chip flow angle at each point selected on the lip (equation 8.17).

As for the chip length ratio, making arbitrarily $t_1/t_2 = 1$ at the outer corner, the variation of $t_1/t_2$ along the lip can be referred to this value.

For the same drill and conditions used for Figure 8.31, the variation of $t_1/t_2$ was computer plotted in Figure 8.32 where it is represented by curve i together with the variation of the chip length ratio, curve ii.

Curve i in Figure 8.32 predicts a sudden increase of the chip thickness close to the chisel corner.

Some full width chips, as in Figure 8.18, show a sudden increase of thickness close to the chisel corner. However, no systematic experiment (with and without pilot holes, for example) has been made

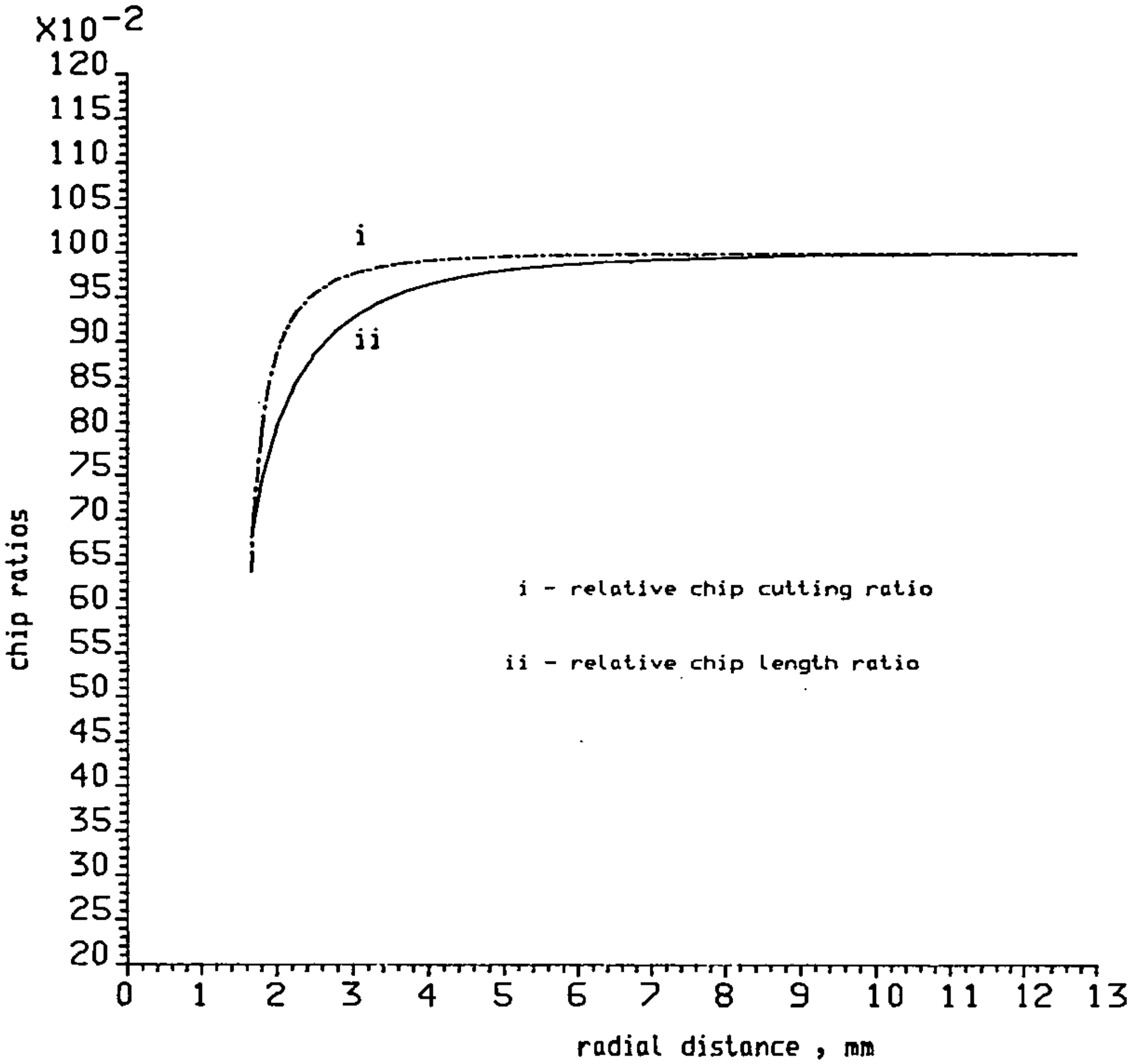


FIGURE 8.32: Variation of the relative cutting ratio and length ratio of drilling chip,along the lip. [Drill features and drilling chip parameters as for FIGURE 8.31]

at this stage to prove that the increase of thickness agrees quantitatively with the predictions.

If the chip yielded by the new design drill could be described for all drill lip points as a full width rigid body (from the outer corner to the chisel corner), the relative cutting ratio to be expected would appear like the one shown in Figure 8.33. In other words, such a chip would show a greater thickness at the middle than at the inner and outer parts.

Few bits of chips produced by the new design drill (Figure 8.26) keep full width. Some of these bits were embedded in resin and press moulded and prepared as shown in Figure 8.18 to be observed and to be measured by the microscope.

The tendency was for the chips to show a higher thickness, thus a lower cutting ratio, at their middle zones. At this stage, however, no systematic experiment has been undertaken in order to provide that the prediction for the new design drill is correct.

### 8.6.4 Fitness of the rigid body drilling chip to the flute face at the drill lip and correlation with experimental data of lip stress and lip temperature reported in the literature for conventional drills

The drill flute is an helical rigid body with an axis which is the drill axis.

The drilling chip is approached in this work as a rigid body with an helical motion with a proper axis, in general not coincident with the drill one, with a maximum diameter determined by the flute/hole space and conically shaped.

The rigid body chip was computed in the previous sections according to the conditions and restrictions imposed on it by the flute geometry.

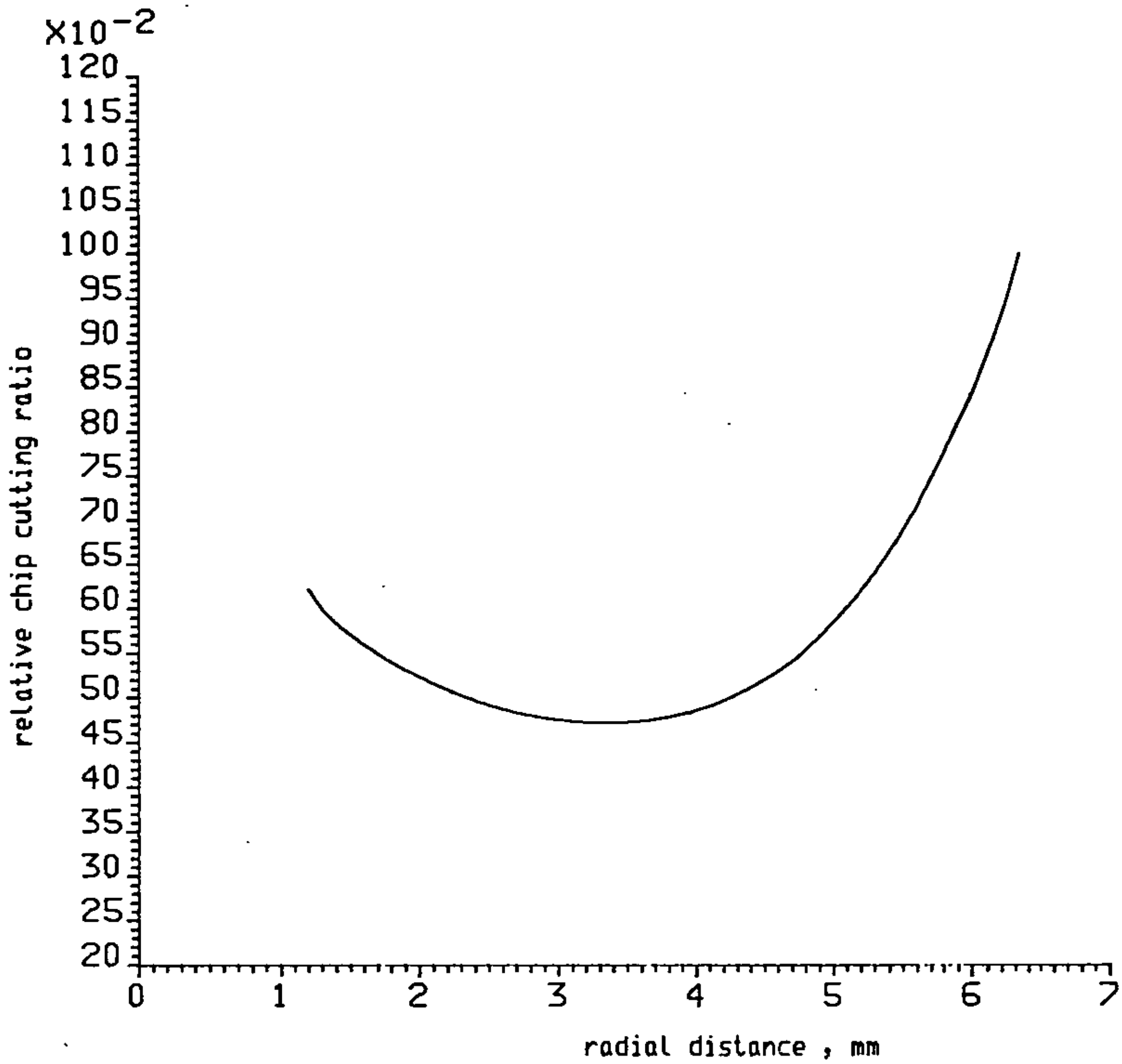


FIGURE 8.33: Variation of the relative chip cutting ratio along the new design drill lip computed from the rigid body chip approach. [Drilling chip parameters as for FIGURE 8.21]

For simplicity of analysis the chip contact length [D.10] is not considered, and one condition to be imposed on the computed rigid body chip should be that it would be tangent to the flute face at the drill lip. However, numerical and graphical investigation revealed that this condition is in conflict with the limits on chip size (flute size). Thus the condition that the rigid body chip should be as tangent as possible to the flute face at the lip was imposed instead.

After a rigid body chip solution is found, the final deviation of the rigid body chip from the tangent to the flute face can be known at each point.

Fitness of the computed drill chip to the flute face is assessed at each lip point by computing the deviation of the chip velocity from the tangent to the flute face (Figure 8.34).

The patterns of contact (Figure 8.34) between the computed chip and the flute face was found to be similar to each other in a very extensive numerical investigation carried out by the author with conventional drills. A perfect tangency between computed chip and the flute face appear at some distance from the outer corner (point A, Figure 8.34), and no tangency between this point and the outer corner as the computed chip velocity points up the flute face. For the points from point A to near the chisel corner, the computed chip velocity points down the flute face as if it was penetrating it.

The referred to pattern of contact between the computed chip and the conventional flute face at the lip is shown in Figure 8.34 by the line (i).

This pattern of contact means that the chip would tend to leave the flute face, behind the lip, near the outer corner, and would tend to penetrate the flute face behind the lip, along the area in the middle of the lip.

This can be shown by using a plan that contains the chip axis and rotates about it producing successive sections of the chip and

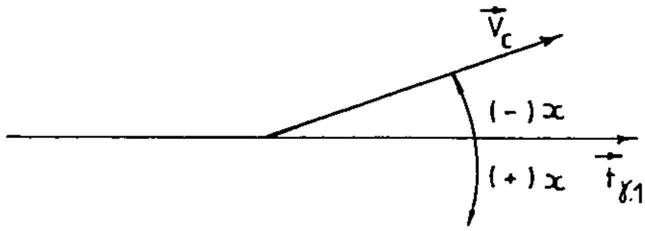


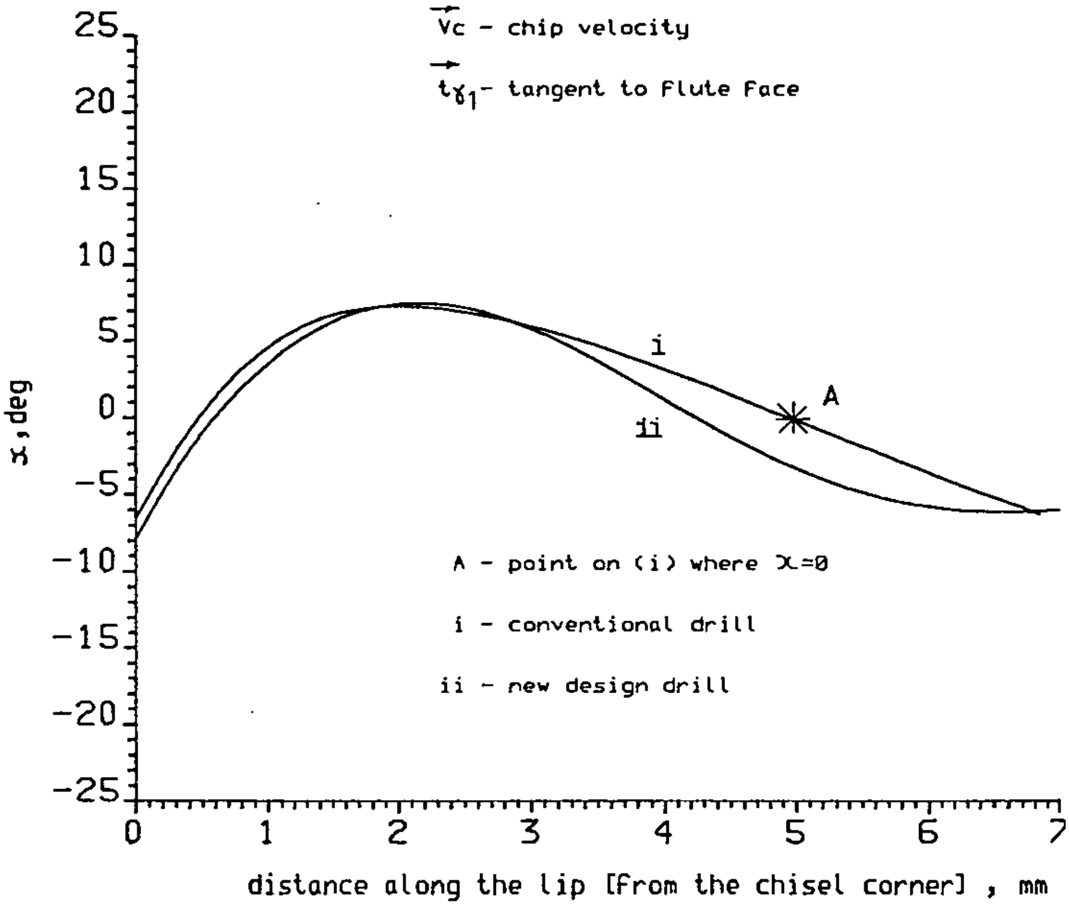


FIGURE 8.34: Pattern of contact between the computed chip and the flute (rake) face at the lip. [Refer to FIGURES 8.19 and 8.21 for drill features and drilling chip parameters]

of the flute behind the lip.

This technique was also implemented in the computer program shown in Appendix 8 and some sections were computer plotted. Figure 8.35 shows the sections yielded by the above referred to plan passing at the outer corner, after rotating $5^{o}$ from the previous position and after rotating $10^{o}$ from the first position.

This pattern of contact of the chip model at the drill lip suggests that, for some stress components on the drill lip resultant from the action of the chip on the flute face, the outer corner and its vicinity should appear alleviated relative to other points further located from the outer corner. This hypothesis seems to be supported and validated by experimental results already reported in literature (41, 57).

Law and co-workers (41) have found by photoelastic methods that the maximum shear stress along the lip presents a pattern shown by line (ii) in Figure 8.36.

These workers specified the drill they used just by its diameter: 78.2 mm (3"). In order to use his model and computing approach to find the pattern of contact between the chip and the flute face at the lip shown by line (i), Figure 8.36, the author assumed the following additional features: 2W = 8 mm (the minimum web for a 76.2 mm diameter drill, according to catalogue C.1 ; $\gamma_f = 30^{o}$ (a common drill helix angle) and $2\kappa = 118^{o}$ (standard drill point angle).

Also Saxena and co-workers (57, 123) have measured the temperature at the drill lip and found it to have the pattern represented by line (iii) in Figure 8.36. This was known to Law and co-workers who wrote in their paper (41): *"It is interesting to note that the maximum shear distribution along the cutting edge is similar to an experimental temperature distribution (57)".*

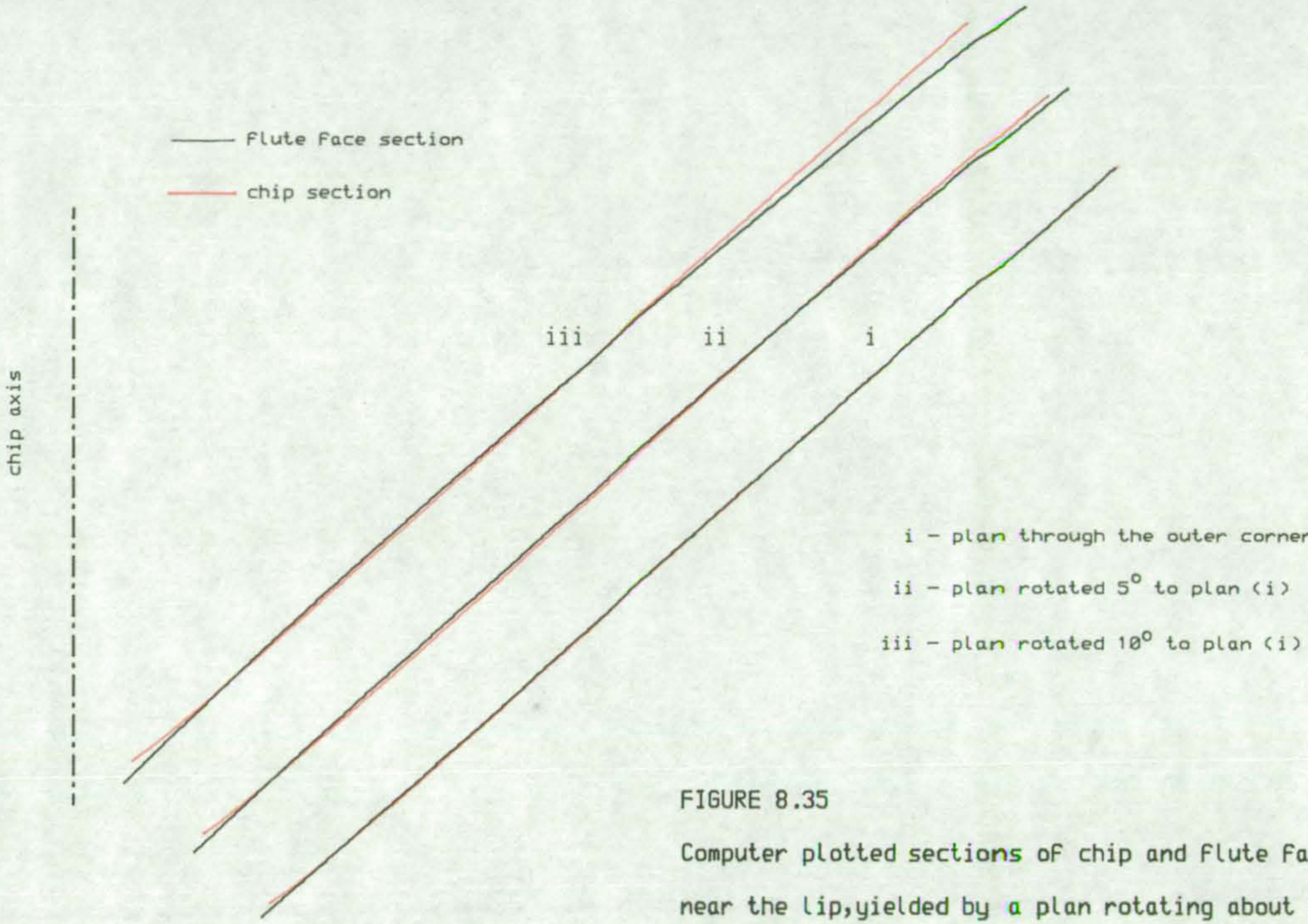


FIGURE 8.35

Computer plotted sections of chip and flute face, near the lip, yielded by a plan rotating about the chip axis, and at three positions : i, ii, iii.

[Refer to FIG 8.19 for chip and drill features]

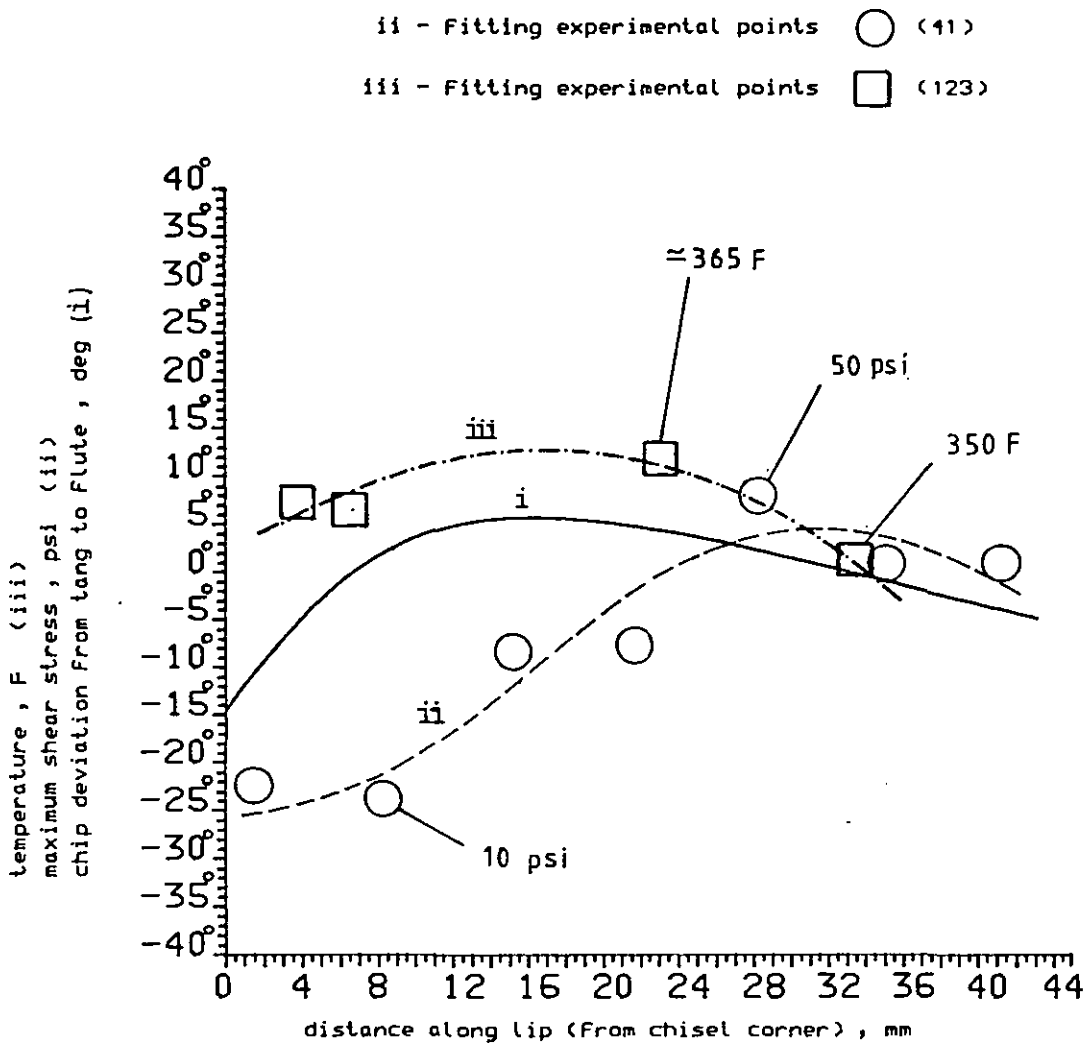


FIGURE 8.36: Computed pattern of contact between chip and flute face at lip (i) - refer to FIGURE 8.34 ; maximum shear stress at the lip (ii)(41) ; temperature near the lip (iii)(123)

## 8.7 Chapter Closure

Chip splitting, seems to correlate with torque increase, thrust decrease and wear rate increase.

Approaches to drilling forces prediction can be found which consist of dividing the main cutting edge in a number of elementary cutting edges, and computing the total force as a summation of the forces on each one of these smaller cutting edges. One of such approaches (12) - claimed to give good predictions with the conventional drill - has been tested by the author (included in computer program shown in Appendix 1) with the new design drill and failed: it predicts higher torques and higher thrusts (experiments show lower thrusts, compared to the conventional drill)(Chapter 7).

Based on the belief (and on the successes reported in this thesis) that the rigid body concept would be a better approach to drilling forces computation, the author could predict a torque increase and a thrust decrease with the new design drill. However, a deeper analysis of the assumptions and method for drilling forces prediction by the author has to be done before a definitive statement can be made.

The author believes that rigid body chips can be formed and flow with different degrees of efficiency within a range of drill lip and drill flute geometries. To base flute design on a rigid body chip criterion seems to the author a direction strongly worthwhile to take.

# CONCLUSIONS AND SUGGESTIONS

# FOR FURTHER WORK

The work reported in this thesis can be divided into the following parts:

i) Analysis of drill geometry (Chapters 2, 3 and 4).

ii) Design of a new drill flute (Chapter 5).

iii) Comparative performance tests between a conventional drill and the new flute drill (Chapters 6 and 7).

iv) Analysis of the drilling chips in relation to the drill lip and drill flute geometry (Chapter 8).

In the present work, twist drills are analysed according to the geometry and cutting angles along the lips rather than according to the traditional drill features such as those referred to in Chapter 1. The main purpose of this approach is to deal with non-straight drill lips either with conventional or non-conventional flute faces.

To deal with twist drills by referring to the cutting angles is more complex than by the traditional drill features as the surfaces determining the drill have to be defined and mathematically modelled and the cutting angles have to be computed by vectorial analysis.

Mathematical models are better dealt with by computing techniques. The advantages of these techniques are multi-fold and some of them have been experienced by the author throughout this work as they:

i) provide for numerical solutions when the analytical ones could hardly be achieved;

ii) allow for numerical investigation;

iii) allow for geometric simulation;

iv) allow for mathematical model testing;

v) allow for reformulation of problems and hypotheses;

vi) enlarge the field of research for the amount of information data that can be dealt with and for the complex relationships that can be analysed.

## Conclusions

1. When the drill lips are straight lines the flute face related cutting angles can be calculated by formula available in literature. For non-straight drill lips the cutting angles either flute face related, or flank surface related, or flute face and flank surface related depend on the lip shape and cannot be computed before defining the surfaces determining the lip.

2. Twist drill surfaces are generally machine generated and can be mathematically modelled.

3. Seven distinct mathematical models (corresponding to the same number of surfaces) can be used to determine and to simulate completely the drill point:
   i) two flute faces
   ii) two flute heels
   iii) two flank surfaces
   iv) one cylindrical surface.

   The complete determination and simulation of the drill point by these mathematical models can be demonstrated by computer aided design techniques.

4. Traditionally a flute face is defined as a ruled surface whose shape depends on four parameters: $r_o$, $2W'$, $\dot{\gamma}_f$ and $\kappa$. For complete definition of the flute profile the flute heel can be mathematically modelled. This model can be defined by one parameter determining the heel profile corner relatively to the face profile corner and by the condition of a common tangent with the face profile at the point on the same helical line as the chisel corner.

5. For convenience the cylindrical grinding was used. The cylindrical grinding surface can be mathematically modelled with four parameters: $d_{og}$, $\nu_g$, $ex_g$ and $\kappa_g$ which allow for free

specification of the drill point features: point angle, chisel edge angle, nominal relief angle and elevation of the heel corner relatively to the outer corner. The freedom to specify the referred to features is achieved at the cost of the lip straightness.

6. The flute face mathematical model and the flank surface mathematical model determine the drill lip and the cutting angles which can be computed by vectorial analysis. The shape and the length of the lip and the chisel edge can be computed from the simulated intersections of the referred to mathematical models. The flank contour on the drill cylindrical surface and the heel point contour can also be computed from these mathematical models and the others referred to in conclusion 3.

7. The configuration of a geometrically simulated drill point depends on the parameters of the mathematical models relative to the surfaces determining the drill point. The cutting angles such as the normal rake angle, the normal clearance angle and the inclination angle along the drill lip also depend on these parameters.

8. The flute face form can be determined on the basis of other conditions rather than to be a ruled surface. To use non-ruled surfaces for the flute face form makes the lip to be curved and makes the cutting angles to be flank surface dependent.

9. The flute form can be determined from the inclination angle law along the lip once the flank surface is known. Iterative numerical methods implemented in a computer program allow for the flute specification to be given in terms of other cutting angles rather than the inclination angle. Such a flute can be determined by successive controlled alterations to an inclination angle law given to a guess.

10. A flute form to yield a uniform wedge angle along the lip produces a normal rake angle law and an inclination angle law different to those of the conventional drill. For some values of the wedge angle, used as a design parameter, little modification is introduced to the effective rake angle as compared to the conventional drill.

11. To modify the flute form, the lip shape and the cutting angles along the lip affects drill performance as far as lip wear, drilling forces and chip form and size are concerned.

12. Lip wear at five equally spaced points on the lip, from the outer corner, for both the conventional drill and the new design drill show similar wear patterns but different intensities as far as drill type, point position and drilling conditions are concerned. Lip wear is smaller for the new design drill at the initial drilling stage, especially for the points closest to the outer corner. For this drill type, the average wear rate during the longer and slower part of the global wear process is in general higher than for the conventional drill.

13. Analysis of variance of the wear rate results shows that:
the points equally spaced on the drill lips, near the outer corner, do not respond in the same way to wear performance;
the points at the same radial distance on the two tested drill types do not respond in the same way either.
The very outer corner of the drill is not so representative of lip wear as referred to drilling factors as other points in its neighbourhood.

14. Analysis of variance of the wear rate results at five points on the drill lips, at the neighbourhood of the outer corner, has shown that the difference between drill types is significant at two intermediate points (points 2 and 3), probably significant at one extreme point (point 1) and at the nearest point to the outer corner (point 4), and non-significant at the outer corner.

15. Analysis of variance has also shown that, for both drill types, the effect of cutting speed is highly significant for the points tested except for the outer corner where it appears to be probably significant. The effect of the drilling feed is highly significant for two intermediate points (points 2 and 3), is significant for points 1 and 4 and non-significant for the outer corner. The effect of the point angle and the effect of the interaction of the drilling factors analysed are non-significant too.
Variability of the wear rate at the very outer corner suggests that other inner points on the lip near the outer corner should be selected when drill lip wear rate measurement is intended.

16. Drilling torque in general is higher and drilling thrust is lower for the new design drill than for the conventional one. The experimental results show that with the new design drill the torque increases between 0 to 10% as the thrust decreases between 5 to 20%.

17. Analysis of variance on the drilling forces results has shown that, for the drilling thrust, the effect of the interaction of drilling feed and drill point angle and drill type is significant. Analysis of variance by drill point angles, for the drilling thrust, has shown that the effect of the interaction of drilling feed and drill type is highly significant, and the analysis of variance by drill types has shown the effect of the interaction of drilling feed and drill point to be also highly significant.

18. Analysis of variance on the drilling thrust results, by drilling feeds, has shown the effect of the interaction of the drill point angle and drill type to be non-significant, and the effect of the drill point angle to be highly significant for low to moderate feeds (240 to 157 RPI) and significant or probably significant for high (70 RPI) and moderate feeds (103 RPI), respectively. The effect of the drill type has shown to be highly significant

to significant for moderate feeds (103 and 157 RPI) and probably significant or non-significant for the extreme feeds (70 and 240 RPI, respectively).

19. Analysis of variance on the drilling torque results has shown the effect of the interaction of the three factors tested, drill type, drill point angle and drilling feed, to be non-significant. Also, the effect of the interaction of the drilling feed and drill point angle, and the interaction of drill type and drill point angle have shown to be non-significant.

20. Analysis of variance on the drilling torque results, by drill types, has shown that the effect of the drilling feed and the effect of the drill point angle are highly significant. Analysis of variance by drilling feeds has shown the effect of the point angle to be highly significant for low to moderate feeds (240 and 157 RPI), and significant to probably significant for high to moderate feeds (70 to 103 RPI). The effect of the drill type has revealed it to be highly significant (103 RPI) to non-significant (240 RPI).

21. To increase the wedge angle - *"heat sink"* - at the outer corner and thereabouts, and designing for the same effective rake angle as for the conventional drill, according to the hypothesis put forward, did not improve drill lip wear rate performance. The departure from the conventional flute reported in this work appears to correlate with wear rate increase, drilling torque increase, thrust decrease and chip splitting.

22. Chips can be analysed from the rigid body concept. Rigid body chips can be mathematically modelled and dealt with by computing techniques.

23. Drilling chip mathematically modelling allow for chip flow simulation and for prediction of variables such as: drilling chip flow angle, relative chip speed, relative chip length ratio and relative cutting ratio. It also allows for the analysis of fitness of a modelled drilling chip to the flute face.

24. Predictions for the chip flow angle by the approach by the author agree with experimental data reported in literature (by Oxford). Predictions for relative chip length ratio by the same approach correlate with experimental data reported in literature (by Armarego).

    Prediction, by the novel approach to drilling chip flow, of the fitness of the modelled chip to the flute face at the drill lip correlates with experimental data relative to shear stress and to temperature near the lip reported in literature (by Law and co-workers and Saxena and co-workers, respectively).

## Suggestions for Further Work

The new flute design - based on the condition of an increased wedge angle at the outer corner when compared to the conventional drill design while leaving the effective rake angle almost unaltered - did not prove to be an improvement in drilling steel relative to the conventional drill.

Drill flute is traditionally designed to yield a straight lip. It seems fortunate that such a purely geometric and empirical criterion has in general succeeded for the many different drilling conditions (feeds, speeds, materials, for instance).

Such a success, in the author's opinion, is due to the fact that the traditional flute design can cope with full width (outer corner to chisel corner) rigid body chips. However, rigid body chips may possibly be produced within a certain range of flute designs though with different chip flow efficiency and different drill performance.

An approach to general flute design and also drill point simulation has been given in the present work. Chip rigid body mathematical modelling and computer aided chip simulation has been given in this work too.

The avenues ahead suggested by the author are:

1. To investigate and establish the range of drill flute (and drill point) designs that can cope with rigid body chips.

2. To introduce in the analysis and simulation the chip contact length and investigate its influence on the range of flute designs established in the previous point.

3. To extend the rigid body chip mathematical model to provide for consideration of drilling feed or rather "drilling feed"/"drill diameter" ratio.

4. To build up an approach to drilling forces prediction based on chip flow (which should predict for torque increase and thrust decrease with flutes similar to the one the author designed and tested).

5. To investigate the possibilities of lip wear prediction (or relative wear along the lip) by a chip flow approach.

6. To base drill design on specifications established according to rigid body drilling chip production.

# REFERENCES

## i) Bibliography


1. OXFORD, C J Jr.
*Fundamentals of drilling, tapping and reaming.*
*Influence of metallurgy on hole making operations.*
Proceedings from an International Symposium of the American Society for Metals, 1978.

2. ERNST, H and HAGGERTY, W A:
*The spiral point drill - a new concept in drill point geometry.*
Transactions of the ASME, 1958. Paper No 57-A-98.

3. GALLOWAY, D F:
*Some experiments on the influence of various factors on drill performance.*
Transactions of the ASME, 1957.
Paper No. 56-SA-18.

4. ARSHINOV, V and ALEKSEEV, G:
*Metal cutting theory and cutting tool design.*
MIR Publishers, Moscow, 1976.

5. TSAI, W D:
*Drill geometry and dynamics of drilling.*
PhD Thesis, University of Wisconsin, Madison, 1977.

6. BILLAU, D J, McGOLDRICK, P F and HEGINBOTHAM, W B:
*The performance of double margin drills with both margins cutting.*
Proceedings of the 19th International Machine Tool Design and Research Conference, Manchester, 1978.

7. LORENZ, G:
*A study of the effect of drill sharpening and sizeability of work-piece material on the process variability in drilling.*
Int. J. Mach. Tool Des. Res. Vol. 10, pp 133-141, Pergamon Press 1970.

8. *Fundamentals of drilling.*
American Machinist, February 1979, McGraw-Hill.

9. KAHNG, C H and HAM, I:
*A study on sequential quality improvement in hole making processes.*
Annals of the CIRP Vol. 24 January 1975.

10. GALLOWAY, D F and MORTON, I S:
*Practical drilling tests.*
Research Department of the Institution of Production Engineers, 1946.

11. BILLAU, D J:
*An investigation relating to double margin drill performance and flank face geometry.*
PhD Thesis, University of Nottingham, 1977.

12. WIRIYACOSOL, S and ARMAREGO, E J A:
*Thrust and torque prediction in drilling from a cutting mechanics approach.*
Annals of the CIRP Vol. 28 January 1979.

13. LYUBIMOV, V E:
*New method of grinding curved-lip drills.*
Machines and Tooling, Vol. XXXIX No. 8, 1968.

14. NAKAYAMA, K and OGAWA, M:
*Basic rules on the form of chip in metal cutting.*
Annals of the CIRP, Vol. 27 January 1978.

15. PERCIVAL, N:
*The use of chip breakers in drilling.*
Metalworking Production, 18/25 Dec. 1968.

16. ARMAREGO, E J A and WRIGHT, J D:
*An analytical study of three point grinding methods for general purpose twist drills.*
Annals of the CIRP, Vol. 29 January 1980.

17. CETIM:
*Guide du perçage au foret hélicoïdal*
CETIM - Service de Coupe, 1977.

18. RODIN, P:
*Design and production of metal-cutting tools.*
MIR Publishers, Moscow, 1968.

19. SPUR, G and MASUHA ,J R:
*Drilling with twist drills of different cross-section profiles.*
Annals of the CIRP Vol. 30 January 1981.

20. OXFORD, C J Jr:
*On the drilling of metals.*
I: Basic Mechanics of the Process.
Transactions ASME, 77, 103, 1955.

21. OXFORD, C J Jr:
*A review of some recent developments in the design and application of twist drills.*
Advances in Machine Tool Design and Research, MTDR Conference, 1964.

22. ARMAREGO, E J A and ROTENBERG, A:
*An investigation of drill point sharpening by straight lip conical grinding method - I. Basic analysis.*
Int. J. Mach. Tool Des. Res. Vol. 13, pp 155-164, Pergamon Press, 1973.

23. MICHELETTI, G F and LEVI, R:
*The effect of several parameters on twist drill performance.*
Advances in Machine Tool Des. and Res. MTDR Conference, 1964.

24. PERA:
*Drilling alloy steel.*
PERA Report No. 53, August 1957.

25. PAL, A K, BHATTACHARYYA, B and SEN, G C:
*Investigation of the torque in drilling ductile materials.*
Int. J. Mach. Tool Des. Res. Vol. 4, pp 205-221, Pergamon Press, 1965.

26. BERA, S and BHATTACHARYYA, A:
*On the determination of torque and thrust during drilling of ductile materials.*
Advances in Machine Tool Des. and Res. MTDR Conference, 1967.

27. SHAW, M C and OXFORD, C J Jr:
*On the drilling of metals, 2 - The torque and thrust in drilling.*
Transactions of the ASME, 1957.

28. LORENZ, G:
*A contribution to the standardization of drill performance tests.*
Annals of the CIRP Vol. 25 January 1977.

29. LORENZ, G:
*Helix angle and drill performance.*
Annals of the CIRP Vol. 28 January 1979.

30. WILLIAMS, R A:
*Dynamic geometry of a twist drill.*
Int. Jnl. Prod. Research, Oct 2, 1968.

31. WALLER, C E:
*Some special equipment and techniques developed for the performance testing of twist drills.*
Annals of the CIRP Vol. XIII, 1966.

32. TOURRET, R:
*Performance of metal-cutting tools.*
Butterworths Scientific Publications, 1958.

33. KANAI, M, IWATA, K, FUJII, S and KANDA, Y:
*Statistical characteristics of drill wear and drill life for the standardized performance tests.*
Annals of the CIRP Vol. 27 January 1978.

34. GALLOWAY, D F:
*Advances in drilling techniques arising from recent research.*
Microtecnic, Vol. IX, No. 3.

35. BILLAU, D J:
*Economic considerations of drill performance.*
MSc Thesis, University of Nottingham, 1964.

36. PERA:
*An investigation into the effects of point thinning and drill stiffness on drill performance.*
PERA Report No. 89, 1962.

37. FUJII, S, DeVRIES, M F and WU, S M:
*Analysis and design of a drill grinder and evaluation of grinding parameters.*
Transactions of the ASME, 1972. Paper No. 71-WA/Prod-5.

38. BHATTACHARYYA, A and HAM, I:
*Design of cutting tools.*
ASTME, 1969.

39. BHATTACHARYYA, A, BHATTACHARYYA, A, CHATTERJEE, A B and HAM, I:
*Modification of drill point for reducing thrust.*
Transactions of ASME, 1971. Paper No. 71-Prod-12.

40. DAGNELL, J:
*Machineability test by a drilling method.*
Annals of the CIRP, Vol XV, pp 301-308.

41. LAW, S S, DeVRIES, M F and WU, S M:
*Analysis of drill stress by three-dimensional photoelasticity.*
Transactions of the ASME, 1972. Paper No. 71-WA/Prod-21.

42. VENKATARAMAM, R:
*Principles and applications of tool simulation in the metal cutting process.*
Int. J. Mach. Tool.Des. Res. Vol. 8, pp 97-106, Pergamon Press, 1968.

43. PALMER, W B and OXLEY, P L B:
*Mechanics of orthogonal machining.*
Proc. Instn. Mech. Engns. Vol. 173, No 24, 1959.

44. MERCHANT, M E:
*Mechanics of the metal cutting process. I: Orthogonal cutting and a type 2 chip.*
Journal of Applied Physics, Vol. 16, No. 5, May 1945.

45. STABLER, G V:
*The fundamental geometry of cutting tools.*
Inst. of Mech. Engrs, Proceedings, 1951, Vol. 165.

46. ARMAREGO, E J A and BROWN, R H:
*The machining of metals.*
Prentice-Hall, Inc.1969.

47. LEE, E H and SHAFFER, B W:
*The theory of plasticity applied to a problem of machining.*
Journal of Applied Mechanics, Dec. 1951, Paper No. 51-A-5.

48. USUI, E and HIROTA, A.
*Lee-Shaffer's type solution for oblique cutting.*
Bull. Japan Soc. of Prec. Engg. Vol. 12, No. 2, June 1978.

49. RAMALINGAM, S:
*Plastic deformation in metal cutting.*
PhD Thesis, 1967. University of Illinois, Mechanical Eng.

50. ENASHE, S, CATRINA, D and STRAFESCU, E:
*Recherches concernant l'influence de la géométrie de l'outil sur les conditions de coupe.*
Annals of the CIRP Vol. 23 January 1974.

51. COLWELL, L V:
*Predicting the angle of chip flow for single-point cutting tool.*
Transactions of the ASME, 1954, Paper No. 53-SA-17.

52. CONNOLLY, R and RUBENSTEIN, C:
*The mechanics of continuous chip formation in orthogonal cutting.*
Int. J. Mach. Tool Des. Res., Vol. 8, pp 159-187, Pergamon Press, 1968.

53. OXFORD, C J Jr:
*Drilling technology.*
Draft for presentation at the Metal Cutting Seminar, May 1958, (American Society of Tool Engineers).

54. WILLIAMS, R A:
*A study of the drilling process.*
Transactions of the ASME, 1974, Paper No. 73-WA/Prod-6.

55. AMARADASA, S R:
*Measurement of twist drill geometry.*
MSc dissertation, UMIST, May 1966.

56. WATANABE, K, YOKOYAMA, K and ICHIMIYA, R:
*Thermal analysis of the drilling process.*
Bull. Japan of Prec. Engg. Vol 11, No. 2, June 1977.

57. SAXENA, U K, DeVRIES, M F and WU, S M:
*Drill temperature distributions by numerical solutions.*
Transactions of the ASME, 1971, Paper No. 70-Prod-E.

58. BHATTACHARYYA, A, CHATTERJEE, A B and MULLICK, B K:
*Geometry and performance of multi-cone and curved-lip twist drills.*
Annals of the CIRP Vol. 22 January 1973.

59. SHAW, M C, COOK, N H and SMITH, P A:
*The mechanics three-dimensional cutting operations.*
Transactions of the ASME, 1952, Paper No. 51-A-61.

60. TSAI, W D and WU, S M:
*Measurement and control of the drill point grinding process.*
Int. J. Mach. Tool Des. Res. Vol. 19, pp 109-120.
Pergamon Press, 1979.

61. *Short drills vs long drills.*
Metal Cutting, July 1954, Vol. 1, No. 4.

62. BELL, R J T:
*An elementary treatise on coordinate geometry of three dimensions.*
Macmillan and Co, London, 1956.

63. BILLAU, D J and HEGINBOTHAM, W B:
*Some aspects of drill performance and testing.*
9th International MTDR Conference Proceedings, 1968.

64. ŠOLAJA, V and STANIÉ, J:
*Selected results from a project on drilling.*
Annals of the CIRP, Vol. 21 January 1972.

65. FUJII, S, DeVRIES, M F and WU, S M:
*An analysis of drill geometry for optimum drill design by computer. Part I: Drill geometry analysis.*
Transactions of the ASME, 1970, Paper No. 70-Prod-5.

66. FUJII, S, DeVRIES, M F and WU, S M:
*An analysis of drill geometry for optimum drill design by computer. Part II: Computer-aided design.*
Transactions of the ASME, 1970, Paper No. 70-Prod-6.

67. ARMAREGO, E J A and ROTENBERG, A:
*An investigation of drill point sharpening by the straight lip conical grinding method - II. A criterion for selecting a solution.*
Int. J. Mach. Tool Des. Res. Vol. 13, pp 165-182.
Pergamon Press, 1973.

68. ARMAREGO, E J A and ROTENBERG, A:
*An investigation of drill point sharpening by the straight lip conical grinding method - III. Drill point grinder design features.*
Int. J. Mach. Tool Des. Res. Vol. 13, pp 233-241.
Pergamon Press, 1973.

69. BILLAU, D J and McGOLDRICK, P F:
*An analysis of the geometry of the periphery of the flank face of twist drills ground with cylindrical and conical forms.*
Int. J. Mach. Tool Des. Res. Vol. 19, pp 69-86.

70. RUSSELL, J K and BROWN, R H:
*The measurement of chip flow direction.*
Int. J. Mach. Tool Des. Res. Vol. 6, pp 129-138, Pergamon Press, 1966.

71. KLUFT, W, LUTTERVELT, C A van, NAKEYAMA, K and PEKELHARING, A J:
*Present knowledge of chip control.*
Annals of the CIRP, Vol. 28 February 1979.

72. ARMAREGO, E J A and CHENG, C Y:
*Drilling with flat rake face and conventional twist drills - I: Theoretical investigation.*
Int. J. Mach. Tool Des. Res. Vol. 12, pp 17-35, Pergamon Press, 1972.

73. SPAANS, C:
*The fundamentals of three-dimensional chip curl, chip breaking and chip control.*
Doctor-thesis, TH Delft, 1971.

74. PATRI, V K and SHING, L W:
*On the estimation of chip flow angle in oblique cutting.*
Microtecnic 2/1977.

75. STABLER, G V:
*The chip flow law and its consequences.*
Advances in Machine Tool Des. and Res, 1964.

76. RAMALINGAM, S:
*What's new in metal cutting research?*
American Machinist, July 1979.

77. SHAW, M C:
*Metal cutting principles.*
MIT Press, 1968.

78. SPIEGEL, M R:
*Vector analysis.*
McGraw-Hill, 1959.

79. NAKAYAMA, K:
*A study on chip-breaker.*
Bulletin of JSME, Vol. 5, No. 17, 1962.

80. ATKIN, R H:
*Classical dynamics.*
Heinemann, London, 1964.

81. STABLER, G V:
*The basic nomenclature of cutting tools.*
Inst. Prod. Engs. Journal, May 1955.

82. VARLEY, G:
*Durability of twist drills machining cast iron.*
The Engineer, 17 August 1934.

83. BURANT, R O and SKINGLE, T J:
*Drilling, tapping Al-Si alloys.*
American Machinist, Oct. 1979.

84. FARNWORTH, G H:
*Evolutionary optimization of machining processes.*
Doctoral Thesis, LUT, 1974.

85. CETIM:
*Le perçage.*
CETIM, Service "Coupe", 1980.

86. SINGPURWALLA, N D and KUEBLER, A A:
*A quantitative evaluation of drill life.*
ASME, 1967. Paper No. 66-WA/Prod-11.

87. WILLIAMS, R A and McGILCHRIST, C A:
*An experimental study of drill life.*
Int. J. Prod. Res. 1972, Vol. 10, No. 2, 175-191.

88. LORENZ, G:
*Comparative drill performance tests.*
Manuscript submitted to the 1978 ASM/SME International Conference on Machineability Testing and Utilization of Machining Data.

89. *Twist drill life testing.*
Metal Cutting, April 1955, Vol. 2, No. 3.

90. IWATA, K and MORIWAKI, T:
*Cutting state identification and in-process tool wear sensing by acoustic emission analysis.*
Bull. Japan Soc. of Prec. Engg, Vol. 12, No. 4, Dec. 1978.

91. WELLER, E J, SCHRIER, H M and WEICHBRODT, B:
*What sound can be expected from a worn tool?*
Transactions of the ASME, 1969, Paper No. 68-WA/Prod-4.

92. IWATA, K and MORIWAKI, T:
*An application of acoustic emission measurement to in-process sensing of tool wear.*
Annals of CIRP Vol. 25 January 1977.

93. *Excessive drilling is expensive.*
Draft of paper with no author reference.

94. SUBRAMANIAN, K and COOK, N H:
*Sensing of drill wear and prediction of drill life.*
Transactions of ASME, 1977, Paper No. 76-WA/Prod-33.

95. TSENG, M M and NOUJAIM, R A:
*On the measurement and propagation of flank wear in cutting tools.*
Transactions of the ASME, 1979, Paper No. 78-WA/Prod-23.

96. KALDOR, S and LENZ, E:
*Investigation in tool life of twist drills.*
Annals of the CIRP, Vol. 29 January 1980.

97. LENZ, E and KATZ, Z:
*A correlation between chip-tool contact length and flank-wear.*
Annals of the CIRP Vol. 22 January 1973.

98. COLDING, B and KÖNIG, W:
*Validity of the Taylor equation in metal cutting.*
Annals of the CIRP 1971, Vol. XVIV, pp 793-812.

99. LENZ, E, MAYER, J E and LEE, D G:
*Investigation in drilling.*
Annals of the CIRP Vol. 27 January 1978.

100. RABINOWICZ, E, McENTIRE, R H and SHIRALKAR, B:
*A technique for accelerated life testing.*
Transactions of the ASME, 1970, Paper No. 70-Prod-10.

101. CHEVALIER, A:
*Étude de la coupe.*
Librairie Delagrave, Paris, 1972.

102. QUENOUILLE, M H:
*The design and analysis of experiment.*
Charles Griffin and Co, London, 1953.

103. FISHER, R A:
*The design of experiments.*
Oliver and Boyd, Edinburgh, 1960.

104. BROWNLEE, K A:
*Industrial experimentation.*
Ministry of Supply. HMSO, London, 1957.

105. MORONEY, M J:
*Facts from figures.*
Penguin Books, England, 1978.

106. HAMBOOLY, A N and KOURA, M M:
*Theoretical determination of the drilling forces for the conventional twist drills.*
Paper manuscript, Ain Shaws University, Cairo.

107. ROADINGER, T J and TOWNSEND, M A:
*Torque and thrust parameters in drilling using dimensional analysis.*
Transactions of the ASME, 1980. Paper No. 79-WA/Prod-4.

108. KALDOR, S, BER, A and LENZ, E:
*On the mechanism of chip breaking.*
Transactions of the ASME, 1979. Paper No. 78-WA/Prod-21.

109. BOOTHROYD, G:
*Fundamentals of metal machining and machine tools.*
McGraw-Hill, Tokyo, 1975.

110. OKUSHIMA, K, HOSHI, T and FUJINAWA, T:
*On the behaviour of chip in steel cutting.*
Part 2, In the case of parallel type chip breaker .
Bulletin of JSME, Vol. 3, No. 10, 1960.

111. OKUSHIMA, K and MINATO, K:
*On the behaviour of chip in steel cutting.*
Bulletin of JSME, Vol. 2, No. 5, 1959.

112. HENRINKSEN, E K:
*Chip breaking - a study of three-dimensional chip flow.*
ASME, 1953, Paper No. 53-S-9.

113. RICE, W B:
*The formation of continuous chips in metal cutting.*
The Engineering Journal, February 1961.

114. COOK, N H and NAYAK, P N:
*The thermal mechanics of tool wear.*
Transactions of the ASME, 1966, Paper No. 65, Prod-9.

115. PONKSHE, G R:
*A new explanation of the phenomenon of chip curling during machining.*
Transactions of the ASME, 1967, Paper No. 66-Prod-E.

116. MAZUR, J C:
*A technique to optimize control of process variables in related studies of causes and effects of metal cutting behaviour.*
Annals of the CIRP, 1967. Vol. XV, pp 287-293.

117. DEWHURST, P:
*Is the machining process uniquely defined?*
Annals of the CIRP. Vol. 27 January 1978.

118. KRONENBERG, M:
*Machining science and application.*
Pergamon Press, England, 1966.

119. WALLACE, W P:
*An investigation on the friction between chip and tool in metal cutting.*
Fellowship thesis, Royal College of Advanced Technology, Salford, April 1962.

120. NAKAYAMA, K:
*Chip curl in metal cutting process.*
Bull. of the Faculty of Engineering, Yokohama National University, Vol. 11, March 1962.

121. ARMAREGO, E J A and CHENG, C Y:
*Drilling with flat rake face and conventional twist drills - II: Experimental investigation.*
Int. J. Mach. Tool Des. Res. Vol. 12, pp 37-54, Pergamon Press, 1972.

122. ZOREV, N N:
*Metal cutting mechanics.*
Pergamon Press, 1966.

123. DeVRIES, M F, SAXENA, U K and WU, S M:
*Temperature distributions in drilling.*
Transactions of the ASME, 1968, Paper No. 67-Prod-16.

124. FINNEY, D J:
*An introduction to the theory of experimental design.*
The University of Chicago Press, 1963.

125. LEVI, R:
*Drill press dynamometers.*
Int. J. Mach. Tool Des. Res. Vol. 7, pp 269-287. Pergamon Press, 1967.

ii) British Standard Specifications

BS 328: Twist drills and combined drills and countersinks,
BS 328: Part 1: 1959.

BS 5533: Geometry of the active part of cutting tools,
BS 5533: Part 1: 1978.

BS 5623: Tool life testing with single point turning tools,
BS 55623: 1979 (identical with ISO 3685: 1977).

iii) Catalogues

C.1 Guhring twist drills, 2nd Edition, Milton, Abingdon.

C.2 Kistler, Two-component measuring platform.
Operating and service instructions.

iv) Films

1. Drill action and drilling chip flow.
Loughborough University of Technology, 16 mm Black and white print.

2. Plastic flow of material during machining.
The College of Aeronautics Cranfield, England.
16 mm Black and white print.

## APPENDIX 1

Computer program for drill point geometric simulation and cutting angles computation for any set of cylindrical grinding conditions and any flute shape (refer to Chapters 2, 3 and 4).

This FORTRAN program uses subroutines from GINO and NAG libraries which are not listed here.

```
C
C
C
C ===============================================
C
C          DRILL POINT SIMULATION AND
C          CUTTING ANGLES COMPUTATION FOR ANY SET OF
C          CYLINDRICAL GRINDING CONDITIONS AND ANY
C          FLUTE SHAPE
C
C          DESIGNED,DEVELOPED AND IMPLEMENTED BY
C          MANUEL DOS SANTOS PAIS
C
C          SUBROUTINES FROM
C          NAG LIBRARY AND
C          GINO LIBRARY ARE USED
C
C ===============================================
C
C
      IMPLICIT DOUBLE PRECISION(A-H,O-Z)
      REAL XWEARG(200),YWEARG(200),ZWEARG(200),DWEARG(200)
      REAL R0H,WEBH,H0H,ROH,EXGH,VGH,RKGH,ROGH
      REAL YELIC8,ZELIC8,ZLIM8,R00,YFLOW,YFHIGH
      REAL RAGE(200),X00POS,Y00POS
      REAL XAXIS,YAXIS,X0POS,Y0POSX,Y0POSY,XCAP
      REAL RAKFS(200),RAKFL(200),RAKFA(200),RAKFB(200)
     $,RAKFK(200)
      REAL XPACG(200),YPACG(200),ZPACG(200)
      REAL DFTR(200),DFNR(200),DFTE(200),DFNSU(200)
      REAL X1(200),Y1(200),Y1N(200),Y1A(200),X1A(200),X1AN(200)
      REAL T1MEU(200),T1WI(200),T1MAU(200)
      REAL XFLU(200),YFLU(200),XCHIG(200),YCHIG(200),ZCHIG(200)
      REAL RAKCHI(200),CHIRAK(200)
      REAL RAKE(200),WEDGE(200),RELIEF(200),AINC(200),CLEAR(200)
      REAL ETAARM(200),ETALEE(200),ETABRO(200),ETAKRO(200)
      REAL RADI(200),XLG(200),YLG(200),DL(200),SSS(200)
      REAL XSTG(200),YSTG(200),ZSTG(200),RSNI(200)
      REAL XCLEA(200),YCLEA(200),ZCLEA(200),PHICLE(200)
      REAL DFPR(200),DFQR(200),DFRR(200),DVSNI(200),ADVSNI(200)
      REAL XHEELG(200),YHEELG(200),ZHEELG(200),XEELG(200)
     $,YEELG(200)
      REAL XSECG(300),YSECG(300),ZSECG(300)
      REAL XSTARG(300),YSTARG(300),ZSTARG(300),YSCFLG(300)
     $,XSCFLG(300)
      REAL VCSIET(200),SVCSIE(200),VVSIIN(200),SVVSII(200)
      REAL XELIC1(200),YELIC1(200),ZELIC1(200)
      REAL XELIC2(200),YELIC2(200),ZELIC2(200)
      DIMENSION XCHI2(200),YCHI2(200)
      DIMENSION ZSTGD(200),XSTGD(200),YSTGD(200)
      DIMENSION THRUS(200),TORQU(200),THRCH(200),TORCH(200)
      DIMENSION RCHISE(200),CHIXA(200)
      DIMENSION DER(14),EREST(14)
      DIMENSION COEF(20)
      DIMENSION XMSU(200),YMSU(200),ZMSU(200)
      DIMENSION XL(200),YL(200),DERIV(200)
      DIMENSION RSTFL(40),PHSTFL(40),COFL(40),XHSTFL(40)
     $,YHSTFL(40)
      DIMENSION CCE1(200),CCE2(200),CCE3(200),CCE3P(200)
      DIMENSION DIDL(200),DRADL(200),VVD(200)
      DIMENSION ZTGHG(200),ETAS(200),WIETA(200)
      DIMENSION CORN(3),RE(3),RU(3),WE0(120)
      DIMENSION FJAC(3,3),SMON(3),V(3,3),IW(1)
      DIMENSION ALAMB(200),PPQQ(200)
      DIMENSION XFLUD(300),YFLUD(300),XEELGD(300),YEELGD(300)
      DIMENSION VCHIP(200)
      DIMENSION XCHID(200),YCHID(200),ZCHID(200)
      DIMENSION XHEELD(200),YHEELD(200),ZHEELD(200)
      DIMENSION XCLEAD(200),YCLEAD(200),ZCLEAD(200)
      COMMON/BLO1/R0,WEB,H0,EXG,VG,RKG,ROG
      COMMON/BLO2/CONS,PI
      COMMON/BLO3/ALPHA,CSVG,SNVG,CSKOI,SNKOI,CSKOU,SNKOU
      COMMON/BLO4/Z,Z0,ZHH
      COMMON/BLO5/S,NPOINT,NLAAP,ISEC,IHE
      COMMON/BLO6/COEF,NCOEF,III
      COMMON/BLO7/XCLE,YCLE,IFL,IHILST,PHIIL2
      COMMON/BLO8/XFLUEE,YFLUEE,DMAR,XSTEEL,YSTEEL,ANGCLE,YEEL
      COMMON/BLO10/CUTRAT,DINC,RAK,FRIC
      COMMON/BLO11/COFL,NSTFLI
      COMMON/BLO12/RSE,PHSE,DSEC,SCE1,SCE2,SCE3
      COMMON/BLO13/XSEC,YSEC,ZSEC,ZMSEC
      COMMON/BLO14/RPACE,PHPA,YPACE1
      COMMON/BLO15/XL0,YL0
      COMMON/BLO16/COEA,COEB
      COMMON/BLO17/XEELA,YEELA,ZWEB
      COMMON/BLO18/XCHID,YCHID,ZCHID
      COMMON/BLO19/XHEELD,YHEELD,ZHEELD
      COMMON/BLO20/XCLEAD,YCLEAD,ZCLEAD
      COMMON/BLO21/XOUT,YOUT
      COMMON/BLO22/RAKFS,RAKFL,RAKFA,RAKFB
      COMMON/BLO23/XSTGD,YSTGD,ZSTGD,RADI,IWEAR,RPI,DZWEAR
      COMMON/BLO24/XWEAR,YWEAR,ZWEAR
      EXTERNAL FAN,FEEL,FIIL,FIN,FLANK,FON,FOUTCR,FPACE,FSCFL
      EXTERNAL FUN,FUNSEC,FWEB,GRIN,GPACE,MONIT,MONUT,RESID
      EXTERNAL RESUD, ROTAC,VIJK
C
C DATA READING
      WRITE(1,6000)
6000  FORMAT('READ PARAMETERS TO CONV FLUTE:R0,WEB,H0,RO')
      READ(1,*)R0,WEB,H0,RO
      WRITE(1,705)
705   FORMAT('GRINDING PARAMETERS')
      READ(1,*)EXG,VG,RKG,ROGG
      ROG=2.*ROGG
      WRITE(1,8060)
8060  FORMAT('READ SPEED  AND FEED ')
      READ(1,*)RPM,RPI
      WRITE(1,8061)
```

```
8061  FORMAT('STABLER (1) OR USUI (2) ?')
      READ(1,*)NSTAB
      WRITE(1,10)
10    FORMAT('READ S=1. FOR SPECIAL DRILL/
     $READ ALSO NPOINT')
      READ(1,*)S,NPOINT
      IF(S .NE. 1.) GO TO 12
      WRITE(1,11)
11    FORMAT('READ  NCOEF')
      READ(1,*)NCOEF
12    WRITE(1,13)
13    FORMAT('READ RADIAL LIMITS TO FLUTE')
      READ(1,*)RSTAN1,RSTAN2
C
      WRITE(1,8004)
8004  FORMAT('DATA FOR CHISEL CORNER COMPUTATION')
      WRITE(1,8000)
8000  FORMAT('IPRINT/(-1)-NO CALL/(1)-EACH ITERATION'
     $,'(0)-FINAL ITER.')
      READ(1,*)IPRINT
C STARTING POINT FOR CHISEL CORNER COMPUTATION
      CORN(1)=WEB/2.
      CORN(2)=-WEB/2.
      CORN(3)=WEB/2.
      WRITE(1,8002)
8002  FORMAT('READ STEP FOR CHISEL CORNER CALCULATION')
      READ(1,*)STEP
C MAXCAL IS THE NUMBER OF ITERATIONS
      MAXCAL=1000
      WRITE(1,8005)
8005  FORMAT('READ STEP FOR PRINTING TABLES')
      READ(1,*)NSALTO
      WRITE(1,8006)
8006  FORMAT('DRILLING FORCES ?')
      READ(1,*)NFORCA
      WRITE(1,7001)
7001  FORMAT('READ HEEL PARAMETER')
      READ(1,*)ANGCLE
      ANGCLE=ANGCLE*CONS
      WRITE(1,7015)
7015  FORMAT(' OPEN  HEEL ?')
      READ(1,*)IHILST
C
      FTOL=1.E-7
      XTOL=1.E-6
      EPS=1.E-7
      EPS1=EPS
      EPV=EPS
      EPV1=EPS
      IFAIL=0
      ZCLE1=1.
      ZCLE2=1.5*R0
      DMAR=0.35
      PI=3.14159265
      CONS=PI/180.
      H0=H0*CONS
C
      CSVG=DCOS(VG*CONS)
      SNVG=DSIN(VG*CONS)
      CSKOI=DCOS(RKG*CONS)
      SNKOI=DSIN(RKG*CONS)
      CSKOU=DCOS(RO*CONS)
      SNKOU=DSIN(RO*CONS)
      Z0=DSQRT(ROG**2-(EXG-WEB/2.)**2)/SNKOI
C COMPUTING THE OUTER CORNER
      P0X=DSQRT(R0**2-(WEB/2.)**2)
      P0Y=-WEB/2.
      P0Z=P0X*CSKOI/SNKOI
      ZOUT1=P0Z-2.
      ZOUT2=P0Z+2.
      CALL C05ACF(ZOUT1,ZOUT2,EPS,EPV,FOUTCR,ZOUT,IFAIL)
      WRITE(1,2780)
2780  FORMAT('OUTER CORNER COMPUTED')
C ==============================================
      IF(S .NE. 1.)GO TO 15
C READING FROM FILE
      READ(5,*)NP
      DO 204 I=1,NP
      READ(5,*)XL(I),YL(I)
204   CONTINUE
      WRITE(1,206)(XL(I),YL(I),I=1,NP)
206   FORMAT(2F10.4)
      CALL E02ACF(XL,YL,NP,COEF,NCOEF,REF)
      XL1=R0/2.
      XL2=R0
      CALL C05ACF(XL1,XL2,EPS,EPV,ROTAC,XLK,IFAIL)
      PHL0=DATAN(YL0/XL0)
      PHLA=DATAN((-WEB/2./R0)/DSQRT(1.-(WEB/2./R0)**2))
      P0X=DSQRT(R0**2-(WEB/2.)**2)
      P0Z=P0X*CSKOU/SNKOU
      PHLB=P0Z/R0*DSIN(H0)/DCOS(H0)
      SISANG=PHL0-PHLA+PHLB
      DO 610 I=1,NP
      XL(I)=XL(I)*DCOS(SISANG)+YL(I)*DSIN(SISANG)
      YL(I)=-XL(I)*DSIN(SISANG)+YL(I)*DCOS(SISANG)
      XLG(I)=XL(I)
      YLG(I)=YL(I)
610   CONTINUE
      SISAN=SISANG/CONS
      WRITE(1,208)(XL(I),YL(I),I=1,NP)
208   FORMAT(2F10.4)
600   CONTINUE
C NON-CONV. FLUTE SECTION
      CALL E02ACF(XL,YL,NP,COEF,NCOEF,REF)
C WEB=-2.*COEF(1) IF WEB WAS MEASURED ALONG Y AXIS
15    M=3
      N=3
      LV=3
```

```
      LJ=3
      LW=120
      LIW=1
      ETA=.5
      IF(S .EQ. 1.) GO TO 8011
C CHISEL CORNER DETERMINATION
      CALL E04FCF(M,N,RESID,MONIT,IPRINT,MAXCAL,ETA,XTOL,
     $STEP,CORN,FE,RE,FJAC,LJ,SMON,V,LV,NITER,NF,IW,LIW,WE0,
     $LW,IFAIL)
C
      GO TO 8014
8011  CALL E04FCF(M,N,RESUD,MONUT,IPRINT,MAXCAL,ETA,XTOL,
     $STEP,CORN,FU,RU,FJAC,LJ,SMON,V,LV,NITER,NF,IW,LIW,WE0,
     $LW,IFAIL)
8014  CONTINUE
      WRITE(1,2779)
2779  FORMAT(/'CHISEL CORNER COMPUTED')
      XCORN=CORN(1)
      YCORN=CORN(2)
      ZCORN=CORN(3)
C
      ZWEB1=0.0
      ZWEB2=ZCORN+1.
      CALL C05ACF(ZWEB1,ZWEB2,EPS,EPV,FWEB,ZWEB,IFAIL)
      WRITE(1,9999)ZWEB
9999  FORMAT('ZWEB=',F10.3)
C =========================================================
C COMPUTING ANGLES,POINT BY POINT
C =========================================================
      DO 5 I=1,NPOINT
      III=I
      NLIP=1
      Z=ZOUT-FLOAT(I-1)*(ZOUT-ZCORN)/FLOAT(NPOINT-1)
38    ALPHA=Z/R0*DSIN(H0)/DCOS(H0)
      ZSTG(I)=Z
      ZSTGD(I)=Z
      IF(S .EQ. 1.)GO TO 30
C FLUTE AND FLANK INTERSECTION
      CALL C05ACF(RSTAN1,RSTAN2,EPS,EPV,FUN,RSTAN,IFAIL)
      GO TO 32
30    CALL C05ACF(RSTAN1,RSTAN2,EPS,EPV,FAN,XST,IFAIL)
      YST=0.0
      DO 75 J=1,NCOEF
      YST=YST+COEF(J)*XST**(J-1)
75    CONTINUE
C
      GO TO 34
32    W2R=WEB/2./RSTAN
      PHST=-(DATAN(W2R/DSQRT(1.-W2R**2))+DSQRT(RSTAN**2
     $-(WEB/2.)**2)*DSIN(H0)/DCOS(H0)/R0*CSKOU/SNKOU)
      XFLU(I)=RSTAN*DCOS(PHST)
      YFLU(I)=RSTAN*DSIN(PHST)
      XFLUD(I)=RSTAN*DCOS(PHST)
      YFLUD(I)=RSTAN*DSIN(PHST)
      IF(I .EQ. 1)XFLUEE=RSTAN*DCOS(PHST)
      IF(I .EQ. 1)YFLUEE=RSTAN*DSIN(PHST)
      PHST=PHST+ALPHA
      XST=RSTAN*DCOS(PHST)
      YST=RSTAN*DSIN(PHST)
      XSTG(I)=XST
      XSTGD(I)=XST
      YSTG(I)=YST
      YSTGD(I)=YST
      RADI(I)=RSTAN
      GO TO 36
34    RSTAN=DSQRT(XST**2+YST**2)
      XFLU(I)=XST
      YFLU(I)=YST
      XFLUD(I)=XST
      YFLUD(I)=YST
      IF(I .EQ. 1)XFLUEE=XST
      IF(I .EQ. 1)YFLUEE=YST
      RADI(I)=RSTAN
      PHST=DATAN(YST/XST)
      PHST=PHST+ALPHA
      XST1=RSTAN*DCOS(PHST)
      YST1=RSTAN*DSIN(PHST)
      XSTG(I)=XST1
      XSTGD(I)=XST1
      YSTG(I)=YST1
      YSTGD(I)=YST1
      XST=XST1
      YST=YST1
36    CONTINUE
C
      CALL GRIN(Z,Z0,AXX,BYY,CXY,DDX,EY,FF)
C
C VECTOR NORMAL TO FLANK
C POINTING OUTWARDS
      DFDX=2.*XST*AXX+YST*CXY+DDX
      DFDY=2.*YST*BYY+CXY*XST+EY
      DFDZ=XST*(-2.*SNKOI*CSKOI*SNVG)+YST*(-2.*SNKOI
     $*CSKOI*CSVG)+SNKOI**2*2.*(Z-Z0)
      DF=DSQRT(DFDX**2+DFDY**2+DFDZ**2)
      DFDX=DFDX/DF
      DFDY=DFDY/DF
      DFDZ=DFDZ/DF
      IF(DFDX .GT. 0.0)GO TO 40
      DFDX=-DFDX
      DFDY=-DFDY
      DFDZ=-DFDZ
C VECTOR NORMAL TO RADIUS AND ON THE FLANK
C POINTING IN THE VELOCITY DIRECTION
40    UR1=DCOS(PHST)
      UR2=DSIN(PHST)
      UR3=0.0
      XFLNR=1.
      YFLNR=-UR1/UR2*XFLNR
```

```
      ZFLNR=(-XFLNR*DFDX-YFLNR*DFDY)/DFDZ
      FLNR=DSQRT(XFLNR**2+YFLNR**2+ZFLNR**2)
      XFLNR=XFLNR/FLNR
      YFLNR=YFLNR/FLNR
      ZFLNR=ZFLNR/FLNR
      IF(YFLNR .GT. 0.0)GO TO 160
      XFLNR=-XFLNR
      YFLNR=-YFLNR
      ZFLNR=-ZFLNR
160   CONTINUE
C VECTOR TANGENT TO FLUTE AT Z
C POINTING OUTWARDS
      NDER=1
      HBASE=1E-5
      IF(S .EQ. 1.)GO TO 130
C DERIVATIVES
      CALL D04AAF(RSTAN,NDER,HBASE,DER,EREST,FON,IFAIL)
      DYDXN=DSIN(PHST)/DCOS(PHST)+RSTAN*DER(1)
      DYDXD=1.-RSTAN*DER(1)*DSIN(PHST)/DCOS(PHST)
      DYDX=DYDXN/DYDXD
      GO TO 140
130   XST=XFLU(I)
      YST=YFLU(I)
      CALL D04AAF(XST,NDER,HBASE,DER,EREST,FIN,IFAIL)
      DYDX=DER(1)
140   DYDXE=DATAN(DYDX)
      XTG=DCOS(DYDXE)
      YTG=DSIN(DYDXE)
      ZTG=0.0
      DERIV(I)=DYDXE/CONS
      IF(XTG .GT. 0.0)GO TO 120
      XTG=-XTG
      YTG=-YTG
C VECTOR TANGENT TO HELIX AND POINTING TO SHANK
C HELIX ANGLE TOO
120   XTGH=-DSIN(PHST)
      YTGH=DCOS(PHST)
      COTH=R0/RSTAN*DCOS(H0)/DSIN(H0)
      XYC=DSQRT(XTGH**2+YTGH**2+COTH**2)
      XTGH=XTGH/XYC
      YTGH=YTGH/XYC
      ZTGH=COTH/XYC
      ZTGH1=DSQRT(1.-ZTGH**2)
      ZTGHG(I)=DATAN(ZTGH1/ZTGH)/CONS
C VECTOR NORMAL TO RAKE FACE POINTING TO SHANK
      XNRA=YTG*ZTGH
      YNRA=-XTG*ZTGH
      ZNRA=XTG*YTGH-XTGH*YTG
      XYZN=DSQRT(XNRA**2+YNRA**2+ZNRA**2)
      XNRA=XNRA/XYZN
      YNRA=YNRA/XYZN
      ZNRA=ZNRA/XYZN
      IF(ZNRA .LT. 0.0)WRITE(1,45)
45    FORMAT('ZNRA IS NEGATIVE')
C VECTOR TANGENT TO CUTTING EDGE
C POINTING OUTWARDS
      CE1=YNRA*DFDZ-ZNRA*DFDY
      CE2=ZNRA*DFDX-XNRA*DFDZ
      CE3=XNRA*DFDY-YNRA*DFDX
      CEE=DSQRT(CE1**2+CE2**2+CE3**2)
      CE1=CE1/CEE
      CE2=CE2/CEE
      CE3=CE3/CEE
C
      CCE1(I)=CE1
      CCE2(I)=CE2
      CCE3(I)=CE3
      CE3A=DSQRT(1.-CE3**2)
      CCE3P(I)=DATAN(CE3A/CE3)/CONS
      IF(CE1 .LT. 0.0)WRITE(1,50)
50    FORMAT('CE1  IS  NEGATIVE')
C VECTOR NORMAL TO THE CUTTING EDGE
C AND ON THE RAKE FACE
C POINTING TO DRILL AXIS
      XTRA=1.
      CZTRA1=(ZNRA*CE2-YNRA*CE3)/(ZNRA*CE2)
      CZTRA2=(YNRA*XTRA*CE1-XNRA*XTRA*CE2)/(CE2*ZNRA)
      ZTRA=CZTRA2/CZTRA1
      YTRA=(-ZTRA*CE3-XTRA*CE1)/CE2
      TRA=DSQRT(XTRA**2+YTRA**2+ZTRA**2)
      XTRA=XTRA/TRA
      YTRA=YTRA/TRA
      ZTRA=ZTRA/TRA
      IF(YTRA .GT. 0.0)GO TO 55
      XTRA=-XTRA
      YTRA=-YTRA
      ZTRA=-ZTRA
C ANGLE BET. TANGENT TO HELIX AND NORMAL TO
C CUTTING EDGE ON THE RAKE FACE
55    AFLO1=XTGH*XTRA+YTGH*YTRA+ZTGH*ZTRA
      AFLO2=DSQRT(1.-AFLO1**2)
      ETAARM(I)=DATAN(AFLO2/AFLO1)/CONS
C VECTOR NORMAL TO CUTTING EDGE AND ON THE
C RAKE FACE,POINTING IN VELOCITY DIRECTION
      XTFLA=1.
      CZFLA1=(DFDZ*CE2-DFDY*CE3)/(DFDZ*CE2)
      CZFLA2=(DFDY*XTFLA*CE1-DFDX*XTFLA*CE2)/(CE2*DFDZ)
      ZTFLA=CZFLA2/CZFLA1
      YTFLA=(-ZTFLA*CE3-XTFLA*CE1)/CE2
      FLA=DSQRT(XTFLA**2+YTFLA**2+ZTFLA**2)
      XTFLA=XTFLA/FLA
      YTFLA=YTFLA/FLA
      ZTFLA=ZTFLA/FLA
      IF(YTFLA .GT. 0.0)GO TO 60
      XTFLA=-XTFLA
      YTFLA=-YTFLA
      ZTFLA=-ZTFLA
C NORMAL WEDGE ANGLE
```

```
60    COSAN=XTRA*XTFLA+YTRA*YTFLA+ZTRA*ZTFLA
      SINAN=DSQRT(1.-COSAN**2)
      ANGC=DATAN(SINAN/COSAN)
      IF(ANGC .GT. 0.0) GO TO 100
      ANGC=PI+ANGC
100   WEDGE(I)=ANGC/CONS
C VECTOR NORMAL TO MACHINED SURFACE
C POINTING TO THE SHANK
      VV1=-2.*PI*RPM/60.*RSTAN*DSIN(PHST)
      VV2=+2.*PI*RPM/60.*RSTAN*DCOS(PHST)
      VV3=25.4/RPI*RPM/60.
      VV=DSQRT(VV1**2+VV2**2+VV3**2)
      VVD(I)=VV
      VV1=VV1/VV
      VV2=VV2/VV
      VV3=VV3/VV
      XNMSU=-VV2*CE3+VV3*CE2
      YNMSU=-VV3*CE1+VV1*CE3
      ZNMSU=-VV1*CE2+VV2*CE1
      SU=DSQRT(XNMSU**2+YNMSU**2+ZNMSU**2)
      XNMSU=XNMSU/SU
      YNMSU=YNMSU/SU
      ZNMSU=ZNMSU/SU
C
      XMSU(I)=XNMSU
      YMSU(I)=YNMSU
      ZMSU(I)=ZNMSU
      TIMEU(I)=.5/RPI*25.4*CE3A
      TIMAU(I)=.5/RPI*25.4*ZNMSU
C VECTOR NORMAL TO CUTTING EDGE,ON THE MACHINED SURFACE
C AND POINTING IN THE VELOCITY DIRECTION
      XTMSU=1.
      CZMSU1=(ZNMSU*CE2-YNMSU*CE3)/(ZNMSU*CE2)
      CZMSU2=(YNMSU*XTMSU*CE1-XTMSU*XNMSU*CE2)/(CE2*ZNMSU)
      ZTMSU=CZMSU2/CZMSU1
      YTMSU=(-ZTMSU*CE3-XTMSU*CE1)/CE2
      TMSU=DSQRT(XTMSU**2+YTMSU**2+ZTMSU**2)
      XTMSU=XTMSU/TMSU
      YTMSU=YTMSU/TMSU
      ZTMSU=ZTMSU/TMSU
      IF(YTMSU .GT. 0.0)GO TO 20
      XTMSU=-XTMSU
      YTMSU=-YTMSU
      ZTMSU=-ZTMSU
C NORMAL CLEARANCE ANGLE
20    COSSN=XTFLA*XTMSU+YTFLA*YTMSU+ZTFLA*ZTMSU
      SINSN=DSQRT(1.-COSSN**2)
      ANSA=DATAN(SINSN/COSSN)
      SIGN3=XNMSU*XTFLA+YNMSU*YTFLA+ZNMSU*ZTFLA
      IF(SIGN3 .GT. 0.0)GO TO 170
      ANSA=-ANSA
170   CLEAR(I)=ANSA/CONS
C VECTOR NORMAL TO THE CUTTING EDGE AND ROTATION VELOCITY
C POINTING TO THE SHANK
      UU1=-DSIN(PHST)
      UU2=DCOS(PHST)
      XVCE=1.
      YVCE=-UU1/UU2*XVCE
      ZVCE=(-CE1*XVCE-CE2*YVCE)/CE3
      VCE=DSQRT(XVCE**2+YVCE**2+ZVCE**2)
      XVCE=XVCE/VCE
      YVCE=YVCE/VCE
      ZVCE=ZVCE/VCE
      IF(ZVCE .GT. 0.0)GO TO 110
      XVCE=-XVCE
      YVCE=-YVCE
      ZVCE=-ZVCE
110   XNMSU1=-UU2*CE3+UU3*CE2
      YNMSU1=-UU3*CE1+UU1*CE3
      ZNMSU1=-UU1*CE2+UU2*CE1
      SU1=DSQRT(XNMSU1**2+YNMSU1**2+ZNMSU1**2)
      XNMSU1=XNMSU1/SU1
      YNMSU1=YNMSU1/SU1
      ZNMSU1=ZNMSU1/SU1
C
80    XTSU=1.
      CTU1=XTSU*XNMSU1*UU2-XTSU*UU1*YNMSU1
      CTU2=YNMSU1*UU3-ZNMSU1*UU2
      ZTSU=CTU1/CTU2
      YTSU=-(XTSU*XNMSU1+ZTSU*ZNMSU1)/YNMSU1
      CTU3=DSQRT(XTSU**2+YTSU**2+ZTSU**2)
      XTSU=XTSU/CTU3
      YTSU=YTSU/CTU3
      ZTSU=ZTSU/CTU3
      IF(ZTSU .GT. 0.0) GO TO 111
      XTSU=-XTSU
      YTSU=-YTSU
      ZTSU=-ZTSU
C INCLINATION ANGLE
111   COSI=UU1*CE1+UU2*CE2
      SINI=DSQRT(1.-COSI**2)
      AIN=DATAN(SINI/COSI)
      AIN=PI/2.-AIN
      AINC(I)=AIN/CONS
C NORMAL RAKE ANGLE
      COSRA=XVCE*XTRA+YVCE*YTRA+ZVCE*ZTRA
      SINRA=DSQRT(1.-COSRA**2)
      SIGN1=XVCE*XNRA+YVCE*YNRA+ZVCE*ZNRA
      SIGN2=DABS(SIGN1)
      SIGN=SIGN1/SIGN2
      RAK=DATAN(SINRA/COSRA)
      RAK=SIGN*RAK
      RAKE(I)=RAK/CONS
C PARALLEL RAKE ANGLE (AS DEFINED BY GALLOWAY)
      CEM1=XOUT-XCORN
      CEM2=YOUT-YCORN
      CEM3=ZOUT-ZCORN
      CEMM=DSQRT(CEM1**2+CEM2**2+CEM3**2)
```

```
      CEM1=CEM1/CEMM
      CEM2=CEM2/CEMM
      CEM3=CEM3/CEMM
C
      XNEG=1.
      YNEG=XNEG*CEM2/CEM1
      ZNEG=-(XNEG*CEM1+YNEG*CEM2)/CEM3
      XYZ=DSQRT(XNEG**2+YNEG**2+ZNEG**2)
      XNEG=XNEG/XYZ
      YNEG=YNEG/XYZ
      ZNEG=ZNEG/XYZ
      COSRA=XNEG*XTRA+YNEG*YTRA+ZNEG*ZTRA
      SINRA=DSQRT(1.-COSRA**2)
      SIGN1=XNEG*XNRA+YNEG*YNRA+ZNEG*ZNRA
      SIGN2=DABS(SIGN1)
      SIGN=SIGN1/SIGN2
      RAG=DATAN(SINRA/COSRA)*SIGN/CONS
      RAGE(I)=RAG
C NOMINAL RELIEF ANGLE (AS DEFINED BY GALLOWAY)
      COREL=UU1*XFLNR+UU2*YFLNR
      SIREL=DSQRT(1.-COREL**2)
      REL=DATAN(SIREL/COREL)
      RELIEF(I)=REL/CONS
C CHIP FLOW ANGLE ACCORDING TO BROWN AND ARMAREGO
      ETAB=DATAN(DSIN(AIN)/DCOS(AIN)*DCOS(RAK))
      ETABRO(I)=ETAB/CONS
C CHIP FLOW ANGLE ACCORDING TO AN OBLIQUE CUTTING
C APPROACH OF USUI TYPE
      IF(NSTAB .EQ. 2) GO TO 8067
      ETA=AIN
      GO TO 8069
8067  ETA=DATAN(1./(DCOS(RAK)+DSIN(RAK))*DSIN(AIN)/DCOS(AIN))
      ETALE=DABS(ETA/CONS)
      ETALEE(I)=ETALE
8069  ETAS(I)=ETA/CONS
      ETAK=DSIN(AIN)/DCOS(AIN)*DSIN(RAK)
      ETAKR=-DATAN(ETAK)/CONS
      ETAKRO(I)=ETAKR
      RSN=RSTAN*DSIN(AIN)
      RSNI(I)=RSN
      IF (I .EQ. 1) GO TO 498
      DL(1)=0.
      DL(I)=DSQRT((XSTGD(I)-XSTGD(I-1))**2+(YSTGD(I)
     $-YSTGD(I-1))**2+(ZSTGD(I)-ZSTGD(I-1))**2)
      SS=SS+DL(I)
      SSS(I)=SS
      IF(NFORCA .EQ. 0) GO TO 1009
C ======================================================
C WIRIYACOSOL PREDICTOR FOR DRILLING FORCES
C ======================================================
C VECTOR NORMAL TO PLANE PARALLEL TO CUTTING EDGE AND TO
C DRILL AXIS,POINTING OUTWARDS
      XNZETA=CE2
      YNZETA=-CE1
      ZNZETA=0.
      CNZETA=DSQRT(XNZETA**2+YNZETA**2+ZNZETA**2)
      XNZETA=XNZETA/CNZETA
      YNZETA=YNZETA/CNZETA
C VECTOR NORMAL TO THE CUTTING EDGE AND ON THE
C PLANE PARALLEL TO DRILL AXIS AND TO CUTTING EDGE
C POINTING TO THE DRILL SHANK
      XTZETA=1.
      YTZETA=-XNZETA/YNZETA*XTZETA
      ZTZETA=1./CE3*(-XTZETA*CE1-YTZETA*CE2)
      CTZETA=DSQRT(XTZETA**2+YTZETA**2+ZTZETA**2)
      XTZETA=XTZETA/CTZETA
      YTZETA=YTZETA/CTZETA
      ZTZETA=ZTZETA/CTZETA
C ZETA ANGLE (WIRIYACOSOL)
      COZETA=XVCE*XTZETA+YVCE*YTZETA+ZVCE*ZTZETA
      IF(COZETA .LT. .0)COZETA=-COZETA
      SIZETA=DSQRT(1.-COZETA**2)
      ZET=DATAN(SIZETA/COZETA)
C FORCES ON THE MAIN LIP
      BW2=DSIN(ETA)/DCOS(ETA)
      DINC=DCOS(AIN)
      SINC=DSIN(AIN)
      RAKU=RAK
      IF(NDESLI .EQ. 0) RAKU=0.
      TAU=(74390.-191.3*RAKU/CONS)*.45359/(25.4)**2
      T1=1./RPI/2.*CE3A*DCOS(ZET)*25.4
      T1WI(I)=T1
      DB=DL(I)*DINC
      DA=T1*DB
      FRIC=32.84+.559*RAK/CONS
      FRICN=DATAN(DSIN(FRIC*CONS)/DCOS(FRIC*CONS)*DCOS(ETA))
      RAKC=RAK
      IF(NCORT .EQ. 0)RAKC=0.
      CUTRAT=.3427+.00292*RAKC/CONS+.00096*VV/25.4/12.*60.
      VCHIP(I)=VVD(I)*CUTRAT
      PHIN1=CUTRAT*(DCOS(ETA)/DINC)*DCOS(RAK)
      PHIN2=1.-CUTRAT*(DCOS(ETA)/DINC)*DSIN(RAK)
      PHIN=DATAN(PHIN1/PHIN2)
      BWIRIY=(DCOS(PHIN+FRICN-RAK))**2
      BWIRY1=(BW2*DSIN(FRICN))**2
      BWIRIY=DSQRT(BWIRIY+BWIRY1)
      BW1=FRICN-RAK
      BW2=BW2
      BW3=DSIN(FRICN)
      BW4=DSIN(PHIN)
      BW5=TAU*DA
C
      DFP=BW5*(DCOS(BW1)*DINC+BW2*SINC*BW3)/BWIRIY/BW4/DINC
      DFPR(I)=DFP
C
      DFQ=BW5*DSIN(BW1)/BWIRIY/BW4/DINC
      DFQR(I)=DFQ
C
```

```
      DFR=BW5*(DCOS(BW1)*SINC-BW2*DINC*BW3)/BWIRIY/BW4/DINC
      DFRR(I)=DFR
C
      RTORQ=(RSTAN+RESQ)/2.
      DK1P=(481.25-7.957*RAK/CONS)*.45359/25.4
      DK1Q=(36Ø.31-4.Ø86*RAK/CONS)*.45359/25.4
C
      CF1=UU1*XTRA+UU2*YTRA+UU3*ZTRA
      CF2=XVCE*XTRA+YVCE*YTRA+ZVCE*ZTRA
      CF3=XTSU*XTRA+YTSU*YTRA+ZTSU*ZTRA
      CF4=UU1*XNRA+UU2*YNRA+UU3*ZNRA
      CF5=XVCE*XNRA+YVCE*YNRA+ZVCE*ZNRA
      CF6=XTSU*XNRA+YTSU*YNRA+ZTSU*ZNRA
      CF7=UU1*CE1+UU2*CE2+UU3*CE3
      CF8=XVCE*CE1+YVCE*CE2+ZVCE*CE3
      CF9=XTSU*CE1+YTSU*CE2+ZTSU*CE3
C
      DFTRA=DFP*CF1+DFQ*CF2-DFR*CF3
      DFTR(I)=DFTRA
C
      DFNRA=-DFP*CF4-DFQ*CF5+DFR*CF6+1ØØØØØ./(RPI)**3
      DFNR(I)=DFNRA
C
      DFTED=-DFP*CF7-DFQ*CF8+DFR*CF9
      DFTED=-DFTED
      DFTE(I)=DFTED
      CF1Ø=UU1*XNMSU+UU2*YNMSU+UU3*ZNMSU
      CF11=XVCE*XNMSU+YVCE*YNMSU+ZVCE*ZNMSU
      CF12=XTSU*XNMSU+YTSU*YNMSU+ZTSU*ZNMSU
      DFNSU(I)=(DFP+DK1P)*CF1Ø+(DFQ+DK1Q)*CF11+DFR*CF12
      DFPU=+DFTRA*CF1-DFNRA*CF4+DFTED*CF7
      DTH=+DFTRA*ZTRA-DFNRA*ZNRA+DFTED*CE3
      THE=2.*DK1Q*DB*COZETA*CE3A
      TOE=2.*RTORQ*DK1P*DB
      THHE=THHE+THE
      TOOE=TOOE+TOE
      THHEE=THHE/.45359
      TOOEE=TOOE/.45359/25.4
      THRUST=THRUST+2.*(DFQ*COZETA*CE3A-DFR*(DINC*CE3+SINC
     $*CE3A*SIZETA))+THE
      TORQUE=TORQUE+2.*RTORQ*DFP+TOE
      THRUS(I)=THRUST/.45359
      TORQU(I)=TORQUE/.45359/25.4
      TRIQUE=TRIQUE+2.*RTORQ*DFPU+TOE
      THRIQ=THRIQ+2.*DTH+THE
      TRUQUE=TRIQUE/Ø.45359/25.4
      THRUQ=THRIQ/Ø.45359
1ØØ9  CONTINUE
C
498   RESQ=RSTAN
      NLUP=I
5     CONTINUE
      WRITE(1,2781)
2781  FORMAT(/'LIP,ANGLES AND FORCES ON THE LIP COMPUTED')
C ==============================================================
C CHISEL POINT - DEAD CENTER
      ZCHIØ=ZØ-DSQRT((ROG**2-EXG**2)/SNKOI**2)
C CHISEL EDGE
C ==============================================================
3Ø3   DO 5ØØ I=1,NPOINT
      NCHI2=2*NPOINT
      ZCHI=ZCORN-FLOAT(I-1)/FLOAT(NPOINT-1)*(ZCORN-ZCHIØ)
      ZCHIG(I)=ZCHI
      ZCHID(I)=ZCHI
C
      AXX=CSVG**2+(CSKOI**2)*(SNVG**2)
      BYY=SNVG**2+CSVG**2*(CSKOI**2)
      CXY=-2.*SNVG*CSVG+2.*(CSKOI**2)*SNVG*CSVG
      DDX=-2.*EXG*1.*CSVG-2.*(ZCHI-ZØ)*SNKOI*CSKOI*SNVG
      EY=2.*1.*EXG*SNVG-2.*(ZCHI-ZØ)*SNKOI*CSKOI*CSVG
      FF=(1.**2)*(EXG**2-ROG**2)+((ZCHI-ZØ)**2)*SNKOI**2
C
      CHI1=BYY+(EY/DDX)**2*AXX-EY/DDX*CXY
      YCHI2(I)=+DSQRT(-FF/CHI1)
      XCHI2(I)=-YCHI2(I)*EY/DDX
      XCHIG(I)=DABS(XCHI2(I))
      YCHIG(I)=-DABS(YCHI2(I))
      XCHID(I)=DABS(XCHI2(I))
      YCHID(I)=-DABS(YCHI2(I))
C
      DFDX=2.*XCHID(I)*AXX+YCHID(I)*CXY-DDX
      DFDY=2.*YCHID(I)*BYY+CXY*XCHID(I)-EY
      DFDZ=XCHID(I)*(-2.*SNKOI*CSKOI*SNVG)+YCHID(I)*(-2.*
     $SNKOI*CSKOI*CSVG)+SNKOI**2*2.*(Z-ZØ)
      DF=DSQRT(DFDX**2+DFDY**2+DFDZ**2)
      DFDX=DFDX/DF
      DFDY=DFDY/DF
      DFDZ=DFDZ/DF
      RAKCHI(I)=-(9Ø.-DATAN(DSQRT(1.-DFDZ**2)/(-DFDZ))/CONS)
      AMOD=DSQRT((XCHI2(I))**2+(YCHI2(I))**2)
      IF(AMOD .EQ. Ø.) AMOD=1.E-8
      XCHIXA=XCHI2(I)/AMOD
      YCHIXA=YCHI2(I)/AMOD
      CIXA=XCHIXA
      IF(CIXA .EQ. Ø.) CIXA=1.E-8
      SIXA=DSQRT(1.-CIXA**2)
      TIXA=SIXA/CIXA
      CHIXA(I)=DATAN(TIXA)/CONS+18Ø.
      RCHISE(I)=DSQRT((XCHID(I))**2+YCHID(I)**2)
      VAXI=RPM/RPI*25.4
      VRAD=2.*PI*RCHISE(I)*RPM/6Ø.
      IF(VRAD .EQ. Ø.)GO TO 2635
      ANG1=DATAN(VAXI/VRAD)/CONS
      GO TO 2636
2635  ANG1=9Ø.
2636  CHIRAK(I)=ANG1-RAKCHI(I)-9Ø.
C
      RCHISE(NPOINT+I)=RCHISE(I)
```

```
C
500   CONTINUE
      WRITE(1,2782)
2782  FORMAT(/'CHISEL EDGE COMPUTED')
C FORCES ON THE CHISEL EDGE
      NCHI1=NPOINT-1
      DO 502 I=1,NCHI1
      RCHI=(RCHISE(I)+RCHISE(I+1))/2.
802   BETAW=DATAN(1./RPI*25.4/2./PI/RCHI)
      GAMAW=DATAN(SNKOI/CSKOI*DSIN((180.-CHIXA(I))*CONS))
      RAKCH=(BETAW-GAMAW)/CONS
      DLCHI=DSQRT((XCHID(I)-XCHID(I+1))**2+(YCHID(I)
     $-YCHID(I+1))**2+(ZCHID(I)-ZCHID(I+1))**2)
      CHILEN=CHILEN+2.*DLCHI
      T1CHI=1./RPI/2.*DCOS(BETAW)
      C1P=55740.*T1CHI**.651*(90.+RAKCH)**.06*.45359/25.4
      C1Q=852500.*T1CHI**.635*(90.+RAKCH)**(-.62)*.45359/25.4
      DFPCHI=C1P*DLCHI
      DFQCHI=C1Q*DLCHI
      THRUCH=THRUCH+2.*DLCHI*(C1P*DSIN(BETAW)+C1Q*DCOS(BETAW))
      TORQCH=TORQCH+2.*RCHI*DLCHI*(C1P*DCOS(BETAW)-C1Q
     $*DSIN(BETAW))
      THRCH(I)=THRUCH/.45359
      TORCH(I)=TORQCH/.45359/25.4
502   CONTINUE
      DO 330 I=2,NLUP
      DRAK=RAKE(I+1)-RAKE(I)
      DRADL(I)=DRAK/DL(I)
330   CONTINUE
C CYLINDRICAL CLEARANCE
      READ(1,*)ZCLE1,ZCLE2
      PHIIL1=DATAN(YSTGD(1)/XSTGD(1))
      DO 1940 IFL=1,NPOINT
      XCLE=R0*DCOS(PHIIL2-FLOAT(IFL-1)/FLOAT(NPOINT-1)*
     $(PHIIL2-PHIIL1))
      YCLE=R0*DSIN(PHIIL2-FLOAT(IFL-1)/FLOAT(NPOINT-1)*
     $(PHIIL2-PHIIL1))
      CALL C05ACF(ZCLE1,ZCLE2,EPS,EPV,FLANK,ZCLE,IFAIL)
      XCLEA(IFL)=XCLE
      YCLEA(IFL)=YCLE
      ZCLEA(IFL)=ZCLE
      XCLEAD(IFL)=XCLE
      YCLEAD(IFL)=YCLE
      ZCLEAD(IFL)=ZCLE
      ZHH=ZCLEA(1)
      IF(ZCLEA(I) .GT. ZHH)ZHH=ZCLEA(I)
      PHICLE(IFL)=(PHIIL2-FLOAT(IFL-1)/FLOAT(NPOINT-1)*(PHIIL2-
     $PHIIL1))/CONS
      IF(IFL .EQ. 1)ZCLEEE=ZCLE
1940  CONTINUE
      WRITE(1,2783)
2783  FORMAT(/'FLANK CONTOUR ON CYLINDRICAL SURFACE COMPUTED')
      IF(IAINCL .EQ. 0)GO TO 2661
      WRITE(6,2662)NPOINT
      WRITE(6,2664)R0,WEB,H0,RO,EXG,VG,RKG,ROG
      WRITE(6,2663)(RADI(I),AINC(I),I=1,NPOINT)
2662  FORMAT(I4,F12.6)
2663  FORMAT(2F12.6)
2664  FORMAT(8F12.6)
2661  WRITE(1,2001)
C ==========================================================
2001  FORMAT(///'RESUME OF RESULTS ?')
C ==========================================================
      READ(1,*)IJK9
      IF(IJK9 .EQ. 0) GO TO 2002
      WRITE(1,200)RKG
200   FORMAT(///'1/2 POINT ANGLE',F7.2)
      WRITE(1,205)VG
205   FORMAT('GRINDING SET ANGLE  VG',F7.2)
      WRITE(1,8042)RELIEF(1)
8042  FORMAT('RELIEF  ANGLE    ',F12.3)
      ZZZCL=ZCLEEE-ZSTGD(1)
      WRITE(1,8070)ZZZCL
8070  FORMAT('CLEARANCE         ',F12.3,'MM')
      WRITE(1,210)R0
210   FORMAT('DRILL RADIUS',F7.2)
      WRITE(1,212)ROG
212   FORMAT('1/2  CAM  RADIUS ',F7.2)
      WRITE(1,215)RPM
215   FORMAT(/'REVS PER MINUTE       ',F8.1)
      WRITE(1,220)RPI
220   FORMAT('REVS PER INCH FEED',F10.0)
      WRITE(1,8044)THRCH(NPOINT-1)
8044  FORMAT(/'THRUST  (CHISEL)     ',F10.3)
      WRITE(1,8046)THRUS(NPOINT)
8046  FORMAT('THRUST  (LIPS  )     ',F10.3)
      THTOT=THRCH(NPOINT-1)+THRUS(NPOINT)
      WRITE(1,8048)THTOT
8048  FORMAT('THRUST  (TOTAL )     ',F10.3,' LB')
      THNOVO=THRCH(NPOINT-1)+THRUQ
      WRITE(1,8049)THNOVO
8049  FORMAT('THRUST NOVO (TOTAL) ',F10.3,' LB')
      WRITE(1,1955)THHEE
1955  FORMAT('THHEE= ',F10.3)
      WRITE(1,8054)TORCH(NPOINT-1)
8054  FORMAT('TORQUE  (CHISEL)     ',F10.3)
      WRITE(1,8056)TORQU(NPOINT)
8056  FORMAT('TORQUE  (LIPS  )     ',F10.3)
      TOTOT=TORCH(NPOINT-1)+TORQU(NPOINT)
      WRITE(1,8058)TOTOT
8058  FORMAT('TORQUE  (TOTAL )     ',F10.3,' LB*IN')
      TONTOT=TORCH(NPOINT-1)+TRUQUE
      WRITE(1,8050)TONTOT
8050  FORMAT('TORQUE NOVO (TOTAL) ',F10.3,' LB*IN')
      WRITE(1,1956)TOOEE
1956  FORMAT('TOOEE= ',F10.3)
      WRITE(1,221)WEB
221   FORMAT('ESPESSURA  WEB ',F10.4)
```

```
      WRITE(1,8022)XSTG(1),YSTG(1),ZSTG(1)
8022  FORMAT(/'XOUTE=',F6.3,'  YOUTE=',F6.3,'  ZOUTE=',F6.3)
      WRITE(1,8020)(CORN(I),I=1,3)
8020  FORMAT('XCORN=',F6.3,'  YCORN=',F6.3,'  ZCORN=',F6.3)
      WRITE(1,8028)ZCHI0
8028  FORMAT('Z VALUE AT  X=0./Y=0.              ',F6.3)
      ZOUCOR=ZSTG(1)-ZCORN
      WRITE(1,8040)ZOUCOR
8040  FORMAT('DIFFERENCE  ZOUTE-ZCORN       ',F6.3)
      ZOUCHI=ZSTG(1)-ZCHI0
      WRITE(1,8032)ZOUCHI
8032  FORMAT('DIFFERENCE  ZOUTE-ZCHI0       ',F6.3)
      ARESTA=DSQRT((XSTGD(1)-XCORN)**2+(YSTGD(1)-YCORN)**2+
     $(ZSTGD(1)-ZCORN)**2)
      ANPTMA=(ZSTGD(1)-ZCORN)/ARESTA
      ANPTME=DSQRT(1.-ANPTMA**2)
      ANPTM=DATAN(ANPTME/ANPTMA)/CONS*2.
      WRITE(1,8033)ANPTM
8033  FORMAT('POINT ANGLE (AVERAGE)                  ',F10.3)
      COCHCO=(-XCHI2(2)-XCORN)*(XSTGD(NPOINT-1)-XCORN)
     $+(-YCHI2(2)-YCORN)*(YSTGD(NPOINT-1)-YCORN)
      RICHCO=DSQRT((-XCHI2(2)-XCORN)**2+(-YCHI2(2)-YCORN)**2)
      RECHCO=DSQRT((XSTGD(NPOINT-1)-XCORN)**2+(YSTGD(NPOINT-1)
     $-YCORN)**2)
      COCHCO=COCHCO/RICHCO/RECHCO
      SICHCO=DSQRT(1.-COCHCO**2)
      AICHCO=DATAN(SICHCO/COCHCO)/CONS+180.
      WRITE(1,8034)AICHCO
8034  FORMAT(/'CHISEL ANGLE AT CORNER              ',F12.2)
      DOCHCO=XCORN*(XSTGD(1)-XCORN)+YCORN*(YSTGD(1)-YCORN)
      FICHCO=DSQRT(XCORN**2+YCORN**2)
      FECHCO=DSQRT((XSTGD(1)-XCORN)**2+(YSTGD(1)-YCORN)**2)
      DOCHCO=DOCHCO/FICHCO/FECHCO
      EOCHCO=DSQRT(1.-DOCHCO**2)
      BICHCO=-DATAN(EOCHCO/DOCHCO)/CONS+180.
C
      WRITE(1,8036)BICHCO
8036  FORMAT('CHISEL ANGLE CHISEL-C/OUTER-C       ',F12.2)
      FOCHCO=XCORN*1.
      FOCHCO=FOCHCO/FICHCO/1.
      GOCHCO=DSQRT(1.-FOCHCO**2)
      FOCHCO=180.-DATAN(GOCHCO/FOCHCO)/CONS
      WRITE(1,8038)FOCHCO
8038  FORMAT('ANGLE BET. CHISEL EDGE AND  XX AXIS',F12.2)
      WRITE(1,8024)CHILEN
8024  FORMAT('CHISEL EDGE LENGTH  ',F6.3)
      WRITE(1,8080)SS
8080  FORMAT('LIP LENGTH    ',F12.3)
2002  CONTINUE
C
      IF(IHILST .EQ. 1)GO TO 7014
      IF(S .EQ. 1.) GO TO 7012
      NSTFLU=40
      DO 7013 J=1,NSTFLU
      RSTFL(J)=WEB/2.+FLOAT(J-1)/FLOAT(NSTFLU-1)*WEB
      W2R=WEB/2./RSTFL(J)
      IF(RSTFL(J) .LE. WEB/2.)GO TO 7020
      PHSTFL(J)=DATAN(W2R/DSQRT(1.-W2R**2))+DSQRT(RSTFL(J)
     $**2-(WEB/2.)**2)*DSIN(H0)/DCOS(H0)/R0*CSKOU/SNKOU
      GO TO 7021
7020  PHSTFL(J)=PI/2.
7021  XHSTFL(J)=RSTFL(J)*DCOS(PHSTFL(J))
      YHSTFL(J)=RSTFL(J)*DSIN(PHSTFL(J))
7013  CONTINUE
      READ(1,*)NSTFLI
      CALL E02ACF(XHSTFL,YHSTFL,NSTFLU,COFL,NSTFLI,REFL)
7012  DO 7000 I=1,NPOINT
      Z=ZCLEEE-FLOAT(I-1)*(ZCLEEE-ZCORN)/FLOAT(NPOINT-1)
      ALPHA=Z/R0*DSIN(H0)/DCOS(H0)
      III=I
      IF(I .NE. 1) GO TO 14
      RHEEL1=-3.
      RHEEL2=R0
14    CALL C05ACF(RHEEL1,RHEEL2,EPS1,EPV1,FEEL,XEEL,IFAIL)
      RHEEL1=XEEL-.8
      RHEEL2=XEEL+1.
      XHEELG(I)=XSTEEL
      YHEELG(I)=YSTEEL
      ZHEELG(I)=Z
      XHEELD(I)=XSTEEL
      YHEELD(I)=YSTEEL
      ZHEELD(I)=Z
      XEELG(I)=XEEL
      YEELG(I)=YEEL
      XEELGD(I)=XEEL
      YEELGD(I)=YEEL
7000  CONTINUE
      GO TO 7022
7014  DO 7016 I=1,NPOINT
      III=I
      Z=ZCLEEE-FLOAT(I-1)*(ZCLEEE-ZCORN)/FLOAT(NPOINT-1)
      ALPHA=Z/R0*DSIN(H0)/DCOS(H0)
      IF(I .NE. 1) GO TO 7017
      RHEEL1=.8*R0
      RHEEL2=1.1*R0
7017  CALL C05ACF(RHEEL1,RHEEL2,EPS1,EPV1,FIIL,RHEEL,IFAIL)
      RHEEL1=.8*RHEEL
      RHEEL2=1.2*RHEEL
      IF(RHEEL1 .LT. WEB/2.)RHEEL1=WEB/2.
      XHEELG(I)=XSTEEL
      YHEELG(I)=YSTEEL
      ZHEELG(I)=Z
      XHEELD(I)=XSTEEL
      YHEELD(I)=YSTEEL
      ZHEELD(I)=Z
      XEELG(I)=XEELA
      YEELG(I)=YEELA
      XEELGD(I)=XEELA
```

```
      YEELGD(I)=YEELA
7Ø16  CONTINUE
7Ø22  CONTINUE
      WRITE(1,6ØØ1)
6ØØ1  FORMAT('HEEL DRILL POINT CONTOUR COMPUTED')
      WRITE(1,9ØØ2)
9ØØ2  FORMAT('PLOTS (2)  OR  TABLES (1) ?')
      READ(1,*)NGRAFI
      IF(NGRAFI .EQ. 2) GO TO 9ØØ5
      WRITE(1,1985)
1985  FORMAT('ANGLES ACROSS LIP ?')
      READ(1,*)IJK1
      IF(IJK1 .EQ. Ø) GO TO 1986
C
      WRITE(1,9Ø)
9Ø    FORMAT(///5X,'RADI',3X,'RAKE',3X,'RAGE',3X,'CLEA',3X,
     $'RLIF',3X,'WEDG',3X,' INC',3X,'ETAS',3X,'RSNI'///)
      WRITE(1,95)(RADI(I),RAKE(I),RAGE(I),CLEAR(I),RELIEF(I)
     $,WEDGE(I),AINC(I),ETAS(I),RSNI(I),I=1,NLUP,NSALTO)
95    FORMAT(2X,9F7.2)
C
1986  WRITE(1,1987)
1987  FORMAT('LIP AND FLUTE ?')
      READ(1,*)IJK2
      IF(IJK2 .EQ. Ø) GO TO 2987
C
      WRITE(1,92)
92    FORMAT(////5X,'RADI',3X,'  X ',3X,'  Y ',3X,'  Z ',3X,
     $'DERI',3X,'XFLU',3X,'YFLU',3X,'CCE3'///)
      WRITE(1,94)(RADI(I),XSTG(I),YSTG(I),ZSTG(I),DERIV(I)
     $,XFLU(I),YFLU(I),CCE3P(I),I=1,NLUP,NSALTO)
94    FORMAT(2X,8F7.2)
C
2987  WRITE(1,2988)
2988  FORMAT('ARC  AND  MACHINED  SURFACE ?')
      READ(1,*)IJK3
      IF(IJK3 .EQ. Ø) GO TO 1989
C
      WRITE(1,93)
93    FORMAT(//////5X,'RADI',3X,' SS ',3X,'XNSU',3X,'YNSU',
     $3X,'ZNSU',3X,'DNSU'//)
      WRITE(1,97)(RADI(I),SSS(I),XMSU(I),YMSU(I),ZMSU(I),
     $DFNSU(I),I=1,NLUP,NSALTO)
97    FORMAT(2X,6F7.2)
C
1989  WRITE(1,199Ø)
199Ø  FORMAT('CHISEL EDGE ?')
      READ(1,*)IJK4
      IF(IJK4 .EQ. Ø) GO TO 1991
C
      WRITE(1,51Ø)
51Ø   FORMAT(//////5X,'XCHI',3X,'YCHI',3X,'ZCHI',4X,'RAKC',
     $3X,'CRAK',3X,'CHIS',4X,'TORQ',4X,'THRU'///)
      WRITE(1,515)(XCHIG(I),YCHIG(I),ZCHIG(I),RAKCHI(I),
```

```
     $CHIRAK(I),CHIXA(I),TORCH(I),THRCH(I),I=1,NPOINT,NSALTO)
515   FORMAT(2X,3F7.2,1X,2F7.2,1X,F7.2,2F8.1)
C
1991  WRITE(1,1992)
1992  FORMAT('DERIVATIVES AND  FORCES ?')
      READ(1,*)IJK5
      IF(IJK5 .EQ. Ø) GO TO 1993
C
      WRITE(1,96)
96    FORMAT(/////,5X,'RADI', 3X,'DIDL',3X,'RADL',3X,'HELI',
     $3X,'HEN',4X,'TORQ',4X,'THRU'/////)
      WRITE(1,52Ø)(RADI(I),DIDL(I),DRADL(I),ZTGHG(I),
     $ETAARM(I),TORQU(I),THRUS(I),I=1,NLUP,NSALTO)
52Ø   FORMAT(2X,5F7.2,2F8.1)
1993  WRITE(1,1994)
1994  FORMAT('SECONDARY CLEARANCE ?')
      READ(1,*)IJK6
      IF(IJK6 .EQ. Ø) GO TO 1995
      WRITE(1,1Ø1Ø)
1Ø1Ø  FORMAT(///,5X,'XCLE',3X,'YCLE',3X,'ZCLE',3X,'PHCL'//)
      WRITE(1,1Ø15)(XCLEA(I),YCLEA(I),ZCLEA(I),PHICLE(I),
     $I=1,NPOINT,NSALTO)
1Ø15  FORMAT(2X,4F7.2)
1995  WRITE(1,1996)
1996  FORMAT('THICKNESS' ?)
      READ(1,*)IJK7
      IF(IJK7 .EQ. Ø) GO TO 9ØØ5
      WRITE(1,1Ø12)
1Ø12  FORMAT(//////5X,'RADI', 3X,'T1WI',3X,'T1ME',3X,'T1MA')
      WRITE(1,1Ø16)(RADI(I),T1WI(I),T1MEU(I),T1MAU(I),
     $I=1,NLUP,NSALTO)
1Ø16  FORMAT(2X,4F7.4)
C FORCES PLOTTING
9ØØ5  WRITE(1,9Ø3Ø)
9Ø3Ø  FORMAT('PLOTTING FORCES DFP,DFP,DFR ?')
      READ(1,*)IFORC
      IF(IFORC .EQ. Ø) GO TO 9Ø33
      WRITE(1,2628)
2628  FORMAT(/'DEVICE - TEK(1),C1Ø(2)')
      READ(1,*)IDEV
      IRØ=IFIX(RØ+1.)
      RØØ=FLOAT(IRØ)
      YFLOW=-2.
      YFHIGH=15.
      NFY=IFIX(YFHIGH)-IFIX(YFLOW)
      YAXIS=12Ø.
      GO TO(2629,263Ø),IDEV
2629  CALL T4Ø1Ø
      XAXIS=16Ø.
      XØPOS=3Ø.
      YØPOSY=3Ø.
      YØPOSX=YØPOSY+YFLOW*YAXIS/FLOAT(NFY)
      GO TO 2631
263Ø  CALL C1Ø51N
```

```
      XAXIS=180.
      X0POS=50.
      Y0POSY=40.
      Y0POSX=Y0POSY+YFLOW*YAXIS/FLOAT(NFY)
      CALL DEVPAP(297.,210.,0)
2631  CALL PICCLE
      CALL WINDOW(2)
      CALL AXIPOS(0,X0POS,Y0POSX,XAXIS,1)
      CALL AXIPOS(0,X0POS,Y0POSY,YAXIS,2)
      CALL AXISCA(2,IR0,0.,R00,1)
      CALL AXISCA(2,NFY,YFLOW,YFHIGH,2)
      CALL AXIDRA(2,1,1)
      CALL AXIDRA(-2,-1,2)
C
      NLOO=NPOINT
      CALL CHASIZ(2.,2.)
      CALL GRASYM(RADI,DFPR,NLOO,4,0)
      CALL GRASYM(RADI,DFQR,NLOO,5,0)
      CALL GRASYM(RADI,DFRR,NLOO,7,0)
      CALL CHAMOD
C
      READ(1,*)SEPARA
9033  WRITE(1,9031)
9031  FORMAT('PLOTTING FORCES DFTR,DFNR,DFTE ?')
      READ(1,*)IFORC
      IF(IFORC .EQ. 0) GO TO 932
      WRITE(1,2623)
2623  FORMAT(/'DEVICE - TEK(1) , C10(2)')
      READ(1,*)IDEV
      IR0=IFIX(R0+1.)
      R00=FLOAT(IR0)
      YFLOW=-2.
      YFHIGH=15.
      NFY=IFIX(YFHIGH)-IFIX(YFLOW)
      GO TO(2624,2625),IDEV
C
2624  CALL T4010
      XAXIS=160.
      YAXIS=120.
      X0POS=30.
      Y0POSY=30.
      Y0POSX=Y0POSY+YFLOW*YAXIS/FLOAT(NFY)
      GO TO 2626
2625  CALL C1051N
      XAXIS=180.
      YAXIS=120.
      X0POS=50.
      Y0POSY=40.
      Y0POSX=Y0POSY+YFLOW*YAXIS/FLOAT(NFY)
      CALL DEVPAP(297.,210.,0)
2626  CALL PICCLE
      CALL WINDOW(2)
      CALL AXIPOS(0,X0POS,Y0POSX,XAXIS,1)
      CALL AXIPOS(0,X0POS,Y0POSY,YAXIS,2)
      CALL AXISCA(2,IR0,0.,R00,1)
      CALL AXISCA(2,NFY,YFLOW,YFHIGH,2)
      CALL AXIDRA(2,1,1)
      CALL AXIDRA(-2,-1,2)
C
      NLOO=NPOINT-2
      CALL CHASIZ(2.,2.)
      CALL GRASYM(RADI,DFTR,NLOO,4,0)
      CALL GRASYM(RADI,DFNR,NLOO,5,0)
      CALL GRASYM(RADI,DFTE,NLOO,7,0)
      CALL GRASYM(RADI,DFNSU,NLOO,8,0)
      CALL CHAMOD
C
      READ(1,*)SEPARA
932   WRITE(1,1978)
1978  FORMAT(/'ANGLES PLOTTING ? '/)
      READ(1,*)IANG
      IF(IANG .EQ. 0) GO TO 2562
      WRITE(1,1988)
1988  FORMAT('RAK(1),RAG(2),REL(3),WED(4),INC(5),RAK AND'/
     $'RAG(6)'/'CLE(7),REL AND CLEA(8)')
      READ(1,*)IANG1
C
      CALL SE281
      CALL PICCLE
      CALL WINDOW(2)
      IF(IANG1 .EQ. 4) GO TO 2505
      CALL AXIPOS(0,20.,50.,180.,1)
      CALL AXIPOS(0,20.,50.,120.,2)
      GO TO 2506
2505  CALL AXIPOS(0,20.,20.,180.,1)
      CALL AXIPOS(0,20.,20.,120.,2)
2506  CALL AXISCA(2,10,0.,10.,1)
      IF(IANG1 .EQ. 4) GO TO 2503
      CALL AXISCA(1,8,-30.,50.,2)
      GO TO 2504
2503  CALL AXISCA(1,5,30.,80.,2)
2504  CALL AXIDRA(2,1,1)
      CALL AXIDRA(-2,-1,2)
      GO TO(1997,1998,1999,2000,2500,2502,2522,2523),IANG1
1997  CALL GRACUR(RADI,RAKE,NPOINT)
      CALL CHAMOD
      GO TO 2501
1998  CALL GRACUR(RADI,RAGE,NPOINT)
      CALL CHAMOD
      GO TO 2501
1999  CALL GRACUR(RADI,RELIEF,NPOINT)
      CALL CHAMOD
      GO TO 2501
2000  CALL GRACUR(RADI,WEDGE,NPOINT)
      CALL CHAMOD
      GO TO 2501
2500  CALL GRACUR(RADI,AINC,NPOINT)
      CALL CHAMOD
```

```
      GO TO 2501
2502  CALL GRACUR(RADI,RAKE,NPOINT)
      CALL GRACUR(RADI,RAGE,NPOINT)
      CALL CHAMOD
      GO TO 2501
2522  CALL GRACUR(RADI,CLEAR,NPOINT)
      CALL CHAMOD
      GO TO 2501
2523  CALL GRACUR(RADI,CLEAR,NPOINT)
      CALL GRACUR(RADI,RELIEF,NPOINT)
      CALL CHAMOD
2501  CONTINUE
C
      READ(1,*)SEPARA
      GO TO 932
C
2562  WRITE(1,2561)
2561  FORMAT(/'EFFECTIVE RAKE PLOTTING?')
      READ(1,*)IRK
      IF(IRK .EQ. 0)GO TO 1979
      WRITE(1,2563)
2563  FORMAT(/'RAKFS(1),RAKFL(2),RAKFA(3),RAKFB(4),RAKFK(5)'/
     $'RAKFS,RAKFL,RAKFA , RAKFB AND RAKFK(6)')
      READ(1,*)IRAKF
C
      CALL SE281
      CALL PICCLE
      CALL WINDOW(2)
      CALL AXIPOS(0,20.,50.,180.,1)
      CALL AXIPOS(0,20.,50.,120.,2)
      CALL AXISCA(2,10,0.,10.,1)
      CALL AXISCA(2,8,-30.,50.,2)
      CALL AXIDRA(2,1,1)
      CALL AXIDRA(-2,-1,2)
C
      DO 2564 I=1,NPOINT
      SRAK1=DSIN(AINC(I)*CONS)**2+DCOS(AINC(I)*CONS)**2*
     $DSIN(RAKE(I)*CONS)
      RAKFS(I)=DATAN(SRAK1/DSQRT(1.-SRAK1**2))/CONS
      SRAK2=DSIN(AINC(I)*CONS)*DSIN(ETALEE(I)*CONS)+DCOS
     $(AINC(I)*CONS)*DCOS(ETALEE(I)*CONS)*DSIN(RAKE(I)*CONS)
      RAKFL(I)=DATAN(SRAK2/DSQRT(1.-SRAK2**2))/CONS
      SRAK3=DSIN(AINC(I)*CONS)*DSIN(ETAARM(I)*CONS)+DCOS
     $(AINC(I)*CONS)*DCOS(ETAARM(I)*CONS)*DSIN(RAKE(I)*CONS)
      RAKFA(I)=DATAN(SRAK3/DSQRT(1.-SRAK3**2))/CONS
      SRAK4=DSIN(AINC(I)*CONS)*DSIN(ETABRO(I)*CONS)+DCOS
     $(AINC(I)*CONS)*DCOS(ETABRO(I)*CONS)*DSIN(RAKE(I)*CONS)
      RAKFB(I)=DATAN(SRAK4/DSQRT(1.-SRAK4**2))/CONS
      SRAK5=DSIN(AINC(I)*CONS)*DSIN(ETAKRO(I)*CONS)+DCOS
     $(AINC(I)*CONS)*DCOS(ETAKRO(I)*CONS)*DSIN(RAKE(I)*CONS)
      RAKFK(I)=DATAN(SRAK5/DSQRT(1.-SRAK5**2))/CONS
2564  CONTINUE
      GO TO (2565,2566,2567,2568,2569,2573),IRAKF
2565  CALL GRACUR(RADI,RAKFS,NPOINT)
      CALL CHAMOD
      GO TO 2570
2566  CALL GRACUR(RADI,RAKFL,NPOINT)
      CALL CHAMOD
      GO TO 2570
2567  CALL GRACUR(RADI,RAKFA,NPOINT)
      CALL CHAMOD
      GO TO 2570
2568  CALL GRACUR(RADI,RAKFB,NPOINT)
      CALL CHAMOD
      GO TO 2570
2569  CALL GRACUR(RADI,RAKFK,NPOINT)
      CALL CHAMOD
      GO TO 2570
2573  CALL GRACUR(RADI,RAKFS,NPOINT)
      CALL GRACUR(RADI,RAKFL,NPOINT)
      CALL GRACUR(RADI,RAKFA,NPOINT)
      CALL GRACUR(RADI,RAKFB,NPOINT)
      CALL GRACUR(RADI,RAKFK,NPOINT)
      CALL CHAMOD
2570  CONTINUE
      READ(1,*)SEPARA
      WRITE(1,2571)
2571  FORMAT(/'MORE EF. RAKE PLOTS ?')
      READ(1,*)IGR
      IF(IGR .NE. 0) GO TO 2562
1979  WRITE(1,2525)
2525  FORMAT('CHIP FLOW ANGLE AGAINST INCLINATION ANGLE ?')
      READ(1,*)ICHFL
      IF(ICHFL .EQ. 0) GO TO 2524
2526  WRITE(1,2527)
2527  FORMAT(/'LEE(1),ARM(2),BRO(3),KRO(4),LEE,ARM,BRO AND'/
     $' KRO(5)')
      READ(1,*)IFLOW
C
      CALL T4010
      CALL PICCLE
      CALL WINDOW(2)
      CALL AXIPOS(0,20.,20.,150.,1)
      CALL AXIPOS(0,20.,20.,120.,2)
      CALL AXISCA(2,6,0.,60.,1)
      CALL AXISCA(2,9,0.,90.,2)
      CALL AXIDRA(2,1,1)
      CALL AXIDRA(-2,-1,2)
C
      GO TO(2528,2529,2530,2533, 2572),IFLOW
2528  CALL GRACUR(AINC,ETALEE,NPOINT)
      GO TO 2531
2529  CALL GRACUR(AINC,ETAARM,NPOINT)
      GO TO 2531
2530  CALL GRACUR(AINC,ETABRO,NPOINT)
      GO TO 2531
2533  CALL GRACUR(AINC,ETAKRO,NPOINT)
      GO TO 2531
```

```
2572  CALL GRACUR(AINC,ETALEE,NPOINT)
      CALL GRACUR(AINC,ETAARM,NPOINT)
      CALL GRACUR(AINC,ETABRO,NPOINT)
      CALL GRACUR(AINC,ETAKRO,NPOINT)
2531  CONTINUE
      CALL GRAMOV(Ø.,Ø.)
      CALL BROKEN(1)
      CALL GRALIN(AINC(NPOINT),AINC(NPOINT))
      CALL CHAMOD
C
      READ(1,*)SEPARA
      WRITE(1,2532)
2532  FORMAT('MORE CHIP FLOW PLOTS ?')
      READ(1,*)IGFL
      IF(IGFL .NE. Ø)GO TO 1979
2524  WRITE(1,933)
933   FORMAT('TOP VIEW OF THE SIMULATED DRILL POINT ?')
      READ(1,*)IPONTA
      IF(IPONTA .EQ. Ø) GO TO 1942
      WRITE(1,1959)
1959  FORMAT(/'READ FACTOR TO COORDINATE AXES')
      READ(1,*)FACT
      XAXIS=FACT*157.89
      YAXIS=FACT*127.53
      WRITE(1,197Ø)
197Ø  FORMAT(/'T4Ø1Ø (1)  OR C1Ø51N (2) ?'/)
      READ(1,*)IDEV
      WRITE(1,25Ø7)
25Ø7  FORMAT('DRAWING  AXES ?')
      READ(1,*)IAX
      IF(IDEV .EQ. 1) GO TO 1971
      XAXIS=FACT*16Ø.
      YAXIS=FACT*12Ø.
      CALL C1Ø51N
      GO TO 1976
1971  CALL T4Ø1Ø
1976  CALL PICCLE
      CALL WINDOW(2)
      CALL AXIPOS(Ø,8Ø.,8Ø.,XAXIS,1)
      CALL AXIPOS(Ø,8Ø.,8Ø.,YAXIS,2)
      CALL AXISCA(2,2Ø,-1Ø.,1Ø.,1)
      CALL AXISCA(2,15,-8.,7.,2)
      IF(IAX .EQ. Ø) GO TO 25Ø8
      CALL AXIDRA(2,1,1)
      CALL AXIDRA(-2,-1,2)
25Ø8  CONTINUE
C
      DO 937 I=1,NPOINT
      XMAX=RØ
      YMAX=RØ
      X1(I)=-(RØ-1.)+FLOAT(I)/FLOAT(NPOINT)*2.*(XMAX-1.)
      Y1(I)=DSQRT(RØ**2-X1(I)**2)
      Y1N(I)=-Y1(I)
      Y1A(I)=-(RØ-1.)+FLOAT(I)/FLOAT(NPOINT)*2.*(YMAX-1.)
      X1A(I)=DSQRT(RØ**2-Y1A(I)**2)
      X1AN(I)=-X1A(I)
937   CONTINUE
      DO 1937 I=1,NPOINT
      XSTG(I)=XSTGD(I)
      YSTG(I)=YSTGD(I)
      XCHIG(I)=XCHID(I)
      YCHIG(I)=YCHID(I)
      XHEELG(I)=XHEELD(I)
      YHEELG(I)=YHEELD(I)
      XSTG(I)=-XSTG(I)
      XHEELG(I)=-XHEELG(I)
1937  CONTINUE
      DO 1938 J=1,NPOINT
      XCHIG(J)=-XCHIG(J)
1938  CONTINUE
      IF(IWFILE .EQ. Ø)GO TO 2657
C WRITE IN FILE
      WRITE(6,2655)RØ,WEB,HØ,RO,EXG,VG,RKG,ROG
2655  FORMAT(8F12.6)
      WRITE(6,2651)NPOINT
      WRITE(6,2652)(X1(I),Y1(I),Y1N(I),Y1A(I),X1A(I),X1AN(I)
     $,XSTG(I),I=1,NPOINT)
      WRITE(6,262Ø)(YSTG(I),XCHIG(I),YCHIG(I),XHEELG(I)
     $,YHEELG(I),I=1,NPOINT)
2651  FORMAT(I4)
2652  FORMAT(7F12.6)
262Ø  FORMAT(5F12.6)
2657  CONTINUE
      DO 2559 IG=1,IL
      CALL GRACUR(XSTG,YSTG,NPOINT)
      CALL GRACUR(XCHIG,YCHIG,NPOINT)
      CALL CHAMOD
      DO 1935 I=1,NPOINT
      XSTG(I)=-XSTG(I)
      YSTG(I)=-YSTG(I)
1935  CONTINUE
      DO 1936 I=1,NPOINT
      XCHIG(I)=-XCHIG(I)
      YCHIG(I)=-YCHIG(I)
1936  CONTINUE
      IF(IWFILE .EQ. Ø)GO TO 2658
      WRITE(6,2653)(XCHIG(I),YCHIG(I),XSTG(I),YSTG(I),
     $I=1,NPOINT)
2658  CONTINUE
C
      CALL GRACUR(XSTG,YSTG,NPOINT)
      CALL GRACUR(XCHIG,YCHIG,NPOINT)
      CALL GRACUR(XHEELG,YHEELG,NPOINT)
      CALL CHAMOD
      DO 7ØØ2 I=1,NPOINT
      XHEELG(I)=-XHEELG(I)
      YHEELG(I)=-YHEELG(I)
7ØØ2  CONTINUE
```

```
      IF(IWFILE .EQ. 0)GO TO 2659
      WRITE(6,2654)(XHEELG(I),YHEELG(I),I=1,NPOINT)
2653  FORMAT(4F12.6)
2654  FORMAT(2F12.6)
2659  CONTINUE
C
      CALL GRACUR(XHEELG,YHEELG,NPOINT)
      CALL GRACUR(X1,Y1,NPOINT)
      CALL GRACUR(X1,Y1N,NPOINT)
      CALL GRACUR(X1A,Y1A,NPOINT)
      CALL GRACUR(X1AN,Y1A,NPOINT)
      CALL CHAMOD
2559  CONTINUE
C
      READ(1,*)SEPARA
      WRITE(1,2518)
2518  FORMAT(/'MORE  VIEWS ?'/)
      READ(1,*)IVIEW
      IF(IVIEW .NE. 0) GO TO 2524
C
1942  WRITE(1,1941)
1941  FORMAT('SIDE VIEW OF THE SIMULATED DRILL POINT ?')
      READ(1,*)IPLADO
      IF(IPLADO .EQ. 0)GO TO 1948
      WRITE(1,2509)
2509  FORMAT('DRAWING  AXES ?')
      READ(1,*)IAX
      WRITE(1,2543)
2543  FORMAT(/'T4010 (1)  OR  C1051N (2) ?')
      READ(1,*)IDEV
      WRITE(1,2515)
2515  FORMAT(/'READ FACTOR TO COORDINATE AXES')
      READ(1,*)FACT
      GO TO(2541,2542),IDEV
2541  XAXIS=FACT*157.89
      YAXIS=FACT*127.53
      CALL T4010
      GO TO 2544
2542  XAXIS=FACT*160.
      YAXIS=FACT*120.
      CALL C1051N
2544  CALL PICCLE
      CALL WINDOW(2)
      CALL AXIPOS(0,90.,20.,XAXIS,1)
      CALL AXIPOS(0,90.,20.,YAXIS,2)
      CALL AXISCA(2,20,-10.,10.,1)
      CALL AXISCA(2,15,-3.,12.,2)
      IF(IAX .EQ. 0) GO TO 2510
      CALL AXIDRA(2,1,1)
      CALL AXIDRA(-2,-1,2)
2510  CONTINUE
C
      ZLIM2=ZCLEA(1)+.5*R0
      DO 2040 I=1,NPOINT
      XSTG(I)=XSTGD(I)
      YSTG(I)=YSTGD(I)
      XHEELG(I)=XHEELD(I)
      YHEELG(I)=YHEELD(I)
      XCLEA(I)=XCLEAD(I)
      XCHIG(I)=XCHID(I)
      ZELIC=ZSTG(1)+FLOAT(I-1)/FLOAT(NPOINT-1)*(ZLIM2-ZSTG(1))
      ZELIC1(I)=ZELIC
      ZELI=ZELIC-ZSTG(1)
      PHLI1=DATAN(YSTG(1)/XSTG(1))
      PHLI=PHLI1+ZELI*DSIN(H0)/DCOS(H0)/R0
      XELIC1(I)=R0*DCOS(PHLI)
      YELIC1(I)=R0*DSIN(PHLI)
2040  CONTINUE
C
      DO 2041 I=1,NPOINT
      ZELIC=ZHEELG(1)+FLOAT(I-1)/FLOAT(NPOINT-1)*(ZLIM2
     $-ZHEELG(1))
      ZELIC2(I)=ZELIC
      ZELI=ZELIC-ZHEELG(1)
      PHLI1=DATAN(YHEELG(1)/XHEELG(1))
      IF(PHLI1 .GE. .0)PHLI1=-(PI-PHLI1)
      PHLI=PHLI1+ZELI*DSIN(H0)/DCOS(H0)/R0
      XELIC2(I)=R0*DCOS(PHLI)
      YELIC2(I)=R0*DSIN(PHLI)
2041  CONTINUE
C
      CALL GRACUR(XSTG,ZSTG,NPOINT)
      CALL GRACUR(XCHIG,ZCHIG,NPOINT)
      CALL GRACUR(XELIC1,ZELIC1,NPOINT)
      CALL CHAMOD
      DO 1945 I=1,NPOINT
      XSTG(I)=-XSTG(I)
      XCLEA(I)=-XCLEA(I)
      XHEELG(I)=-XHEELG(I)
      XELIC1(I)=-XELIC1(I)
1945  CONTINUE
      DO 1946 J=1,NPOINT
      XCHIG(J)=-XCHIG(J)
1946  CONTINUE
      CALL GRACUR(XSTG,ZSTG,NPOINT)
      CALL GRACUR(XCHIG,ZCHIG,NPOINT)
      CALL GRACUR(XCLEA,ZCLEA,NPOINT)
      CALL GRACUR(XHEELG,ZHEELG,NPOINT)
      CALL GRACUR(XELIC1,ZELIC1,NPOINT)
      CALL GRACUR(XELIC2,ZELIC2,NPOINT)
      CALL CHAMOD
C
      READ(1,*)SEPARA
      WRITE(1,2519)
2519  FORMAT(/'MORE  VIEWS ?'/)
      READ(1,*)IVIEW
      IF(IVIEW .NE. 0) GO TO 1942
1948  WRITE(1,1947)
```

```
1947  FORMAT('SIDE VIEW AFTER 9Ø DEGREES ROTATION ? ')
      READ(1,*)IPLADØ
      IF(IPLADØ .EQ. Ø) GO TO 934
      WRITE(1,2511)
2511  FORMAT('DRAWING  AXES ?')
      READ(1,*)IAX
      WRITE(1,2545)
2545  FORMAT(/'T4Ø1Ø (1)  OR  C1Ø51N (2) ?')
      READ(1,*)IDEV
      WRITE(1,2516)
2516  FORMAT(/'READ FACTOR TO COORDINATE AXES')
      READ(1,*)FACT
      GO TO(2546,2547),IDEV
2546  XAXIS=FACT*157.89
      YAXIS=FACT*127.53
      CALL T4Ø1Ø
      GO TO 2548
2547  XAXIS=FACT*16Ø.
      YAXIS=FACT*12Ø.
      CALL C1Ø51N
2548  CALL PICCLE
      CALL WINDOW(2)
      CALL AXIPOS(Ø,9Ø.,2Ø.,XAXIS,1)
      CALL AXIPOS(Ø,9Ø.,2Ø.,YAXIS,2)
      CALL AXISCA(2,2Ø,-1Ø.,1Ø.,1)
      CALL AXISCA(2,15,-3.,12.,2)
      IF(IAX .EQ. Ø) GO TO 2512
      CALL AXIDRA(2,1,1)
      CALL AXIDRA(-2,-1,2)
2512  CONTINUE
C
      DO 1977 I=1,NPOINT
      YSTG(I)=YSTGD(I)
      YCHIG(I)=YCHID(I)
      YHEELG(I)=YHEELD(I)
1977  CONTINUE
      CALL GRACUR(YCHIG,ZCHIG,NPOINT)
      CALL CHAMOD
      DO 195Ø I=1,NPOINT
      YCHIG(I)=-YCHIG(I)
195Ø  CONTINUE
      CALL GRACUR(YCHIG,ZCHIG,NPOINT)
      CALL CHAMOD
      IF(YSTG(NPOINT) .LT. Ø.) GO TO 1953
      DO 1954 I=1,NPOINT
      YSTG(I)=-YSTG(I)
1954  CONTINUE
1953  CONTINUE
      CALL GRACUR(YSTG,ZSTG,NPOINT)
      CALL GRACUR(YHEELG,ZHEELG,NPOINT)
      CALL GRACUR(YELIC1,ZELIC1,NPOINT)
      CALL GRACUR(YELIC2,ZELIC2,NPOINT)
      YELIC8=YELIC2(1)
      ZELIC8=ZELIC2(1)
```

```
      ZLIM8=ZLIM2
      CALL GRAMOV(YELIC8,ZELIC8)
      CALL GRALIN(YELIC8,ZLIM8)
      CALL CHAMOD
      DO 1951 I=1,NPOINT
      YHEELG(I)=-YHEELG(I)
      YELIC2(I)=-YELIC2(I)
1951  CONTINUE
      CALL GRACUR(YHEELG,ZHEELG,NPOINT)
      CALL GRACUR(YCLEA,ZCLEA,NPOINT)
      YELIC8=YELIC2(1)
      CALL GRAMOV(YELIC8,ZELIC8)
      CALL GRALIN(YELIC8,ZLIM8)
      CALL CHAMOD
C
      READ(1,*)SEPARA
      WRITE(1,252Ø)
252Ø  FORMAT(/'MORE  VIEWS ?'/)
      READ(1,*)IVIEW
      IF(IVIEW .NE. Ø) GO TO 1948
934   WRITE(1,2575)
2575  FORMAT(/'THREE SIMULTANEOUS VIEWS ?')
      READ(1,*)IPONTA
      IF(IPONTA .EQ. Ø) GO TO 2574
      WRITE(1,2576)
2576  FORMAT(/'READ FACTOR TO COORDINATE AXES')
      READ(1,*)FACT
      XAXIS=FACT*157.89
      YAXIS=FACT*127.53
C
      WRITE(1,2577)
2577  FORMAT(/'T4Ø1Ø (1)  OR C1Ø51N (2) ?'/)
      READ(1,*)IDEV
      WRITE(1,2578)
2578  FORMAT('DRAWING  AXES ?')
      READ(1,*)IAX
      IF(IDEV .EQ. 1) GO TO 2579
      XAXIS=FACT*16Ø.
      YAXIS=FACT*12Ø.
      CALL C1Ø51N
      GO TO 258Ø
2579  CALL T4Ø1Ø
258Ø  CALL PICCLE
      CALL WINDOW(2)
      CALL AXIPOS(Ø,5Ø.,4Ø.,XAXIS,1)
      CALL AXIPOS(Ø,5Ø.,4Ø.,YAXIS,2)
      CALL AXISCA(2,2Ø,-1Ø.,1Ø.,1)
      CALL AXISCA(2,15,-8.,7.,2)
      IF(IAX .EQ. Ø) GO TO 2581
      CALL AXIDRA(2,1,1)
      CALL AXIDRA(-2,-1,2)
2581  CONTINUE
      DO 2582 I=1,NPOINT
      XMAX=RØ
```

```
      YMAX=RØ
      X1(I)=-(RØ-1.)+FLOAT(I)/FLOAT(NPOINT)*2.*(XMAX-1.)
      Y1(I)=DSQRT(RØ**2-X1(I)**2)
      Y1N(I)=-Y1(I)
      Y1A(I)=-(RØ-1.)+FLOAT(I)/FLOAT(NPOINT)*2.*(YMAX-1.)
      X1A(I)=DSQRT(RØ**2-Y1A(I)**2)
      X1AN(I)=-X1A(I)
2582  CONTINUE
      DO 2583 I=1,NPOINT
      XSTG(I)=XSTGD(I)
      YSTG(I)=YSTGD(I)
      XCHIG(I)=XCHID(I)
      YCHIG(I)=YCHID(I)
      XHEELG(I)=XHEELD(I)
      YHEELG(I)=YHEELD(I)
      XSTG(I)=-XSTG(I)
      XHEELG(I)=-XHEELG(I)
2583  CONTINUE
      DO 2584 J=1,NPOINT
      XCHIG(J)=-XCHIG(J)
2584  CONTINUE
C
      CALL GRACUR(XSTG,YSTG,NPOINT)
      CALL GRACUR(XCHIG,YCHIG,NPOINT)
      CALL CHAMOD
C
      DO 2587 I=1,NPOINT
      XSTG(I)=-XSTG(I)
      YSTG(I)=-YSTG(I)
2587  CONTINUE
C
      DO 2588 I=1,NPOINT
      XCHIG(I)=-XCHIG(I)
      YCHIG(I)=-YCHIG(I)
2588  CONTINUE
C
      CALL GRACUR(XSTG,YSTG,NPOINT)
      CALL GRACUR(XCHIG,YCHIG,NPOINT)
      CALL GRACUR(XHEELG,YHEELG,NPOINT)
      CALL CHAMOD
C
      DO 2589 I=1,NPOINT
      XHEELG(I)=-XHEELG(I)
      YHEELG(I)=-YHEELG(I)
2589  CONTINUE
      CALL GRACUR(XHEELG,YHEELG,NPOINT)
      CALL GRACUR(X1,Y1,NPOINT)
      CALL GRACUR(X1,Y1N,NPOINT)
      CALL GRACUR(X1A,Y1A,NPOINT)
      CALL GRACUR(X1AN,Y1A,NPOINT)
      CALL CHAMOD
C
      CALL AXIPOS(Ø,5Ø.,9Ø.,XAXIS,1)
      CALL AXIPOS(Ø,5Ø.,9Ø.,YAXIS,2)
      CALL AXISCA(2,2Ø,-1Ø.,1Ø.,1)
      CALL AXISCA(2,15,-3.,12.,2)
      IF(IAX .EQ. Ø) GO TO 259Ø
      CALL AXIDRA(2,1,1)
      CALL AXIDRA(-2,-1,2)
259Ø  CONTINUE
C
      ZLIM2=ZCLEA(1)+.5*RØ
      DO 2591 I=1,NPOINT
      XSTG(I)=XSTGD(I)
      YSTG(I)=YSTGD(I)
      XHEELG(I)=XHEELD(I)
      YHEELG(I)=YHEELD(I)
      XCLEA(I)=XCLEAD(I)
      XCHIG(I)=XCHID(I)
      ZELIC=ZSTG(1)+FLOAT(I-1)/FLOAT(NPOINT-1)*(ZLIM2-
     $ZSTG(1))
      ZELIC1(I)=ZELIC
      ZELI=ZELIC-ZSTG(1)
      PHLI1=DATAN(YSTG(1)/XSTG(1))
      PHLI=PHLI1+ZELI*DSIN(HØ)/DCOS(HØ)/RØ
      XELIC1(I)=RØ*DCOS(PHLI)
      YELIC1(I)=RØ*DSIN(PHLI)
2591  CONTINUE
C
      DO 2592 I=1,NPOINT
      ZELIC=ZHEELG(1)+FLOAT(I-1)/FLOAT(NPOINT-1)*(ZLIM2-ZHEELG(1))
      ZELIC2(I)=ZELIC
      ZELI=ZELIC-ZHEELG(1)
      PHLI1=DATAN(YHEELG(1)/XHEELG(1))
      IF(PHLI1 .GE. .Ø)PHLI1=-(PI-PHLI1)
      PHLI=PHLI1+ZELI*DSIN(HØ)/DCOS(HØ)/RØ
      XELIC2(I)=RØ*DCOS(PHLI)
      YELIC2(I)=RØ*DSIN(PHLI)
2592  CONTINUE
C
      CALL GRACUR(XSTG,ZSTG,NPOINT)
      CALL GRACUR(XCHIG,ZCHIG,NPOINT)
      CALL GRACUR(XELIC1,ZELIC1,NPOINT)
      CALL CHAMOD
      DO 2593 I=1,NPOINT
      XSTG(I)=-XSTG(I)
      XCLEA(I)=-XCLEA(I)
      XHEELG(I)=-XHEELG(I)
      XELIC1(I)=-XELIC1(I)
2593  CONTINUE
C
      DO 2594 J=1,NPOINT
      XCHIG(J)=-XCHIG(J)
2594  CONTINUE
C
      CALL GRACUR(XSTG,ZSTG,NPOINT)
      CALL GRACUR(XCHIG,ZCHIG,NPOINT)
      CALL GRACUR(XCLEA,ZCLEA,NPOINT)
```

```
      CALL GRACUR(XHEELG,ZHEELG,NPOINT)
      CALL GRACUR(XELIC1,ZELIC1,NPOINT)
      CALL GRACUR(XELIC2,ZELIC2,NPOINT)
      CALL CHAMOD
C
      DO 2604 I=1,NPOINT
      XSTG(I)=-XSTG(I)
      XCLEA(I)=-XCLEA(I)
      XHEELG(I)=-XHEELG(I)
      XELIC1(I)=-XELIC1(I)
2604  CONTINUE
C
      CALL AXIPOS(0,130.,90.,XAXIS,1)
      CALL AXIPOS(0,130.,90.,YAXIS,2)
      CALL AXISCA(2,20,-10.,10.,1)
      CALL AXISCA(2,15,-3.,12.,2)
      IF(IAX .EQ. 0) GO TO 2595
      CALL AXIDRA(2,1,1)
      CALL AXIDRA(-2,-1,2)
2595  CONTINUE
C
      DO 2596 I=1,NPOINT
      YSTG(I)=YSTGD(I)
      YCHIG(I)=YCHID(I)
      YHEELG(I)=YHEELD(I)
2596  CONTINUE
      CALL GRACUR(YCHIG,ZCHIG,NPOINT)
      CALL CHAMOD
C
      DO 2597 I=1,NPOINT
      YCHIG(I)=-YCHIG(I)
2597  CONTINUE
      CALL GRACUR(YCHIG,ZCHIG,NPOINT)
      CALL CHAMOD
C
      IF(YSTG(NPOINT) .LT. 0.) GO TO 2598
      DO 2599 I=1,NPOINT
      YSTG(I)=-YSTG(I)
2599  CONTINUE
2598  CONTINUE
      CALL GRACUR(YSTG,ZSTG,NPOINT)
      CALL GRACUR(YHEELG,ZHEELG,NPOINT)
      CALL GRACUR(YELIC1,ZELIC1,NPOINT)
      CALL GRACUR(YELIC2,ZELIC2,NPOINT)
      YELIC8=YELIC2(1)
      ZELIC8=ZELIC2(1)
      ZLIM8=ZLIM2
      CALL GRAMOV(YELIC8,ZELIC8)
      CALL GRALIN(YELIC8,ZLIM8)
      CALL CHAMOD
C
      DO 2600 I=1,NPOINT
      YHEELG(I)=-YHEELG(I)
      YELIC2(I)=-YELIC2(I)
2600  CONTINUE
      CALL GRACUR(YHEELG,ZHEELG,NPOINT)
      CALL GRACUR(YCLEA,ZCLEA,NPOINT)
      YELIC8=YELIC2(1)
      CALL GRAMOV(YELIC8,ZELIC8)
      CALL GRALIN(YELIC8,ZLIM8)
      CALL CHAMOD
C
      READ(1,*)SEPARA
      WRITE(1,2601)
2601  FORMAT(/'MORE  VIEWS ?'/)
      READ(1,*)IVIEW
      IF(IVIEW .NE. 0) GO TO 934
2574  WRITE(1,938)
938   FORMAT('SECTION NORMAL TO DRILL AXIS ?')
      READ(1,*)IFLUT
      IF(IFLUT .EQ. 0) GO TO 939
      WRITE(1,2513)
2513  FORMAT('DRAWING  AXES ?')
      READ(1,*)IAX
      WRITE(1,2560)
2560  FORMAT(/'BROKEN LINES  ?')
      READ(1,*)IBRO
      WRITE(1,2549)
2549  FORMAT(/'T4010 (1)  OR  C1051N (2) ?')
      READ(1,*)IDEV
      WRITE(1,2517)
2517  FORMAT(/'READ FACTOR TO COORDINATE AXES')
      READ(1,*)FACT
      R0H=R0
      WEBH=WEB
      H0H=H0/CONS
      READ(1,*)X0POS,XCAP
      GO TO(2550,2551),IDEV
2550  XAXIS=FACT*157.89
      YAXIS=FACT*127.53
      CALL T4010
      GO TO 2552
2551  XAXIS=FACT*160.
      YAXIS=FACT*120.
      CALL C1051N
2552  CALL PICCLE
      CALL WINDOW(2)
      CALL AXIPOS(0,X0POS,80.,XAXIS,1)
      CALL AXIPOS(0,X0POS,80.,YAXIS,2)
      CALL AXISCA(2,20,-10.,10.,1)
      CALL AXISCA(2,15,-8.,7.,2)
      IF(IAX .EQ. 0) GO TO 2514
      CALL AXIDRA(2,1,1)
      CALL AXIDRA(-2,-1,2)
C
2514  CONTINUE
      DO 7006 I=1,NPOINT
      XFLU(I)=XFLUD(I)
```

```
      YEELG(I)=YEELGD(I)
      XFLU(I)=-XFLU(I)
      YEELG(I)=-YEELGD(I)
7ØØ6  CONTINUE
      CALL GRACUR(XFLU,YFLU,NPOINT)
      CALL BROKEN(IBRO)
      CALL GRACUR(XEELG,YEELG,NPOINT)
      CALL CHAMOD
C
      DO 7ØØ7 I=1,NPOINT
      XFLU(I)=-XFLU(I)
      YFLU(I)=-YFLU(I)
      XEELG(I)=-XEELG(I)
      YEELG(I)=-YEELG(I)
      IF(NORSEC .EQ. Ø)GO TO 7ØØ7
C WRITE IN FILE
      WRITE(6,2638)XFLU(I),YFLU(I),XEELG(I),YEELG(I)
7ØØ7  CONTINUE
      CALL BROKEN(Ø)
      CALL GRACUR(XFLU,YFLU,NPOINT)
      CALL BROKEN(IBRO)
      CALL GRACUR(XEELG,YEELG,NPOINT)
      CALL CHAMOD
      DO 7ØØ8 I=1,NPOINT
      Y1D=-YEELG(1)+FLOAT(I-1)/FLOAT(NLUP-1)*(YFLU(1)+YEELG(1))
      X1D=DSQRT(RØ**2-Y1D**2)
      Y1AD=-YFLU(1)+FLOAT(I-1)/FLOAT(NLUP-1)*(YEELG(1)+YFLU(1))
      X1AD=-DSQRT(RØ**2-Y1AD**2)
      Y1(I)=Y1D
      X1(I)=X1D
      Y1A(I)=Y1AD
      X1A(I)=X1AD
      IF(NORSEC .EQ. Ø)GO TO 7ØØ8
      WRITE(6,2638)Y1(I),X1(I),Y1A(I),X1A(I)
7ØØ8  CONTINUE
2638  FORMAT(4F1Ø.4)
      CALL CHAMOD
      CALL BROKEN(Ø)
      CALL GRACUR(X1,Y1,NPOINT)
      CALL GRACUR(X1A,Y1A,NPOINT)
      CALL CHAMOD
C
      READ(1,*)SEPARA
      WRITE(1,2521)
2521  FORMAT(/'MORE  VIEWS ?'/)
      READ(1,*)IVIEW
      IF(IVIEW .NE. Ø) GO TO 934
939   WRITE(1,7Ø4Ø)
7Ø4Ø  FORMAT(' CIRCLE INSIDE THE FLUTE ?')
      READ(1,*)IFLUT
      IF(IFLUT .EQ. Ø) GO TO 94Ø
      DO 7Ø41 I=1,NPOINT
      XFLU(I)=XFLUD(I)
      YFLU(I)=YFLUD(I)
      YEELG(I)=YEELGD(I)
      YEELG(I)=-YEELG(I)
7Ø41  CONTINUE
7Ø28  CONTINUE
      WRITE(1,7Ø26)
7Ø26  FORMAT(/'READ RCØ,XCØ AND YCØ'/)
      READ(1,*)RCØ,XCØ,YCØ
      CALL SE281
C     CALL C1Ø51N
      CALL PICCLE
      CALL WINDOW(2)
      CALL AXIPOS(Ø,9Ø.,8Ø.,157.89,1)
      CALL AXIPOS(Ø,9Ø.,8Ø.,127.53,2)
      CALL AXISCA(2,2Ø,-1Ø.,1Ø.,1)
      CALL AXISCA(2,15,-8.,7.,2)
      CALL AXIDRA(2,1,1)
      CALL AXIDRA(-2,-1,2)
C
      DO 7Ø31 I=1,NPOINT
      XMAX=RØ
      YMAX=RØ
      X1(I)=-(RØ-1.)+FLOAT(I)/FLOAT(NPOINT)*2.*(XMAX-1.)
      Y1(I)=DSQRT(RØ**2-X1(I)**2)
      Y1N(I)=-Y1(I)
      Y1A(I)=-(RØ-1.)+FLOAT(I)/FLOAT(NPOINT)*2.*(YMAX-1.)
      X1A(I)=DSQRT(RØ**2-Y1A(I)**2)
      X1AN(I)=-X1A(I)
7Ø31  CONTINUE
C
      CALL GRACUR(XFLU,YFLU,NPOINT)
      CALL GRACUR(XEELG,YEELG,NPOINT)
      CALL GRACUR(X1,Y1,NPOINT)
      CALL GRACUR(X1,Y1N,NPOINT)
      CALL GRACUR(X1A,Y1A,NPOINT)
      CALL GRACUR(X1AN,Y1A,NPOINT)
      CALL CHAMOD
C
7Ø44  YMIN=YCØ-RCØ
      YMAX=YCØ+RCØ
      XMIN=XCØ-RCØ
      XMAX=XCØ+RCØ
      DO 7Ø32 I=1,NPOINT
      Y1D=YMIN+.2+FLOAT(I-1)/FLOAT(NPOINT-1)*(2.*RCØ-.4)
      X1D=XCØ+DSQRT(RCØ**2-(Y1D-YCØ)**2)
      X1AD=XMIN+.2+FLOAT(I-1)/FLOAT(NPOINT-1)*(2.*RCØ-.4)
      Y1AD=YCØ+DSQRT(RCØ**2-(X1AD-XCØ)**2)
      Y1(I)=Y1D
      X1(I)=X1D
      Y1A(I)=Y1AD
      X1A(I)=X1AD
7Ø32  CONTINUE
      CALL GRACUR(X1,Y1,NPOINT)
      CALL GRACUR(X1A,Y1A,NPOINT)
      CALL CHAMOD
```

```
C
      DO 7030  I=1,NPOINT
      X1(I)=2.*XC0-X1(I)
      Y1A(I)=2.*YC0-Y1A(I)
7030  CONTINUE
      CALL GRACUR(X1,Y1,NPOINT)
      CALL GRACUR(X1A,Y1A,NPOINT)
      CALL CHAMOD
C
      READ(1,*)SEPARA
      IF(IFLUT .EQ. 0) GO TO 7045
      WRITE(1,7024)
7024  FORMAT(/'CIRCLE  AGAIN ?'/)
      READ(1,*)IFLUT
      IF(IFLUT .EQ. 1) GO TO 7028
      ALPHA=ZOUT/R0*DSIN(H0)/DCOS(H0)
      PHC0=DATAN(YC0/XC0)
      PHC=PHC0+ALPHA
      RXYC0=DSQRT(XC0**2+YC0**2)
C COORDINATES OF THE CENTER OF THE CIRCLE
      ZEM=ZOUT
      XEM=RXYC0*DCOS(PHC)
      YEM=RXYC0*DSIN(PHC)
      XC0=XEM
      YC0=YEM
      GO TO 7044
7045  WRITE(1,7042)XEM,YEM,ZEM
7042  FORMAT(/'XEM=',F8.4,3X,'YEM=',F8.4,3X,'ZEM=',F8.4/)
940   WRITE(1,1964)
1964  FORMAT('SECTIONS ACROSS THE FLUTE ?')
      READ(1,*)ISEC
      IF(ISEC .EQ. 0) GO TO 2011
1962  WRITE(1,1961)
1961  FORMAT('AT WHICH POINT IS THE SECTION WANTED ?')
      READ(1,*)NSEC
      XSE1=XSTGD(NSEC)
      YSE1=YSTGD(NSEC)
      ZSE1=ZSTGD(NSEC)
      PHSEC1=-50.*CONS
      PHSEC2=89.9*CONS
      WRITE(1,1973)
1973  FORMAT('SECTION NORMAL TO LINE CHISEL C-OUTER C LIP ?')
      READ(1,*)ILIP
      IF(ILIP .EQ. 0) GO TO 1975
      SCE4=XSTGD(1)-XCORN
      SCE5=YSTGD(1)-YCORN
      SCE6=ZSTGD(1)-ZCORN
      SCE0=DSQRT(SCE4**2+SCE5**2+SCE6**2)
      SCE1=SCE4/SCE0
      SCE2=SCE5/SCE0
      SCE3=SCE6/SCE0
      GO TO 1974
1975  WRITE(1,2535)
2535  FORMAT(/'SECTION NORMAL TO ACTUAL CUTTING EDGE ?')
      READ(1,*)INAL
      IF(INAL .EQ. 0) GO TO 2536
      SCE1=CCE1(NSEC)
      SCE2=CCE2(NSEC)
      SCE3=CCE3(NSEC)
      GO TO 1974
2536  WRITE(1,2557)
2557  FORMAT(/'SECTION NORMAL TO THE TANGENT TO HELIX ?')
      READ(1,*)IHE
      IF(IHE .EQ. 0)GO TO 2558
      PHH1=DATAN(YSTGD(1)/XSTGD(1))
      PHH2=PHH1-(PI-ANGCLE)/2.
      XHH2=R0*DCOS(PHH2)
      YHH2=R0*DSIN(PHH2)
      HRX=-YHH2
      HRY=XHH2
      XSE1=XHH2
      YSE1=YHH2
      ZSE1=ZSTGD(1)
      RRXY=DSQRT(HRX**2+HRY**2)
      HRX=HRX/RRXY
      HRY=HRY/RRXY
      SCE1=HRX
      SCE2=HRY
      SCE3=DCOS(H0)/DSIN(H0)
      SCE=DSQRT(SCE1**2+SCE2**2+SCE3**2)
      SCE1=SCE1/SCE
      SCE2=SCE2/SCE
      SCE3=SCE3/SCE
      GO TO 1974
C
2558  WRITE(1,2537)
2537  FORMAT(/'FOR OTHER SECTION READ COORDINATES'/
     $'TO 2 POINTS')
      READ(1,*)XPO1,YPO1,ZPO1,XPO2,YPO2,ZPO2
      SCE1=XPO2-XPO1
      SCE2=YPO2-YPO1
      SCE3=ZPO2-ZPO1
      SCE=DSQRT(SCE1**2+SCE2**2+SCE3**2)
      SCE1=SCE1/SCE
      SCE2=SCE2/SCE
      SCE3=SCE3/SCE
1974  CONTINUE
      CALL VIJK(SCE1,SCE2,SCE3,VJ1,VJ2,VJ3,VI1,VI2,VI3)
      WRITE(1,1982)
1982  FORMAT('READ LIMITS (2) TO FLANK SECTION AND NLEEP')
      READ(1,*)YSCFL1,YSCFL2,NLEEP
      WRITE(1,2534)
2534  FORMAT(/'READ DELTAY')
      READ(1,*)DELTAY
      NLOOSC=2*NPOINT
      NLEEP=NSEC+NLEEP
      ISEC=0
      NLAAP=NSEC
```

```
      DO 1966 I=NSEC,NLOOSC
      IF(I .GT. NPOINT) GO TO 1957
      XSE=XFLUD(I)
      YSE=YFLUD(I)
      GO TO 1972
1957  J=2*NPOINT-I+1
      XSE=-XEELGD(J)
      YSE=-YEELGD(J)
1972  CONTINUE
      IF(XSE .NE. Ø.)GO TO 1949
      WRITE(1,1958)I
1958  FORMAT('XSECTION IS Ø.Ø AT POINT ',I4)
      CALL EXIT
1949  PHSE=DATAN(YSE/XSE)
      IF(PHSE .GT. Ø.) PHSE=PHSE-PI
      RSE=DSQRT(XSE**2+YSE**2)
      DSEC=-(SCE1*XSE1+SCE2*YSE1+SCE3*ZSE1)
      CALL CØ5ACF(PHSEC1,PHSEC2,EPS,EPV,FUNSEC,PHSEC,IFAIL)
      PHSEC1=PHSEC-1Ø.*CONS
      PHSEC2=PHSEC+1Ø.*CONS
      XSECG(I)=XSEC
      YSECG(I)=YSEC
      ZSECG(I)=ZSEC
      XMSEC=XSEC
      ZMSEC=ZSEC
C
      CALL GRIN(ZSEC,ZØ,AXX,BYY,CXY,DDX,EY,FF)
C
3     F2=AXX*XSEC**2+BYY*YSEC**2+CXY*XSEC*YSEC-DDX*XSEC
     $-EY*YSEC+FF
      IF(I .GT. NPOINT .AND. F2 .GT. Ø.Ø) GO TO 1981
      XSTAR=(XSEC-XSE1)*VI1+(YSEC-YSE1)*VI2+(ZSEC-ZSE1)*VI3
      YSTAR=(XSEC-XSE1)*VJ1+(YSEC-YSE1)*VJ2+(ZSEC-ZSE1)*VJ3
C FOR VERIFICATION ZSTAR COULD BE PRINTED
      ZSTAR=(XSEC-XSE1)*VK1+(YSEC-YSE1)*VK2+(ZSEC-ZSE1)*VK3
      XSTARG(I)=XSTAR
      YSTARG(I)=YSTAR
      ZSTARG(I)=ZSTAR
      IF(I .GT. NLEEP) GO TO 2ØØ5
      CALL CØ5ACF(YSCFL1,YSCFL2,EPS,EPV,FSCFL,YSCFL,IFAIL)
      YSCFL1=YSCFL-DELTAY
      YSCFL2=YSCFL+DELTAY
      YSCFLA=(XSEC-XSE1)*VJ1+(YSCFL-YSE1)*VJ2+(ZSEC-ZSE1)*VJ3
      YSCFLG(I)=YSCFLA
      XSCFLG(I)=XSTARG(I)
2ØØ5  NLAAP=I
1966  CONTINUE
1981  NLOOSC=NLAAP
      WRITE(1,1944)
1944  FORMAT(/'LOOP 1966 FINISHED')
      WRITE(1,1952)
1952  FORMAT('READ YSCFL1 , YSCFL2  AND  XDIF')
      READ(1,*)YSCFL1,YSCFL2,XDIF
      NABC1=NLOOSC+1
      NABC2=NLOOSC+2Ø
      DO 2ØØ4 ISEC=NABC1,NABC2
      XSEC=XMSEC-FLOAT(ISEC-NABC1)/FLOAT(NABC2-NABC1)*XDIF
      CALL CØ5ACF(YSCFL1,YSCFL2,EPS,EPV,FSCFL,YSCFL,IFAIL)
      YSCFL1=YSCFL-.5
      YSCFL2=YSCFL+.5
      ZSEC=(-SCE1*XSEC-SCE2*YSCFL-DSEC)/SCE3
      YSCFLA=(XSEC-XSE1)*VJ1+(YSCFL-YSE1)*VJ2+(ZSEC-ZSE1)*VJ3
      YSCFLG(ISEC)=YSCFLA
      XSTAR=(XSEC-XSE1)*VI1+(YSCFL-YSE1)*VI2+(ZSEC-ZSE1)*VI3
      XSCFLG(ISEC)=XSTAR
2ØØ4  CONTINUE
C
      WRITE(1,2539)
2539  FORMAT(/'DRAWING AXES ?')
      READ(1,*)IAX
      WRITE(1,2553)
2553  FORMAT(/'T4Ø1Ø (1) , C1Ø51N (2) OR SE281(3) ?')
      READ(1,*)IDEV
      WRITE(1,254Ø)
254Ø  FORMAT(/'READ FACTOR TO COORDINATE AXES')
      READ(1,*)FACT
      GO TO(2554,2555,265Ø),IDEV
2554  XAXIS=FACT*157.89
      YAXIS=FACT*127.53
      CALL T4Ø1Ø
      GO TO 2556
2555  XAXIS=FACT*16Ø.
      YAXIS=FACT*12Ø.
      CALL C1Ø51N
      GO TO 2556
265Ø  XAXIS=FACT*16Ø.
      YAXIS=FACT*12Ø.
      CALL SE281
2556  CALL PICCLE
      CALL WINDOW(2)
      CALL AXIPOS(Ø,121.578,8Ø.,XAXIS,1)
      CALL AXIPOS(Ø,121.578,8Ø.,YAXIS,2)
      CALL AXISCA(2,2Ø,-14.,6.,1)
      CALL AXISCA(2,15,-8.,7.,2)
      IF(IAX .EQ. Ø) GO TO 2538
      CALL AXIDRA(2,1,1)
      CALL AXIDRA(-2,-1,2)
C
2538  CONTINUE
      NLOO=NLOOSC-NSEC+1
      NLIIP=NLEEP-NSEC-1
      NNLL=NABC2-NABC1+1
      CALL GRAPOL(XSTARG(NSEC),YSTARG(NSEC),NLOO)
      CALL GRAPOL(XSCFLG(NSEC),YSCFLG(NSEC),NLIIP)
      CALL GRAPOL(XSCFLG(NABC1),YSCFLG(NABC1),NNLL)
      CALL CHAMOD
C
      READ(1,*)SEPARA
```

```
      WRITE(1,1967)
1967  FORMAT('MORE SECTIONS ?')
      READ(1,*)MSEC
      IF(MSEC .NE. 0) GO TO 1962
2011  WRITE(1,2010)
2010  FORMAT('SECTIONS PARALLEL TO THE LIP ?')
      READ(1,*)ISEPAR
      IF(ISEPAR .EQ. 0) GO TO 2031
      WRITE(1,2012)
2012  FORMAT('READ Y AT WHICH IS THE PLANE PAR. TO CUT. EDG.')
      READ(1,*)YPACE1
      PHPAC1=0.0
      PHPAC2=89.9*CONS
      DO 2013 I=1,NPOINT
      RPACE=DSQRT(XFLUD(I)**2+YFLUD(I)**2)
      PHPA=DATAN(YFLUD(I)/XFLUD(I))
      CALL C05ACF(PHPAC1,PHPAC2,EPS,EPV,FPACE,PHPACE,IFAIL)
      XPACE=RPACE*DCOS(PHPACE+PHPA)
      YPACE=RPACE*DSIN(PHPACE+PHPA)
      ZPACE=PHPACE*R0*DCOS(H0)/DSIN(H0)
      XPACG(I)=XPACE
      YPACG(I)=YPACE
      ZPACG(I)=ZPACE
2013  CONTINUE
C
      CALL SE281
      CALL PICCLE
      CALL WINDOW(2)
      CALL AXIPOS(0,90.,80.,157.89,1)
      CALL AXIPOS(0,90.,80.,127.53,2)
      CALL AXISCA(2,20,-10.,10.,1)
      CALL AXISCA(2,15,-8.,7.,2)
      CALL AXIDRA(2,1,1)
      CALL AXIDRA(-2,-1,2)
      CALL GRACUR(XPACG,ZPACG,NPOINT)
      CALL CHAMOD
C
      READ(1,*)SEPARA
      WRITE(1,2018)
2018  FORMAT('MORE SECTIONS ?')
      READ(1,*)MORE
      IF(MORE .NE. 0) GO TO 2011
C
2031  WRITE(1,2032)
2032  FORMAT('SECTIONS ON A VERTICAL ROTATING PLANE ?')
      READ(1,*)ISEPAR
      IF(ISEPAR .EQ. 0) GO TO 1900
      WRITE(1,2033)
2033  FORMAT('READ ANGLE OF ROTATION OF THE PLANE')
      READ(1,*)ROT
      COEA=DSIN(ROT*CONS)/DCOS(ROT*CONS)
      COEB=-WEB/2.*(DSIN(ROT*CONS)*COEA+DCOS(ROT*CONS))
      PHPAC1=.0*CONS
      PHPAC2=89.9*CONS
      DO 2034 I=1,NPOINT
      RPACE=DSQRT(XFLUD(I)**2+YFLUD(I)**2)
      PHPA=DATAN(YFLUD(I)/XFLUD(I))
      CALL C05ACF(PHPAC1,PHPAC2,EPS,EPV,GPACE,PHPACE,IFAIL)
      XPACE=RPACE*DCOS(PHPACE+PHPA)
      YPACE=RPACE*DSIN(PHPACE+PHPA)
      ZPACE=PHPACE*R0*DCOS(H0)/DSIN(H0)
      XPACG(I)=XPACE
      YPACG(I)=YPACE
      ZPACG(I)=ZPACE
2034  CONTINUE
      CALL SE281
      CALL PICCLE
      CALL WINDOW(2)
      CALL AXIPOS(0,90.,80.,157.89,1)
      CALL AXIPOS(0,90.,80.,127.53,2)
      CALL AXISCA(2,20,-10.,10.,1)
      CALL AXISCA(2,15,-8.,7.,2)
      CALL AXIDRA(2,1,1)
      CALL AXIDRA(-2,-1,2)
      CALL GRACUR(XPACG,ZPACG,NPOINT)
      CALL CHAMOD
C
      READ(1,*)SEPARA
      WRITE(1,2036)
2036  FORMAT('MORE SECTIONS ?')
      READ(1,*)MORE
      IF(MORE .NE. 0) GO TO 2031
C
2023  CALL DEVEND
      CALL EXIT
      END
C
C ===================================================
C          FUNCTIONS AND SUBROUTINES
C ===================================================
C
      FUNCTION FAN(XST)
      IMPLICIT DOUBLE PRECISION(A-H,O-Z)
      DIMENSION COEF(20)
      COMMON/BLO1/R0,WEB,H0,EXG,VG,RKG,ROG
      COMMON/BLO2/CONS,PI
      COMMON/BLO3/ALPHA,CSVG,SNVG,CSKOI,SNKOI,CSKOU,SNKOU
      COMMON/BLO4/Z,Z0,ZHH
      COMMON/BLO6/COEF,NCOEF,III
C
      CALL GRIN(Z,Z0,AXX,BYY,CXY,DDX,EY,FF)
C
      YST=0.0
      DO 70 J=1,NCOEF
      YST=YST+COEF(J)*XST**(J-1)
70    CONTINUE
      PHST=DATAN(YST/XST)
      RSTAN=DSQRT(XST**2+YST**2)
```

```
      PHST=PHST+ALPHA
      XST1=RSTAN*DCOS(PHST)
      YST1=RSTAN*DSIN(PHST)
C
      FAN=AXX*XST1**2+BYY*YST1**2+CXY*XST1*YST1+DDX*XST1
     $+EY*YST1+FF
C
      RETURN
      END
C ==================================================
      FUNCTION FEEL(XEEL)
      IMPLICIT DOUBLE PRECISION(A-H,O-Z)
      DIMENSION COEF(20),COEEL(3),COFL(40)
      COMMON/BLO1/R0,WEB,H0,EXG,VG,RKG,ROG
      COMMON/BLO2/CONS,PI
      COMMON/BLO3/ALPHA,CSVG,SNVG,CSKOI,SNKOI,CSKOU,SNKOU
      COMMON/BLO4/Z,Z0,ZHH
      COMMON/BLO5/S,NPOINT,NLAAP,ISEC,IHE
      COMMON/BLO6/COEF,NCOEF,III
      COMMON/BLO8/XFLUEE,YFLUEE,DMAR,XSTEEL,YSTEEL,ANGCLE,YEEL
      COMMON/BLO11/COFL,NSTFLI
C
      CALL GRIN(Z,Z0,AXX,BYY,CXY,DDX,EY,FF)
C
      YEELDV=COEF(2)
      IF(S .NE. 1.)YEELDV=0.
      XEEL1=0.
      YEEL1=WEB/2.
      IF(S .EQ. 1.)YEEL1=-COEF(1)
      XEEL2=-YFLUEE
      YEEL2=XFLUEE
      PHEEL=DATAN(YEEL2/XEEL2)
      PHIIL=PHEEL+(ANGCLE-PI/2.)
      XEEL2=DSQRT(XEEL2**2+YEEL2**2)*DCOS(PHIIL)
      YEEL2=DSQRT(XEEL2**2+YEEL2**2)*DSIN(PHIIL)
      COEEL(1)=YEEL1
      COEEL(2)=YEELDV
      COEEL(3)=(YEEL2-XEEL2*COEEL(2)-COEEL(1))/XEEL2**2
      IF(XEEL .GE. .0)GO TO 1
      IF(S .EQ. 1. .AND. XEEL .LT. 0.) GO TO 5
      YEEL=0.
      XEELL=-XEEL
      DO 6 J=1,NSTFLI
      YEEL=YEEL+COFL(J)*XEELL**(J-1)
6     CONTINUE
      YEELL=-YEEL
      PHST=DATAN(YEELL/XEELL)+3.14159265
      GO TO 2
5     YEEL=0.
      XEELL=-XEEL
      DO 7 J=1,NCOEF
      YEEL=YEEL+COEF(J)*XEELL**(J-1)
7     CONTINUE
      YEELL=+YEEL
      PHST=DATAN(YEELL/XEELL)+3.14159265
      YEEL=-YEEL
      GO TO 2
1     YEEL=COEEL(1)+COEEL(2)*XEEL+COEEL(3)*XEEL**2
      PHST=DATAN(YEEL/XEEL)
2     RSTAN=DSQRT(XEEL**2+YEEL**2)
      PHST=PHST+ALPHA
      XST1=RSTAN*DCOS(PHST)
      YST1=RSTAN*DSIN(PHST)
      XSTEEL=XST1
      YSTEEL=YST1
C
      FEEL=AXX*XST1**2+BYY*YST1**2+CXY*XST1*YST1+DDX*XST1
     $+EY*YST1+FF
C
      RETURN
      END
C ==================================================
      FUNCTION FIIL(RHEEL)
      IMPLICIT DOUBLE PRECISION(A-H,O-Z)
      DIMENSION COEF(20),COEEL(3),COFL(40)
      COMMON/BLO1/R0,WEB,H0,EXG,VG,RKG,ROG
      COMMON/BLO2/CONS,PI
      COMMON/BLO3/ALPHA,CSVG,SNVG,CSKOI,SNKOI,CSKOU,SNKOU
      COMMON/BLO4/Z,Z0,ZHH
      COMMON/BLO5/S,NPOINT,NLAAP,ISEC,IHE
      COMMON/BLO6/COEF,NCOEF,III
      COMMON/BLO8/XFLUEE,YFLUEE,DMAR,XSTEEL,YSTEEL,ANGCLE,YEEL
      COMMON/BLO11/COFL,NSTFLI
      COMMON/BLO17/XEELA,YEELA,ZWEB
C
      CALL GRIN(Z,Z0,AXX,BYY,CXY,DDX,EY,FF)
C
      W2R=WEB/2./RHEEL
      IF(RHEEL .LE. WEB/2.) GO TO 1
      ANG=DATAN(W2R/DSQRT(1.-W2R**2))
      PHST=ANG+DSQRT(RHEEL**2-(WEB/2.)**2)*DSIN(H0)/DCOS(H0)
     $/R0*CSKOU/SNKOU
      IF(Z .LT. ZWEB)PHST=PI-PHST
      GO TO 2
1     PHST=PI/2.
2     XEELA=RHEEL*DCOS(PHST)
      YEELA=RHEEL*DSIN(PHST)
      PHST=PHST+ALPHA
      XST1=RHEEL*DCOS(PHST)
      YST1=RHEEL*DSIN(PHST)
      XSTEEL=XST1
      YSTEEL=YST1
C
      FIIL=AXX*XST1**2+BYY*YST1**2+CXY*XST1*YST1+DDX*XST1
     $+EY*YST1+FF
C
      RETURN
      END
```

```
C ================================================
      FUNCTION FIN(XST)
      IMPLICIT DOUBLE PRECISION(A-H,O-Z)
      DIMENSION COEF(20)
      COMMON/BLO3/ALPHA,CSVG,SNVG,CSKOI,SNKOI,CSKOU,SNKOU
      COMMON/BLO6/COEF,NCOEF,III
C
      YST=0.0
      DO 150 J=1,NCOEF
      YST=YST+COEF(J)*XST**(J-1)
150   CONTINUE
      PHST=DATAN(YST/XST)
      RSTAN=DSQRT(XST**2+YST**2)
      PHST=PHST+ALPHA
      XST1=RSTAN*DCOS(PHST)
      YST1=RSTAN*DSIN(PHST)
      FIN=YST1
C
      RETURN
      END
C ================================================
      FUNCTION FLANK(ZCLE)
      IMPLICIT DOUBLE PRECISION(A-H,O-Z)
      DIMENSION COEF(20)
      COMMON/BLO1/R0,WEB,H0,EXG,VG,RKG,ROG
      COMMON/BLO2/CONS,PI
      COMMON/BLO3/ALPHA,CSVG,SNVG,CSKOI,SNKOI,CSKOU,SNKOU
      COMMON/BLO4/Z,Z0,ZHH
      COMMON/BLO6/COEF,NCOEF,III
      COMMON/BLO7/XCLE,YCLE,IFL,IHILST,PHIIL2
      COMMON/BLO8/XFLUEE,YFLUEE,DMAR,XSTEEL,YSTEEL,ANGCLE,YEEL
C
      IF(IFL .NE. 1) GO TO 1
      PHEEL=DATAN(YFLUEE/XFLUEE)
      PHIIL=PHEEL+ANGCLE
      IF(IHILST .NE. 1) GO TO 2
      W2R=WEB/2./R0
      PHIIL=DATAN(W2R/DSQRT(1.-W2R**2))+DSQRT(R0**2
     $-(WEB/2.)**2)*DSIN(H0)/DCOS(H0)/R0*CSKOU/SNKOU
2     ALPHA=ZCLE/R0*DSIN(H0)/DCOS(H0)
      PHST=PHIIL+ALPHA
      XCLE=R0*DCOS(PHST)
      YCLE=RO*DSIN(PHST)
      PHIIL2=DATAN(YCLE/XCLE)
1     Z=ZCLE
C
      CALL GRIN(Z,Z0,AXX,BYY,CXY,DDX,EY,FF)
C
      FLANK=AXX*XCLE**2+BYY*YCLE**2+CXY*XCLE*YCLE+DDX*XCLE
     $+EY*YCLE+FF
C
      RETURN
      END
C ================================================
      FUNCTION FON(RSTAN)
      IMPLICIT DOUBLE PRECISION(A-H,O-Z)
      COMMON/BLO1/R0,WEB,H0,EXG,VG,RKG,ROG
      COMMON/BLO2/CONS,PI
      COMMON/BLO3/ALPHA,CSVG,SNVG,CSKOI,SNKOI,CSKOU,SNKOU
C
      W2R=WEB/2./RSTAN
      PHST=-(DATAN(W2R/DSQRT(1.-W2R**2))+DSQRT(RSTAN**2
     $-(WEB/2.)**2)*DSIN(H0)/DCOS(H0)/R0*CSKOU/SNKOU)
      FON=PHST+ALPHA
C
      RETURN
      END
C ================================================
      FUNCTION FOUTCR(ZOUT)
      IMPLICIT DOUBLE PRECISION(A-H,O-Z)
      COMMON/BLO1/R0,WEB,H0,EXG,VG,RKG,ROG
      COMMON/BLO2/CONS,PI
      COMMON/BLO3/ALPHA,CSVG,SNVG,CSKOI,SNKOI,CSKOU,SNKOU
      COMMON/BLO4/Z,Z0,ZHH
      COMMON/BLO5/S,NPOINT,NLAAP,ISEC,IHE
      COMMON/BLO21/XOUT,YOUT
C
      ALPHA=ZOUT/R0*DSIN(H0)/DCOS(H0)
      W2R=WEB/2./R0
      PHST=-(DATAN(W2R/DSQRT(1.-W2R**2))+DSQRT(R0**2
     $-(WEB/2.)**2)*DSIN(H0)/DCOS(H0)/R0*CSKOU/SNKOU)
      PHST=PHST+ALPHA
      XST=R0*DCOS(PHST)
      YST=R0*DSIN(PHST)
      XOUT=XST
      YOUT=YST
C
      CALL GRIN(Z,Z0,AXX,BYY,CXY,DDX,EY,FF)
C
      FOUTCR=AXX*XST**2+BYY*YST**2+CXY*XST*YST+DDX*XST
     $+EY*YST+FF
C
      RETURN
      END
C ================================================
      FUNCTION FPACE(PHPACE)
      IMPLICIT DOUBLE PRECISION(A-H,O-Z)
      COMMON/BLO14/RPACE,PHPA,YPACE1
C
      YPACE=RPACE*DSIN(PHPACE+PHPA)
      FPACE=YPACE-YPACE1
C
      RETURN
      END
C ================================================
      FUNCTION FSCFL(YSCFL)
      IMPLICIT DOUBLE PRECISION(A-H,O-Z)
      COMMON/BLO1/R0,WEB,H0,EXG,VG,RKG,ROG
```

```
      COMMON/BLO2/CONS,PI
      COMMON/BLO3/ALPHA,CSVG,SNVG,CSKOI,SNKOI,CSKOU,SNKOU
      COMMON/BLO4/Z,ZØ,ZHH
      COMMON/BLO5/S,NPOINT,NLAAP,ISEC,IHE
      COMMON/BLO12/RSE,PHSE,DSEC,SCE1,SCE2,SCE3
      COMMON/BLO13/XSEC,YSEC,ZSEC,ZMSEC
C
      IF(ISEC .GT. NLAAP)ZSEC=(-SCE1*XSEC-SCE2*YSCFL-DSEC)/
     $SCE3
      CALL GRIN(Z,ZØ,AXX,BYY,CXY,DDX,EY,FF)
      IF(ISEC .LT. NLAAP) GO TO 2
      IF(ZMSEC .LE. ZHH) GO TO 3
      FSCFL=RØ**2-XSEC**2-YSCFL**2
      GO TO 1
C
3     FSCFL=AXX*XSEC**2+BYY*YSCFL**2+CXY*XSEC*YSCFL-DDX*XSEC
     $-EY*YSCFL+FF
      GO TO 1
2     FSCFL=AXX*XSEC**2+BYY*YSCFL**2+CXY*XSEC*YSCFL+DDX*XSEC
     $+EY*YSCFL+FF
1     IF(IHE .NE. 1) GO TO 4
      FSCFL=RØ**2-XSEC**2-YSCFL**2
C
4     CONTINUE
      RETURN
      END
C ==================================================
      FUNCTION FUN(RSTAN)
      IMPLICIT DOUBLE PRECISION(A-H,O-Z)
      INTEGER NPOINT
      COMMON/BLO1/RØ,WEB,HØ,EXG,VG,RKG,ROG
      COMMON/BLO2/CONS,PI
      COMMON/BLO3/ALPHA,CSVG,SNVG,CSKOI,SNKOI,CSKOU,SNKOU
      COMMON/BLO4/Z,ZØ,ZHH
      COMMON/BLO5/S,NPOINT,NLAAP,ISEC,IHE
C
      W2R=WEB/2./RSTAN
      PHST=-(DATAN(W2R/DSQRT(1.-W2R**2))+DSQRT(RSTAN**2
     $-(WEB/2.)**2)*DSIN(HØ)/DCOS(HØ)/RØ*CSKOU/SNKOU)
      PHST=PHST+ALPHA
      XST=RSTAN*DCOS(PHST)
      YST=RSTAN*DSIN(PHST)
C
      CALL GRIN(Z,ZØ,AXX,BYY,CXY,DDX,EY,FF)
C
      FUN=AXX*XST**2+BYY*YST**2+CXY*XST*YST+DDX*XST
     $+EY*YST+FF
C
      RETURN
      END
C ==================================================
      FUNCTION FUNSEC(PHSEC)
      IMPLICIT DOUBLE PRECISION(A-H,O-Z)
      COMMON/BLO1/RØ,WEB,HØ,EXG,VG,RKG,ROG
      COMMON/BLO2/CONS,PI
      COMMON/BLO12/RSE,PHSE,DSEC,SCE1,SCE2,SCE3
      COMMON/BLO13/XSEC,YSEC,ZSEC,ZMSEC
C
      XSEC=RSE*DCOS(PHSEC+PHSE)
      YSEC=RSE*DSIN(PHSEC+PHSE)
      ZSEC=PHSEC*RØ*DCOS(HØ)/DSIN(HØ)
      FUNSEC=SCE1*XSEC+SCE2*YSEC+SCE3*ZSEC+DSEC
      RETURN
      END
C ==================================================
      FUNCTION FWEB(ZWEB)
      IMPLICIT DOUBLE PRECISION(A-H,O-Z)
      DIMENSION COEF(2Ø),COEEL(3),COFL(4Ø)
      COMMON/BLO1/RØ,WEB,HØ,EXG,VG,RKG,ROG
      COMMON/BLO2/CONS,PI
      COMMON/BLO3/ALPHA,CSVG,SNVG,CSKOI,SNKOI,CSKOU,SNKOU
      COMMON/BLO4/Z,ZØ,ZHH
      COMMON/BLO5/S,NPOINT,NLAAP,ISEC,IHE
      COMMON/BLO6/COEF,NCOEF,III
      COMMON/BLO8/XFLUEE,YFLUEE,DMAR,XSTEEL,YSTEEL,ANGCLE,YEEL
      COMMON/BLO11/COFL,NSTFLI
C
      CALL GRIN(Z,ZØ,AXX,BYY,CXY,DDX,EY,FF)
C
      ALPHA=ZWEB/RØ*DSIN(HØ)/DCOS(HØ)
      PHST=PI/2.+ALPHA
      XST1=WEB/2.*DCOS(PHST)
      YST1=WEB/2.*DSIN(PHST)
C
      FWEB=AXX*XST1**2+BYY*YST1**2+CXY*XST1*YST1+DDX*XST1
     $+EY*YST1+FF
C
      RETURN
      END
C ==================================================
      SUBROUTINE GRIN(Z,ZØ,AXX,BYY,CXY,DDX,EY,FF)
      IMPLICIT DOUBLE PRECISION(A-H,O-Z)
      COMMON/BLO1/RØ,WEB,HØ,EXG,VG,RKG,ROG
      COMMON/BLO3/ALPHA,CSVG,SNVG,CSKOI,SNKOI,CSKOU,SNKOU
C
      AXX=CSVG**2+(CSKOI**2)*(SNVG**2)
      BYY=SNVG**2+CSVG**2*(CSKOI**2)
      CXY=-2.*SNVG*CSVG+2.*(CSKOI**2)*SNVG*CSVG
      DDX=-2.*EXG*CSVG-2.*(Z-ZØ)*SNKOI*CSKOI*SNVG
      EY=2.*EXG*SNVG-2.*(Z-ZØ)*SNKOI*CSKOI*CSVG
      FF=EXG**2-ROG**2+((Z-ZØ)**2)*SNKOI**2
C
      RETURN
      END
C ==================================================
      FUNCTION GPACE(PHPACE)
      IMPLICIT DOUBLE PRECISION(A-H,O-Z)
      COMMON/BLO14/RPACE,PHPA,YPACE1
```

```
      COMMON/BLO16/COEA,COEB
C
      YPACE=RPACE*DSIN(PHPACE+PHPA)
      XPACE=RPACE*DCOS(PHPACE+PHPA)
      YPACE1=COEA*XPACE+COEB
      GPACE=YPACE-YPACE1
C
      RETURN
      END
C ==================================================
      SUBROUTINE MONIT(M,N,CORN,RE,FJAC,LJC,SMON,IGR,NITER
     $,NF,IW,LIW,WE0,LW)
      IMPLICIT DOUBLE PRECISION(A-H,O-Z)
      DIMENSION CORN(3),RE(3),FJAC(3,3),SMON(3),IW(1),WE0(120)
      FE=RE(1)**2+RE(2)**2+RE(3)**2
      WRITE(1,20)NITER,FE
20    FORMAT('AFTER',I4,' ITERATIONS',2X,'THE SUM OF SQ. IS'
     $,F9.3)
      WRITE(1,22)(CORN(I),I=1,N)
22    FORMAT('AT THE POINT',F10.4)
      RETURN
      END
C ==================================================
      SUBROUTINE MONUT(M,N,CORN,RU,FJAC,LJC,SMON,IGR,NITER
     $,NF,IW,LIW,WE0,LW)
      IMPLICIT DOUBLE PRECISION(A-H,O-Z)
      DIMENSION CORN(3),RU(3),FJAC(3,3),SMON(3),IW(1),WE0(120)
      FU=RU(1)**2+RU(2)**2+RU(3)**2
      WRITE(1,20)NITER,FU
20    FORMAT('AFTER',I4,' ITERATIONS',2X,'THE SUM OF SQ. IS'
     $,F9.3)
      WRITE(1,22)(CORN(I),I=1,N)
22    FORMAT('AT THE POINT',F10.4)
      RETURN
      END
C ==================================================
      SUBROUTINE RESID(IFLAG,M,N,CORN,RE,IW,LIW,WE0,LW)
      IMPLICIT DOUBLE PRECISION(A-H,O-Z)
      DIMENSION RE(3),CORN(3),IW(1),WE0(120)
      COMMON/BLO1/R0,WEB,H0,EXG,VG,RKG,ROG
      COMMON/BLO2/CONS,PI
      COMMON/BLO3/ALPHA,CSVG,SNVG,CSKOI,SNKOI,CSKOU,SNKOU
      COMMON/BLO4/Z,Z0,ZHH
C
      XCORN=CORN(1)
      YCORN=CORN(2)
      ZCORN=CORN(3)
      RSTAN=DSQRT(XCORN**2+YCORN**2)
      ALPHA=ZCORN/R0*DSIN(H0)/DCOS(H0)
      IF(RSTAN .LE. WEB/2.)GO TO 1
      W2R=WEB/2./RSTAN
      PHST=-(DATAN(W2R/DSQRT(1.-W2R**2))+DSQRT(RSTAN**2
     $-(WEB/2.)**2)*DSIN(H0)/DCOS(H0)/R0*CSKOU/SNKOU)
      GO TO 2
1     PHST=-PI/2.
2     PHSTXY=-DATAN(YCORN/XCORN)
C
      CALL GRIN(Z,Z0,AXX,BYY,CXY,DDX,EY,FF)
C
      RE(1)=AXX*XCORN**2+BYY*YCORN**2+CXY*XCORN*YCORN+DDX
     $*XCORN+EY*YCORN+FF
      RE(2)=AXX*XCORN**2+BYY*YCORN**2+CXY*XCORN*YCORN-DDX
     $*XCORN-EY*YCORN+FF
      RE(3)=PHST+PHSTXY+ALPHA
C
      RETURN
      END
C ==================================================
      SUBROUTINE RESUD(IFLAG,M,N,CORN,RU,IW,LIW,WE0,LW)
      IMPLICIT DOUBLE PRECISION(A-H,O-Z)
      DIMENSION COEF(20),RU(3),CORN(3),IW(1),WE0(120)
      COMMON/BLO1/R0,WEB,H0,EXG,VG,RKG,ROG
      COMMON/BLO2/CONS,PI
      COMMON/BLO3/ALPHA,CSVG,SNVG,CSKOI,SNKOI,CSKOU,SNKOU
      COMMON/BLO4/Z,Z0,ZHH
      COMMON/BLO6/COEF,NCOEF,III
C
      XCORN=CORN(1)
      YCORN=CORN(2)
      ZCORN=CORN(3)
C
      CALL GRIN(Z,Z0,AXX,BYY,CXY,DDX,EY,FF)
C
      RSTAN=DSQRT(XCORN**2+YCORN**2)
      PHSTXY=-DATAN(YCORN/XCORN)
      ALPHA=ZCORN/R0*DSIN(H0)/DCOS(H0)
      PHST=-PHSTXY-ALPHA
      XST1=RSTAN*DCOS(PHST)
      YST1=RSTAN*DSIN(PHST)
      YST=0.0
      DO 70 J=1,NCOEF
      YST=YST+COEF(J)*XST1**(J-1)
70    CONTINUE
C
      RU(1)=AXX*XCORN**2+BYY*YCORN**2+CXY*XCORN*YCORN+DDX
     $*XCORN+EY*YCORN+FF
      RU(2)=AXX*XCORN**2+BYY*YCORN**2+CXY*XCORN*YCORN-DDX
     $*XCORN-EY*YCORN+FF
      RU(3)=YST-YST1
C
      RETURN
      END
C ==================================================
      FUNCTION ROTAC(XLK)
      IMPLICIT DOUBLE PRECISION(A-H,O-Z)
      DIMENSION COEF(20)
      COMMON/BLO1/R0,WEB,H0,EXG,VG,RKG,ROG
      COMMON/BLO2/CONS,PI
```

```
      COMMON/BLO6/COEF,NCOEF,III
      COMMON/BLO15/XLØ,YLØ
C
      YLK=Ø.
      DO 75 J=1,NCOEF
      YLK=YLK+COEF(J)*XLK**(J-1)
75    CONTINUE
      R=DSQRT(XLK**2+YLK**2)
      ROTAC=R-RØ
      XLØ=XLK
      YLØ=YLK
C
      RETURN
      END
C ===================================================
      SUBROUTINE VIJK(SCE1,SCE2,SCE3,VJ1,VJ2,VJ3,VI1,VI2,VI3)
      IMPLICIT DOUBLE PRECISION(A-H,O-Z)
C
      VK1=SCE1
      VK2=SCE2
      VK3=SCE3
C
      VJ2=1.
      VJ1=-(VJ2*VK2)/VK1
      VJ3=Ø.
      VJ=DSQRT(VJ1**2+VJ2**2+VJ3**2)
      VJ1=VJ1/VJ
      VJ2=VJ2/VJ
      VJ3=VJ3/VJ
C
      VI1=1.
      VI2=-(VI1*VJ1)/VJ2
      VI3=-(VI1*VK1+VI2*VK2)/VK3
      VI=DSQRT(VI1**2+VI2**2+VI3**2)
      VI1=VI1/VI
      VI2=VI2/VI
      VI3=VI3/VI
C
      RETURN
      END
C
C
C
C *END*END*END*END*END*END*END*END*END*END*END*END*END*
```

# APPENDIX 2

Computer geometric simulation of drill point showing the effect of flute design and cylindrical grinding parameters on drill point design (refer to Chapter 4).

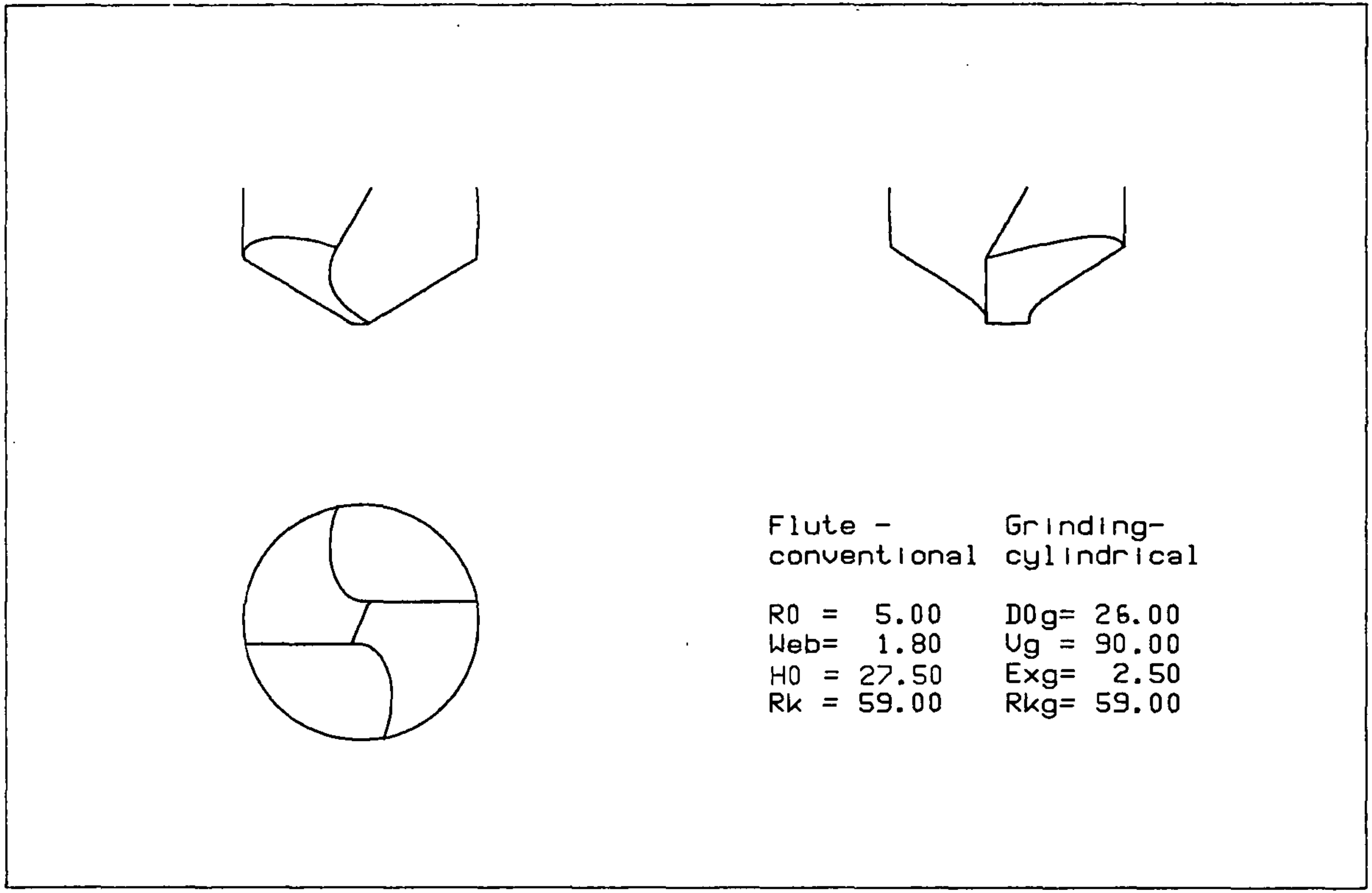


Computer geometric simulation of drill point

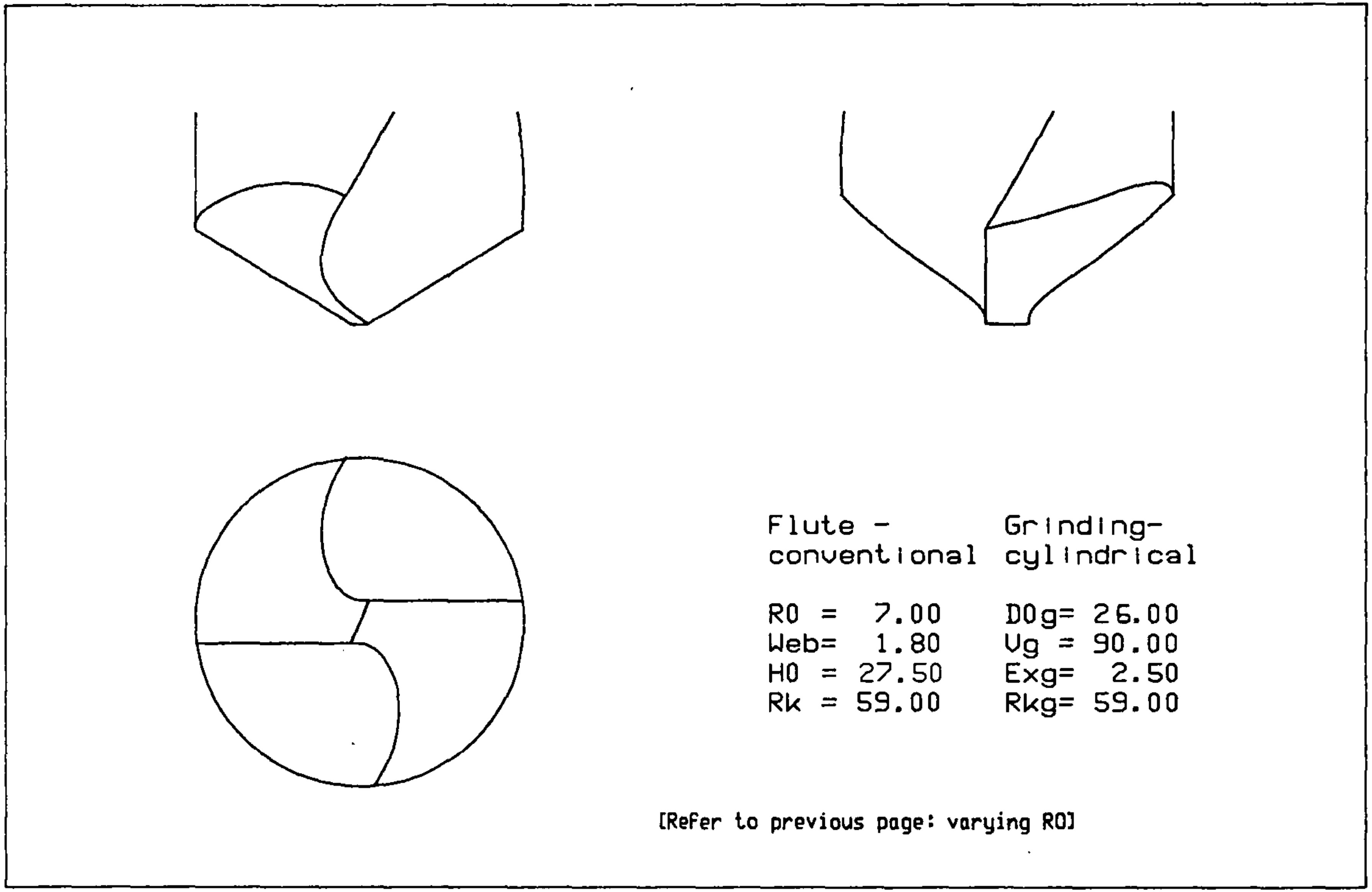


Computer geometric simulation of drill point

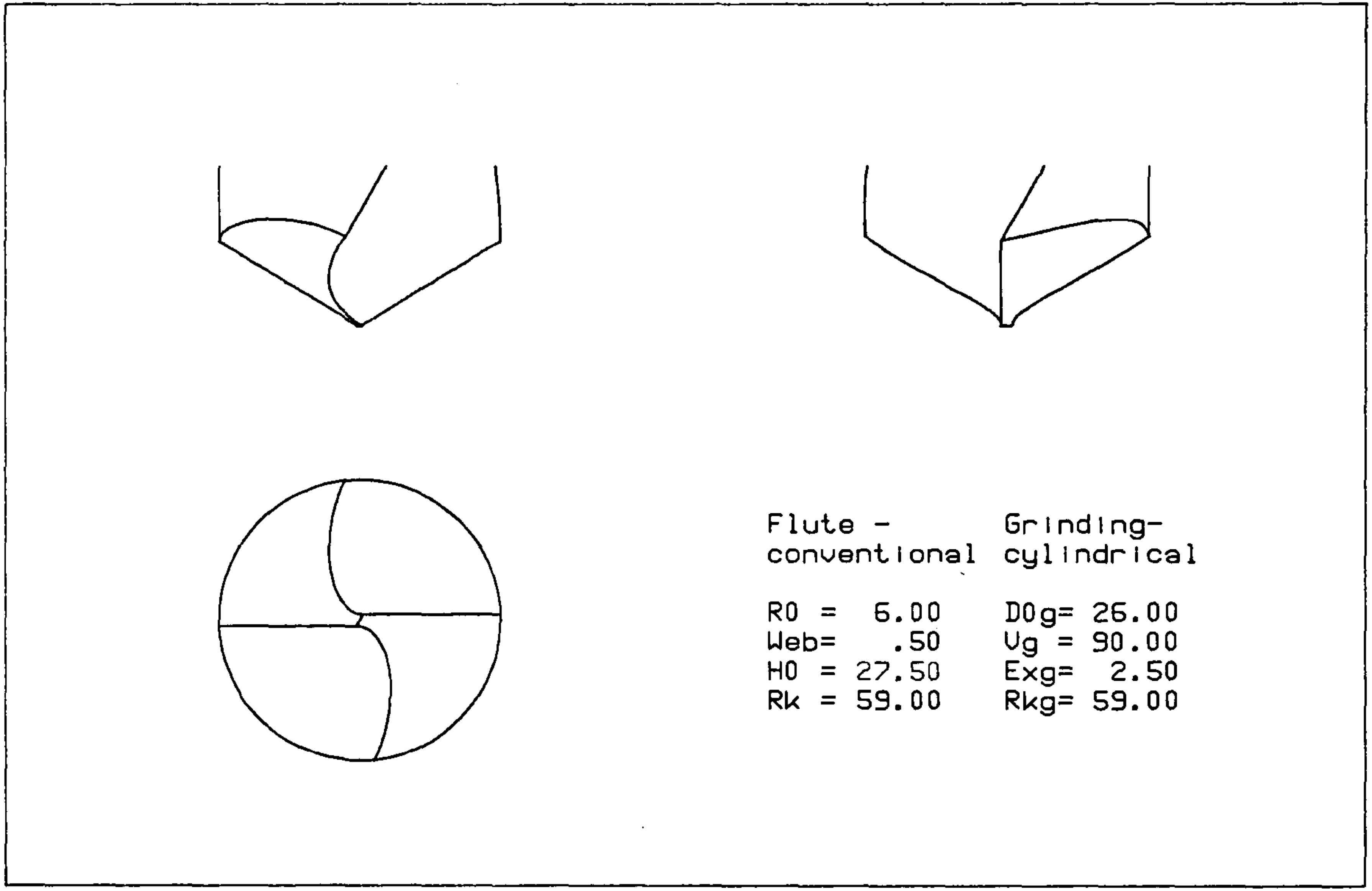


Computer geometric simulation of drill point

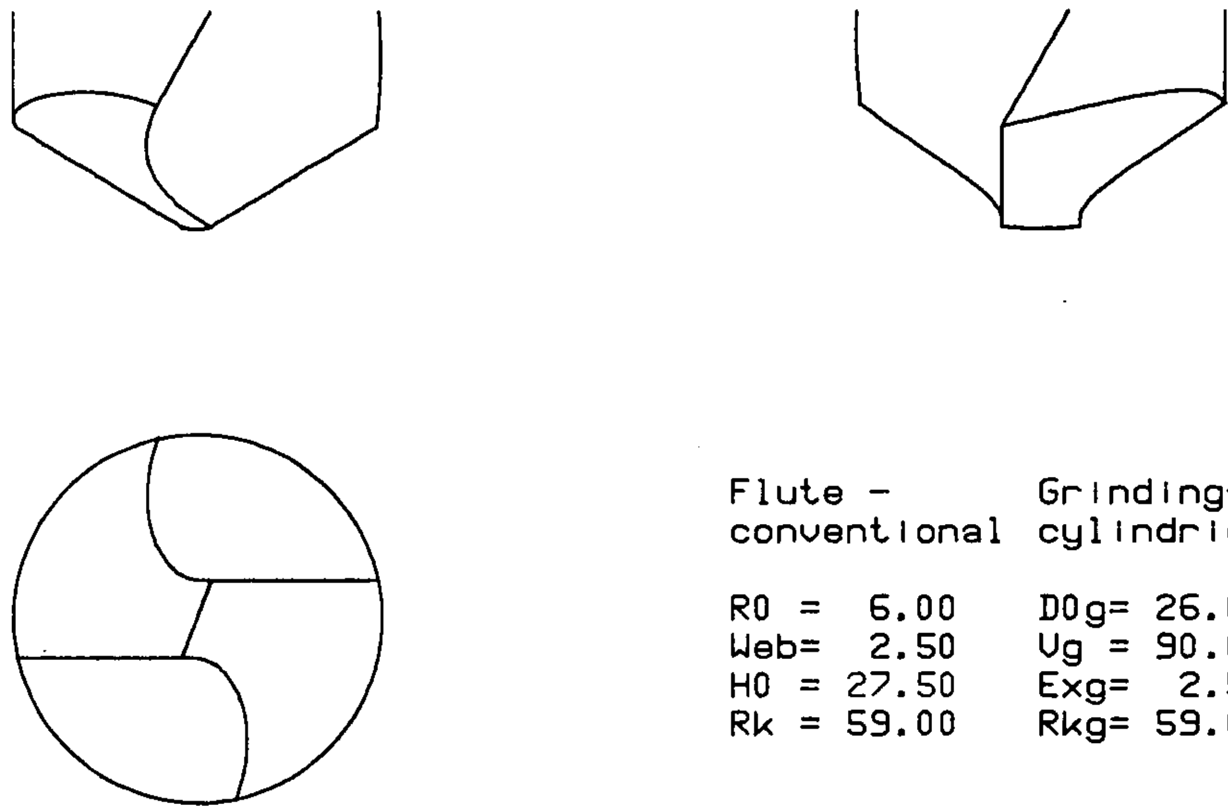

| | |
|---|---|
| Flute - conventional | Grinding- cylindrical |
| R0 = 6.00 | D0g= 26.00 |
| Web= 2.50 | Vg = 90.00 |
| H0 = 27.50 | Exg= 2.50 |
| Rk = 59.00 | Rkg= 59.00 |

[Refer to previous page: varying Web]

Computer geometric simulation of drill point

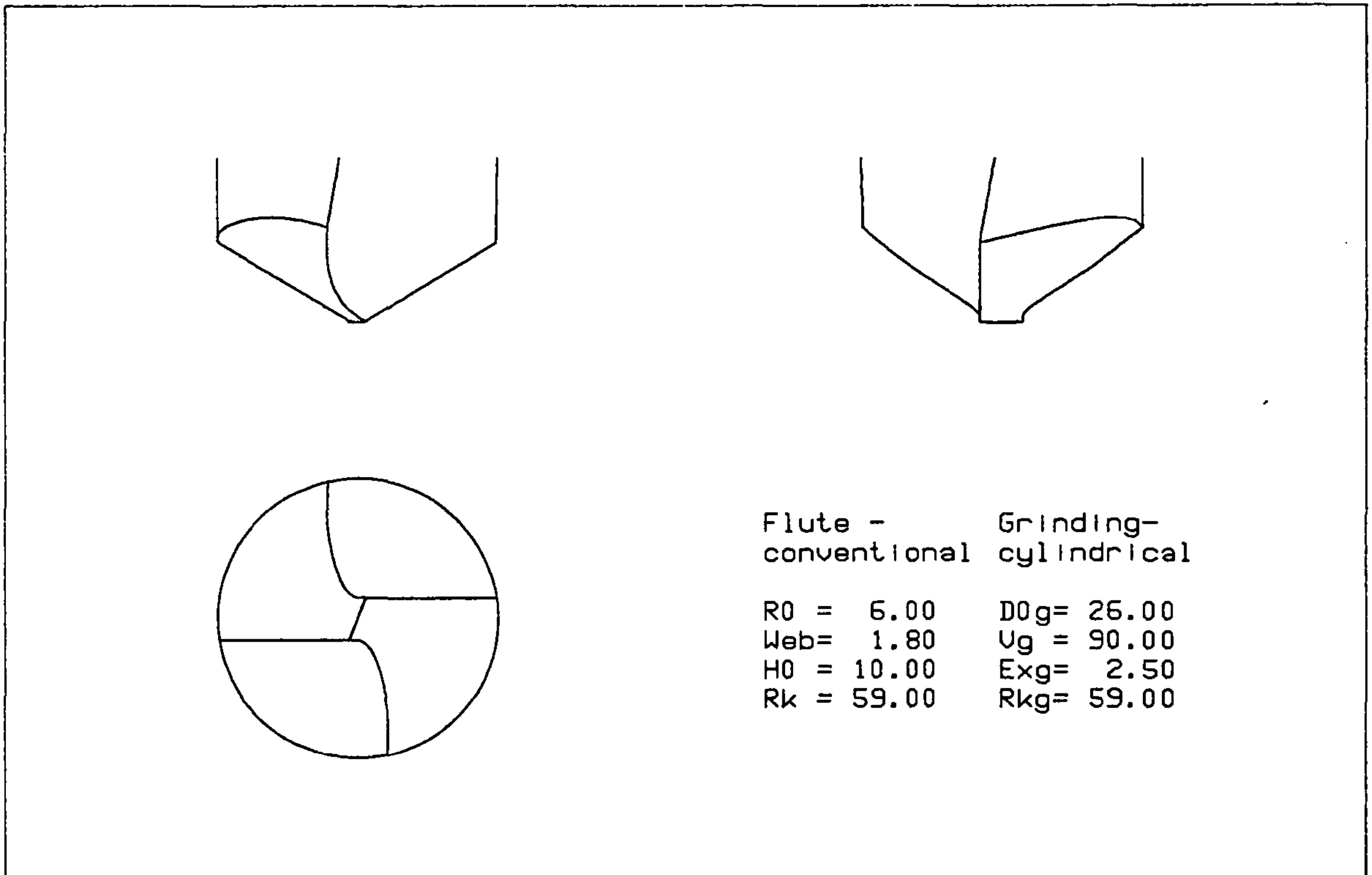


Computer geometric simulation of drill point

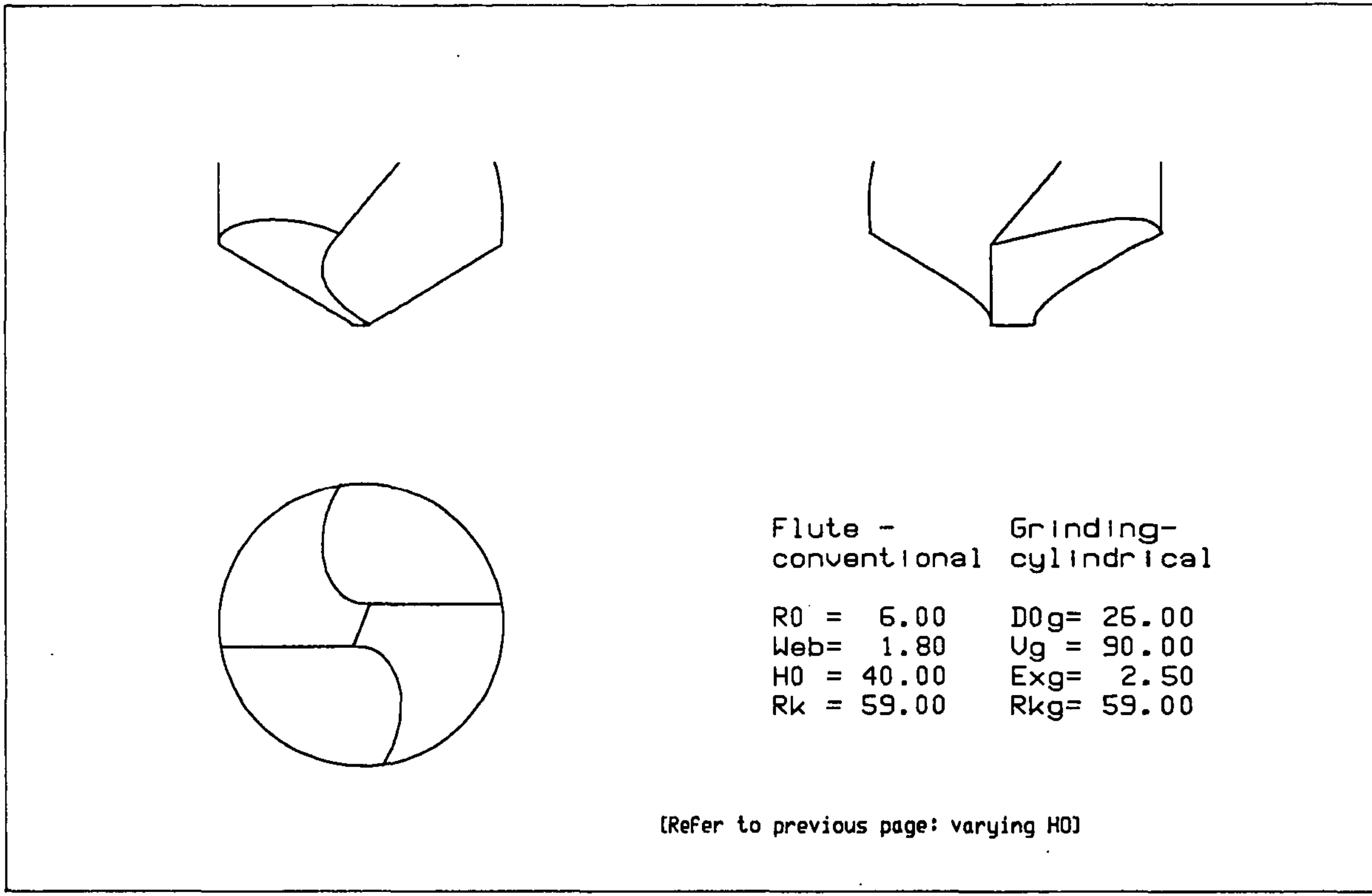


Computer geometric simulation of drill point

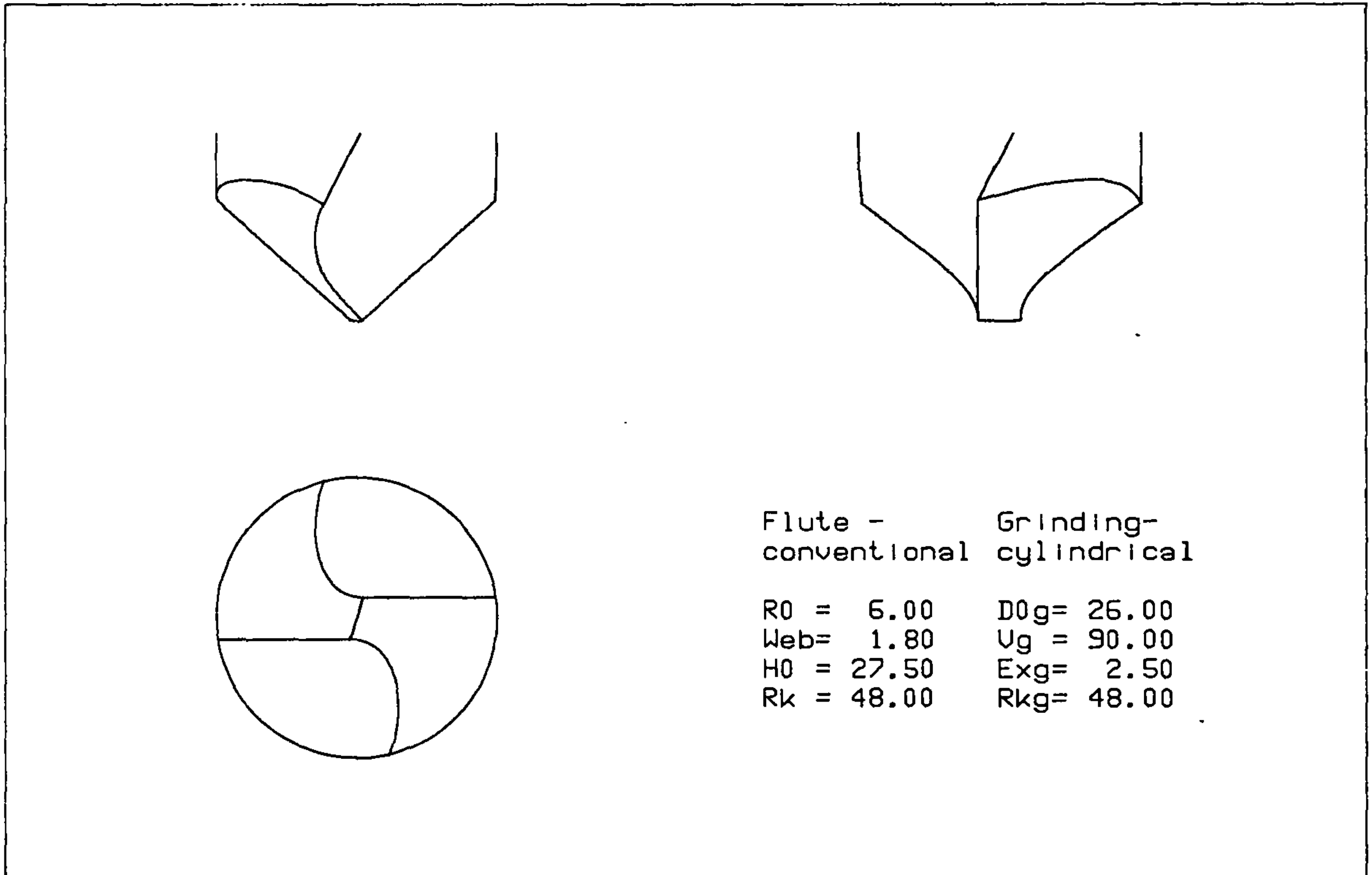


Computer geometric simulation of drill point

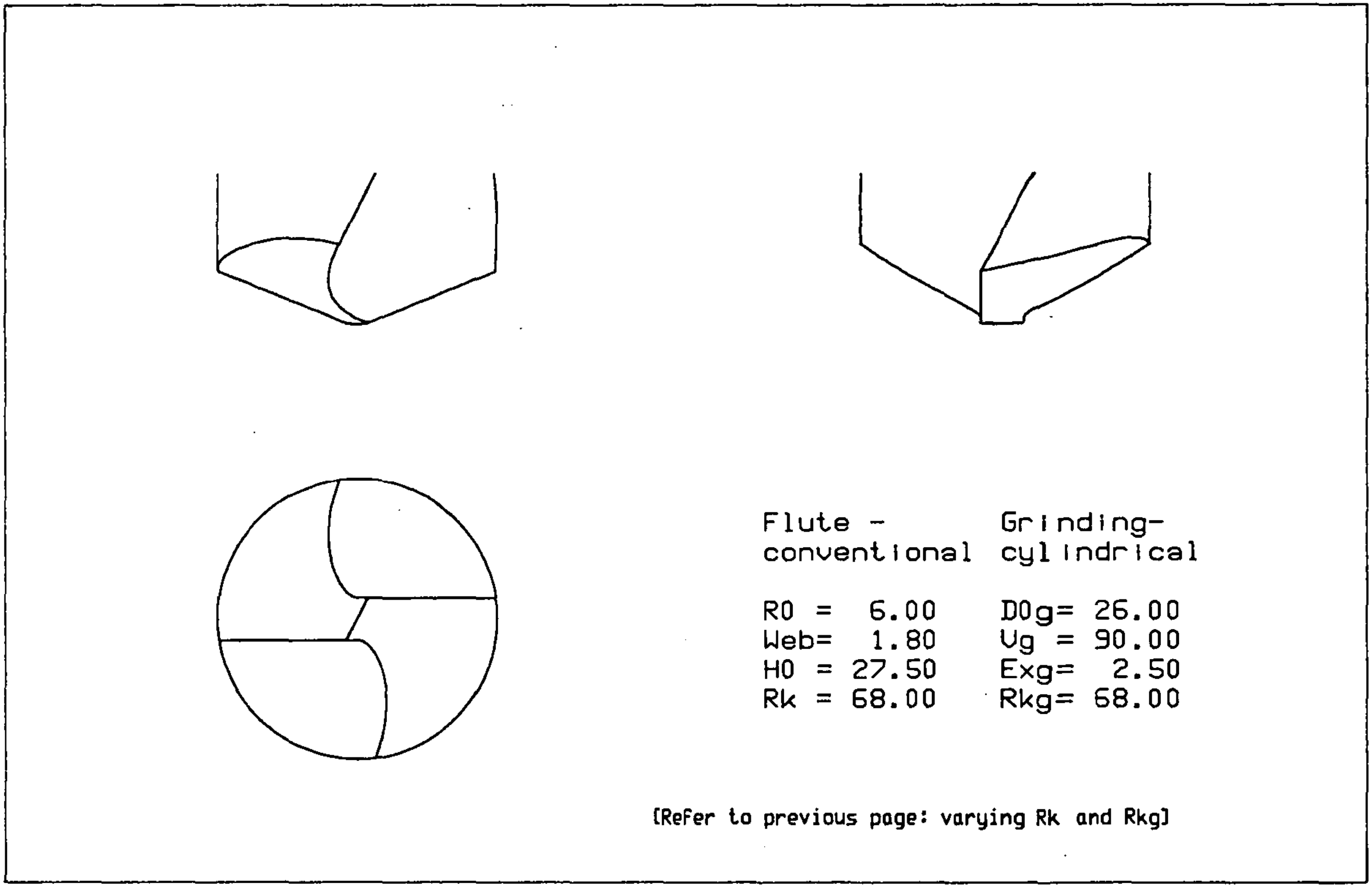


Computer geometric simulation of drill point

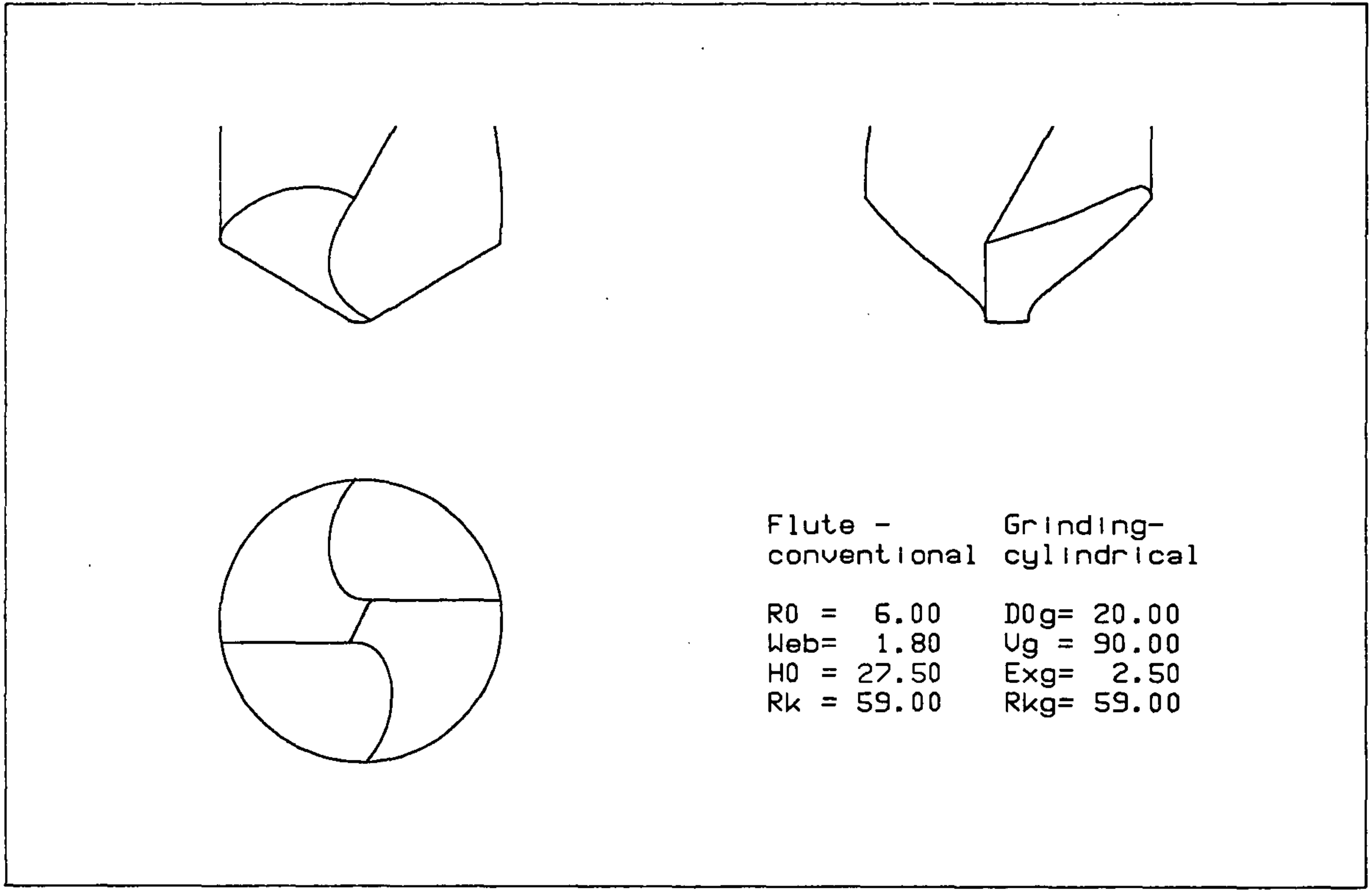


Computer geometric simulation of drill point

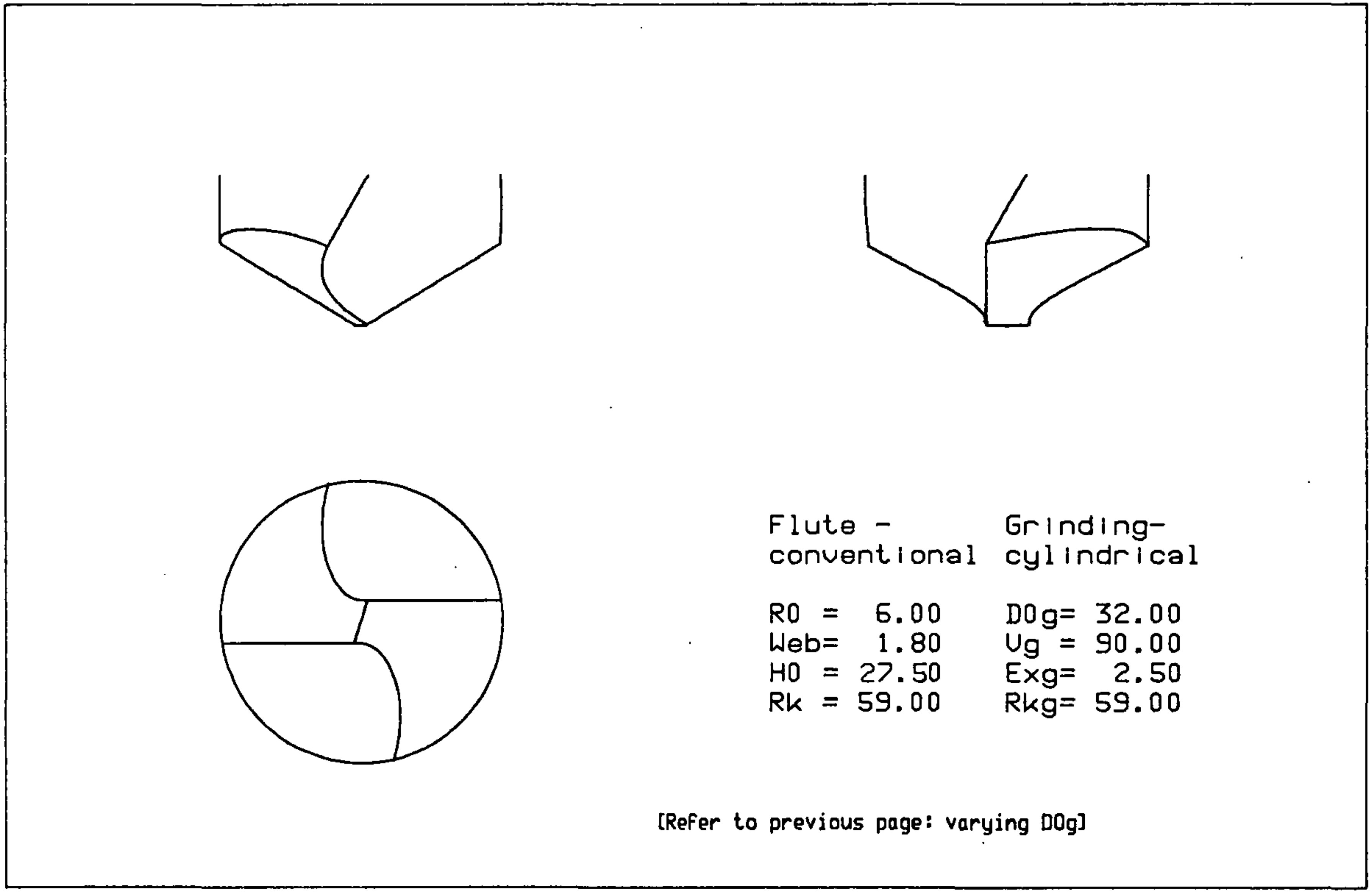


Computer geometric simulation of drill point

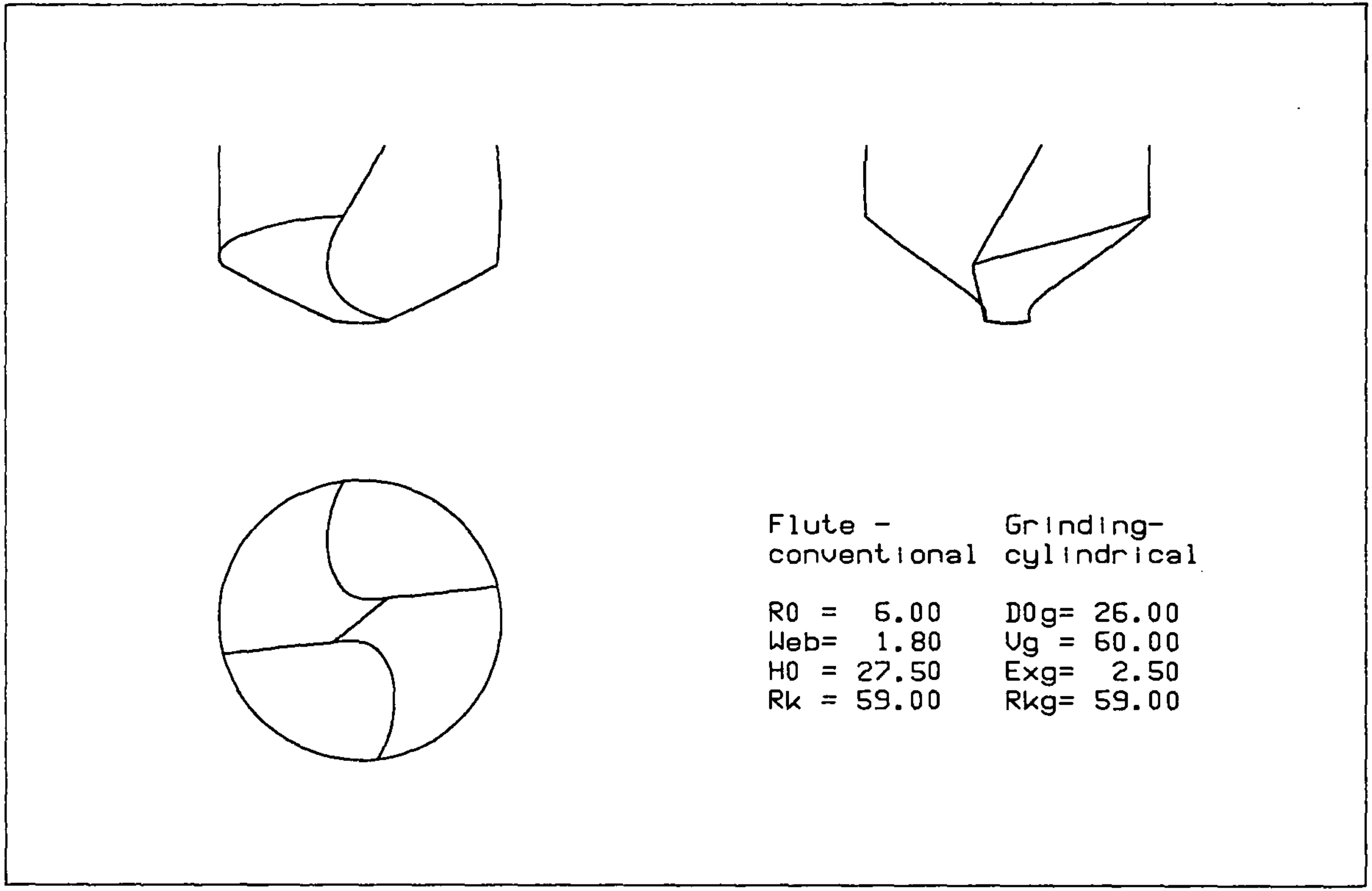


Computer geometric simulation of drill point

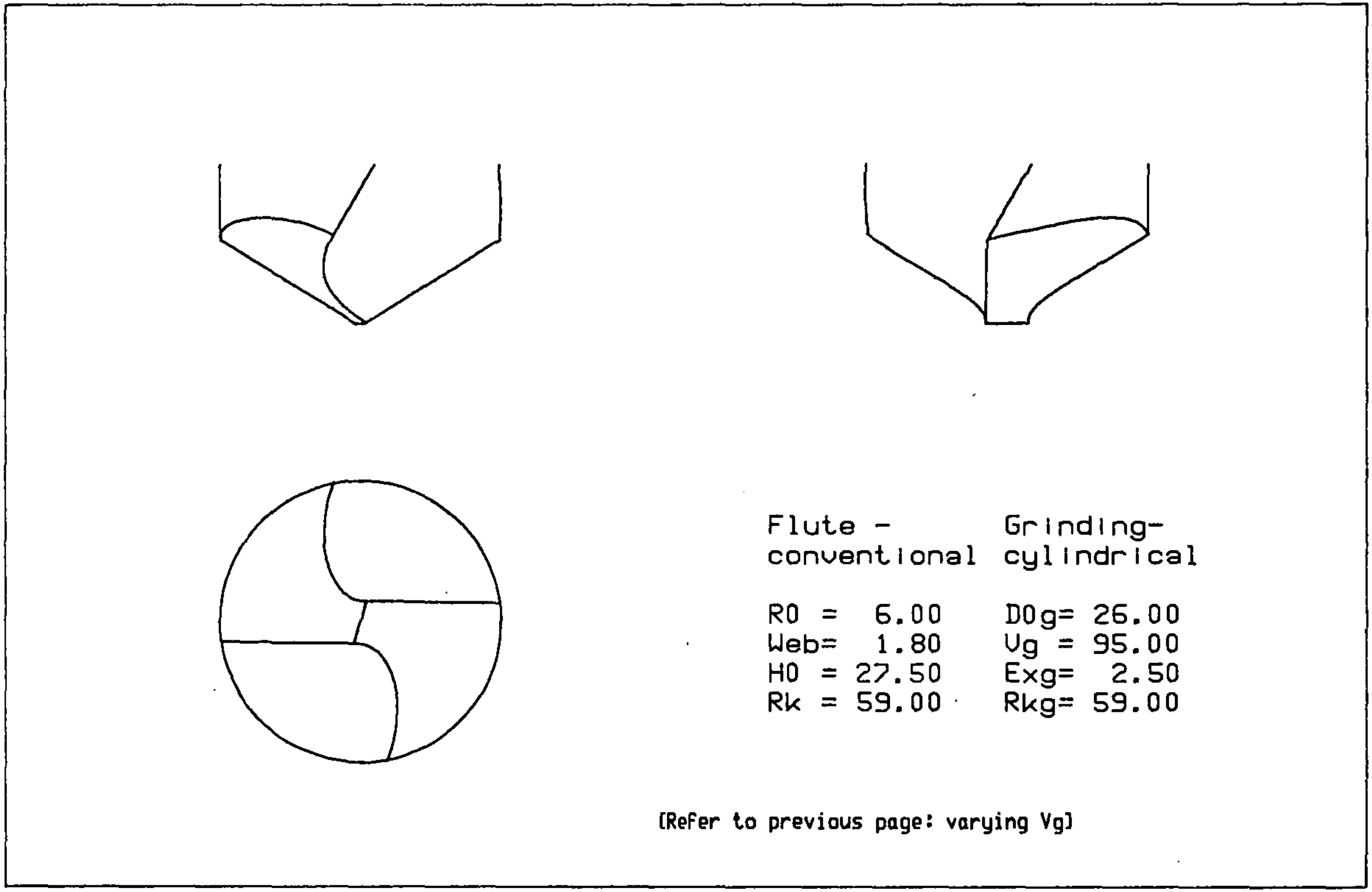


Computer geometric simulation of drill point

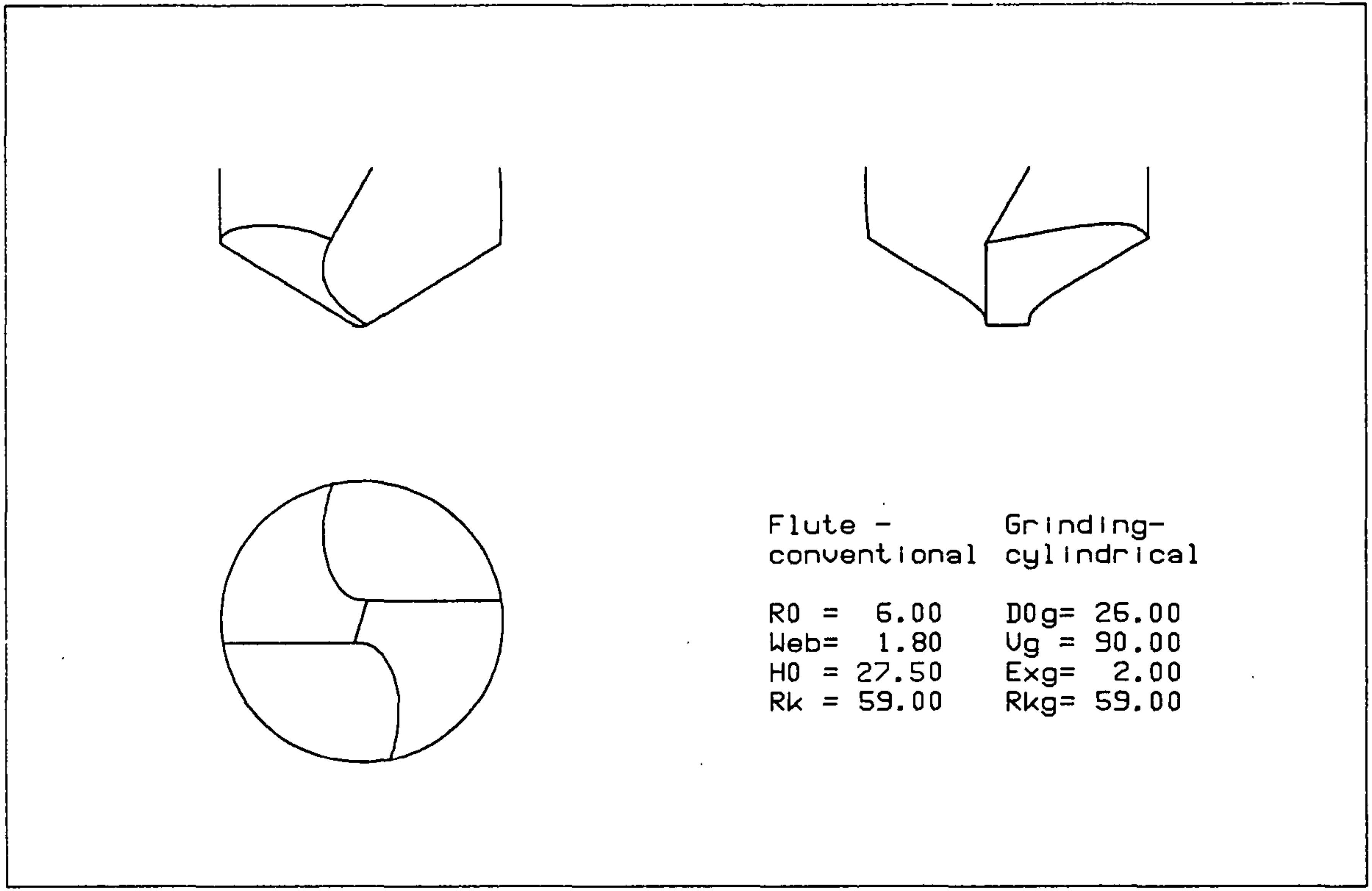


Computer geometric simulation of drill point

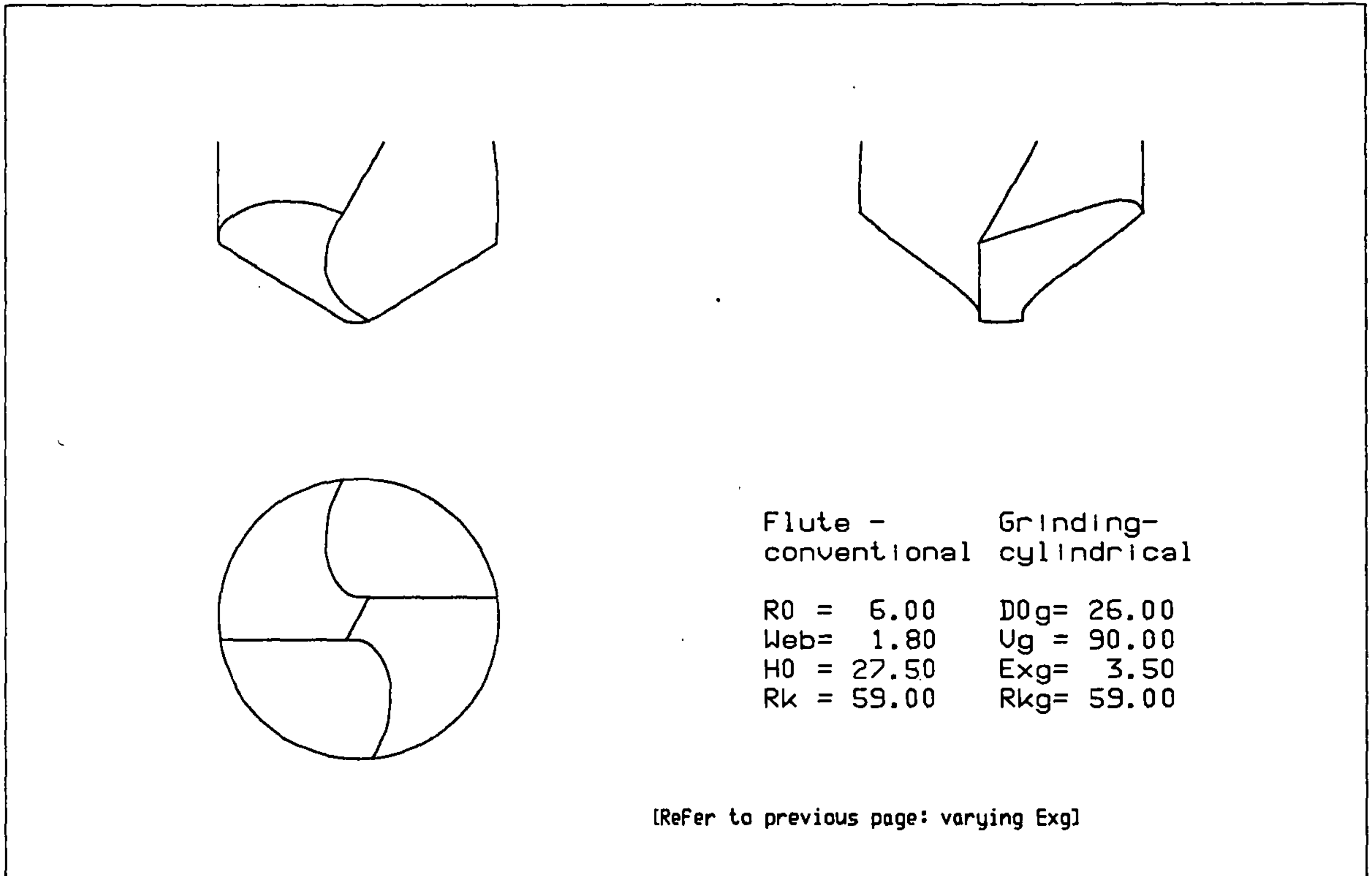


Computer geometric simulation of drill point

## APPENDIX 3

Computer plots of normal rake angle against radial distance showing the effect of flute design and cylindrical grinding parameters on the rake angle variation (refer to Chapter 4).

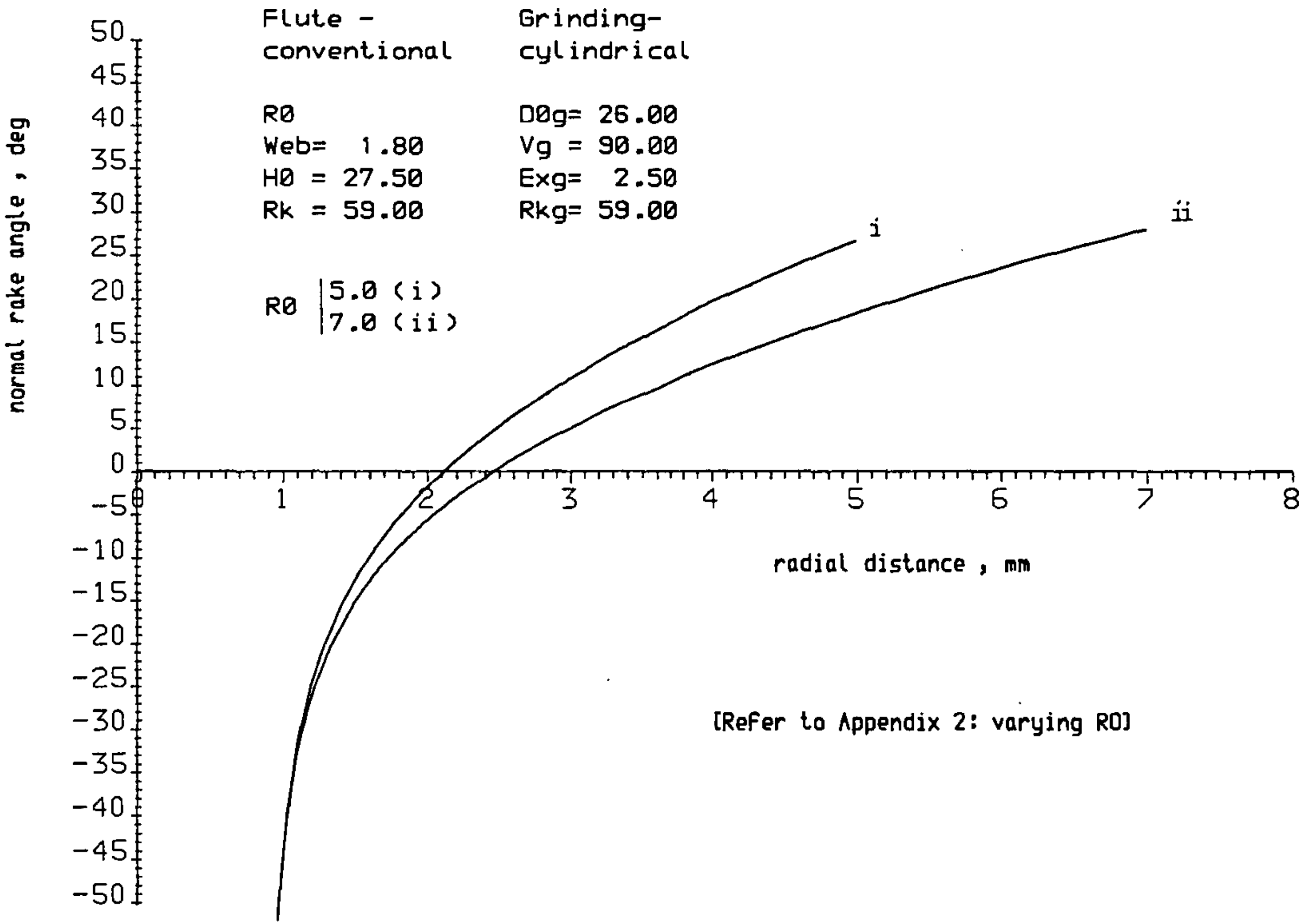
Flute - conventional
Grinding- cylindrical
R0
Web= 1.80
H0 = 27.50
Rk = 59.00
D0g= 26.00
Vg = 90.00
Exg= 2.50
Rkg= 59.00
R0 | 5.0 (i) | 7.0 (ii)
i
ii
normal rake angle , deg
radial distance , mm
50
45
40
35
30
25
20
15
10
5
0
-5
-10
-15
-20
-25
-30
-35
-40
-45
-50
0
1
2
3
4
5
6
7
8
[Refer to Appendix 2: varying R0]

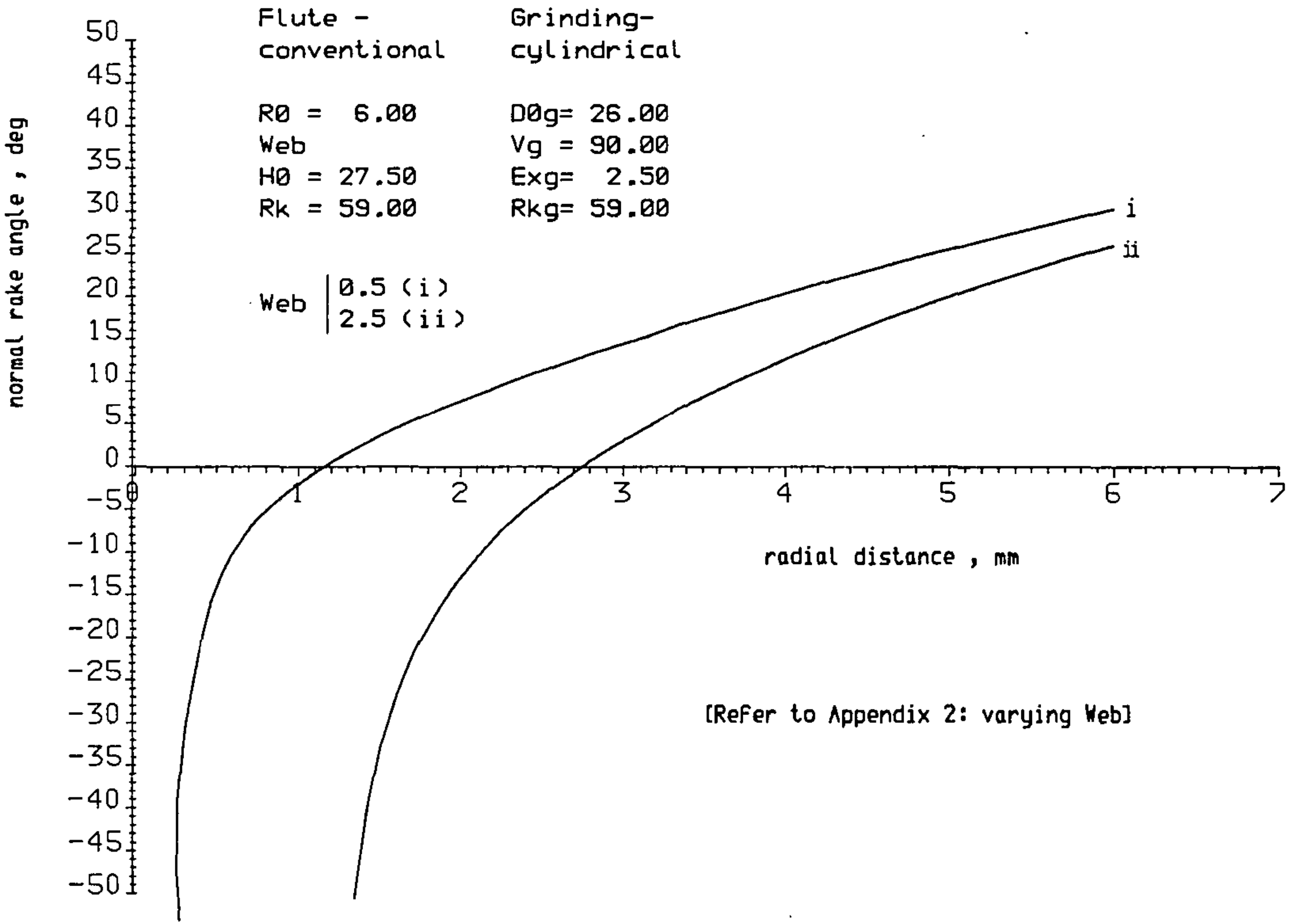
Flute -
conventional
Grinding-
cylindrical
R0 = 6.00
Web
H0 = 27.50
Rk = 59.00
D0g= 26.00
Vg = 90.00
Exg= 2.50
Rkg= 59.00
Web | 0.5 (i)
2.5 (ii)
i
ii
normal rake angle , deg
radial distance , mm
[Refer to Appendix 2: varying Web]

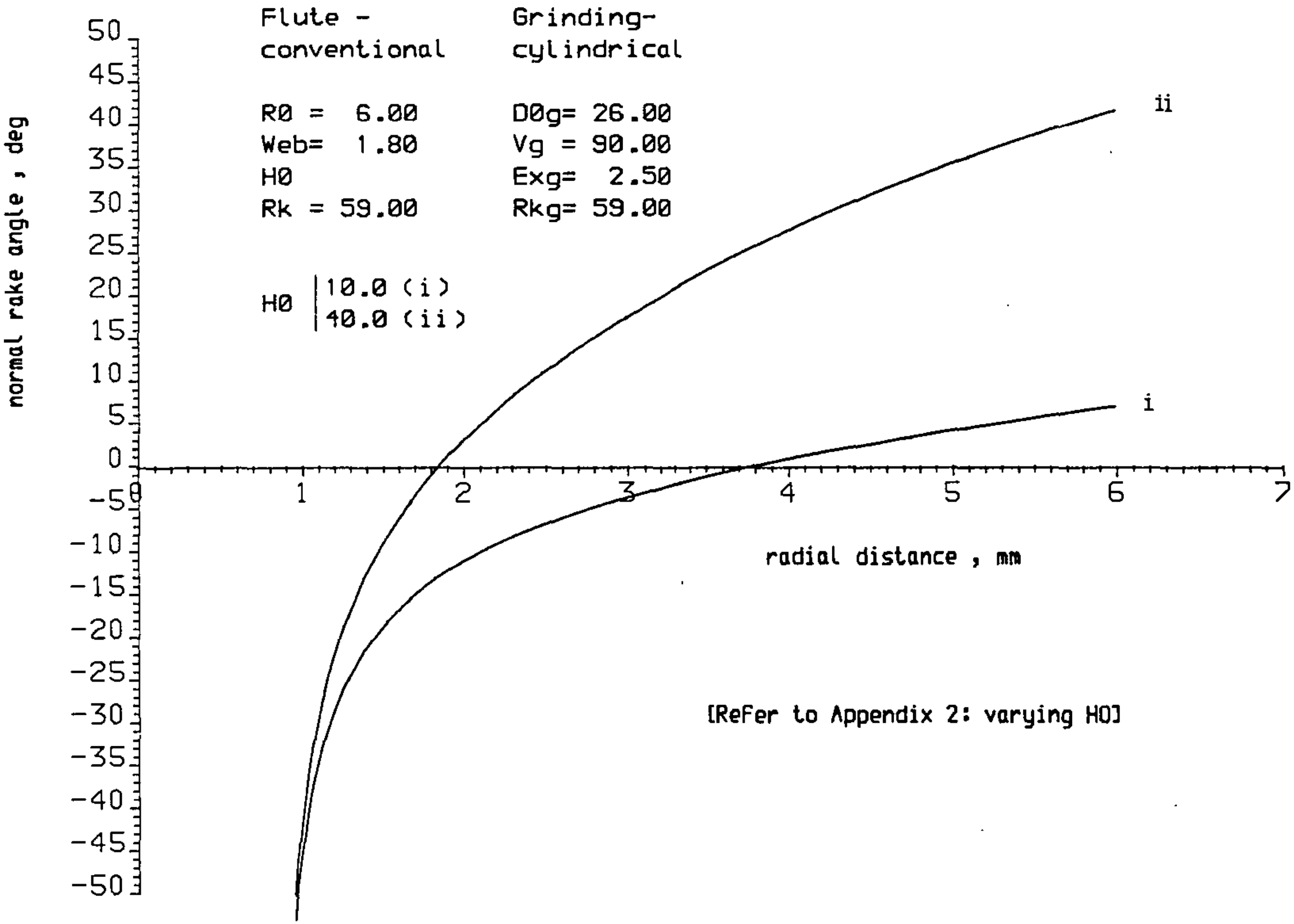
Flute -
conventional
Grinding-
cylindrical
R0 = 6.00
Web= 1.80
H0
Rk = 59.00
D0g= 26.00
Vg = 90.00
Exg= 2.50
Rkg= 59.00
H0 | 10.0 (i) | 40.0 (ii)
normal rake angle , deg
radial distance , mm
i
ii
50
45
40
35
30
25
20
15
10
5
0
-5
-10
-15
-20
-25
-30
-35
-40
-45
-50
0
1
2
3
4
5
6
7
[Refer to Appendix 2: varying H0]

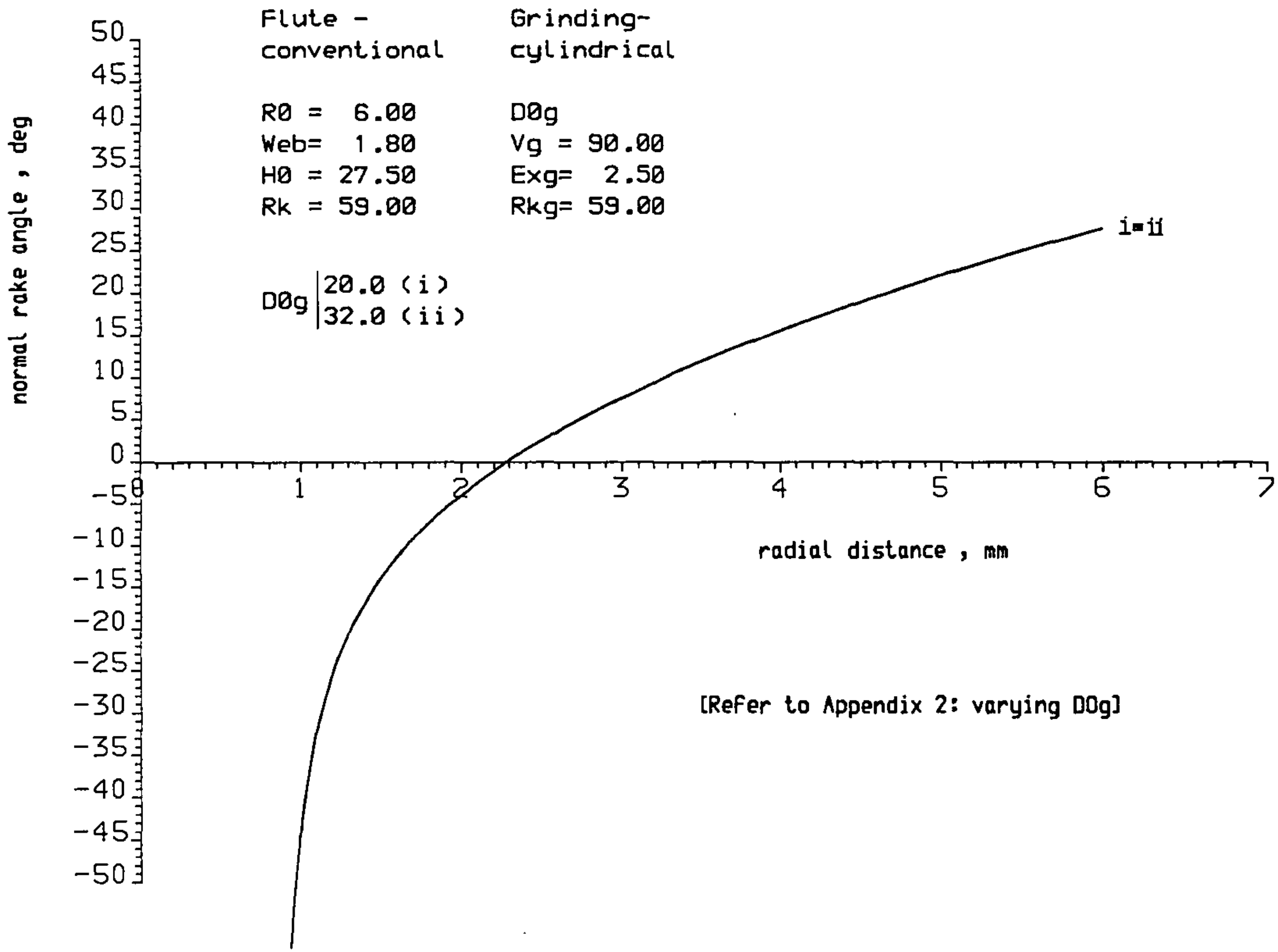
Flute -
conventional
Grinding-
cylindrical
R0 = 6.00
Web= 1.80
H0 = 27.50
Rk = 59.00
D0g
Vg = 90.00
Exg= 2.50
Rkg= 59.00
D0g 20.0 (i)
32.0 (ii)
i=ii
normal rake angle , deg
radial distance , mm
[Refer to Appendix 2: varying D0g]

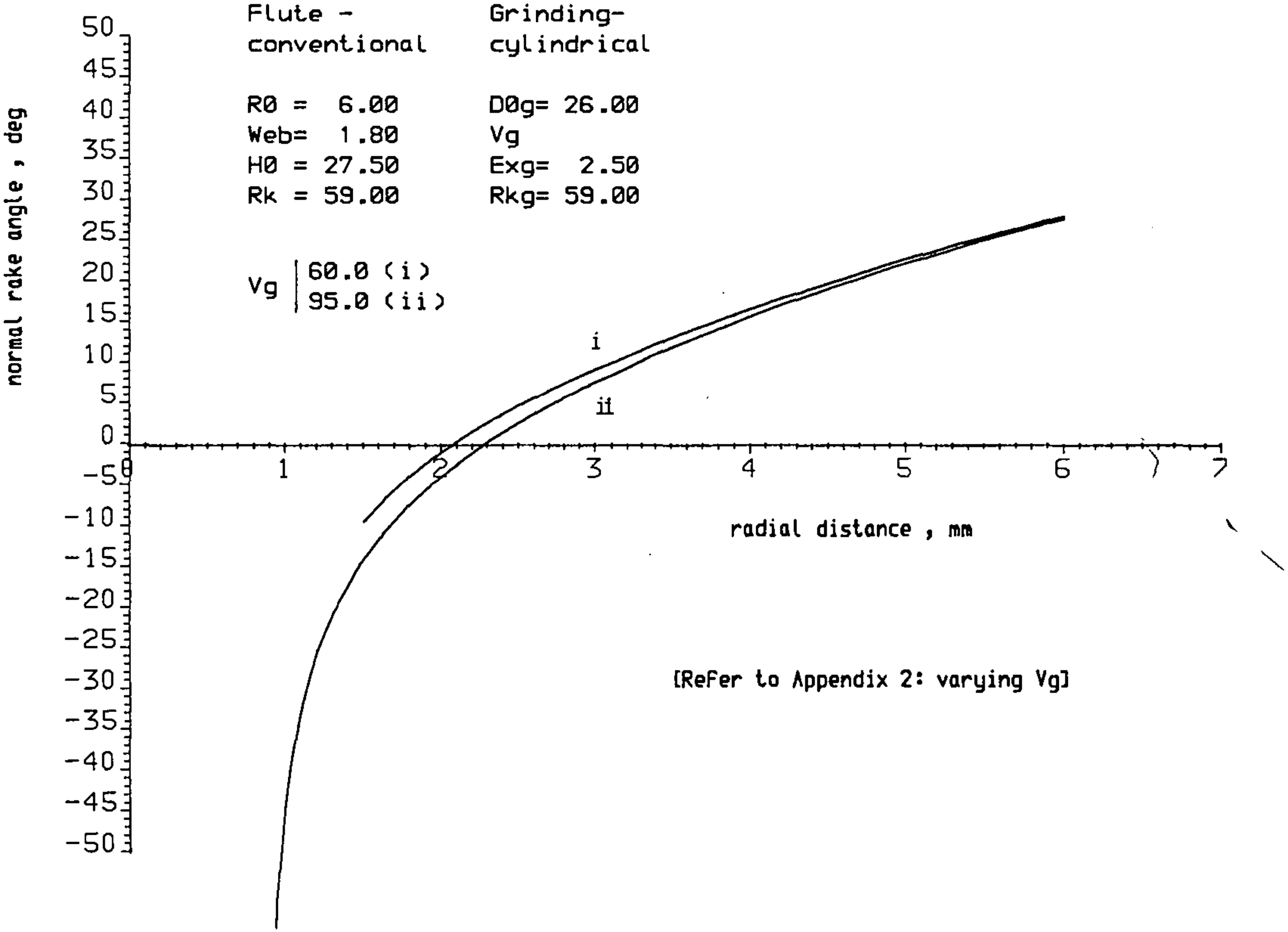

Flute -
conventional
Grinding-
cylindrical
R0 = 6.00
Web= 1.80
H0 = 27.50
Rk = 59.00
D0g= 26.00
Vg
Exg= 2.50
Rkg= 59.00
Vg | 60.0 (i)
95.0 (ii)
normal rake angle , deg
radial distance , mm
i
ii
50
45
40
35
30
25
20
15
10
5
0
-5
-10
-15
-20
-25
-30
-35
-40
-45
-50
0
1
2
3
4
5
6
7
[Refer to Appendix 2: varying Vg]

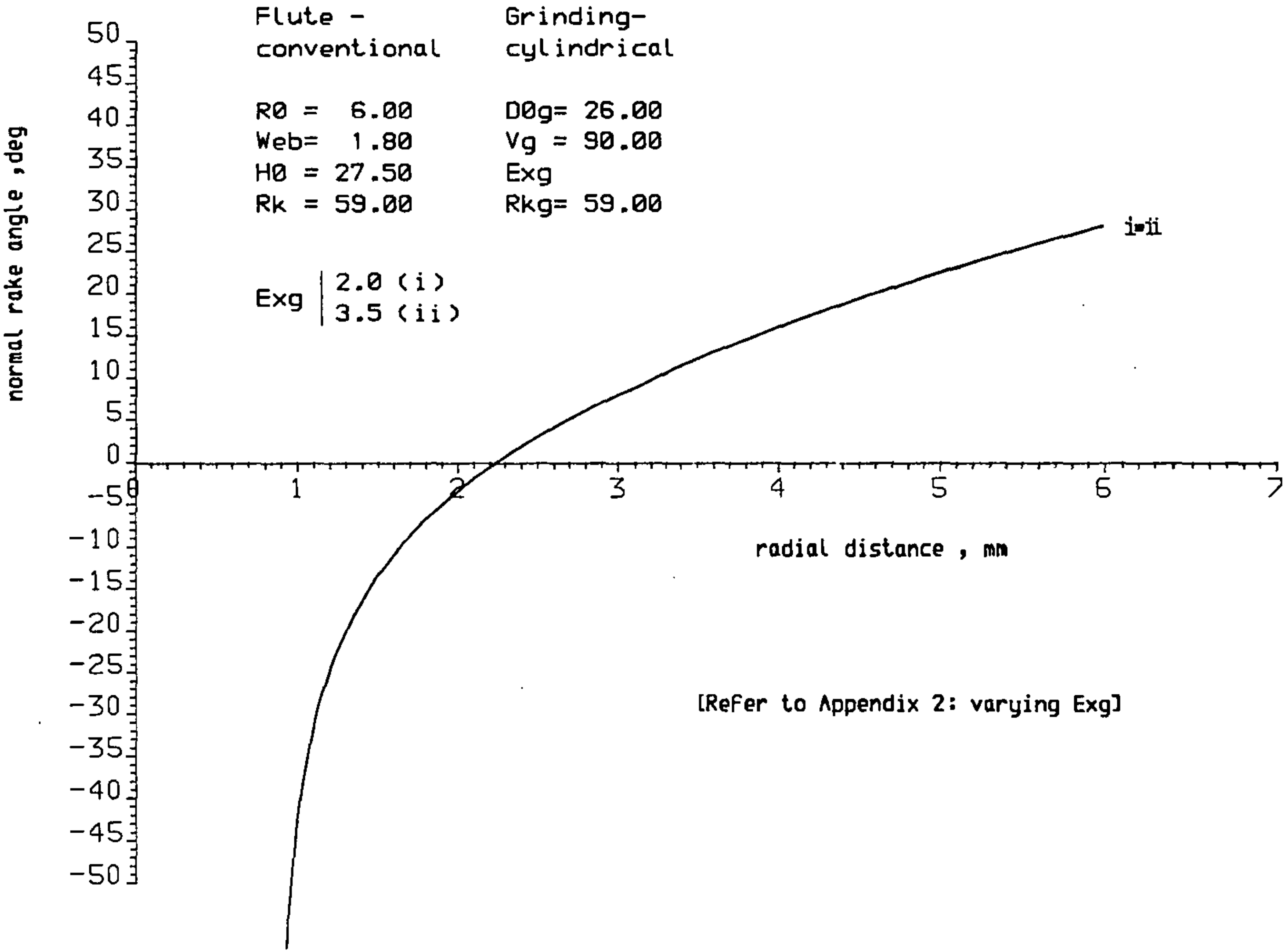

Flute -
conventional
Grinding-
cylindrical
R0 = 6.00
Web= 1.80
H0 = 27.50
Rk = 59.00
D0g= 26.00
Vg = 90.00
Exg
Rkg= 59.00
Exg | 2.0 (i)
| 3.5 (ii)
i=ii
normal rake angle ,deg
radial distance , mm
50
45
40
35
30
25
20
15
10
5
0
-5
-10
-15
-20
-25
-30
-35
-40
-45
-50
0
1
2
3
4
5
6
7
[Refer to Appendix 2: varying Exg]

# APPENDIX 4

Computer plots of normal clearance angle against radial distance showing the effect of flute design and cylindrical grinding parameters on clearance angle variation (refer to Chapter 4).

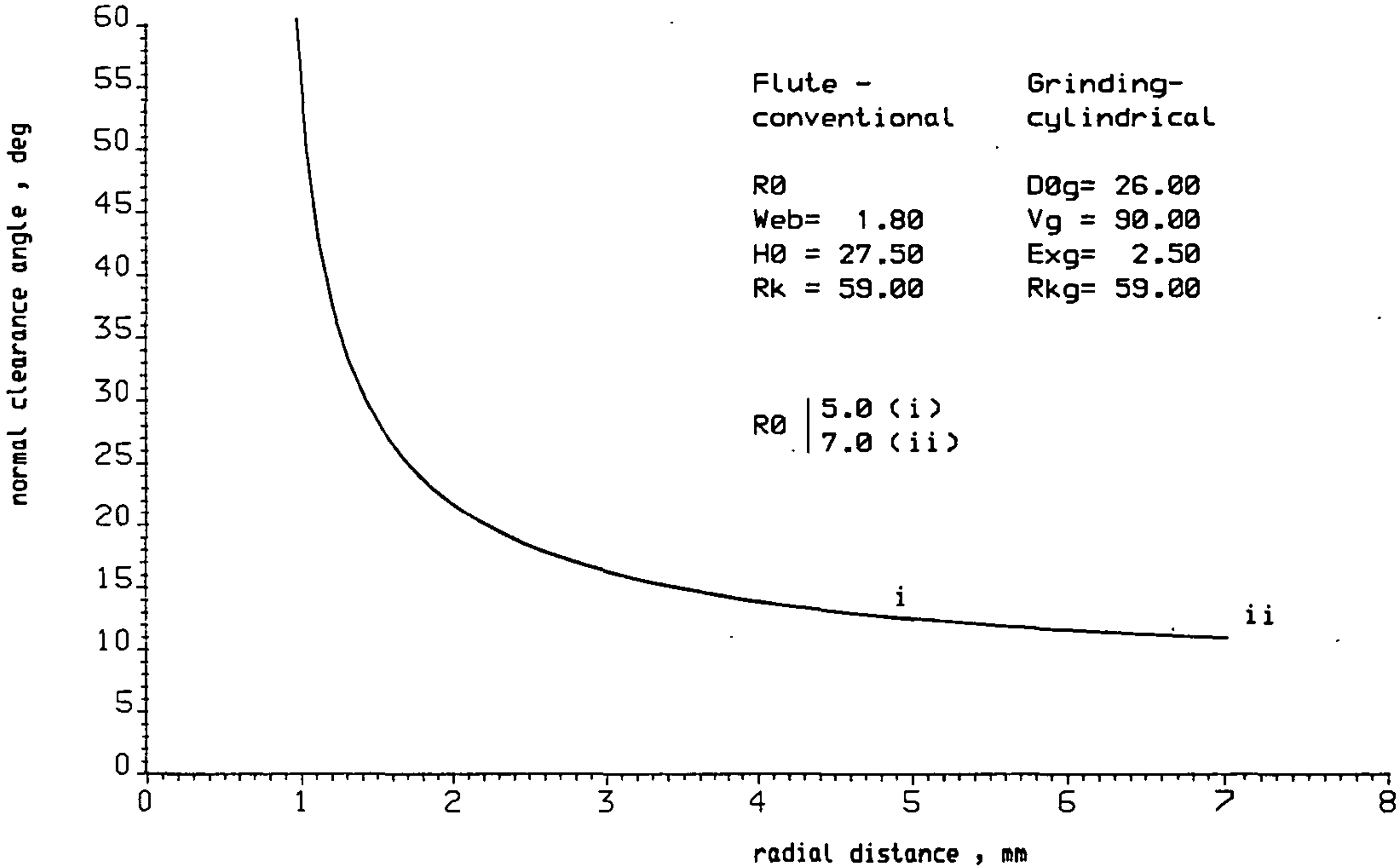


[Refer to Appendix 2: varying RO]

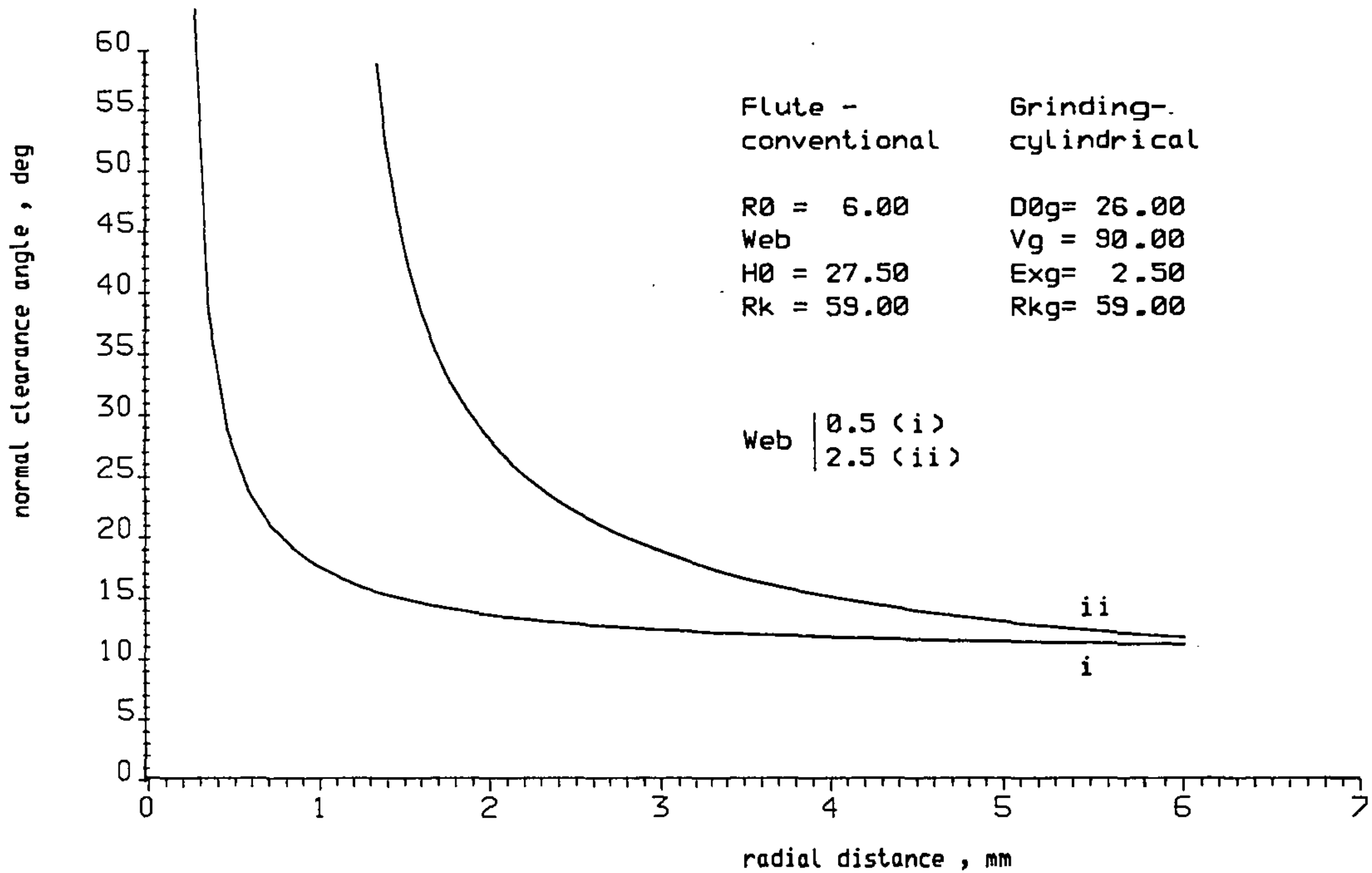


[Refer to Appendix 2: varying Web]

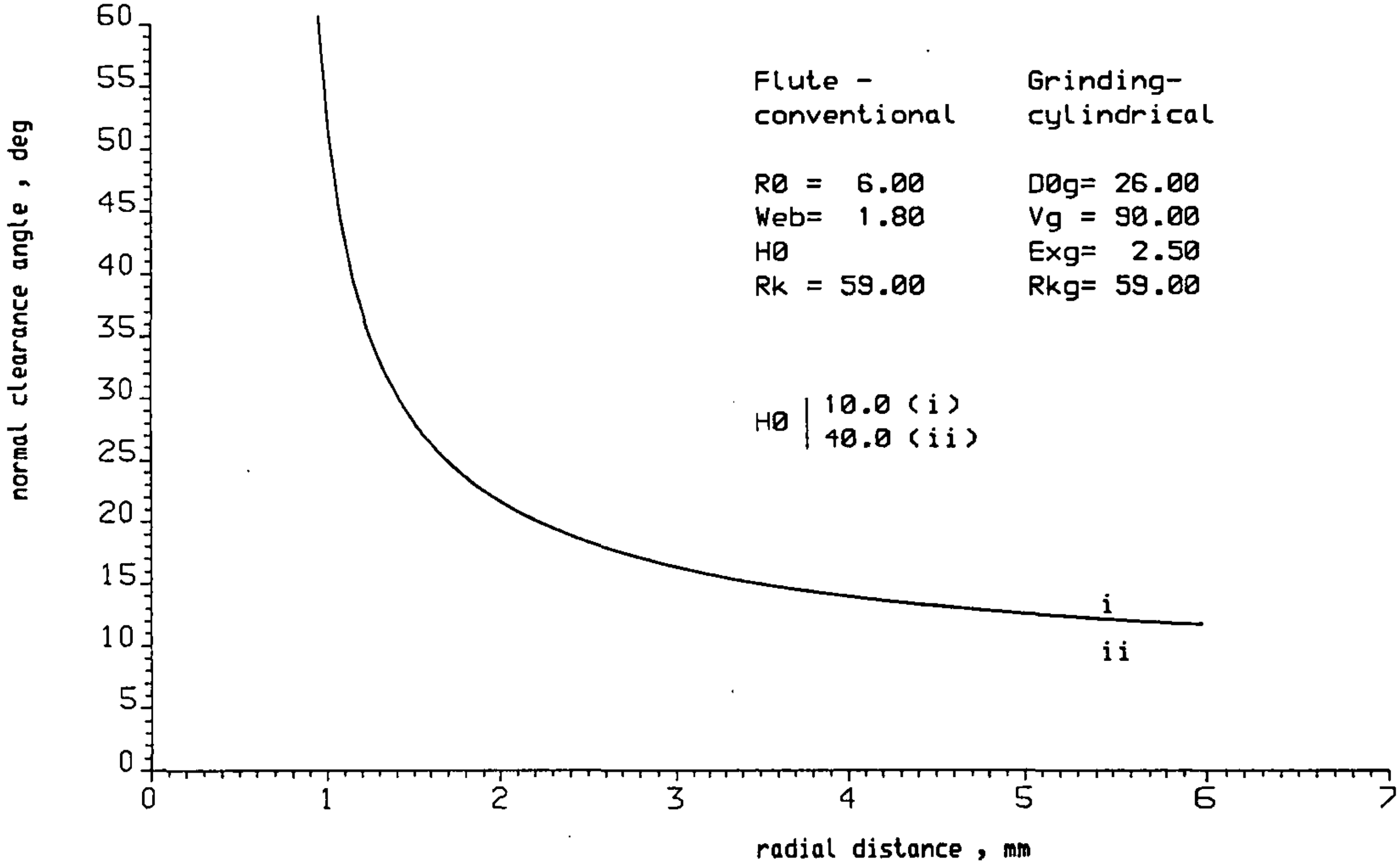


[Refer to Appendix 2: varying HO]

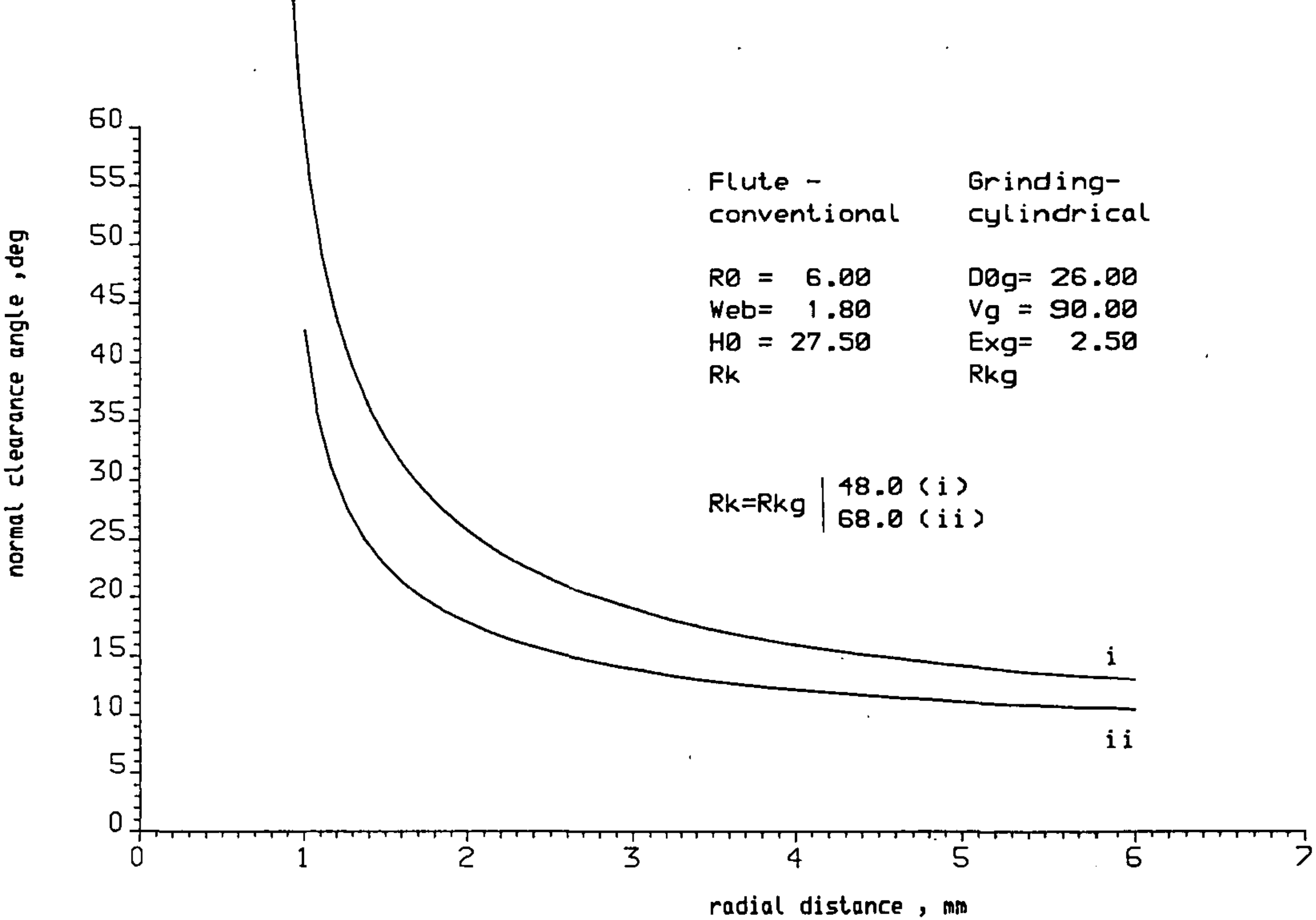


[Refer to Appendix 2: varying Rk and Rkg]

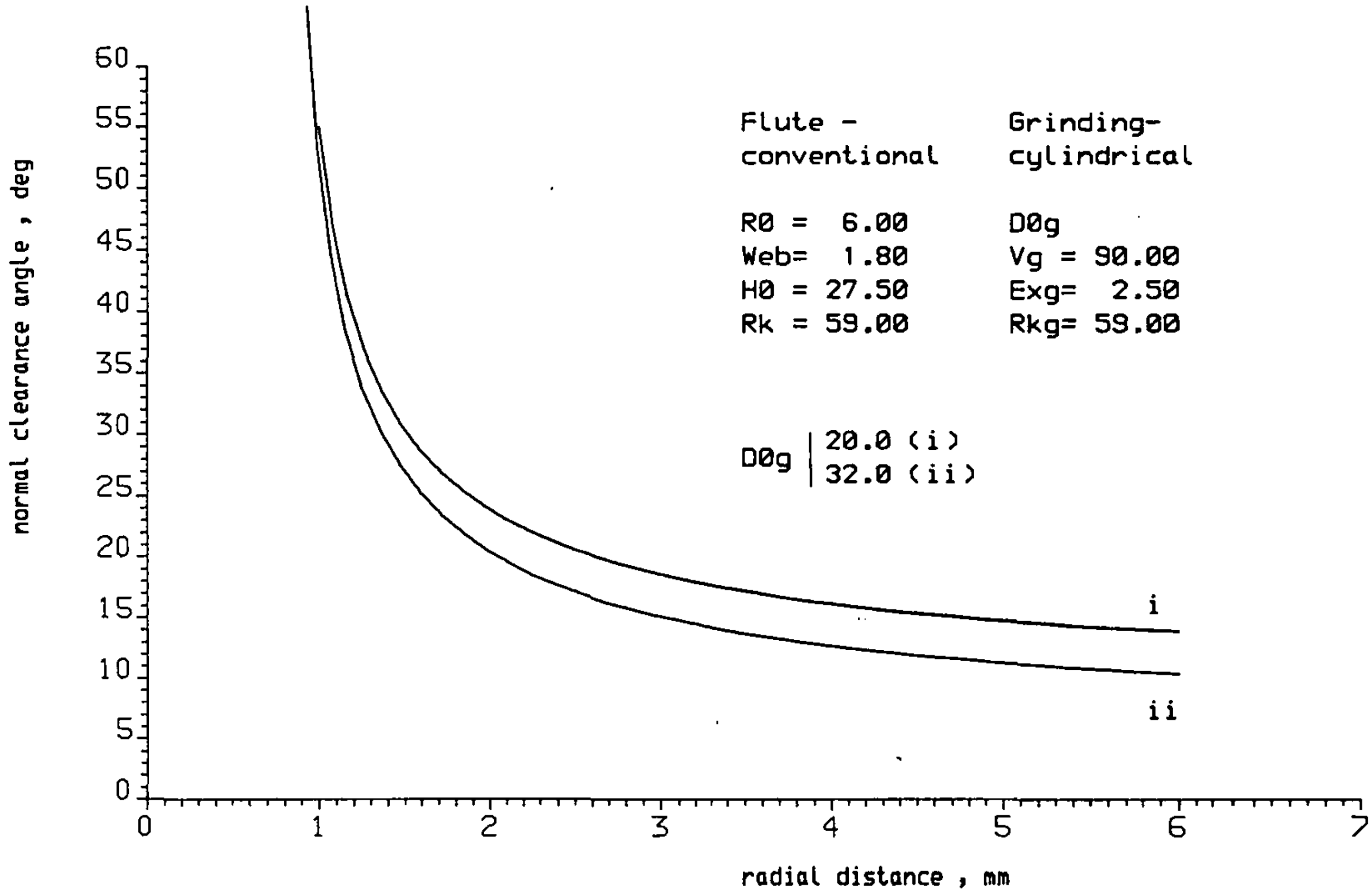


[Refer to Appendix 2: varying D0g]

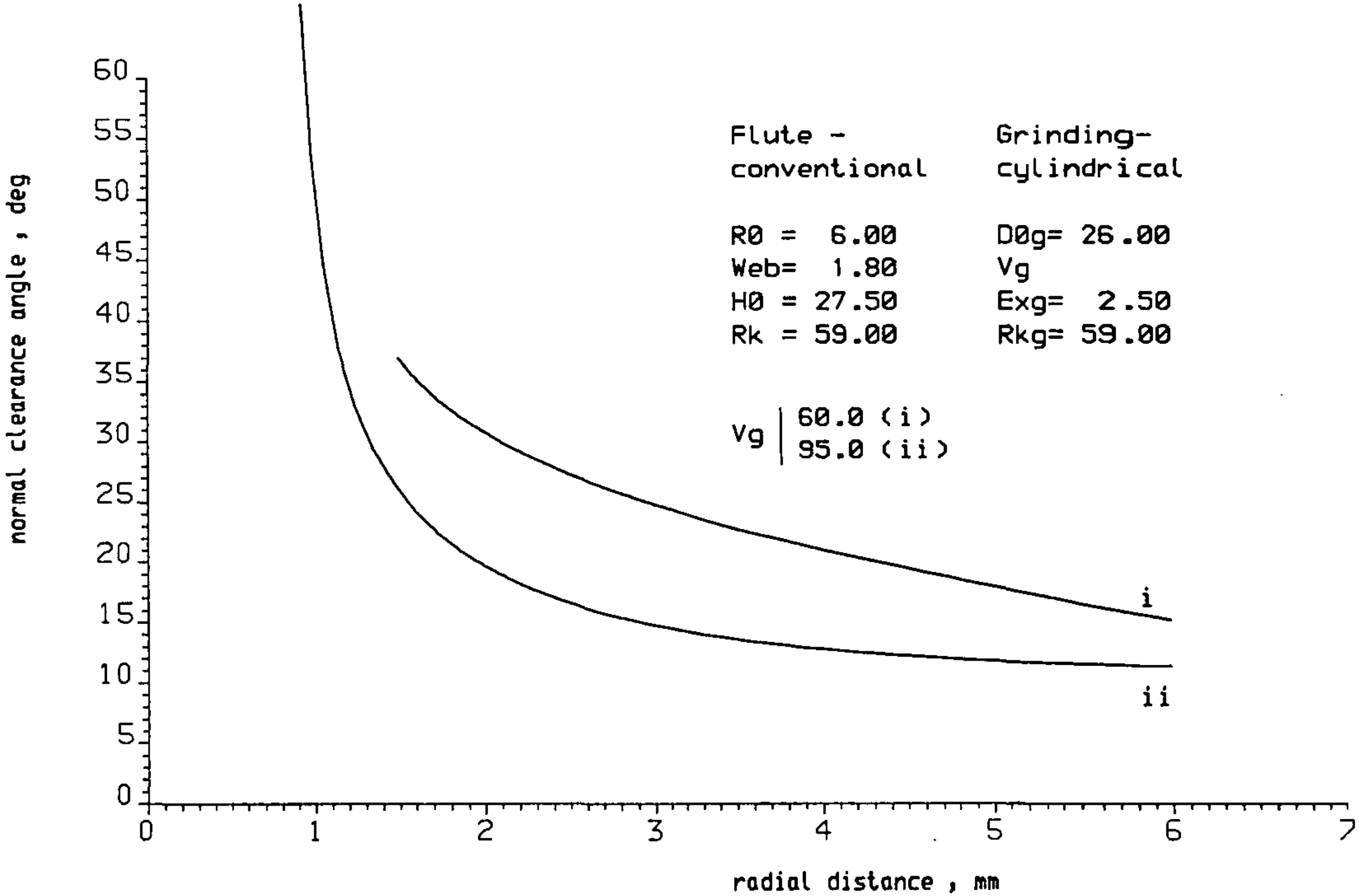


[Refer to Appendix 2: varying Vg]

# APPENDIX 5

Computer plots of inclination angle against radial distance showing the effect of flute design and cylindrical grinding parameters on inclination angle variation (refer to Chapter 4).

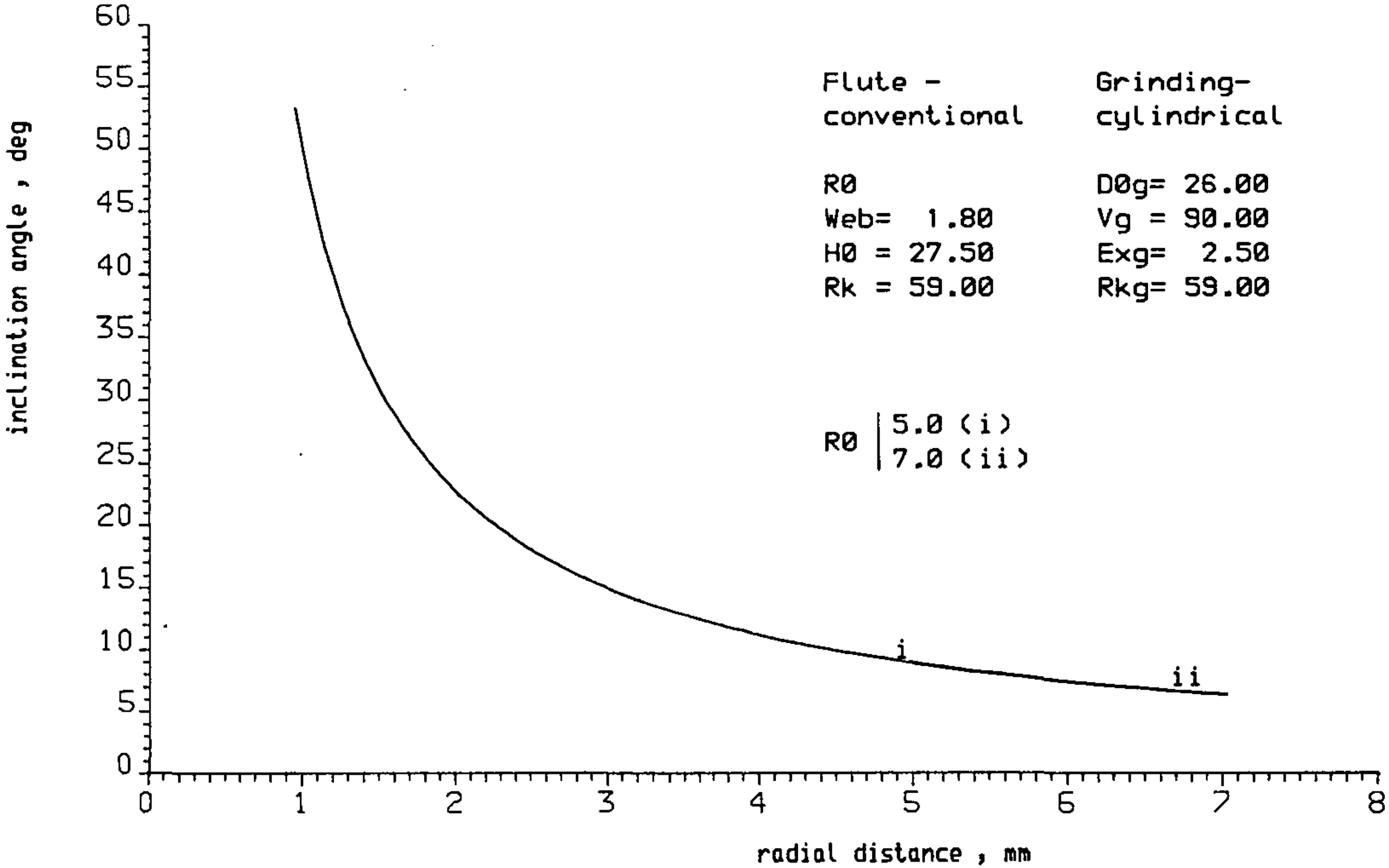


[Refer to Appendix 2: varying RO]

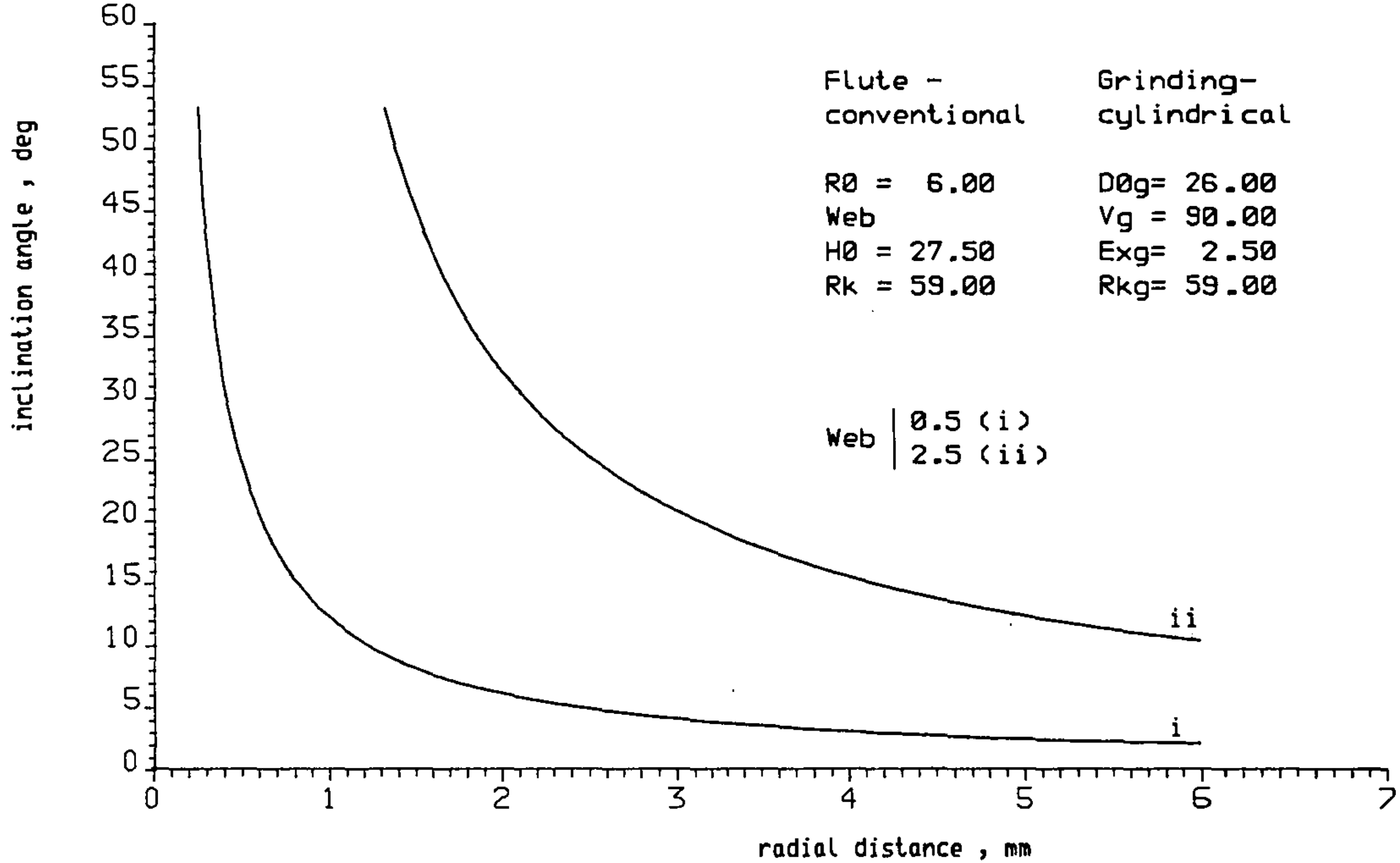


[Refer to Appendix 2: varying Web]

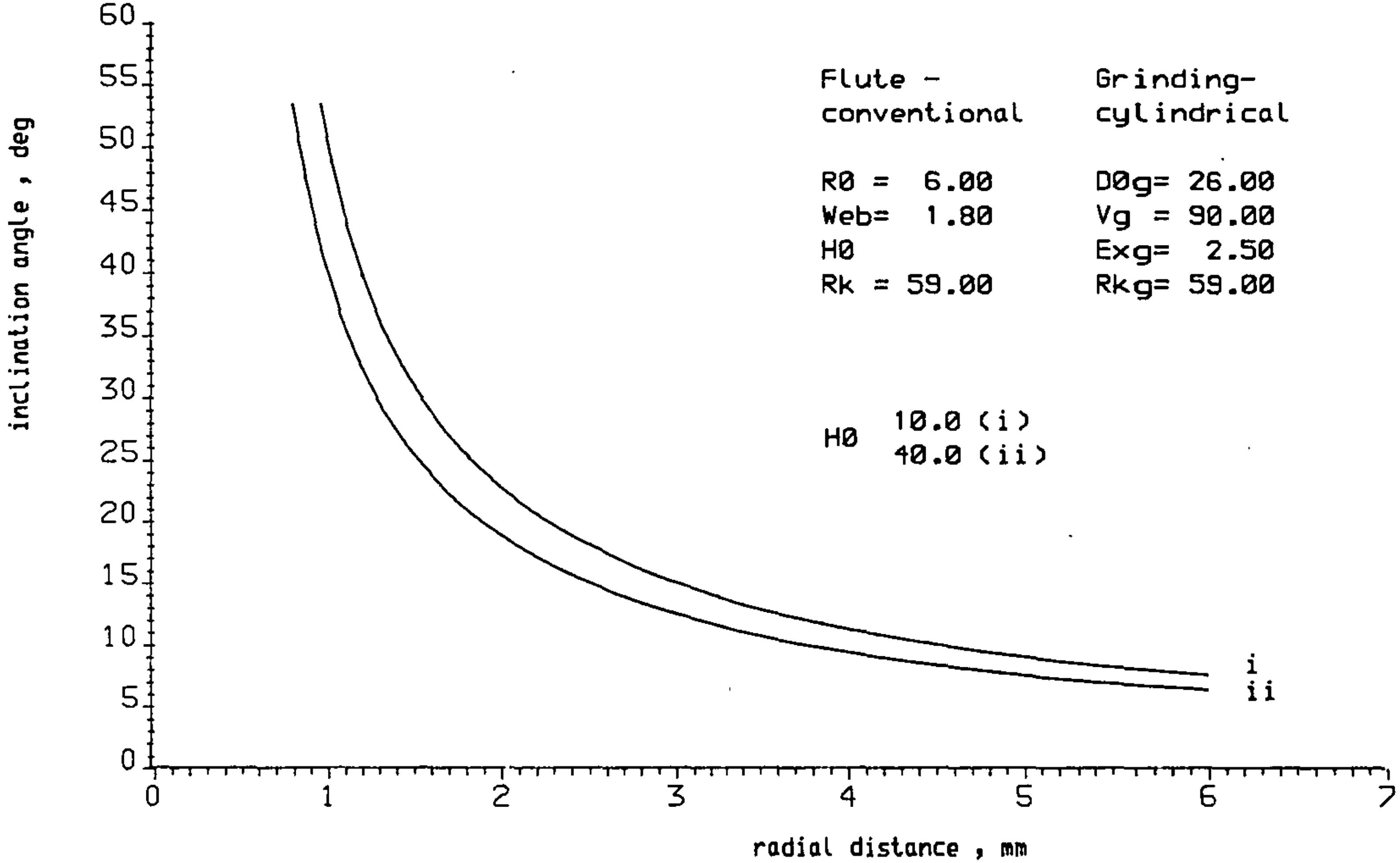


[Refer to Appendix 2: varying H0]

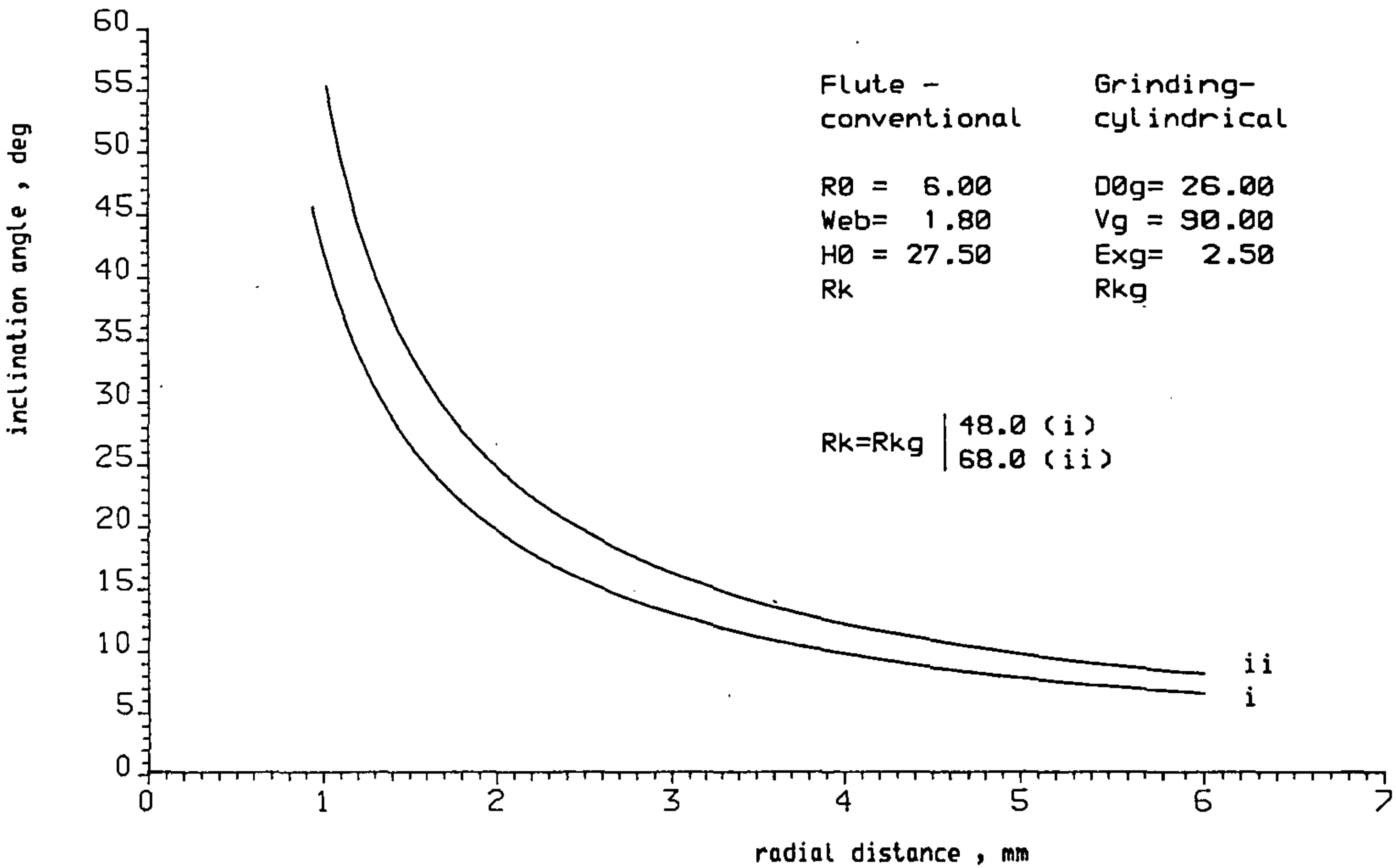


[Refer to Appendix 2: varying Rk and Rkg]

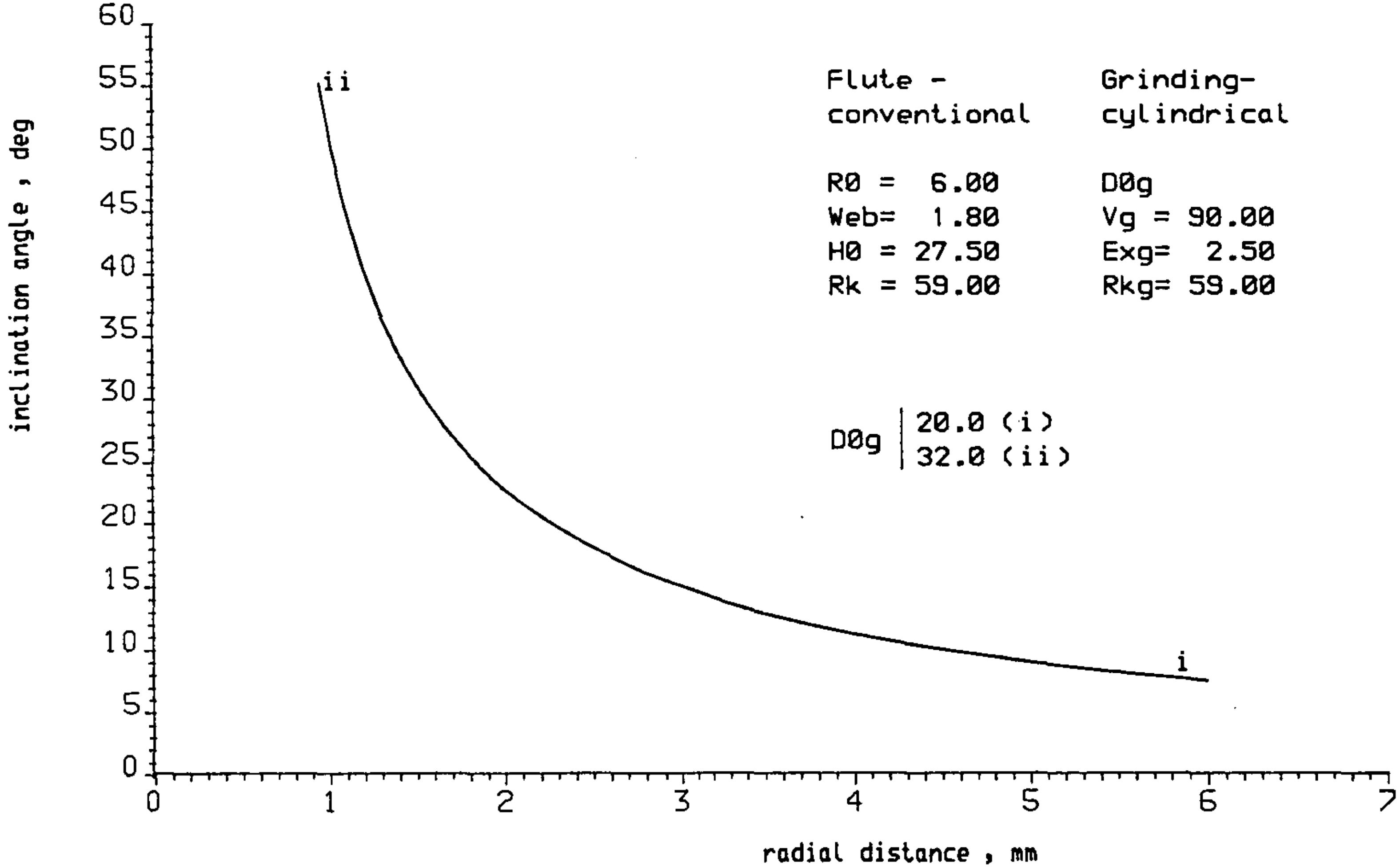


[Refer to Appendix 2: varying D0g]

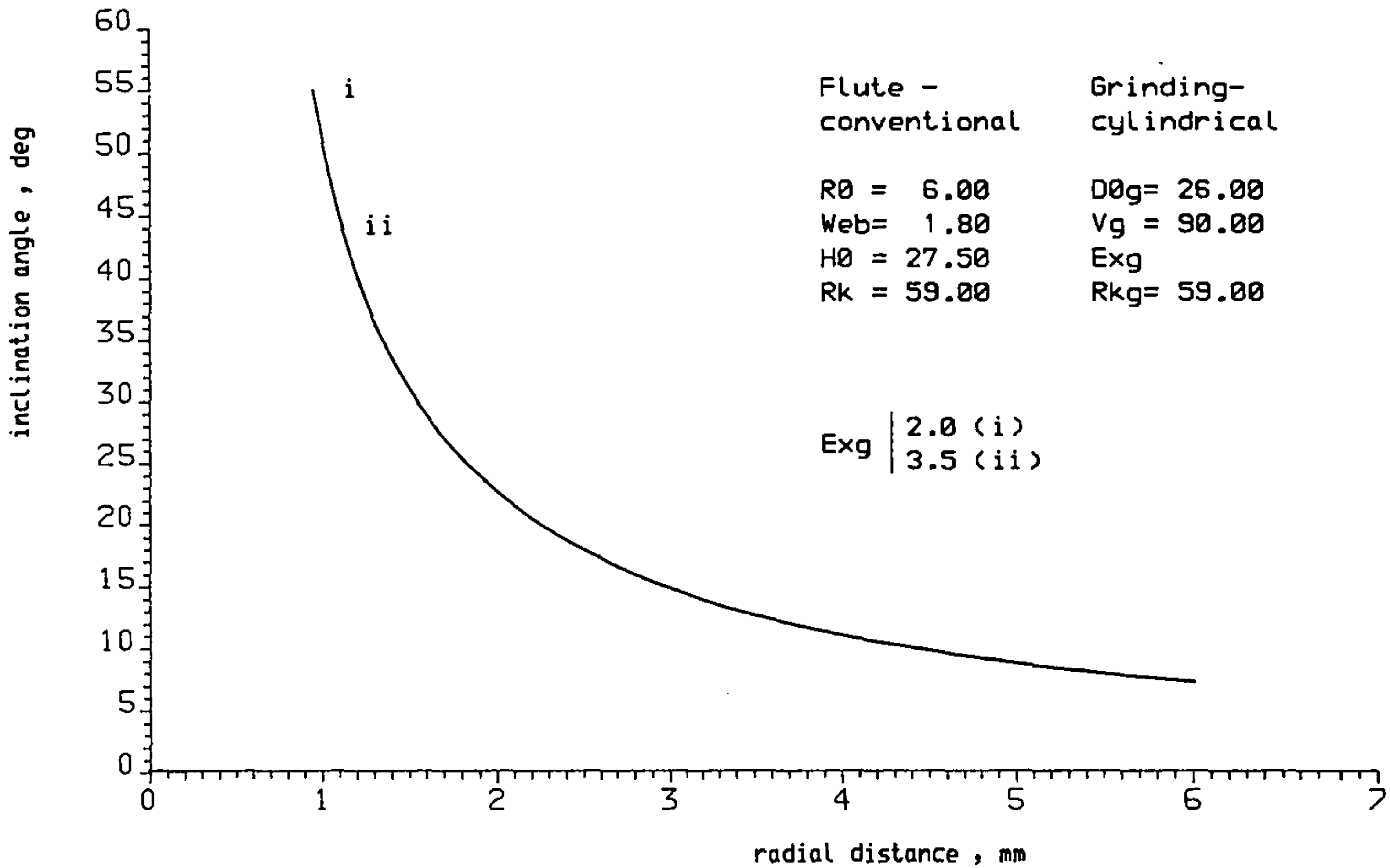


[Refer to Appendix 2: varying Exg]

# APPENDIX 6

Computer program for non-conventional (and conventional) flute generation.
General flute design according to the cutting angles along the drill lip (refer to Chapter 5).
This FORTRAN program uses subroutines from GINO and NAG libraries which are not listed here.

```
C
C
C ================================================
C
C        NON-CONVENTIONAL (AND CONVENTIONAL)
C        FLUTE GENERATION
C
C        GENERAL FLUTE DESIGN ACCORDING TO THE
C        CUTTING ANGLES ALONG THE DRILL LIP
C
C        DESIGNED,DEVELOPED AND IMPLEMENTED BY
C        MANUEL DOS SANTOS PAIS
C
C ================================================
C
C
      IMPLICIT DOUBLE PRECISION (A-H,O-Z)
      REAL R0P,R0N
      REAL XEEL(200),YEEL(200),XAXIS,YAXIS,XCOR,YCOR
      REAL XCIRE(200),YCIRE(200),XCIRD(200),YCIRD(200)
      REAL XCHIG(200),YCHIG(200),ZCHIG(200)
      REAL XFLU(200),YFLU(200),XS(200),YS(200)
      REAL XSTG(200),YSTG(200),ZSTG(200)
      REAL DINCC(200),WEDGE(200),RSINC(200)
      DIMENSION XCHI2(200),YCHI2(200)
      DIMENSION RU(7),T1PR(200),T2PR(200),STEPXY(7),WW(400)
      DIMENSION WS(3,7),REAU(200),REAUX(200)
      DIMENSION DDIS(200)
      DIMENSION VAR(3)
      DIMENSION DF2(3),C12(4),C21(7)
      DIMENSION RE(4),STEPMX(4),W(120)
      DIMENSION SSS(200)
      DIMENSION FJAC(4,4),SMON(4),V(4,4),IW(1),WE0(120)
      DIMENSION GAMAA(200),CLEAA(200),GAMAE(200)
      DIMENSION RADI(200),T211(200),ETAA(200),VVCA(200)
      DIMENSION ETACHA(200),RCA(200),GEMEA(200)
      EXTERNAL DERIV2,GRIN,MONIT,RESID
      COMMON/BLO0/XFLU,YFLU,CWEDGE,RCA,ETACHA,XSTG,YSTG,ZSTG
      COMMON/BLO1/NPOINT,MAXCAL,T1PR,T2PR,NLOOP
      COMMON/BLO2/DFDX,DFDY,DFDZ,CE1,CE2,CE3
      COMMON/BLO3/PA,REVAB,VG,RKG,EXG
      COMMON/BLO4/SNVG,CSVG,SNKOI,CSKOI
      COMMON/BLO5/SENETA,CSGAMA,VVCV,SGAMAE,GEMEA,SGAMA
      COMMON/BLO6/DINCC,GAMAA,CLEAA,GAMAE,ETAA,VVCA
      COMMON/BLO7/RADI,T211,SSS
      COMMON/BLO8/H0,CONS,R0,WEB,R0G,IWRITE,PI
      COMMON/BLO10/C12,C21
      COMMON/BLO11/DIDS,Z0
      COMMON/BLO12/BAFTOL
      COMMON/BLO14/XCE,YCE,ZCE,XCORN,YCORN,ZCORN,ZX0Y0
      COMMON/BLO15/ISTINS,J
      COMMON/BLO20/XST0,YST0,ZST0,RC0
      COMMON/BLO21/XS,YS
C
C READING DATA
      WRITE(1,73)
73    FORMAT('READ R0,WEB,H0,EXG,VG,RKG,R0G'/
     $'FOR DRILL BODY AND POINT ARCHITECTURE')
      READ(1,*)R0,WEB,H0,EXG,VG,RKG,R0G
      WRITE(1,71)
71    FORMAT(/'READ NUMBER OF POINTS ON THE LIP')
      READ(1,*)NPOINT
      NLOOP=3*NPOINT
C
      PI=3.14159265
      CONS=3.141593/180.
      H0=H0*CONS
C
      CSVG=DCOS(VG*CONS)
      SNVG=DSIN(VG*CONS)
      CSKOI=DCOS(RKG*CONS)
      SNKOI=DSIN(RKG*CONS)
C CONVENTIONAL PROFILE - FOR COMPARISON
C ===================================
      DO 9147 NS=1,NLOOP
      RSTAN=R0-FLOAT(NS-1)*(R0-WEB/2.)/(NLOOP-1)
      W2R=WEB/2./RSTAN
      IF(W2R .GE. 1.) GO TO 79
      PHST=DATAN(W2R/DSQRT(1.-W2R**2))+DSQRT(RSTAN**2-
     $(WEB/2.)**2)*DSIN(H0)/DCOS(H0)/R0*CSKOI/SNKOI
      GO TO 80
79    PHST=PI/2.
80    XST=RSTAN*DCOS(PHST)
      YST=-RSTAN*DSIN(PHST)
      XS(NS)=XST
      YS(NS)=YST
9147  CONTINUE
C
      Z0=DSQRT((2.*R0G)**2-(EXG-WEB/2.)**2)/DSIN(RKG*CONS)
C REFERENCE  POINTS
C ===================
      YCE=-WEB/2.
      XCE=DSQRT(R0**2-YCE**2)
C
      AXX=CSVG**2+(CSKOI**2)*(SNVG**2)
      BYY=SNVG**2+CSVG**2*(CSKOI**2)
      CXY=-2.*SNVG*CSVG+2.*(CSKOI**2)*SNVG*CSVG
C
      POZ1=(-2.*SNKOI*CSKOI*SNVG)*XCE
      POZ2=(-2.*SNKOI*CSKOI*CSVG)*YCE
      POZ3=(-2.*EXG*CSVG+2.*Z0*SNKOI*CSKOI*SNVG)*XCE
      POZ4=(2.*EXG*SNVG+2.*Z0*SNKOI*CSKOI*CSVG)*YCE
      POZ5=EXG**2-(2.*R0G)**2+Z0**2*SNKOI**2
      POZ6=-2.*Z0*SNKOI**2
C
      POZA=SNKOI**2
      POZB=POZ1+POZ2+POZ6
      POZC=AXX*XCE**2+BYY*YCE**2+CXY*YCE*XCE+POZ3+POZ4+POZ5
```

```
C
      POZ10=(-POZB+DSQRT(POZB**2-4.*POZA*POZC))/2./POZA
      POZ20=(-POZB-DSQRT(POZB**2-4.*POZA*POZC))/2./POZA
      ZCE=POZ20
C OUTER CORNER
C ==================
      POX=XCE
      POY=YCE
      POZ=ZCE
      POZA=SNKOI**2
      POZB=POZ6
      POZC=POZ5
      POZ10=(-POZB+DSQRT(POZB**2-4.*POZA*POZC))/2./POZA
      POZ20=(-POZB-DSQRT(POZB**2-4.*POZA*POZC))/2./POZA
C CHISEL POINT - DEAD CENTRE
C ========================
      ZX0Y0=POZ20
      WRITE(1,406)ZX0Y0
406   FORMAT(//'   ZX0Y0=',F10.3//)
      FFL=-2.*SNKOI*CSKOI*CSVG
      HFL=2.*SNKOI*CSKOI*CSVG*Z0+2.*EXG*SNVG
      CFL=SNKOI**2
      FLI=-2.*Z0*SNKOI**2
      EFL=-2.*SNKOI*CSKOI*SNVG
      GFL=2.*SNKOI*CSKOI*SNVG*Z0-2.*EXG*CSVG
C
      CU1=2.*(FFL*ZX0Y0+HFL)*(2.*CFL*ZX0Y0+FLI)
      CU2=-2.*(EFL*ZX0Y0+GFL)*(2.*CFL*ZX0Y0+FLI)
      CU3=0.0
      CU=DSQRT(CU1**2+CU2**2)
      CU1=CU1/CU
      CU2=CU2/CU
C
      PHCHI=-DATAN(DSQRT(1.-CU1**2)/CU1)
      PHCHIG=PHCHI/CONS
C CHISEL CORNER  [ APROXIMATION ]
C ============================
      YCORN=YCE
      XCORN=WEB/2.*DCOS(PHCHI)/DSIN(PHCHI)
C
      POZ1=(-2.*SNKOI*CSKOI*SNVG)*XCORN
      POZ2=(-2.*SNKOI*CSKOI*CSVG)*YCORN
      POZ3=(-2.*EXG*CSVG+2.*Z0*SNKOI*CSKOI*SNVG)*XCORN
      POZ4=(2.*EXG*SNVG+2.*Z0*SNKOI*CSKOI*CSVG)*YCORN
      POZ5=EXG**2-(2.*R0G)**2+Z0**2*SNKOI**2
      POZ6=-2.*Z0*SNKOI**2
C
      POZA=SNKOI**2
      POZB=POZ1+POZ2+POZ6
      POZC=AXX*XCORN**2+BYY*YCORN**2+CXY*YCORN*XCORN+POZ3+
     $POZ4+POZ5
      POZ10=(-POZB+DSQRT(POZB**2-4.*POZA*POZC))/2./POZA
      POZ20=(-POZB-DSQRT(POZB**2-4.*POZA*POZC))/2./POZA
      ZCORN=POZ20
      IF(POZ10 .LT. POZ20)ZCORN=POZ10
      ZEB=ZCORN
      ZEM=ZCE
C CHISEL EDGE
C ============
      DO 5 I=1,NLOOP
      ZCHI=ZCORN-FLOAT(I-1)/FLOAT(NLOOP-1)*(ZCORN-ZX0Y0)
C
      CALL GRIN(ZCHI,Z0,AXX,BYY,CXY,DDX,EY,FF)
C
      CHI1=BYY+(EY/DDX)**2*AXX-AXX-EY/DDX*CXY
      NCHI=I
      IF(-FF/CHI1 .GE. 0.0) GO TO 408
      WRITE(1,410)NCHI
410   FORMAT(//'    NCHI= ',I4//)
      GO TO 405
408   YCHI2(I)=+DSQRT(-FF/CHI1)
      XCHI2(I)=-YCHI2(I)*EY/DDX
      XCHIG(I)=DABS(XCHI2(I))
      YCHIG(I)=-DABS(YCHI2(I))
5     CONTINUE
405   CONTINUE
C INITIAL CONDITIONS TO THE PROFILE TO BE FOUND
C ==========================================
      SS=0.0
      XST=XCE
      YST=YCE
      ZST=ZCE
C
C READING WEDGE ANGLE
      WRITE(1,75)
75    FORMAT('READ  CWEDGE')
      READ(1,*)CWEDGE
      WRITE(1,70)
70    FORMAT('READ TO A GUESS STARTING COEFFICIENTS TO'/
     $'INCLINATION ANGLE LAW AND STEP')
      READ(1,*)C12(1),C12(2),C12(3),C12(4),STEP
      WRITE(1,74)
74    FORMAT('READ MAXCAL,IFAIL,IWRITE')
      READ(1,*)MAXCAL,IFAIL,IWRITE
      WRITE(1,76)
76    FORMAT('READ BAFTOL,XTOL,ETA,IPRINT')
      READ(1,*)BAFTOL,XTOL,ETA,IPRINT
      WRITE(1,77)
77    FORMAT(/'CONVENTIONAL FLUTE INSTEAD ?')
      READ(1,*)ISTINS
C PARAMETERS TO SUBROUT E04FCF
C =========================
      M4F=4
      N4F=4
      LJ=4
      LV=4
      LIW=1
      LW=120
```

```
C
      PHI1=DATAN(YST/XST)
      PHI=PHI1-ZST/R0*DSIN(H0)/DCOS(H0)
      XSTG(1)=XST
      YSTG(1)=YST
      WRITE(1,113)
113   FORMAT(/'CALLING E04FCF'/)
C
      CALL E04FCF(M4F,N4F,RESID,MONIT,IPRINT,MAXCAL,ETA,XTOL,
     $STEP,C12,FE,RE,FJAC,LJ,SMON,V,LV,NITER,NF,IW,LIW,WE0,LW,
     $IFAIL)
C
      CALL EXIT
      END
C
C ================================================
C                   S U B R O U T I N E S
C ================================================
C
C
C ========================================================
      SUBROUTINE RESID(IFLAG,M4F,N4F,C12,RE,IW,LIW,WE0,LW)
      IMPLICIT DOUBLE PRECISION (A-H,O-Z)
      REAL R0N,R0P,XCOR,YCOR
      EXTERNAL DERIV2
      REAL XCIRE(200),YCIRE(200),XCIRD(200),YCIRD(200)
      REAL XEEL(200),YEEL(200),XAXIS,YAXIS
      REAL XSTG(200),YSTG(200),ZSTG(200)
      REAL XCHIG(200),YCHIG(200),ZCHIG(200)
      REAL XFLU(200),YFLU(200),XS(200),YS(200)
      REAL VERIG(200),RRG(200),GAMI(200)
      REAL DINCC(200),WEDGE(200),RSINC(200)
      REAL GAMAA(200),CLEAA(200),GAMAE(200)
      DIMENSION EIX(100,5),FEAT(100,4),THETA(5,4),B(4),AM(5,5)
      DIMENSION SOLU(4),C(100,5),IPIV(5),WK1(5,5),WK2(100)
      DIMENSION WKS2(4),WKS1(32),SIGSQ(4)
      DIMENSION XNMSD(200),YNMSD(200),ZNMSD(200)
      DIMENSION PHU(200),SENOEE(200)
      DIMENSION CCE1(200),CCE2(200),CCE3(200)
      DIMENSION A(3,3),DCOOR(3)
      DIMENSION XSTGD(200),YSTGD(200),ZSTGD(200)
      DIMENSION XNRAD(200),YNRAD(200),ZNRAD(200)
      DIMENSION XFLUD(200),YFLUD(200)
      DIMENSION XCHI2(200),YCHI2(200)
      DIMENSION REAU(200),REAUX(200)
      DIMENSION IW(1),WE0(120),WS(3,7)
      DIMENSION VAR(3)
      DIMENSION DF2(3),C12(4),T1PR(200),T2PR(200)
      DIMENSION RE(4),STEPMX(3),W(120),DDIS(200)
      DIMENSION SSS(200)
      DIMENSION GAMN(200),GCD(200),AKCD(200),HCD(200)
      DIMENSION RADI(200),T211(200),ETAA(200),VVCA(200)
      DIMENSION ETACHA(200),RCA(200),GEMEA(200)
      COMMON/BLO0/XFLU,YFLU,CWEDGE,RCA,ETACHA,XSTG,YSTG,ZSTG
      COMMON/BLO1/NPOINT,MAXCAL,T1PR,T2PR,NLOOP
      COMMON/BLO2/DFDX,DFDY,DFDZ,CE1,CE2,CE3
      COMMON/BLO3/PA,REVAB,VG,RKG,EXG
      COMMON/BLO4/SNVG,CSVG,SNKOI,CSKOI
      COMMON/BLO5/SENETA,CSGAMA,VVCV,SGAMAE,GEMEA,SGAMA
      COMMON/BLO6/DINCC,GAMAA,CLEAA,GAMAE,ETAA,VVCA
      COMMON/BLO7/RADI,T211,SSS
      COMMON/BLO8/H0,CONS,R0,WEB,R0G,IWRITE,PI
      COMMON/BLO11/DIDS,Z0
      COMMON/BLO12/BAFTOL
      COMMON/BLO14/XCE,YCE,ZCE,XCORN,YCORN,ZCORN,ZX0Y0
      COMMON/BLO15/ISTINS,J
      COMMON/BLO16/RPACE,PHPA,YPACE1
      COMMON/BLO17/COEA,COEB
      COMMON/BLO18/R0CHIP,H0CHIP,A
      COMMON/BLO19/RSTAR,PHSTAR,ZSTAR,XSTROT,YSTROT,ZSTROT
      COMMON/BLO20/XST0,YST0,ZST0,RC0
      COMMON/BLO21/XS,YS
C
      POZ=ZCE
C SS IS THE LENGTH ALONG THE CUTTING EDGE,
C FROM THE OUTER CORNER
      VARX=XCE
      VAR(1)=0.0
      VAR(2)=YCE
      VAR(3)=ZCE
      DVARX=(XCE-XCORN)/FLOAT(NPOINT-2)
C
      NBAF=3
      IFAUL=0
      WRITE(1,114)
114   FORMAT(/'STARTING LOOP 40 AND CALLING D02ABF'/)
      DO 40 J=1,NPOINT
      IF(J .GE. 2) GO TO 42
      VARX1=XCE
      VARX2=VARX1+DVARX
      GO TO 43
42    VARX1=XCE-FLOAT(J-3)*DVARX
      VARX2=VARX1-DVARX
43    TOL=BAFTOL
C
      CALL D02BAF(VARX1,VARX2,NBAF,VAR,TOL,DERIV2,
     $WS,IFAUL)
C
      SS=VAR(1)
      XST=VARX2
      YST=VAR(2)
      ZST=VAR(3)
      PHI1=DATAN(YST/XST)
      PHU(J)=PHI1
      UU1=-DSIN(PHI1)
      UU2=+DCOS(PHI1)
      UU3=0.0
      RR=DSQRT(XST**2+YST**2)
```

```
      VV=2.*PI*RR
      COTH=R0*DCOS(H0)/DSIN(H0)/RR
      SENOI=C12(1)*(RR/R0)**2+C12(2)*RR/R0+C12(3)+C12(4)/RR
      IF(ISTINS .EQ. 1)SENOI=WEB/2./RR*SNKOI
      SENOEE(J)=SENOI
C
      CCE1(J)=CE1
      CCE2(J)=CE2
      CCE3(J)=CE3
C VECTOR NORMAL TO THE MACHINED SURFACE
      XNMS=+UU2*CE3
      YNMS=-UU1*CE3
      ZNMS=-CE1*UU2+UU1*CE2
      SU=DSQRT(XNMS**2+YNMS**2+ZNMS**2)
      DFD=DSQRT(DFDX**2+DFDY**2+DFDZ**2)
      CSCLEA=(XNMS*DFDX+YNMS*DFDY+ZNMS*DFDZ)/SU/DFD
      TGCLEA=DSQRT(1.-CSCLEA**2)/CSCLEA
      CLEAR=DATAN(TGCLEA)/CONS
C
      XNMS=-XNMS
      YNMS=-YNMS
      ZNMS=-ZNMS
C
      XNMSD(J)=XNMS
      YNMSD(J)=YNMS
      ZNMSD(J)=ZNMS
C
      SALPHA=DABS(ZNMS/SU)
      CALPHA=DSQRT(1.-SALPHA**2)
C ========================
C RAKE ANGLE COMPUTATION
C ========================
196   COTH=R0*DCOS(H0)/DSIN(H0)/RR
      VVCOTH=DSQRT(UU1**2+UU2**2+COTH**2)
C
C VECTOR NORMAL TO RAKE FACE
      XNRA=UU2*CE3-CE2*COTH
      YNRA=CE1*COTH-UU1*CE3
      ZNRA=UU1*CE2-UU2*CE1
      XYZN=DSQRT(XNRA**2+YNRA**2+ZNRA**2)
      TGTETA=RR/R0*DSIN(H0)/DCOS(H0)
      XNRA=XNRA/XYZN
      YNRA=YNRA/XYZN
      ZNRA=ZNRA/XYZN
      XNRAD(J)=XNRA
      YNRAD(J)=YNRA
      ZNRAD(J)=ZNRA
      COSGN=(-XNRA*CE2+YNRA*CE1)/DSQRT(CE2**2+CE1**2)
      GAMNN=DATAN(DSQRT(1.-COSGN**2)/COSGN)
C
      IF(XNRA .NE. .0) GO TO 3300
      WRITE(1,3313)
3313  FORMAT('    XNRA   IS  NUL  ')
      CALL EXIT
C
3300  AR2=DSQRT(XNRA**2/(XNRA**2+YNRA**2))
      AR1=-AR2*YNRA/XNRA
      BR1=XST/RR
      BR2=YST/RR
      CSBETA=AR1*BR1+AR2*BR2
      SNBETA=DSQRT(1.-CSBETA**2)
      BETA=DATAN(SNBETA/CSBETA)
      SIGN1=XNRA*XST+YNRA*YST
      SIGN2=DABS(SIGN1)
      IF(SIGN2 .NE. 0.) GO TO 3001
      WRITE(1,3003)
3003  FORMAT('     SIGN2=  0.0')
      CALL EXIT
C
3001  SIGN=SIGN1/SIGN2
      BETA=SIGN*DABS(BETA)
      TGBETA=DSIN(BETA)/DCOS(BETA)
      TGETA=SALPHA*TGTETA+TGBETA*CALPHA
      TGGAMA=DSQRT(1.-SENOI**2)*TGETA
      CSGAMA=(1.+TGGAMA**2)**(-1.)
      GAMA=DATAN(TGGAMA)/CONS
      SGAMA=DSIN(GAMA*CONS)
      PHI1=DATAN(YST/XST)
      PHI=PHI1-ZST/R0*DSIN(H0)/DCOS(H0)
      XFLUT=RR*DCOS(PHI)
      YFLUT=RR*DSIN(PHI)
      XFLUD(J)=XFLUT
      YFLUD(J)=YFLUT
C
      XFLU(J)=XFLUT
      YFLU(J)=YFLUT
      IF(SENOI .LT. 1.) GO TO 4311
      WRITE(1,4316)
4316  FORMAT('     SENOI  .GE.  1.')
      CALL EXIT
C
4311  TINC=SENOI/DSQRT(1.-SENOI**2)
      DINC=DATAN(TINC)
      DINC1=DINC/CONS
C
      IF(J .NE. 2) GO TO 117
      XST0=XST
      YST0=YST
      ZST0=ZST
C
117   RRG(J)=RR
      RADI(J)=RR
      RSINC(J)=SENOI*RR
      XSTG(J)=XST
      YSTG(J)=YST
      ZSTG(J)=ZST
      XSTGD(J)=XST
      YSTGD(J)=YST
```

```
      ZSTGD(J)=ZST
      SSS(J)=SS-SSS(2)
      DINCC(J)=DINC1
      GAMAA(J)=GAMA
      GAMN(J)=GAMNN/CONS
      CLEAA(J)=CLEAR
      GAMAA(1)=GAMAA(2)
      WEDGE(J)=9Ø.-GAMA-CLEAR
      HCD(J)=HC/CONS
      ETACHA(J)=ETACH
      DDIS(J)=DIDS*CONS
      GAMIE=(SIN(DINCC(J)*CONS))**2+(COS(DINCC(J)*CONS))**2*
     $SIN(GAMAA(J)*CONS)
      GAMI(J)=ATAN(GAMIE/SQRT(1.-GAMIE))/CONS
C
      REAUX(1)=Ø.Ø
      REAU(J)=DABS(9Ø.-CWEDGE-GAMAA(J)-CLEAA(J))
      IF(J .EQ. 1)GO TO 4Ø
      REAUX(J)=REAUX(J-1)+REAU(J)*DVARX
4Ø    CONTINUE
      WRITE(1,115)
115   FORMAT(/'LOOP 4Ø FINISHED'/)
C
      SSS(2)=Ø.
      RE(1)=REAU(2)
      RE(2)=(YSTGD(NPOINT)+WEB/2.)
      RE(3)=REAUX(NPOINT-3)/DVARX/FLOAT(NPOINT-3)
      RE(4)=REAU(NPOINT-3)
C
      IF(IWRITE .EQ. Ø)GO TO 4Ø2
1Ø9   WRITE(1,94Ø)
94Ø   FORMAT('IF GRAPHICS ONLY, READ 1')
      READ(1,*)IGRA
      IF(IGRA .EQ. 1) GO TO 935
      READ(1,*)SEPARA
C TABLES
C SECTION AND COORDINATES TO NEW DESIGN FLUTE
      WRITE(1,8Ø)
8Ø    FORMAT(3X,'RADI',3X,' SS ',3X,' X  ',3X,' Y  ',3X,
     $' Z  ',3X,'XFLU',3X,'YFLU'///)
C
      DO 41 J=2,NPOINT
      WRITE(1,92)RADI(J),SSS(J),XSTG(J),YSTG(J),ZSTG(J),
     $XFLU(J),YFLU(J)
92    FORMAT(1ØF7.2)
41    CONTINUE
C
C ANGLES ALONG LIP
      WRITE(1,2Ø4)
2Ø4   FORMAT(///3X,'RADI',3X,' INC',3X,'GAMA',3X,
     $'GAMN',3X,'GAMI',3X,'CLEA',3X,'WEDG'///)
C
      WRITE(1,2Ø5)(RADI(I),DINCC(I),GAMAA(I),GAMN(I),
     $GAMI(I),CLEAA(I),WEDGE(I),I=1,NPOINT)
2Ø5   FORMAT(7F7.2)
      READ(1,*)SEPARA
C
C FINAL PARAMETERS TO INCLINATION ANGLE LAW
      WRITE(1,921)C12(1),C12(2),C12(3)
921   FORMAT(///6X,'C12(1)=',F8.4,3X,'C12(2)=',F8.4,3X,/
     $'C12(3)=',2F8.4)
C
C NOW , PLOTS
      WRITE(1,6Ø)
6Ø    FORMAT(//'   GRAPHICS ?'//)
      READ(1,*)IGRAF
      IF(IGRAF .EQ. Ø)CALL EXIT
935   CONTINUE
C
      WRITE(1,142)
142   FORMAT(/' T4Ø1Ø (1) , C1Ø51N (2) OR SE281(3) ?'/)
      READ(1,*)IDEVIC
      WRITE(1,232)
232   FORMAT('CHISEL EDGE ?')
      READ(1,*)ICHIS
      IF(ICHIS .EQ. Ø)GO TO 112
C
C CHISEL EDGE COMPUTATION
C
      DO 5 I=1,NLOOP
      ZCHI=ZCORN-FLOAT(I-1)/FLOAT(NLOOP-1)*(ZCORN-ZXØYØ)
      ZCHIG(I)=ZCHI
C
      CALL GRIN(ZCHI,AXX,BYY,CXY,DDX,EY,FF)
C
      CHI1=BYY+(EY/DDX)**2*AXX-AXX-EY/DDX*CXY
      RADIC=-FF/CHI1
      IF(RADIC .GE. Ø)GO TO 233
      WRITE(1,231)
231   FORMAT(/'RADIC < Ø')
      CALL EXIT
233   YCHI2(I)=+DSQRT(RADIC1)
      XCHI2(I)=-YCHI2(I)*EY/DDX
C
      XCHIG(I)=DABS(XCHI2(I))
      YCHIG(I)=-DABS(YCHI2(I))
5     CONTINUE
      WRITE(1,1Ø1)
1Ø1   FORMAT(/'CHISEL EDGE COMPUTED'/)
112   CONTINUE
      RØP=RØ+1.
      IRØ=RØP
      RØP=IRØ
      RØN=-RØP
      IRØ=2*IRØ
C
C COMPUTING FLUTE HEEL
      WRITE(1,2ØØ)
```

```
200   FORMAT(/'READ ANGLE FOR HEEL')
      READ(1,*)ANGCLE
      YEEL(1)=RØ*SIN(ATAN(YFLU(2)/XFLU(2))-PI+ANGCLE*CONS)
      XEEL(1)=RØ*COS(ATAN(YFLU(2)/XFLU(2))-PI+ANGCLE*CONS)
      RCORN=DSQRT(XCORN**2+YCORN**2)
      PHICO=ZCORN/RCORN*DSIN(HØ)/DCOS(HØ)
      PHICOR=DATAN(YCORN/XCORN)-PHICO
      YCOR=RCORN*SIN(PHICOR)
      XCOR=RCORN*COS(PHICOR)
      AEEL=(YEEL(1)-YCOR)/(XEEL(1)-XCOR)**2
      BEEL=-2.*AEEL*XCOR
      CEEL=YEEL(1)-AEEL*(XEEL(1)**2-2.*XCOR*XEEL(1))
      DO 201 I=1,NLOOP
      XEEL(I)=XEEL(1)+FLOAT(I-1)/FLOAT(NLOOP-1)*(XCOR
     $-XEEL(1)+1.)
      YEEL(I)=AEEL*XEEL(I)**2+BEEL*XEEL(I)+CEEL
      YCIRE(I)=YEEL(1)+FLOAT(I-1)/FLOAT(NLOOP-1)
     $*(1.-YEEL(1))
      XCIRE(I)=-SQRT(RØ**2-YCIRE(I)**2)
      YCIRD(I)=YFLU(2)+FLOAT(I-1)/FLOAT(NLOOP-1)*(1.-YFLU(2))
      XCIRD(I)=SQRT(RØ**2-YCIRD(I)**2)
201   CONTINUE
C
      NPOINT=NPOINT-1
222   WRITE(1,215)
215   FORMAT(/'FLUTE CROSS SECTION ?')
      READ(1,*)IFLUSE
      IF(IFLUSE .EQ. Ø)GO TO 216
      GO TO(202,143,144),IDEVIC
C
202   CALL T4010
      XAXIS=158.
      YAXIS=128.
      GO TO 44
143   CALL C1051N
      XAXIS=20.*RØP
      YAXIS=20.*RØP
      GO TO 44
144   CALL SE281
      XAXIS=20.*RØP
      YAXIS=20.*RØP
44    CALL PICCLE
      CALL WINDOW(2)
      CALL AXIPOS(Ø,13Ø.,1ØØ.,XAXIS,1)
      CALL AXIPOS(Ø,13Ø.,1ØØ.,YAXIS,2)
      CALL AXISCA(2,IRØ,RØN,RØP,1)
      CALL AXISCA(1,IRØ,RØN,RØP,2)
      CALL AXIDRA(2,1,1)
      CALL AXIDRA(-2,-1,2)
C
      CALL GRAPOL(XFLU(2),YFLU(2),NPOINT)
      CALL GRAPOL(XEEL,YEEL,NLOOP)
      CALL GRACUR(XCIRE,YCIRE,NLOOP)
      CALL GRACUR(XCIRD,YCIRD,NLOOP)
      CALL DASHED(-2,6.,3.,1.)
      CALL GRAPOL(XS,YS,NLOOP)
      CALL BROKEN(Ø)
      CALL GRAMOV(XCOR,YCOR)
      CALL CHASIZ(6.,6.)
      CALL SYMBOL(5)
      CALL CHAMOD
      CALL GRAMOV(Ø.,Ø.)
      CALL CHAMOD
      WRITE(1,206)XCOR,YCOR
206   FORMAT(2F1Ø.3)
C
      IRØ=IRØ/2
      READ(1,*)SEPARA
216   WRITE(1,217)
217   FORMAT(/'INCLINATION ANGLE PLOTTING?')
      READ(1,*)INCANG
      IF(INCANG .EQ. Ø)GO TO 218
      IRØ=RØP
      RØP=IRØ
      RØN=-RØP
      GO TO(207,208,209),IDEVIC
C
207   CALL T4010
      XAXIS=158.
      YAXIS=128.
      GO TO 210
208   CALL C1051N
      XAXIS=15Ø.
      YAXIS=15Ø.
      GO TO 210
209   CALL SE281
      XAXIS=18Ø.
      YAXIS=11Ø.
210   CALL PICCLE
      CALL WINDOW(2)
      CALL AXIPOS(Ø,5Ø.,5Ø.,XAXIS,1)
      CALL AXIPOS(Ø,5Ø.,5Ø.,YAXIS,2)
      CALL AXISCA(2,IRØ,Ø.,RØP,1)
      CALL AXISCA(1,12,Ø.,6Ø.,2)
      CALL AXIDRA(2,1,1)
      CALL AXIDRA(-2,-1,2)
C
      CALL GRACUR(RRG(2),DINCC(2),NPOINT)
C     CALL AXISCA(1,6,Ø.,6.,2)
C     CALL GRACUR(RRG(2),RSINC(2),NPOINT)
C     CALL AXIPOS(Ø,35.,4Ø.,YAXIS,2)
C     CALL AXISCA(1,6,Ø.,6.,2)
C     CALL AXIDRA(-2,-1,2)
      CALL CHAMOD
C
      READ(1,*)SEPARA
218   WRITE(1,220)
220   FORMAT(/'WEDGE PLOTTINGANGLE ?')
```

```
      READ(1,*)IWED
      IF(IWED .EQ. 0)GO TO 219
C
      R0P=R0+1.
      IR0=R0P
      R0P=IR0
      R0N=-R0P
      GO TO(211,212,213),IDEVIC
C
211   CALL T4010
      XAXIS=158.
      YAXIS=128.
      GO TO 214
212   CALL C1051N
      XAXIS=150.
      YAXIS=150.
      GO TO 214
213   CALL SE281
      XAXIS=180.
      YAXIS=120.
214   CALL PICCLE
      CALL WINDOW(2)
      CALL AXIPOS(0,50.,50.,XAXIS,1)
      CALL AXIPOS(0,50.,50.,YAXIS,2)
      CALL AXISCA(2,IR0,0.,R0P,1)
      CALL AXISCA(1,8,40.,80.,2)
      CALL AXIDRA(2,1,1)
      CALL AXIDRA(-2,-1,2)
C
      CALL GRACUR(RRG(2),WEDGE(2),NPOINT)
      CALL CHAMOD
C
219   CONTINUE
      READ(1,*)SEPARA
      WRITE(1,224)
224   FORMAT('EFFECTIVE RAKE PLOTTING ?')
      READ(1,*)IRAKE
      IF(IRAKE .EQ. 0)GO TO 223
      R0P=R0+1.
      IR0=R0P
      R0P=IR0
      R0N=-R0P
      CALL SE281
2705  CALL PICCLE
      CALL WINDOW(2)
      CALL AXIPOS(0,50.,80.,180.,1)
      CALL AXIPOS(0,50.,80.,135.,2)
      CALL AXISCA(2,IR0,0.,R0P,1)
      CALL AXISCA(2,16,-40.,40.,2)
      CALL AXIDRA(2,1,1)
      CALL AXIDRA(-2,-1,2)
      CALL GRACUR(RRG(2),GAMAA(2),NPOINT)
      CALL CHAMOD
C
      READ(1,*)SEPARA
223   WRITE(1,221)
221   FORMAT(/'MORE PLOTS ?')
      READ(1,*)IPLOT
C
C PLOTTING DRILL LIP
      IF(IPLOT .EQ. 1)GO TO 222
      IF(IDEVIC .EQ. 2) GO TO 45
      CALL T4010
      GO TO 46
45    CALL C1051N
46    CALL PICCLE
      CALL WINDOW(2)
      CALL AXIPOS(0,100.,20.,200.,1)
      CALL AXIPOS(0,100.,20.,150.,2)
      CALL AXISCA(2,20,-10.,10.,1)
      CALL AXISCA(2,15,-3.,12.,2)
      CALL AXIDRA(2,1,1)
      CALL AXIDRA(-2,-1,2)
C
      CALL GRACUR(XSTG(2),ZSTG(2),NPOINT)
      CALL GRACUR(XCHIG,ZCHIG,NLOOP)
      CALL CHAMOD
      READ(1,*)SEPARA
C
      CALL DEVEND
402   CONTINUE
      RETURN
      END
C
      SUBROUTINE DERIV2(XVAR,VAR,DF2)
C ====================================
      IMPLICIT DOUBLE PRECISION (A-H,O-Z)
      DIMENSION VAR(3)
      DIMENSION DF2(3),C12(4),VERUF(200),C21(7)
      DIMENSION ZX(200),ZY(200),ZZ(200),SSS(200)
      COMMON/BLO2/DFDX,DFDY,DFDZ,CE1,CE2,CE3
      COMMON/BLO3/PA,REVAB,VG,RKG,EXG
      COMMON/BLO4/SNVG,CSVG,SNKOI,CSKOI
      COMMON/BLO8/H0,CONS,R0,WEB,R0G,IWRITE,PI
      COMMON/BLO10/C12,C21
      COMMON/BLO11/DIDS,Z0
      COMMON/BLO15/ISTINS,J
C
      XST=XVAR
      YST=VAR(2)
      ZST=VAR(3)
C
      RR=DSQRT(XST**2+YST++2)
      SENOI=C12(1)*(RR/R0)**2+C12(2)*RR/R0+C12(3)+C12(4)/RR
      IF(DABS(SENOI) .LT. 1.)GO TO 230
      WRITE(1,231)
231   FORMAT('DABS(SIN(INC)) >= 1 ')
      CALL EXIT
```

```
230   IF(ISTINS .EQ. 1)SENOI=WEB/2./RR*SNKOI
      PHI1=DATAN(YST/XST)
      UU1=-DSIN(PHI1)
      UU2=+DCOS(PHI1)
      UU3=Ø.Ø
      IF(UU1 .NE. Ø.Ø .AND. RR .NE. Ø.Ø) GO TO 1789
      WRITE(1,1791)
1791  FORMAT('   UU1   OR    RR  IS  NUL')
      CALL EXIT
1789  CONTINUE
C
      CALL GRIN(ZST,ZØ,AXX,BYY,CXY,DDX,EY,FF)
C
      DFDX=2.*XST*AXX+YST*CXY+DDX
      DFDY=2.*YST*BYY+CXY*XST+EY
      DFDZ=XST*(-2.*SNKOI*CSKOI*SNVG)+YST*(-2.*SNKOI
     $*CSKOI*CSVG)+SNKOI**2*2.*(ZST-ZØ)
C
      IF(UU1 .NE. .Ø) GO TO 7654
      WRITE(1,7656)
7656  FORMAT('      UU1  =  Ø.Ø')
      CALL EXIT
7654  CO1CE1=SENOI/UU1
      CO2CE1=-UU2/UU1
      CO1CE3=-(DFDX*SENOI)/(DFDZ*UU1)
      CO2CE3=(DFDX*UU2)/(DFDZ*UU1)-DFDY/DFDZ
C
      COTH=RØ*DCOS(HØ)/DSIN(HØ)/RR
      ACE2=1.+CO2CE1**2+CO2CE3**2
      BCE2=2.*(CO1CE1*CO2CE1+CO1CE3*CO2CE3)
      CCCE2=-1.+CO1CE1**2+CO1CE3**2
      RADIC5=BCE2**2-4.*ACE2*CCCE2
      IF(RADIC5 .GE. Ø.Ø) GO TO 185
      WRITE(1,187)RADIC5
187   FORMAT('(187)    RADIC5   IS   NEGATIVE =',F12.6)
185   CONTINUE
C
      IF(ACE2 .NE. .Ø) GO TO 41ØØ
      WRITE(1,4ØØ9)
4ØØ9  FORMAT('   ACE2  IS  NUL  ')
      CALL EXIT
C
41ØØ  CE2=(-BCE2-DSQRT(RADIC5))/(2.*ACE2)
      CE1=CO1CE1+CO2CE1*CE2
      CE3=CO1CE3+CO2CE3*CE2
C
      DF2(1)=-1./CE1
      DF2(2)=CE2/CE1
      DF2(3)=CE3/CE1
      IF(J .EQ. 1)DF2(1)=-DF2(1)
C
      RETURN
      END
C
C ==============================================================
      SUBROUTINE GRIN(Z,ZØ,AXX,BYY,CXY,DDX,EY,FF)
      IMPLICIT DOUBLE PRECISION(A-H,O-Z)
      COMMON/BLO3/PA,REVAB,VG,RKG,EXG
      COMMON/BLO4/SNVG,CSVG,SNKOI,CSKOI
      COMMON/BLO8/HØ,CONS,RØ,WEB,RØG,IWRITE,PI
C
      AXX=CSVG**2+(CSKOI**2)*(SNVG**2)
      BYY=SNVG**2+CSVG**2*(CSKOI**2)
      CXY=-2.*SNVG*CSVG+2.*(CSKOI**2)*SNVG*CSVG
      DDX=-2.*EXG*CSVG-2.*(Z-ZØ)*SNKOI*CSKOI*SNVG
      EY=2.*EXG*SNVG-2.*(Z-ZØ)*SNKOI*CSKOI*CSVG
      FF=EXG**2-(2.*RØG)**2+((Z-ZØ)**2)*SNKOI**2
C
      RETURN
      END
C
C ==============================================================
      SUBROUTINE MONIT(M4F,N4F,C12,RE,FJAC,LJC,SMON,IGR,NITER,
     $NF,IW,LIW,WEØ,LW)
      IMPLICIT DOUBLE PRECISION(A-H,O-Z)
      DIMENSION C12(4),RE(4),FJAC(4,4),SMON(4),IW(1),WEØ(12Ø)
      FE=RE(1)**2+RE(2)**2+RE(3)**2+RE(4)**2
      WRITE(1,2Ø)NITER,FE
2Ø    FORMAT('AFTER',I4,'   ITERATIONS',2X,'THE SUM OF SQ. IS'
     $,F9.3)
      WRITE(1,22)(C12(I),I=1,4)
22    FORMAT('AT THE POINT',4F1Ø.4)
      RETURN
      END
C
C
C
C *END*END*END*END*END*END*END*END*END*END*END*END*END*
```

## APPENDIX 7

Wear loss at points 2, 3, 4 and 5 (outer corner) along the drill lips for both tested drilling conditions. For point 1 refer to Chapter 6.

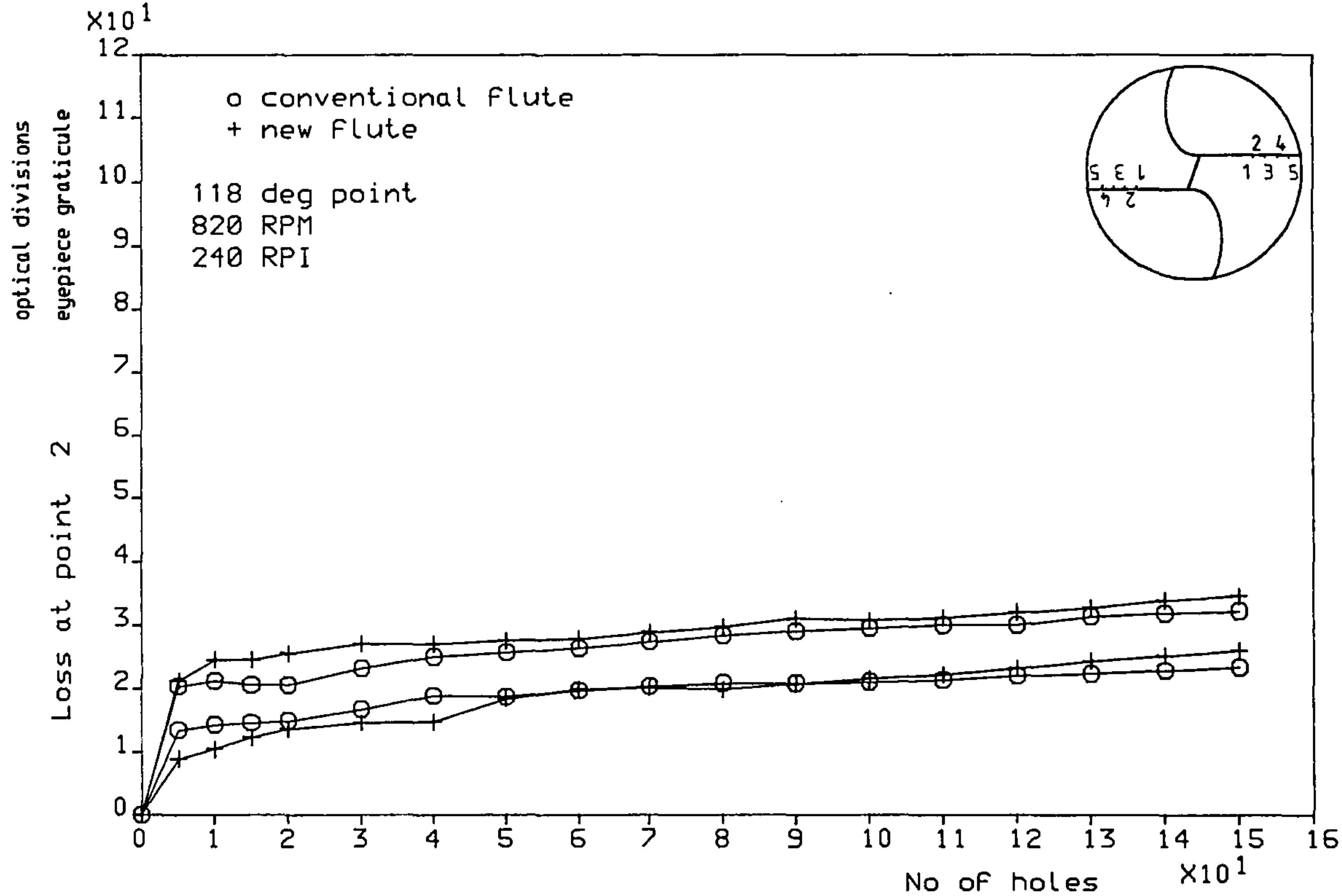


Wear loss at point 2 of each drill lip

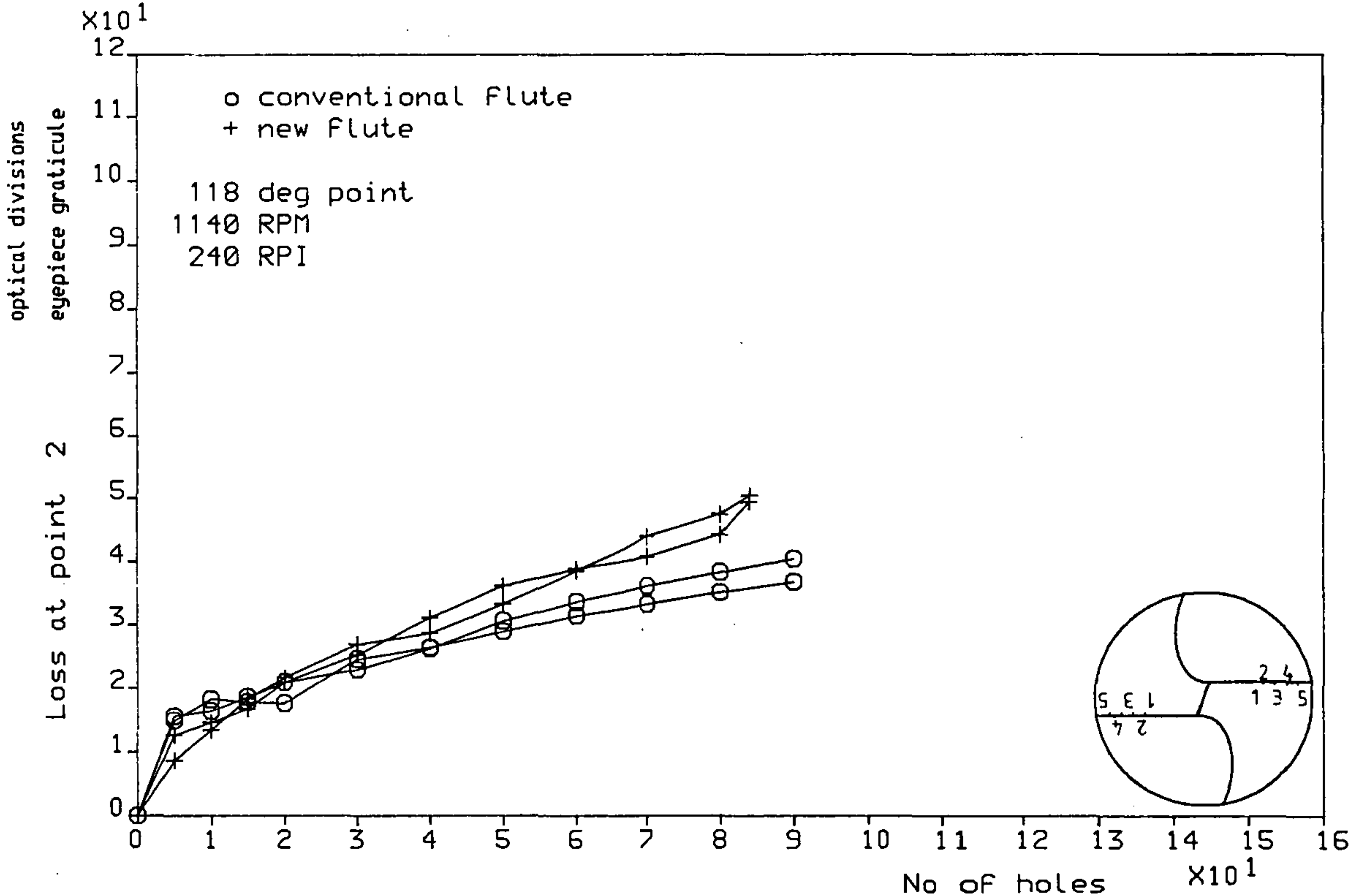


Wear loss at point 2 of each drill lip

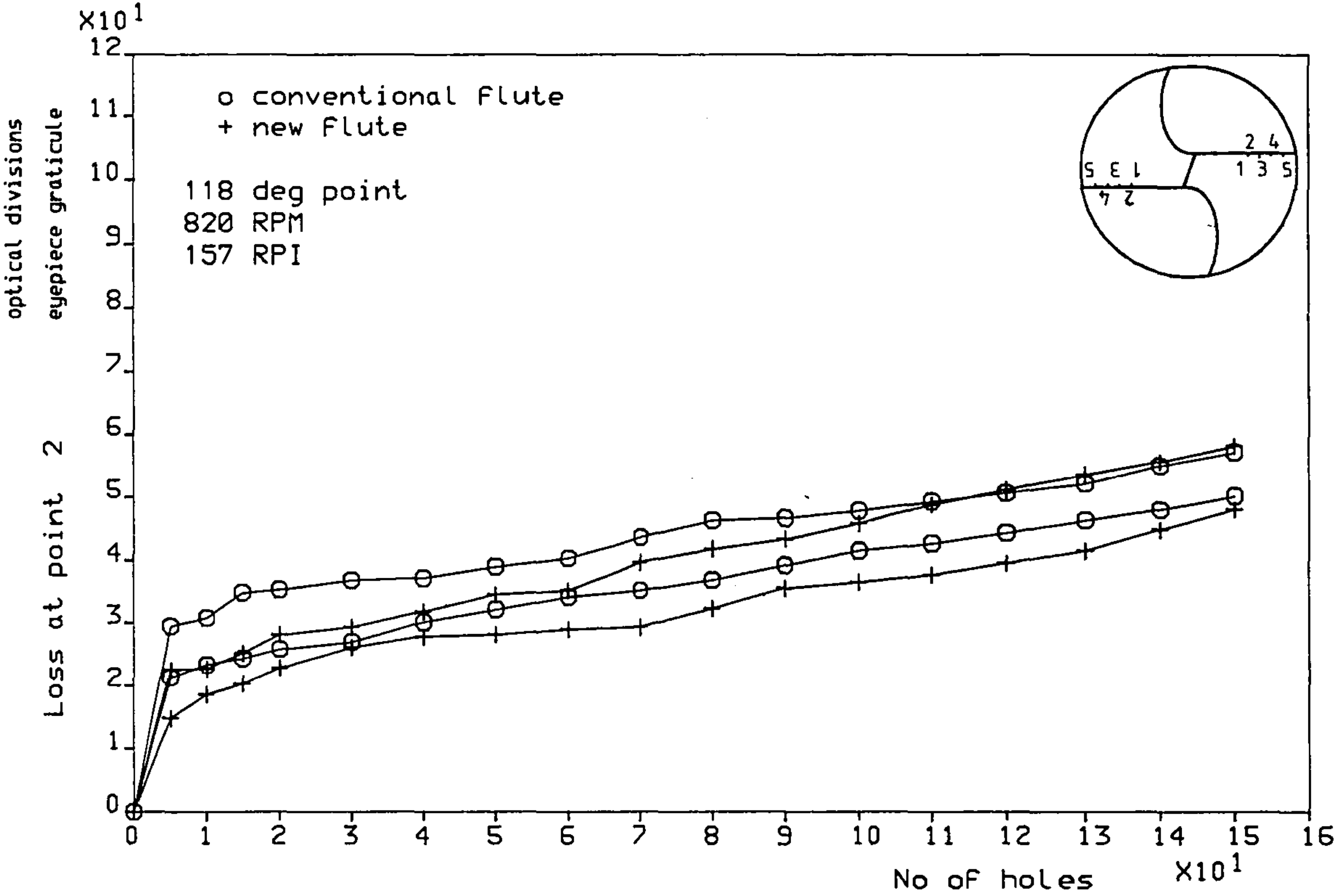


Wear loss at point 2 of each drill lip

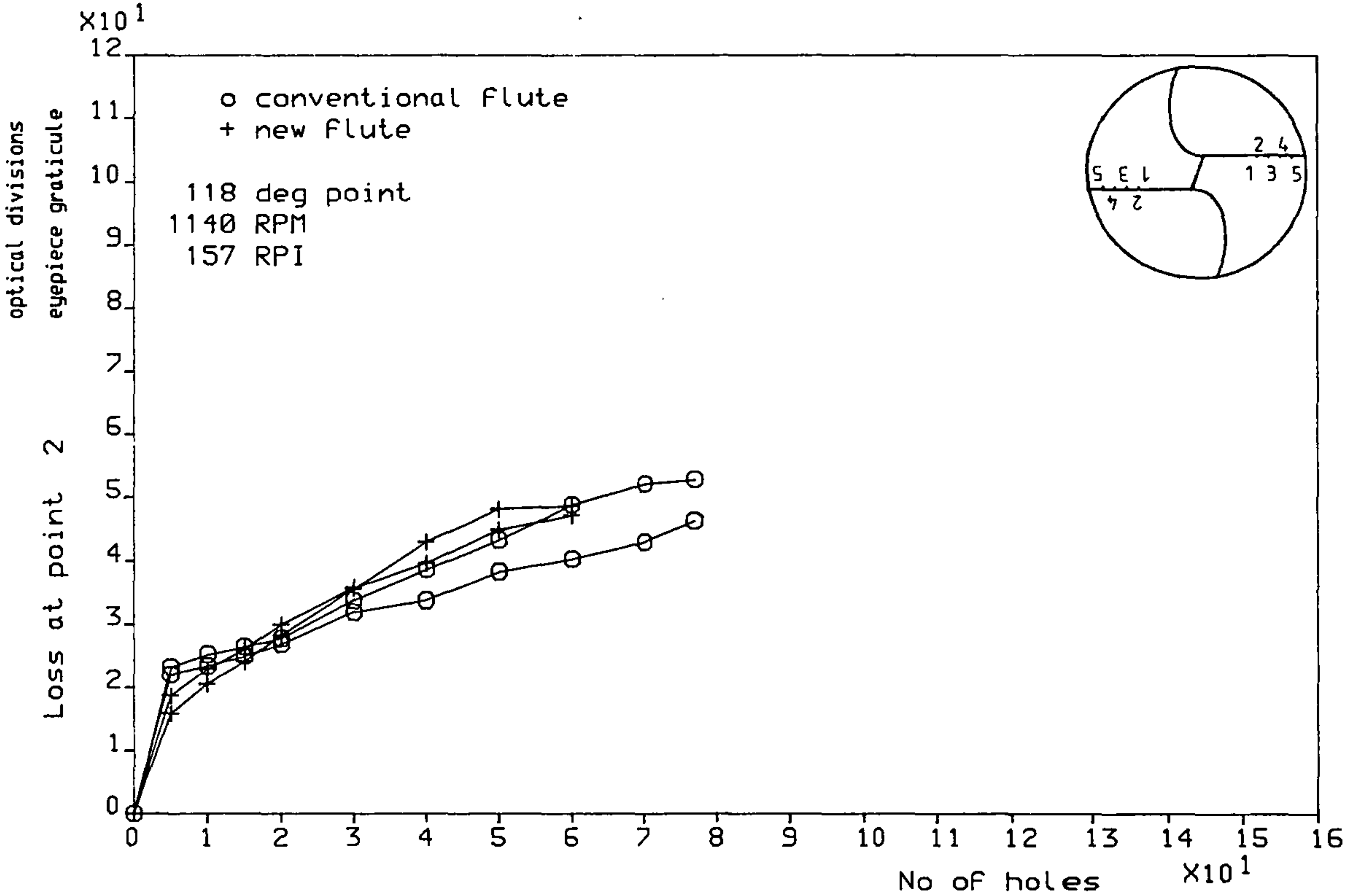


Wear loss at point 2 of each drill lip

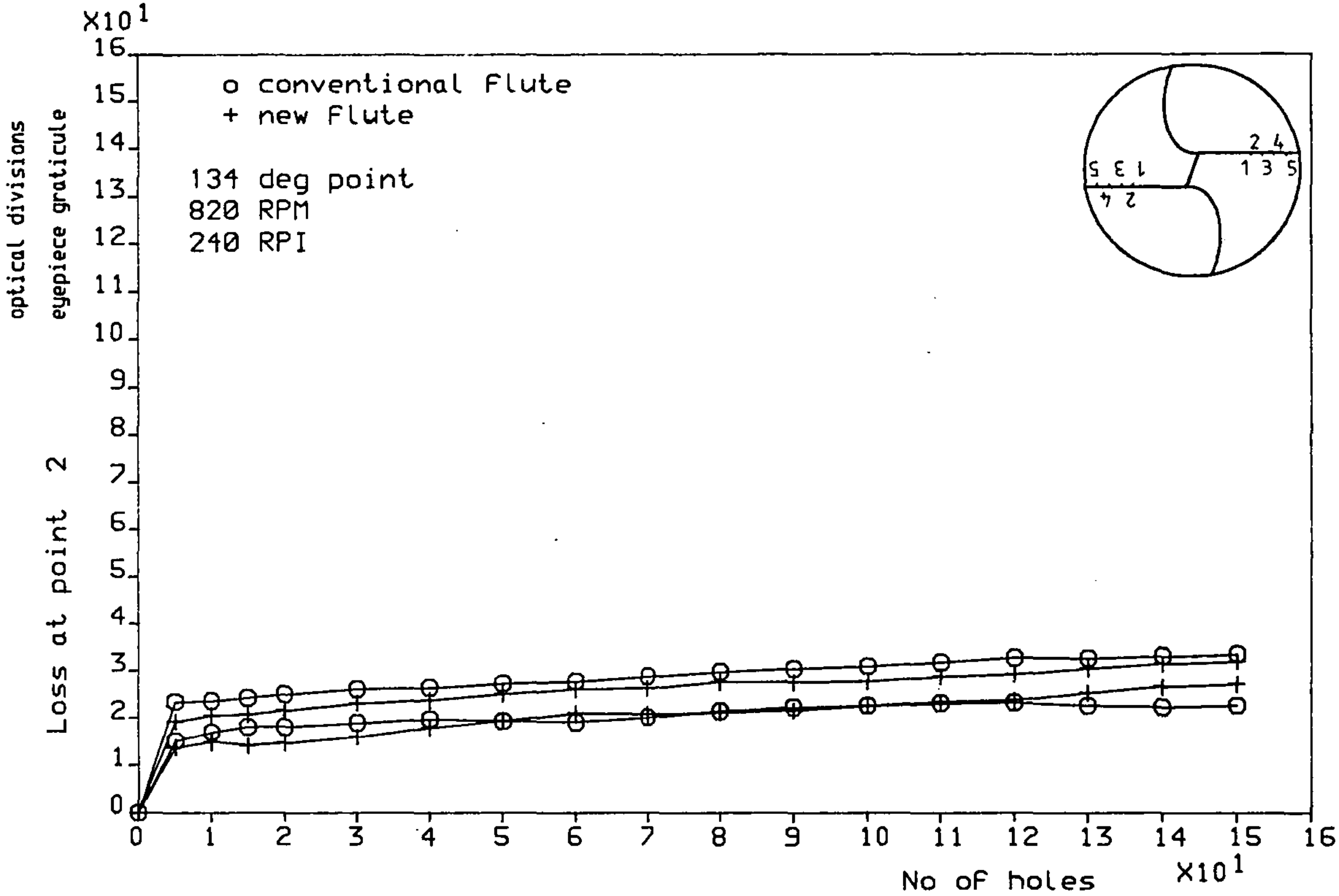


Wear loss at point 2 of each drill lip

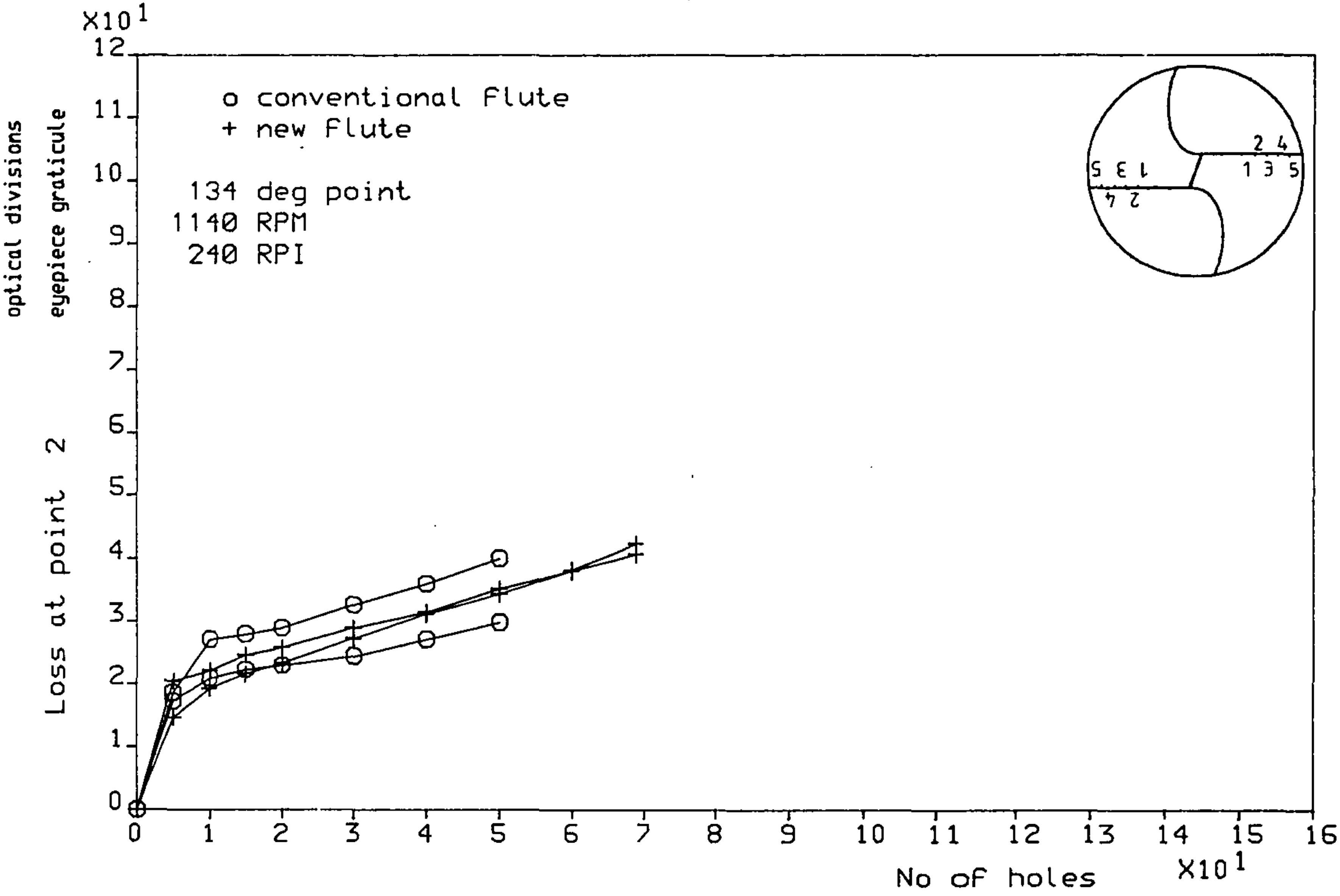


Wear loss at point 2 of each drill lip

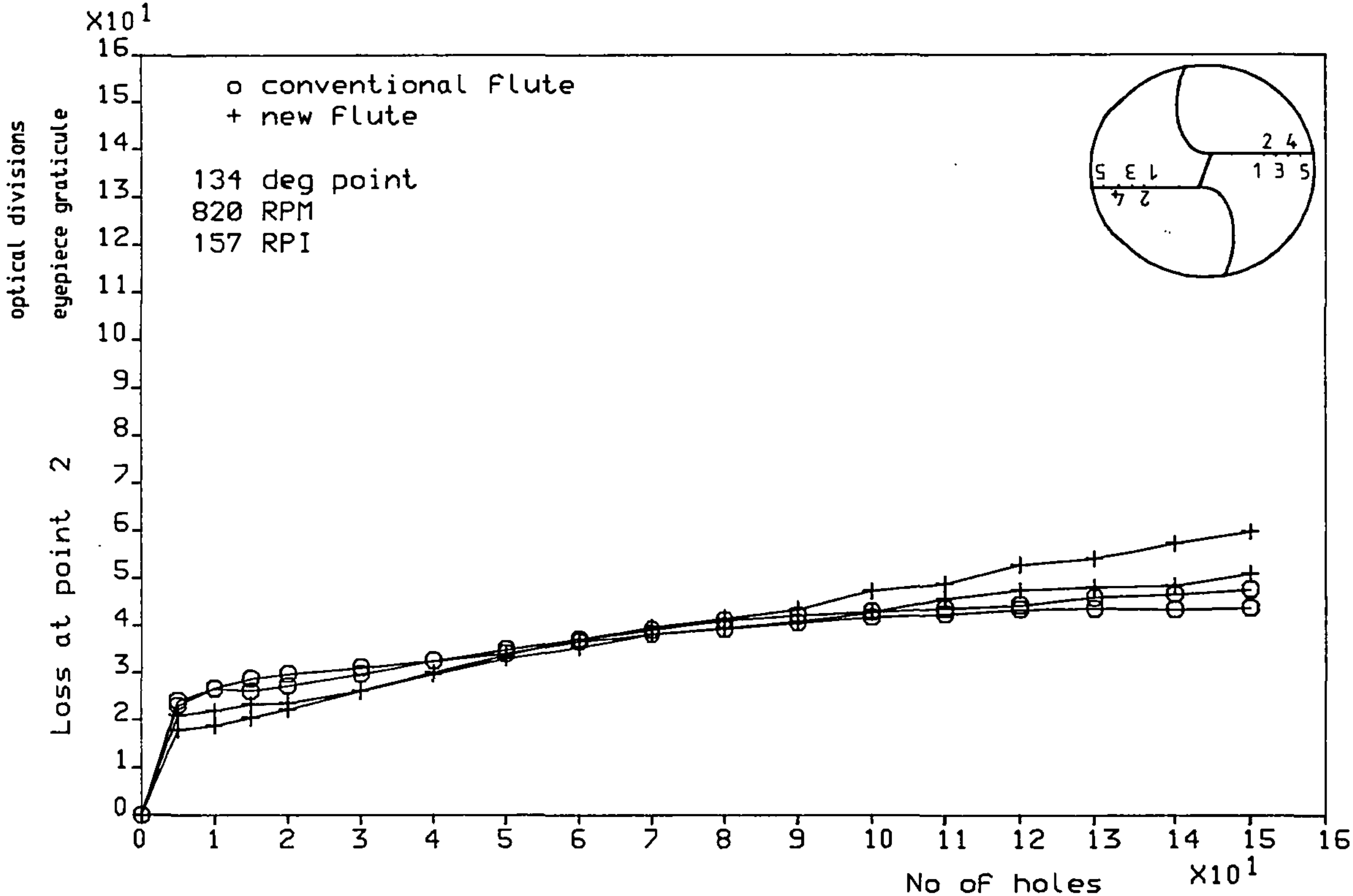


Wear loss at point 2 of each drill lip

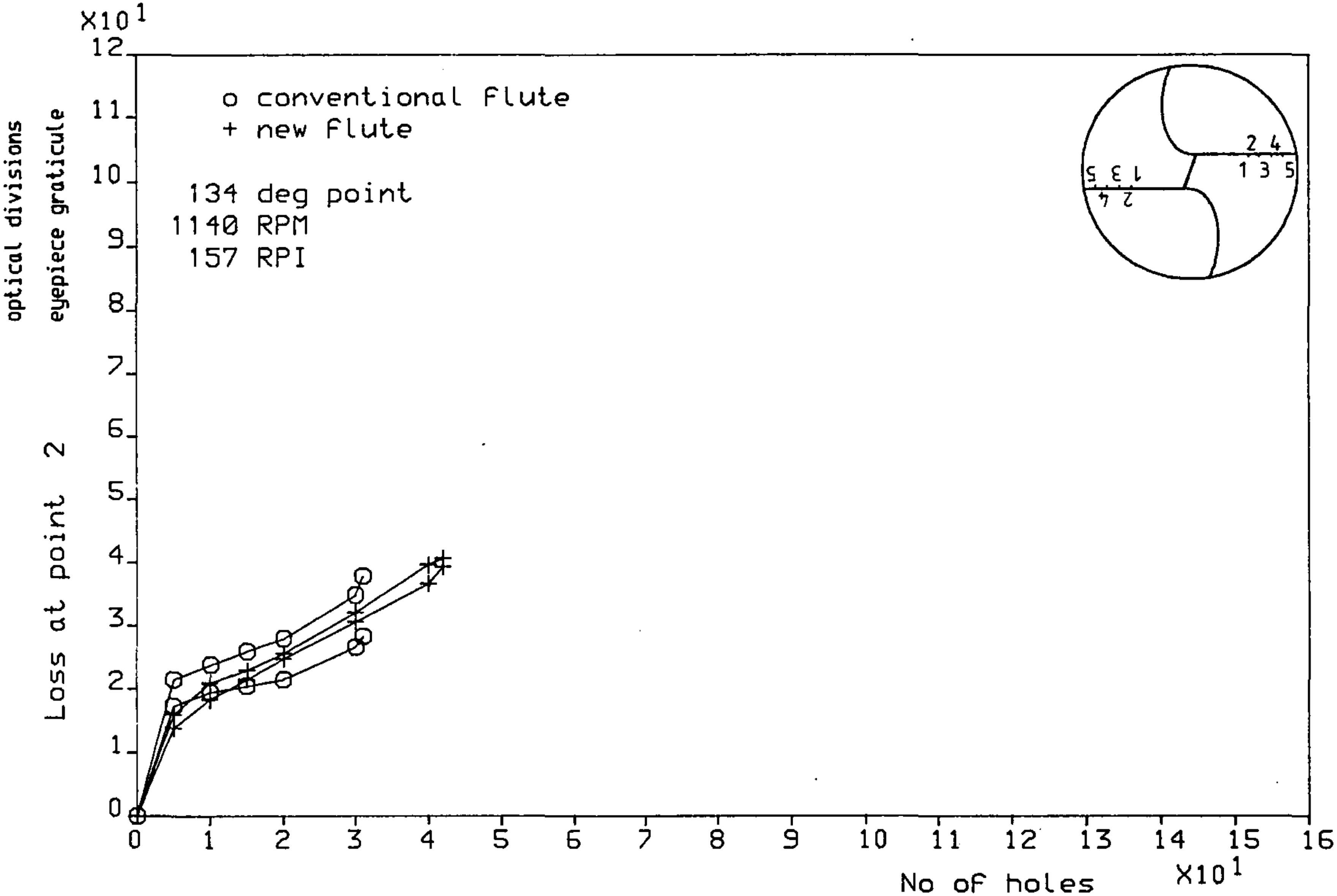


Wear loss at point 2 of each drill lip

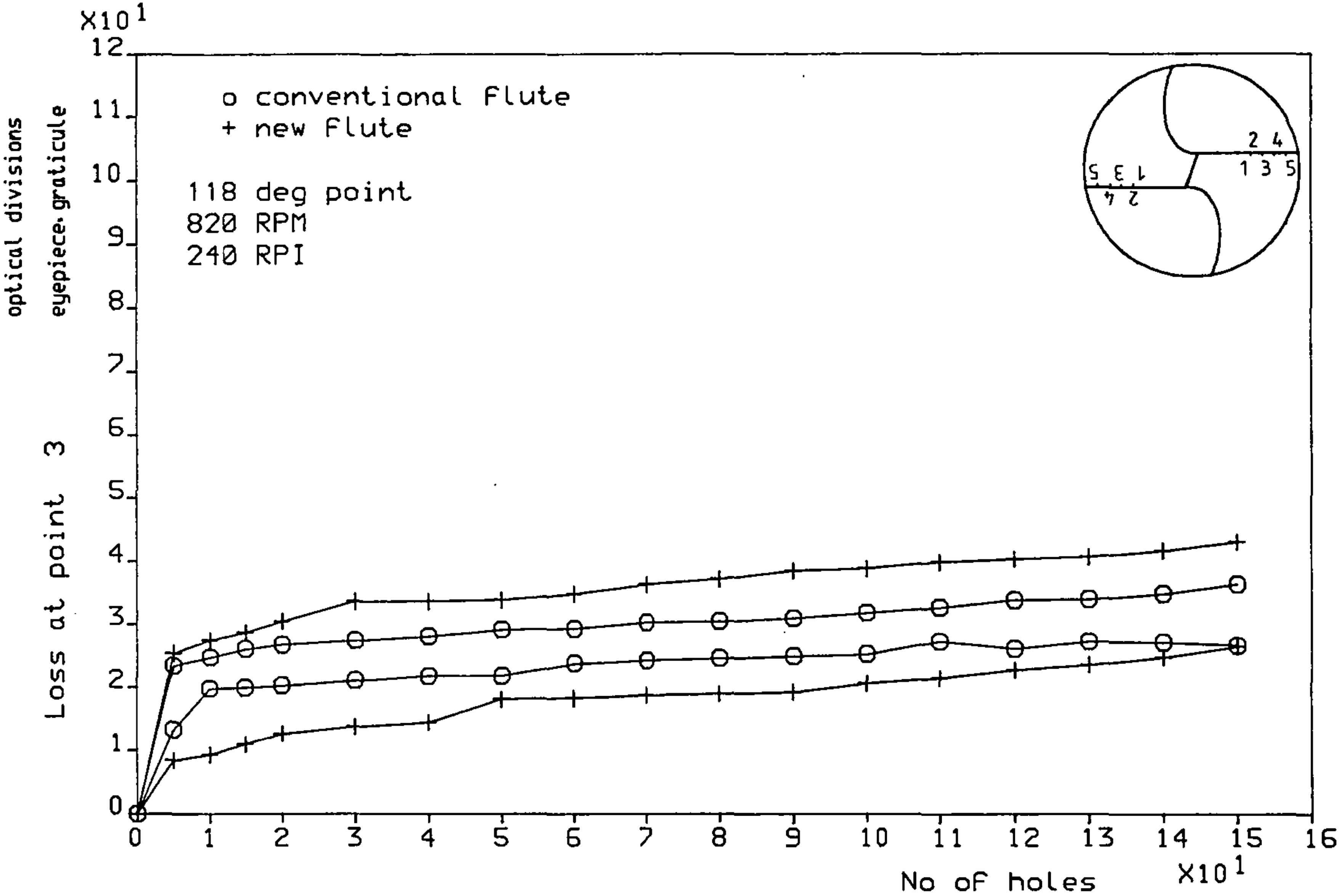


Wear loss at point 3 of each drill lip

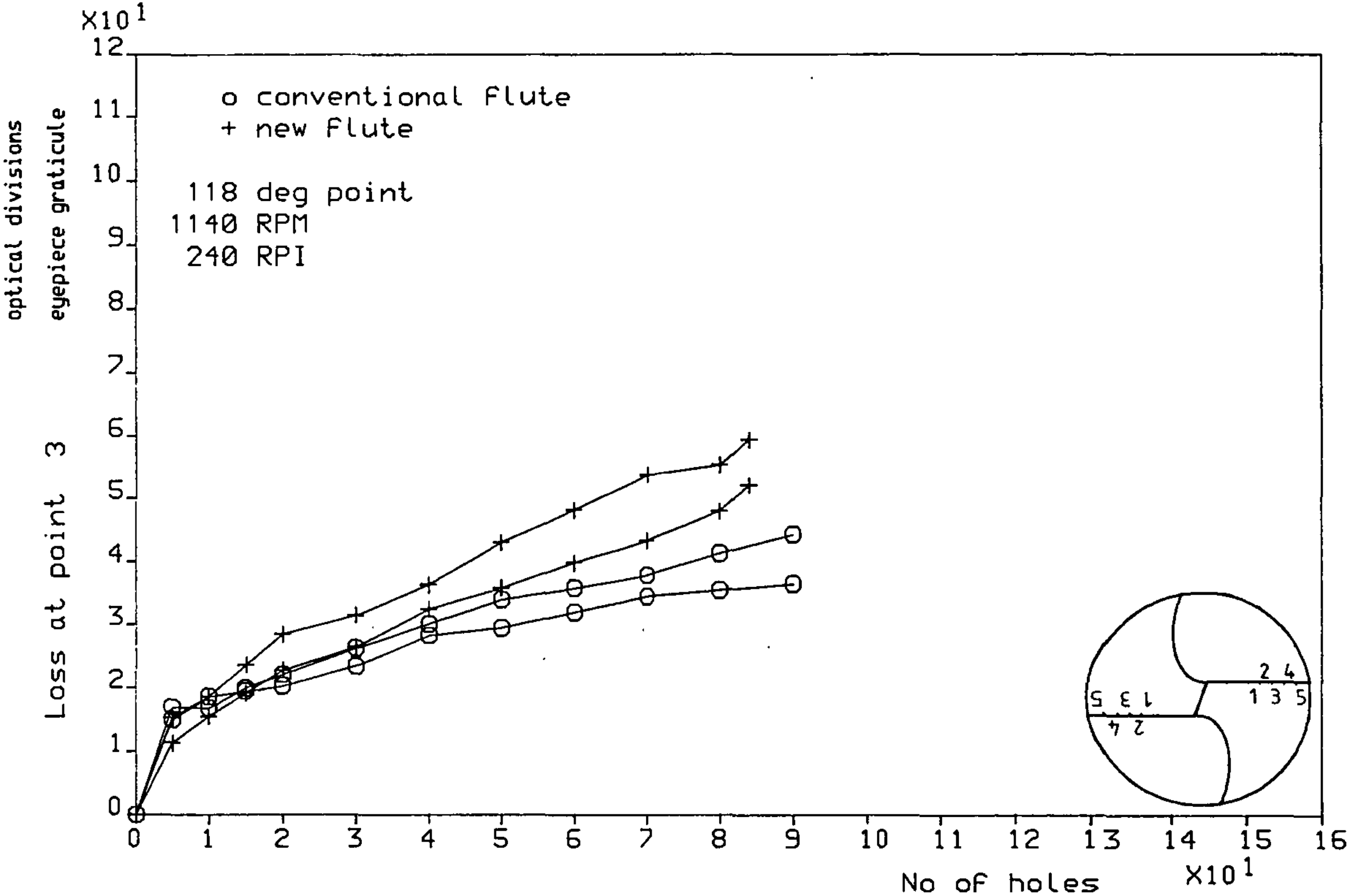


Wear loss at point 3 of each drill lip

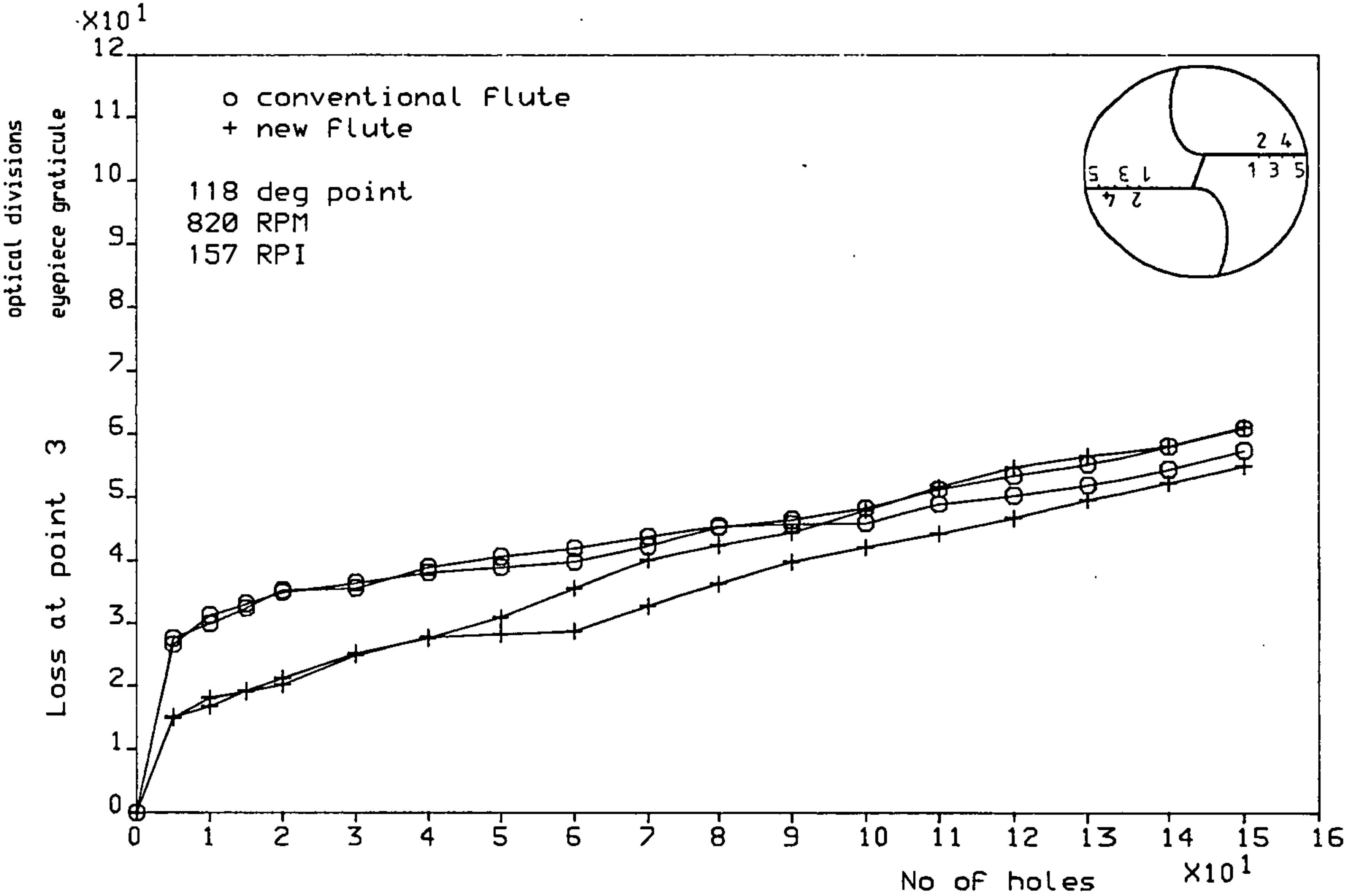


Wear loss at point 3 of each drill lip

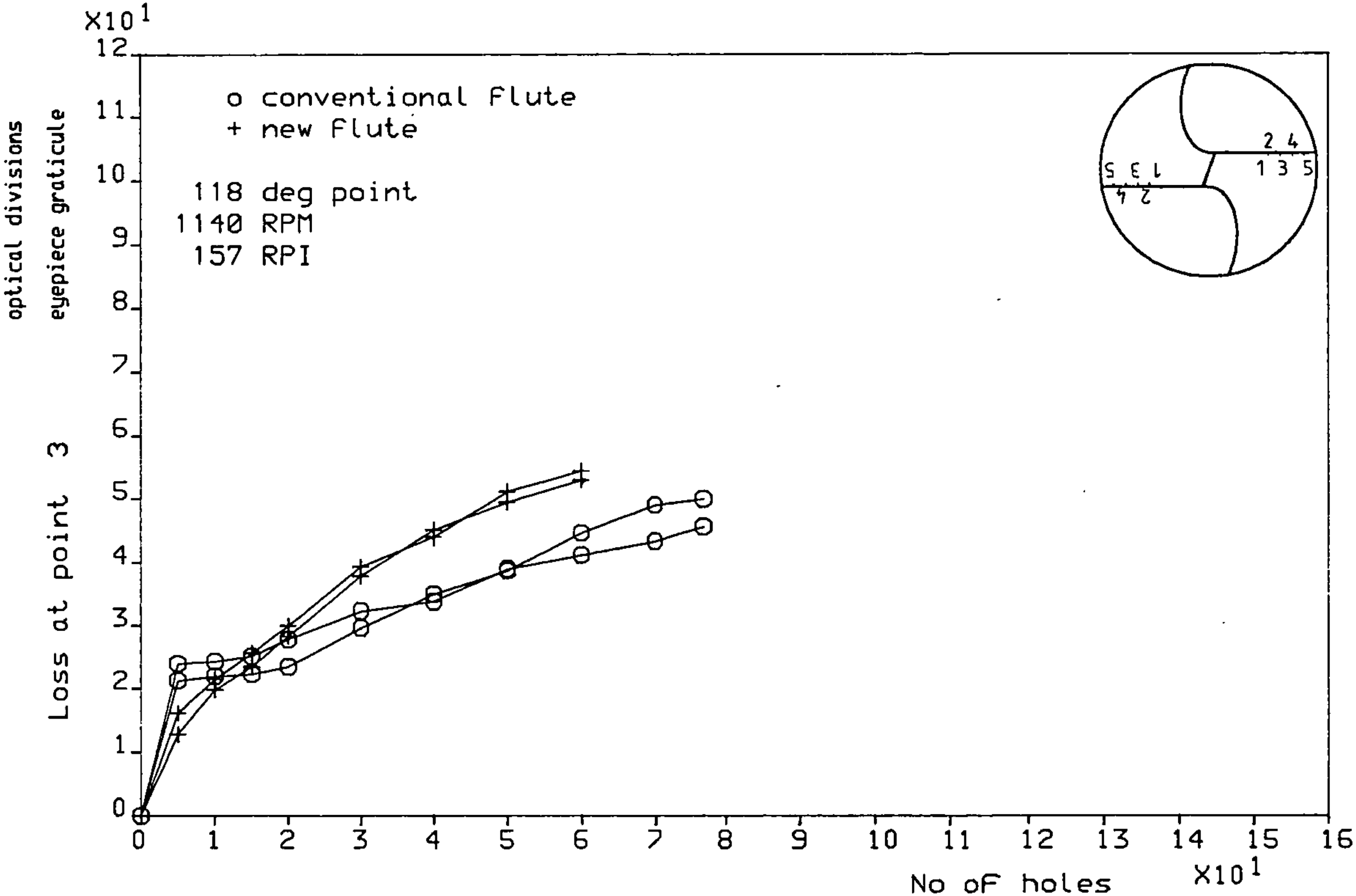


Wear loss at point 3 of each drill lip

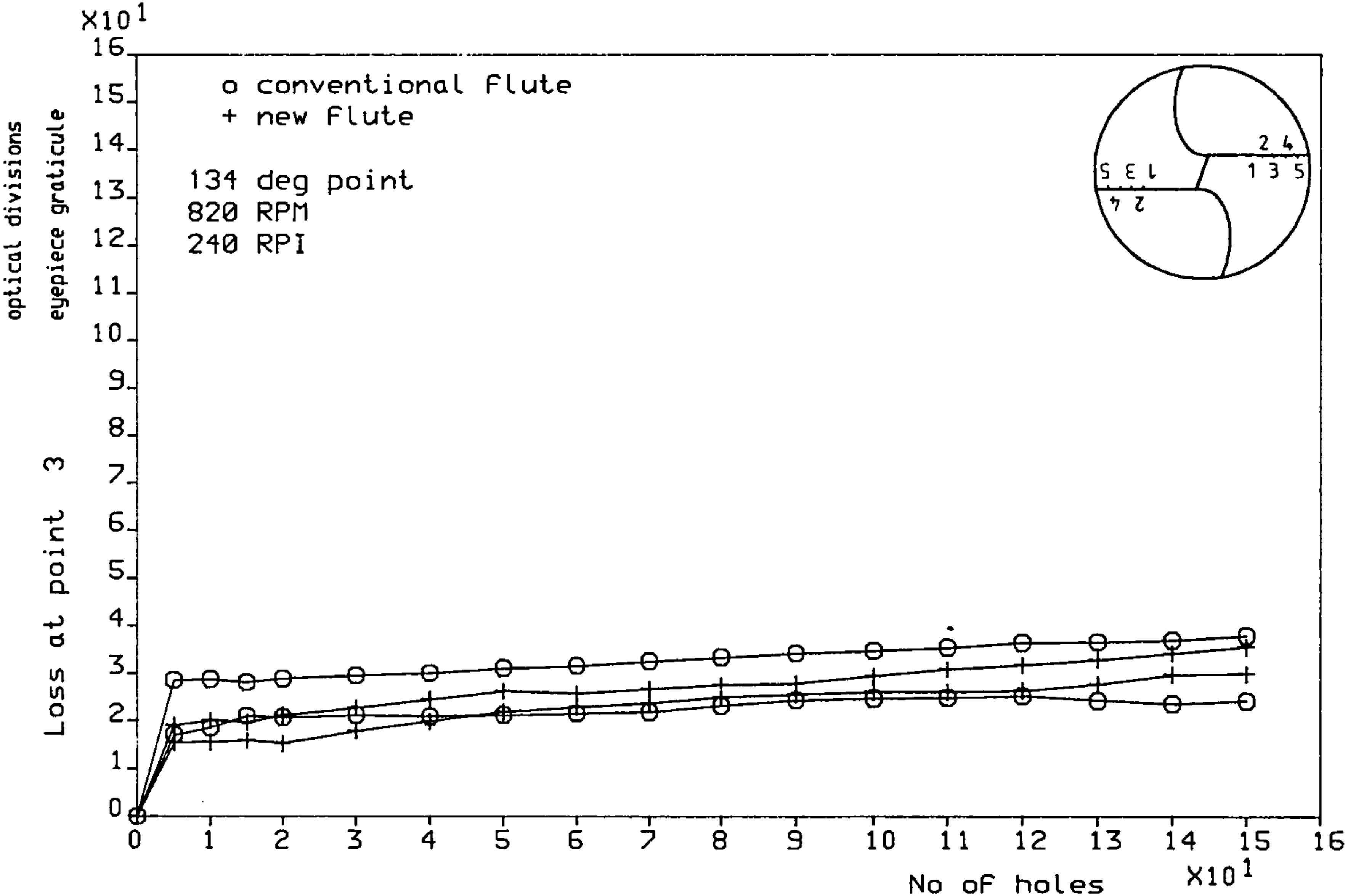


Wear loss at point 3 of each drill lip

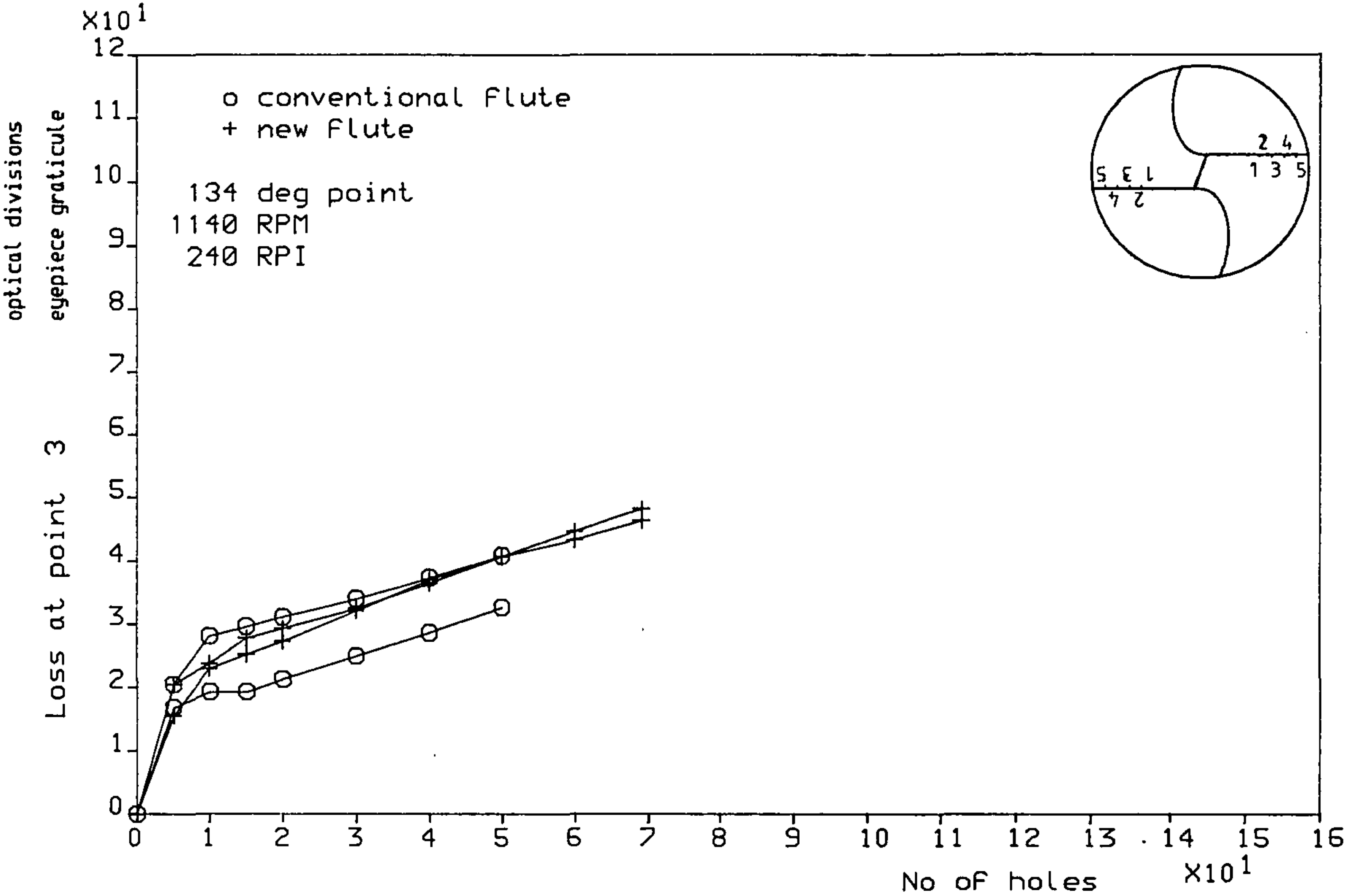


Wear loss at point 3 of each drill lip

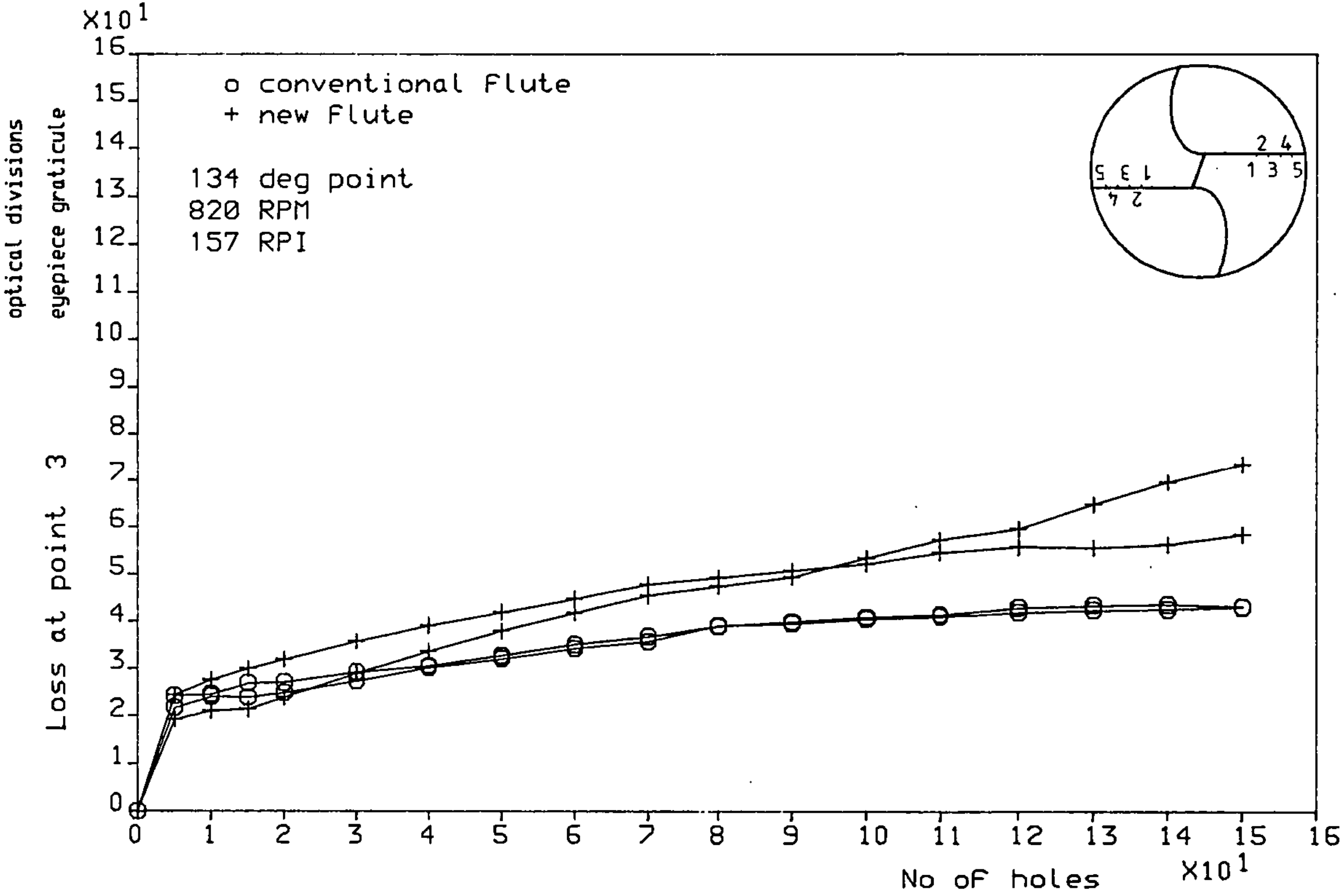


Wear loss at point 3 of each drill lip

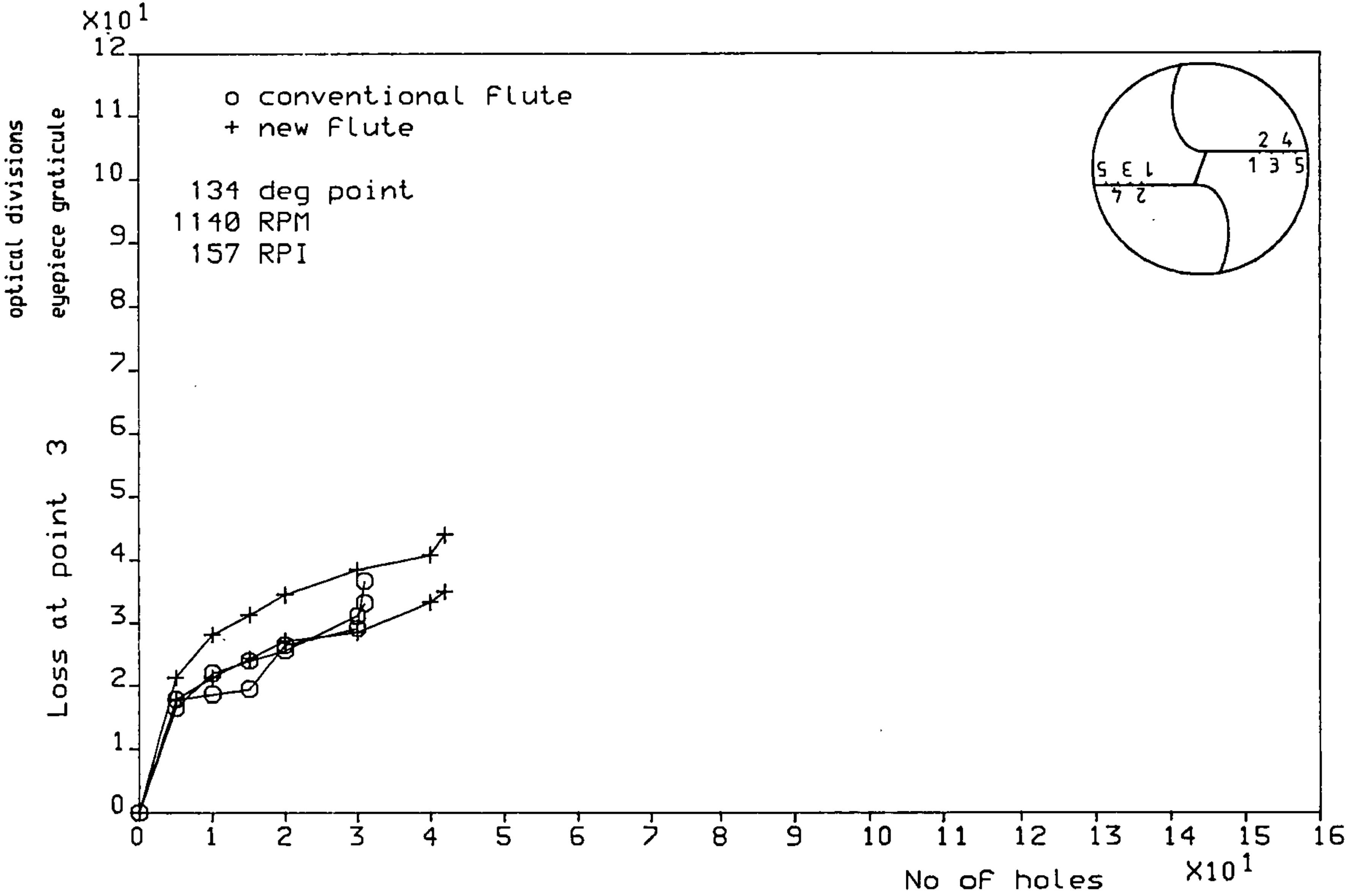


Wear loss at point 3 of each drill lip

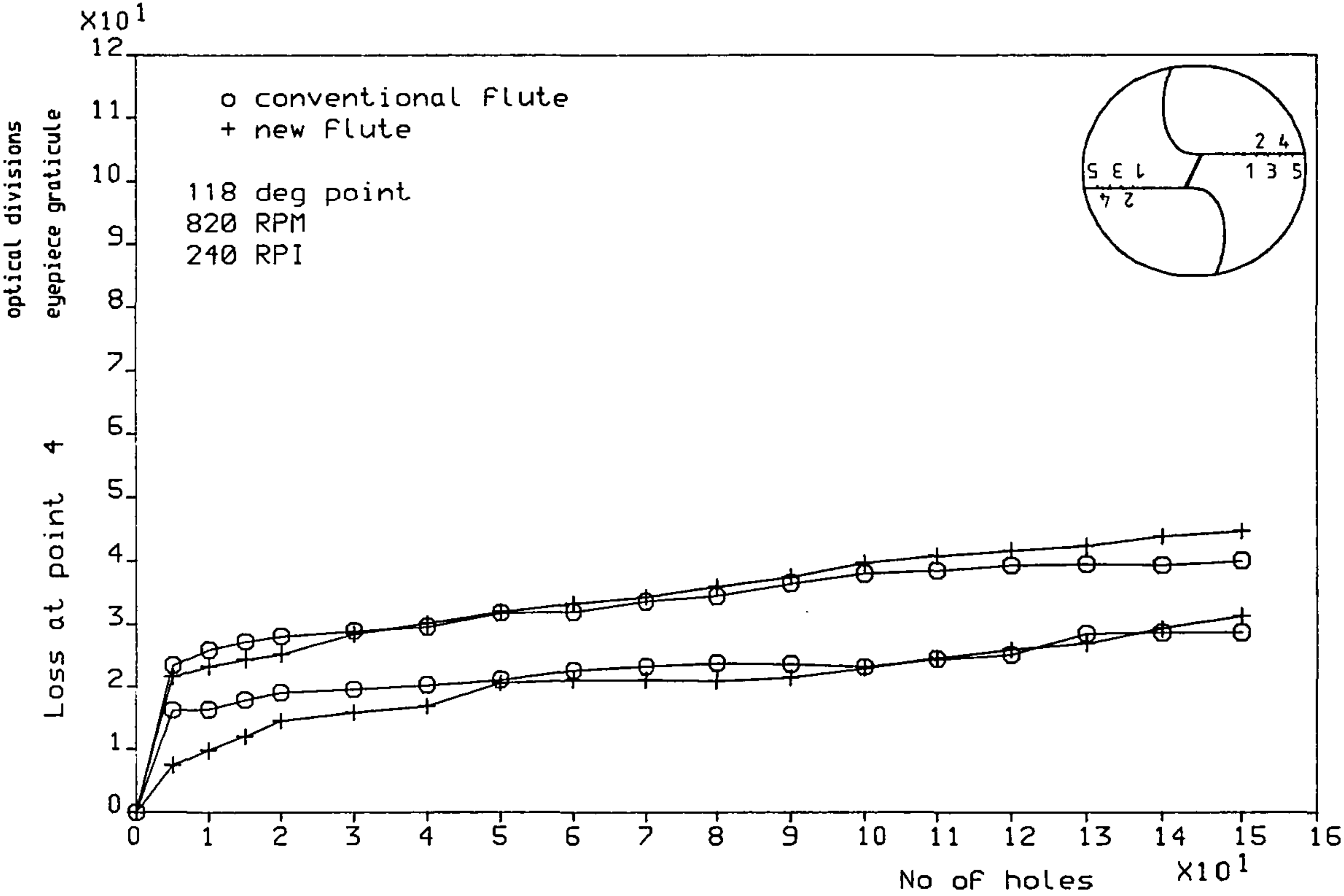


Wear loss at point 4 of each drill lip

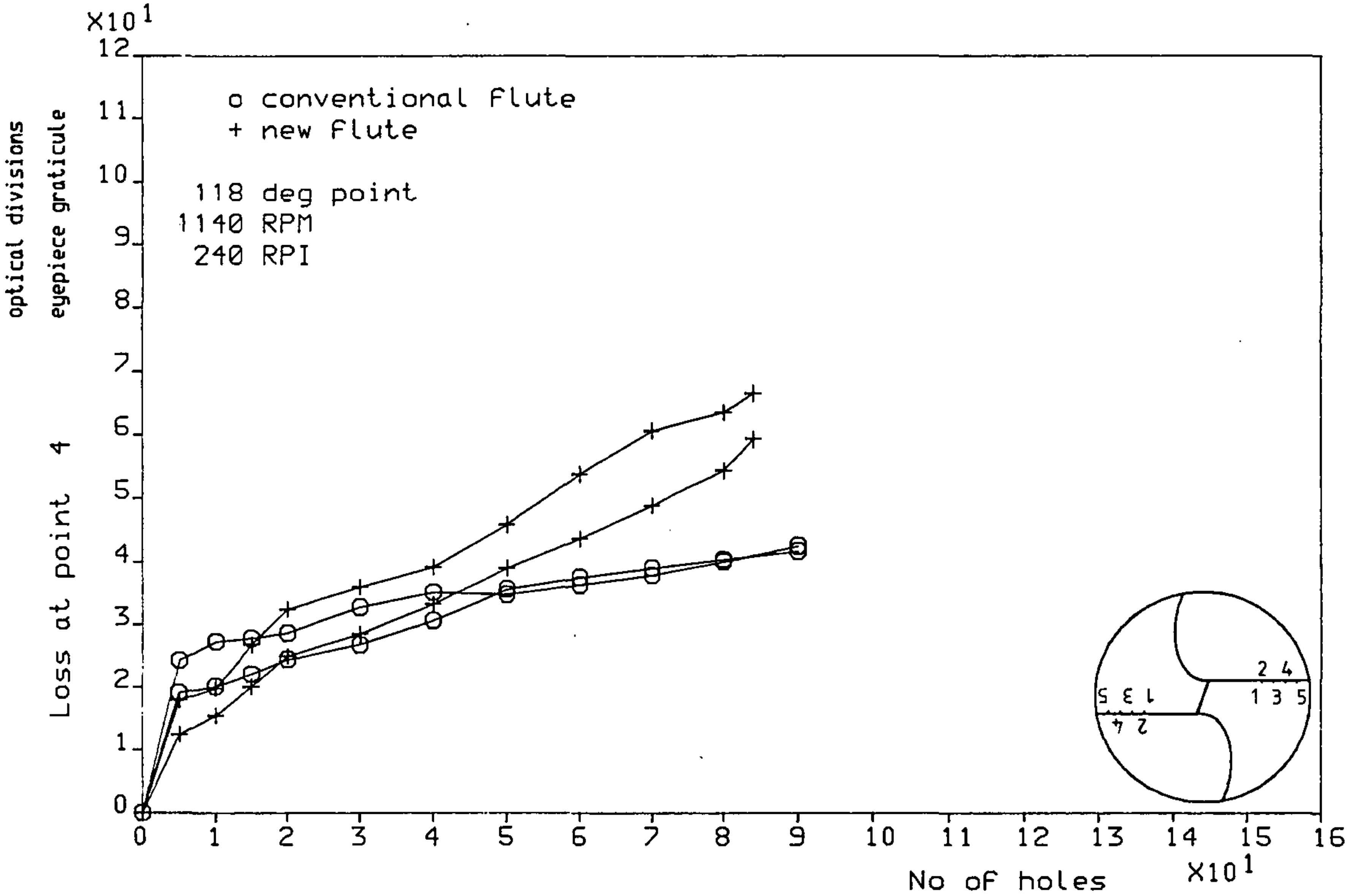


Wear loss at point 4 of each drill lip

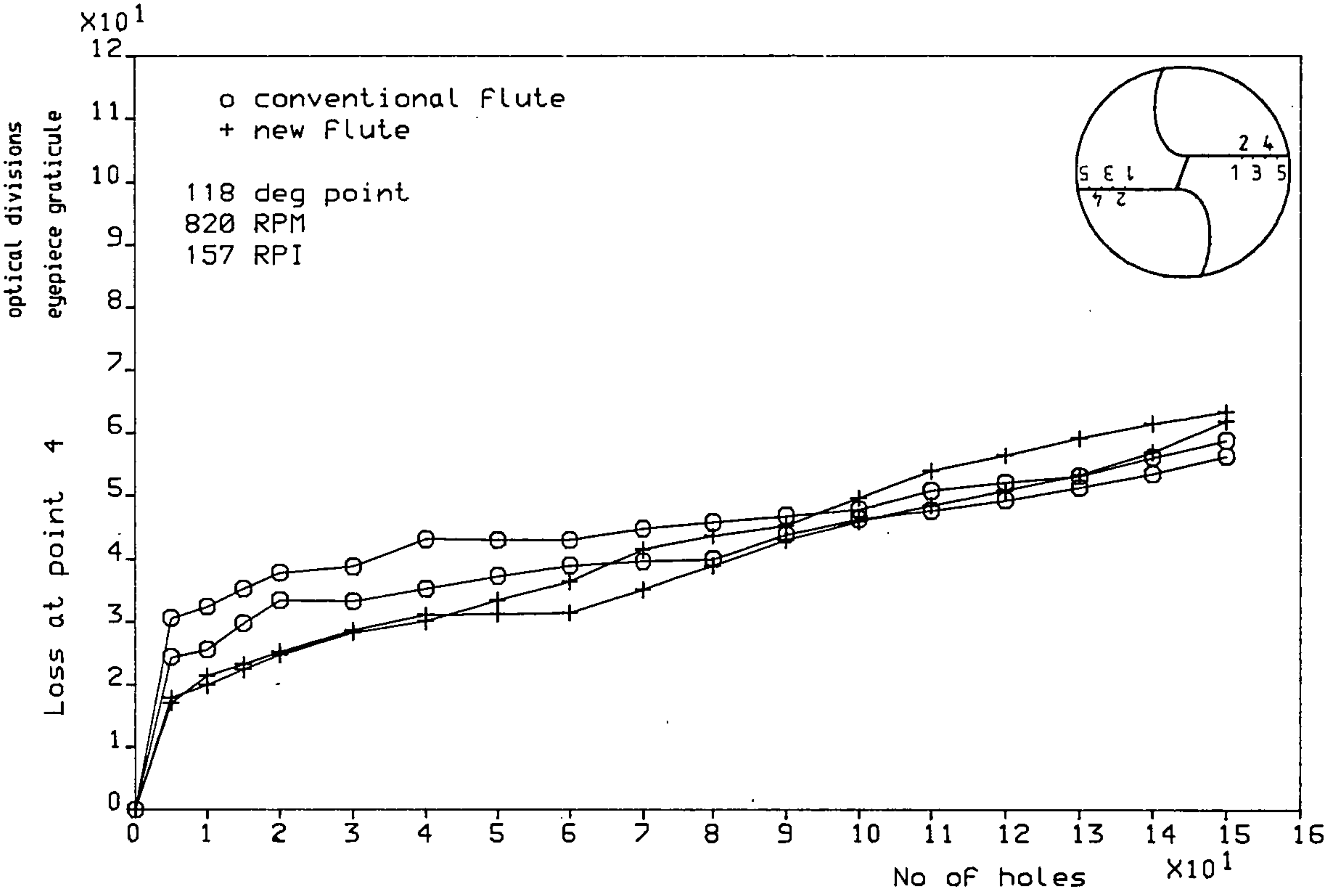

Wear loss at point 4 of each drill lip

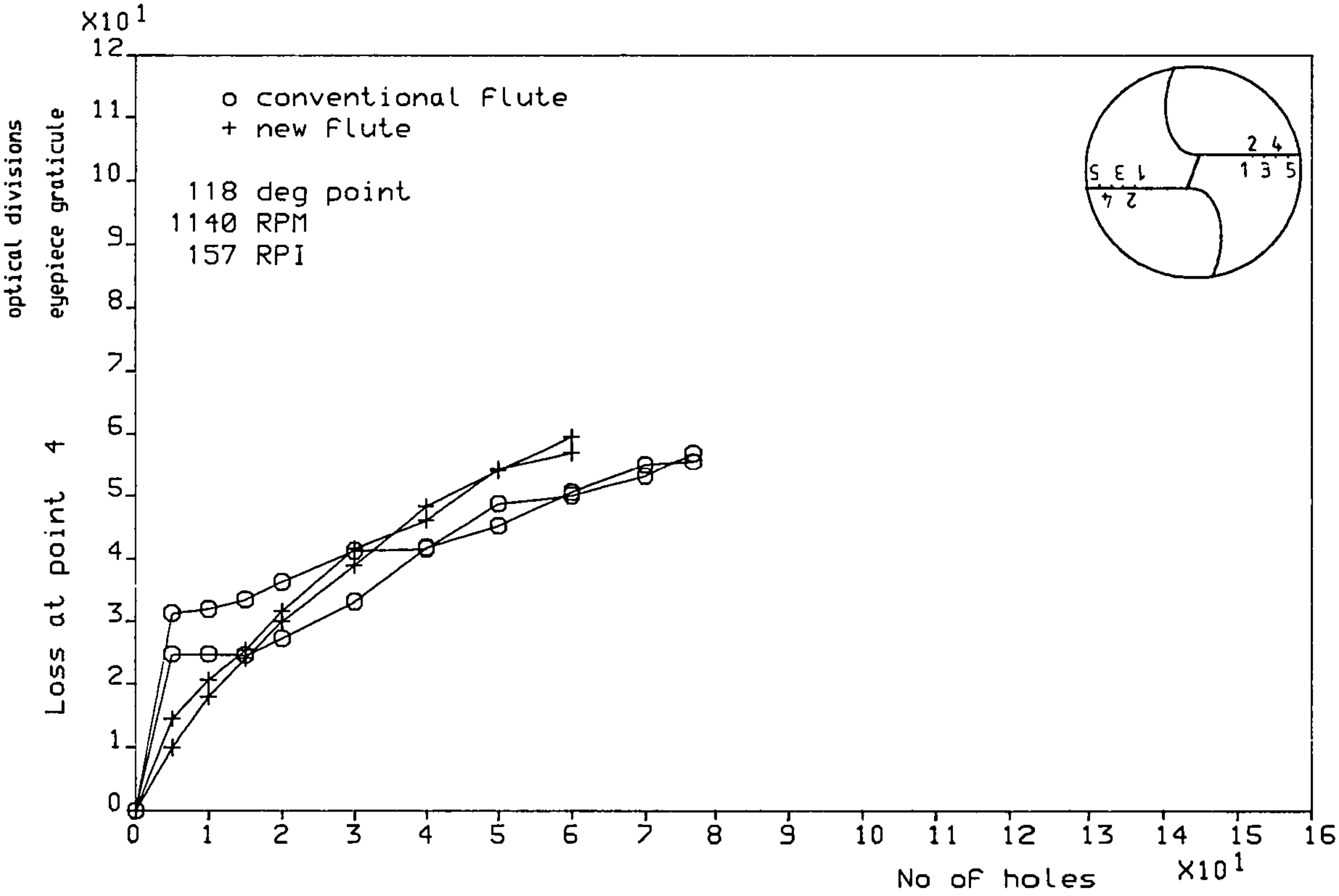


Wear loss at point 4 of each drill lip

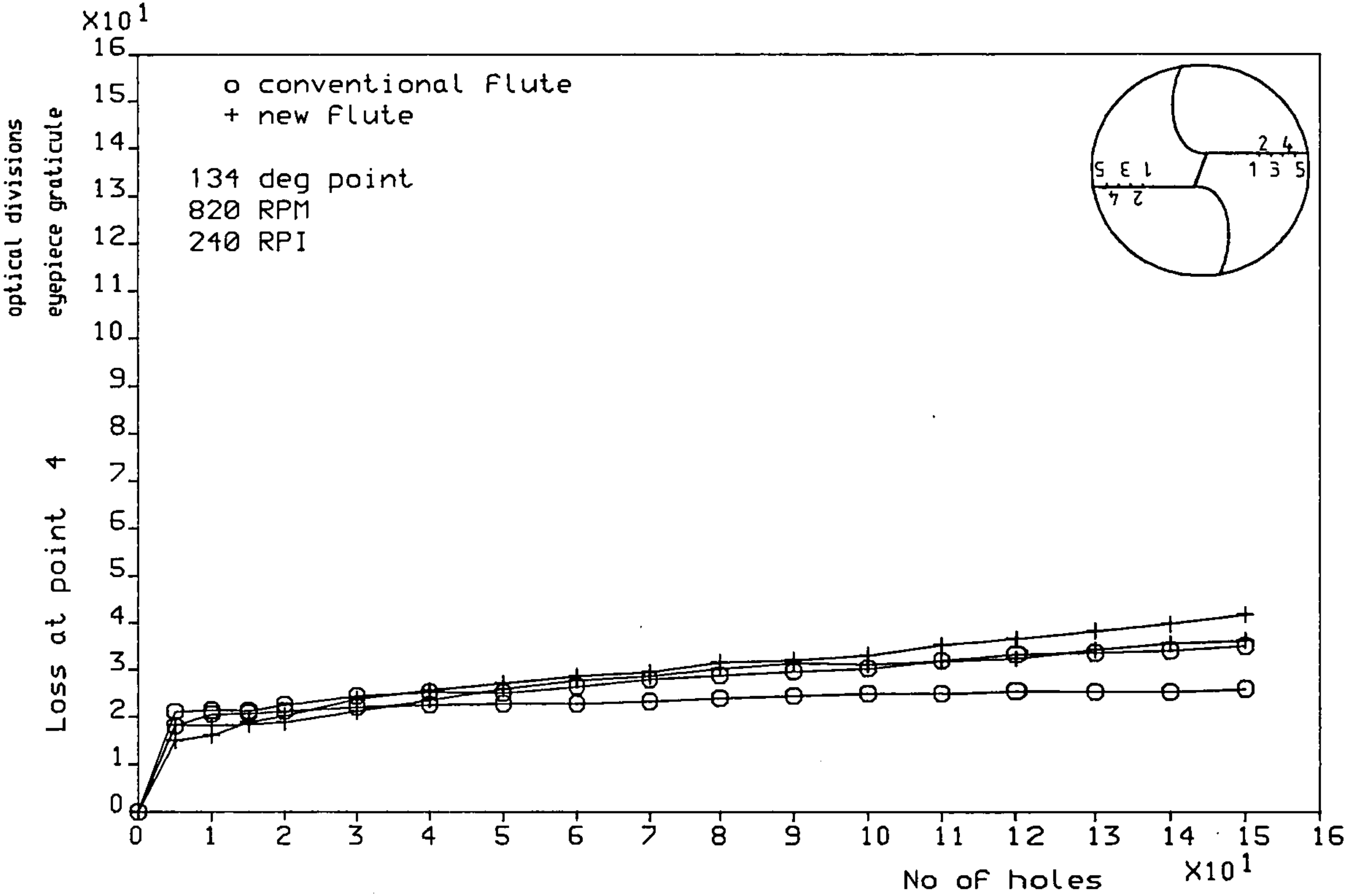


Wear loss at point 4 of each drill lip

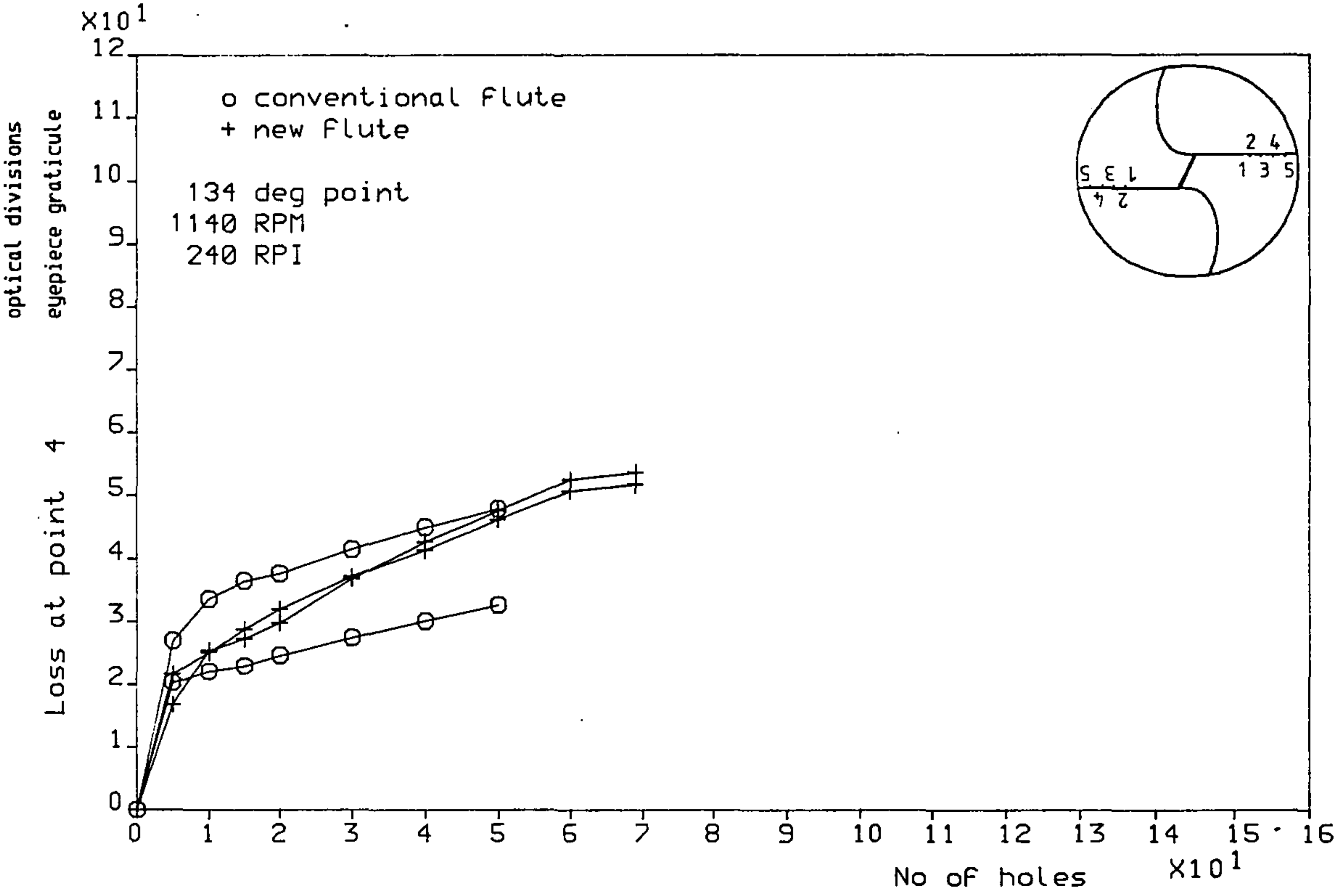


Wear loss at point 4 of each drill lip

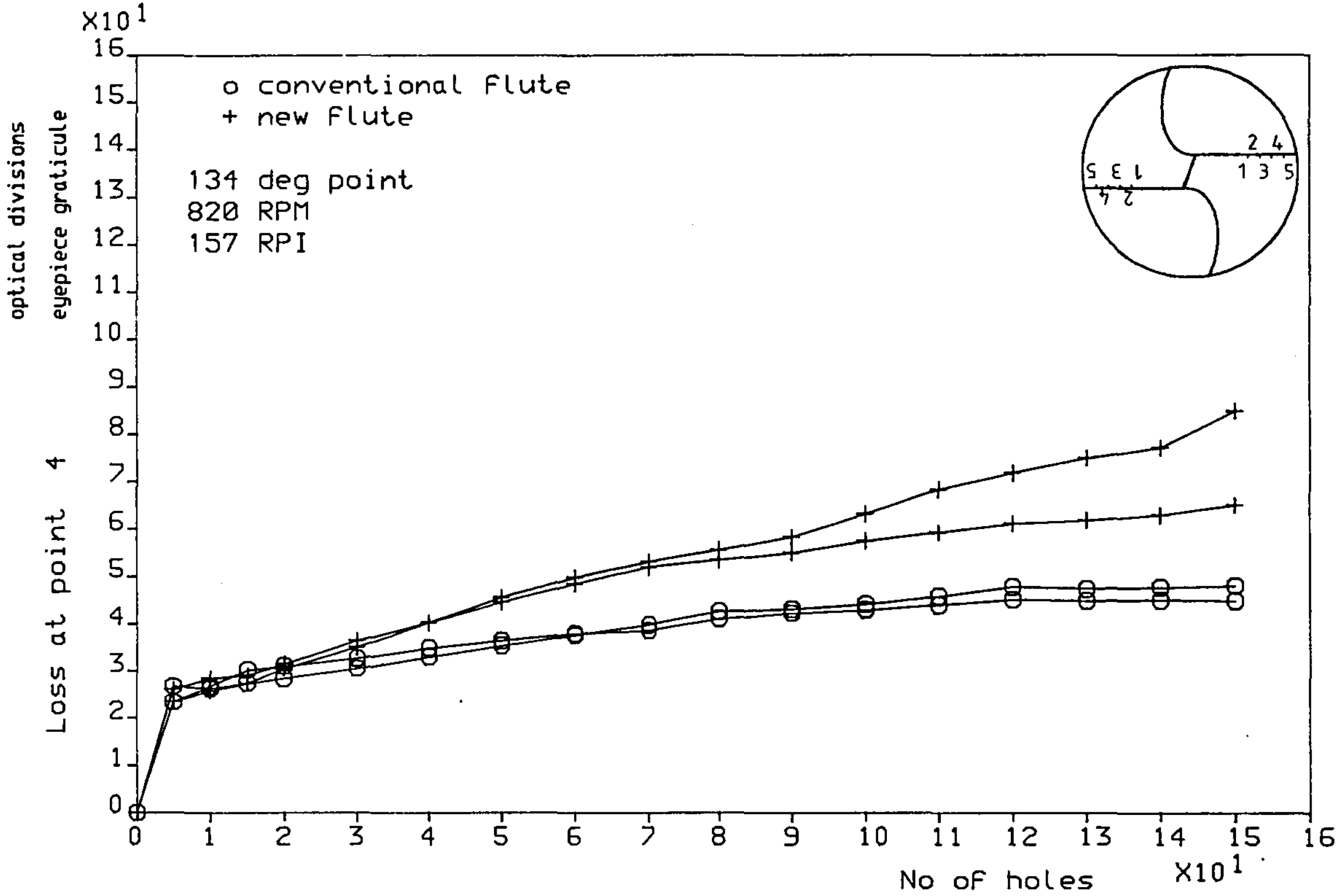


Wear loss at point 4 of each drill lip

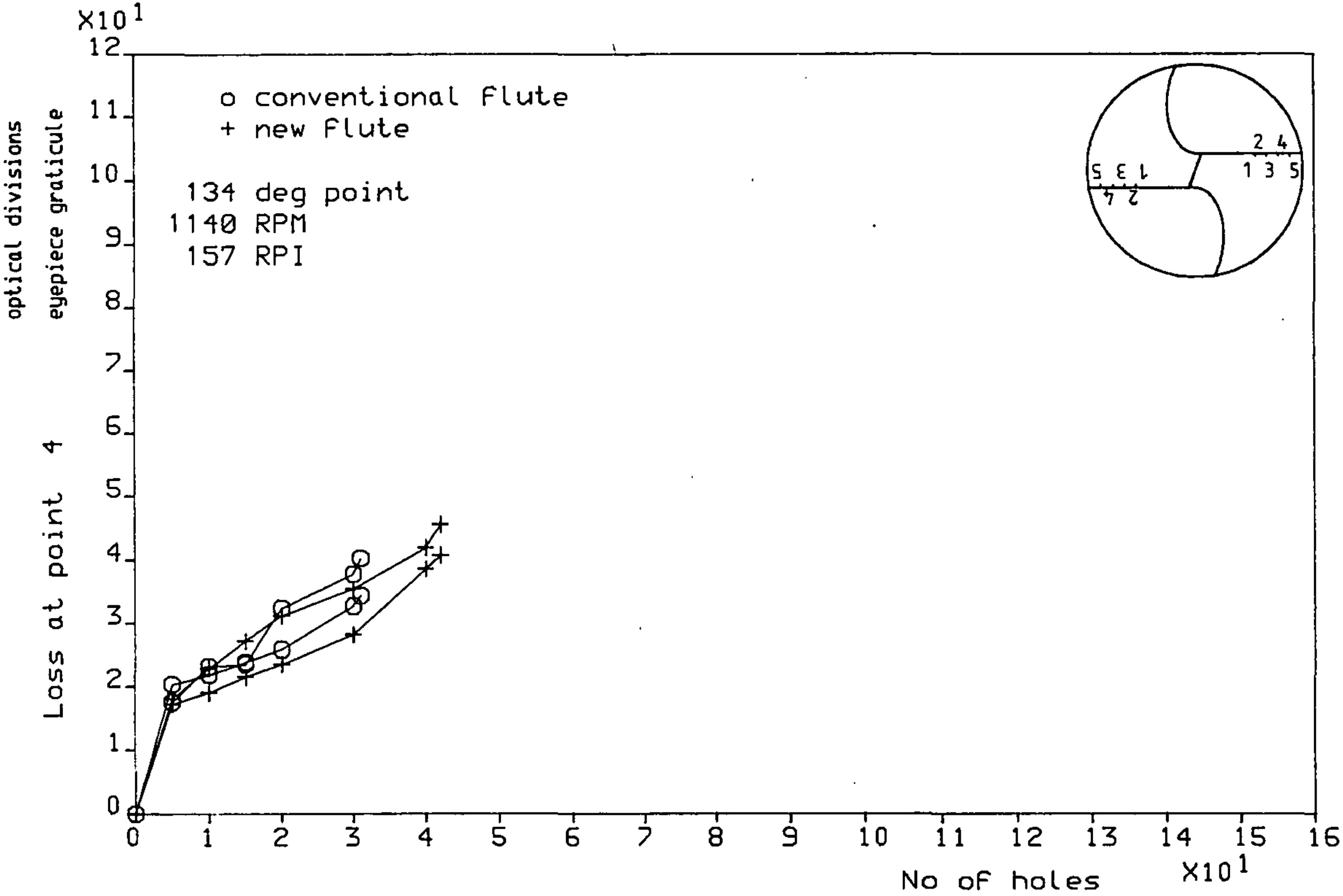

Wear loss at point 4 of each drill lip

405

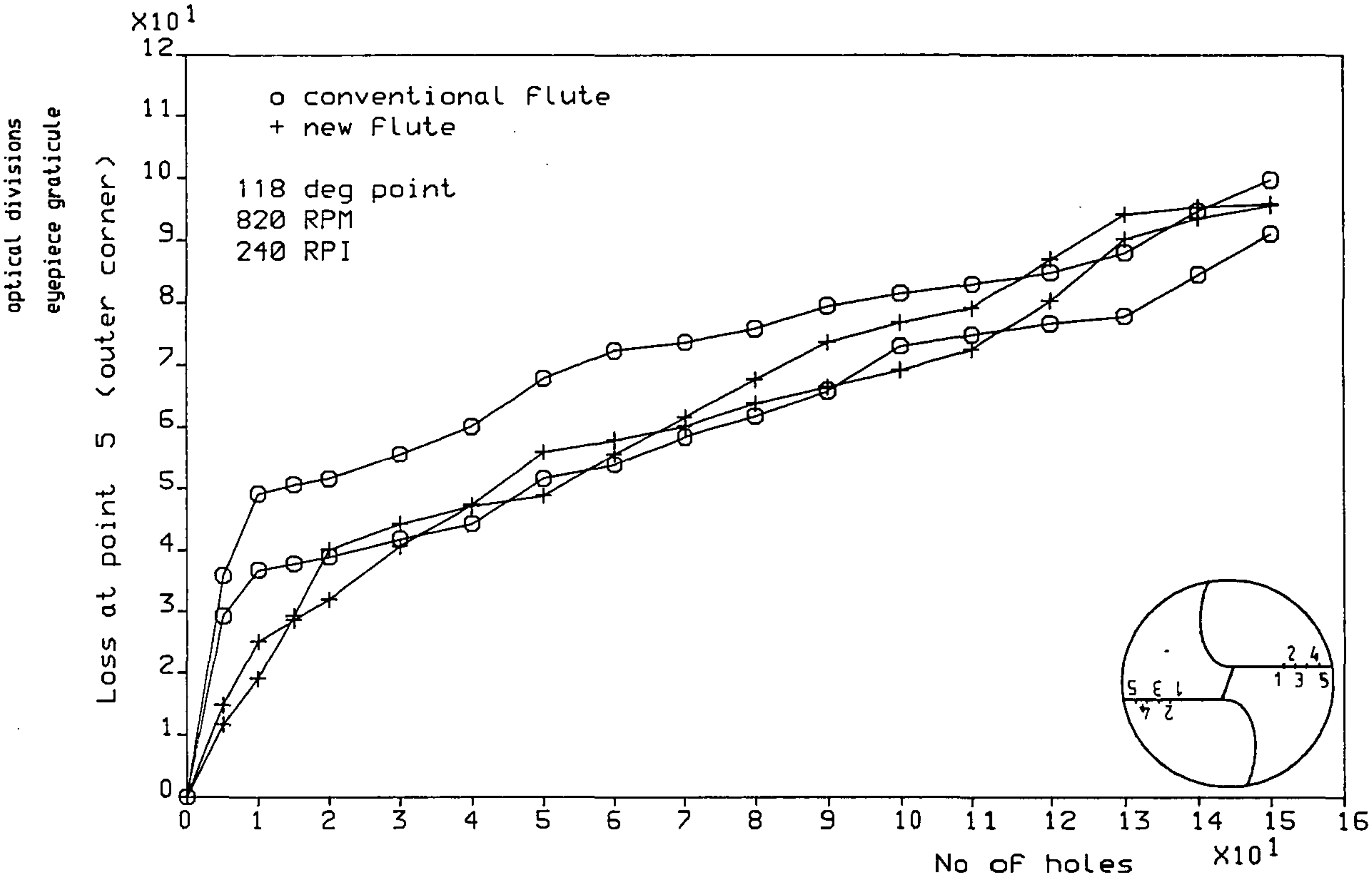


Wear loss at point 5 - outer corner - of each drill lip

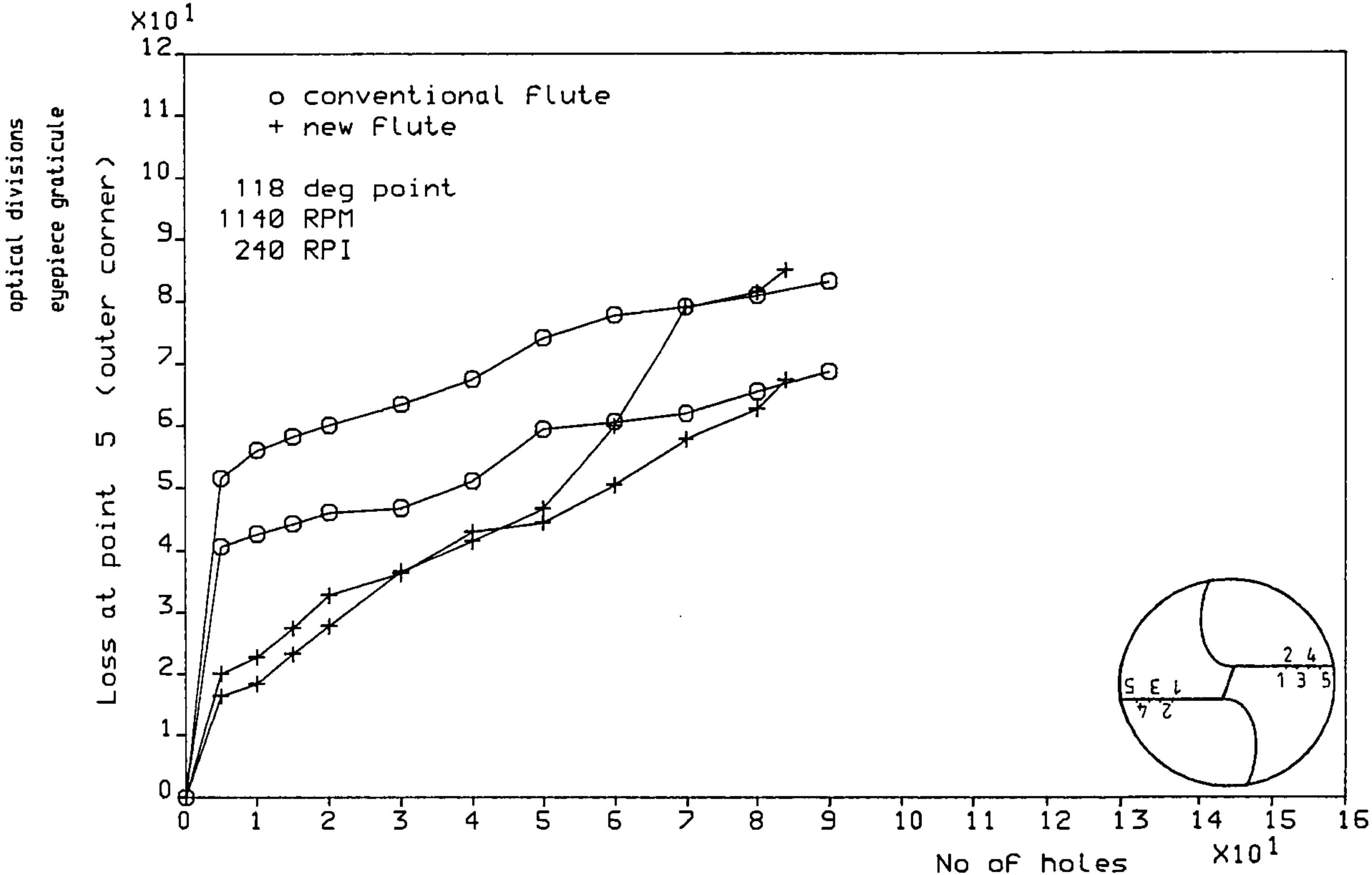


Wear loss at point 5 - outer corner - of each drill lip

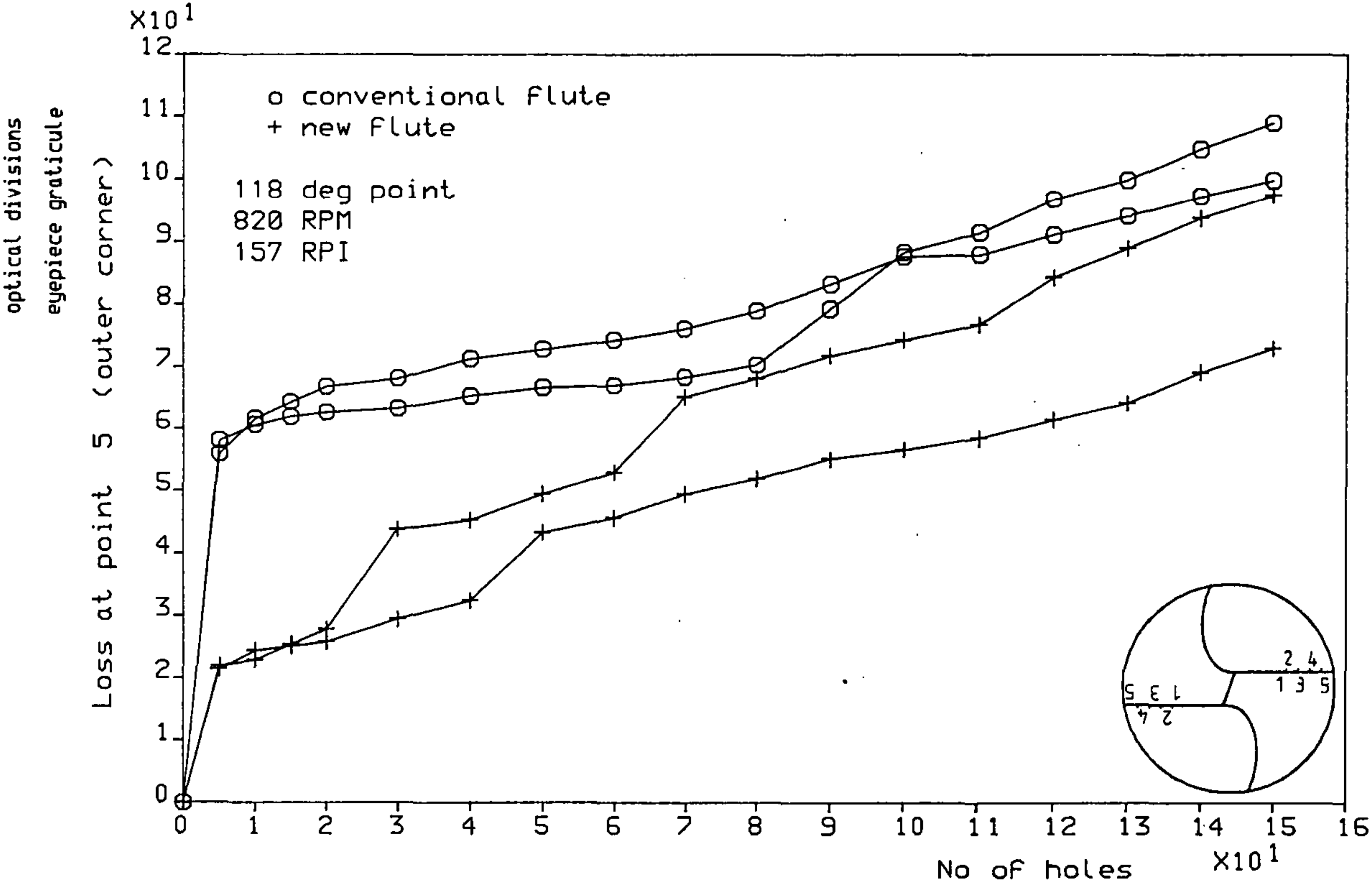


Wear loss at point 5 - outer corner - of each drill lip

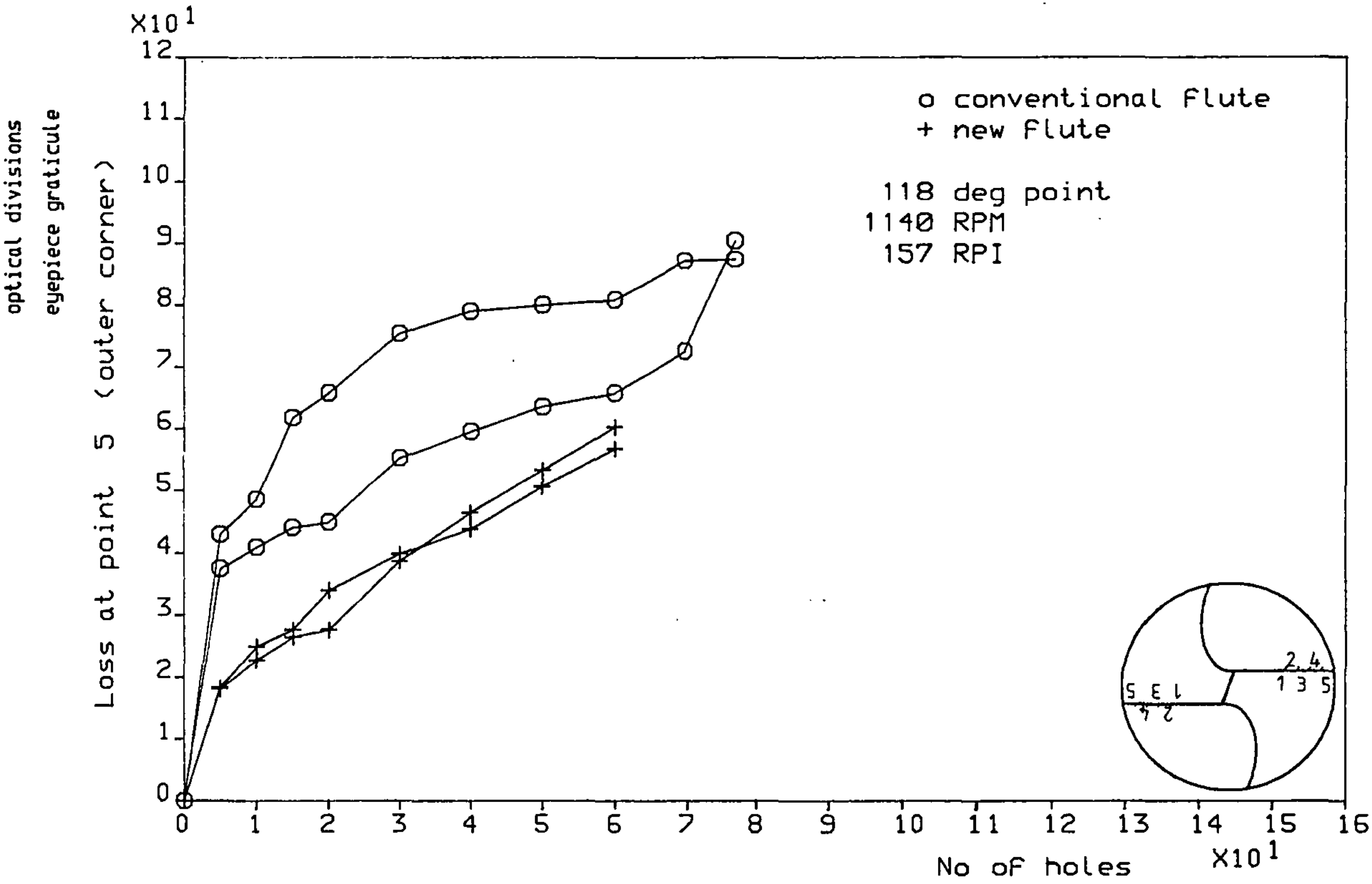


Wear loss at point 5 - outer corner - of each drill lip

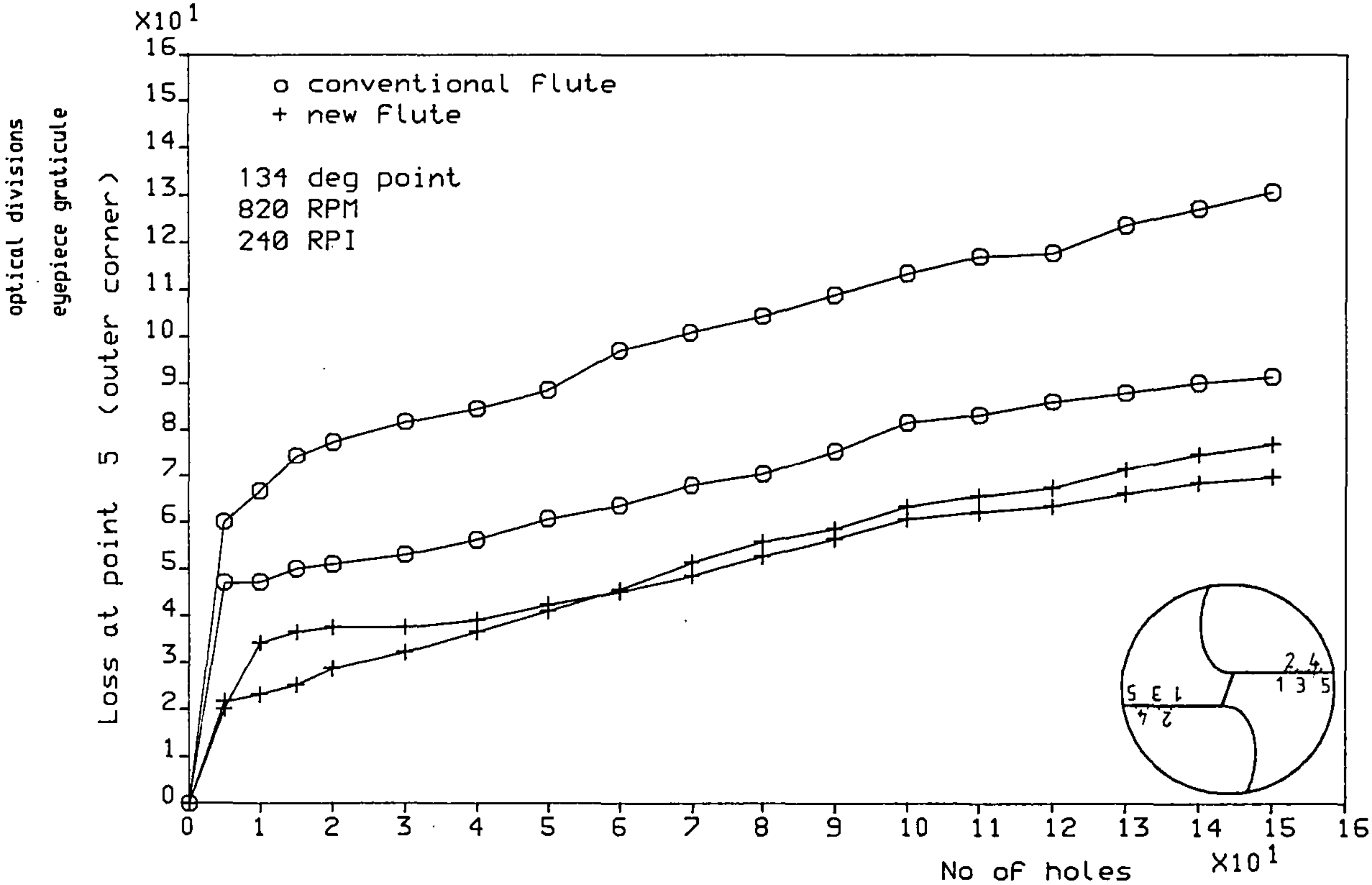


Wear loss at point 5 - outer corner - of each drill lip

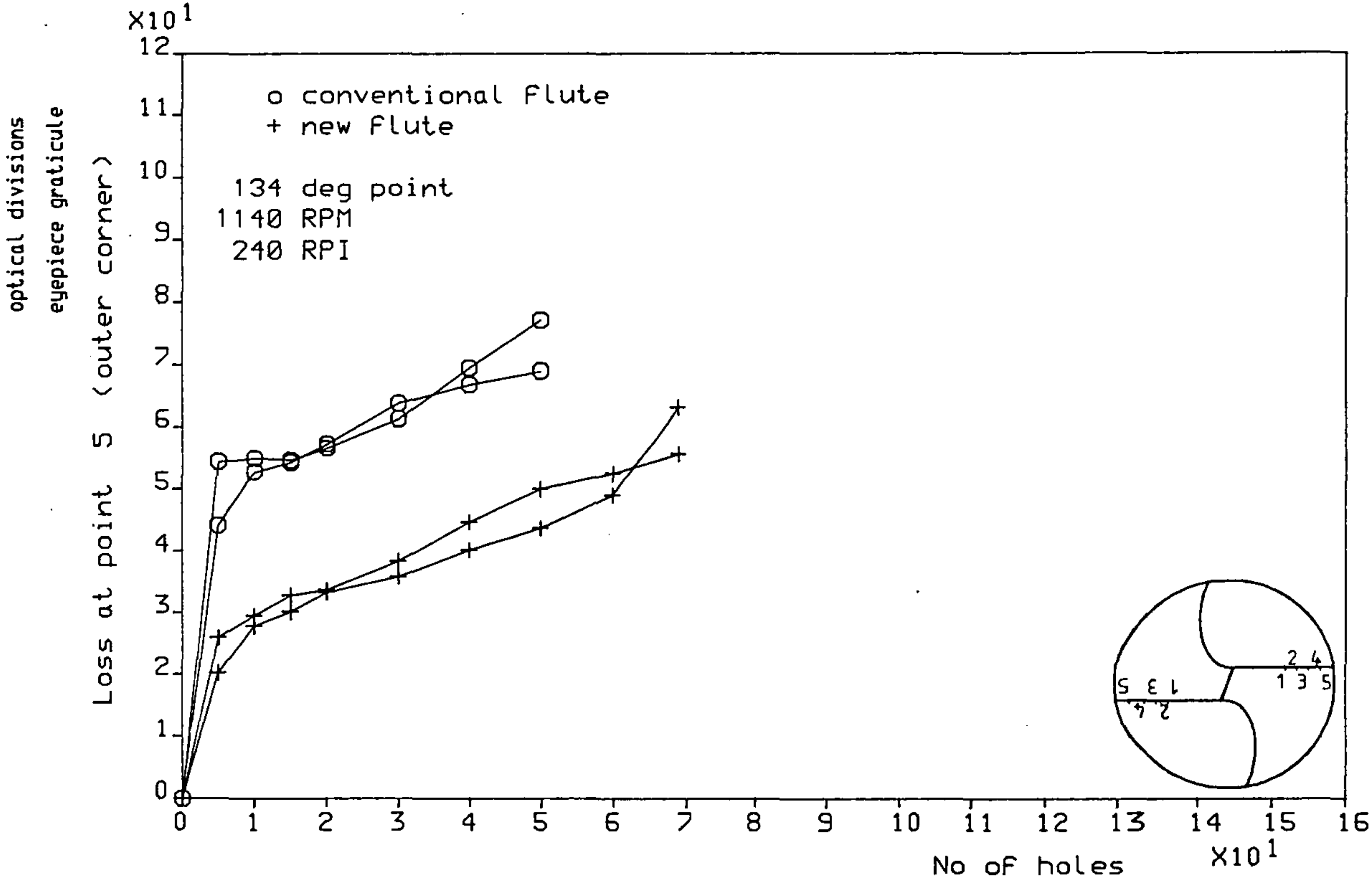


Wear loss at point 5 - outer corner - of each drill lip

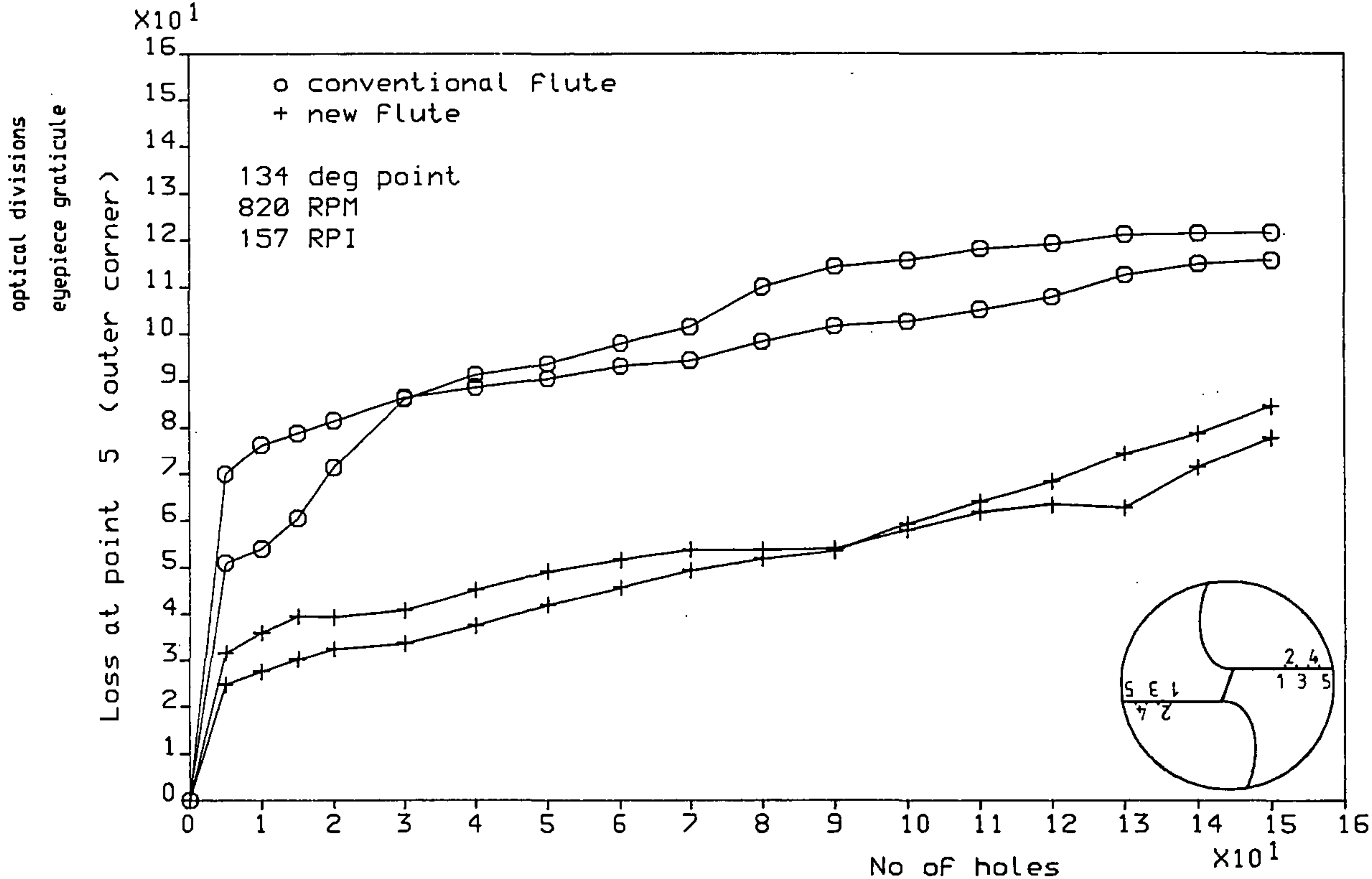


Wear loss at point 5 - outer corner - of each drill lip

# APPENDIX 8

Computer program for chip geometric simulation with any flute shape and any set of cylindrical grinding conditions providing for chip flow angle prediction, cutting ratio prediction and other chip related variables (refer to Chapter 8).

This FORTRAN program uses subroutines from GINO and NAG libraries which are not listed here.

```
C
C
C ==============================================
C
C
C           CHIP SIMULATION FOR
C           ANY SET OF CYLINDRICAL GRINDING
C           CONDITIONS AND ANY FLUTE SHAPE
C
C
C           PROGRAM DESIGNED,DEVELOPED AND IMPLEMENTED BY
C           MANUEL DOS SANTOS PAIS
C
C
C           SUBROUTINES FROM GINO AND NAG
C           LIBRARIES ARE USED
C
C
C ==============================================
      IMPLICIT DOUBLE PRECISION(A-H,O-Z)
      REAL ETARIG(100),SSS(100),CEL(100)
      REAL XAXIS,YAXIS,R0P,R0N
      REAL XPACG(100),YPACG(100),ZPACG(100),RSTO(100)
      REAL X1(100),Y1(100),Y1N(100),Y1A(100),X1A(100)
      DIMENSION X1AN(100)
      REAL T1MEU(100),T1WI(100),T1MAU(100)
      REAL XFLU(100),YFLU(100),XCHIG(100),YCHIG(100),ZCHIG(100)
      REAL RAKE(100),ANSAI(100),AINC(100),ANSI(100)
      REAL RADI(100),XLG(100),YLG(100)
      REAL XSTG(100),YSTG(100),ZSTG(100),RSNI(100),DL(100)
      REAL DVSNI(100),ADVSNI(100)
      REAL XHEELG(100),YHEELG(100),ZHEELG(100),XEELG(100)
      DIMENSION YEELG(100)
      REAL VCSIET(100),SVCSIE(100),VVSIIN(100),SVVSII(100)
      REAL XRIGG(100),YRIGG(100),ZRIGG(100),ZRIGGD(100)
      REAL VERIG(100),RCAG(100),T1PR(100),T2PR(100),VVCA(100)
      DIMENSION A(3,3),DCOOR(3),CAAR(3),EIX(4)
      DIMENSION VERIF(100)
      DIMENSION CLEAA(100),GAMAE(100)
      DIMENSION GAMN(100),GCD(100),AKCD(100),HCD(100)
      DIMENSION RRN(100),T211(100),ETAA(100)
      DIMENSION RCA(100),GEMEA(100)
      DIMENSION XCHI2(100),YCHI2(100)
      DIMENSION ZSTGD(100),XSTGD(100),YSTGD(100)
      DIMENSION XNRAD(100),YNRAD(100),ZNRAD(100)
      DIMENSION RCHISE(100),CHIXA(100)
      DIMENSION DER(14),EREST(14),COEF(20)
      DIMENSION XMSU(100),YMSU(100),ZMSU(100)
      DIMENSION XL(100),YL(100),DERIV(100),RELIEF(100)
      DIMENSION RSTFL(40),PHSTFL(40),COFL(40),XHSTFL(40)
      DIMENSION YHSTFL(40)
      DIMENSION CCE1(100),CCE2(100),CCE3(100),CCE3P(100)
      DIMENSION DIDL(100),VVD(100)
      DIMENSION ZTGHG(100),HENR(100),ETAS(100),WIETA(100)
      DIMENSION CORN(3),RE(8),RU(3),WE0(120)
      DIMENSION FJAC(8,8),SMON(8),V(8,8),IW(1)
      DIMENSION XFLUD(100),YFLUD(100),XEELGD(100),YEELGD(100)
      DIMENSION XCHID(100),YCHID(100),ZCHID(100),VCHIP(100)
      DIMENSION XHEELD(100),YHEELD(100)
      COMMON/BLO1/R0,R0G,WEB,H0,RKG
      COMMON/BLO2/CONS,RCAM,EXG,VG
      COMMON/BLO3/ALPHA,CSVG,SNVG,CSKOI,SNKOI,CSKOU,SNKOU
      COMMON/BLO4/Z,Z0,ZHH
      COMMON/BLO5/S,NPOINT,NLAAP,ISEC
      COMMON/BLO6/COEF,NCOEF,III,IYN,IYO
      COMMON/BLO7/XCLE,YCLE,IFL,IHILST,PHIIL2
      COMMON/BLO8/XFLUEE,YFLUEE,DMAR,XSTEEL,YSTEEL,DPHEEL,YEEL
      COMMON/BLO10/CUTRAT,DINC,RAK,FRIC
      COMMON/BLO11/COFL,NSTFLI
      COMMON/BLO12/RSE,PHSE,DSEC,SCE1,SCE2,SCE3
      COMMON/BLO13/XSEC,YSEC,ZSEC,ZMSEC
      COMMON/BLO14/RPACE,PHPA,ZPACE1
      COMMON/BLO15/XL0,YL0
      COMMON/BLO16/COEA,COEB,COEC,COED
      COMMON/BLO17/XEELA,YEELA,ZWEB
      COMMON/BLO18/XCHID,YCHID,ZCHID
      COMMON/BLO19/XHEELD,YHEELD,ZHEELD
      COMMON/BLO20/XCLEAD,YCLEAD,ZCLEAD
      COMMON/BLO21/ZEB,XEB,YEB,XEM,YEM,ZEM
      COMMON/BLO22/R0CHIP,H0CHIP,A
      COMMON/BLO23/RSTAR,PHSTAR,ZSTAR,XSTROT,YSTROT,ZSTROT
      COMMON/BLO24/PA,PI,RC0,RC1
      COMMON/BLO25/XSTGD,YSTGD,ZSTGD
      COMMON/BLO26/RRN
      COMMON/BLO27/XNRAD,YNRAD,ZNRAD
      COMMON/BLO28/XPACE,YPACE,ZPACE
      EXTERNAL FAN,FEEL,FIIL,FIN,FLANK,FON,FOUTCR,FPACE,FUN
      EXTERNAL FUNSEC,GPACE,GRIN,MONAT,MONIT,MONUT,RESAD,RESID
      EXTERNAL RESUD,ROTAC
C
C DATA READING
      WRITE(1,704)
704   FORMAT('READ R0,WEB,H0 AND RO - DRILL PARAMETERS')
      READ(1,*)R0,WEB,H0,RO
      WRITE(1,705)
705   FORMAT(/'GRINDING PARAMETERS')
      READ(1,*)EXG,VG,RKG,R0G
      WRITE(1,10)
10    FORMAT('READ S=1. FOR NON-CONV. DRILL'/
     $'READ ALSO NPOINT')
      READ(1,*)S,NPOINT
      IF(S .NE. 1.) GO TO 12
C READ FROM FILE
      READ(5,*)NP
      WRITE(1,11)
11    FORMAT('READ NCOEF')
      READ(1,*)NCOEF
12    RSTAN1=1E-4
```

```
      IF(S .EQ. .Ø)RSTAN1=WEB/2.+1.E-6
      RSTAN2=RØ+1.
      HBASE=1E-5
      NCHI=NPOINT
      ZCLE1=2.
      ZCLE2=1.2*RØ
      DMAR=Ø.35
C
      WRITE(1,813)
813   FORMAT('READ RPM AND RPI ')
      READ(1,*)RPM,RPI
C
      PI=3.14159265
      CONS=PI/18Ø.
      HØ=HØ*CONS
C
      CSVG=DCOS(VG*CONS)
      SNVG=DSIN(VG*CONS)
      CSKOI=DCOS(RKG*CONS)
      SNKOI=DSIN(RKG*CONS)
      CSKOU=DCOS(RO*CONS)
      SNKOU=DSIN(RO*CONS)
      DIST =DSQRT((2.*RØG)**2-EXG**2)
      ZØ=DSQRT((2.*RØG)**2-(EXG-WEB/2.)**2)/DSIN(RKG*CONS)
C
      WRITE(1,8ØØ4)
8ØØ4  FORMAT('DATA FOR THE COMPUTATION THE CHISEL CORNER')
      WRITE(1,8ØØØ)
8ØØØ  FORMAT('IPRINT /(-1)-NO CALL / (1)-EACH ITERATIØN' /
     $'(Ø)-FINAL ITERATION')
      READ(1,*)IPRINT
      FTOL=1.E-7
      XTOL=1.E-6
C CHISEL CORNER - STARTING POINT
      CORN(1)=WEB/2.
      CORN(2)=-WEB/2.
      CORN(3)=1.
      WRITE(1,8ØØ2)
8ØØ2  FORMAT('READ STEP FOR CHISEL CORNER CALCULATION')
      READ(1,*)STEP
      MAXCAL=1ØØØ
C
      WRITE(1,8ØØ5)
8ØØ5  FORMAT(/'SELECT POINT STEP FOR PRINTING')
      READ(1,*)NSALTO
      WRITE(1,7Ø1Ø)
7Ø1Ø  FORMAT('ANGULAR DIFFERENCE MARGIN/HEEL')
      READ(1,*)DPHEEL
      DPHEEL=DPHEEL*CONS
      WRITE(1,8ØØ9)
8ØØ9  FORMAT('MAIN DATA READ')
C
      WRITE(1,7Ø15)
7Ø15  FORMAT(/' VERY OPEN  HEEL ?')
      READ(1,*)IHILST
C
      WRITE(1,734)
734   FORMAT(/'WRITE INTO  FILE ? IF YES READ 6')
      READ(1,*)IFILE
C
      EPS=1.E-7
      EPS1=1.E-7
      EPV1=1.E-7
      EPV=1.E-7
      IFAIL=Ø
      IF(S .NE. 1.)GO TO 15
      DO 2Ø4 I=1,NP
      READ(5,*)XL(I),YL(I)
2Ø4   CONTINUE
      WRITE(1,2Ø6)(XL(I),YL(I),I=1,NP)
2Ø6   FORMAT(2F1Ø.4)
      CALL EØ2ACF(XL,YL,NP,COEF,NCOEF,REF)
      XL1=RØ/2.
      XL2=RØ+.1
      CALL CØ5ACF(XL1,XL2,EPS,EPV,ROTAC,XLK,IFAIL)
      PHLØ=DATAN(YLØ/XLØ)
      PHLA=DATAN((-WEB/2./RØ)/DSQRT(1.-(WEB/2./RØ)**2))
      PØX=DSQRT(RØ**2-(WEB/2.)**2)
      PØZ=PØX*CSKOU/SNKOU
      PHLB=PØZ/RØ*DSIN(HØ)/DCOS(HØ)
      SISANG=PHLØ-PHLA+PHLB
C
      DO 61Ø I=1,NP
      XL(I)=XL(I)*DCOS(SISANG)+YL(I)*DSIN(SISANG)
      YL(I)=-XL(I)*DSIN(SISANG)+YL(I)*DCOS(SISANG)
      XLG(I)=XL(I)
      YLG(I)=YL(I)
61Ø   CONTINUE
      SISAN=SISANG/CONS
      WRITE(1,2Ø7)SISAN
2Ø7   FORMAT(/' SISANG=',F8.2/)
      WRITE(1,2Ø8)(XL(I),YL(I),I=1,NP)
2Ø8   FORMAT(2F1Ø.4)
6ØØ   CONTINUE
C NON-CONV. FLUTE SECTION
      CALL EØ2ACF(XL,YL,NP,COEF,NCOEF,REF)
C
15    M=3
      N=3
      LV=3
      LJ=3
      LW=12Ø
      LIW=1
      ETA=.5
      IF(S .EQ. 1.) GO TO 8Ø11
C DETERMINING THE CHISEL CORNER
      CALL EØ4FCF(M,N,RESID,MONIT,IPRINT,MAXCAL,ETA,XTOL,STEP,
     $CORN,FE,RE,FJAC,LJ,SMON,V,LV,NITER,NF,IW,LIW,WEØ,LW,IFAIL)
```

```
C
      GO TO 8Ø14
C
8Ø11  CALL EØ4FCF(M,N,RESUD,MONUT,IPRINT,MAXCAL,ETA,XTOL,STEP,
     $CORN,FU,RU,FJAC,LJ,SMON,V,LV,NITER,NF,IW,LIW,WEØ,LW,IFAIL)
C
8Ø14  CONTINUE
C DETERMINING THE OUTER CORNER
      PØX=DSQRT(RØ**2-(WEB/2.)**2)
      PØY=-WEB/2.
      PØZ=PØX*CSKOI/SNKOI
      ZOUT=PØZ
      XCORN=CORN(1)
      YCORN=CORN(2)
      ZCORN=CORN(3)
      ZOUT1=PØZ-2.
      ZOUT2=PØZ+2.
      CALL CØ5ACF(ZOUT1,ZOUT2,EPS,EPV,FOUTCR,ZOUT,IFAIL)
      ZEB=ZCORN
      ZEM=ZOUT
C COMPUTING LIP AND FLUTE SURFACE
      DO 5 I=1,NPOINT,1
      III=I
      NLIP=1
      Z=ZOUT-FLOAT(I-1)*(ZOUT-ZCORN)/FLOAT(NPOINT-1)
38    ALPHA=Z/RØ*DSIN(HØ)/DCOS(HØ)
      ZSTG(I)=Z
      ZSTGD(I)=Z
      IF(S .EQ. 1.)GO TO 3Ø
      CALL CØ5ACF(RSTAN1,RSTAN2,EPS,EPV,FUN,RSTAN,IFAIL)
      GO TO 32
3Ø    CALL CØ5ACF(RSTAN1,RSTAN2,EPS,EPV,FAN,XST,IFAIL)
      YST=Ø.Ø
      DO 75 J=1,NCOEF
      YST=YST+COEF(J)*XST**(J-1)
75    CONTINUE
      GO TO 34
C
32    W2R=WEB/2./RSTAN
      PHST=-(DATAN(W2R/DSQRT(1.-W2R**2))+DSQRT(RSTAN**2-(WEB/2.)**2
     $*DSIN(HØ)/DCOS(HØ)/RØ*CSKOU/SNKOU)
      XFLU(I)=RSTAN*DCOS(PHST)
      YFLU(I)=RSTAN*DSIN(PHST)
      XFLUD(I)=RSTAN*DCOS(PHST)
      YFLUD(I)=RSTAN*DSIN(PHST)
      IF(I .EQ. 1)XFLUEE=RSTAN*DCOS(PHST)
      IF(I .EQ. 1)YFLUEE=RSTAN*DSIN(PHST)
      PHST=PHST+ALPHA
      XST=RSTAN*DCOS(PHST)
      YST=RSTAN*DSIN(PHST)
      XSTG(I)=XST
      XSTGD(I)=XST
      YSTG(I)=YST
      YSTGD(I)=YST
      RRN(I)=RSTAN
      RADI(I)=RSTAN
      GO TO 36
C
34    RSTAN=DSQRT(XST**2+YST**2)
      XFLU(I)=XST
      YFLU(I)=YST
      XFLUD(I)=XST
      YFLUD(I)=YST
      IF(I .EQ. 1)XFLUEE=XST
      IF(I .EQ. 1)YFLUEE=YST
      RRN(I)=RSTAN
      RADI(I)=RSTAN
      PHST=DATAN(YST/XST)
      PHST=PHST+ALPHA
      XST1=RSTAN*DCOS(PHST)
      YST1=RSTAN*DSIN(PHST)
      XSTG(I)=XST1
      XSTGD(I)=XST1
      YSTG(I)=YST1
      YSTGD(I)=YST1
      XST=XST1
      YST=YST1
36    CONTINUE
C
      CALL GRIN(Z,ZØ,AXX,BYY,CXY,DDX,EY,FF)
C VECTOR NORMAL TO FLANK POINT - POINTING OUT
      DFDX=2.*XST*AXX+YST*CXY+DDX
      DFDY=2.*YST*BYY+CXY*XST+EY
      DFDZ=XST*(-2.*SNKOI*CSKOI*SNVG)+YST*(-2.*SNKOI
     $*CSKOI*CSVG)+SNKOI**2*2.*(Z-ZØ)
      DF=DSQRT(DFDX**2+DFDY**2+DFDZ**2)
      DFDX=DFDX/DF
      DFDY=DFDY/DF
      DFDZ=DFDZ/DF
      IF(DFDX .GT. Ø.Ø)GO TO 4Ø
      DFDX=-DFDX
      DFDY=-DFDY
      DFDZ=-DFDZ
C VECTOR ON THE FLANK AND NORMAL TO RADIUS
C POINTING IN VELOCITY DIRECTION
4Ø    UR1=DCOS(PHST)
      UR2=DSIN(PHST)
      UR3=Ø.Ø
      XFLNR=1.
      YFLNR=-UR1/UR2*XFLNR
      ZFLNR=(-XFLNR*DFDX-YFLNR*DFDY)/DFDZ
      FLNR=DSQRT(XFLNR**2+YFLNR**2+ZFLNR**2)
      XFLNR=XFLNR/FLNR
      YFLNR=YFLNR/FLNR
      ZFLNR=ZFLNR/FLNR
      IF(YFLNR .GT. Ø.Ø)GO TO 16Ø
      XFLNR=-XFLNR
      YFLNR=-YFLNR
```

```
      ZFLNR=-ZFLNR
C VECTOR TANGENT TO THE FLUTE AT Z=ZSTGD(I)
C POINTING OUT
16Ø   CONTINUE
      NDER=1
      IF(S .EQ. 1.)GO TO 13Ø
      CALL DØ4AAF(RSTAN,NDER,HBASE,DER,EREST,FON,IFAIL)
      DYDXN=DSIN(PHST)/DCOS(PHST)+RSTAN*DER(1)
      DYDXD=1.-RSTAN*DER(1)*DSIN(PHST)/DCOS(PHST)
      DYDX=DYDXN/DYDXD
      GO TO 14Ø
13Ø   XST=XFLU(I)
      YST=YFLU(I)
      CALL DØ4AAF(XST,NDER,HBASE,DER,EREST,FIN,IFAIL)
      DYDX=DER(1)
14Ø   DYDXE=DATAN(DYDX)
      XTG=DCOS(DYDXE)
      YTG=DSIN(DYDXE)
      ZTG=Ø.Ø
      DERIV(I)=DYDXE/CONS
      IF(XTG .GT. Ø.Ø)GO TO 12Ø
      XTG=-XTG
      YTG=-YTG
C VECTOR TANGENT TO THE HELIX POINTING UPWARDS
C ALSO HELIX ANGLE
12Ø   XTGH=-DSIN(PHST)
      YTGH=DCOS(PHST)
      COTH=RØ/RSTAN*DCOS(HØ)/DSIN(HØ)
      XYC=DSQRT(XTGH**2+YTGH**2+COTH**2)
      XTGH=XTGH/XYC
      YTGH=YTGH/XYC
      ZTGH=COTH/XYC
C
      ZTGH1=DSQRT(1.-ZTGH**2)
      ZTGHG(I)=DATAN(ZTGH1/ZTGH)/CONS
C VECTOR NORMAL TO RAKE FACE
C POINTING UPWARDS
      XNRA=YTG*ZTGH
      YNRA=-XTG*ZTGH
      ZNRA=XTG*YTGH-XTGH*YTG
      XYZN=DSQRT(XNRA**2+YNRA**2+ZNRA**2)
      XNRA=XNRA/XYZN
      YNRA=YNRA/XYZN
      ZNRA=ZNRA/XYZN
      IF(ZNRA .LT. Ø.Ø)WRITE(1,45)
45    FORMAT(/'NORMAL TO RAKE FACE POINTING DOWNWARDS')
      XNRAD(I)=XNRA
      YNRAD(I)=YNRA
      ZNRAD(I)=ZNRA
C VECTOR TANGENT TO THE LIP
C POINTING TO THE OUTER CORNER
      CE1=YNRA*DFDZ-ZNRA*DFDY
      CE2=ZNRA*DFDX-XNRA*DFDZ
      CE3=XNRA*DFDY-YNRA*DFDX
      CEE=DSQRT(CE1**2+CE2**2+CE3**2)
      CE1=CE1/CEE
      CE2=CE2/CEE
      CE3=CE3/CEE
C
      CCE1(I)=CE1
      CCE2(I)=CE2
      CCE3(I)=CE3
      CE3A=DSQRT(1.-CE3**2)
      CCE3P(I)=DATAN(CE3A/CE3)/CONS
      IF(CE1 .LT. Ø.Ø)CALL EXIT
C VECTOR ON THE RAKE FACE,NORMAL TO THE CUTTING EDGE
C POINTING IN THE VELOCITY DIRECTION
      XTRA=1.
      CZTRA1=(ZNRA*CE2-YNRA*CE3)/(ZNRA*CE2)
      CZTRA2=(YNRA*XTRA*CE1-XNRA*XTRA*CE2)/(CE2*ZNRA)
      ZTRA=CZTRA2/CZTRA1
      YTRA=(-ZTRA*CE3-XTRA*CE1)/CE2
      TRA=DSQRT(XTRA**2+YTRA**2+ZTRA**2)
      XTRA=XTRA/TRA
      YTRA=YTRA/TRA
      ZTRA=ZTRA/TRA
      IF(YTRA .GT. Ø.Ø)GO TO 55
      XTRA=-XTRA
      YTRA=-YTRA
      ZTRA=-ZTRA
C ANGLE BETWEEN THE TANGENT TO THE HELIX AND THE
C NORMAL TO THE CUTTING EDGE ON THE RAKE FACE
55    AFLO1=XTGH*XTRA+YTGH*YTRA+ZTGH*ZTRA
      AFLO2=DSQRT(1.-AFLO1**2)
      HENR(I)=DATAN(AFLO2/AFLO1)/CONS
C VECTOR ON THE FLANK POINT,NORMAL TO THE CUTTING EDGE
C POINTING IN THE VELOCITY DIRECTION
      XTFLA=1.
      CZFLA1=(DFDZ*CE2-DFDY*CE3)/(DFDZ*CE2)
      CZFLA2=(DFDY*XTFLA*CE1-DFDX*XTFLA*CE2)/(CE2*DFDZ)
      ZTFLA=CZFLA2/CZFLA1
      YTFLA=(-ZTFLA*CE3-XTFLA*CE1)/CE2
      FLA=DSQRT(XTFLA**2+YTFLA**2+ZTFLA**2)
      XTFLA=XTFLA/FLA
      YTFLA=YTFLA/FLA
      ZTFLA=ZTFLA/FLA
      IF(YTFLA .GT. Ø.Ø)GO TO 6Ø
      XTFLA=-XTFLA
      YTFLA=-YTFLA
      ZTFLA=-ZTFLA
C VECTOR NORMAL TO THE MACHINED SURFACE
C POINTING UPWARDS
6Ø    VV1=-2.*PI*RPM/6Ø.*RSTAN*DSIN(PHST)
      VV2=+2.*PI*RPM/6Ø.*RSTAN*DCOS(PHST)
      VV3=25.4/RPI*RPM/6Ø.
      VV=DSQRT(VV1**2+VV2**2+VV3**2)
      VVD(I)=VV
      VV1=VV1/VV
```

```
      VV2=VV2/VV
      VV3=VV3/VV
      XNMSU=-VV2*CE3+VV3*CE2
      YNMSU=-VV3*CE1+VV1*CE3
      ZNMSU=-VV1*CE2+VV2*CE1
      SU=DSQRT(XNMSU**2+YNMSU**2+ZNMSU**2)
      XNMSU=XNMSU/SU
      YNMSU=YNMSU/SU
      ZNMSU=ZNMSU/SU
C
      XMSU(I)=XNMSU
      YMSU(I)=YNMSU
      ZMSU(I)=ZNMSU
C
      T1MEU(I)=.5/RPI*25.4*CE3A
      T1MAU(I)=.5/RPI*25.4*ZNMSU
C VECTOR ON THE MACHINED SURFACE,NORMAL TO THE CUTTING EDGE
C POINTING IN THE VELOCITY DIRECTION
      XTMSU=1.
      CZMSU1=(ZNMSU*CE2-YNMSU*CE3)/(ZNMSU*CE2)
      CZMSU2=(YNMSU*XTMSU*CE1-XTMSU*XNMSU*CE2)/(CE2*ZNMSU)
      ZTMSU=CZMSU2/CZMSU1
      YTMSU=(-ZTMSU*CE3-XTMSU*CE1)/CE2
      TMSU=DSQRT(XTMSU**2+YTMSU**2+ZTMSU**2)
      XTMSU=XTMSU/TMSU
      YTMSU=YTMSU/TMSU
      ZTMSU=ZTMSU/TMSU
      IF(YTMSU .GT. 0.0)GO TO 20
      XTMSU=-XTMSU
      YTMSU=-YTMSU
      ZTMSU=-ZTMSU
C VECTOR NORMAL TO CUTTING EDGE AND VELOCITY
C POINTING UPWARDS
20    UU1=-DSIN(PHST)
      UU2=DCOS(PHST)
      XVCE=1.
      YVCE=-UU1/UU2*XVCE
      ZVCE=(-CE1*XVCE-CE2*YVCE)/CE3
      VCE=DSQRT(XVCE**2+YVCE**2+ZVCE**2)
      XVCE=XVCE/VCE
      YVCE=YVCE/VCE
      ZVCE=ZVCE/VCE
      IF(ZVCE .GT. 0.0)GO TO 110
      XVCE=-XVCE
      YVCE=-YVCE
      ZVCE=-ZVCE
C
110   XNMSU1=-UU2*CE3+UU3*CE2
      YNMSU1=-UU3*CE1+UU1*CE3
      ZNMSU1=-UU1*CE2+UU2*CE1
      SU1=DSQRT(XNMSU1**2+YNMSU1**2+ZNMSU1**2)
      XNMSU1=XNMSU1/SU1
      YNMSU1=YNMSU1/SU1
      ZNMSU1=ZNMSU1/SU1
C VECTOR ON THE MACHINED SURFACE
C NORMAL TO VELOCITY AND POINTING UPWARDS
80    XTSU=1.
      CTU1=XTSU*XNMSU1*UU2-XTSU*UU1*YNMSU1
      CTU2=YNMSU1*UU3-ZNMSU1*UU2
      ZTSU=CTU1/CTU2
      YTSU=-(XTSU*XNMSU1+ZTSU*ZNMSU1)/YNMSU1
      CTU3=DSQRT(XTSU**2+YTSU**2+ZTSU**2)
      XTSU=XTSU/CTU3
      YTSU=YTSU/CTU3
      ZTSU=ZTSU/CTU3
      IF(ZTSU .GT. 0.0) GO TO 111
      XTSU=-XTSU
      YTSU=-YTSU
      ZTSU=-ZTSU
C INCLINATION ANGLE
111   COSI=UU1*CE1+UU2*CE2
      SINI=DSQRT(1.-COSI**2)
      AIN=DATAN(SINI/COSI)
      AIN=PI/2.-AIN
      AINC(I)=AIN/CONS
C NORMAL RAKE ANGLE
      COSRA=XVCE*XTRA+YVCE*YTRA+ZVCE*ZTRA
      SINRA=DSQRT(1.-COSRA**2)
      SIGN1=XVCE*XNRA+YVCE*YNRA+ZVCE*ZNRA
      SIGN2=DABS(SIGN1)
      SIGN=SIGN1/SIGN2
      RAK=DATAN(SINRA/COSRA)
      RAK=SIGN*RAK
      RAKE(I)=RAK/CONS
8067  ETA=DATAN(1./(DCOS(RAK)+DSIN(RAK))*DSIN(AIN)/DCOS(AIN))
8069  ETAS(I)=ETA/CONS
      RSN=RSTAN*DSIN(AIN)
      RSNI(I)=RSN
      IF (I .EQ. 1) GO TO 498
      DL(1)=0.
      DL(I)=DSQRT((XSTGD(I)-XSTGD(I-1))**2+(YSTGD(I)-YSTGD(I-1)
     $)**2+(ZSTGD(I)-ZSTGD(I-1 ))**2)
      SS=SS+DL(I)
      SSS(I)=SS
498   RESQ=RSTAN
C
      NLUP=I
5     CONTINUE
      DO 714 I=1,NPOINT
      CEL(I)=SSS(NPOINT-I+1)
714   CONTINUE
C ====================================
C CHIP COMPUTATION
C ====================================
C READ CHIP AXIS TO A GUESS
      WRITE(1,119)
119   FORMAT('READ XEB,YEB,XEM,YEM,RC1 ')
      READ(1,*)XEB,YEB,XEM,YEM,RC1
```

```
708    WRITE(1,709)
709    FORMAT(/'READ CHIP LEAD AND CHIP DIAMETER')
       READ(1,*)PA,RC0
       NLOO1=IFIX(FLOAT(NPOINT)/3.)
       EIX(1)=XEB
       EIX(2)=YEB
       EIX(3)=XEM
       EIX(4)=YEM
       M=8
       N=4
       LJ=8
       LV=4
       LIW=1
       LW=120
       IFAIL=0
       MAXCAL=1000
       WRITE(1,817)
817    FORMAT(/'READ IPRANT,STEP,XTOL AND ETA'/)
       READ(1,*)IPRANT,STEP,XTOL,ETA
C
       CALL E04FCF(M,N,RESAD,MONAT,IPRANT,MAXCAL,ETA,XTOL,STEP,
      $EIX,FE,RE,FJAC,LJ,SMON,V,LV,NITER,NF,IW,LIW,WE0,LW,IFAIL)
C
       WRITE(1,819)XEB,YEB,ZEB,XEM,YEM,ZEM
819    FORMAT(/'XEB=',F10.5/'YEB=',F10.5/'ZEB=',F10.5/'XEM=',
      $F10.5/'YEM=',F10.5/'ZEM=',F10.5/)
816    DO 810 I=1,NPOINT
       SENOI=DSIN(AINC(I)*CONS)
       CE1=CCE1(I)
       CE2=CCE2(I)
       CE3=CCE3(I)
       XST=XSTGD(I)
       YST=YSTGD(I)
       ZST=ZSTGD(I)
       PHI1=DATAN(YST/XST)
       XNRA=-XNRAD(I)
       YNRA=-YNRAD(I)
       ZNRA=-ZNRAD(I)
       XNMSU=XMSU(I)
       YNMSU=YMSU(I)
       ZNMSU=ZMSU(I)
C COMPUTATION FOR CHIP VELOCITY
       DBM=DSQRT((XEM-XEB)**2+(YEM-YEB)**2+(ZEM-ZEB)**2)
       AAA=(XEM-XEB)/DBM
       BBB=(YEM-YEB)/DBM
       CCC=(ZEM-ZEB)/DBM
       REVAB=3.
       WAA=2.0*PI*REVAB
       V1=REVAB*PA
       ABC1=BBB*(ZST-ZEM)-CCC*(YST-YEM)
       ABC2=CCC*(XST-XEM)-AAA*(ZST-ZEM)
       ABC3=AAA*(YST-YEM)-BBB*(XST-XEM)
       VC1=AAA*V1+WAA*ABC1
       VC2=BBB*V1+WAA*ABC2
       VC3=CCC*V1+WAA*ABC3
       VC=DSQRT(VC1**2+VC2**2+VC3**2)
       VC1=VC1/VC
       VC2=VC2/VC
       VC3=VC3/VC
       VV=2.*PI*RRN(I)
       VVCV=VC/VV
       IF(ABC1 .NE. 0.0) GO TO 9148
       WRITE(1,9149)
9149   FORMAT('          ABC1   IS   NUL')
       CALL EXIT
C FINDING CHIP RADIUS AT EACH POINT OF THE LIP
9148   ZEXEAC=-ABC3/ABC1*AAA+CCC
       YEXEAB=-ABC2/ABC1*AAA+BBB
C
       IF(YEXEAB .NE. 0.0) GO TO 9151
       WRITE(1,9152)
9152   FORMAT(' YEXEAB  IS   NUL')
       CALL EXIT
9151   ZEYEXE=ZEXEAC*ABC2/YEXEAB/ABC1-ABC3/ABC1
       ZEZEYE=1.+ZEYEXE**2+(ZEXEAC/YEXEAB)**2
       CONSTA=(XEB-XST)*ZEYEXE-(YEB-YST)*ZEXEAC/YEXEAB
      $+(ZEB-ZST)
       IF(ZEZEYE .NE. 0.0) GO TO 9153
       WRITE(1,9154)
9154   FORMAT('ZEZEYE     IS  NUL')
       CALL EXIT
9153   VN3=-CONSTA/ZEZEYE
       VN2=-ZEXEAC/YEXEAB*VN3
       VN1=ZEYEXE*VN3
       RC=DSQRT(VN1**2+VN2**2+VN3**2)
       IF(I .EQ. 1)R0CHIP=RC
       COSK=AAA*CE1+BBB*CE2+CCC*CE3
       SENK=DSQRT(1.-COSK**2)
       AKC=DATAN(SENK/COSK)
       ABTV=AAA*(XEB-XST)+BBB*(YEB-YST)+CCC*(ZEB-ZST)
       CETV=CE1*(XST-XEB)+CE2*(YST-YEB)+CE3*(ZST-ZEB)
       CECOSI=(-CETV-COSK*ABTV)/(1.-COSK**2)
       CECOSU=COSK*CECOSI-ABTV
       PARDA=(AAA*CECOSU+XEB-CE1*CECOSI-XST)
       PARDB=(BBB*CECOSU+YEB-CE2*CECOSI-YST)
       PARDC=(CCC*CECOSU+ZEB-CE3*CECOSI-ZST)
       PARD1=PARDA**2
       PARD2=PARDB**2
       PARD3=PARDC**2
       BCCE1=BBB*CE3-CCC*CE2
       BCCE2=CCC*CE1-AAA*CE3
       BCCE3=AAA*CE2-BBB*CE1
       SIGNM=PARDA*BCCE1+PARDB*BCCE2+PARDC*BCCE3
       SIGNN=DABS(SIGNM)
       SIGNO=SIGNN/SIGNM
       GC=DSQRT(PARD1+PARD2+PARD3)
C COMPUTATION FOR CHIP FLOW ANGLE
       HC=DATAN(2.*PI*RC/PA)
```

```
      IF(I .EQ. 1)H0CHIP=HC
      SETACH=GC*SIGNO/RC*DSIN(HC)*SENK+COSK*DCOS(HC)
      CETACH=DSQRT(1.-SETACH**2)
      TETACH=SETACH/CETACH
      ETACH=DATAN(TETACH)/CONS
C VERIFICATION FOR ETA
      SENETA=VC1*CE1+VC2*CE2+VC3*CE3
      COSETA=DSQRT(1.-SENETA**2)
      TGETA=SENETA/COSETA
      ETA=DATAN(TGETA)/CONS
      T2A=DCOS(AINC(I)*CONS)/VVCV/COSETA
      T211(I)=1./T2A
C T211(I) IS T1/T2
      T1PR(I)=ZNMSU/RPI*25.4
      VT1I=DCOS(AINC(I)*CONS)*VV*T1PR(I)
      VT2E=CETACH*VC
      T2PR(I)=VT1I/VT2E
      UU1=-DSIN(PHI1)
      UU2=+DCOS(PHI1)
      UU3=0.
      SGAMAE=UU1*VC1+UU2*VC2
      CGAMAE=DSQRT(1.-SGAMAE**2)
      TGGAME=SGAMAE/CGAMAE
      GAME=DATAN(TGGAME)/CONS
      SGAMA=DSIN(RAKE(I)*CONS)
      SINGEM=SENOI*SENETA+DSQRT(1.-SENOI**2)*COSETA*SGAMA
      COSGEM=DSQRT(1.-SINGEM**2)
      GEME=DATAN(SINGEM/COSGEM)/CONS
C
      VERIF1=VC1*XNRA
      VERIF2=VC2*YNRA
      VERIF3=VC3*ZNRA
C
      COSV=VERIF1+VERIF2+VERIF3
      VER=DATAN(DSQRT(1.-COSV**2)/COSV)
      VERI=(PI/2.-VER)/CONS
      IF(VERI .GT. 90.)VERI=VERI-180.
      VERIF(I)=VERI
      VERIG(I)=VERI
      GCD(I)=GC
      AKCD(I)=AKC/CONS
      GEMEA(I)=GEME
      HCD(I)=HC/CONS
      ETARIG(I)=ETACH
C
      ETAA(I)=ETA
      RCA(I)=RC
      RCAG(I)=RC
      GAMAE(I)=GAME
      VVCA(I)=VVCV
810   CONTINUE
C
      IREL=1
      DO 735 I=1,NPOINT
      T2PR(I)=T211(I)/T211(IREL)
      T1PR(I)=VVCA(I)/VVCA(IREL)
735   CONTINUE
C
C WRITING IN FILE
      IF(IFILE .EQ. 0)GO TO 732
      WRITE(IFILE,1733)XEB,YEB,ZEB,XEM,YEM,ZEM
      NNPP=10
1733  FORMAT(6F10.5)
      WRITE(IFILE,733)(NNPP,XSTG(I),YSTG(I),ZSTG(I),RCA(I),
     $I=1,NPOINT,3)
733   FORMAT(I3,4F12.4)
      WRITE(1,1744)
1744  FORMAT('FILE WRITTEN')
732   CONTINUE
      WRITE(1,703)
703   FORMAT(/'TABLES FOR CHIP  ?')
      READ(1,*)IT
      IF(IT .EQ. 0) GO TO 706
      WRITE(1,116)
116   FORMAT(///30X,'CHIP')
      WRITE(1,925)
925   FORMAT(///3X,' RR ',3X,'GAME',3X,' ETA',3X,'ETAC',3X,
     $'VVCV',3X,' RCA',3X,'HCDD',3X,'GEME',3X,'VERI'///)
      DO 141 JN=1,NPOINT,NSALTO
      WRITE(1,923)RRN(JN),GAMAE(JN),ETAA(JN),ETARIG(JN),
     $T1PR(JN),RCA(JN),HCD(JN),GEMEA(JN),VERIF(JN)
923   FORMAT(9F7.2)
141   CONTINUE
      READ(1,*)SEPARA
      WRITE(1,952)
952   FORMAT(////3X,' RRN',3X,' T21',3X,'T1PR',3X,'T2PR',3X,
     $'AKCD',3X,'GCDD'///)
      DO 1441 J=1,NPOINT,NSALTO
      WRITE(1,959)RRN(J),T211(J),T1PR(J),T2PR(J),AKCD(J),GCD(J)
959   FORMAT(6F7.2)
1441  CONTINUE
      READ(1,*)SEPARA
      WRITE(1,711)
711   FORMAT(/'MORE TABLES  ?')
      READ(1,*)ITA
      IF(ITA .NE. 0) GO TO 708
706   WRITE(1,707)
707   FORMAT(/'CHIP FLOW ANGLE  VS INC. ANG(1),EDGE LENG.(2)' /
     $'NONE (0)')
      READ(1,*)IEI
      IF(IEI .EQ. 0) GO TO 2031
      IR0=R0+2
      R0P=IR0
      CALL SE281
      CALL PICCLE
      CALL WINDOW(2)
      CALL AXIPOS(0,40.,50.,135.,1)
      CALL AXIPOS(0,40.,50.,190.,2)
```

```
      GO TO (715,716),IEI
715   CALL AXISCA(2,12,0.,60.,1)
      GO TO 717
716   CALL AXISCA(2,IR0,0.,R0P,1)
717   CONTINUE
      CALL AXISCA(2,18,0.,90.,2)
      CALL AXIDRA(2,1,1)
      CALL AXIDRA(-2,-1,2)
C
      GO TO(718,719),IEI
718   CALL GRACUR(AINC,ETARIG,NPOINT)
      CALL GRAMOV(0.,0.)
      CALL BROKEN(1)
      CALL GRALIN(AINC(NPOINT),AINC(NPOINT))
      CALL CHAMOD
C
      GO TO 720
719   CALL GRACUR(CEL,ETARIG,NPOINT)
      CALL BROKEN(1)
      CALL GRACUR(CEL,AINC,NPOINT)
      CALL CHAMOD
720   CONTINUE
      READ(1,*)SEPARA
      WRITE(1,710)
710   FORMAT(/'MORE GRAPHS  ?')
      READ(1,*)IGR
      IF(IGR .NE. 0) GO TO 708
C
2031  WRITE(1,2032)
2032  FORMAT(///'SECTIONS ON A ROTATING PLANE FOR INTERF ?')
      READ(1,*)ISEPAR
      IF(ISEPAR .EQ. 0) GO TO 109
107   CONTINUE
      WRITE(1,712)
712   FORMAT(/'CHANGE CHIP DATA  ?')
      READ(1,*)ICH
      IF(ICH .NE. 0) GO TO 708
      WRITE(1,2033)
2033  FORMAT('READ ROTATION OF THE PLANE  ')
      READ(1,*)ROT
      PHPAC1=-45.*CONS
      PHPAC2=89.9*CONS
C
      EPS=1E-8
      EPV=1E-8
      IFAIL=0
C COORDINATES TRANSFORMATION
C
C TRANSFORMATION MATRIX
      A(1,3)=AAA
      A(2,3)=BBB
      A(3,3)=CCC
C
      A(2,2)=1.
      A(1,2)=-A(2,3)*A(2,2)/A(1,3)
      A(3,2)=.0
C
      AT=DSQRT(1.+A(1,2)**2+A(3,2)**2)
C
      A(1,2)=A(1,2)/AT
      A(2,2)=A(2,2)/AT
      A(3,2)=A(3,2)/AT
C
      A(1,1)=1.
      A(2,1)=-A(1,1)*A(1,2)/A(2,2)
      A(3,1)=-(A(1,1)*A(1,3)+A(2,1)*A(2,3))/A(3,3)
C
      ATT=DSQRT(A(1,1)**2+A(2,1)**2+A(3,1)**2)
C
      A(1,1)=A(1,1)/ATT
      A(2,1)=A(2,1)/ATT
      A(3,1)=A(3,1)/ATT
C
      DCOOR(1)=XSTGD(1)-XEB
      DCOOR(2)=YSTGD(1)-YEB
      DCOOR(3)=ZSTGD(1)-ZEB
      XSTAR=.0
      YSTAR=.0
      ZSTAR=.0
C
      DO 102 K=1,3
      XSTAR=XSTAR+A(K,1)*DCOOR(K)
      YSTAR=YSTAR+A(K,2)*DCOOR(K)
      ZSTAR=ZSTAR+A(K,3)*DCOOR(K)
102   CONTINUE
C
      IF(XSTAR .EQ. .0 .AND. YSTAR .GT. .0)PHSTAR=PI/2.
      IF(XSTAR .EQ. .0 .AND. YSTAR .LT. .0)PHSTAR=-PI/2.
      IF(XSTAR .EQ. .0) GO TO 808
C
      PHSTAR=DATAN(YSTAR/XSTAR)
      IF(PHSTAR .LT. .0 .AND. YSTAR .GT. .0)PHSTAR=PI+PHSTAR
      IF(PHSTAR .GT. .0 .AND. YSTAR .LT. .0)PHSTAR=-(PI-PHSTAR)
808   RSTAR=DSQRT(XSTAR**2+YSTAR**2)
C
      PHROT=PHSTAR+ROT*CONS
      XROT=R0CHIP*DCOS(PHROT)
      YROT=R0CHIP*DSIN(PHROT)
      ZROT=ZSTAR+(PHROT-PHSTAR)*R0CHIP*DCOS(H0CHIP)/DSIN(H0CHIP)
      CAAR(1)=XROT
      CAAR(2)=YROT
      CAAR(3)=ZROT
C
      XOUTR=0.
      YOUTR=0.
      ZOUTR=0.
      DO 1 I=1,3
      XOUTR=XOUTR+A(1,I)*CAAR(I)
```

```
      YOUTR=YOUTR+A(2,I)*CAAR(I)
      ZOUTR=ZOUTR+A(3,I)*CAAR(I)
1     CONTINUE
C
      XOUTR=XOUTR+XEB
      YOUTR=YOUTR+YEB
      ZOUTR=ZOUTR+ZEB
C
      COEA=BBB*(ZOUTR-ZEM)-CCC*(YOUTR-YEM)
      COEB=CCC*(XOUTR-XEM)-AAA*(ZOUTR-ZEM)
      COEC=AAA*(YOUTR-YEM)-BBB*(XOUTR-XEM)
      COED=-XEM*COEA-YEM*COEB-ZEM*COEC
C
      DO 2034 I=1,NPOINT
      DCOOR(1)=XSTGD(I)-XEB
      DCOOR(2)=YSTGD(I)-YEB
      DCOOR(3)=ZSTGD(I)-ZEB
      XSTAR=.Ø
      YSTAR=.Ø
      ZSTAR=.Ø
      DO 826 K=1,3
      XSTAR=XSTAR+A(K,1)*DCOOR(K)
      YSTAR=YSTAR+A(K,2)*DCOOR(K)
      ZSTAR=ZSTAR+A(K,3)*DCOOR(K)
826   CONTINUE
C
      IF(XSTAR .EQ. .Ø .AND. YSTAR .GT. .Ø)PHSTAR=PI/2.
      IF(XSTAR .EQ. .Ø .AND. YSTAR .LT. .Ø)PHSTAR=-PI/2.
      IF(XSTAR .EQ. .Ø) GO TO 827
C
      PHSTAR=DATAN(YSTAR/XSTAR)
      IF(PHSTAR .LT. .Ø .AND. YSTAR .GT. .Ø)PHSTAR=PI+PHSTAR
      IF(PHSTAR .GT. .Ø .AND. YSTAR .LT. .Ø)PHSTAR=-(PI-PHSTAR)
827   RSTAR=DSQRT(XSTAR**2+YSTAR**2)
      DZ=(PHROT-PHSTAR)*RØCHIP*DCOS(HØCHIP)/DSIN(HØCHIP)
      ZSTAR=ZSTAR+DZ
      ZRIGG(I)=ZSTAR
      RPACE=DSQRT(XSTGD(I)**2+YSTGD(I)**2)
      PHPA=DATAN(YSTGD(I)/XSTGD(I))
      ZPACE1=ZSTGD(I)
      CALL CØ5ACF(PHPAC1,PHPAC2,EPS,EPV,GPACE,PHPACE,IFAIL)
      DCOOR(1)=XPACE-XEB
      DCOOR(2)=YPACE-YEB
      DCOOR(3)=ZPACE-ZEB
      XSTAR=.Ø
      YSTAR=.Ø
      ZSTAR=.Ø
      DO 828 K=1,3
      XSTAR=XSTAR+A(K,1)*DCOOR(K)
      YSTAR=YSTAR+A(K,2)*DCOOR(K)
      ZSTAR=ZSTAR+A(K,3)*DCOOR(K)
828   CONTINUE
C
      RSTO(I)=RSTOR
      IF(I .GT. 1 .AND. RSTO(I) .GT. RSTO(I-1))RSTO(I)=-RSTO(I)
      XPACG(I)=XSTAR
      YPACG(I)=YSTAR
      ZPACG(I)=ZSTAR
2034  CONTINUE
      IF(IROT .EQ. 1)GO TO 737
109   WRITE(1,940)
940   FORMAT('IF GRAPHICS ONLY, READ 1')
      READ(1,*)IGRA
      IF(IGRA .EQ. 1) GO TO 935
C TABLES
      WRITE(1,807)
807   FORMAT(3X,' SS ',3X,' X  ',3X,' Y  ',3X,' Z  ',3X,'XFLU',
     $3X,'YFLU',3X,' INC',3X,'RAKE',3X,'GAMN',3X,'ETAL'///)
      DO 41 J=1,NPOINT
      READ(1,*)SEPARA
      WRITE(1,92)SSS(J),XSTG(J),YSTG(J),ZSTG(J),XFLU(J),YFLU(J),
     $AINC(J),RAKE(J),GAMN(J),ETAS(J)
92    FORMAT(10F7.2)
41    CONTINUE
      READ(1,*)SEPARA
      WRITE(1,722)
722   FORMAT(//3X,'XNRA',3X,'YNRA',3X,'ZNRA'//)
      DO 723 I=1,NPOINT
      AXNRA=ATAN(SQRT(1.-XNRAD(I)**2)/XNRAD(I))/CONS
      AYNRA=ATAN(SQRT(1.-YNRAD(I)**2)/YNRAD(I))/CONS
      AZNRA=ATAN(SQRT(1.-ZNRAD(I)**2)/ZNRAD(I))/CONS
      WRITE(1,724)AXNRA,AYNRA,AZNRA
723   CONTINUE
724   FORMAT(3F7.2)
C
      WRITE(1,806)
806   FORMAT(//' GRAPHICS FOR CHIP ?'//)
      READ(1,*)IGRAF
      IF(IGRAF .EQ. Ø)GO TO 815
935   CONTINUE
C ========================================
C GRAPHICS
C ========================================
      WRITE(1,7001)
7001  FORMAT(/'VERIF X SSS ?')
      READ(1,*)IVER
      IF(IVER .NE. 1)GO TO 7002
      RØP=1.2*RØ
      IRØ=RØP
      RØP=IRØ
      XAXIS=120
      CALL SE281
      CALL PICCLE
      CALL WINDOW(2)
      CALL AXIPOS(Ø,5Ø.,12Ø.,11Ø.,1)
      CALL AXIPOS(Ø,5Ø.,17Ø.,1ØØ.,2)
      CALL AXISCA(2,IRØ,Ø.,45.,1)
      CALL AXISCA(2,16,-4Ø.,4Ø.,2)
```

```
      CALL AXIDRA(2,1,1)
      CALL AXIDRA(-2,-1,2)
      CALL GRACUR(CEL,VERIG,NPOINT)
      CALL CHAMOD
      READ(1,*)SEPARA
7ØØ2  WRITE(1,8Ø5)
8Ø5   FORMAT(/'CHIP INTERFERENCE ? '/)
      READ(1,*)INTE
      IF(INTE .EQ. Ø) GO TO 112
C
      WRITE(1,713)
713   FORMAT(/'READ XFACT AND YFACT ')
      READ(1,*)XFACT,YFACT
      XAXIS=XFACT*15Ø.
      YAXIS=YFACT*15Ø.
      RØP=RØCHIP+1.
      IRØ=RØP
      RØP=IRØ
C
      CALL SE281
      CALL PICCLE
      CALL WINDOW(2)
      CALL AXIPOS(Ø,4Ø.,5Ø.,XAXIS,1)
      CALL AXIPOS(Ø,4Ø.,5Ø.,YAXIS,2)
      CALL AXISCA(2,IRØ,Ø.,RØP,1)
      CALL AXISCA(2,1Ø,Ø.,1Ø.,2)
C DO NOT PLOT AXES
C     CALL AXIDRA(2,1,1)
C     CALL AXIDRA(-2,-1,2)
C
737   CONTINUE
C CHANGE PEN COLOUR
      CALL PENSEL(1,.2,4)
      CALL GRAPOL(RSTO(1),ZPACG(1),NPOINT)
C     CALL GRACUR(CEL,ZPACG,NPOINT)
C     CALL DASHED(1,3.,2.,Ø.)
      CALL PENSEL(2,.2,4)
      DO 738 I=1,NPOINT
      ZRIGGD(I)=ZPACG(I)+5.*(ZRIGG(I)-ZPACG(I))
738   CONTINUE
      CALL GRAPOL(RCAG(1),ZRIGG(1),NPOINT)
C     CALL GRACUR(CEL,ZRIGG,NPOINT)
      CALL DASHED(2,6.,3.,.5)
      CALL GRAMOV(Ø.,Ø.)
      CALL GRALIN(Ø.,5.)
      CALL BROKEN(Ø)
      CALL CHAMOD
C
      READ(1,*)SEPARA
      WRITE(1,1Ø6)
1Ø6   FORMAT(/'MORE ROTATING SECTIONS ?'/)
      READ(1,*)IROT
      IF(IROT .EQ. 1) GO TO 1Ø7
112   WRITE(1,142)
142   FORMAT(/'RELATIVE CUTTING RATIO ?')
      READ(1,*)IRELCR
      IF(IRELCR .EQ. Ø) GO TO 815
C
      RØP=RØ+1.
      IRØ=RØP
      RØP=IRØ
      CALL SE281
44    CALL PICCLE
      CALL WINDOW(2)
      CALL AXIPOS(Ø,4Ø.,1ØØ.,13Ø.,1)
      CALL AXIPOS(Ø,4Ø.,1ØØ.,12Ø.,2)
      CALL AXISCA(2,IRØ,Ø.,RØP,1)
      CALL AXISCA(2,2Ø,.2,1.2,2)
      CALL AXIDRA(2,1,1)
      CALL AXIDRA(-2,-1,2)
C
      CALL GRACUR(RADI,T1PR,NPOINT)
      CALL DASHED(2,4.,2.,.5)
      CALL GRACUR(RADI,T2PR,NPOINT)
      CALL BROKEN(Ø)
      CALL CHAMOD
C
      READ(1,*)SEPARA
815   ZCHIØ=ZØ-DSQRT(((2.*RØG)**2-EXG**2)/SNKOI**2)
3Ø3   DO 5ØØ I=1,NPOINT
      NCHI2=2*NCHI
      ZCHI=ZCORN-FLOAT(I-1)/FLOAT(NCHI-1)*(ZCORN-ZCHIØ)
      ZCHIG(I)=ZCHI
      ZCHID(I)=ZCHI
C
      CALL GRIN(ZCHI,ZØ,AXX,BYY,CXY,DDX,EY,FF)
C
      CHI1=BYY+(EY/DDX)**2*AXX-EY/DDX*CXY
      YCHI2(I)=+DSQRT(-FF/CHI1)
      XCHI2(I)=-YCHI2(I)*EY/DDX
      XCHIG(I)=DABS(XCHI2(I))
      YCHIG(I)=-DABS(YCHI2(I))
      XCHID(I)=DABS(XCHI2(I))
      YCHID(I)=-DABS(YCHI2(I))
      AMOD=DSQRT((XCHI2(I))**2+(YCHI2(I))**2)
      IF(AMOD .EQ. Ø.) AMOD=1E-8
      XCHIXA=XCHI2(I)/AMOD
      YCHIXA=YCHI2(I)/AMOD
      CIXA=XCHIXA
      IF(CIXA .EQ. Ø.) CIXA=1E-8
      SIXA=DSQRT(1.-CIXA**2)
      TIXA=SIXA/CIXA
      CHIXA(I)=DATAN(TIXA)/CONS+18Ø.
      RCHISE(I)=DSQRT((XCHID(I))**2+YCHID(I)**2)
      RCHISE(NCHI+I)=RCHISE(I)
C
5ØØ   CONTINUE
      WRITE(1,1965)
```

```
1965  FORMAT('LOOP 500 FINISHED')
C HEEL CORNER ELEVATION
      PHIIL1=DATAN(YSTGD(1)/XSTGD(1))
      IFL=1
      XCLE=R0*DCOS(PHIIL1)
      YCLE=R0*DSIN(PHIIL1)
      CALL C05ACF(ZCLE1,ZCLE2,EPS,EPV,FLANK,ZCLE,IFAIL)
C
      ZHH=ZCLE
      ZCLEEE=ZCLE
1940  CONTINUE
936   CONTINUE
      IF(IHILST .EQ. 1)GO TO 7014
      IF(S .EQ. 1.) GO TO 7012
      NSTFLU=40
      DO 7013 J=1,NSTFLU
      RSTFL(J)=WEB/2.+FLOAT(J-1)/FLOAT(NSTFLU-1)*WEB
      W2R=WEB/2./RSTFL(J)
      IF(RSTFL(J) .LE. WEB/2.)GO TO 7020
      PHSTFL(J)=DATAN(W2R/DSQRT(1.-W2R**2))+DSQRT(RSTFL(J)
     $**2-(WEB/2.)**2)*DSIN(H0)/DCOS(H0)/R0*CSKOU/SNKOU
      GO TO 7021
7020  PHSTFL(J)=PI/2.
7021  XHSTFL(J)=RSTFL(J)*DCOS(PHSTFL(J))
      YHSTFL(J)=RSTFL(J)*DSIN(PHSTFL(J))
7013  CONTINUE
      WRITE(1,7033)
7033  FORMAT('READ NO. COEF. TO POLY. STAN')
      READ(1,*)NSTFLI
      CALL E02ACF(XHSTFL,YHSTFL,NSTFLU,COFL,NSTFLI,REFL)
7012  DO 7000 I=1,NPOINT
      Z=ZCLEEE-FLOAT(I-1)*(ZCLEEE-ZCORN)/FLOAT(NPOINT-1)
      ALPHA=Z/R0*DSIN(H0)/DCOS(H0)
      III=I
      IF(I .NE. 1) GO TO 14
      RHEEL1=-3.
      RHEEL2=R0
14    CALL C05ACF(RHEEL1,RHEEL2,EPS1,EPV1,FEEL,XEEL,IFAIL)
      RHEEL1=XEEL-.8
      RHEEL2=XEEL+1.
      XHEELG(I)=XSTEEL
      YHEELG(I)=YSTEEL
      ZHEELG(I)=Z
      XHEELD(I)=XSTEEL
      YHEELD(I)=YSTEEL
      XEELG(I)=XEEL
      YEELG(I)=YEEL
      XEELGD(I)=XEEL
      YEELGD(I)=YEEL
7000  CONTINUE
      GO TO 7022
C
7014  DO 7016 I=1,NPOINT
      III=I
      Z=ZCLEEE-FLOAT(I-1)*(ZCLEEE-ZCORN)/FLOAT(NPOINT-1)
      ALPHA=Z/R0*DSIN(H0)/DCOS(H0)
      IF(I .NE. 1) GO TO 7017
      RHEEL1=.8*R0
      RHEEL2=1.1*R0
7017  CALL C05ACF(RHEEL1,RHEEL2,EPS1,EPV1,FIIL,RHEEL,IFAIL)
      RHEEL1=.8*RHEEL
      RHEEL2=1.2*RHEEL
      IF(RHEEL1 .LT. WEB/2.)RHEEL1=WEB/2.
C
      XHEELG(I)=XSTEEL
      YHEELG(I)=YSTEEL
      ZHEELG(I)=Z
      XHEELD(I)=XSTEEL
      YHEELD(I)=YSTEEL
      XEELG(I)=XEELA
      YEELG(I)=YEELA
      XEELGD(I)=XEELA
      YEELGD(I)=YEELA
7016  CONTINUE
7022  CONTINUE
      READ(1,*)SEPARA
C
      ALPHA=ZOUT/R0*DSIN(H0)/DCOS(H0)
      PHC0=DATAN(YC0/XC0)
      PHC=PHC0+ALPHA
      RXYC0=DSQRT(XC0**2+YC0**2)
      ZEM=ZOUT
      XEM=RXYC0*DCOS(PHC)
      YEM=RXYC0*DSIN(PHC)
      XC0=XEM
      YC0=YEM
      GO TO 7044
C
7045  WRITE(1,7042)XEM,YEM,ZEM
7042  FORMAT(/'XEM=',F8.4,3X,'YEM=',F8.4,3X,'ZEM=',F8.4/)
2023  CALL DEVEND
      CALL EXIT
      END
C ========================================================
C          FUNCTIONS AND SUBROUTINES
C ========================================================
C
      FUNCTION FAN(XST)
      IMPLICIT DOUBLE PRECISION(A-H,O-Z)
      DIMENSION COEF(20)
      COMMON/BLO1/R0,R0G,WEB,H0,RKG
      COMMON/BLO2/CONS,RCAM,EXG,VG
      COMMON/BLO3/ALPHA,CSVG,SNVG,CSKOI,SNKOI,CSKOU,SNKOU
      COMMON/BLO4/Z,Z0,ZHH
      COMMON/BLO6/COEF,NCOEF,III,IYN,IYO
C
      IF(IYN .EQ. 1) WRITE(1,71)III
71    FORMAT(5X,I4,' TH  STEP  IN  COURSE (FUNCTION FAN)')
```

```
C
      CALL GRIN(Z,Z0,AXX,BYY,CXY,DDX,EY,FF)
C
      YST=0.0
      DO 70 J=1,NCOEF
      YST=YST+COEF(J)*XST**(J-1)
70    CONTINUE
      PHST=DATAN(YST/XST)
      RSTAN=DSQRT(XST**2+YST**2)
      PHST=PHST+ALPHA
      XST1=RSTAN*DCOS(PHST)
      YST1=RSTAN*DSIN(PHST)
C
      FAN=AXX*XST1**2+BYY*YST1**2+CXY*XST1*YST1+DDX*XST1
     $+EY*YST1+FF
C
      RETURN
      END
C ==================================================
      FUNCTION FEEL(XEEL)
      IMPLICIT DOUBLE PRECISION(A-H,O-Z)
      DIMENSION COEF(20),COEEL(3),COFL(40)
      COMMON/BLO1/R0,R0G,WEB,H0,RKG
      COMMON/BLO2/CONS,RCAM,EXG,VG
      COMMON/BLO3/ALPHA,CSVG,SNVG,CSKOI,SNKOI,CSKOU,SNKOU
      COMMON/BLO4/Z,Z0,ZHH
      COMMON/BLO5/S,NPOINT,NLAAP,ISEC
      COMMON/BLO6/COEF,NCOEF,III,IYN,IYO
      COMMON/BLO8/XFLUEE,YFLUEE,DMAR,XSTEEL,YSTEEL,DPHEEL,YEEL
      COMMON/BLO11/COFL,NSTFLI
C
      PI=3.14159265
      IF(IYO .EQ. 1) WRITE(1,71)III
71    FORMAT(5X,I4,' TH  STEP  IN  COURSE (FUNCTION FEEL)')
C
      CALL GRIN(Z,Z0,AXX,BYY,CXY,DDX,EY,FF)
C
      YEELDV=COEF(2)
      IF(S .NE. 1.)YEELDV=0.
      XEEL1=0.
      YEEL1=WEB/2.
      IF(S .EQ. 1.)YEEL1=-COEF(1)
      XEEL2=-YFLUEE
      YEEL2=XFLUEE
      PHEEL=DATAN(YEEL2/XEEL2)
      PHIIL=PHEEL+DPHEEL
      XEEL2=DSQRT(XEEL2**2+YEEL2**2)*DCOS(PHIIL)
      YEEL2=DSQRT(XEEL2**2+YEEL2**2)*DSIN(PHIIL)
      COEEL(1)=YEEL1
      COEEL(2)=YEELDV
      COEEL(3)=(YEEL2-XEEL2*COEEL(2)-COEEL(1))/XEEL2**2
      IF(XEEL .GE. .0)GO TO 1
      IF(S .EQ. 1. .AND. XEEL .LT. 0.) GO TO 5
      YEEL=0.
      XEELL=-XEEL
      DO 6 J=1,NSTFLI
      YEEL=YEEL+COFL(J)*XEELL**(J-1)
6     CONTINUE
      YEELL=-YEEL
      PHST=DATAN(YEELL/XEELL)+PI
      GO TO 2
5     YEEL=0.
      XEELL=-XEEL
      DO 7 J=1,NCOEF
      YEEL=YEEL+COEF(J)*XEELL**(J-1)
7     CONTINUE
      YEELL=+YEEL
      PHST=DATAN(YEELL/XEELL)+PI
      YEEL=-YEEL
      GO TO 2
C
1     YEEL=COEEL(1)+COEEL(2)*XEEL+COEEL(3)*XEEL**2
      PHST=DATAN(YEEL/XEEL)
2     RSTAN=DSQRT(XEEL**2+YEEL**2)
      PHST=PHST+ALPHA
      XST1=RSTAN*DCOS(PHST)
      YST1=RSTAN*DSIN(PHST)
      XSTEEL=XST1
      YSTEEL=YST1
C
      FEEL=AXX*XST1**2+BYY*YST1**2+CXY*XST1*YST1+DDX*XST1
     $+EY*YST1+FF
C
      RETURN
      END
C ==================================================
      FUNCTION FIIL(RHEEL)
      IMPLICIT DOUBLE PRECISION(A-H,O-Z)
      DIMENSION COEF(20),COEEL(3),COFL(40)
      COMMON/BLO1/R0,R0G,WEB,H0,RKG
      COMMON/BLO2/CONS,RCAM,EXG,VG
      COMMON/BLO3/ALPHA,CSVG,SNVG,CSKOI,SNKOI,CSKOU,SNKOU
      COMMON/BLO4/Z,Z0,ZHH
      COMMON/BLO5/S,NPOINT,NLAAP,ISEC
      COMMON/BLO6/COEF,NCOEF,III,IYN,IYO
      COMMON/BLO8/XFLUEE,YFLUEE,DMAR,XSTEEL,YSTEEL,DPHEEL,YEEL
      COMMON/BLO11/COFL,NSTFLI
      COMMON/BLO17/XEELA,YEELA,ZWEB
C
      PI=3.14159265
C
      CALL GRIN(Z,Z0,AXX,BYY,CXY,DDX,EY,FF)
C
      W2R=WEB/2./RHEEL
      IF(RHEEL .LE. WEB/2.) GO TO 1
      ANG=DATAN(W2R/DSQRT(1.-W2R**2))
      PHST=ANG+DSQRT(RHEEL**2-(WEB/2.)**2)*DSIN(H0)/DCOS(H0)/R0
     $*CSKOU/SNKOU
```

```
      IF(Z .LT. ZWEB)PHST=PI-PHST
      GO TO 2
1     PHST=PI/2.
2     XEELA=RHEEL*DCOS(PHST)
      YEELA=RHEEL*DSIN(PHST)
      PHST=PHST+ALPHA
      XST1=RHEEL*DCOS(PHST)
      YST1=RHEEL*DSIN(PHST)
      XSTEEL=XST1
      YSTEEL=YST1
C
      PIIL=AXX*XST1**2+BYY*YST1**2+CXY*XST1*YST1+DDX*XST1
     $+EY*YST1+FF
C
      RETURN
      END
C ================================================
      FUNCTION FIN(XST)
      IMPLICIT DOUBLE PRECISION(A-H,O-Z)
      DIMENSION COEF(2Ø)
      COMMON/BLO3/ALPHA,CSVG,SNVG,CSKOI,SNKOI,CSKOU,SNKOU
      COMMON/BLO6/COEF,NCOEF,III,IYN,IYO
C
      YST=Ø.Ø
      DO 15Ø J=1,NCOEF
      YST=YST+COEF(J)*XST**(J-1)
15Ø   CONTINUE
      PHST=DATAN(YST/XST)
      RSTAN=DSQRT(XST**2+YST**2)
      PHST=PHST+ALPHA
      XST1=RSTAN*DCOS(PHST)
      YST1=RSTAN*DSIN(PHST)
      FIN=YST1
C
C
      RETURN
      END
C ================================================
      FUNCTION FLANK(ZCLE)
      IMPLICIT DOUBLE PRECISION(A-H,O-Z)
      DIMENSION COEF(2Ø)
      COMMON/BLO1/RØ,RØG,WEB,HØ,RKG
      COMMON/BLO2/CONS,RCAM,EXG,VG
      COMMON/BLO3/ALPHA,CSVG,SNVG,CSKOI,SNKOI,CSKOU,SNKOU
      COMMON/BLO4/Z,ZØ,ZHH
      COMMON/BLO6/COEF,NCOEF,III,IYN,IYO
      COMMON/BLO7/XCLE,YCLE,IFL,IHILST,PHIIL2
      COMMON/BLO8/XFLUEE,YFLUEE,DMAR,XSTEEL,YSTEEL,DPHEEL,YEEL
C
      IF(IFL .NE. 1) GO TO 1
      XEEL2=-YFLUEE
      YEEL2=DSQRT(RØ**2-XEEL2**2)
      PHEEL=DATAN(YEEL2/XEEL2)
      PHIIL=PHEEL+DPHEEL
      IF(IHILST .NE. 1) GO TO 2
      W2R=WEB/2./RØ
      PHIIL=DATAN(W2R/DSQRT(1.-W2R**2))+DSQRT(RØ**2-(WEB/2.)**2)
     $*DSIN(HØ)/DCOS(HØ)/RØ*CSKOU/SNKOU
2     ALPHA=ZCLE/RØ*DSIN(HØ)/DCOS(HØ)
      PHST=PHIIL+ALPHA
      XCLE=RØ*DCOS(PHST)
      YCLE=RØ*DSIN(PHST)
      PHIIL2=DATAN(YCLE/XCLE)
1     Z=ZCLE
C
      CALL GRIN(Z,ZØ,AXX,BYY,CXY,DDX,EY,FF)
C
      FLANK=AXX*XCLE**2+BYY*YCLE**2+CXY*XCLE*YCLE+DDX*XCLE
     $+EY*YCLE+FF
C
      RETURN
      END
C ================================================
      FUNCTION FON(RSTAN)
      IMPLICIT DOUBLE PRECISION(A-H,O-Z)
      COMMON/BLO1/RØ,RØG,WEB,HØ,RKG
      COMMON/BLO3/ALPHA,CSVG,SNVG,CSKOI,SNKOI,CSKOU,SNKOU
C
      W2R=WEB/2./RSTAN
      PHST=-(DATAN(W2R/DSQRT(1.-W2R**2))+DSQRT(RSTAN**2-(WEB/2.)**2)
     $*DSIN(HØ)/DCOS(HØ)/RØ*CSKOU/SNKOU)
      FON=PHST+ALPHA
C
      RETURN
      END
C ================================================
      FUNCTION FOUTCR(ZOUT)
      IMPLICIT DOUBLE PRECISION(A-H,O-Z)
      COMMON/BLO1/RØ,RØG,WEB,HØ,RKG
      COMMON/BLO2/CONS,RCAM,EXG,VG
      COMMON/BLO3/ALPHA,CSVG,SNVG,CSKOI,SNKOI,CSKOU,SNKOU
      COMMON/BLO4/Z,ZØ,ZHH
      COMMON/BLO5/S,NPOINT,NLAAP,ISEC
      COMMON/BLO21/XOUT,YOUT
C
      ALPHA=ZOUT/RØ*DSIN(HØ)/DCOS(HØ)
      W2R=WEB/2./RØ
      PHST=-(DATAN(W2R/DSQRT(1.-W2R**2))+DSQRT(RØ**2-(WEB/2.)**2)
     $*DSIN(HØ)/DCOS(HØ)/RØ*CSKOU/SNKOU)
      PHST=PHST+ALPHA
      XST=RØ*DCOS(PHST)
      YST=RØ*DSIN(PHST)
C
      CALL GRIN(ZOUT,ZØ,AXX,BYY,CXY,DDX,EY,FF)
C
      FOUTCR=AXX*XST**2+BYY*YST**2+CXY*XST*YST+DDX*XST
     $+EY*YST+FF
C
```

```
      RETURN
      END
C
C =================================================
      FUNCTION FPACE(PHPACE)
      IMPLICIT DOUBLE PRECISION(A-H,O-Z)
      COMMON/BLO14/RPACE,PHPA,ZPACE1
C
      YPACE=RPACE*DSIN(PHPACE+PHPA)
      FPACE=YPACE-YPACE1
C
      RETURN
      END
C =====================================================
      FUNCTION FUN(RSTAN)
      IMPLICIT DOUBLE PRECISION(A-H,O-Z)
      INTEGER NPOINT
      COMMON/BLO1/R0,R0G,WEB,H0,RKG
      COMMON/BLO2/CONS,RCAM,EXG,VG
      COMMON/BLO3/ALPHA,CSVG,SNVG,CSKOI,SNKOI,CSKOU,SNKOU
      COMMON/BLO4/Z,Z0,ZHH
      COMMON/BLO5/S,NPOINT,NLAAP,ISEC
C
      W2R=WEB/2./RSTAN
      PHST=-(DATAN(W2R/DSQRT(1.-W2R**2))+DSQRT(RSTAN**2-
     $(WEB/2.)**2)*DSIN(H0)/DCOS(H0)/R0*CSKOU/SNKOU)
      PHST=PHST+ALPHA
      XST=RSTAN*DCOS(PHST)
      YST=RSTAN*DSIN(PHST)
C
      CALL GRIN(Z,Z0,AXX,BYY,CXY,DDX,EY,FF)
C
      FUN=AXX*XST**2+BYY*YST**2+CXY*XST*YST+DDX*XST
     $+EY*YST+FF
C
      RETURN
      END
C ==================================================
      FUNCTION GPACE(PHPACE)
      IMPLICIT DOUBLE PRECISION(A-H,O-Z)
      COMMON/BLO1/R0,R0G,WEB,H0,RKG
      COMMON/BLO14/RPACE,PHPA,ZPACE1
      COMMON/BLO16/COEA,COEB,COEC,COED
      COMMON/BLO28/XPACE,YPACE,ZPACE
C
      ZPACE=PHPACE*R0*DCOS(H0)/DSIN(H0)+ZPACE1
      YPACE=RPACE*DSIN(PHPACE+PHPA)
      XPACE=RPACE*DCOS(PHPACE+PHPA)
      GPACE=COEA*XPACE+COEB*YPACE+COEC*ZPACE+COED
C
      RETURN
      END
C ====================================================
      SUBROUTINE GRIN(Z,Z0,AXX,BYY,CXY,DDX,EY,FF)
      IMPLICIT DOUBLE PRECISION(A-H,O-Z)
      COMMON/BLO1/R0,R0G,WEB,H0,RKG
      COMMON/BLO2/CONS,RCAM,EXG,VG
      COMMON/BLO3/ALPHA,CSVG,SNVG,CSKOI,SNKOI,CSKOU,SNKOU
C
      AXX=CSVG**2+(CSKOI**2)*(SNVG**2)
      BYY=SNVG**2+CSVG**2*(CSKOI**2)
      CXY=-2.*SNVG*CSVG+2.*(CSKOI**2)*SNVG*CSVG
      DDX=-2.*EXG*CSVG-2.*(Z-Z0)*SNKOI*CSKOI*SNVG
      EY=2.*EXG*SNVG-2.*(Z-Z0)*SNKOI*CSKOI*CSVG
      FF=EXG**2-(2.*R0G)**2+((Z-Z0)**2)*SNKOI**2
C
      RETURN
      END
C
C ====================================================
      SUBROUTINE MONAT(M,N,EIX,RE,FJAC,LJC,SMON,IGR,NITER,NF,IW,
     $LIW,WE0,LW)
      IMPLICIT DOUBLE PRECISION(A-H,O-Z)
      DIMENSION EIX(4),RE(8),FJAC(8,8),SMON(8),IW(1),WE0(120)
      FE=RE(1)**2+RE(2)**2+RE(3)**2+RE(4)**2+RE(5)**2+RE(6)**2
     $+RE(7)**2+RE(8)**2
      WRITE(1,20)NITER,FE
20    FORMAT('AFTER',I4,'   ITERATIONS',2X,'THE SUM OF SQ. IS'
     $,F12.6)
      WRITE(1,22)(EIX(I),I=1,N)
22    FORMAT('AT THE POINT',F10.4)
C
      RETURN
      END
C ====================================================
      SUBROUTINE MONIT(M,N,CORN,RE,FJAC,LJC,SMON,IGR,NITER,
     $NF,IW,LIW,WE0,LW)
      IMPLICIT DOUBLE PRECISION(A-H,O-Z)
      DIMENSION CORN(3),RE(3),FJAC(3,3),SMON(3),IW(1),WE0(120)
      FE=RE(1)**2+RE(2)**2+RE(3)**2
      WRITE(1,20)NITER,FE
20    FORMAT('AFTER',I4,'   ITERATIONS',2X,'THE SUM OF SQ. IS'
     $,F9.3)
      WRITE(1,22)(CORN(I),I=1,N)
22    FORMAT('AT THE POINT',F10.4)
      RETURN
      END
C
C ====================================================
      SUBROUTINE MONUT(M,N,CORN,RU,FJAC,LJC,SMON,IGR,NITER,
     $NF,IW,LIW,WE0,LW)
      IMPLICIT DOUBLE PRECISION(A-H,O-Z)
      DIMENSION CORN(3),RU(3),FJAC(3,3),SMON(3),IW(1),WE0(120)
      FU=RU(1)**2+RU(2)**2+RU(3)**2
      WRITE(1,20)NITER,FU
20    FORMAT('AFTER',I4,'   ITERATIONS',2X,'THE SUM OF SQ. IS'
     $,F9.3)
      WRITE(1,22)(CORN(I),I=1,N)
```

```
22    FORMAT('AT THE POINT',F10.4)
C
      RETURN
      END
C
C ==================================================
      SUBROUTINE RESAD(IFLAG,M,N,EIX,RE,IW,LIW,WE0,LW)
      IMPLICIT DOUBLE PRECISION(A-H,O-Z)
      DIMENSION XSTGD(100),YSTGD(100),ZSTGD(100)
      DIMENSION XNRAD(100),YNRAD(100),ZNRAD(100)
      DIMENSION RRN(100),RCA(100)
      DIMENSION VERIF(100),EIX(4),RE(8)
      COMMON/BLO5/S,NPOINT,NLAA,ISEC  .
      COMMON/BLO21/ZEB,XEB,YEB,XEM,YEM,ZEM
      COMMON/BLO24/PA,PI,RC0,RC1
      COMMON/BLO25/XSTGD,YSTGD,ZSTGD
      COMMON/BLO26/RRN
      COMMON/BLO27/XNRAD,YNRAD,ZNRAD
C
      NLOO1=IFIX(NPOINT/3)
      NLOO3=4
      NLOO2=2*NLOO1
      XEB=EIX(1)
      YEB=EIX(2)
      XEM=EIX(3)
      YEM=EIX(4)
C
      DO 1 J=1,5
      GO TO(10,11,12,13,15),J
10    I=1
      GO TO 14
11    I=NLOO1
      GO TO 14
12    I=NLOO2
      GO TO 14
13    I=NPOINT
      GO TO 14
15    I=NLOO3
14    CONTINUE
C
      DBM=DSQRT((XEM-XEB)**2+(YEM-YEB)**2+(ZEM-ZEB)**2)
      AAA=(XEM-XEB)/DBM
      BBB=(YEM-YEB)/DBM
      CCC=(ZEM-ZEB)/DBM
C
      REVAB=3.
      WAA=2.0*PI*REVAB
      V1=REVAB*PA
      ABC1=BBB*(ZSTGD(I)-ZEM)-CCC*(YSTGD(I)-YEM)
      ABC2=CCC*(XSTGD(I)-XEM)-AAA*(ZSTGD(I)-ZEM)
      ABC3=AAA*(YSTGD(I)-YEM)-BBB*(XSTGD(I)-XEM)
      VC1=AAA*V1+WAA*ABC1
      VC2=BBB*V1+WAA*ABC2
      VC3=CCC*V1+WAA*ABC3
      VC=DSQRT(VC1**2+VC2**2+VC3**2)
      VC1=VC1/VC
      VC2=VC2/VC
      VC3=VC3/VC
      IF(ABC1 .NE. 0.0) GO TO 9148
      WRITE(1,9149)
9149  FORMAT('          ABC1   IS   NUL')
      CALL EXIT
9148  ZEXEAC=-ABC3/ABC1*AAA+CCC
      YEXEAB=-ABC2/ABC1*AAA+BBB
      IF(YEXEAB .NE. 0.0) GO TO 9151
      WRITE(1,9152)
9152  FORMAT('         YEXEAB  IS   NUL')
      CALL EXIT
9151  ZEYEXE=ZEXEAC*ABC2/YEXEAB/ABC1-ABC3/ABC1
      ZEZEYE=1.+ZEYEXE**2+(ZEXEAC/YEXEAB)**2
      CONSTA=(XEB-XSTGD(I))*ZEYEXE-(YEB-YSTGD(I))
     $*ZEXEAC/YEXEAB+(ZEB-ZSTGD(I))
      IF(ZEZEYE .NE. 0.0) GO TO 9153
      WRITE(1,9154)
9154  FORMAT('ZEZEYE     IS  NUL')
      CALL EXIT
C
9153  VN3=-CONSTA/ZEZEYE
      VN2=-ZEXEAC/YEXEAB*VN3
      VN1=ZEYEXE*VN3
      RCA(I)=DSQRT(VN1**2+VN2**2+VN3**2)
      VERIF1=VC1*XNRAD(I)
      VERIF2=VC2*YNRAD(I)
      VERIF3=VC3*ZNRAD(I)
      COSV=VERIF1+VERIF2+VERIF3
      VER=DATAN(DSQRT(1.-COSV**2)/COSV)
      VERI=(PI/2.-VER)
      IF(VERI .GT. PI/2.)VERI=VERI-PI
      VERIF(I)=VERI
1     CONTINUE
C
      RE(1)=RCA(1)-RC0
      RE(2)=VERIF(1)
      RE(3)=VERIF(NLOO1)
      RE(4)=VERIF(NLOO2)
      RE(5)=VERIF(NPOINT)
      RE(6)=VERIF(NLOO3)
      RE(7)=VERIF(NLOO2)
      RE(8)=RCA(NPOINT)-RC1
C
      RETURN
      END
C ================================================
      SUBROUTINE RESID(IFLAG,M,N,CORN,RE,IW,LIW,WE0,LW)
      IMPLICIT DOUBLE PRECISION(A-H,O-Z)
      DIMENSION RE(3),CORN(3),IW(1),WE0(120)
      COMMON/BLO1/R0,R0G,WEB,H0,RKG
      COMMON/BLO2/CONS,RCAM,EXG,VG
```

```
      COMMON/BLO3/ALPHA,CSVG,SNVG,CSKOI,SNKOI,CSKOU,SNKOU
      COMMON/BLO4/Z,ZØ,ZHH
C
      PI=3.14159265
      XCORN=CORN(1)
      YCORN=CORN(2)
      ZCORN=CORN(3)
C
      RSTAN=DSQRT(XCORN**2+YCORN**2)
      ALPHA=ZCORN/RØ*DSIN(HØ)/DCOS(HØ)
      IF(RSTAN .LE. WEB/2.)GO TO 1
      W2R=WEB/2./RSTAN
      PHST=-(DATAN(W2R/DSQRT(1.-W2R**2))+DSQRT(RSTAN**2-
     $(WEB/2.)**2)*DSIN(HØ)/DCOS(HØ)/RØ*CSKOU/SNKOU)
      GO TO 2
1     PHST=-PI/2.
2     PHSTXY=-DATAN(YCORN/XCORN)
      CALL GRIN(ZCORN,ZØ,AXX,BYY,CXY,DDX,EY,FF)
C
      RE(1)=AXX*XCORN**2+BYY*YCORN**2+CXY*XCORN*YCORN+DDX*XCORN
     $+EY*YCORN+FF
      RE(2)=AXX*XCORN**2+BYY*YCORN**2+CXY*XCORN*YCORN-DDX*XCORN
     $-EY*YCORN+FF
      RE(3)=PHST+PHSTXY+ALPHA
C
      RETURN
      END
C ======================================================
      SUBROUTINE RESUD(IFLAG,M,N,CORN,RU,IW,LIW,WEØ,LW)
      IMPLICIT DOUBLE PRECISION(A-H,O-Z)
      DIMENSION COEF(2Ø),RU(3),CORN(3),IW(1),WEØ(12Ø)
      COMMON/BLO1/RØ,RØG,WEB,HØ,RKG
      COMMON/BLO2/CONS,RCAM,EXG,VG
      COMMON/BLO3/ALPHA,CSVG,SNVG,CSKOI,SNKOI,CSKOU,SNKOU
      COMMON/BLO4/Z,ZØ,ZHH
      COMMON/BLO6/COEF,NCOEF,III,IYN,IYO
C
      XCORN=CORN(1)
      YCORN=CORN(2)
      ZCORN=CORN(3)
C
      CALL GRIN(ZCORN,ZØ,AXX,BYY,CXY,DDX,EY,FF)
C
      RSTAN=DSQRT(XCORN**2+YCORN**2)
      PHSTXY=-DATAN(YCORN/XCORN)
      ALPHA=ZCORN/RØ*DSIN(HØ)/DCOS(HØ)
      PHST=-PHSTXY-ALPHA
      XST1=RSTAN*DCOS(PHST)
      YST1=RSTAN*DSIN(PHST)
      YST=Ø.Ø
      DO 7Ø J=1,NCOEF
      YST=YST+COEF(J)*XST1**(J-1)
7Ø    CONTINUE
C
      RU(1)=AXX*XCORN**2+BYY*YCORN**2+CXY*XCORN*YCORN+DDX*XCORN
     $+EY*YCORN+FF
      RU(2)=AXX*XCORN**2+BYY*YCORN**2+CXY*XCORN*YCORN-DDX*XCORN
     $-EY*YCORN+FF
      RU(3)=YST-YST1
C
      RETURN
      END
C
C ======================================================
      FUNCTION ROTAC(XLK)
      IMPLICIT DOUBLE PRECISION(A-H,O-Z)
      DIMENSION COEF(2Ø)
      COMMON/BLO1/RØ,RØG,WEB,HØ,RKG
      COMMON/BLO6/COEF,NCOEF,III,IYN,IYO
      COMMON/BLO15/XLØ,YLØ
C
      YLK=Ø.
      DO 75 J=1,NCOEF
      YLK=YLK+COEF(J)*XLK**(J-1)
75    CONTINUE
      R=DSQRT(XLK**2+YLK**2)
      ROTAC=R-RØ
      XLØ=XLK
      YLØ=YLK
C
      RETURN
      END
C
C *END*END*END*END*END*END*END*END*END*END*END*END*END*
```